Generation of induced Pluripotent Stem Cell derived Endothelial Cells from Fibrodysplasia Ossificans Progressiva patients-

a disease model of ActivinA and BMP-induced ALK2 receptor activation

Inaugural-Dissertation

to obtain the academic degree

Doctor rerum naturalium (Dr. rer. nat.)

submitted to the Department of Biology, Chemistry and Pharmacy

of Freie Universität Berlin

by

Susanne Hildebrandt

Berlin, 2020

This PhD thesis was prepared from September 2015 to December 2020 in the group of Prof. Dr. Petra Knaus, Institute of Chemistry and Biochemistry, Freie Universität Berlin.

First supervisor: Prof. Dr. Petra Knaus
Institut für Chemie und Biochemie
Freie Universtiät Berlin
Thielallee 63,14195 Berlin
E-Mail: petra.knaus@fu-berlin.de

Second supervisor: Prof. Dr. Sigmar Stricker
Institut für Chemie und Biochemie
Freie Universtiät Berlin
Thielallee 63,14195 Berlin
E-Mail: sigmar.stricker@fu-berlin.de

Date of disputation: 05.03.2021

Contents

List of Figures

List of Tables

Summary

Fibrodysplasia Ossificans Progressiva (FOP) is a rare disease characterized by episodic bone formation outside of the skeleton (ectopic bone) in soft tissues in a process called heterotopic ossification (HO). Independent of the location and initial triggers, ectopic bone in FOP forms via a complex-multi-stage process, which mimics the developmental process of endochondral bone formation. Bone is a highly vascularized organ and its formation requires a tightly controlled interplay of osteogenesis and angiogenesis. Blocking or loss of pro-angiogenic factors (e.g. VEGFA) impairs bone formation by disturbed angiogenesis and decreased ossification. FOP patient biopsies revealed that HO lesions are highly angiogenic with aberrations in vascular markers and morphology suggesting the involvement of pathological angiogenesis and Endothelial to Mesenchymal Transition (EndMT). However, it remains elusive, which molecular mechanisms orchestrate the vasculature in ectopic bone formation and which signals are responsible for the aberrant vascular phenotype in FOP lesions.

FOP is caused by mutations in the BMP type I receptor ALK2 leading to hypersensitive signaling and aberrant SMAD1/5 activation by ActivinA. In FOP mice, blocking of ActivinA prevents HO indicating a central role of this ligand in the disease.

Whether signaling responses of Activin or BMP ligands cause the vascular phenotype in human FOP biopsies is unknown. The endothelium represents a fundamental component of the vasculature by forming the initial tubular structure.

In the present study a patient derived endothelial cell (EC) model was generated by using induced Pluripotent Stem Cells (iPSCs) in a combinatorial cryopreservation and differentiation method. FOP iECs recapitulated the pathomechanism of aberrant ActivinA/SMAD1/5 signaling and additionally showed aberrant BMP/SMAD2 responses in an ALK2 dependent manner. ActivinA transduced a BMP like response only in FOP iECs and a comprehensive transcriptome analysis identified a FOP-specific genetic profile interlinking ActivinA with BMP/NOTCH pathways, blood vessel formation and EndMT.

Collectively, the results propose a model in which ActivinA primes FOP ECs in favor of pathological angiogenesis and EndMT in presence of angiogenic and inflammatory factors as 2nd triggers.

ActivinA induced only partial EndMT and alterations in angiogenesis were only observed in presence of VEGFA suggesting a *second hit* model for pathological endothelial function in FOP lesions. Thus, I propose that the ActivinA induced FOP specific transcriptome (1st trigger) pre-patterns the FOP endothelium and thereby challenges endothelial identity and plasticity, which leads to pathological angiogenesis and EndMT in presence of 2nd triggers.

Drug testing in the FOP endothelial disease model demonstrated that the kinase inhibitor Saracatinib rescued aberrant signaling responses and the ActivinA-induced transcriptome in FOP iECs to WT levels, suggesting a preventive effect on pathological vascularization in pre-osseous FOP lesions.

Zusammenfassung

Fibrodysplasia Ossificans Progressiva (FOP) ist eine seltene Erkrankung, die durch episodische Knochenbildung außerhalb des Skeletts (ektopischer Knochen) gekennzeichnet ist. Der Prozess der Knochenbildung in Weichteilgewebe wird heterotope Ossifikation genannt (HO). Unabhängig von der Lokalisation und den anfänglichen Auslösern bildet sich der ektopische Knochen bei FOP über einen komplexen, mehrstufigen Prozess, der die endochondrale Knochenbildung nachahmt. Der Knochen ist ein stark vaskularisiertes Organ und seine Bildung erfordert ein eng kontrolliertes Zusammenspiel von Knochen- (Osteogenese) und Blutgefäßbildung (Angiogenese).

Die Inhibierung oder der Verlust von pro-angiogenen Faktoren (z.B. VEGFA) beeinträchtigt die Angiogenese und verringert die Knochenbildung. Biopsien von FOP-Patienten enthüllten, dass sich in Läsionen der HO viele Blutgefäße bilden, welche veränderte Markerproteine und Morphologie aufweisen. Dies lässt eine pathologischen Angiogenese und eine Endothelial-mesenchymale Transition (EndMT) vermuten. Es bleibt jedoch unklar, welche molekularen Mechanismen die Blutgefäße während der ektopischen Knochenbildung steuern und welche Signale für den vaskulären Phänotyp in FOP-Läsionen verantwortlich sind.

FOP wird durch Mutationen im BMP-Typ-I-Rezeptor ALK2 verursacht, die zu einer hypersensitiven Signalübertragung und einer aberranten SMAD1/5-Aktivierung durch ActivinA führen. In FOP-Mäusen verhindert die Blockierung von ActivinA die HO, was auf eine zentrale Rolle dieses Liganden bei FOP hinweist. Ob Signalübertragungen von Activin- oder BMP-Liganden den vaskulären Phänotyp in menschlichen FOP-Biopsien verursachen, ist unbekannt. Das Endothel stellt eine fundamentale Komponente der Vaskulatur dar und bildet die initiale tubuläre Struktur von Blutgefäßen.

In der vorliegenden Studie wurde ein FOP-Endothelzellmodell mittels kombinatorischer Kryokonservierungs- und Differenzierungsmethode generiert. Dafür wurden von FOP Patienten stammende induzierte pluripotente Stammzellen (iPSZ) verwendet. Die aus FOP iPSZ generierten Endothelzellen rekapitulierten den Pathomechanismus der aberranten ActivinA/SMAD1/5-Signalübertragung und zeigten zusätzlich aberrante BMP/SMAD2-Signalantworten in einer ALK2-abhängigen Weise.

ActivinA transduzierte eine BMP-ähnliche Antwort nur in FOP Enothelzellen und eine umfassende Transkriptomanalyse identifizierte ein FOP-spezifisches genetisches Profil, das ActivinA mit BMP/NOTCH-Signalwegen, Blutgefäßbildung und EndMT verknüpft. ActivinA induzierte nur teilweise EndMT und veränderte die Angiogenese nur in Gegenwart von VEGFA, was auf ein *second hit* Modell für die pathologische Endothelfunktion in FOP-Läsionen hindeutet.

Auf Basis des *second hit* Modells wird angenommen, dass ActivinA als erster Auslöser ein FOP-spezifisches Transkriptom induziert, welches das FOP-Endothel vorstrukturiert. In Gegenwart des zweiten Triggers wird die endotheliale Identität und Plastizität herausgefordert und mündet in pathologische Angiogenese und EndMT. Medikamententests im FOP-Endothelmodell zeigten, dass der Kinaseinhibitor Saracatinib die aberranten Signalantworten und das ActivinA-induzierte Transkriptom in FOP-Endothelzellen auf WT-Niveau hält. Dies deutet auf eine präventive Wirkung auf eine mögliche pathologischen Vaskularisierung in frühen FOP-Läsionen hin, bevor der ektopische Knochen entsteht.

1. Introduction

1.1 Bone is a vascularized organ

The formation of the endoskeleton is a unique feature of embryonic development in vertebrates. The skeletal system is complex and consists of bones, joint, ligaments and tendons and is mostly described as a framework of the body, which enables support, movement and protection of inner organs. Skeletal structures derive from mesenchyme precursors and most bones develop from a cartilage intermediate, which becomes gradually replaced by bone through endochondral ossification between the sixth and seventh week of human embryonic development. Only flat bone of the skull, clavicle and most cranial bones form directly from mesenchymal tissue to bone via intramembranous ossification (Breeland et al., 2020). At birth the majority of cartilage is replaced by bone but ossification proceeds throughout growth until the age of about 25 (Breeland et al., 2020). However, those developmental bone formation programs become re-activated in cases of injury to regenerate bone in fracture healing (Hu et al., 2017). Bone is a vital organ composed of mineralized connective tissue and specialized cells, which maintain bone homeostasis, involving essential physiological processes such as mineral storage and hematopoiesis (Al-Bari and Mamun, 2020).

After development and growth, bone in skeletal structures is constantly formed and resorbed in a process called ***remodeling***, which maintains organ homeostasis by bone matrix forming osteoblasts and resorbing osteoclasts accompanied by osteocytes (Hattner et al., 1965). The complex remodeling process adapts to changing biomechanical forces and the average turnover of bone is 10% per year, corresponding to estimations of complete renewal of the skeleton every ten years (Manolagas and Parfitt, 2010). Already in the 1869 Julius Wolff observed that **bones are living, highly vascularized structures** (Figure 1.1) that shape during life (remodel) and adapt to mechanical loads (White et al., 2011).

Today, it has become increasingly clear that different bone compartments are not only nourished by an integrated **vascular network**. In fact, the vasculature is indispensable as a functional component for bone development, repair, hematopoiesis, mineral storage and endocrine functions (Filipowska et al., 2017). Recent evidence suggest different vasculature in specific bone regions and even the existence of specialized bone vessel sub-types (Sivaraj and Adams, 2016). Increasing evidence demonstrates

that **osteogenesis** and **vascularization** is tightly coupled but the underlying molecular mechanisms remain poorly understood (Grosso et al., 2017).

The following chapters will introduce the essential role of the vasculature in bone formation and how molecular mechanisms of single cell types may navigate the vasculature in this process. This is of interest in context of the **rare disease Fibrodysplasia Ossificans Progressiva (FOP)**, which is characterized by a severe form of ectopic bone formation in soft tissues outside of the skeleton.

In the present study the establishment of a FOP disease model will demonstrate how the overactivation of the molecular signaling pathway of **Bone Morphogenetic Proteins (BMPs)** changes vascular cell responses and how this may contribute to the initiation of ectopic bone formation in FOP.

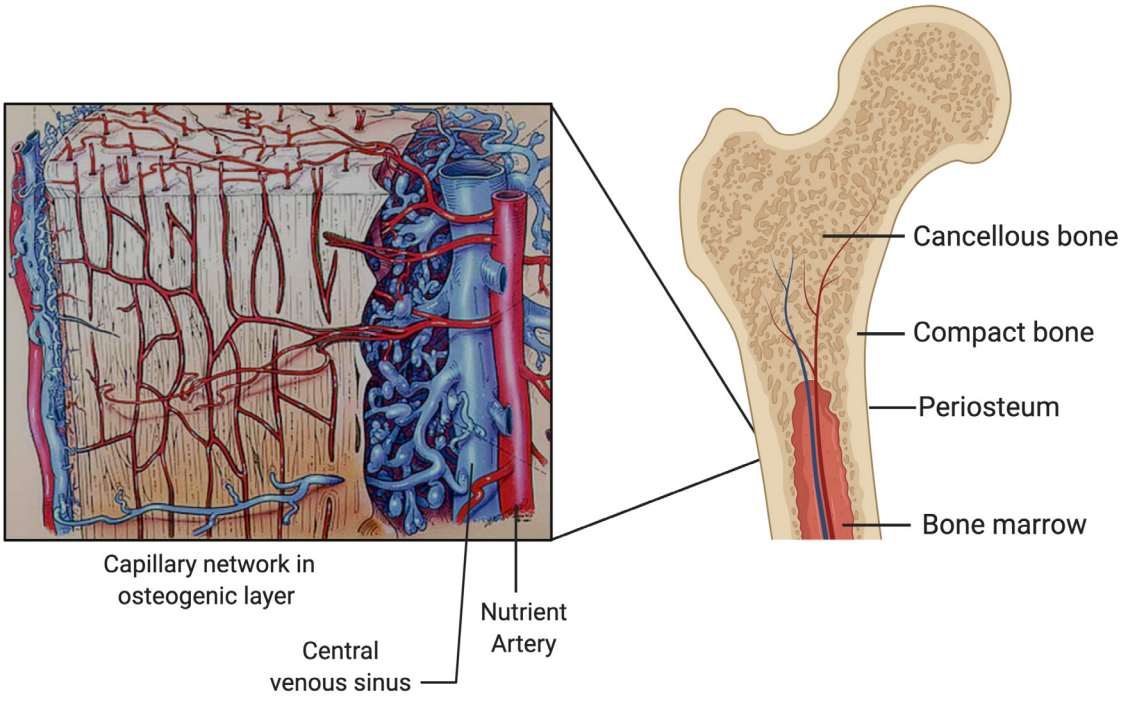

Figure 1.1 Vascular networks in bone. Schematic depiction of the head (Epiphysis) and a part of the lower shaft (Diaphysis) of a long bone (right image) and the integrated blood vessel connections between bone marrow, cortical bone and the outer connective tissue layer (periosteum) (right and left image). The left image is adapted from (Cowin and Cardoso, 2015).

1.2 Blood vessels form vascular networks

The vascular system of an organism permits circulation of blood to ensure oxygen and nutrition supply and waste removal from all tissues to sustain growth and viability and to support and maintain diverse organ functions (Filipowska et al., 2017).

This requires the establishment of a complex vessel network, which maintains blood flow and reaches every tissue. Thereby, the vascular system connects the heart with all other organs and needs to quickly adapt to acute and chronic changes in tissues. In fact, the cardiovascular system is the first functional organ, which is formed in development of vertebrates (Udan et al., 2013). Defects in vascular development and vessel formation may cause embryonic lethality and contribute to vascular pathologies (Chappell and Bautch, 2010).

The vasculature can be subdivided in the arterial, venous and lymphatic vessel systems. The arterial system transports blood away from the heart and is composed of large but also smaller diameter arteries and arterioles. In contrast, the venous system transports blood back to the heart through larger venules and veins. The heart is connected through the pulmonary arteries and veins to the rest of the vasculature to circulate blood to and from the lungs. The arterial and venous vascular beds form a closed circulatory system by a hierarchical vascular tree with large arteries and veins that are connected to progressively smaller, thin capillaries (Figure 1.2A, C).

In contrast, the lymphatic system is not closed and forms a unidirectional network that begins as blind-ended lymphatic capillaries that transport interstitial fluid from tissues and organs into larger collecting vessels (Jiang et al., 2018). The endothelium can be considered as the fundamental building block of the vascular system by forming the initial tubular structure.

Endothelial cells (ECs) line the inner wall of blood vessels and form via intercellular junctions a dynamic barrier between circulating blood and tissue (Figure 1.2B). The endothelium is supported by mural cells, which include smooth muscle cells and pericytes. Larger vessels are surrounded by thicker layers of smooth muscle cells and an outer layer of connective tissues, which maintain stability and allow dynamic responses to blood flow and contractility (Taylor and Bordoni, 2020; Udan et al., 2013) (Figure 1.2B). Different vascular beds and vessel types can be distinguished by specific molecules and pathways of the endothelium, which specifiy cellular function and morphology on organ and tissue demands (Rocha and Adams, 2009). However, up to date the heterogeneity of the endothelium remains incompletely understood.

But in recent years the knowledge has increased based on data from single-cell sequencing allowing the characterization of cellular heterogeneity by whole genome profiles (Chavkin and Hirschi, 2020). For example, a very recent study mapped endothelial heterogeneity of the adult lung and identified a new EC subpopulation by using single cell analytics (Niethamer et al., 2020). Moreover, transcriptomic analysis identified an endothelial cell subtype in embryonic and early postnatal long bones, which strongly supports osteoblast cells (Langen et al., 2017).

New blood vessels can form *de novo* from endothelial progenitors by **vasculogenesis** or from pre-existing vessels by **sprouting angiogenesis**. Both processes are essential in vascular development in embryogenesis but also postnatally.

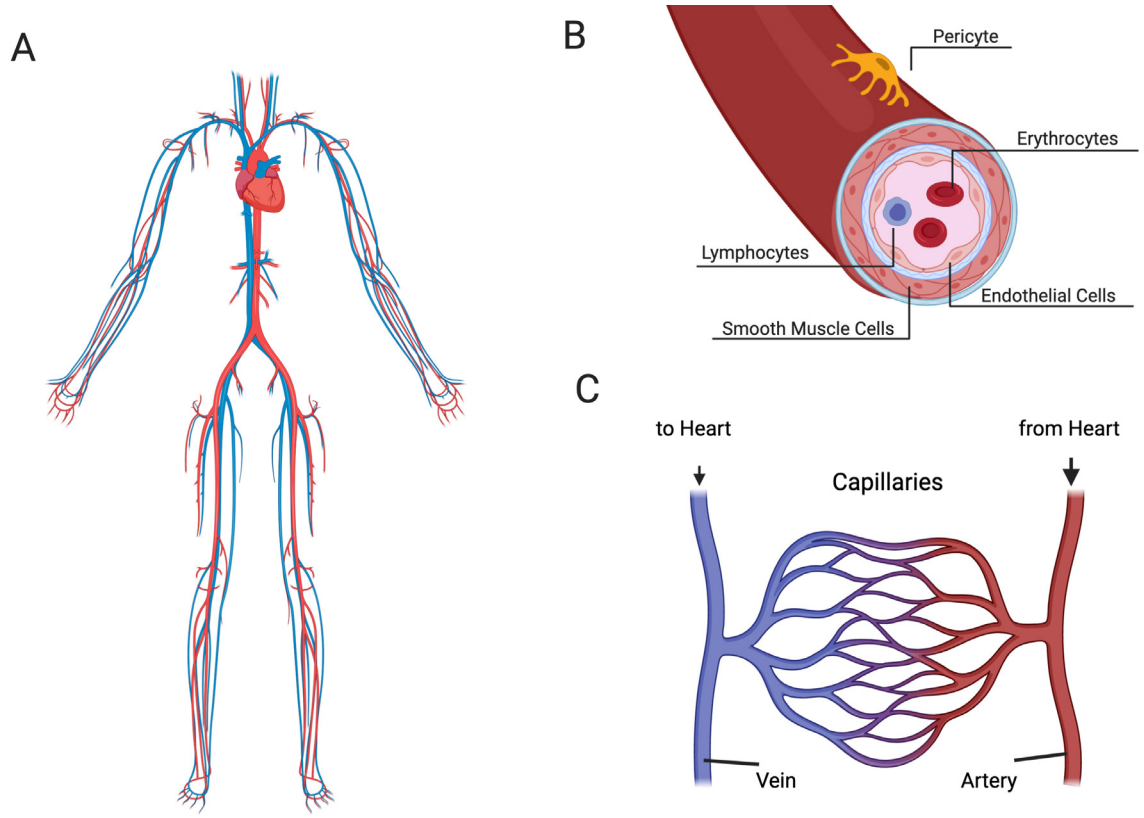

Figure 1.2 The vascular system and its cellular components. (**A**) The vasculature can be subdivided in the arterial, venous systems. (**B**) Vessel size and wall characteristics are very heterogenous but each vessel consists of three main cell types: Endothelial cells, which line the inner wall of blood vessels and form a dynamic barrier between the tissue and the circulating blood containing Erythrocytes and Lymphocytes. The endothelium is supported by mural cells, which include smooth muscle cells and pericytes. (**C**) The arterial and venous circulatory system is connected by smaller venous and arterial capillaries.

1.2.1 **Embryonic blood vessel development**

In embryonic development first blood vessels form *de novo* via **vasculogenesis** shortly after gastrulation from mesoderm. Mesoderm becomes induced between ectoderm and endoderm during gastrulation involving **BMP4** expression from the epiblast (Figure 1.3A). The epiblast (primitive ectoderm) derives together with the

hypoblast (primitive endoderm) from the inner cell layer of the blastocyst (Dyer and Patterson, 2010). Shortly after gastrulation, the **mesoderm** becomes further specified in axial, paraxial and lateral domains. High levels of BMP signaling specify the formation of **lateral plate mesoderm**, which constitutes the progenitors for the heart, cardiovascular system, blood, kidneys, smooth muscle lineage and also for the limb skeleton (Prummel et al., 2020).

BMP4 is essential in mesoderm formation as *Bmp4* deficient mice die at (E7.5-E9.5) due to mesodermal defects in gastrulation (Winnier et al., 1995). Interestingly, some homozygous mutants developed beyond this stage, indicating that Bmp2, which has 92% sequence identity of the mature region may in some cases compensate for the absence of Bmp4 as both ligands are expressed in embryos from embryonic developmental stage E6.5 to E10.5 (Winnier et al., 1995). This is supported by the observation that mice deficient in *Alk3*, the high affinity binding receptor for Bmp2 and Bmp4, did not develop beyond gastrulation (Winnier et al., 1995). However, mice deficient in either *Alk3*, *Bmp2* or *Bmp4* are embryonic lethal (Sun et al., 2007; Wang et al., 2014).

Moreover, studies with human embryonic stem cells (ESCs) demonstrated that BMP4 was required for mesoderm induction and the formation of primitive vascular networks (Boyd et al., 2007; Zhang et al., 2008). In contrast, BMP2 stimulation of ESC resulted in extra-embryonic endoderm (Pera et al., 2004) suggesting that primarly BMP4 is required for mesoderm induction in human ESCs. However, BMP4 directly induces vascular endothelial growth factor receptor 2 (*VEGFR2/FLK1/KDR*) and stem cell leukemia (*SCL*) in human and murine ESCs, which are markers for **hemangioblasts**, the precursors of endothelial and hematopoietic cells (Chung et al., 2002; Park et al., 2004) (Figure 1.3B). This is in line with *in vivo* data showing that BMP4 positively regulates VEGFR2 expression in the lateral plate mesoderm of developing quail and zebrafish embryos (He and Chen, 2005; Nimmagadda et al., 2005). *VEGFR2* expression is required for vasculogenesis, the differentiaton of endothelial progenitor cells (**angioblasts**) into *de novo* endothelial cells (Vieira et al., 2010) (Figure 1.3B).

Thus, BMP signaling is activated upstream of the vasculogenesis cascade and is required for mesoderm induction and further specification of the hemangioblasts.

Commitment to endothelial progenitors (angioblasts) and **vasculogenesis** is regulated by signals from extraembryonic endoderm, such as Indian hedgehog (IHH) (Dyer et al., 2001) and vascular endothelial growth factor A (**VEGFA**). VEGFA treatment directs

mesodermal cells to the endothelial lineage by further upregulation of **VEGFR2** as shown in Japanese quail embryos (Giles et al., 2005). Both, VEGFA and VEGFR2 are essential for vasculogenesis as the lack of either one causes embryonic lethality and failed blood vessel formation (Ferrara et al., 1996; Shalaby et al., 1995).

Primitive ECs coalesce into an initial primitive vascular network and form the major embryonic vessels, the dorsal aorta and the cardinal vein (Figure 1.3)**.** Endothelial barriers are stabilized by the cell-cell proteins junctional VE-Cadherin and PECAM1, which also mark endothelial identity (Dyer and Patterson, 2010).

Arterial and venous identity is further specialized through **arteriovenous differentiation,** driven by the activation of specific arterial (e.g. *EPHRINB2, HEY1/2*) and venous (e.g. *EPHB4, COUP-TFII*) gene markers (Fang and Hirschi, 2019; Kume, 2010). After arterial and venous specification the primitive vasculature matures into a hierarchical network of large arteries and veins that connects into a more extensive network of small capillaries via extensive **remodeling** (Towbin, 2015; Udan et al., 2013) (Figure 1.3). This remodeling process results in a mature blood vessel network and is characterized by lumen formation, cell proliferation, **mural cell recruitment** and the formation of new blood vessels from pre-existing ones, named **angiogenesis**.

In addition, mechanical forces by blood flow are crucial for proper vascular remodeling of initial vessels such as the aortic arches and the umbilical vessels (Campinho et al., 2020; Udan et al., 2013). But also in mature arterial networks the vessel walls continue to remodel in response to **mechanical** and **hemodynamic stimuli** (Van Varik et al., 2012).

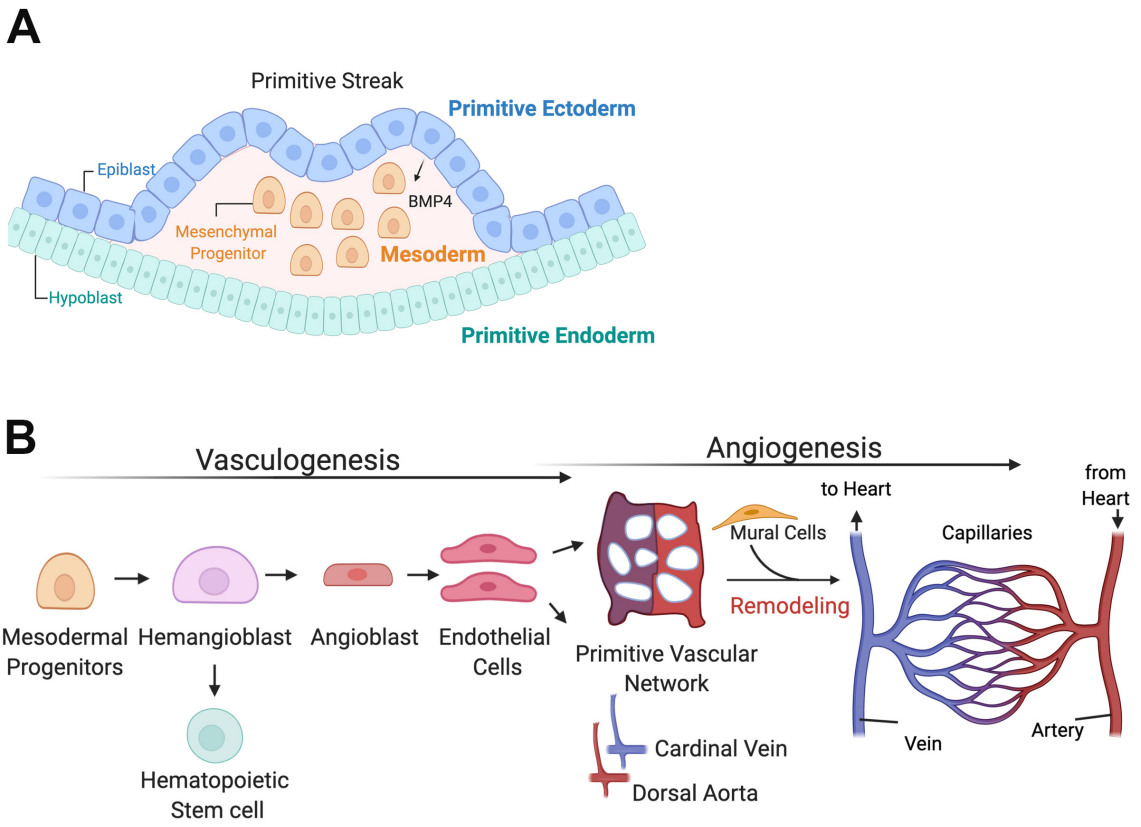

Figure 1.3 Development of vascular networks involves Vasculogenesis and Angiogenesis. (**A**) Simplified scheme of mesoderm formation in gastrulation triggered by epiblast (Primitive Ectoderm) derived BMP4. Adapted from (Dyer and Patterson, 2010) (**B**) A subset of mesodermal progenitors become hemangioblasts, which are the precursors of hematopoietic stem cells and endothelial cells. The endothelial progenitors (angioblasts) are committed for endothelial differentiation and result in endothelial cells aggregate and form primitive vascular networks and undergo arteriovenous differentiation. The major embryonic vessels, the dorsal aorta and the cardinal vein are formed. The complex vasculature network is formed via extensive remodeling including regression mural cell recruitment and formation of new vessel branches via angiogenesis. Remodeling of the primitive vascular network with large diameter arteries connects to smaller diameter capillary networks.

1.2.2 **New blood vessel formation in adults**

New adult blood vessels mainly form through activation of pre-existing vessels by **angiogenesis**. Additionally, *de novo* blood vessel formation may occur through **vasculogenesis**. About two decades ago the identification of endothelial progenitors (EPCs) or also called endothelial colony forming cells (**ECFCs**) in peripheral blood (Asahara et al., 1997), has changed the dogma that vasculogenesis is restricted to embryonic development. ECFCs form new blood vessels and incorporate into resident mature vessels upon various stimuli such as ischemia (Keighron et al., 2018). The extent of ECFC contribution to new blood vessel formation remains controversial (Naito et al., 2020). Moreover, it has been proposed that the vascular wall of tissue resident vessel contains a subset of ECs with high proliferative potential and even stem/progenitor cell characteristics (Naito et al., 2020).

Correct blood vessel maintenance and organization of new structures requires pro- and anti-angiogenic factors, which balance the interplay of several signaling pathways (explained in more detail in chapter 1.11) to maintain vessel quiescence or activation of angiogenesis and remodeling (Figure 1.4). Mostly, the vasculature remains in quiescent state maintaining tissue homeostasis. However, in **physiological** settings such as growth and the female reproductive cycle proangiogenic gradients trigger ECs to form new vessels in adult tissues. But also pathological conditions result in pro-angiogenic environments, which aberrantly activate signaling pathways leading to **pathological angiogenesis,** which then forms malformed vessels for example in wound healing, vascular diseases, cancer and chronic inflammation (Chung et al., 2010; Góth et al., 2003). Moreover, disbalance in signaling may also cause increased endothelial apoptosis and vessel regression in complications such as retinopathy in diabetes (Watson et al., 2017) (Figure 1.4).

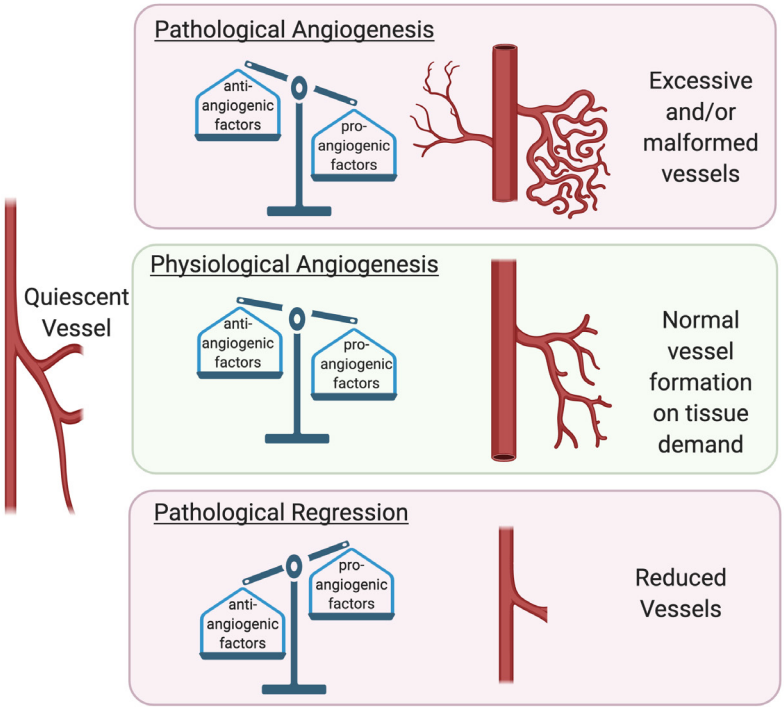

Figure 1.4 Blood vessel formation in adult tissues. Schematic model of quiescent vessels in adult tissues, which become activated by pro-and anti-angiogenic factors for angiogenesis or regression in physiological and pathological tissue context. In healthy tissue homeostasis pro- and anti-angiogentic factors balance the interplay of several signaling pathways to maintain vessel quiescence or activation of angiogenesis and remodeling depending on the tissue demands. Pathological triggers impair this balance and aberrantly deregulate signaling pathways, which results in vasculature defects and malformation by angiogenesis or aberrant vessel regression.

1.2.3 **Blood vessel remodeling**

Initial blood vessel formation by primitive ECs in vasculogenesis and angiogenesis, requires subsequent processes of remodeling, which alter structure and arrangement of vessels diameter and density to develop a mature blood vessel network (Figure 1.3). In addition to vessel growth and mural cell recruitment **pruning of excessive blood vessels and regression** are essential steps to develop and but also to maintain mature vascular network structures in changing tissue environments. However, compared to sprouting angiogenesis, mechanisms of vascular pruning and regression are poorly understood. In fact, all neovascularization processes initially result in excessive vascular density, which requires pruning for effective perfusion of blood into tissues (Ricard and Simons, 2015). Physiological processes may require the regression of entire blood vessels networks, such as the breast endothelium after lactation (Andres and Djonov, 2010). Moreover, vascular regression is required for vessel patterning in multiple organs as well as for wound healing and tissue repair (Korn and Augustin, 2015). Remodeling of the vessel walls in mature arterial networks is constantly triggered by **mechanical** and **hemodynamic stimuli** (Van Varik et al., 2012). In sum, ECs represent the major building block of blood vessels and initially derived from mesenchymal tissue in embryonic development via vasculogenesis and angiogenesis. New blood vessels also form in adult tissues mostly via angiogenesis, which is triggered by pro-angiogenic factors in physiological and pathological context.

1.3 Skeletal development

Bone is a highly **vascularized organ** and requires coupled vascularization in development. All bones develop from three embryonic lineages: neural crest, paraxial mesoderm and lateral plate mesoderm.

Most bones are formed by **endochondral ossification,** which starts with an avascular phase of intermediate cartilage generation, which is replaced by a phase of **coupled osteogenesis and angiogenesis** (Figure 1.5). (**1**) Bone and joint formation is initiated by expansion and condensation of mesenchymal Prx1+ (Paired-related homeobox gene1) progenitors, which originate from the lateral plate mesoderm and produce hyaline cartilage (Logan et al., 2002). (**2**) Upon subsequent chondrogenic differentiation, cells in the future primary ossification center proliferate rapidly and produce cartilaginous matrix including type II collagen. (**3**) In the next phase, chondrocytes increase their volume, become hypertrophic and later undergo

apoptosis. The release of matrix-metalloprotease 13 (MMP13) enables the removal of transverse septa of dead chondrocytes and cartilage extracellular matrix (ECM), which creates a permissive environment for **blood vessel invasion** (Stickens et al., 2004). Interestingly, when a mutant type I collagen with resistance to cleavage by MMPs was used in explants, migration of ECs and vessel formation was prevented (Stickens et al., 2004; Zijlstra et al., 2004). Additionally, hypertrophic chondrocytes produce osteogenic factors and VEGF, which further attracts invasion of blood vessels, osteoclasts and osteogenic cells**.** (**4**) Thereby, hypertrophic chondrocytes create a permissive environment in the central part of the developing bone (primary ossification center) and foster the transition from cartilage to bone by **coupling chondrogenesis to osteogenesis and angiogenesis** (Chung, 2004; Kronenberg, 2003; Sivaraj and Adams, 2016). In developing murine long bones, blood vessel invasion of the avascular cartilage is initiated at embryonic day (E) 13.5-14.5. By E15.5 the primary ossification center contains a branched vascular network (Langen et al., 2017; Sivaraj and Adams, 2016). (**4**) Bone formation spreads along the shafts towards both ends and secondary centers start to ossify accompanied by blood vessel attraction. Bone remodeling forms the marrow cavity and maintains growth and maturation of compact and spongy bone, which is accompanied by expansion and establishment of vascular networks. (**5**) Bone and vascular remodeling occur as growth continues and replaces the cartilaginous tissue, except the cartilage in the epiphyseal plates, which remains until growth plate fusion (Figure 1.5).

Especially the two isoforms VEGF165 and VEGF188, which are produced by alternative exon splicing of VEGFA (Robinson and Stringer, 2001) (for more details about VEGF signaling see chapter 1.11.2) are essential for endochondral bone formation. Loss of VEGF165 and VEGF188 in transgenic mice resulted in disturbed vascular patterning, growth plate morphogenesis and decreased hypertrophic chondrocyte differentiation (Liu and Olsen, 2014; Maes et al., 2002).

Whereas loss of VEGF165 impaired differentiation of osteoblasts and osteoclast, VEGF165 overexpression caused bone overgrowth (Maes et al., 2010). The important role of VEGF to couple angiogenesis with endochondral bone formation is supported by an early study, which showed that the administration of a soluble VEGF receptor suppressed blood vessel invasion in endochondral bone formation of young mice resulting in impaired ossification in the hypertrophic chondrocyte zone (Gerber et al., 1999). Moreover, scanning electron microscopy (SEM) studies in 13-22-week old

human fetuses visualized the process of **cartilage vascularization** in the proximal femoral epiphysis (Skawina et al., 1994). In the initial phase, hairpin-like vascular loops were observed in the perichondrium, the surrounding layer of cartilage in developing bone (Figure 1.5 (1) (2)). Subsequently, a capillary plexus in form of a node formed, which grew into a capillary network of elongating sprouts with interconnections (Skawina et al., 1994). More recent 3D confocal imaging techniques, transcriptomics and Flow cytometry enabled the high-resolved visualization and characterization respectively of vascular networks. In skeletal tissue, an **adult vessel subtype** (**type H**) and **juvenile vessel subtype** (**type E**) were identified, which are involved in the coupling of angiogenesis and osteogenesis (Kusumbe et al., 2015, 2014; Langen et al., 2017). Type H (H for `high´) vessels are characterized by high CD31 (PECAM1) and endomucin expression levels and were found in association with osteoprogenitors in the epiphyseal growth plate, which declines during aging (Kusumbe et al., 2014). In contrast, type L (L for `low´) vessels form the bone marrow vessel network and have lower levels of CD31 and endumucin and are not associated with osteoprogenitors (Kusumbe et al., 2014). Type E vessels were named after their high abundance in E16.5 and maintain osteoblast support (Langen et al., 2017).

Coupled vascularization is also observed in the development of **intramembranous ossification**, the developmental process of flat bones, such as most cranial facial bones. Cells from the neural crest and paraxial mesoderm directly differentiate into mineralizing osteoblast, which contrasts with endochondral bone formation. Studies in chick embryos showed that shortly before the first ossification, mesenchymal cells in the condensation center secrete VEGF, which attracts small capillary invasion into the outer layer of loose mesenchyme (Thompson et al., 1989). Loss of VEGFA isoforms reduced mineralization and osteoblastic marker expression in intramembranous bones (Zelzer et al., 2002).

Thus, angiogenesis is tightly linked to osteogenesis and is essential for bone formation.

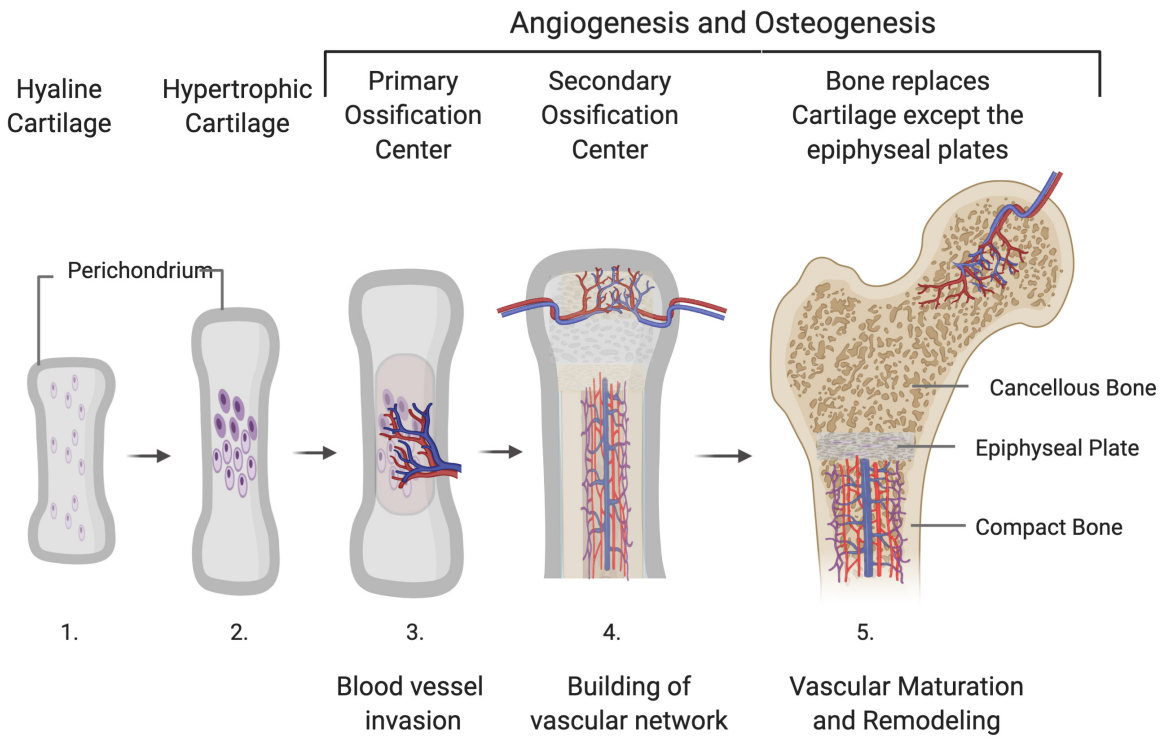

Figure 1.5 Endochondral Bone formation. (**1**) Hyaline cartilage develops from proliferating Prx1+ cells of the lateral plate mesoderm, which condense in the future primary ossification center and produce cartilaginous matrix. (**2**) In the next phase chondrocytes increase their volume, become hypertrophic. (**3**) Hypertrophic chondrocytes create a permissive environment in the central part of the developing bone (primary ossification center) for blood vessel invasion and osteogenic progenitors thereby initiating coupled angiogenesis and osteogenesis. (**4**) Production of bone matrix and cavity via bone remodeling is accompanied by vascularization. Bone formation and blood vessel invasion starts at a secondary ossification center (**5**) Growth and maturation of the developing bone is achieved by bone and vascular remodeling. Formation of compact and spongy bone replaces the cartilage except the epiphyseal plates.

1.4 Bone regeneration and fracture healing

In addition to embryonic bone development and growth in adolescence intramembranous and endochondral bone formation are important in adult tissue regeneration programs, which become activated in fracture healing.

The fracture heals either by direct intramembranous bone formation or by endochondral bone formation and is accompanied by immunological processes (Hu et al., 2017). Bone repair requires regeneration of mineralized tissue and blood vessels for successful restoration of the vascularized organ.

During fracture healing, blood vessels are not only involved in bone formation but also in the initial acute inflammatory response as well as in restoration of local blood supply in disrupted tissue (Hankenson et al., 2011). Blood vessel growth is induced by a variety of growth factors, such as VEGF, which are secreted by immune cells and stromal cells. New blood vessels form mostly by angiogenesis via outgrowth from preexisting vessels but alternatively also by vasculogenesis from endothelial progenitors (Hankenson et al., 2011). However, the remodeling and reorganization of

blood vessels as well as the underlying molecular mechanisms during bone repair remain incompletely understood (Sivaraj and Adams, 2016).

Bone regeneration in fracture healing involves four main stages reviewed in (Einhorn and Gerstenfeld, 2015). In brief, (**1**) Several blood vessels supplying the bone are disrupted and cause **hematoma formation**. The hematoma consists of cells from bone marrow, peripheral blood and intramedullary blood. This injury causes secretion of inflammatory cytokines which results in an **inflammatory response**, which is crucial for the bone healing process and lasts for 7 days with a peak after 24 hours (Marsell and Einhorn, 2011). Macrophages, monocytes and lymphocytes remove damaged, necrotic tissue. (**2**) Additionally, **bone progenitor cells** and fibrous cells are recruited within the hematoma and **angiogenesis** is initiated. A fibrocartilaginous network spanning the fracture ends forms a callus. (**3**) Subsequently the cartilaginous callus undergoes **endochondral ossification**. (**4**) In the following months the newly formed bone is constantly remodeled to regenerate the normal bone structure and regain proper functionality.

1.5 Extraskeletal bone

All postnatal bone forming processes in growth, remodeling or regeneration in fracture healing take only place within the skeletal structure, which was already defined early in embryonic development. However, there are pathologies where **extraskeletal bone** forms outside of the skeleton (**ectopic bone**) in soft tissues in a process called **heterotopic ossification** (**HO**). The word “heterotopic” is derived from Greek: “Hetero” and “topos” mean “other place” (Meyers et al., 2019). Interestingly, besides a wrong location, ectopic bone resembles normal bone in the skeleton and mimics processes of bone formation in development and postnatal bone regeneration during fracture healing. In fact, extraskeletal bone is the only example of complete recapitulation of an entire organ system with mineralized tissue, vasculature and marrow elements in postnatal life (Pignolo and Foley, 2005). HO is a major impairment of health due to mobility impairment and pain. It can be divided in rare **inherited forms** and more common **nongenetic forms**. Non-hereditary HO arises in response to severe tissue trauma, following injury by severe burns, hip replacement surgery, joint dislocation and central nervous system injury (Pignolo and Foley, 2005). The incidence of nonhereditary HO varies with certain predisposing conditions from 30% after bone fracture or dislocation to up to 90% for severe traumatic amputation (Meyers et al.,

2019). Non-hereditary HO can form by both **endochondral and intramembranous bone formation**. In contrast, inherited forms show progressive HO formation via endochondral bone formation in **Fibrodysplasia Ossificans Progressive (FOP)** (see chapter 1.6) or via intramembranous bone formation in progressive osseous hetero plasia (POH) as well as in albright inherited osteodystrophy (AHO). Even though, there are no effective treatment option up to date, anti-inflammatory drugs remain the most commonly used treatment agents, which may suppress HO at early stage. Once ectopic bone has formed and completed its maturation, the option of surgical removal accounts mainly for non-hereditary forms because in FOP this mechanical intervention triggers regrowth of new bone (Meyers et al., 2019).

1.6 Fibrodysplasia Ossificans Progressiva - when soft swellings become stiff and turn into bone

FOP is a severe ultra-rare, autosomal dominant disorder leading to progressive HO throughout life. FOP cases most likely existed ever since in human history. The first known description of a FOP patient was published by the London physician John Freke in 1740. He reported on a 14-year-old ‘boy of healthy look’ with ‘many large swellings on his back (Hüning and Gillessen-Kaesbach, 2014). In 1868, the condition received the name **Myositis Ossificans Progressiva** by von Dusch. In the following decade the **great toe malformations** were recognized by Frankel and Helferich. Based on the involvement of connective tissue, tendons, ligaments and fascia the name **Fibrodysplasia Ossificans Progressiva** (FOP) was proposed by Bauer and Bode in 1940, which was later adopted by McKusick (Kaplan et al., 2020; McKusick, 1959).

Independent of FOP, ectopic bone was studied by Marshal Urist, who artificially induced ectopic bone in skeletal muscle of animals by implantation of a demineralized bone substance. After three weeks the resulting transplant resulted in highly vascularized, inflammatory and fibrous tissue, which developed bone within 8-16 weeks via endochondral ossification. This was the first evidence, which suggested that recalcification and new bone formation can occur in skeletal muscle (Katagiri et al., 2018; Urist, 1965). Marshal Urist established the concept of a substance in bone which is responsible for bone formation and fracture healing and named it **Bone Morphogenetic Protein (**BMP) (Urist, 1965). Throughout the 1970s the involvement of BMPs in endochondral and intramembranous bone formation and bone fracture healing was demonstrated (Grgurevic et al., 2017). Advances in molecular biology in

the 1980s and 1990s enabled the sequencing and cloning of BMPs and associated them to the Transforming Growth Factor β (TGFβ) superfamily (Wozney et al., 1988). Moreover, recombinant BMP2 was shown to induce heterotopic cartilage *in vivo* (Wozney et al., 1988). Shortly later, the first BMP and TGFβ receptors were cloned (Attisano et al., 1993; Franzén et al., 1993; Koenig et al., 1994; Rosenzweig et al., 1995; Tsuchida et al., 1993; Yamaji et al., 1994).

The characteristics of the FOP disease were compared with developmental BMP patterns in a drosophila model and suggested an association of FOP with BMPs (Kaplan et al., 1990).

In 2006 Eileen Shore, Fred Kaplan and colleagues discovered mono-allelic gain of function mutations in the ACVR1 receptor as the genetic cause of FOP (E. M. Shore et al., 2006). By 2006 progress in BMP research has increased the knowledge about the mechanistic action of BMPs and its receptors in signal transduction as well as its diverse role in processes during development and adult tissue homeostasis and disease. The association of FOP to the BMP pathway increased awareness and a broader research interest to the ultra-rare disease. In fact, the gene discovery of FOP has paved the way to investigate the underlying molecular mechanisms in animal and patient cell disease models aiming to develop targeted treatment strategies for FOP. Despite recent discoveries and clinical investigations of compounds counteracting HO, there is no approved effective therapy up to date.

1.6.1 **Clinical symptoms**

Most FOP patients develop inflammatory **soft tissue swellings** in their first decade of life, which transform soft tissues (skeletal muscles, tendons, fascia, ligaments, aponeuroses) via **endochondral ossification** into **extraskeletal bone (**Figure 1.6A) as described in 1.6.3. Different stages of HO resemble events in embryonic skeletal development and regeneration during fracture healing. The tissue swelling start spontaneously in episodes and are also called ***flare ups***. Interestingly, flare ups can regress but are irreversible once bone has formed.

The disease progression is characterized by spontaneous and episodic HO formation with unknown triggers. However, HO can also be triggered by minor soft tissue injury, such as muscle fatigue, bruises, intramuscular injections or viral illnesses. Of note, bone fractures in FOP patients in the normal skeletal bone or ectopic bone undergo normal but accelerated fracture healing with no indication of additional HO (Shore and

Kaplan, 2010). Disease progression and intensity is very heterogenous among patients, which indicates that secondary mechanisms modulate FOP. Extraskeletal bone formation at distinct locations causes progressive immobilization of whole-body parts, which may even include ankylosis of the jaw. Thus, most patients require already in young age lifelong assistance in daily life (Kaplan et al., 2008).

In addition to progressive HO postnatally, a second clinical hallmark of FOP are prenatal **great toe malformations (**Figure 1.6B). A general dysregulation in skeletal development in FOP is supported by a very recent study, which identified even more **widespread joint malformations**, including joint fusion and even continued decreased joint health in adulthood in the majority of FOP patients (Towler et al., 2020). Thus, FOP is not only characterized by HO but also by degenerative joint disease (Kaplan et al., 2020). In the study by Towler and colleagues, in half of the participating patients the costo-vertebral joints, which connect the ribs to the vertebral column, were ankylosed, which is associated with chest wall disease and restricted breathing independent of HO. In fact, a primary cause of death in FOP patients is thoracic insufficiency, in which normal respiration is impaired by the chest walls (Kaplan et al., 2010; Towler et al., 2020).

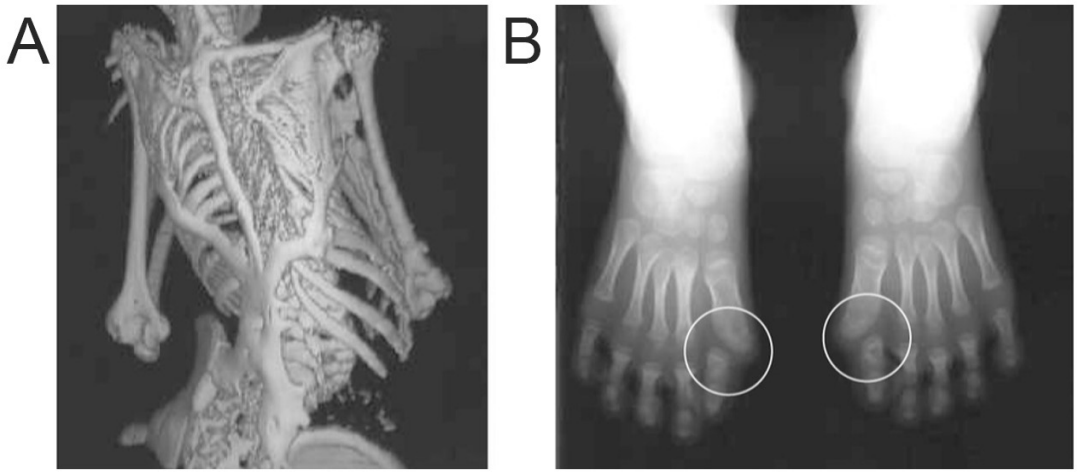

Figure 1.6 Clinical feature and genetic cause of FOP. (**A**) Typical ectopic bone formation on the back from a 12-year old child shown by a Computed Tomography (CT) scan. Heterotopic ossification (HO) in FOP progresses in a well-defined spatial pattern that fuse the joints and axial and appendicular skeletons. (**B**) Anteroposterior radiograph of the feet of a 3-year old child showing the symmetrical big toe joint malformations (circled). Modified after (Shore and Kaplan, 2010).

1.6.2 **Challenge of diagnosis and prevalence**

Since newborns with FOP appear normal except the great toe malformation, it is an important indication for early diagnosis. Nevertheless, often the soft tissue swellings are not associated with the symmetric great toe malformations. Consequently, most individuals become diagnosed with FOP very late and it is often misdiagnosed with tissue sarcomas, lymphoedema and aggressive juvenile fibromatosis. Unfortunately, this involves unnecessary and harmful tissue biopsies, which severely accelerate disease progression (Kaplan et al., 2008). Even though genetic transmission of FOP is autosomal dominant and can be inherited from a parent, most cases are a result of spontaneous/sporadic mutations and only less than ten multigenerational FOP families were reported worldwide (Shore et al., 2005). Thus, in most cases classic family medical history information does not lead to diagnostic molecular testing as for other inherited genetic diseases. The population frequency of FOP has been estimated to 1.0 in two million (Morales-Piga et al., 2014). However, recent record linkage of two national databases in France estimated the FOP prevalence to up to **1.36 per one million** (Baujat et al., 2017). Since there are no ethnic, gender or geographic predispositions known, this study suggests a much higher prevalence of FOP patients worldwide. As an ultra-rare disease many physicians have never heard from FOP. Initiatives by international patient organizations and research advances have increased the awareness in the last two decades. However, in many geographic regions FOP is largely unknown and people suffering from FOP are not diagnosed. Correct diagnosis is crucial for optimal care, prevention of biopsies and provision of potential treatment options in future. Up to date, there is no proven treatments available, which prevents, halts or even reverses progressive HO. However, several treatment strategies are in development and clinical investigations in phase II and phase III clinical trials. Currently, immunosuppressant therapy with anti-inflammatory drugs is often used to counteract the intense immune cell infiltration in the early stage of HO, which is applied within 24 hours of a *flare up* (Glaser and Kaplan, 2005).

1.6.3 **HO is a multi-stage process and accompanied by vascularization**

HO is a severe pathogenesis which involves several different cell and tissue types. It still remains poorly understood how a wound healing process in soft tissue turns into a process of bone formation over time. FOP is characterized by progressive HO formation via **endochondral bone formation** (for details see chapter 1.3), which

occurs in episodes and often spontaneous without known triggers. This contrasts with non-hereditary HO, which is initiated subsequent severe injury or trauma.

Histologic images represent valuable *snap shots* of the complex multi-stage process and enable analysis of common characteristics among the heterogenous spectrum of HO (Figure 1.7). Independent of injury or spontaneous induced HO, the initial lesion is characterized by an influx of inflammatory cells, which often involves localized pain and swelling. **Inflammatory responses** within the tissue are associated with tissue destruction, which is followed by **angiogenesis** and **fibroproliferative responses**. Subsequent stages are characterized by a replacement phase of new tissue development into bone via endochondral ossification (Figure 1.7). The stages of bone formation via endochondral processes resemble the events that occur in embryonic skeletal development and in bone regeneration during fracture healing (Meyers et al., 2019; Shore and Kaplan, 2010).

Thus, ectopic bone also requires coupled vascularization and bone formation as in previously described bone developmental processes (see 1.3).

In addition, the vasculature is an essential component of inflammatory processes which are a hallmark in the initial process of HO. However, surprisingly only a few studies have reported on the vasculature in ectopic bone formation. An early study analyzed lesional biopsies of eleven children, which were taken before diagnosis with FOP. Histological tissue analysis encountered that `numerous small blood vessels were a prominent feature of early lesions and were an integral part of the fibroblastic proliferation´ (Kaplan et al., 1993). Based on erythema formation, it was assumed that high abundant, primitive vascular cells have altered permeability (Kaplan et al., 1993). This is supported by another study, which detected **leaky and hemorrhagic vessels** in FOP lesions by electron microscopy (el-Labban et al., 1995). Moreover in 2017, vascular patterns were analyzed in genetic and non-hereditary forms of HO across the histologic spectrum using patient biopsies (Cocks et al., 2017). Each stage of HO showed a characteristic vascular morphology: Especially early **pre-osseous HO lesions** were **highly angiogenic** and displayed the highest number of thin-walled capillaries. Interestingly, the vessel area increased in mature lesions of woven and lamellar bone, whereas cartilaginous areas remained mostly avascular (Cocks et al., 2017). In sum, pre-osseous lesions are highly angiogenic and fibroproliferative, followed by an avascular chondrogenic stage and subsequent formation of mature,

vascularized heterotopic bone through endochondral ossification (Cocks et al., 2017; Kaplan et al., 1993; Shore and Kaplan, 2010).

Thus, the different stages of HO are accompanied by different patterns of vascularization, which suggests **coupled pathophysiologic processes of osteogenesis and angiogenesis** (Cocks et al., 2017).

Moreover, a recent study uncovered a differential vascular phenotype with increased vessel number, area and size in genetic *versus* non-hereditary forms in human HO biopsies such as FOP (Ware et al., 2019).

Collectively, in all forms of HO blood vessels undergo rapid and dynamic changes, but it remains elusive which mechanisms orchestrate the vasculature in the aberrant tissue repair processes and which signals cause the **aberrant vascular phenotype** in FOP lesions.

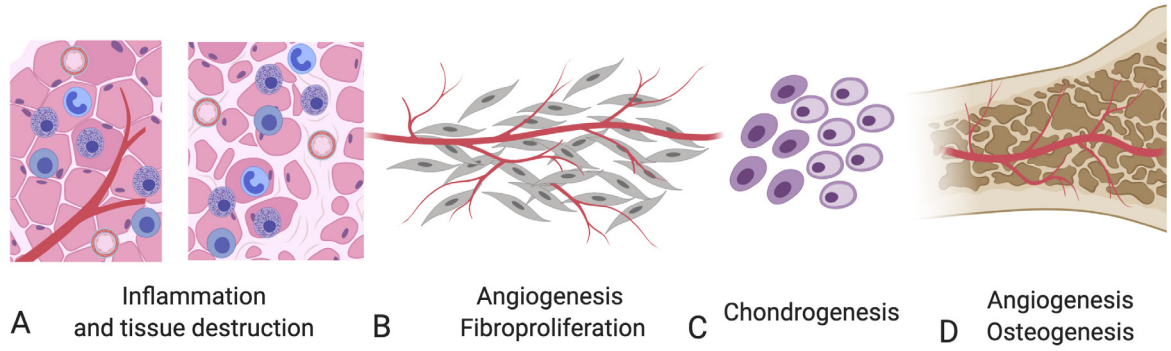

Figure 1.7 Dynamic changes of the vasculature in ectopic bone formation. Schematic depiction of ectopic bone formation via heterotopic ossification (HO) based on histologic evidence (Shore and Kaplan, 2010). HO is a complex, multi-stage process involving various cell types. (**A**) HO is initiated by inflammation in soft tissues (e.g. skeletal muscle) with characteristic lymphocyte infiltration. This involves the vasculature, which enables the transmigration of lymphocytes from the circulatory system to the tissue. Inflammation causes tissue destruction, (**B**) which is followed by a replacement phase with fibroproliferative cells and angiogenesis. (**C**) Subsequent chondrogenesis is avascular whereas (**D**) later stages of osteogenesis are tightly linked to angiogenesis to form mature vascularized bone.

1.6.4 The causative gene of FOP encodes the BMP receptor ALK2

The causative gene underlying FOP encodes the transmembrane receptor ALK2 or also called ACVR1, which belongs to one of the seven type I receptor family members, essential for the BMP signaling pathway. ALK2 is composed of an extracellular ligand binding domain (ECD), an intracellular glycine-serine (GS) rich domain and a kinase domain (KD) (Figure 1.8). Several heterozygous gain of function mutations have been identified in the *ALK2* gene of FOP patients (Haupt et al., 2018). The most prevalent one is a point mutation, which causes a substitution of the amino acid arginine to histidine (R206H) in the glycine serine rich domain of the receptor (Figure 1.8) (Shore et al., 2006). A small number of patients carry heterozygous mutations in other

positions of the GS domain but also in the kinase domain (Figure 1.8) (Haupt et al., 2018). In sum, all mutations cluster around the GS domain and the ATP binding pocket and lead to a destabilization of the inactive state of the ALK2 receptor. This favors the activation of the BMP/SMAD signaling pathway (Chaikuad et al., 2012), which is described in more detail in chapter 1.8.

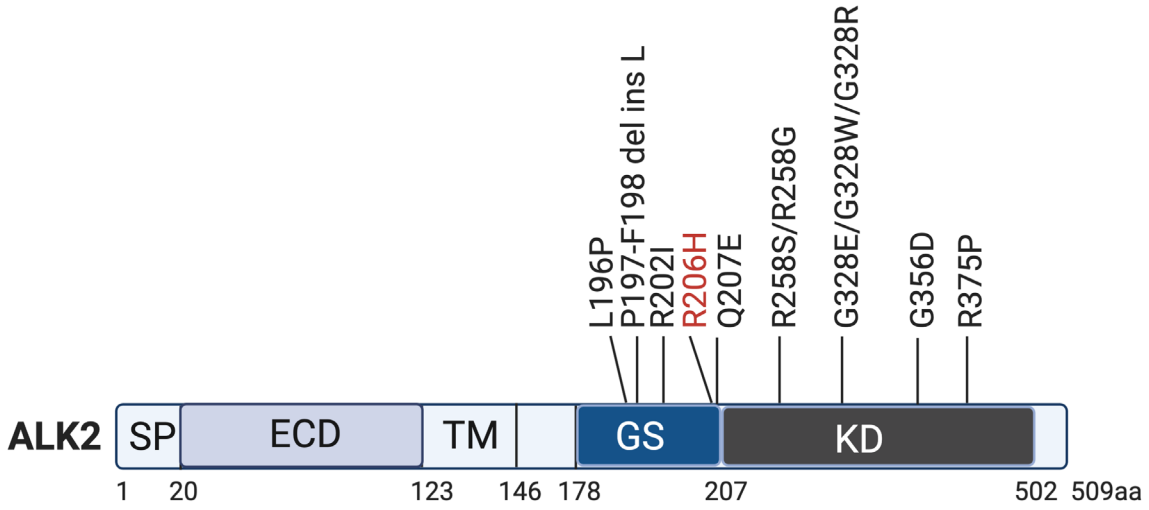

Figure 1.8 Genetic cause of FOP. Scheme of the ALK2 domain structure with indicated mutations identified in FOP patients. The most common mutation R206H is highlighted in red. Signal Peptide (SP); Extracellular Domain (ECD), Transmembrane domain (TM), Glycine-Serine rich (GS) domain and Kinase Domain (KD).

1.6.5 **Animal models to study FOP pathology**

To investigate the consequences of ALK2 mutant signaling on the FOP pathology requires appropriate animal models, which recapitulate the disease phenotype and its progression over time. The episodic formation of ectopic bone spontaneously or upon trauma is an important clinical characteristic. Interestingly, conditions of ectopic bone have been described in several animals and were associated with FOP disease even before the identification of the causative gene for human FOP, including cats (Asano et al., 2006; Valentine et al., 1992; Warren and Carpenter, 1984), dogs (Guilliard, 2001), pigs (Seibold and Davis, 1967), and even whale (Sala et al., 2012). But none of these have been confirmed with the presence of an mutation in respective ACVR1 orthologs in these animals (LaBonty and Yelick, 2018).

The ALK2 is highly conserved in evolution and protein orthologs can be found in evolutionary history in the earliest metazoans like *Hydra* (Mortzfeld et al., 2019) or in invertebrate class of insects, such as the *Drosophila melanogaster* (fruit fly). BMP signaling via heteromeric receptor complexes is conserved in drosophila and offers a

valuable model system to investigate basic mechanisms in BMP signaling (Brummel et al., 1994). A fruit fly model carrying the R206H mutation recapitulated the mutant ALK2 dependent overactivation of BMP signaling (Le and Wharton, 2012). Additional transgenic animals with mutations in ALK2 have been generated, including zebrafish, and mouse (LaBonty and Yelick, 2018).

However, since BMP signaling plays pleiotropic roles during embryonic development such as patterning in vertebrates (Kishigami and Mishina, 2005), loss or overactivation of ALK2 causes embryonic or perinatal lethality in many animals. A heat-inducible system enabled the generation of a FOP zebrafish model harboring the ALK2-Q204D mutation (LaBonty et al., 2017), which is homologous to the ultra-rare human GS variant mutation ALK2 Q207E mutation causing FOP (Haupt et al., 2014).

To overcome lethality in FOP mice, strategies of chimeric/mosaic animals or the application of conditional gene expression systems, such as Cre-Lox recombination have been applied in recent years (LaBonty and Yelick, 2018).

Genetic FOP mouse models

Historically, a mouse model expressing the constitutive active ALK2 variant Q207D was generated before the discovery of the causative gene for FOP (Fukuda et al., 2006). Based on HO development upon induction of global ALK2-Q207D expression, several groups used these mice to model FOP (Bagarova et al., 2013; Shimono et al., 2011; H. Wang et al., 2016; Yu et al., 2008a). However, the Q207D mutation is not naturally occurring in human FOP patients. In 2012, the first mouse model with the classical ALK2-R206H mutation using chimeric mice was generated, which developed the characteristic clinical features of FOP patients, including the embryonic skeletal malformations and postnatal HO (Chakkalakal et al., 2012). Three years later the first global ALK2-R206H mouse model at the endogenous locus was generated, which bypassed the perinatal lethality with a Cre-dependent-conditional on Knock In system. Those FOP mice developed progressive HO without injury at anatomical sites similar to human FOP patients (Hatsell et al., 2015).

Non-genetic mouse models of heterotopic ossification

HO has also been investigated in mouse models independent of ALK2 mutations, which are also commonly used in research of non-hereditary forms of HO.

Those include implantation, injection and overexpression of BMP ligands (e.g. BMP2 and BMP4) or toxins which trigger HO by an initial inflammatory response and subsequent stages which resemble phenotypes of non-hereditary HO and FOP (Kan

and Kessler, 2011; Lees-Shepard and Goldhamer, 2018). Since BMP implantation models typically do not incorporate injury apart from the mild injury by injection, other models have been established to recapitulate trauma and injury induced HO. Those include, burn or trauma induced models and the achilles tenotomy model although this site is uncommon for human HO (Kan and Kessler, 2011; Peterson et al., 2014).

1.6.6 **Progenitor cells of ectopic bone**

Above mentioned mouse models have been intensively used to discover progenitor cell populations contributing to the development of HO. Early studies have used BMP2 injection and delivery methods to trigger HO in mice and identified that **Tie2+ cells** contributed largely to endochondral bone formation (Lounev et al., 2009). The contribution of Tie2+ cells to HO was confirmed in the ALK2-Q207D mouse model (the classical constitutive ALK2 mutation, not found in FOP though) (Medici et al., 2010) and the ALK2-R206H chimeric mouse model (Chakkalakal et al., 2012). In addition to the contribution of Tie2+ cells to HO in mice, there is evidence of strong coexpression of Tie2 and the EC marker von-Willebrand Factor (vWF) with chondrogenic and osteogenic markers in human and murine HO lesions but not in normal bone. Based on this, the authors proposed that **ECs** contribute to HO via **endothelial to mesenchymal transition** (EndMT) (Medici et al., 2010).

However, since Tie2 is expressed in several cell types, the identity of the ectopic bone forming Tie+ cells had been under debate. Further studies defined a Tie2+ multipotent cell population (CD45-/CD31-/PDGFRα+/SCA1+) in the muscle interstitium that was uniquely capable of osteogenic differentiation and distinct from endothelial and hematopoietic cells (Wosczyna et al., 2012). In addition, intramuscular transplantation of cells positive for the EC marker CD31 (Pecam-1) and Tie2 did not contribute to BMP2-induced HO whereas Tie2+/CD31- cells incorporated in osteogenic and chondrogenic lesions (Wosczyna et al., 2012).

The usage of the classic endothelial marker CD144 (VE-Cadherin) as a Cre driver supported this assumption and showed that ECs did not contribute to BMP2-induced HO in mice (Wosczyna et al., 2012). In line with this, EC specific expression of ALK2-Q207D (Dey et al., 2016) or ALK2-R206H (Lees-Shepard et al., 2018) using VE - Cadherin-Cre did not result in spontaneous or injury induced HO.

However, another report using VE-Cadherin Cre mice described EC contribution to HO via EndMT following burn injury and tendonectomy, supported by EC transplantation into the tendon injury site, which underwent EndMT and contributed to HO (Agarwal et

al., 2016). Moreover, a recent publication demonstrated in VE-Cadherin Cre mice that monocyte depletion in the injured muscle partially shifted the fate of ECs towards endochondral differentiation, which resulted in increased BMP2-induced HO (Tirone et al., 2019). This highlights the plasticity of ECs and that complex local environments build a niche, which triggers cellular fate shift.

However, the contribution of ECs to HO remains controversial and requires further investigation. Interestingly, ECs were additionally reported to contribute to lesional angiogenesis (Wosczyna et al., 2012) highlighting the interlink of osteogenesis and angiogenesis and the indirect contribution of EC in ectopic bone formation.

The Tie2 cell population in the muscle interstitium contributing to HO was further defined by the following markers Tie2+/PDGFRα+/SCA1+/CD31-/CD45- (Wosczyna et al., 2012), which is identical or represents a subpopulation of so called **fibro/adipogenic progenitors (FAPs)** (Lees-Shepard and Goldhamer, 2018).

FAPs are mesenchymal progenitor cells, which were identified in the muscle interstitium with fibro/adipogenic and chondro-osteogenic capacities (Joe et al., 2010; Uezumi et al., 2010). FAPs become activated upon injury but in contrast to muscle progenitors they lack myogenic potential and rather fulfil a supportive role to establish an environment for muscle regeneration (Joe et al., 2010; Akiyoshi Uezumi et al., 2014). FAPs are commonly defined with the markers Sca1+ and PDGFRα+ (Akiyoshi Uezumi et al., 2014). Importantly, FAPs exist also in humans and were isolated as **PDGFRα+** cells from muscle tissue (A. Uezumi et al., 2014). FAPs are derived from cells that express the transcription factor **Osr1** during development (Vallecillo-García et al., 2017). Adult FAPs have low levels of Osr1, which becomes upregulated upon injury and marks activated FAPs (Stumm et al., 2018). Thus, Osr1 represents a valuable marker to distinguish quiescent FAPs from activated FAPs. A recent study showed in a number of comprehensive experiments including conditional ALK2-R206H mouse with PDGFRα-Cre that FAPs contributed to heterotopic cartilage and bone in FOP (Lees-Shepard et al., 2018). FAPs contribution was observed in injury and spontaneous HO at the major anatomical sites described in FOP patients (back, tendons ligaments, major joints, jaw) (Lees-Shepard et al., 2018). Moreover, cell specific expression of ALK2-R206H in satellite cells, ECs, and FAPs resulted only in HO upon muscle pinch in mice expressing ALK2-R206H in FAPs.

Another study used ALK2-Q207D and ALK2-R206H mice and proposed that two distinct non-overlapping cell progenitor populations are responsible for the diverse HO

phenotype. **Tendon-derive progenitors** (Scx+) that mediate HO of ligaments and joints without exogenous injury and **muscle resident interstitial progenitors** (Mx1+) population that mediate intramuscular, injury-dependent HO (Dey et al., 2016). Scx+ cells were also identified to contribute to HO by another study but in contrast to the previous study Scx+ were found to mediate intramuscular injury-induced HO in muscle (Agarwal et al., 2017). However, PDGFR+ (FAPs) cells represented a small subpopulation of both, Mx1+ and Scx+ populations and were also present in most other lineage-tracing studies that identified contributors to HO (Lees-Shepard and Goldhamer, 2018).

In sum, this suggests that FAPs represent a major progenitor cell type in ectopic bone formation but it is not excluded that additional progenitor populations also contribute to HO. Besides tissue resident progenitor cells, circulating progenitors may also contribute to ectopic bone formation. **Circulating, bone-marrow derived osteogenic progenitors (COP)** (ColI+/CD45+) were identified in early pre-osseous fibroproliferative lesions in FOP patients. Direct contribution of FOP COPs to HO was shown in a murine implantation model (Suda et al., 2009). Interestingly, higher levels of COP cells were detected in blood of patients with active episodes of HO (Suda et al., 2009). Thus, bone progenitor cells may not only derive from mesenchymal but also hematopoietic lineages. A summary of suggested bone forming progenitors in context of FOP are depicted in (Figure 1.9B).

Interestingly, it was reported that FAPs are not restricted to muscle tissue and are present in a wide range of organs, also those which are not susceptible to undergo HO (Lees-Shepard and Goldhamer, 2018; Wosczyna et al., 2012). This suggests that FAPs and likely other tissue resident progenitors require (1) a permissive environment (niche) and (2) inducing trigger(s), which enable osteogenic differentiation.

Interestingly, independent of the organ and tissue, FAPs are often observed in close association with the vasculature (Uezumi et al., 2010; Wosczyna et al., 2012) (Figure 1.9A). The broad localization of FAPs in diverse tissues strengthens the need to investigate the local environment of progenitor cells. This includes other cell types, ECM architecture and signaling molecules to understand the mechanisms, which trigger a physiological niche towards a pathological niche of bone formation. Details about the close association of FAPs to the vasculature remain unexplored but it is tempting to speculate that vascular changes and vascular bed specific differences may influence the activity and fate of FAPs.

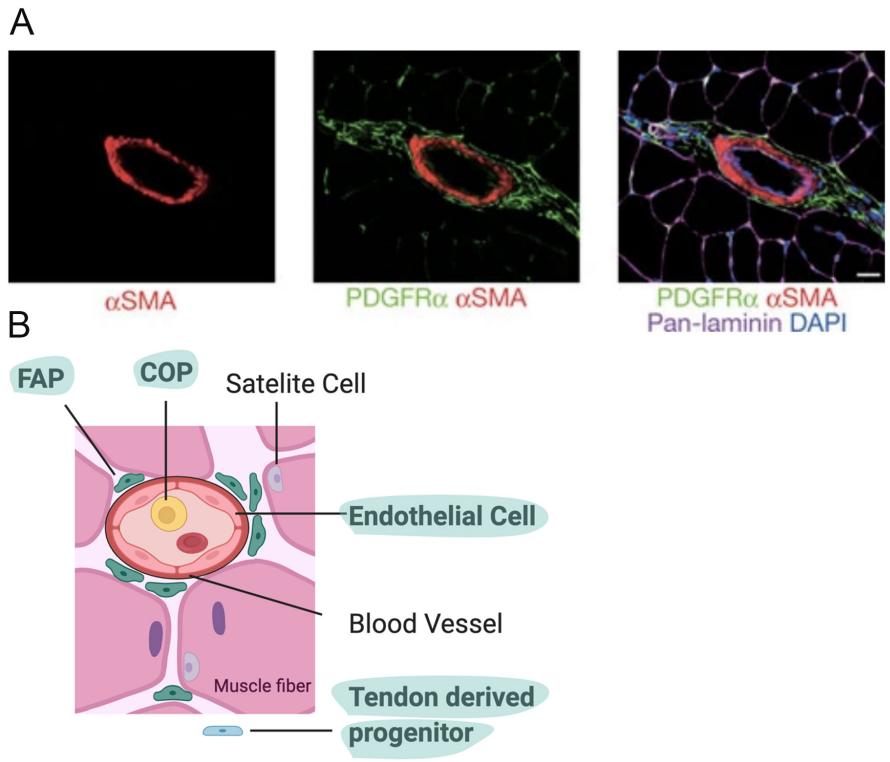

Figure 1.9 Potential progenitors of heterotopic bone in skeletal muscle tissue. (**A**) Murine skeletal muscle section stained with antibodies against αSMA, PDGFRα, Pan-laminin and DAPI. PDGFRα+ cells (FAPs) localized circumferentially around vessels (αSMA+ for Smooth muscle cells) (Uezumi et al., 2010). (**B**) Summary scheme of potential progenitors of heterotopic bone in FOP (marked in light green). Interstitial FAPs, Endothelial cells, circulating osteogenic progenitors (COP) and Tendon derived progenitors.

1.6.7 **Human cell models to study FOP**

Above mentioned animal models are valuable tools to study ALK2 mutant signaling and FOP pathology, which recapitulates important clinical characteristic. However, species differences may limit the full recapitulation of the human disease phenotype, especially the phenotypic variability among patients with the same mutation. Even though genetic tools enable to overcome the embryonic lethality of FOP mice, the contribution of ALK2 mutation in embryonic development to postnatal phenotypes is absent in these mice but evident in FOP of humans. A recent review highlights that in addition to ectopic bone formation, developmental and postnatal defects on joints are an additional hallmark of the disease, which affect far more skeletal defects than the great toe malformation (Kaplan et al., 2020). Moreover, most investigations of the progenitor cells contributing to the formation of heterotopic bone are based on studies in mice and cell models of ALK2 mutant overexpression.

The establishment of patient-derived models of FOP has been challenging due to the limited number of patients and the risk to trigger HO upon tissue biopsy sampling. Therefore, many FOP human cell models are based on ALK2 mutant overexpression.

Only in recent years, a few approaches achieved the isolation of primary cells from FOP patients, such as stem cells from human exfoliated deciduous teeth (SHED) (Kaplan et al., 2012), skin fibroblasts (Micha et al., 2016) or periodontal ligaments (de Vries et al., 2018) as well as ECFCs (Sánchez-Duffhues et al., 2019c), lymphocytes (Fiori et al., 2006) and monocytes (Barruet et al., 2018) from peripheral blood.

Induced pluripotent stem cells

In addition, induced pluripotent stem cells (iPSCs) were generated from FOP patient derived dermal fibroblasts (Hamasaki et al., 2012; Hayashi et al., 2016; Kim et al., 2016; Matsumoto et al., 2013), urine cells (Cai et al., 2015; Hildebrand et al., 2016a) and periodontal ligament fibroblasts (Sánchez-Duffhues et al., 2019b). Two studies from above reported contradicting result whether the BMP signaling of FOP dermal fibroblasts impairs the generation of iPSCs. One approach was not successful in generating iPSCs from FOP patient dermal fibroblasts without using the BMP type I receptor inhibitor LDN (Hamasaki et al., 2012). In contrast, another study suggested that the active BMP signaling in FOP dermal fibroblasts increases iPSC generation efficiency (Hayashi et al., 2016). However, other approaches have not observed FOP dependent impaired efficiencies, which suggests that rather different reprogramming techniques, culture conditions could have influenced the efficiency in iPSC generation (Barruet and Hsiao, 2018).

The discovery of iPSC generation from somatic cells has revolutionized the stem cell research. In 2006, Shinya Jamanaka and his group at Kyoto University in Japan generated iPSCs from mouse fibroblasts (Takahashi and Yamanaka, 2006) and in 2007 from human fibroblasts for the first time (Takahashi et al., 2007). The generation of iPSCs from somatic cells is achieved by reprograming the somatic cells via expression of a defined set of transcription factors, named `Yamanaka factors´: OCT4, SOX2, KLF4 and c-MYC (Takahashi et al., 2007; Takahashi and Yamanaka, 2006). In 2012, Shinya Yamanaka and John B. Gurdon received the Nobel prize in Physiology and Medicine for the discovery that mature somatic cells can be reprogrammed to pluripotent cells (“The Nobel Prize in Physiology or Medicine 2012,”).

Even though the delivery methods for reprogramming factors have been improved from retro- and lentiviral to non-integration viral transduction as well as non-viral approaches, the underlying mechanisms of reprogramming remain poorly understood (Liu et al., 2020; Takahashi and Yamanaka, 2016). The Yamanka transcription factors have indirect and direct effects on regulatory elements of many genes, which causes

the silencing of the somatic and the activation of the pluripotency transcriptional program as well as the reorganization of chromatin architecture (Apostolou and Stadtfeld, 2018). As a consequence, the transcriptional and epigenetic state of the somatic cell is converted to a pluripotent stem cell, which closely resembles embryonic stem cells (ESCs) in many aspects, including morphology, pluripotency, proliferation and global gene expression profiles (Bilic and Izpisua Belmonte, 2012). In fact, iPSCs have a similar developmental potential as ESCs and can differentiate into the three germ layers (Bilic and Izpisua Belmonte, 2012).

Ongoing research investigates differences between iPSC and ESCs as genetic memory was suggested to remain in iPSCs, which potentially affects lineage-specific differentiation capacities. And it remains to be clarified how genetic memory distinguishes different cell types and tissues (Bilic and Izpisua Belmonte, 2012; Liu et al., 2020). The pluripotency state is maintained by the core transcription factors OCT4, NANOG and SOX2, which occupy the genome at their own promoters and at promoters of other key genes, which are either repressed or induced in favor of pluripotency (Yeo and Ng, 2013).

FGF signaling and TGFβ/Activin signaling are two major pathways controlling pluripotency in ESCs (Fathi et al., 2017; James et al., 2005; Mossahebi-Mohammadi et al., 2020; Mullen and Wrana, 2017). Importantly, mechanistic actions of TGFβ family signaling in pluripotency and self-renewal are divergent between human and mouse (m) ESCs (Watabe and Miyazono, 2009). BMP signaling and leukemia inhibitory factor (LIF) enforce the pluripotency network in mESCs (Ying et al., 2003) whereas TGFβ/Activin signaling promotes pluripotency in human ESCs (L. Vallier et al., 2009) (Mullen and Wrana, 2017). In fact, BMPs inhibit self-renewal in human ESCs and induce differentiation into mesodermal lineages (Chadwick et al., 2003; James et al., 2005; Kennedy et al., 2007; Schuldiner et al., 2000; Xu et al., 2005).

Thus, BMP signaling has divergent functions in mouse and human ESCs: BMP pathway activation promotes differentiation and specification in human ESCs and pluripotency in mouse ESC.

Various directed *in vitro* differentiation protocols have been developed to generate mature tissues from iPSC monolayers and embryoid bodies via defined culture conditions supplemented with specific growth factors and small molecules. Directed differentiation of iPSCs has been achieved towards diverse cell types such as neural cells (Chambers et al., 2012; Zhang et al., 2001), cardiomyocytes (Lian et al., 2013),

skeletal muscle (Chal et al., 2015; Shelton et al., 2014) and vascular cells including endothelial cells, smooth muscle cells and pericytes (Descamps and Emanueli, 2012; Klein, 2018; Williams and Wu, 2019). These methods are continuously improved to overcome challenges of low and heterogenous differentiation efficiencies as well as to model the diverse cell types of the human body. In addition, iPSCs enable to study healthy and diseased human cell types of various human tissues, which overcome the restrictions of primary sources from patients and the limited expansion potential of primary cells *in vitro*. This is especially evident for limited patient material in FOP. A major advantage of patient derived cell models is the expression of physiological levels of the mutated ALK2 receptor, which enables to recapitulate the disease phenotype and relevant mechanisms in different cell types as well as drug testing approaches (Barruet and Hsiao, 2018).

Patient iPSCs can contribute to model HO as an important clinical phenotype in FOP and to elucidate the underlying developmental process of endochondral bone formation. Indeed, the FOP mutation in iPSCs causes increased chondrogenesis and mineral deposition *in vitro* (Matsumoto et al., 2013). However, the contribution of specific cell types in this process and the generation of 3D tissue structures remains less explored.

Collectively, divergent roles of BMP and TGFβ signaling between human and mouse ESCs highlight the importance of patient derived human cell models for FOP in addition to FOP mice. FOP patient cell models largely contribute to a better understanding of FOP pathology and the mechanistic action of potential drug candidates.

1.7 BMP and TGFβ signal transduction

Independent of the tissue and organ context, the sequence homology and conservation of Transforming Growth Factor β (TGFβ) family members propose a shared basic molecular mechanism of Bone Morphogenetic Protein (BMP) and TGFβ signal transduction (Figure 1.10). In brief, dimeric BMP, Activin and TGFβ ligands bind to heteromeric transmembrane signaling complexes, which consist of **serine/threonine kinase receptors** which are divided in functional groups of **type I and type II receptors**. Sequence and structural based affinities between the over 30 ligands and between the seven type I and five type II receptors enable the formation of diverse ligand-receptor complexes. Constitutive active kinases of the type II receptors activate type I receptor kinases by phosphorylation of the type I receptor GS domain, once they are complexed with their respective ligand. **Sons of mothers against decapentaplegic** (**SMADs**) are the main effectors of canonical BMP and TGFβ signaling and act as transcription factors upon translocation to the nucleus. Dependent on their kinase substrate specificity (interaction of the **L3 loop** in SMADs with the **L45 loop** in the type I receptor kinase (Cárcamo et al., 1994; Feng and Derynck, 1997; Lo et al., 1998; Persson et al., 1998), type I receptors are divided in **SMAD2/3-activating** Activin receptor-like kinase (ALK) **(ALK4/5/7)- and SMAD1/5/8-activating (ALK2/3/6) type I receptors**. The receptor associated SMAD proteins (R-SMADs) become activated by C-terminal phosphorylation by respective type I receptors. Two phosphorylated R-SMADs form a complex with Co-SMAD4, which enables the translocation to the nucleus. DNA binding motifs in most SMAD proteins regulate target gene transcription by binding to specific SMAD binding elements (SBEs) (Derynck and Budi, 2019). Moreover, BMP/TGFβ signaling cascades are associated with cytoskeletal rearrangements and migration, which are induced within minutes and are independent of transcriptional SMAD mechanisms. These pathways are named **non-SMAD pathways**, where BMP and TGFβ receptor complexes induce the activation of several non-SMAD substrates, such as mitogen-activated protein (MAP) kinases, Rho-like GTPases, PI3Kinase and AKT (Dörpholz et al., 2017; Hiepen et al., 2014; Zhang, 2017). MAP kinases induce immediate architectural changes of the cytoskeleton and cell junctions as well as activate transcription factors (e.g. TWIST1), which modulate gene transcription (Zhang, 2017).

Moreover, there is also increasing evidence that mechanical stimulation integrates via **mechanosensors,** such as integrins into BMP/TGFβ signaling on multiple levels (da Silva Madaleno et al., 2020). These pathways are modulated and fine-tuned by several extra-and intracellular signaling components, such as antagonists, co-receptors, ligand prodomains and three dimensional (3D) ECM macromolecules in space and time. In sum, these modulators expand the diversity of signaling events and further specify the basic mode of ligand receptor complex formation with varying affinities in the TGFβ superfamily (da Silva Madaleno et al., 2020; Derynck and Budi, 2019; Hiepen et al., 2020; Nickel et al., 2018). The advances in BMP/TGFβ research depict signaling networks with increasing complexity, which may better explain the diverse and complex function in multicellular organisms.

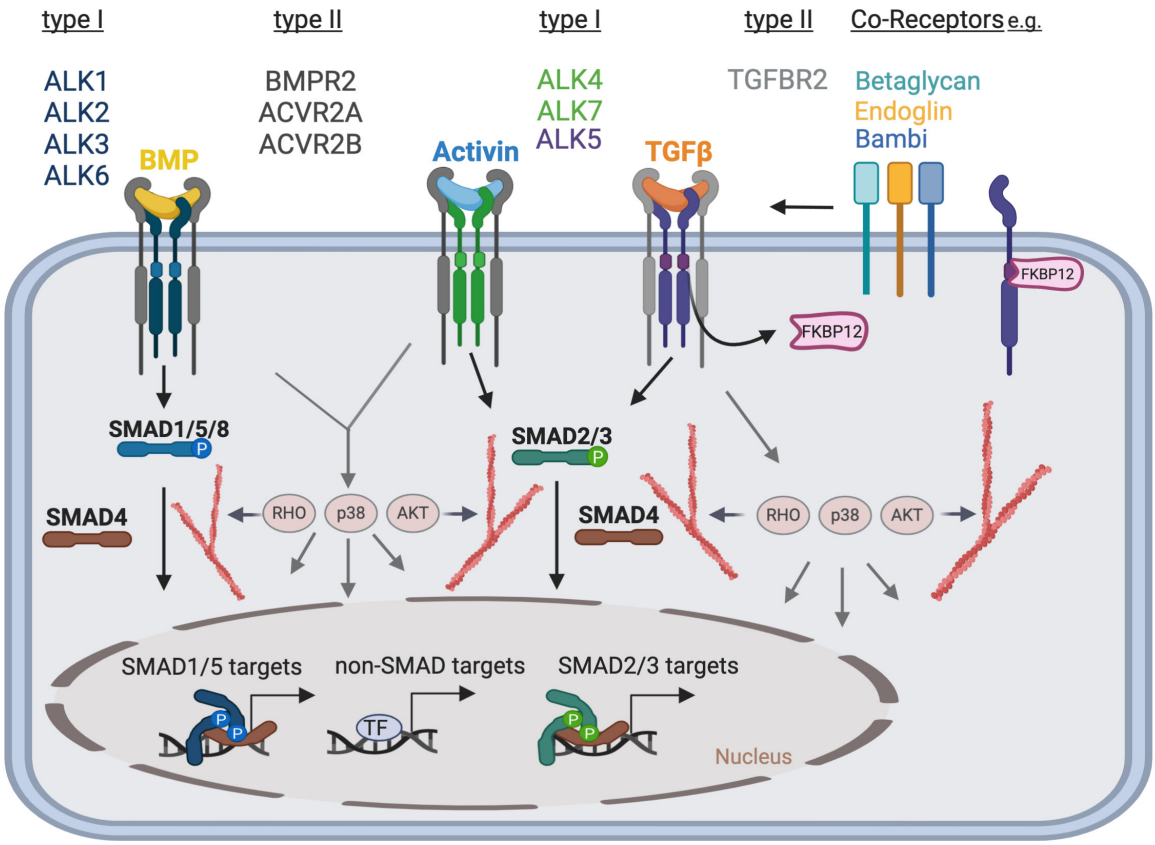

Figure 1.10 Simplistic model of BMP and TGFβ signal transduction. Signal transduction is initiated via binding of dimeric TGFβ family ligands to a heterotetrameric receptor complex composed of two type I and two type II serine/threonine kinase receptors. Constitutive active kinases of the type II receptors activate type I receptor kinases via phosphorylation of the type I receptor glycine serine-rich (GS) domain. Dependent on their kinase substrate specificity type I receptors are divided in SMAD2/3-activating- and SMAD1/5/8-activating type I receptors. The receptor associated SMAD proteins (R-SMADs) become activated by C-terminal phosphorylation by respective type I receptors. Activated R-SMADs form a trimeric complex with Co-SMAD4, which enables the translocation to the nucleus to regulate target gene transcription. Moreover, ligand binding activates mitogen-activated protein (MAPK) cascades downstream of the BMP type I receptors, including RHO, p38 and AKT signaling, which directly modulate the cytoskeletal architecture as well as gene transcription via activation of transcription factors (TF) such as TWIST1.

1.7.1 **Ligands**

The human genome encodes at least 33 unique TGFβ family ligands. All TGFβ family ligands are synthesized as a **precursor protein (pro-form)**, which consist of a **mature signaling domain** (~110 residues) with **a large pro-domain** (~250 residues) with a **N-terminal signal peptide** for secretion (Figure 1.11A-B).

For maturation, the pro-domains are cleaved by furin-like proteases, which releases the mature signaling domain. The location of the processing via proteolytic cleavage is less clear and may occur intracellularly in the trans-Golgi network or the endoplasmic reticulum, at the plasma membrane or even extracellularly (Hinck et al., 2016; Yadin et al., 2016).

Monomeric mature ligand domains are in shape of a **hand** with **α-helix** (**wrist)** and four antiparallel **β-strands** (**fingers**) (Figure 1.11C). Two mature ligand domains (monomers) assemble into a mature homodimeric or heterodimeric ligand with a symmetrical, **butterfly-like structure** (Figure 1.11D). Two disulfide bonds form a ring (cysteine knot) which contributes with an additional interchain disulfide bond to stability and folding of the ligand. TGFβ family ligands are classically organized into three main classes according functional and structural characteristics. (1) BMPs and Growth and Differentiation Factors (GDFs) form the largest class, (2) the second class is composed of Activin/Inhibin/Nodal ligands and (3) TGFβ ligands form the third class(Yadin et al., 2016). However, based on phylogenetic and sequence divergence, three new ligand classes with several subfamilies have been suggested which associate some GDFs rather to the Activins than to the BMP class: **BMP class**: (BMP5/6/7/8), (BMP2/4), (BMP9/10), (GDF5/6/7), (GDF9/BMP15), (GDF1/GDF3), (Nodal). **Activin class**: (ActivinA/B/C/E), (GDF8/GDF11), (BMP3/GDF10). **TGFβ class:** (TGFβ1/2/3) (Hinck, 2012; Hinck et al., 2016).

Three-dimensional (3D) structures have been resolved for over 15 TGFβ family members reviewed in (Gipson et al., 2020; Goebel et al., 2019b). Despite similarities in the overall structure, there are important differences in residues which are not critical for folding but define specificity for receptor interaction and functionality. The regions of highest variability occur at the back face of the ligand fingers (**knuckle region**), its **fingertips** and the **prehelix loop (wrist region)**, which are important for receptor specificity and binding (Gipson et al., 2020; Goebel et al., 2019b) (Figure 1.11C-E).

Moreover, sequence variation may result in charge and shape differences. Mature BMP ligands are positively charged, which enables direct interaction with heparin or

heparan sulfate proteoglycans, which restricts their mobility. In contrast, other ligands, such as ActivinA are negatively charged at neutral pH and diffuse more readily (Goebel et al., 2019b). Even though all ligands exhibit a dimer butterfly-like shape, the relative position of each monomer is divergent. In BMP2,3,6,7 and 9 ligands the dimer interface and the wrist region are well-ordered, which leads to a more rigid conformation. In contrast, several ligands from the TGFβ and Activin class have a more flexible wrist region, which enables free rotation around the intermolecular disulfide bond (Goebel et al., 2019b; Yadin et al., 2016). In fact, TGFβ3 or ActivinA were crystalized in multiple conformations (Bocharov et al., 2002; Greenwald et al., 2004; Thompson et al., 2003), which suggests an additional functional model to modify receptor binding specificity.

History and Nomenclature of Activins

ActivinA and ActivinB homo- and heterodimers were initially discovered in porcine follicular fluid and named Activins because they activated the release of follicle-stimulating hormone (FSH) (Ling et al., 1986), whereas their counterparts, the Inhibins blocked this effect (Setchell and Jacks, 1974). Inhibins antagonize Activin signaling by the formation of inactive signaling complexes with Activin type I (ALK4) and type II receptors (ACVR2A/B) and in conjunction with the co-receptor Betaglycan (Namwanje and Brown, 2016; Zhu et al., 2012).

ActivinC and ActivinE were discovered later and are mainly described as inhibitors for ActivinA signaling by forming heterodimers with ActivinA (Mellor et al., 2003). Activins are composed of two dimerized β subunits (ββ homodimers) as the other TGFβ family ligands. In contrast, the Inhibins occur as αβ heterodimers. Because Inhibins were isolated before Activins the Activin β monomers are also sometimes named Inhibins βA (ActivinA) and Inhibins βA (ActivinB), respective the gene names *INHBA, INHBB* (Namwanje and Brown, 2016).

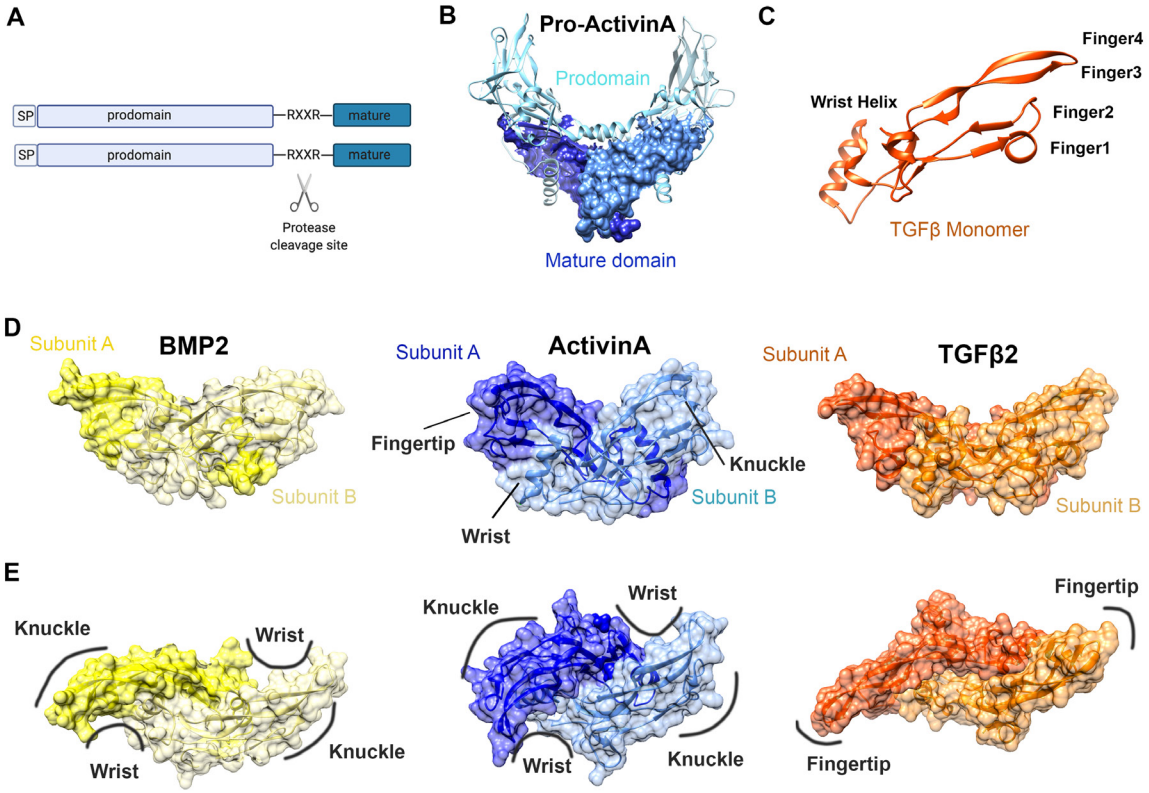

Figure 1.11 Structures of BMP, Activin and TGFβ class ligands. (**A**) TGFβ family ligands are synthesized as a precursor protein (pro-form). For maturation and activation, the pro-domains are cleaved by furin-like proteases. (**B**) Quarternary structure of pro-ActivinA with mature domains in dark blue and prodomains in light blue (X. Wang et al., 2016). (**C**) Folding of the BMP/Activin/TGFβ monomer resembles a hand model. (**D**) Two ligand monomers (subunits) assemble in a symmetric butterfly-shape dimer (BMP2 (Seeherman et al., 2019); ActivinA (Harrington et al., 2006); TGFβ2 (Del Amo-Maestro et al., 2019). (**E**) Dimeric ligands of D are rotated around the x axis by 90°. Binding epitopes of type I (Wrist) and type II receptors (Knuckle), (Fingers) are indicated. Crystal structures were exported from the Protein Data Bank (PDB ID: 5HLZ; 6OMN; 2ARV; 6I9J) and rendered in Chimera software (Pettersen et al., 2004).

Ligand Prodomains

Association with the pro-domains may influence ligand stability, storage, localization and signaling activity but remains poorly understood (Constam, 2014)

The large size and sequence variability of pro-domains, which is less conserved compared to the mature signaling domain, suggests diverse functions of pro-domains within the TGFβ ligand family (Figure 1.11A-B). In fact, upon cleavage several mature dimeric BMP ligands remain non-covalently associated with their pro-domains and are targeted to ECM components (Sengle et al., 2011, 2008).

Most insight about pro-domain function comes from the TGFβ1 ligand, where the pro-domain (Latency associated peptide (LAP)) confers latency, meaning after cleavage the pro-domain remains associated with mature part of TGFβ to keep it in an inactive state (Wakefield et al., 1989). By forming a straightjacket around the mature TGFβ1

the pro-domain blocks the receptor binding sites and enables binding to the ECM via latent binding proteins (LTBP) or fibrillin (Shi et al., 2011). Besides pro-TGFβ1, latency by pro-domains has only been shown for pro-myostatin (pro-GDF8) (Wolfman et al., 2003) and GDF11 (Pepinsky et al., 2017). To achieve full signaling activity pro-TGFβ1 undergoes an ECM and integrin-driven mechanical activation (Shi et al., 2011) and pro-myostatin sequential proteolytic cleavage (Cotton et al., 2018; Wolfman et al., 2003).

In contrast, structural resolution of pro-BMP9 (Mi et al., 2015) and pro-ActivinA (X. Wang et al., 2016) (Figure 1.11B) revealed that both ligands have equivalent signaling activity compared to their free, mature ligand forms, suggesting a weaker, non-inhibitory function of pro-domains. Studies with pro-ActivinA show that the pro-domain increased the solubility (X. Wang et al., 2016), extended the half-life of the mature growth factor *in vivo* (Johnson et al., 2016) and facilitated binding to heparan sulfate proteoglycans of the ECM (Li et al., 2010).

Thus, the ligand precursor (pro-form) allows additional, post-translational activation mechanisms in the extracellular space. This suggests an additional way to control ligand availability within tissues and to modulate signaling responses in time and space and demands further investigations on the less conserved pro-domain of the TGFβ ligand family.

1.7.2 **Ligand receptor interactions**

Once specific epitopes become accessible in the pro- or mature form of a ligand, transmembrane receptors with serine/threonine kinases bind to the ligand and form a heteromeric receptor complex (Figure 1.12B).

TGFβ family receptors are structurally and functionally grouped into seven **type I** (ALK1, ALK2, ALK3, ALK4, ALK5, ALK6, ALK7) and five **type II** (ACVR2A, ACVR2B, BMPR2, TGFBR2, AMHR2) receptors. Type I and type II receptors share a similar domain structure, which consists of a cysteine-rich **extracellular domain** (**ECD**) that mediates ligand binding, a **transmembrane domain** (**TMD**) and an intracellular part of a **serine/threonine kinase domain (KD)** (Figure 1.12A)**.** Key difference between type I and type II receptors is a **serine-glycine rich sequence (GS-domai**n) N-terminal to the kinase domain of type I receptors, which is absent in type II receptors (Figure 1.12A). For type I receptor activation the type II receptors phosphorylate conserved serine and threonine residues in the **helix-loop-helix motif** (**GS loop**) within the GS-

domain. This enables type I kinase activity for downstream target. Close to the GS domain lies a cytoplasmic loop segment, called the **L45 loop**, which defines type I receptor substrate specificity (Feng and Derynck, 1997) via a corresponding loop segment (called L3 loop) in the SMAD C-terminal domain (Lo et al., 1998). The SMAD proteins SMAD1, 5, 8 are substrates of the type I receptors ALK1, ALK2, ALK3 and ALK6 and SMAD2 and 3 become phosphorylated by ALK4, ALK5 and ALK7 (Mueller and Nickel, 2012).

The discrepancy between number in ligands and number of receptors implies that single receptors bind to more than one ligand and in fact a particular ligand can also bind so several receptors. This is called **ligand-receptor promiscuity**.

The receptors bind to specific ligand epitopes. Type I receptor bind to the so called **wrist epitope** and type II receptors at the back face of the fingers, named **knuckle epitope**, except for the TGFBR2, which recognizes its ligands by two conserved residues in the **fingertips** (Yadin et al., 2016) (Figure 1.11C-E).

Until now, structural characterization of several ECDs alone (ACVR2A, TGFBR2, BMPR2; ALK1, ALK3, ALK5) or in a ligand receptor complex (ACVR2A, ACVR2B, TGFBR2, BMPR2, ALK1, ALK3, ALK5, ALK6) have contributed insight into the molecular basis for ligand receptor specificity (Goebel et al., 2019b). Each type I and type II receptor ECD consist of about 100 residues with three β-strands with a high degree of homology, except the three **extended β-sheets loops**, which define specificity for ligand interaction (Goebel et al., 2019b).

In addition to **structural data**, binding specificities and affinities between ligands and receptors have been analyzed by chemical **crosslinking** of radioactively labeled ligands with receptors in cells and by **cell-free surface plasmon resonance** studies (Biacore; Biosensor analysis using surface plasmon resonance) using receptor ectodomains (Aykul and Martinez-Hackert, 2019; Danielpour, 2000).

Besides the measurement of the affinity of the receptor-ligand interactions, the crosslinking technique enabled also the initial identification and characterization of TGFβ receptors as high affinity cell surface TGFβ binding proteins by incubating the cells with radiolabeled TGFβ (Cheifetz et al., 1986; Massagué and Like, 1985; Rodriguez et al., 1995; Wang et al., 1991).

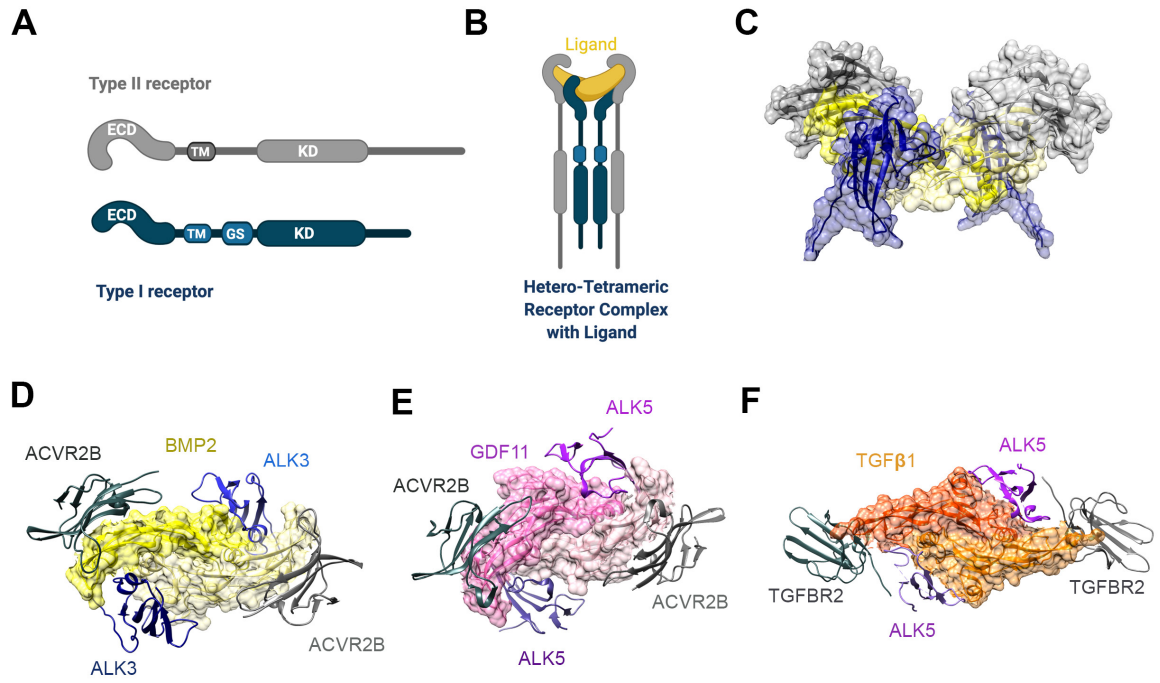

Figure 1.12 Ternary Ligand-Receptor complexes. (**A**) Schematic depiction of the domain organization of type I and type II receptors (Extracellular Domain (ECD); Transmembrane Domain (TM); Glycin-Serin rich domain (GS-domain); Kinase Domain (KD)) and (**B**) a Hetero-Tetrameric Receptor Complex with a ligand. (**C-D**) Ternary ligand-receptor complex of BMP2 with ECD of ACVR2B and ALK3 (Weber et al., 2007) (**E**) GDF11 with ECD of ACVR2B and ALK5 (Goebel et al., 2019a) (**F**) and TGFβ1 in complex with TGFBR2 and ALK5 (Radaev et al., 2010). Crystal structures were exported from the Protein Data Bank (PDB ID: 2H64; 6MAC; 3KFD) and rendered in Chimera software (Pettersen et al., 2004).

Type II receptors

At the back face of the two ligand fingers, named **knuckle epitope**, TGFβ family ligands bind type II receptors. Even though type II receptors bind ligands at the same epitope, there are preferences for specific ligands (Yadin et al., 2016).

ACVR2A and ACVR2B interact with BMP ligands as well as Activins. BMPR2 is mainly known for its binding to BMP ligands but it was also shown to bind and signal via Activins (Aykul et al., 2017; Rejon et al., 2013). Therefore, those type II receptors can engage in various signaling complexes leading to different SMAD responses.

In general, Activin and TGFβ class ligands bind type II receptors with higher affinities compared to BMP ligands. Whereas **BMPs** and **GDFs** (BMP2/4/5/6/7/8 and GDF5/6/7) were shown to bind with rather low micromolar affinities to all three type II receptors (ACVR2A, ACVR2B, BMPR2), **Activins** bind with very high nanomolar affinities to **ACVR2A** and **ACVR2B** but also with lower affinity to **BMPR2** (Heinecke et al., 2009). This suggests a competitive environment of BMP/GDF versus Activin ligand binding to type II receptors. Several studies have shown that ActivinA competes with BMPs for

binding to ACVR2A and ACVR2B (Aykul and Martinez-Hackert, 2016; Hatsell et al., 2015; Olsen et al., 2015; Piek et al., 1999; Seher et al., 2017). And recently, based on native PAGE analysis and signaling experiments with recombinant extracellular domains it was reported that ActivinA has no preference for interaction with ACVR2A or ACVR2B, whereas GDF11 preferred ACVR2B over ACVR2A (Goebel et al., 2019a). Interestingly, **BMP9** also has a preference for **ACVR2B** in comparison to the other type II receptors (BMPR2, ACVR2A) and this is even reflected in a similar binding affinity as for its high affinity receptor ALK1 (Townson et al., 2012).

In contrast, **TGFBR2** is fully restricted for interaction with TGFβ ligands. TGFBR2 binds the ligands at their **fingertips**, where they have specific residues for binding, which prevent binding to other type II receptors and are not present in BMP and Activin ligands (Yadin et al., 2016).

However, for BMP and Activin type II receptor interactions it is not completely clear from structural data why binding at the same knuckle epitope achieves for some a highly specific while for others a promiscuous interaction interface. Studies with BMP2 for example have shown, that the binding interface to ACVR2A is dominated by hydrophobic interfaces, which enable promiscuous interactions with low affinity. In addition to the hydrophobic interface, ligands with high affinity to type II receptors, such as Activins have specific residues, which shielding hydrogen bonds from the solvent and foster binding (Yadin et al., 2016). This could be demonstrated by exchange of single residues in BMP2 with equivalent residues from ActivinA, which turned BMP2 into a high affinity ligand for ACVR2B. Mutation of two other residues led to high affinity binding of BMP2 to BMPR2 (Weber et al., 2007).

Thus, it is proposed that type II receptor binding affinity and specificity is mediated by **single residues** within the **knuckle** of the ligand that determine **hot spots** of binding with the **hydrophobic interfaces** of type II receptors (Clackson and Wells, 1995; Yadin et al., 2016).

Type I receptors with a particular role for ALK2

Compared to type II receptors, ligand binding to type I receptors is mediated via a binding interface, which lies between the ligand fingertips and the wrist helix and is therefore named **wrist epitope**.

Interestingly, the interaction between the SMAD2/3-activating type I receptors (ALK4, ALK5, ALK7) to their corresponding ligands is low affinity. Despite the same epitope, ligands binding to SMAD1/5/8 activating type I receptors have a much higher affinity (Heinecke et al., 2009; Rodriguez et al., 1995).

Key structural differences, which define ligand-receptor binding and recognition are the length of the **β4-β5 loops** in **type I receptors** and the **prehelix loop** within the wrist epitope of the ligand (Gipson et al., 2020; Goebel et al., 2019b)

ALK5 is the primary type I receptor for **TGFβ** and has extremely low affinity to the ligand when not bound to TGFBR2 (Groppe et al., 2008). In contrast to other type I receptors, ALK5 directly interacts with TGBFR2, which is enabled by TGFβ shifting the type II binding interface towards the fingertip (Goebel et al., 2019b).

The **Activin class** ligands are more promiscuous and use **ALK4, ALK5, ALK7** type I receptors for signaling but also bind with low affinities (Attisano et al., 1996; Heinecke et al., 2009). The highly flexible wrist region of Activin ligands is suggested to cause the low affinity to its type I receptors. Specificity for the Activin ligand class is facilitated by a four amino acid extensions at β4-β5 loops, which interact with the ligand fingertip (Gipson et al., 2020). **ActivinA** utilizes **ALK4** as its primarily type I receptor in complex with type II receptors ACVR2A, ACVR2B and to a lesser extend BMPR2 (Aykul et al., 2017; Willis et al., 1996). **ActivinB** and **ActivinAB** can signal via **ALK4** or **ALK7** (Attisano et al., 1996; Bernard et al., 2006; Tsuchida et al., 2004). **ActivinC** is suggested to be non-signaling and to have an inhibitory function by forming ActivinAC heterodimers (Mellor et al., 2003, 2000).

ALK7 was originally discovered as an orphan receptor with a similar kinase domain to ALK4 and ALK5 but a very different ECD (Rydén et al., 1996). Later ALK7 was defined as a receptor for Nodal (Reissmann et al., 2001) and some members of the activin subgroup GDF8, GDF11 as well as GDF1, GDF3 (Yadin et al., 2016). Constitutive active ALK7 mutants confirmed ALK7 as a SMAD2/3 activating type I receptors (Jörnvall et al., 2001; Watanabe et al., 1999).

Low affinity binding of TGFβ and Activin ligands to type I receptors and high affinity binding to type II receptors is reversed for most BMPs and GDFs, which bind type I receptors much stronger than their type II receptors.

The static nature of **BMPs** offers a rigid preformed binding pocket in the **wrist region**, which is suggested to facilitate the high affinity type I receptor binding (Gipson et al., 2020). In fact, sequence differences in the **pre-helix loop segment** suggest a discrimination between binding specificity to SMAD2/3-or SMAD1/5/8-activating type I receptors and even between ALK2, ALK3 and ALK6 (Cash et al., 2009; Keller et al., 2004; Nickel et al., 2005; Saremba et al., 2008; Yadin et al., 2016).

For example **BMP2** and **BMP4** have high affinity to **ALK3** and **ALK6** and relatively low to type II receptors (Heinecke et al., 2009). **ALK1** represents the high affinity receptor for **BMP9** (Brown et al., 2005). Recent evidence suggests that BMP9 signaling also occurs via **ALK2** that could be blocked by a specific ALK2 antibody in myeloma cells, which are devoid of ALK1 (Olsen et al., 2018, 2015). This is supported by binding of pro-BMP9 and the BMP9 growth factor domain to ALK2-Fc (Salmon et al., 2020).

Compared to ALK3 and ALK6 the BMP type I receptor ALK2 binds BMP ligands with very low affinities *in vitro* using cell free ligand-receptor interaction studies (Biacore) (Heinecke et al., 2009; Yadin et al., 2016).

However, in several cell based crosslinking and functional studies it was proofed that **ALK2** is an essential type I receptor for **BMP6** and **BMP7** signaling (Ebisawa et al., 1999; Hong et al., 2009; Macías-Silva et al., 1998; ten Dijke et al., 1994b).

In fact, **BMP6** incorporates a specific **glycosylation motif** (hot spot) in the wrist region, which determines binding to ALK2 and does not play a role in binding to ALK3 or ALK6. When this motif was deleted, BMP6 was defective in ALK2 binding but remained normal affinities to ALK3 and ALK6. As a consequence, essential cellular function such as BMP induced ALP expression in C2C12 cells was disrupted without compensation of other type I receptors (Saremba et al., 2008).

Interestingly, **ALK2** was originally described as a **Activin type I receptor** because of its ability to bind ActivinA in complex with **ACVR2A or ACVR2B** (Attisano et al., 1993; Tsuchida et al., 1993). Two independent studies confirmed binding of ActivinA to murine Alk2 and human ALK2 and a corresponding ACVR2 receptor (Ebner et al., 1993; ten Dijke et al., 1994a). ALK2 co-expression with ACVR2A or ACVR2B resulted in transcriptional activation of a SMAD2/3 reporter (3TP) compared to solely ACVR2A/B overexpression (Attisano et al., 1993; Yamashita et al., 1995). The 3TP

reporter contains portions of the promoter region of the target gene plasminogen activator inhibitor 1 (PAI-1) (Wrana et al., 1992). However, this was not confirmed on endogenous PAI-1 protein levels (ten Dijke et al., 1994a).
Later ALK2 was also found in complex with BMP7 and type II receptors and SMAD downstream responses were only detected for BMP7 and not for ActivinA in the used systems (Macías-Silva et al., 1998). Moreover, ALK2 associated with SMAD1 and efficiently phosphorylated SMAD1/5/8 but not SMAD2 (Macías-Silva et al., 1998).
Based on the inability of ActvinA to activate ALK2 in comparison to BMP7, ALK2 was then re-categorized as a **BMP type I receptor**. Of note, all ALK2 ligands share the low affinity binding to ALK2 in absence of type II receptors, as shown for BMP6 (Saremba et al., 2008), BMP7 and ActivinA (Heinecke et al., 2009).
Even though ActivinA was initially not assigned to activate ALK2, it was later reported to functionally antagonize BMP7 for ALK2 binding as highlighted by crosslinking studies (Piek et al., 1999). This is supported by recent evidence from ALK2-WT myeloma cells, which suggest that ActivinA antagonizes BMP6 and BMP9 induced ACVR2A/ACVR2B/ALK2 signaling but not BMP2 and BMP4 induced BMPR2/ALK3 or BMPR2/ALK6 signaling (Olsen et al., 2015). Moreover, co-treatment of ALK2-WT ESCs with BMP6 and ActivinA reduced pSMAD1/5 levels (Hatsell et al., 2015).
Thus, ActivinA does not only compete with BMPs for type II receptor binding as mentioned above but also for binding to ALK2.

1.7.3 Receptor ligand assembly paradigms

Based on binding specificities and affinities, two different receptor-ligand assemble paradigms have been established for the TGFβ superfamily, which were recently expanded by a third paradigm (Goebel et al., 2019a). The assembling of a dimeric ligand and two type I and two type II receptors aims to form a functional heterotetrameric complex for signal transduction. For BMP ligands the **high-affinity lock and key mechanism** has been proposed (Figure 1.13). Based on the rigid, open and butterfly-like structure of BMP ligands, a rigid binding pocket facilitates the high affinity interactions with type I receptors and symmetrically binding of type II receptors to the convex surface (Allendorph et al., 2006; Weber et al., 2007; Yadin et al., 2016). In contrast, TGFβ utilizes a **cooperative mechanism** with initial high affinity binding of the ligand to type II receptors, which then recruit the type I receptors into the complex with a unique type I and type II receptor binding interface (Groppe et al., 2008) (Figure

1.13). Only recently, a third mechanism for the Activin family members was proposed, which shares the type II receptor affinities of the TGF class and the receptor orientations of the BMP class. In the so-called **conformational selection model**, the type II receptor bind and enrich the Activin ligands on the cell surface to facilitate interactions with the low affinity type I receptors (Figure 1.13).

For the BMP family the ligand receptor assembly paradigm was further specified into two modes: (1) The formation of **ligand-independent preformed complexes (PFCs)**, which consist of homo- or heterodimeric type I and type II as well as heterotetrameric type I and type II complexes (Gilboa et al., 2000; Nohe et al., 2002) (2) And a **ligand-dependent BMP-induced signaling complex (BISC)**, which results from binding of a BMP dimer to two high affinity type I receptors and subsequent recruitment of type II receptors into the complex (Nohe et al., 2002). This was supported by single particle tracking studies, which showed that BMP receptors have different lateral mobilities in the plasma membrane (Guzman et al., 2012). Whereas the BMP type I and II receptors ALK3, ALK6 and BMPR2 had a confined movement, showed a subpopulation of BMPR2 a high lateral mobility, which was only stabilized upon ligand-induced complex formation with type I receptors using BMP2 (Guzman et al., 2012). Moreover, based on receptor mutant studies and endocytosis experiments it was proposed that PFCs promote SMAD dependent intracellular signaling whereas BISCs form in cholesterol rich membranes and require confined type I receptors to induce non-SMAD signaling (Guzman et al., 2012; Hartung et al., 2006). However, those investigational studies are lacking for the ALK2 receptor and it remains to be shown, if receptor complexes with ALK2 form via the same modes. The characteristic differences in ALK2 ligand binding affinities suggest a different mode of receptor oligomerization.

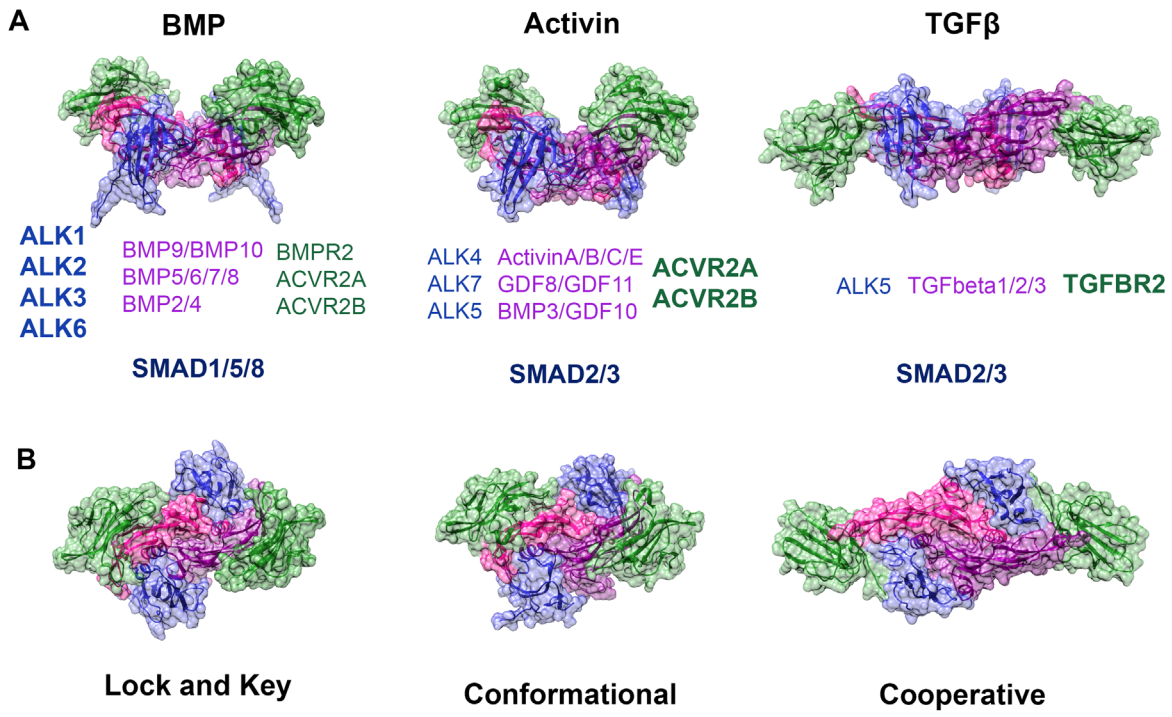

Figure 1.13 Receptor-Ligand assembly paradigms of the BMP, Activin and TGFβ Class. (**A**) Exemplary signaling complex structures of each ligand class comprised of a dimeric ligand and the ECD of two type I and two type II receptors. Below are the ligands and receptor types listed. High ligand affinity receptors are depicted in bold. (**B**) Signaling complexes of A are rotated around the x axis by 90° and receptor binding mechanisms are indicated below. Crystal structures (PDB ID: 2H64; 6MAC; 3KFD) were exported from the Protein Data Bank and rendered in Chimera software (Pettersen et al., 2004).

1.7.4 Antagonists and Co-Receptors modulate BMP/TGF signaling

Additional regulation of signaling responses is mediated by other transmembrane receptors and soluble antagonists, which modulate the BMP/TGFβ pathway very distinctly.

Co-receptors

Several transmembrane or membrane bound proteins have been shown to also bind TGFβ family ligands and to associate with their receptors such as Endoglin, Neuropillins, Cripto, Betaglycan, BAMBI or Integrins (Nickel et al., 2018).

Endoglin is a well expressed transmembrane protein in ECs and was shown to bind several TGFβ ligand family members in presence of corresponding type II receptors, including TGFβ1, TGFβ3, BMP2, BMP7 and ActivinA (Barbara et al., 1999; Letamendía et al., 1998; Nickel et al., 2018). BMP9 and BMP10 bind Endoglin with high affinities at type II receptor binding sites even in absence of other type I and II receptors (Alt et al., 2012; Castonguay et al., 2011).

Ligand bound Endoglin was isolated in complex with several type I (ALK1, ALK2, ALK3, ALK4, ALK5, ALK6) and type II receptors (ACVR2, BMPR2, TGFBR2) (Nickel et al.,

2018) indicating modulation of SMAD responses. TGFβ induced SMAD2/3 signaling was inhibited in presence of Endoglin, which is suggested to occur via the dissociation of ALK5 from the signaling complex with TGFBR2 (Guerrero-Esteo et al., 2002).
This supports the cooperative receptor assembly model of TGFβ ligands, which requires the type I and type II receptor binding interface. This is in line with another study, which also reported inhibited TGFβ/ALK5 signaling in presence of Endoglin but interestingly the promotion of TGFβ/ALK1 SMAD1/5 signaling was also observed (Lebrin et al., 2004).
A recent structural data suggests that Endoglin bound to BMP9 still enables the binding of ALK1 but not ACVR2B (Saito et al., 2017). Therefore, it remains unclear how the blocking of type II receptor binding by Endoglin facilitates the activation of type I receptors in this complex. Saito et al., proposed a transient model, where Endoglin enriches BMP9 at the plasma membrane for complex formation with ALK1, which is followed by Endoglin dissociation to enable type II receptor binding (Saito et al., 2017). Another possibility could be that Endoglin may displace the GS domain bound FKBP12, which destabilizes the inactive type I receptor kinase. However, for efficient type I receptor kinase activation the GS-domain has to undock from the kinase N-lobe requiring the phosphorylation of serine and threonine residues in the GS-domain (see chapter 1.7.5). Thus, the distinct receptor-ligand assembly paradigms enable co-receptors as Endoglin to modify SMAD2/3 and SMAD1/5 responses differently. But how active and inactive co-receptor-ligand complexes are formed remains incompletely understood.
Interestingly, in contrast to BMP9 and BMP10 Endoglin binding to BMP7 and ActivinA requires type II receptors (Barbara et al., 1999) suggesting that Endoglin does not bind to type II receptor epitopes on those ligands, which should be explored by structural data in future.
Other abundant co-receptors in the endothelium are **Neuropillins** (NRP1, NRP2), which have been reported to suppress the stalk cell phenotype in sprouting angiogenesis by limiting SMAD2/3 signaling through ALK1 and ALK5 (Aspalter et al., 2015). On the other hand it was also demonstrated that NRP1 enhances SMAD2/3 signaling by promoting the oligomerization of TGF type I and type II receptors suggesting a context dependent function of NRP1 (Glinka et al., 2011).
So far, there is no structural evidence how NRP1 inhibits SMAD2/3 signaling. Based on binding of NRP1 to TGFβ, Aspalter and colleagues proposed that NRP1 acts as a

decoy, which may inhibit interaction between type I and type II receptors (Aspalter et al., 2015). Since NRP1 and Endoglin have a PDZ-binding motif, both co-receptors may also share similar mechanisms for the modulation of TGFβ signaling (Nickel et al., 2018). Moreover, in the endothelia context, an important function of NRP1 is the binding to VEGFA, which induces complex formation with VEGFR2 and is essential for proper VEGF signaling (Lanahan et al., 2010; Prahst et al., 2008; Salikhova et al., 2008).

Betaglycan or also called TGFBR3, has a similar structure as Endoglin and binds TGFβ ligands with high affinities. However, in contrast to Endoglin it binds the ligands even in absence of corresponding type II receptors (López-Casillas et al., 1993). Betaglycan has also been reported to bind BMP2, BMP4, BMP7, GDF5 with lower affinities (Kirkbride et al., 2008) and with high affinities to Inhibins (Lewis et al., 2000). Betaglycan enhances TGFβ signaling by enriching the ligand at the membrane, which presents them to type II receptors and also enhancing the binding to type II receptors (Nickel et al., 2018). Mediating enhanced ligand binding to TGFBR2 is especially crucial for TGFβ2 because it has a much lower affinity to TGFBR2 than TGFβ1 and TGFβ3 (De Crescenzo et al., 2006).

BMP activin membrane-bound inhibitor (**BAMBI**) is another co-receptor which inhibits BMP, Activin and TGF heterotetrameric β signaling (Onichtchouk et al., 1999). The intracellular domain of BAMBI resembled the homodimerization interface of type I receptors. Indeed BAMBI binds all TGF-β/BMP Type I receptors except for ALK2 and is suggested to act as a decoy receptor preventing the formation of signaling-competent receptor complexes (Nickel et al., 2018).

Cripto1 plays a pivotal role in embryonic development and is involved in body axis specification. Thus, Cripto is mainly expressed in pluripotent stem cells and only shows minor expression in adult tissues. However, upon certain triggers it becomes upregulated, such as in several neoplasia (de Castro et al., 2010). Cripto is essential for Nodal signaling by facilitating the interaction of Nodal, ACVR2A/B and ALK4/7 signaling complexes. Direct binding to Nodal and ALK4 was reported as well as to ActivinA and ActivinB but only in presence of ACVR2A/B. In contrast to Nodal, binding of Cripto to Activins results in signaling inhibition (Gray et al., 2003; Nickel et al., 2018). Moreover, Cripto also binds to TGFβ1, which reduces its binding to ALK5 (Gray et al., 2006).

In sum, TGFβ family ligands do not only bind to their classic type I and II receptors, but additionally to other transmembrane proteins, which activate or antagonize signaling responses and thus function as a **co-receptor** or **decoy receptor** respectively. Some co-receptors also exist as a soluble form with different functions. An example is the **soluble form** of Betaglycan, which functions as a very potent neutralizing agent for TGFβ (Mendoza et al., 2009). Extracellular antagonism by ligand neutralization and thereby blocking the receptor binding sites is also mediated by ligand antagonists (Goebel et al., 2019b).

Antagonists

A wide range of structurally diverse antagonists inhibit ligands through different binding mechanisms. Mostly, two antagonists inhibit the ligand by blocking each one type I and one type II receptor binding site, which prevents receptor assembly and signaling. In 2002 the first structure of an antagonist was solved and showed how the homodimer **Noggin** inhibits BMP7 by blocking all four receptor binding sites (Groppe et al., 2002) (Figure 1.14A). Noggin also binds BMP6 and with even higher affinity BMP2 and BMP4 (Gipson et al., 2020). Three years later the antagonist-ligand complex of Activin and **Follistatin** was solved (Thompson et al., 2005a) (Figure 1.14C). Follistatin consist of multiple domains, one N-terminal domain (ND) (blocking type I receptor binding site) and three tandem follistatin domains (FSD) (covering type II receptor binding sites). The ND exhibits different conformations, which enables the blocking of the wrist region of different ligand groups (ActivinA/B, GDF8/11, BMP2/4/6/7). Thus, compared to Noggin Follistatin is promiscuous and targets multiple ligand classes. Over ten years later the structure of **Gremlin-2, a member of the Gremlin antagonist family,** in complex with GDF5 was solved (Nolan et al., 2016) (Figure 1.14B). In contrast to Noggin two Gremlin-2 dimers are required to block the receptor binding sites, which bind as an H shape at each end of the ligand dimer (Goebel et al., 2019b). While TGFβ family ligands show a high degree of structural conservation, their antagonists are very heterogenous in their structure. However, the structurally distinct antagonists Noggin, Follistatin and Gremlin-2 have in common that they block all four receptor binding epitopes, which prevents ligand binding and the formation of functional signaling complexes.

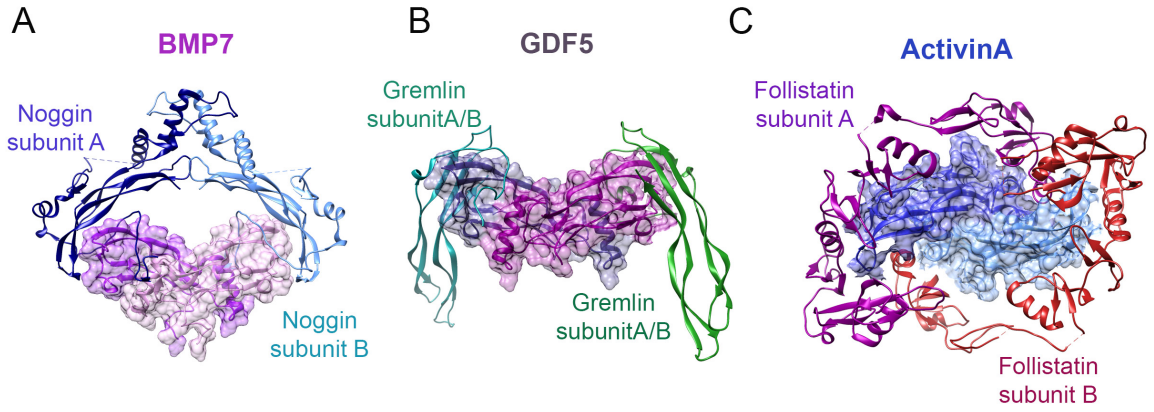

Figure 1.14 Heterogenous antagonist structures for BMP and Activin ligands. (**A**) Dimeric BMP7 ligand bound to two monomers of Noggin (Groppe et al., 2002). (**B**) Two Gremlin-2 dimers bind in H shape to dimeric GDF5 and block receptor binding sites (Nolan et al., 2016). (**C**) Two monomers of Follistatin bind dimeric ActivinA in a ring-like structure (Thompson et al., 2005b). Crystal structures (PDB ID: 1M4U; 5HK5; 2B0U) were exported from the Protein Data Bank and rendered in Chimera software (Pettersen et al., 2004).

1.7.5 **Receptor activation**

BMP and TGFβ ligands bind to serine/threonine kinase transmembrane receptors, which are structurally and functionally grouped into seven type I receptors and five type II receptors. Type I and type II receptors share a similar domain structure, which consists of a cysteine-rich extracellular domain that mediates ligand binding, a transmembrane domain and an intracellular part of a **serine/threonine kinase domain**. The kinase domains consist of **N-and C-terminal subdomains (lobes)**, which are connected by a shorth hinge, which enables their rearrangements to facilitate ATP exchange and substrate binding. The **N-lobe** contains five stranded β-sheets and a single α-helix (αC) whereas the **C-lobe** consist of α-helices (Yadin et al., 2016) (Figure 1.15). Key difference between type I and type II receptors is a serine-glycine rich sequence (GS-domain) N-terminal to the kinase domain of type I receptors, which is absent in type II receptors. For type I receptor activation the type II receptors phosphorylate conserved serine and threonine residues in the **helix-loop-helix motif** (**GS loop**) within the GS-domain (Figure 1.15). Thereby, the GS-domain undocks from the kinase N-lobe, which switches the type I receptor kinase active and allows subsequent SMAD phosphorylation. In contrast to type I receptor, type II receptor have an active conformation with reoriented **helix αC**, which enables constitutive kinase activity (Kornev et al., 2006), as shown by autophosphorylation *in vitro* (Hassel et al., 2004; Lin et al., 1992).

The **inactive state** of type I receptors is maintained by critical residues, which bind the GS domain to the kinase N-terminal subdomains (N-lobe), thereby the GS loop is protected from phosphorylation.

Moreover, complex formation with the cytoplasmic peptidyl-prolyl cis-trans isomerase **FKBP12** (FK506 binding protein 12) stabilizes the inactive conformation of type I receptors. FKBP12 binds to the GS domain and **shields the GS loop** from phosphorylation of type II receptor kinases (Huse et al., 1999; Wang et al., 1996, 1994). FKBP12 binding forces the GS loop to insert into the kinase domain where it forms an inhibitory connection between the amino lobe β sheet and the αC helix, which causes an inactive conformation of the kinase. The inhibitory receptor conformation is stabilized by a number of arginine residues, which are highly conserved among type I receptors (Chaikuad and Bullock, 2016). In sum, **FKBP12** binds to the **GS domain,** shielding the GS loop and pushing it against the kinase domain, locking the position and orientation of the **αC helix**, which keeps the type I receptor **kinase** in an **inactive conformation**. Thus, for type I receptor activation, FKBP12 has to dissociate first to enable subsequent phosphorylation of serine threonine residues in the GS domain by the type II receptor kinase. Based on the conserved structural similarity among type I receptors this mechanism applies to all type I receptors (Yadin et al., 2016).

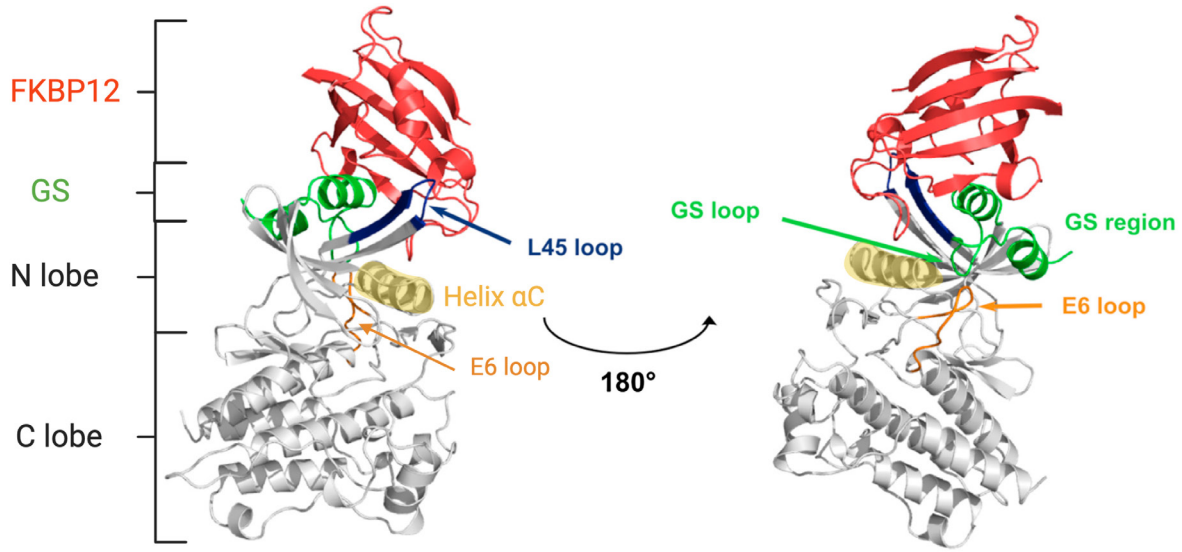

Figure 1.15 Structure of the inactive type I receptor kinase in complex with FKBP12. Structure of ALK5 glycine-serine rich (GS) (green) and kinase (grey) domains in complex with inhibitory protein FKBP12 (red). The type I receptors have a typical kinase architecture consisting of N-and C-terminal subdomains (lobes), αC helix, E6 loop and L45 loop (blue), which defines type I receptor substrate specificity. Modified after (Yadin et al., 2016).

1.7.6 **BMP/TGFβ signal transduction via SMAD proteins**

Receptor SMADS and Co-SMAD4

Activation of type I receptor kinases leads to the phosphorylation of R-SMADs at a C-terminal SXS motif. This enables complex formation with the co-SMAD4 into a heterotrimeric complex consisting of two phosphorylated R-SMADs, which translocates to the nucleus to regulate target gene transcription. Each R-SMAD and the Co-SMAD4 have a conserved N-terminal **MH1** and a C-terminal **MH2 domain**. The **linker sequence** between the MH1 and MH2 domain includes phosphorylation sites and is target for several kinases, which control stability and function of the SMADs (Derynck and Budi, 2019). The C-terminal **MH2 domain** mediates the interaction with type I receptors via a specific **L3 loop** (Lo et al., 1998). Binding of the L3 loop to a specific, corresponding **L45 loop** in type I receptors defines receptor SMAD specificity and facilitates the phosphorylation of SMADs on two C-terminal serines (**SXS motif**) by type I receptors (Cárcamo et al., 1994; Feng and Derynck, 1997; Persson et al., 1998). Accordingly, the SMAD proteins SMAD1, 5, 8 are substrates of the type I receptors ALK1, ALK2, ALK3 and ALK6 and SMAD2 and 3 become phosphorylated by ALK4, ALK5 and ALK7 (Mueller and Nickel, 2012). The MH2 domain and the phosphorylated SXS motif facilitate the interaction with other SMADs and the Co-SMAD4 to form heterotrimeric complexes.

In addition to R-SMADS interact also the **inhibitory (I) SMADS** with type I receptors via their MH2 domain. Thereby two kinds of I-SMADs, named **SMAD6** and **SMAD7**, inhibit the binding of R-SMADs to type I receptors and prevent their C-terminal phosphorylation. In addition, I-SMADs also complex with SMAD4 via the MH2 domain and thereby antagonize R-SMADS for SMAD4 complex formation. Moreover, I-SMADS are capable to recruit E3 ubiquitin ligases, which ubiquitinate type I receptors for proteasomal degradation. SMAD7 interacts with ALK2, ALK3, ALK4 and ALK5 receptors whereas SMAD6 preferentially with ALK3 and ALK6. (Miyazawa and Miyazono, 2017). SMAD6 is a direct target gene of SMAD1 and SMAD5 and SMAD7 expression is induced by binding of SMAD3 to its promoter (Ishida et al., 2000; Nagarajan et al., 1999). However, the expression of SMAD6 and SMAD7 can be induced by various TGFβ family ligands and other stimuli, such as by fluid shear stress in the vascular endothelium (Afrakhte et al., 1998; Miyazawa and Miyazono, 2017; Topper et al., 1997).

Upon phosphorylation of R-SMADs by type I receptors a nuclear localization signal in the **MH1 domain** becomes exposed and enables translocation to the nucleus. The β-hairpin structure in the N-terminal **MH1 domain** mediates direct DNA binding of SMADs (Xiao et al., 2000).

Active R-SMAD in the nucleus become eventually dephosphorylated, which results in their dissociation from SMAD4 and the recycle back to the cytoplasm. In fact, during active signaling R-SMADs and SMAD4 constantly shuttle between the cytoplasm and the nucleus, otherwise they retain in the cytoplasm (Derynck and Budi, 2019; Hata and Chen, 2016; Inman et al., 2002).

SMAD2 has generally been considered as the only non-DNA-binding SMAD protein (Dennler et al., 1998; Derynck and Zhang, 2003; Yagi et al., 1999). The most commonly expressed SMAD2 isoform has an E3 insert in the MH1 domain, which has been considered to prevent DNA binding (Yagi et al., 1999). However, very recent evidence from biochemical and structural studies shows that SMAD2 indeed binds to the DNA but this is highly dependent on the conformation of the E3 insert, which is unique to SMAD2 and can hinder DNA binding by a closed conformation form, which is observed in recombinant and tagged SMAD2 protein (Aragón et al., 2019).

BMP and TGFβ SMADs bind preferentially to specific target sequences. **SMAD1** and **SMAD5** bind preferentially to so called SMAD binding elements (SBEs), which consist of GC-rich motives such as GGCGCC or GGAGCC (**GC-SBE**), while **SMAD3** and **SMAD4** bind to **CAGAC** (SBE) motifs, which are found in many BMP and TGFβ target genes (Morikawa et al., 2013, 2011). Interestingly, recent evidence from structural studies showed that in embryonic stem cells all SMADs were able to bind to GC rich motifs, which suggests that specific target gene regulation is dependent on additional lineage-determining factors (Martin-Malpartida et al., 2017). SMAD proteins offer via the MH2 domain various contact points to partner with other transcription factors, coactivators and repressors, which modulates target gene transcription and repression (Macias et al., 2015).

Examples of well-known **SMAD1 co-factors** include **RUNX2**, which modulates the expression of osteogenic genes e.g. in chondrocyte differentiation (Drissi et al., 2003), the intracellular domain of NOTCH (**NICD**), which control endothelial cell function in crosstalk with NOTCH signaling (Itoh et al., 2004) and **YAP** during BMP suppressed neural differentiation (Alarcón et al., 2009).

Moreover, trimeric SMAD complexes consist of different R-SMADs. And it was shown that a complex of two identical R-SMADs induced different targets genes compared to a complex consisting of SMAD2, SMAD3 and SMAD4 (Lucarelli et al., 2018). There is emerging evidence of **mixed SMAD complex formation** consisting of BMP and TGFβ SMADs (Byfield and Roberts, 2004; Daly et al., 2008; Hiepen et al., 2019; Ramachandran et al., 2018).

These various combinatorial possibilities to form SMAD transcription factor complexes more likely reflect the complex upstream signaling and enable the demand of cell type specific and fine-tuned gene expression. Thus, SMAD signaling is very heterogenous and depends on upstream ligand-receptor complex formation as well as intracellular modulators in the cytoplasm and nucleus, which result in highly specific transcriptional responses.

1.8 Consequences of FOP mutations on ALK2 receptor activity

1.8.1 FOP mutations destabilize the inactive receptor and trigger hypersensitivity

Structural localization of FOP causing mutations in the BMP type I receptor ALK2 revealed, that they cluster around the GS domain and ATP pocket of the kinase domain (Figure 1.16A). The affected residues normally form critical interactions to stabilize the inhibitory complex with FKBP12 and the inactive conformation of the receptor. Therefore, it has been predicted that the FOP mutations break these inhibitory interactions, which cause a shift to the active conformation (Groppe et al., 2007). The most common **mutation R206H** involves residues, which **connects the GS domain** to the kinase **N-lobe and stabilize the interactions with FKBP12**. Arg-206 forms a hydrogen bond with Asp-269 and an additional hydrogen bond with the backbone oxygen of Met-270 (Figure 1.16B). Replacement of the conserved arginine with histidine at residue 206 of ALK2 breaks these interaction (Chaikuad et al., 2012). A more recent *in silico* analysis found that R206H also destabilizes the D354-R375 salt-bridge, which normally acts as a lock to prevent coordination of ATP to the catalytic site (Botello-Smith et al., 2017).

This is in line with other **FOP mutations,** that **break inhibitory bonds** of the inactive state of the receptor, which enables freedom for the GS loop to move away from the kinase N-lobe, **promoting an active kinase conformation** (Chaikuad et al., 2012).

This introduced the concept of constitutive receptor activity based on **impaired interaction of mutant ALK2 to FKBP12** and hyperactive signaling in response to BMP ligands as shown by a number of studies using models of receptor overexpression (Chaikuad et al., 2012; Fukuda et al., 2009; Shen et al., 2009a; Song et al., 2010a; van Dinther et al., 2010). Constitutive activating receptors are able to recruit downstream effectors in the absence of ligand stimulation and type II receptors as shown for constitutive active ALK5-T204D when mutated in the GS domain (Wieser et al., 1995). Later the artificial constitutive ALK2-Q207D mutation (not naturally occurring in FOP) was designed accordingly (Fukuda et al., 2006). However, until 2012 it hasn't been proven whether the activity of ALK2 mutants is also independent of type II receptors. Studies in a FOP Drosophila model and type II receptor deficient mice confirmed that GS domain ALK2 mutants (R206H, Q207D) signal independent of ligand stimulation but require expression of at least one type II receptor (Bagarova et al., 2013; Le and Wharton, 2012). Interestingly, the ALK2 and type II receptor ligand binding domain (LBD) was not needed for ALK2 mutant activation (Le and Wharton, 2012). Importantly, mutant ALK2 signaling is even **independent of type II receptor kinase activity** (Bagarova et al., 2013), indicating that **type II receptors** are mainly required for **scaffolding** to form a functional ALK2 signaling complex. Therefore, **mutant ALK2 receptor** responses **require type II receptor cooperation** and can rather be described as **hypersensitive** with increased (`leaky´) basal signaling and hyperactivated signaling in response to ligands.

A comparative analysis confirmed increased basal signaling and hyperactivated signaling in response to BMP ligands for all FOP causing mutations compared to WT ALK2 in overexpression (Haupt et al., 2018). But this study also highlighted that mutant ALK2 signaling showed variations in different cell types and that signaling responses between GS domain and kinase domain ALK2 mutants were different for high and low ligand concentrations (Haupt et al., 2018). This underlines the possibility that secondary so far unknown component(s) or mechanism(s) contribute to ALK2 signaling outcomes, which may also explain the phenotypic variations observed in FOP patients.

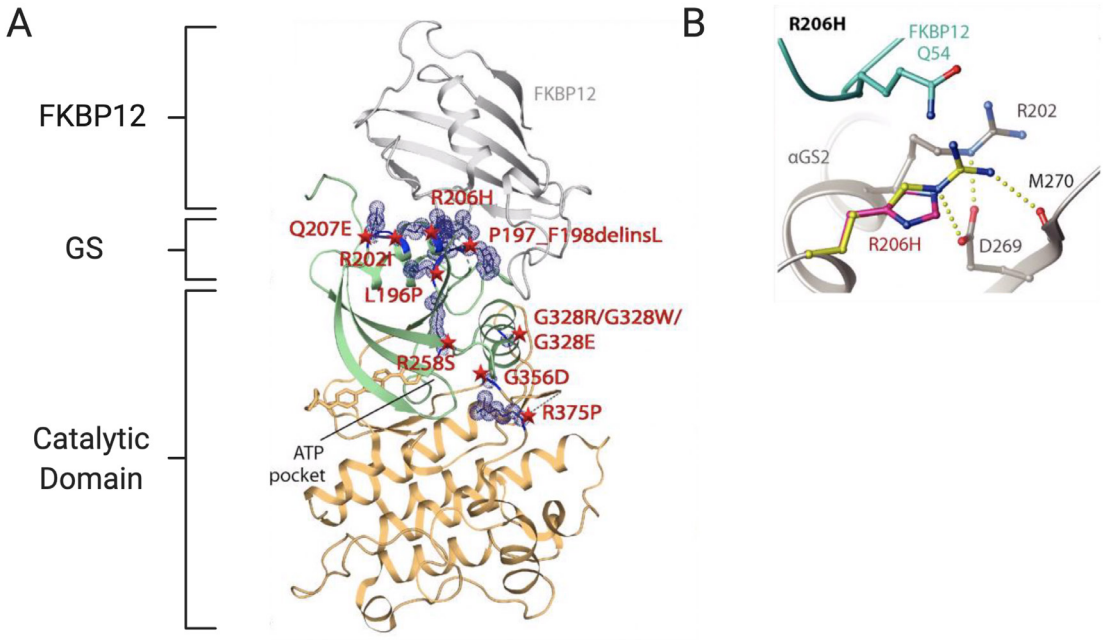

Figure 1.16 FOP mutations destabilize the inactive state of ALK2. (**A**) FOP causing mutations (red) cluster around the GS domain and the ATP pocket of the catalytic domain of ALK2 and break interactions with the inhibitory protein FKBP12 (grey). (**B**) Structural modeling of R206H mutation shows changes in mutant structure (pink) overlaid onto wild-type (WT) residue (yellow). Hydrogen bonds in the WT are shown by yellow spheres between Arg-206 and Asp-269 and an additional hydrogen bond with the backbone oxygen of Met-270. Modified after (Chaikuad et al., 2012).

1.8.2 **FOP mutations foster ALK2 activation in response to Activins**

In 2015, two independent research teams discovered that ALK2-R206H gains responsiveness to Activin ligands by aberrantly transducing SMAD1/5 signaling (Hatsell et al., 2015; Hino et al., 2015). Normally, Activin ligands transduce SMAD2/3 signaling via the type I receptors ALK4 and ALK7 (Yadin et al., 2016). By overexpressing AK2-R206H in BMP-responsive-element luciferase (BRE-Luc) reporter HEK293 cells, this reporter responded with SMAD1/5 signaling to ActivinA, ActivinB, ActivinAB and ActvinAC ligands, whereas ALK2-WT showed no response. This observation was confirmed in human FOP iPSC derived Mesenchymal Stem Cells (iMSCs) under endogenous receptor expression conditions upon ActivinA treatment. ActivinA induced canonical SMAD2/3 signaling in both ALK2-WT and ALK2-R206H expressing cells to similar levels (Hatsell et al., 2015; Hino et al., 2015). In ALK2-WT cells ActivinA does not only induce SMAD2/3 signaling, it was also reported to inhibit BMP signaling by competing with BMPs for receptor binding in HEK cells and myeloma cells (Hatsell et al., 2015; Olsen et al., 2015).

Downstream responses of ActivinA/SMAD1/5 signaling induced expression of classical BMP target genes such as *ID1/2/3* only in FOP cells suggesting that ActivinA aberrantly transduced BMP signaling in FOP cells (Hino et al., 2015).

Binding of ALK2-WT to ActivinA in presence of type II receptors ACVR2A/B was already reported when ALK2 was initially described as an Activin receptor. But then ALK2 was categorized as a BMP type I receptors because of its inability to transduce any downstream SMAD signaling in response to ActivinA (see chapter 1.7.2) (Attisano et al., 1993; Macías-Silva et al., 1998; Tsuchida et al., 1993).

The binding of ALK2 to Activins was confirmed for several homo- and heterodimeric Activin ligands (ActivinA, ActivinB, ActivinAB, ActivinAC) in presence of ACVR2A or ACVR2B (Hatsell et al., 2015). This is in line with crosslinking studies, which showed that ALK2-WT and ALK2-R206H do not bind to ActivinA alone but only when ACVR2A or ACVR2B were co-expressed (Hino et al., 2015). Interestingly, in these conditions the binding affinity of ALK2-R206H to ActivinA was slightly higher compared to ALK2-WT. However, treatment of soluble ECD of ALK2 (ALK2-Fc), which is the same for ALK2-WT and ALK2-R206H did not alter the ActivinA/SMAD1/5 response, whereas treatment with ACVR2A-Fc and ACVR2B-Fc abrogated the Activin response (Hino et al., 2015).

The localization of FOP causing mutations in the intracellular domain of ALK2 already suggested that intracellular mediators such as FKBP12 are involved in the hyperactivated signaling responses of mutant ALK2 (see chapter 1.8.1). Whether the reduced binding of FKBP12 to ALK2-R206H contributes to Activin/SMAD1/5 signaling is under debate. Two studies have evaluated if WT cells may gain ActivinA/SMAD1/5 response if binding of FKBP12 is reduced by the FKBP12 inhibitor FK506. One study conferred an ActivinA/SMAD1/5 response in WT cells by FK506 treatment (Hino et al., 2015) whereas the other did not and excluded a contribution of FKBP12 to the mechanism of Activin/SMAD1/5 signaling (Hatsell et al., 2015). Of note, Hatsell and colleagues used lower FK506 concentrations, which may explain the different results compared to the aforementioned study.

Until now, the aberrant ActivinA induced SMAD1/5 signaling was confirmed for all FOP causing mutations in overexpression studies (Haupt et al., 2018).

However, the tissue and cell types which gain ActivinA/SMAD1/5 responsiveness endogenously as well as the source of ActivinA and its triggers for production remain poorly understood.

To proof whether the aberrant Activin/SMAD1/5 signaling of mutant ALK2 has a physiological relevance, a conditional FOP-ALK2-R206H mouse model was used. FOP mice developed HO within 4 weeks after tamoxifen induction, which could be prevented by treatment with BMP and Activin ligand blockers using ACVR2A-Fc and ACVR2B-Fc alone or in combination (Hatsell et al., 2015). This suggested, that HO is a ligand dependent process in FOP mice. To further discriminate the role of Activins and BMPs, a monoclonal Antibody against ActivinA was used. Whereas control mice developed HO, ActivinA antibody treatment the prevented HO formation as efficient as ACVR2A-Fc treated mice, indicating a central role of this ligand in the disease (Hatsell et al., 2015). A recent study confirmed the inhibition of injury-induced and spontaneous HO in ALK2-R206H mice by an ActivinA blocking antibody, which even provided long-term protection against spontaneous HO (Lees-Shepard et al., 2018). Moreover, ActivinA was required for HO driven by progenitor cells (FAPs) harboring the ALK2-R206H mutation when transplanted into murine muscle tissue. Isolated FAPs were responsive to BMP2 but only FOP FAPs responded with SMAD1/5 phosphorylation to ActivinA (Lees-Shepard et al., 2018). However, tissue specific downstream consequence of Activin/SMAD1/5 signaling remain poorly understood. Long-term ActivinA treatment to FOP iMSCs gave first insight that chondrogenic pathways were upregulated in the osteogenic progenitor cell type, which resulted in increased chondrogenesis *in vitro*. Moreover, transplantation of iMSCs in muscle tissue of conditional ActivinA mice only induced HO when ActivinA was expressed and FOP iMSCs were transplanted (Hino et al., 2015). But, the cell and tissue source of ActivinA and its triggers for production remains elusive. Interestingly, monocytes from FOP patient blood showed no ActivinA/SMAD1/5 response (Barruet et al., 2018).

This suggests that not all mutant ALK2 expressing cells respond with aberrant SMAD1/5 signaling to Activins. In fact, Activin induced SMAD1/5 signaling was also observed in ALK2 WT cells, such as myeloma cells and hepatocytes (Besson-Fournier et al., 2012; Canali et al., 2016; Olsen et al., 2018) and in immortalized mouse embryonic fibroblasts (iMEFs) under ectopic ALK2 WT expression (Haupt et al., 2018). In general, the tissue and cell type specific responses of Activins and the underlying mechanism of SMAD1/5 signaling by Activins remain poorly understood. But current evidence suggests that the ALK2 receptor is an important component of the signaling complex (Canali et al., 2016; Hatsell et al., 2015; Hino et al., 2015; Olsen et al., 2020, 2018).

1.9 BMP receptor mutations in other human diseases

Based on the pleiotropic effects of BMPs from embryonic development to adult tissue homeostasis, genetic defects in signaling components lead to severe human disorders (Wang et al., 2014).

Even though clinical symptoms occur in different tissue types the diseases share basic mechanisms, which disrupt fine-tuned steps within the signaling cascade and the crosstalk to other pathways. In the following, disease causing mutations in BMP receptors and co-receptors which are associated with cardiovascular, musculoskeletal diseases and various types of cancer will be briefly mentioned. Mutations in ALK1, Endoglin, BMPR2, ALK6, SMAD4 or BMP9 cause the rare autosomal dominant vascular disease **Hereditary Hemorrhagic Telangiectasia** (**HHT**), which is characterized by mucocutaneous telangiectases and arteriovenous malformations in the gastrointestinal tract, liver, lung and brain. A common symptom are nose bleeds (Gomez-Puerto et al., 2019). **Pulmonary Arterial Hypertension** (**PAH**) is a chronic disease of increased pulmonary arterial pressure leading to life threatening right heart failure with shortness of breath. More than 70% of patients with familial PAH and 20% of patients with idiopathic PAH have heterozygous mutations that impair BMPR2 function. Moreover, mutations in BMP9, ALK1, Endoglin and SMAD8 are also associated with PAH (Gomez-Puerto et al., 2019).

Defects in ALK2 mediated signaling by mutations in the *ALK2* gene or impaired expression are responsible for **cardiac defects** (Joziasse et al., 2011; Smith et al., 2009; Thomas et al., 2012) and mutations in *ACVR2B* are associated with heart malformations in humans (Kosaki et al., 1999).

In addition to aforementioned genetic diseases, are other vascular diseases associated with aberrant expression of BMP receptors such as **atherosclerosis**, **anemia** and **vascular calcification** (Gomez-Puerto et al., 2019). In addition to FOP other genetic bone diseases have been associated with mutated BMP receptors. For example **Acromesomelic dysplasia**, a form of dwarfism affecting the bones of forearms, lower legs as well as hands and feet show mutations in ALK6 (Stange et al., 2015). Mutations in ALK6 also lead to the rare skeletal condition called **Brachydactyly type B** which is characterized by incomplete or absence of the outermost bones of fingers and toes (distal phalanges) (Racacho et al., 2015).

Moreover, the progression and poor diagnosis of specific **cancers** correlates with aberrant expression of BMP receptors and some genetic mutations in BMP receptors

are directly associated with some cancer disorders. The severe pediatric brain cancer **Diffuse Intrinsic Pontine Glioma** (**DIPG**) is connected to mutations in histone3 variants in the majority of patients and interestingly about 25% of the patients additionally have ALK2 activating mutations (Hoeman et al., 2019). Mutations in ACVR2B and ALK6 are associated with pancreatic cancer and BMPR2 and ACVR2 mutations were described in colon cancers. But also indirect contribution of BMP and TGFβ receptors to cancer progression has also been described for **tumor angiogenesis** and tumor microenvironment (Pickup et al., 2017; Ye and Jiang, 2016). In sum, this highlights the pleiotropic functions of BMP signaling in a variety of physiological processes of various tissues. And ultimately strengthens the essential mechanisms of fine-tuning pathway activation crosstalk on different levels. Any imbalance in ligand availability, co-receptor activity and/or expression lacking compensation often impairs cellular functions and cause secondary defects, which results in severe diseases.

1.10 Inhibition of BMP pathway components by pharmacological agents

Based on the aforementioned pleiotropic physiological effects of BMPs in different tissues and organs the targeting of pathological signaling defects should be achieved as specific as possible to avoid undesirable side effects.

During the last decades several potential agents have been developed to target different levels in the BMP signaling cascades. Those therapeutic agents include molecules that interfere with ligand availability (natural soluble antagonists, specific antibodies and ECD ligand traps), inhibitors of BMP receptor expression (siRNAs, anti-sense oligonucleotides), molecules that prevent BMP receptor activation (kinase inhibitors, antibodies) and intracellular SMAD inhibitors (Sánchez-Duffhues et al., 2020). In the following I will focus on small molecules that inhibit BMP receptor kinase activation.

The last two decades protein kinases have been an important class of drug target in pharmaceutical and academic research and several kinase inhibitors have been approved especially as drugs for cancer diseases. The structural similarity of the ATP-binding pocket in the over 500 human protein kinases has been considered a major challenge (Cohen and Alessi, 2013).

In recent years, several BMP type I receptor kinase inhibitors have been developed, which are useful tools in research but also offer great potential in clinical application as therapies for receptor associated diseases. Most of the type I receptor inhibitors interact with the ATP catalytic binding pocket from the kinase domain. The first potent BMP type I receptor kinase inhibitor **Dorsomorphin** was discovered in a screen that interfered with BMP regulated dorsoventral axis formation in zebrafish development (Yu et al., 2008b). However, dorsomorphin required high concentrations and showed off-target effects to VEGFR kinases, which led to the development of other kinases inhibitors based on the (pyrazolo-[1,5-a]pyrimidine) backbone of Dorsomorphin, such as **LDN-193189** and **DMH1** (Yadin et al., 2016). LDN-193189 was the first kinase inhibitor used in context of FOP, which achieved a reduction of HO in ALK2-Q207D mice (Yu et al., 2008a). However, LDN also targets the VEGFR kinases and inhibits all BMP type I receptors whereas DMH1 shows more specificity to ALK2 but less potency. Thus, efforts have been made to develop compounds with a similar efficacy than LDN-193189 but greater specificity to single type I receptors, especially ALK2 (Yadin et al., 2016). In an *in vitro* kinase compound library screen **K02288** was discovered with preferential inhibition of ALK1 (IC_{50} = 1.8 nM) and ALK2 (IC_{50} = 1,1 nM) compared to ALK3 (IC_{50} = 34.4 nM) (Sanvitale et al., 2013). Structural comparison of the ALK2 kinase in complex with LDN-193189 or K02288 revealed additional contacts with peripheral residues in the proximity of the ATP binding site for the K02288 complex (Sanvitale et al., 2013). Based on the 2-aminopyridine compound K02288 Mohedas *et al.* developed related compounds with increases potency and selectivity for ALK2. Especially the derivate **LDN-212854** showed increased selectivity for BMP type I receptors compared to TGFβ type I receptors and exhibits *in vitro* selectivity for ALK1 (IC_{50} = 2.4 nM) and ALK2 (IC_{50} = 1.3 nM) compared to ALK3 (IC_{50} = 85.8 nM) with slight a preference for ALK2. Moreover, LDN-212854 was as potent as LDN-193189 to inhibit HO in the majority of ALK2-Q207D mice (Mohedas et al., 2013).

Interestingly, several molecules originally developed for other purposes were discovered to also interfere with BMP receptor activity. For example, **Saracatinib** (AZD0530), which was originally developed as an anti-tumor drug targeting the tyrosine kinases of the SRC family and ABL tyrosine kinases (Hennequin et al., 2006). In 2013, Saracatinib treatment of colon cancer cells showed additional inhibitory effects on SMAD1/5 phosphorylation and *ID1* expression, which were independent of SRC (Lewis and Prywes, 2013). Saracatinib as a BMP type I receptor inhibitor was

confirmed in an *in vitro* kinase assay (ALK1 (IC_{50} = 3.2 nM), ALK2 (IC_{50} = 17.4 nM), ALK3 (IC_{50} = 30.7 nM), ALK6 (IC_{50} = 295 nM), ALK5 (IC_{50} = 665 nM), ALK4 (IC_{50} = 816 nM)) (Lewis and Prywes, 2013). Three years later, Saracatinib has first been shown to also effectively prevent HO in FOP mouse models, which was published as a patent (Yu et al., 2016). In 2018, the inhibitory effect on HO in FOP mice was confirmed by a another study in (Hino et al., 2018). Interestingly, Saracatinib was well tolerated in mice whereas treatment with LDN-193189 or LDN-212854 was associated with weight loss up to 25% relative to vehicle controls (Yu et al., 2016).

Weight loss effects may not be of importance for mechanistic investigational studies *in vitro*, which primarily are interested in targeting specific receptor by specific inhibitors. However*, in vitro* and *in vivo* animal studies and clinical investigations, which aim to develop treatment strategies for human diseases rely on save drugs with low off target effects on systemic physiological mechanisms.

1.11 BMP signaling in the endothelium

The endothelium can be considered as the fundamental building block of the vascular system, which ensures oxygen, nutrition supply of all organs. ECs line the inner wall of blood vessels and form a dynamic barrier between circulating blood and tissue. Controlled blood vessel formation and function is crucial in embryonic development and adult tissue homeostasis (see chapter 1.2), which requires the orchestration of multiple signaling cascades, including vascular endothelial growth factor (VEGF), NOTCH, fibroblast growth factor (FGF), TGFβ and BMP pathways. Increasing evidence suggests that VEGF and NOTCH regulate sprouting angiogenesis and vascular patterning collectively with BMP signaling (Bautch, 2019; Beets et al., 2013; Jin et al., 2014). Genetic defects in BMP signaling components lead to human disorders (see chapter 1.9) including cardiovascular diseases.

Moreover, aberrations in vasculature function are interlinked to pathological conditions such as cancer, chronic inflammation (Chung et al., 2010) and was recently also connected to HO (Cocks et al., 2017). Thus, balanced BMP signaling is required for the maintenance of healthy vasculature.

Genetic deletion of BMP pathway components in animal models highlight the role of BMP signaling in vascular development. Deletion of *Smad1* and *Smad5* in mice causes embryonic lethality due to defects in vascular development, characterized by enlarged blood vessels and decreased number of smooth muscle cells (Goumans and Mummery, 2000; Tremblay et al., 2001)

Moreover, deficiency of single BMP ligands or receptors often lead to embryonic lethality before the formation of the vasculature or causes vascular malformations in the developing embryo (Pardali et al., 2010). For example, mice deficient in *Bmp2* (Zhang and Bradley, 1996), *Bmp4* (Winnier et al., 1995) as well as deficiency in *Alk2* (Gu et al., 1999; Mishina et al., 1999) or *Alk3* (Mishina et al., 1995) cause lethality immediately after gastrulation before the onset of cardiovascular morphogenesis. *Alk1* deficient mice die at midgestation and have severe vascular abnormalities and leaky vessels (Oh et al., 2000). Interestingly, the lack of *Alk5, Tgfbr2* and *Endoglin* have very similar phenotypes to *Alk1* deficient mice, which also highlight the importance of TGFβ signaling in the vascular system (Goumans et al., 2009).

Moreover, BMP6 and BMP7 are required for cushion formation and septation in the developing mouse heart (Kim et al., 2001). In line with this, *Alk2* as the corresponding type I receptor was reported to mediate atrioventricular cushion transformation in the

developing mouse heart (Wang et al., 2005) and deficient Alk2 signaling caused defects in aortic valve development (Thomas et al., 2012). The endocardial cushion is a subset of cells in the developing heart tube, which originates from ECs transdifferentiating to mesenchymal cells in a process called endothelial to mesenchymal transition (EndMT) (Kinsella and Fitzharris, 1980). EndMT is also a common observation in adult BMP associated vascular pathologies such as atherosclerosis, vessel calcification and PAH (Evrard et al., 2016; Hiepen et al., 2019; Sánchez-Duffhues et al., 2019a).

Many of the same pathways and mechanisms that regulate vascular development are reactivated in response to injury and vascular pathologies, which highlights the role of BMP signaling in vascular homeostasis and disease in adults.

1.11.1 Blood vessel formation by Sprouting Angiogenesis

The main mechanism underlying new blood vessel formation in adult tissue growth, regeneration and pathologies is sprouting angiogenesis by ECs.

Angiogenesis is defined as new blood vessel formation from pre-existing vessels. Endothelial sprouting is initiated by signals from the tissue environment such as growth factors, hypoxia or mechanical cues (Hofmann and Heineke, 2018). In sprouting angiogenesis ECs become activated by angiogenic factors, such as VEGF. ECs dynamically shuffle between tip and stalk cell competence at the leading edge of vessel sprouts. The **tip cell** is located at the distal end of each sprout and is characterized by a migratory and polarized phenotype. **Stalk cells** proliferate and facilitate sprout elongation and stability (Figure 1.17) (Chen et al., 2019). Together with mural cells ECs and mural cells undergo a complex multistage process, which was first described in 1977 by Ausprunk and Folkman (Ausprunk and Folkman, 1977) (Figure 1.17) (**1**) First the basement membrane is locally degraded by matrix metalloproteinases (MMPs). (**2**) The loosening of cell-cell junctional contacts of the endothelial barrier cooperates with the (**3**) dynamic selection of a filopodia forming EC (tip cell), which starts to migrate. (**4**) The surrounding ECM is remodeled via proteolytic enzymes to develop a angiogenic substratum, on which selected tip cells anchor and are subsequently pulled by contraction of actin filaments along angiogenic stimuli. (**5**) Endothelial stalk cells follow behind the tip cell causing sprout elongation and simultaneously a lumen is formed within a series of stalk cells, which allows perfusion with blood. (**6**) The sprout increases in size and new tip cells start branching (**7**) Eventually, the new formed blood vessel network undergoes maturation by

remodeling, which involves the recruitment of pericytes and mural cells, ECM deposition, shear stress and other mechanical signals. These processes requires a number of different cellular function including migration, proliferation, cell junctional remodeling and specialization, which is coordinated and controlled by multiple signaling cascades (Adair and Montani, 2010; Gerhardt, 2008; Ribatti and Crivellato, 2012).

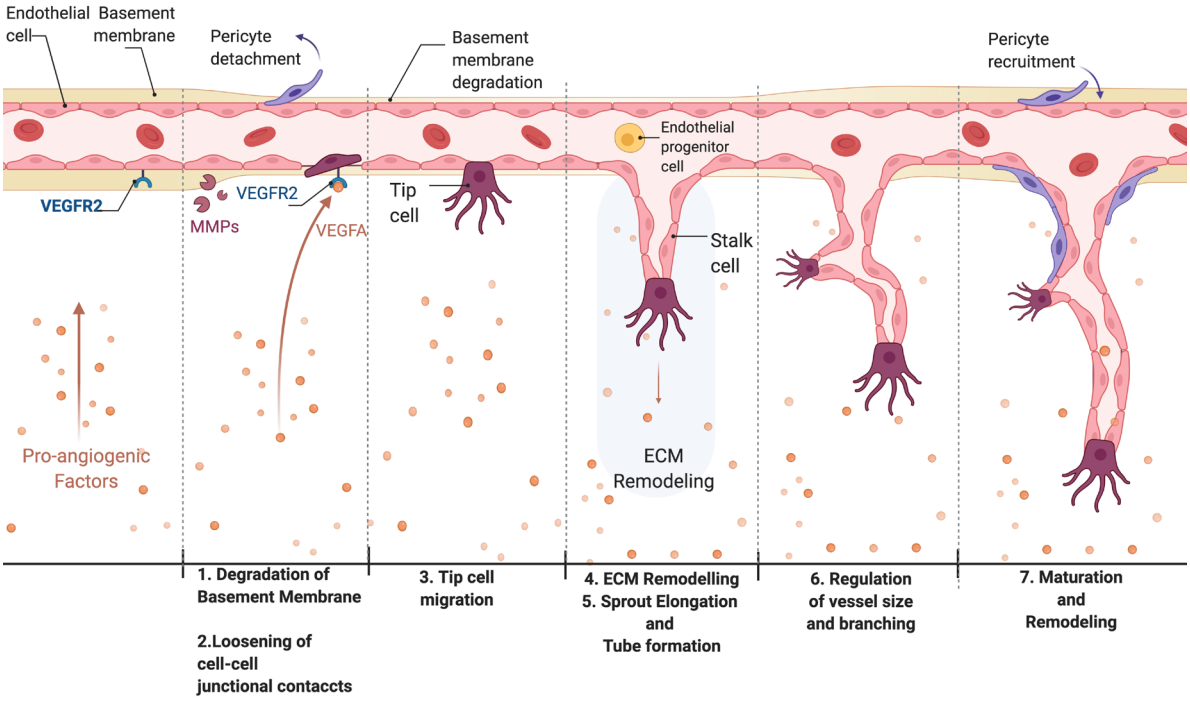

Figure 1.17 Sprouting Angiogenesis. Proangiogenic factors such as VEGFA induce Sprouting Angiogenesis (SA). (**1-2**) SA is initiated by the degradation of the basement membrane and the loosening of cell-cell junctional contacts. (**3**) Tip cell markers become upregulated and the tip cell starts to migrate out of the endothelial barrier. (**4**) The surrounding ECM becomes remodeled via proteolytic enzymes to develop an angiogenic substratum, which favors (**5**) cell proliferation and thus sprout elongation and tube formation. (**6**) The sprout increases in size and new tip cells start branching. (**7**) New formed blood vessel network undergoes maturation by remodeling, which involves the recruitment of pericytes and mural cells, ECM deposition, shear stress and other mechanical signals. Adapted from „Tumor Vascularization" by BioRender.com (2020). Retrieved from app.biorender.com/biorender-templates.

1.11.2 VEGF and NOTCH signaling regulate endothelial patterning in blood vessel formation

VEGF Signaling

VEGF signaling can be considered as the most studied pathway in regulating vasculogenesis and angiogenesis during development, physiological homeostasis and disease (Apte et al., 2019). VEGF signaling comprises a family of ligands (VEGF-B, VEGF-C, VEGF-D, VEGF-E) and three tyrosine receptor kinases **VEGFR1** (FLT1), **VEGFR2 (KDR)** and VEGFR3. As for BMP ligands, VEGF ligands also show different binding preferences to their receptors. **VEGFA** signals via VEGFR1 and VEGFR2 whereas VEGFC and VEGFD preferentially bind to VEGFR3 and are primarily involved in lymphangiogenesis (Alitalo et al., 2005). VEGFR1 and VEGFR2 are predominately expressed in ECs and are used as EC markers. However, even though VEGFR1 (de Vries et al., 1992) is the high affinity receptor, the lower affinity VEGFR2 is the main signaling receptor in ECs (Terman et al., 1992). An alternative splice isoform of VEGFR1 is a soluble form, which functions as a decoy receptor and binds to VEGFA with high affinity (Koch and Claesson-Welsh, 2012).

VEGFA undergoes alternative exon splicing that produces several isoforms including VEGF121, VEGF165, VEGF189, and VEGF206. The isoforms can be distinguished by absence or presence of 1-2 heparin-binding domains, which determine ligand availability and ECM interactions (Koch and Claesson-Welsh, 2012).

Moreover, only the isoform VEGF165 binds to the co-receptor Neuropillin 1 (NRP1), which promotes VEGFR2 signaling (Robinson and Stringer, 2001). VEGF165 (in the following be referred as VEGFA) is abundantly expressed in most tissues and the physiological relevant isoform regulating angiogenesis and disease (Apte et al., 2019). The downstream signaling responses of VEGF includes the activation of several kinases including PI3K, AKT, MAPK p38 and the activation of SRC and small GTPases like RhoA (Koch and Claesson-Welsh, 2012).

VEGFA is a very potent angiogenic factor and signaling via VEGFR1/2 regulates the multistage process of **sprouting angiogenesis** which comprises of cell proliferation, migration, survival and **vascular permeability** (Apte et al., 2019). VEGFA induces the activation of the endothelium including the cell-cell junctional disintegration leading to permeability of the EC barrier. **VE-Cadherin** is a single-span transmembrane protein, which forms homomeric dimers with VE-cadherin molecules of adjacent cells and is a

main component of endothelial adherens junctions (Lampugnani et al., 1995). Via the cytoplasmic domain VE-Cadherin interacts with members of the actin-binding catenin family and is thereby linked to the cytoskeleton (Iyer et al., 2004; Lampugnani et al., 1995). The VEGFA mediated phosphorylation of VEGFR2 enables activation of the tyrosine kinase **SRC** via recruitment of the SRC binding T cell-specific adaptor (Sun et al., 2012). The tyrosine kinase SRC phosphorylates VE-Cadherin at a specific residue (Y685) (Wallez et al., 2007; Wessel et al., 2014), which triggers VE-Cadherin internalization and typically disrupts the interaction of VE-Cadherin to catenins and consequently causes permeability and reduction in endothelial barrier integrity (Gavard and Gutkind, 2006) (Figure 1.18). Besides VEGFA other permeability inducing factors, such as TNFα (Angelini et al., 2006), histamin (Andriopoulou et al., 1999) lead to barrier disintegration. Upon local disintegration of endothelial junctions ECs loose their integrity and are stimulated for migration and proliferation by proangiogenic gradients. VEGFA induces tip cell selection and filopodia formation, which includes the upregulation of the tip cell marker DLL4. The transmembrane NOTCH ligand DLL4 activates Notch signaling in neighboring cells and thereby facilitates stalk cell identity (Lobov et al., 2007) (Figure 1.18).

NOTCH signaling

NOTCH signaling is a highly conserved pathway, which mediated cell contact dependent signaling between neighboring cells (Zhang et al., 2014). In the vasculature NOTCH signaling is essential and regulates multiple processes ranging from **sprouting angiogenesis**, force transmission and **arterial differentiation** to quiescence (Mack and Iruela-Arispe, 2018).

NOTCH ligands (DLL1-4, JAG1-2) and receptors (NOTCH 1-2) are transmembrane proteins, which trigger sequential NOTCH receptor cleavage by the proteases ADAM17 and γ-secretase upon mechano-sensitive ligand-receptor interaction. In fact, force generation is required for NOTCH receptor cleavage, which releases a NOTCH intracellular domain (NICD) polypeptide from the membrane to the cytoplasm. Molecular force measurements revealed the force requirements for NOTCH activation (Chowdhury et al., 2016; Kovall et al., 2017). Translocation of NICD to the nucleus facilitates binding to the transcription factor recombination signal-binding protein-J kappa (RBPJ), which activates the expression of specific **NOTCH target genes** (Kovall et al., 2017). Such as the **HES** (Hairy and enhancer of split) family transcription factors

HES1 and the related but distinct **HEY** (Hes-related repressor protein) family including HEY1, HEY2 and HEYL (Borggrefe and Oswald, 2009; Iso et al., 2003).
HEY and HEY proteins belong to the helix-loop-helix transcription factors that mediate transcriptional repression (Iso et al., 2003).
In the angiogenic vasculature, the transmembrane ligand **DLL4** is upregulated by VEGFA in endothelial tip cells and activates NOTCH signaling in adjacent stalk cells (Benedito et al., 2009; Hellström et al., 2007) (Figure 1.18). HEY1 levels in cells with active NOTCH signaling (stalk cells) **downregulate *VEGFR2*** expression (Henderson et al., 2001), whereas the **VEGFA decoy receptor *VEGFR1*** becomes **upregulated** (Kappas et al., 2008) (Figure 1.18).
Thus, DLL4 induced NOTCH signaling in stalk cells locally reduces or **restricts VEGFA responsiveness in ECs** (Phng and Gerhardt, 2009). However, simultaneously NOTCH signaling induces the gene expression of another notch ligand, named **JAG1**, which is strongly expressed in stalk cells (Hofmann and Iruela-Arispe, 2007) (Figure 1.18). JAG1, is in contrast to DLL4 proangiogenic and antagonizes DLL4-NOTCH signaling through NOTCH1, which **sustains VEGFR2 expression** (Benedito et al., 2009; Pedrosa et al., 2015)
Thus, ECs with high JAG1 levels inhibit DLL4-NOTCH signaling in adjacent tip cells but also stalk cells and thereby maintain their VEGF responsiveness, which promotes proliferation and dynamic tip cell selection (Benedito et al., 2009).
In sum, collective regulation of VEGF and NOTCH signaling dynamically regulates tip and stalk cell identity, which is permanently shuffled during sprouting angiogenesis (Benedito et al., 2009; Blanco and Gerhardt, 2013; Jakobsson et al., 2010) (Figure 1.17 and Figure 1.18).

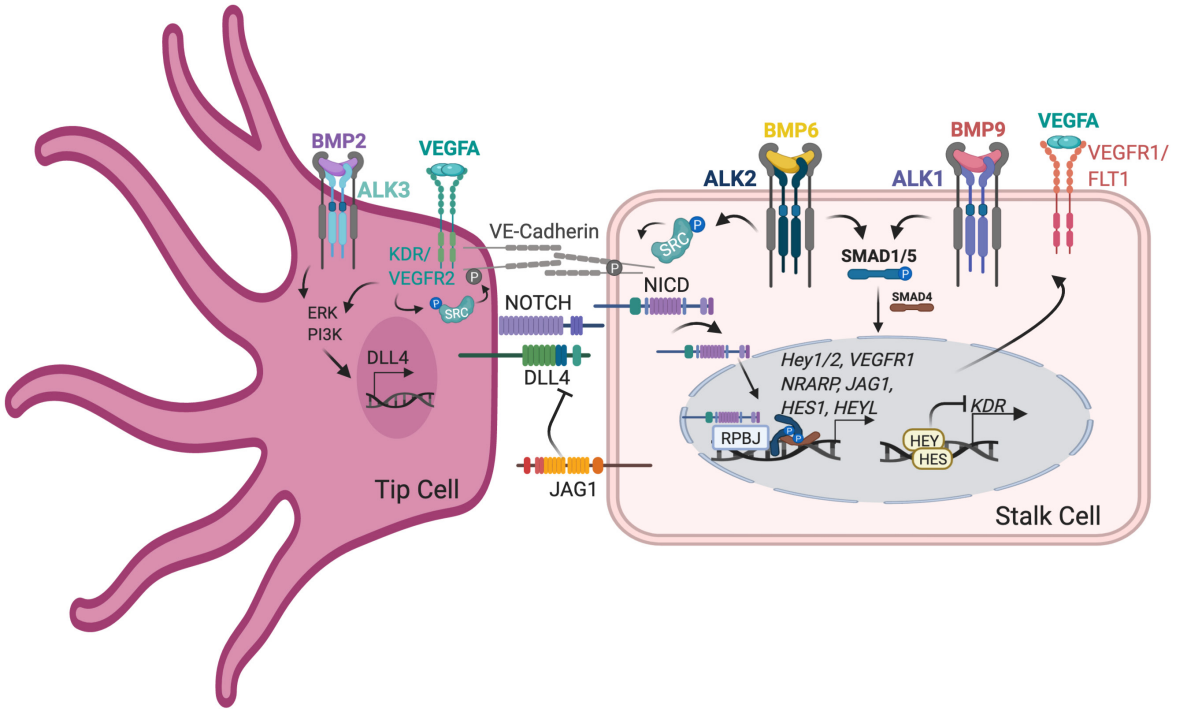

Figure 1.18 Tip and Stalk cell competence in sprouting Angiogenesis. In Sprouting Angiogenesis VEGFA binds to VEGFR2 and activates PI3K and ERK signaling, which leads to the upregulation of *DLL4.* DLL4 binds NOTCH receptors of neighboring stalk cells, which triggers the release of the NOTCH intracellular domain (NICD) upon sequential cleavage. In conjunction which co-factors NICD induces the expression of NOTCH target genes such as *HEY* and *HES* transcription factors and the *VEGFR1*. HES and HEY transcription factors inhibit the transcription of VEGFR2, which limits the responsiveness to VEGFA. Moreover, VEGFA induces SRC-dependent phosphorylation of the junctional protein VE-Cadherin leading to destabilization and internalization. In a similar manner does BMP6 activate via ALK2 SRC-dependent phosphorylation of VE-Cadherin. In addition, BMP2 induces DLL4 expression in tip cells via p38 and BMP induced SMAD1/5 signaling induces stalk cell specification synergistically with NOTCH.

1.11.3 BMP signaling as an additional orchestrator in blood vessel formation

Previous mentioned genetic studies from mice and humans have already highlighted the crucial role of BMP signaling in physiological and pathophysiological cardiovascular function. In 2002 the first study demonstrated the mechanistic effects of BMPs on cultured ECs and showed the activation of endothelial SMAD1/5 signaling (Valdimarsdottir et al., 2002). Induction of endothelial migration and tube formation by BMP pathway activation via BMP6 stimulation and overexpression of constitutive active ALK2, ALK3 or ALK6 introduced BMPs as proangiogenic factors (Valdimarsdottir et al., 2002). At that time BMPs were mainly studied in the context of bone and interestingly the authors commented that BMPs may not only induce bone formation but also angiogenesis in endochondral ossification (Valdimarsdottir et al., 2002). Moreover, the initial study of endothelial BMP signaling already revealed that the expression of BMP receptors (ALK2, ALK3, ALK6 and BMPR2) and

phosphorylated SMAD1/5 is very heterogenous in the endothelium of blood vessels among diverse tissues (Valdimarsdottir et al., 2002).

ALK1 is an endothelial BMP receptor

Among the BMP type I receptors, ALK1 shows a remarkable vascular specific expression profile (S. Paul Oh et al., 2000; Roman and Hinck, 2017) and is implicated in arterial differentiation (Somekawa et al., 2012). Originally, ALK1 was first described in modulating TGFβ signaling via ALK5/TGFBR2 or ALK1/TGFBR2 in angiogenesis (S. Paul Oh et al., 2000). TGFβ mediated signaling via ALK1 and ALK5 was mechanistically elucidated and termed **lateral signaling**. Here, ALK5 becomes recruited and phosphorylated by TGFBR2 bound to TGFβ, which enables the lateral phosphorylation of ALK1 by ALK5 (Goumans et al., 2003). Later BMP9 and BMP10 were identified as the main signaling ligands of ALK1 and shown to maintain endothelial homeostasis, quiescence and to counteract angiogenesis (David et al., 2008, 2007; Scharpfenecker et al., 2007). In addition, BMP9/BMP10 ALK1 signaling was also reported to have proangiogenic effect on ECs (Suzuki et al., 2010) and application of an anti-ALK1 or anti-BMP9 antibody inhibited angiogenic sprouting of HUVEC-coated beads in a fibrin gel in full medium conditions (van Meeteren et al., 2012). ALK1 signaling synergizes with NOTCH to induce **NOTCH** and **stalk cell related genes** in sprouting angiogenesis (Kerr et al., 2015; Larrivée et al., 2012) (Figure 1.18). A recent study demonstrated BMP9 induced sprouting angiogenesis of human ESC derived ECs via ALK1/SMAD1/5 signaling leading to the upregulation of EGFL7, a mediator of NOTCH and ECM remodeling (Richter et al., 2019).

In line with the *in vitro* data, blocking of BMP9 and BMP10 signaling in young mice reduced vascular expansion but increased vascular density in the retina, which highlights the role of BMP9/BMP10 ALK1 signaling in postnatal blood vessel remodeling (Ricard et al., 2012).

Whereas *in vivo* data clearly suggest important functions for BMP9, BMP10-ALK1 signaling in vascular development and postnatal vascular remodeling, the cellular roles based on *in vitro* studies in ECs are not completely understood. Concentrations dependent and vascular bed specific effects were suggested to contribute to pro- and anti-angiogenic effects of endothelial BMP9/BMP10-ALK1 signaling (García de Vinuesa et al., 2016). Moreover, a very recent study highlights the importance to

analyze BMP9 and BMP10-ALK1 signaling in their prodomain forms, which is the predominant form of circulating BMP9 BMP10 ligands *in vivo* (Salmon et al., 2020).

ALK2, ALK3 and ALK6 fine tune endothelial function

In contrast to BMP9/BMP10, the ligands BMP2/BMP4 and BMP6/BMP7 signal primarily via ALK3 ALK6 and ALK2, which show a more heterogeneous expression in diverse vascular beds compared to ubiquitous endothelial ALK1 expression. For example ALK3 expression is low in venous ECs (HUVECs), intermediate in aortic ECs (HAECs) and high in microvascular ECs (HPMECs) whereas ALK1 and interestingly also ALK2 was present at similar levels in all three EC types (Benn et al., 2017).

In line with the ALK2 expression profile, **BMP6** activated SMAD1/5 signaling in ECs derived from human aortic, venous and microvascular beds (Benn et al., 2017).

Moreover, SMAD1/5 dependent signaling by BMP6 was shown to induce stalk cell genes in venous ECs (Benn et al., 2017) (Figure 1.18). This is in line with observations in a functional HUVEC sprouting assay where BMP6 increased pSMAD1/5 levels in stalk cells but only minorly in tip cells, which already had high pSMAD1/5 levels in untreated conditions (Mouillesseaux et al., 2016).

Endothelial specific inactivation of *Smad1/5* in mouse embryos increased the numbers of tip cells at the expense of stalk cells (Moya et al., 2012). In fact, BMP induced SMAD1/5 signaling synergizes with activated NOTCH to induce stalk cell genes (Larrivée et al., 2012; Moya et al., 2012) (Figure 1.18). Moreover, BMP and NOTCH regulate selected target genes even cooporately via complex formation of pSMAD1/5 with the NOTCH downstream effector NICD (NOTCH Intracellular Domain) (Itoh et al., 2004).

Several studies report BMP6/SMAD signaling as pro-angiogenic and show BMP6 induced tube formation, migration and sprouting in ECs derived from venous, arterial and microvascular beds (Benn et al., 2017; Ren et al., 2007; Valdimarsdottir Gudrun et al., 2002). In line with this, the overall BMP6 induced lateral branching was reduced upon knockdown of SMAD1/5 (Mouillesseaux et al., 2016).

BMP7 from the same ligand group was also described to induce tube formation in HUVECs (Akiyama et al., 2014) and angiogenesis in the chorioallantoic membrane of chick eggs (Ramoshebi and Ripamonti, 2000). *Bmp6* and *Bmp7* expression is enriched in murine postnatal retinal angiogenesis and retinal vessels of BMP responsive

elements (BRE)-GFP mice, showed broad GFP detection within the vascular front in tip as well as stalk cells (Lee et al., 2017).

BMP2 and **BMP4** were reported to induce pro-angiogenic effects *in vitro* as well as *in vivo*, such as migration and tube formation in human aortic ECs and HUVECs (García de Vinuesa et al., 2016; Langenfeld and Langenfeld, 2004). Pro-angiogenic effects of BMP2 have been described to be mediated by SMAD1/5 signaling as well as via non-Smad dependent mechanisms through p38, ERK or Cdc42 activation (Benn et al., 2017; Wakayama et al., 2015; Wiley et al., 2011). BMP2 upregulated tip cell associated genes (*DLL4, VEGFR2*) and induces migration via an p38 dependent mechanism in venous ECs (Benn et al., 2017) (Figure 1.18).

Bmp2 and *Bmp4* and *Alk3* were highly expressed in the developing vein and Alk3 signaling was suggested to mediate venous identity via Smad1/5 dependent induction of the venous markers Ephb4 and Coup-TFII in murine and zebrafish vascular development (Neal et al., 2019). Interestingly, BMP-SMAD dependent promotor activity is active in arterial and venous ECs in BRE reporter mice, indicating that type I receptor signaling fine tune arteriovenous differentiation (Moya et al., 2012).

As described in chapter 1.2.1 BMP4 is a prominent player in mesoderm formation and subsequent differentiation of vascular progenitors and thus an inducer of vasculogenesis even upstream of VEGFA, reviewed in (Benn et al., 2017). Postnatally, BMP4 induces angiogenesis, e.g. in microvascular ECs (Rothhammer et al., 2007) and in HUVECs via ERK1/2 dependent and SMAD4 independent mechanisms (Zhou et al., 2007). The essential role for **ALK2** and **ALK3** in angiogenesis was recently elucidated by endothelial specific deletion of *Alk2* and *Alk3*, which demonstrated a substantial reduction in vessel expansion and density in mouse retinas. These vascular characteristics were in line with phenotypic observations in endothelial-specific *Bmpr2* depleted endothelium (Lee et al., 2017). In contrast, retinal ECs deficient of *Alk1* showed no change in vessel expansion but increased vascular density (Lee et al., 2017). Interestingly, Bmpr2, Alk1 and Alk3 were specifically enriched in the vascular front whereas Alk2 was absent. This is in line with the observation that only depletion of *Bmpr2* and *Alk3* resulted in reduced number of sprouts. However, *Alk2* depletion caused a significant reduction in vascularized area, suggesting a role in mediating vascular branching behind the vascular front (Lee et al., 2017).

In fact, **ALK2** was shown to control **barrier destabilization** by cell-cell junctional disintegration in human venous ECs (HUVECs) (Benn et al., 2016), an initial step in

sprouting angiogenesis and branching. Mechanistically, in an ALK2 dependent manner BMP6 induced similar to VEGFA a SRC-dependent phosphorylation (Thr416) and subsequent internalization of VE-Cadherin (Benn et al., 2016) (Figure 1.18). In the same cell type (HUVECs) ALK2 knockdown resulted in hypersprouting and a significant increase in tip cell number, whereas ALK3 depletion inhibited sprouting angiogenesis (Benn et al., 2017). This is in line with the previous study in mice, showing that *Alk3* depleted ECs form reduced sprouts in postnatal retinal angiogenesis (Lee et al., 2017). Observations for endothelial *Alk2* depletion in mice show no significant change in sprout number but substantial reduction in vascular area and density (Lee et al., 2017), thereby contrasting the hypersprouting *in vitro* data in human ECs (Benn et al., 2017).

Collectively, increasing evidence demonstrates that BMP signaling has essential functions in endothelial homeostasis and angiogenesis by regulating downstream components collectively with VEGF and NOTCH.

Endothelial signaling of BMP2/4/6/7 via ALK2 and ALK3 were mostly reported to direct pro-angiogenic proliferation, sprouting and migration whereas the ALK1 ligands BMP9 and BMP10 are known homeostatic factors. However, concentration and vascular bed dependent effects underlying different BMP receptor expression profiles suggests that **BMPs context dependently function as pro**- as well as **anti-angiogenic factors**.

1.11.4 Endothelial to mesenchymal transition (EndMT)

EndMT was originally described in **embryonic heart development** in which endocardial cushion tissue originates from transdifferentiating ECs to mesenchymal cells. EndMT is essential for the formation of the anatomical heart structures, such as the ventricular septum, which separates the two lower chambers (ventricles) of the heart from each other (Eisenberg and Markwald, 1995; Kinsella and Fitzharris, 1980). In recent years, EndMT was reported as a frequent mechanism in **pathological conditions** in human vascular, malignant, inflammatory and fibrotic diseases (Piera-Velazquez and Jimenez, 2019). The mechanisms of the **transdifferentiation** of ECs to mesenchymal cells in EndMT is complex and not completely understood involving multiple cellular processes. ECs lose their markers (VE-Cadherin, VEGFR, PECAM1), cell-cell junctional integrity and acquire a mesenchymal spindle-shaped migratory phenotype, including expression of N-Cadherin, fibronectin and fibroblast-specific protein 1 (FSP-1) (Piera-Velazquez and Jimenez, 2019). These phenotypic changes are orchestrated by several signaling pathways. **TGFβ** is considered as the main

EndMT inducer but also the contribution of **BMP, WNT, FGF, TNFα, NOTCH** pathways as well as mechanical and hypoxic triggers have been described. These pathways commonly induce similar EndMT associated transcription factors such as **SNAIL, SLUG**, **TWIST** and **MSX2** which repress cadherins (Benn et al., 2017; Chen et al., 2008; Gong et al., 2017; Piera-Velazquez and Jimenez, 2019; Sánchez-Duffhues et al., 2018; Weinstein et al., 2020). In fact, SMAD1/5/8 were shown to directly bind to the SLUG promoter via Chromatin Immunoprecipitation Sequencing (ChiP-Seq) (Richter et al., 2014). Furthermore, SMAD4 as a mediator of TGFβ and BMP signaling was found to be essential in EndMT as *Smad4* deficiency in mice prevents EndMT of endorcardial cells in valve development (Moskowitz et al., 2011; Yoshimatsu and Watabe, 2011). Several studies show the contribution of EndMT to the initiation and progression of **cardiovascular diseases**, such as vascular calcification in atherosclerosis, PAH (Pulmonary arterial hypertension), organ fibrosis and report the contribution of BMP signaling (Sánchez-Duffhues et al., 2018). For example human biopsies of advanced atherosclerotic lesions show high levels of phosphorylated SMAD1 and SLUG (Sánchez-Duffhues et al., 2015). Although BMP signaling is generally known to induce EndMT, it also has a protective function to maintain endothelial homeostasis and identity. For example ALK1 can antagonize TGFβ/ALK5 SMAD2/3 signaling (Goumans et al., 2003).

Moreover, **BMPR2** was proposed as a **gatekeeper** to protect ECs from increased TGFβ signaling and EndMT (Hiepen et al., 2019).

In an endothelial PAH model BMPR2 deficiency increased formation of TGFβ binding receptor complexes enabling SMAD2/3 signaling but also ALK5 mediated lateral SMAD1/5 signaling via BMP type I receptors, which favored EndMT and ECM production. This is in line with another study, which showed that TNFα triggered EndMT was accompanied by the downregulation of BMPR2 levels in an atherosclerotic model. Absence of BMPR2 favored the formation of BMP9 binding receptor complexes involving ACVR2A, which promoted EndMT and thus osteogenic potential of human aortic ECs (Sánchez-Duffhues et al., 2019a).

This demonstrates another example where BMP9 has an endothelial activating role instead of promoting homeostasis.

In contrast the expression and activity of **ALK2** was reported to promote EndMT. In fact, ALK2 is required for EndMT as demonstrated in endothelial specific *Alk2* knockout mice, which fail to undergo EndMT in heart development (Wang et al., 2005). This is

in line with ALK2 knockdown in human venous and microvascular ECs, which prevented TGFβ and BMP4 induced EndMT (Medici et al., 2010). Moreover, stable expression of the FOP mutant ALK2-R206H receptor in ECs or FOP patient derived iPSC-ECs and ECFCs were prone to undergo EndMT *in vitro* (Barruet et al., 2016; Cai et al., 2015;Medici et al., 2010; Sánchez-Duffhues et al., 2019c).

Importantly, **human FOP biopsies** of HO lesions showed **co-expression** of TIE2, and the EC marker **vWF** with **chondrogenic and osteogenic markers** whereas normal bone derived from the hip showed no co-expression, suggesting involvement of EndMT in HO formation (Medici et al., 2010). In addition to ALK2 the expression of **ALK5** was required in ECs (HUVEC, ECFC) undergoing EndMT (Medici et al., 2010; Moonen et al., 2010). Thus, in contrast to BMPR2, ALK2 and ALK5 are considered as EndMT regulators and several compounds targeting ALK2 or ALK5 have been shown to inhibit EndMT implicating their therapeutic potential in EndMT associated pathologies (Man et al., 2019).

Interestingly, EndMT was triggered by BMP4 and TGFβ *in vitro* and induced interaction of ALK5 with ALK2 but in contrast BMP7 inhibited EndMT and did not mediate ALK2/ALK5 interactions (Medici et al., 2010; Zeisberg et al., 2007).

Collectively, these insights highlight the requirement of balanced BMP and TGFβ signaling in the endothelium to maintain physiological tissue homeostasis.

Imbalanced signaling likely results from specific environmental tissue conditions, which facilitates the expression and formation of distinct BMP/TGFβ receptor complexes. Those receptor complexes transduce signaling responses in ECs that activate a transcriptional and functional machinery in favor of EndMT and other pathological processes.

1.12 Aim

FOP is a rare disease characterized by episodic bone formation outside of the skeleton (ectopic bone) in soft tissues in a complex-multi-stage process called heterotopic ossification (HO). Bone is a highly vascularized organ and its formation requires osteogenesis and angiogenesis, a coupled process, which remains incompletely understood. Investigations of HO lesion biopsies show aberrations of vascular morphology suggesting involvement of pathogenic angiogenesis and Endothelial to Mesenchymal Transition (EndMT) but underlying mechanisms and signals remain elusive. The endothelium represents a fundamental component of the vasculature by forming the initial tubular structure. The genetic cause of FOP is a gain of function mutation in the BMP receptor ALK2 with R206H being the most common point mutation, located in the intracellular glycine-serine rich domain. Mutant ALK2 leads to hyperactivated SMAD1/5 signaling in response to BMP ligands. ALK2 signaling in the endothelium remains poorly understood compared to the well-studied endothelial BMP receptor ALK1.

At the start of this study two independent groups discovered that ActivinA aberrantly transduces SMAD1/5 signaling in ALK2-R206H expressing cells (Hatsell et al., 2015; Hino et al., 2015). Blocking of ActivinA prevented HO, indicating a central role of this ligand in the disease (Hatsell et al., 2015). However, the tissue and cell types which gain ActivinA/SMAD1/5 responsiveness endogenously remain poorly understood. Importantly, at this time point, no patient derived FOP endothelial cell model was available and thus the effect of ActivinA on FOP endothelium remained unknown. Therefore, this doctoral thesis aimed to address one key question:

Do Activin and BMP ligands activate ALK2 signaling in the FOP endothelium and how does it influence cellular function?

To answer this question the following aims were addressed:

1. The establishment of a patient derived FOP endothelial cell model
2. Investigation of Activin and BMP ligand effects on ALK2 signaling and functional cues of angiogenesis and EndMT in FOP endothelial cells
3. Usage of FOP endothelial disease model for drug testing.

2. Materials and Methods

2.1 Materials

2.1.1 Cell culture materials, reagents and media

Sterile cell culture plastic ware was purchased from Greiner Bio-One GmbH, Hartenstein Laborbedarf and Corning.

Table 1: Cell Culture Media and reagents

Medium	Preparation	Manufacturer
E8-Medium	Basal medium: DMEM/F12 64 mg/l L-ascorbic acid 2 phosphate magnesium salt 14 µg/l Sodium selenite 100 µg/l FGF2 19.4 mg/l Insulin 543 mg/l $NaHCO_3$ 10.7 mg/l Transferrin 2 µg/l TGFβ1 (Chen et al., 2011)	 Thermo Fisher Scientific Sigma Sigma PeproTech Sigma Sigma Sigma R&D
E6-Medium	E6-Medium w/o FGF2 and TGFβ1	Thermo Fisher Scientific
Mesoderm Induction Medium	Basal medium: 50% DMEM/F12, 50% Neurobasal medium 2% B27 supplement, minus VitaminA 1% N-2 Supplement 50 µM β-Mercaptoethanol 2 mM GlutaMAX 6-7µM CHIR 99021 solution 25ng/ml hBMP4	 Thermo Fisher Scientific Thermo Fisher Scientific Thermo Fisher Scientific Thermo Fisher Scientific Thermo Fisher Scientific Thermo Fisher Scientific Biovision PeproTech
Endothelial Induction Medium	Basal medium: StemPro-34 basal medium 2.6% StemPro-34 supplement 1% Penicillin-Streptomycin (100 U/ml) 2 mM GlutaMax 200 ng/µl VEGFA 165 2 µM Forskolin	 Thermo Fisher Scientific Thermo Fisher Scientific Thermo Fisher Scientific Thermo Fisher Scientific PeproTech Abcam
Endothelial Expansion Medium	Basal medium: Endothelial Basal Medium (EBM-2)	 Lonza

	20% FCS	Biochrom
	2 ml hFGF-B	Lonza
	0.5 ml VEGF	Lonza
	0.5 ml R3-IGF-1	Lonza
	0.5 ml Ascorbic Acid	Lonza
	0.5 ml hEGF	Lonza
	0.5 ml Heparin	Lonza
	1% Penicillin-Streptomycin (100 U/ml)	Thermo Fisher Scientific
	10 µM SB431542	Selleck Chemicals
Endothelial Growth Medium modified (EGM2)	Basal medium:	
	EBM-2	PromoCell
	10% FCS	Biochorom
	10 ng/mL hFGF-B	PromoCell
	0,5 ng/mL VEGF	PromoCell
	20 ng/mL R3-IGF-1	PromoCell
	1 µg/ml Ascorbic Acid	PromoCell
	5 ng/ml hEGF	PromoCell
	22,5 µg/mL Heparin	PromoCell
	0.2 µg/ml Hydrocortisone	PromoCell
	1% Penicillin-Streptomycin (100 U/ml)	PAA-laboratories
Endothelial Growth Medium modified (EGM2-m)	Basal medium:	
	EBM-2	PromoCell
	20% FCS	Biochorom
	10 ng/mL hFGF-B	PromoCell
	0,5 ng/mL VEGF	PromoCell
	20 ng/mL R3-IGF-1	PromoCell
	1 µg/ml Ascorbic Acid	PromoCell
	5 ng/ml hEGF	PromoCell
	22,5 µg/mL Heparin	PromoCell
	1% Penicillin-Streptomycin (100 U/ml)	PAA-laboratories
Endothelial Starvation Medium (ESM)	Basal medium:	
	EBM-2	PromoCell
	0.5% FCS	Biochrom
Endothelial Growth Medium- Knock Down (EGM2-KD)	Basal medium:	
	EBM-2	PromoCell
	2% FCS	PromoCell
	10 ng/mL hFGF-B	PromoCell
	0,5 ng/mL VEGF	PromoCell
	20 ng/mL R3-IGF-1	PromoCell
	1 µg/ml Ascorbic Acid	PromoCell
	5 ng/ml hEGF	PromoCell
	22,5 µg/mL Heparin	PromoCell
M199 Medium	Basal medium:	
	M199 basal medium	Sigma Aldrich
	20% FCS	Biochrom

	2 mM L-Glutamine 25 ng/ml Heparin 1% Penicillin-Streptomycin (100 U/ml)	PAN Biotech Sigma Aldrich PAN Biotech
DMEM Basal Media (DBM)	Basal medium: DMEM 2 mM L-Glutamine 1% Penicillin-Streptomycin (100 U/ml)	 PAN Biotech PAN Biotech PAN Biotech
DMEM Growth Media (DGM)	Basal medium: DMEM 2 mM L-Glutamine 10% FCS 1% Penicillin-Streptomycin (100 U/ml)	 PAN Biotech PAN Biotech Biochrom PAN Biotech
Cryopreservation medium for iPSC	FreSR-S medium	Stem Cell Technologies

Table 2: Cell culture reagents

Product	Manufacturer
TrypLE Select	Thermo Fisher Scientific
Dulbecco's Phosphate Buffered Saline (DPBS)	PAN Biotech
Trypsin 0,05%/ EDTA 0,02% in PBS w/o Ca, Mg	PAN Biotech
Matrigel Growth Factor Reduced Basement Membrane Matrix	Corning
Methylcellulose	Sigma-Aldrich
EDTA ($Na_2EDTA• 2H_2O$) solution 0.5 M	Thermo Fisher Scientific
0.1% Gelatin Solution	EmbryoMax, Sigma-Aldrich
FCR Blocking Reagent	Miltenyi Biotec
CD144 MicroBeads	Miltenyi Biotec
Accutase	Stem Cell Technologies
Methylcellulose	Sigma Aldrich
DMSO	Sigma-Aldrich

Table 3: Cell Culture Material

Product	Manufacturer
Culture plastic ware (Plates: 6-well, 12-well, 24-well, 96-well)	Greiner Bio-One GmbH, Falcon
Culture plastic ware (Flasks: 75 cm^2, 175 cm^2)	Greiner Bio-One GmbH, Falcon
Cell scraper	Sarstedt
LS columns	Miltenyi Biotec
Perfusion set with 1,6 mm, tubing sets for FSS assays with the ibidi Pump System	ibidi
Terumo Syringe Luer-Lock Tip without Needle 10 mL, medium reservoir for FSS assays	ibidi

96-well round-well, non-adhesive (#650161)	Greiner Bio-One
Gold electrode 8W10E arrays for ECIS measurements	ibidi

2.1.2 Patient Material and cell lines

Table 4: Patient material and cell lines

Cell line	Cell type	Tissue origin	Source
BCRTi005-A (WT-1)	induced Pluripotent Stem Cell (iPSC)	Urine	Charité Universitätsmedizin Berlin https://hpscreg.eu
BCRTi004-A (WT-2)	induced Pluripotent Stem Cell (iPSC)	Urine	Charité Universitätsmedizin Berlin https://hpscreg.eu
BCRTi001-A (FOP-1)	induced Pluripotent Stem Cell (iPSC)	Urine	Charité Universitätsmedizin Berlin https://hpscreg.eu
BCRTi001-A (FOP-2)	induced Pluripotent Stem Cell (iPSC)	Urine	Charité Universitätsmedizin Berlin https://hpscreg.eu
HUVEC	Human Umbilical Vein Endothelial Cell	Umbilical cord	AG Knaus cell bank
HUAEC	Human Arterial Vein Endothelial Cell	Umbilical cord	PromoCell, Lot #397Z038.1
C2C12	Myoblast		AG Knaus cell bank

2.1.3 Recombinant growth factors

Growth Factor	Source	Manufacturer
Recombinant human (rh)BMP2	produced in *E.coli*	Gift from Walter Sebald (Ruppert et al., 1996)
rhBMP6	produced in CHO cells	Gift from Slobodan Vukicevic (Simic et al., 2006)
rhBMP9 /GDF2	produced in CHO cells	PeproTech
rhTGFβ1	produced in CHO cells	PeproTech
rhActivinA	produced in CHO cells	R&D
rhVEGFA-165	produced in *E.coli*	PeproTech
rhTNFα	produced in *E.coli*	ImunoTools

2.1.4 Inhibitors

Inhibitor	Description	Manufacturer
K02288	ALK1 & ALK2 kinase inhibitor	Selleckchem
SB431542	ALK4, ALK5, ALK7 kinase inhibitor	Selleckchem
Saracatinib	ALK1, ALK2 and SRC kinase inhibitor	Selleckchem

BMS-345541	Catalytic subunits of IKK-2, IKK-1	Selleckchem
FK506/Tacrolimus	Binds to immunophilins (FK506 binding proteins)	Selleckchem
ROCK Y-27632	Rho-associated, coiled-coil containing protein kinase inhibitor	Stem Cell Technologies

2.1.5 Antibodies and Fluorescent dyes

Table 5: Antibodies

Antibody	Species	Manufacturer (Clone)	Dilution
Primary antibodies			
GAPDH	Rabbit	Cell Signaling (14C10)	1:1000 (1)
ID1	Rabbit	Santa Cruz (C-20)	1:1000 (1)
Phosphorylated (p)SMAD1/5 (Ser463/465)	Rabbit	Cell Signaling (41D10)	1:1000 (1)
pSMAD2 (Ser465/467)	Rabbit	Cell Signaling (138D4)	1:1000 (1)
pSRC family (Tyr416)	Rabbit	Cell Signaling (D49G4)	1:1000 (1)
SRC	Rabbit	Cell Signaling (32G6)	1:1000 (1)
VE-Cadherin XP	Rabbit	Cell Signaling (D87F2)	1:1000 (1)
pVE-Cadherin (Tyr685)	Rabbit	ECM Biosciences	1:1000 (1)
p38 MAPK XP	Rabbit	Cell Signaling (D13EI)	1:1000 (1)
pp38 (Thr180/Tyr182)	Mouse	Cell Signaling (D3F9)	1:1000 (1)
PECAM1	Mouse	Cell Signaling	1:1000 (1), 1:200 (2)
SMAD2	Rabbit	Cell Signaling (86F7)	1:1000 (1)
SMAD1 XP	Rabbit	Cell Signaling (6944)	1:1000 (1)
FKBP12	Mouse	Santa Cruz (H-5)	1:1000 (1)
AKT (AKT1, AKT3) (pan)	Mouse	Cell Signaling (5G3)	1:1000 (1)
pAKT (Ser473)	Rabbit	Cell Signaling (193H12)	1:1000 (1)
Cofilin	Rabbit	Cell Signaling	1:1000 (1)
Conjugated antibodies			
CD144(VE-Cadherin)-FITC	Human	Miltenyi Biotec (REA199)	1:50 (3)
CD31(PECAM1)-APC	Human	Miltenyi Biotec (AC128)	1:50 (3)
mouse IgG, conjugated to HRP	Goat	Dianova/Jackson ImmunoResearch	1:5000 (1)
rabbit IgG, conjugated to HRP	Goat	Dianova/Jackson ImmunoResearch	1:5000 (1)
Alexa Fluor 488 F(ab')2 fragment of α-mouse IgG	Goat	Invitrogen	1:300 (2)
Alexa Fluor 594 F(ab')2 fragment of α-mouse IgG	Goat	Life Technologies	1:300 (2)
Alexa Fluor 594 α-rabbit IgG	Goat	Invitrogen	1:300 (2)
Alexa Fluor 647 α-rabbit IgG	Goat	Life Technologies	1:300 (2)

Antibodies were diluted in in 3% BSA/ TBS-T, 0,1% NaN3 for Western Blotting (1) or in blocking solution for immunofluorescence staining (2) or FACS (3).

Table 6: Fluorescent dyes

Product	Application	Manufacturer	Dilution
4'6-Diamino-2-phenylindole dihydrochloride (DAPI)	Nuclei staining, 1:1000	Sigma-Aldrich	1:1000
Phalloidin CruzFluor 594 Conjugate	F-actin staining, 1:200	Santa Cruz	1:200
Phalloidin CruzFluor 647 Conjugate	F-actin staining, 1:200	Santa Cruz	1:200

2.1.6 Oligonucleotides

Table 7: siRNA sequences

Target gene	Target Sequence	Manufacturer
Accell Non-targeting siRNA	UGGUUUACAUGUCGACUAA	Dharmacon (D-001910-01-05)
Accell FKBP1A	GCUUGAAGAUGGAAAGAAA	Dharmacon (A-009494-15-0010

Table 8: Real-time PCR Primer

Human gene	Primer name	Primer Sequence (5'→3')
RSP9	RSP9 forward RSP9 reverse	CTGCTGACGCTTGATGAGAA CAGCTTCATCTTGCCCTCAT
ID1	ID1 forward ID1 reverse	GCTGCTCTACGACATGAACG GCTGCTCTACGACATGAACG
ID2	ID2 forward ID2 reverse	GTGGCTGAATAAGCGGTGTT TGTCCTCCTTGTGAAATGGTT
ID3	ID3 forward ID3 reverse	CTTCCGGCAGGAGAGGTT AAAGGAGCTTTTGCCACTGA
SMAD6	SMAD6 forward SMAD6 reverse	TGATGAGGGAGTTGGTACCC ACCTCCCTACTCTCGGCTGT
ACVRL1	ACVRL1 forward ACVRL1 reverse	ACAACATCCTAGGCTTCATCGC GGTTTGCCCTGTGTACCG
ACVR1	ACVR1 forward ACVR1 reverse	AAGCCTGGAGCATTGGTAA TCACTGGGGTACTCGGAGA
BMPR1A	BMPR1A forward BMPR1A reverse	CATCTTGGAGGAGTCGTAAGAA TTCTGTCCTTGAACACGAGAAA
BMPR1B	BMPR1B forward BMPR1B reverse	CTGCCATAAGTGAGAAGCAAAC ACAACGCAAGACCTTTGGAC
ACVR1B	ACVR1B forward ACVR1B reverse	TGCAACAGGATCGACTTGAG ATGATGCCTACCAGCTCCAC
ACVR1C	ACVR1C forward ACVR1C reverse	ACTTGTGCCATAGCGGACTTA GGTTCCCACTTTAGGATTCTGAG
TGFBR1	TGFBR1 forward TGFBR1 reverse	ACTGTAAAGTCATCACCTGGC GTGAATGACAGTGCGGTTGT

BMPR2	BMPR2 forward BMPR2 reverse	CATGGAGATGCGTAGCTGTC GGTTCTGAGGAAGTGCGAGT
ACVR2A	ACVR2A forward ACVR2A reverse	CCTGACAGCTTGCATTGCTGACTT TCTGCGTCGTGATCCCAACATTCT
ACVR2B	ACVR2B forward ACVR2B reverse	TGAAGCACGAGAACCTGCTACAGT GGCATACATGTCAATGCGCAGGAA
TGFBR2	TGFBR2 forward TGFBR2 reverse	GTTCAGAAGTCGGATGTGGAA TCTGGTTGTCACAGGTGGAA
INHBA	INHBA forward INHBA reverse	CCTCCCAAAGGATGTACCCAA CTCTATCTCCACATACCCGTTCT
NOG	NOG forward NOG reverse	GCGAGATCAAAGGGCTAGAG TAACTTCCTCCGCAGCTTCT
KDR	KDR forward KDR reverse	AGCGATGGCCTCTTCTGTAA ACACGACTCCATGTTGGTCA
CDH5	CDH5 forward CDH5 reverse	CAGCCCAAAGTGTGTGAGAA CGGTCAAACTGCCCATACTT
PECAM1	PECAM1 forward PECAM1 reverse	GAGTCCTGCTGACCCTTCTG TCAGGTTCTTCCCATTTTGC
ICAM1	ICAM1 forward ICAM1 reverse	CAAGGCCTCAGTCAGTGTGA CCTCTGGCTTCGTCAGAATC
vWF	vWF forward vWF reverse	ACTCATGGGCTCTGAGCAGT GCTCTTCAGAAGCTGGCACT
VEGFR1	VEGFR1 forward VEGFR1 reverse	GTTCAAGGAACCTCGGACAA GCTCACACTGCTCATCCAAA
NRP1	NRP1 forward NRP1 reverse	GCCTGCAACTTGGGAAACTGG CCTTGGTTGGATGATGTGATCTGG
ENG	ENG forward ENG reverse	ATGAGGCGGTGGTCAATATC AGGAAGTGTGGGCTGAGGTA
NEDD9	NEDD9 forward NEDD9 reverse	ATGGCAAGGGCCTTATATGACA TTCTGCTCTATGACGGTCAGG
PMEPA1	PMEPA1 forward PMEPA1 reverse	TGTCAGGCAACGGAATCCC CAGGTACGGATAGGTGGGC
UNC5B	UNC5B forward UNC5B reverse	GGTTTCCACCCCGTCAACTT GGGGATTTTGTCGGTGGAGT
SGK1	SGK1 forward SGK1 reverse	AGGATGGGTCTGAACGACTTT GCCCTTTCCGATCACTTTCAAG
SMAD9	SMAD9 forward SMAD9 reverse	GTTCACCACGGCTTTGAAGT TGACATCCTGGCGATGATAC
HEY2	HEY2 forward HEY2 reverse	TTGAAGATGCTTCAGGCAACAGGG TCAGGTACCGCGCAACTTCTGTTA
JAG1	JAG1 forward JAG1 reverse	GGGAACCCGATCAAGGAAATCAC CAGCAAGGGAACAAGGAAATCTGT
LFNG	LFNG forward LFNG reverse	CTGCACCATCGGCTACATCG GGCGTTCCGCTTGTTTTCAA

DLL4	DLL4 forward DLL4 reverse	GACCACTTCGGCCACTATGT TTGCTGCAGTAGCCATTCTG
EFNB2	EFNB2 forward EFNB2 reverse	TGGACAAGATGCAAGTTCTGCT CTGTTGCCGTCTGTGCTAGA
EPHB4	EPHB4 forward EPHB4 reverse	CCCGCGCGGAGTATCG CGTCCACCTGAGGGAATGTC
COUP-TFII	COUP-TFII forward COUP-TFII reverse	TGCCTGTGGTCTCTCTGATG CCTACCAAACGGACGAAAAA
SNAI1	SNAI1 forward SNAI1 reverse	CCAGTGCCTCGACCACTATG CTGCTGGAAGGTAAACTCTGG
NRP1	NRP1 forward NRP1 reverse	GCCTGCAACTTGGGAAACTGG CCTTGGTTGGATGATGTGATCTGG
ENG	ENG forward ENG reverse	ATGAGGCGGTGGTCAATATC AGGAAGTGTGGGCTGAGGTA
MSX2	MSX2 forward MSX2 reverse	ATGGCTTCTCCGTCCAAAGG CGGCTTCTTGTCGGACATGA
FOXC2	MSX2 forward MSX2 reverse	CCTCCTGGTATCTCAACCACA GAGGGTCGAGTTCTCAATCCC
CDH2	CDH2 forward CDH2 reverse	AGGCTTCTGGTGAAATCGCA TGCAGTTGCTAAACTTCACATTG
RHOB	RHOB forward RHOB reverse	CTGCTGATCGTGTTCAGTAAGG TCAATGTCGGCCACATAGTTC
HEYL	HEYL forward HEYL reverse	ATGCAAGCCAGGAAGAAACGCAGA AGCTTGGAAGAGCCCTGTTTCTCA
NRARP	NRARP forward NRARP reverse	TCAACGTGAACTCGTTCGGG TCAACGTGAACTCGTTCGGG
PTGS2	PTGS2 forward PTGS2 reverse	CTGGCGCTCAGCCATACAG CGCACTTATACTGGTCAAATCCC
JAG2	JAG2 forward JAG2 reverse	TGGGACTGGGACAACGATAC AGTGGCGCTGTAGTAGTTCTC
ADM	ADM forward ADM reverse	AAGAAGTGGAATAAGTGGGCT TGTGAACTGGTAGATCTGGT
TCIM	TCIM forward TCIM reverse	ATGAAAGCAAAGCGAAGCCAC TCAGTGAACTTTGATGGAATA
FKBP1A	FKBP1A forward FKBP1A reverse	CTCCAGATTATGCCTATGGTGC AGCTCCACATCGAAGACGAGA
TDGF1	TDGF1 forward TDGF1 reverse	CACGATGTGCGCAAAGAGAA TGACCGTGCCAGCATTTACA
NFKBIE	NFKBIE forward NFKBIE reverse	TCTGGCATTGAGTCTCTGCG AGGAGCCATAGGTGGAATCAG
wtACVR1	wtACVR1 forward wtACVR1 reverse	TGGTACAAAGAACAGTGGCTAG CCATACCTGCCTTTCCCGA
mutantACVR1	mutantACVR1 forward mutantACVR1 reverse	TGGTACAAAGAACAGTGGCTTA CCATACCTGCCTTTCCCGA

2.1.7 Commercial Kits

Kit	Manufacturer
NucleoSpin Gel and PCR Clean-up	Macherey-Nagel
NucleoSpin RNA II isolation Kit	Machery-Nagel
Pierce BCA Protein Assay Kit	Thermo Fisher Scientific

2.1.8 Chemicals and reagents

Standard chemicals and reagents were purchased from Sigma-Aldrich, VWR, neoLab, NEB or Carl Roth GmbH, unless stated otherwise.

Table 9: Buffers and solutions

Buffers or Solutions	Preparation or supplier
10X TBE	121.1 g Tris Base, 61.8 g Boric acid, 27.5 g EDTA ad 1 l dH_2O, pH 8.0
Blocking Buffer	5% NGS, 3% BSA in DPBS
Laemmli buffer (6x)	375 mM Tris-HCl, 25% SDS, 45% Glycerol, 12.5% 2-Mercaptoethanol, 0.01% Bromphenol blue in H_2O
Lower Tris (4x)	1.5 M Tris, 0.4% SDS in H_2O, pH 8.8
RIPA lysis buffer	150 mM NaCl, 50 mM Tris, 0.1% SDS, 1% NP-40 Alternative. Add freshly before usage: 1 mM Phenylmethylsulfonyl fluoride, 2 mM Sodium orthovanadate, 500 mM Sodium fluoride, 20 mM Sodium pyrophosphate, 1x Protease Inhibitor Cocktail/50 mL in H_2O, pH 7.5
SDS-PAGE running buffer	10% Rotiphorese 10x SDS-PAGE in H_2O
TBS	100 mM Tris pH 7.5 150 mM NaCl
TBS-T (0.1%)	0.5% Tween 20, 5% 20x TBS buffer in H_2O
Upper Tris (4x)	0.5 M Tris, 0.4% SDS in H_2O, pH 6.8
Western Blot transfer buffer	24 mM Tris, 196 mM Glycine, 20% Methanol in H_2O
Fluoromount-G	Southern Biotech

All buffers and solutions were prepared with Milli-Q water unless stated otherwise.

2.1.9 Technical devices, software and online tools

Table 10: Technical devices

Device	Type	Company
Camera	Axiocam ERc 5s	Carl Zeiss Microscopy
CCD-based detection system	FUSION FX7	Vilber Lourmat
Cell Counter	CASY Model TT	Roche
Cell Counter	Countess II FL Automated Cell Counter	Thermo Fisher Scientific

Cooling Centrifuge	Centrifuge 5418 R and Rotor FA-45-18-11	Eppendorf
Electrophoresis power supply	PowerPac High Current	Bio-Rad
Electrophoresis system	Mini-PROTEAN Tetra Cell Systems	Bio-Rad
Microscope (bright-field)	Axiovert 40 CFL	Carl Zeiss Microscopy
Microscope (epifluorescence)	Axiovert Observer 7, Axiovert 200M	Carl Zeiss Microscopy
Real-Time PCR System	Applied Biosystems StepOnePlus	Life Technologies
Spectrophotometer	NanoDrop ND-1000	NanoDrop Technologies
Wet/Tank Blotting system	Trans-Blot Cell	Bio-Rad
Impedance Sensor	Electric cell-substrate impedance sensing (ECIS) Zθ instrument	Applied BioPhysics, ibidi
Pump system with 4 Fluidic Units for the cultivation of cells under flow	ibidi Pump System Quad	Ibidi
Flow Cytometer	MACS Quant VYB	Miltenyi
Magnetic cell separator	MiniMACS Separator	Miltenyi

Table 11: Software and online tools

Software/Online Tool	Application	Company/Source
Adobe Photoshop CC	Image Processing	Adobe
AxioVision	Image acquisition	Zeiss
BioRender	Generation of illustrations and schemes	BioRender (biorender.com)
Chimera1.13.1	Molecular modelling of crystal structures	University of California, San Francisco
CCTop	CRISPR/Cas9 target online predictor	crispr.cos.uni-heidelberg.de
FCS Express V6	FACS analysis	De Novo Software
FusionCapt Advance FX7	Immunoblot image acquisition	Vilber Lourmat
Ensemble genome browser	cDNA sequence export	ensembl.org/index.html
Galaxy Europe	RNA Sequencing data analysis	Open Source (usegalaxy.eu)
Gene Expression Omnibus (GEO) database	Export of published RNASeq data	ncbi.nlm.nih.gov/geo
ImageJ FIJI	Image processing and quantification	Open Source (imagej.net/Fiji)
Microsoft Office	Text editing	Microsoft
Primer BLAST	Primer design	ncbi.nlm.nih.gov/tools/primer-blast/
Prism8	Analysis and graphing of data	GraphPad
Snapgene	DNA viewer and digital cloning	Snapgene
StepOne Software2.3	qRT-PCR evaluation	Thermo Fisher Scientific
Zotero	Management of bibliography	Open Source (zotero.org)

2.2 Methods

2.2.1 Cell culture

All cell types were expanded and maintained at 37°C and 5% CO_2 atmosphere and cell numbers were determined using a CasyTT cell counter or Countess™ automated cell counter. For starvation and passaging, the cells were previously washed with Dulbecco´s phosphate buffered saline (DPBS) and subsequently kept in growth or starvation medium. Details of the medium compositions are listed in Table 1.

Induced pluripotent Stem Cells (iPSCs)

Cell lines iPSC-WT-1 (BCRTi005-A), iPSC-WT-2 (BCRTi004-A), iPSC-FOP-1 (BCRTi001-A), iPSC FOP-2 (BCRTi002-A) are registered, including ethical statements at the global human iPSC registry https://hpscreg.eu.

iPSCs were grown in colonies and maintained in defined conditions in **E8-Medium** (Chen et al., 2011) and routinely passaged in colony clumps at a ratio of ~1:20 every 4–5 days using 0.5 mM EDTA. iPSCs were seeded on Geltrex-coated 6-well plates. Therefore, Geltrex was diluted 1:11 in DMEM/F12 and stored in aliquots at -20°C. Before usage of Geltrex, aliquots were diluted 1:6 in DMEM/F12 and 6 well plates were coated with 1 ml/well and incubated at 37°C for 30 min. After seeding, a daily medium change was performed and spontaneous differentiated cells were removed manually with a tip using a microscope under the fume hood. For single cell seeding, iPSCs were harvested with Accutase and subsequently the growth medium was supplemented with 10 µM ROCK inhibitor for 24 hours.

Endothelial Cells (ECs)

Upon thawing iPSC derived ECs (iECs) were cultured in **EGM2-mod** on 0.1% Gelatin coated culture flasks and used for all experiments in passage 2. HUAECs were routinely cultured in **EGM2** and HUVECs in **M199 Medium.** Before seeding culture plates or flasks were incubated with 0.1% Gelatin Solution (e.g. 12-well plate 0.5 ml/well) and incubated at 37°C for 30 min.

2.2.2 Cell stimulation with growth factors and inhibitors

Cells were starved prior growth factor stimulation for 5 hours. iPSCs were starved in **E6-Medium** and iECs in Endothelial Starvation Medium 2 (**ESM**). Small-molecule kinase inhibitors (SMKI) were added to cells 1 hour prior ligand stimulation with

indicated concentrations unless stated otherwise. Growth factors and SMKIs were reconstituted and stored according to manufacturer instructions.

2.2.3 **Cryopreservation of iPSC for differentiation (*CryoPause*)**

iPSCs, which were cryopreserved according the CryoPause method in a controlled-rate freezer (Wong et al., 2017). In brief, iPSCs were harvested with Accutase for 30 min at 37°C. Cells were washed with E8-Medium and centrifuged at 200 g for 5 min at room temperature. The medium was aspirated and the pellet was washed again with E8-Medium followed by a centrifugation step as described above. The supernatant was aspirated and iPSCs were resuspended FresSR-S medium to reach a cell number of 10 million cells/ml. The cell suspension was transferred to pre-chilled cryotubes and transferred to a temperature controlled-rate freezer with the following program:

Step 1: wait at 4°C; Step 2: 1.2°C/min (sample) to -4°C; Step 3: 25°C/min (chamber) to -40°C; Step 4: 10°C/min (chamber) to -12°C; Step 5: 1.0°C/min (chamber) to -40°C; Step 6: 10°C/min (chamber) to -90°C; Step 7: wait at -90°C. Cryotubes were rapidly transferred to a liquid nitrogen tank once the controlled rate freezer reached -90°C.

2.2.4 **Differentiation of iECs from iPSCs**

Cryopreserved iPSCs as described in chapter 2.2.3 were thawed and immediately seeded for EC differentiation. iPSCs were differentiated into iECs using a modified version of a cell monolayer approach (Patsch et al., 2015). In brief, iPSCs were thawed in E8-Medium supplemented with 10 µM ROCK and seeded in at a density of 2-3 x 10^5 cells/well on Geltrex coated 6-well plates. About 24 hours after seeding the medium was changed to mesoderm induction **Mesodermal induction medium.** The preparation of the different medias is listed in Table 1.Optimal concentration of Glycogen Synthase Kinase 3-β (GSK3-β) inhibitor CHIR99021 and cell density was established separately for each iPSC line by measuring the differentiation efficiency (see Table 15).

On day 4 and day 5 the medium was changed to **Endothelial induction medium**. On day 6, cells were dissociated by TrypLE and centrifuged at 300 g for 5 min. The cell pellet was resuspended in MACS-buffer containing DPBS with 0.5% BSA and 2 mM EDTA and a single cell suspension was prepared by using a 40 µM cell strainer. 5 x 10^4 cells were stained with CD144-FITC (Miltenyi Biotec) for subsequent FACS analysis. The rest of the cells was centrifuged at 300 g for 5 min at 4°C. The

supernatant was removed and the cell pellet was resuspended and a cell count performed. Up to 1 x 10^7 cells were gently resuspended in 60 µl MACS buffer containing 20 µl FCR Blocking Reagent (Miltenyi Biotec) and 20 µl CD144 MicroBeads (Miltenyi Biotec) and incubated for 15 min at 4 °C. Upon a washing step in MACS buffer, the cells were resuspended in 500 µl and applied on the eliquibrated LS columns (Miltenyi Biotec) attached to the magnetic rack. Upon collection of the negative fraction and three washing steps, the positive fraction (CD144+) was eluted in a separate tube in absence of the magnet. The cell pellet was resuspended in **Endothelial Expansion Medium** and 4 x 10^4 cells per cm^2 were seeded on 0.1% Gelatin coated culture flasks. Upon confluency, cells were split (max. 1:3) or frozen in freezing medium containing 90% FCS and 10% DMSO. Upon thawing iECs were cultured in **EGM2** and seeded for all experiments in passage 2.

2.2.5 Cryopreservation of Endothelial Cells

iECs were harvested with Trypsin and washed with DGM. Cells were centrifuged at 300 g for 4 min and the cell pellet was resuspended in freezing medium (90% FCS and 10% DMSO) to reach a cell number of 1.5-2.0 million cells/ml for each vial. Cryotubes were rapidly transferred to a freezing container, which was located at -80 °C to reach a cool rate of approximately -1°C/min. Other ECs were cryopreserved according the same method but the freezing medium contained 90% full growth medium and 10% DMSO.

2.2.6 Fluid Shear Stress (FSS) experiments with iPSC derived ECs (iECs)

For FSS experiments, 1x10^5 iECs were seeded on 0.1% Gelatin coated µ-Slides I 0.4 Luer (ibidi) and cultured for 48 hours at 37°C and 5% CO_2 atmosphere in 100 µl **EGM2**. Due to the small medium amount, the µ-Slides were flushed with fresh medium twice a day. Optimal cell growth and density was controlled before and after FSS by phase contrast microscopy. On day 2, FSS was applied by connecting the µ-Slides to the ibidi pneumatic pump system. After a 6 hours ramp phase to reach step-wise 30 dyne/cm^2 in full medium (EGM2, 10 ml), iECs were stimulated with FSS for 24 hours. The ramp phase is included to avoid detachment of the cells. For ligand stimulation ActivinA was diluted in 1 ml EGM2 and added to the medium reservoir. For static controls iECs were seeded in the same densities in silicone chambers with equal dimensions as the µ-slides and exposed to equal volume of medium. Before seeding the silicone, chambers were mounted on 0.1% Gelatin coated culture plates. For harvesting the cells, the

µ- slides were put on an ice and washed three times with ice-cold PBS to wash out the remaining serum containing medium. For protein isolation iECs were lysed in RIPA buffer. Protein concentrations were measured by a BCA Protein Assay Kit according to the manufacturer's instructions and adjusted for Western Blot analysis. For RNA isolation, iECs were lysed in RA-1 lysis buffer from NucleoSpin RNA II (Macherey-Nagel) according to manufacturer instructions.

2.2.7 **siRNA delivery**

For targeted knockdown experiments $1.3x10^5$ iECs were seeded in one well of a 0.1% Gelatin coated 12-well plate in **EGM2**. After 24 hours cells were washed with calcium and magnesium containing PBS. Accell siRNA was diluted in serum reduced growth medium (**EGM2-KD**) to a final concentration of 0.5 µM or 1.0 µM and added to the cells. After 48 hours the medium was changed to endothelial starvation medium **ESM**. After 5 hours the cells were stimulated with respective growth factors and lysed in RIPA buffer. Protein concentrations were measured by a BCA Protein Assay Kit according to the manufacturer's instructions and adjusted for Western Blot by which knockdown efficiency was analyzed.

2.2.8 **Endothelial barrier function**

Endothelial barrier function was assessed by Electric Cell-substrate Impedance Sensing (ECIS) using the ECIS Zθ instrument (Applied BioPhysics, ibidi). Before cell seeding for an experiment, gold electrode arrays 8W10E (ibidi) were cleaned and stabilized to prevent well-to-well reproducibility and signal-to noise-ratio. Therefore, electrodes were pre-treated with 200 µl 10 mM L-cysteine for 15 min at room temperature followed by a two washing steps with Milli-Q water. Afterwards arrays were coated with 0.1% Gelatin for 30 min at 37°C. 3×10^4 cells/ well were grown to confluence for 72 hours. Cells were starved for 5 hours before stimulation with respective growth factors and PBS as control. Barrier function was assessed by ECIS measurement of resistance at 4000 Hz (Szulcek et al., 2014).

2.2.9 **Tube formation assay**

iECs were seeded in growth medium on growth factor reduced Matrigel (Corning) coated 96 well culture plates (3×10^4/well). After an incubation for 24 hours at 37°C in 5% CO_2 images were taken using phase-contrast microscopy.

2.2.10 Spheroid assay

For endothelial spheroid generation 3000 cells were resuspended in 50 µL EGM2: Methocel solution (3:1). Beforehand, Methocel was prepared with 12 g/L Methylcellulose in EBM2. 50 µl cell suspension was seeded on non-adhesive 96-well round bottom plates and incubated at 37°C and 5% CO_2 for 24 hours. Then spheroids were harvested, washed twice with DPBS and embedded in 25% growth factor–reduced Matrigel diluted in ESM. The Matrigel was thawed on 4°C beforehand. Spheroids were seeded in 150 µl on 96-well flat bottom plates and incubated for 2 hours at 37°C and 5% CO_2. Subsequently, spheroids were stimulated with respective growth factors and/or inhibitors for 24 hours. The next day, excess medium was removed and the spheroids were fixed with 4% paraformaldehyde (PFA) in DPBS for 10 min and subsequently permeabilized in 0.5% Triton X100/DPBS for 15 min. Then spheroids were stained with Alexa Fluor™ 594 Phalloidin and DAPI in a 1:1000 dilution in DPBS for 30 min. After a washing step in DPBS, spheroids were imaged. At least three spheroids per experimental condition were imaged with an epifluorescence microscope Axio Observer 7. Spheroid outgrowth area (SOA) was measured and normalized to spheroid size using ImageJ.

2.2.11 Adhesion molecule expression assay

iECs were exposed to tumor necrosis factor-alpha (TNF-α) (0.6 nM) for 2 hours. RNA was isolated and expression of *ICAM-1* was analyzed by qPCR.

2.2.12 Western Blot analysis

Cells were lysed in Laemmli or RIPA protein lysis buffer and frozen at -20 °C. Upon thawing, lysates were subjected to SDS-PAGE and transferred to PVDF membranes by Western Blotting. Membranes were blocked in 0.1% TBS-T containing 3% w/v BSA for 1 hour at RT, washed three times in 0.1% TBS-T and incubated with indicated primary antibodies (Table 5) overnight at 4°C following manufacturer's instructions. For protein detection the Horseradish peroxidase (HRP)-based method was used and membranes were incubated with secondary HRP conjugated antibodies (Table 5). Chemiluminescent reactions were processed using WesternBright Quantum HRP substrate (advansta) and documented by using a ChemiSmart5000 digital imaging system (Vilber-Lourmat).

2.2.13 Immunofluorescence staining

3×10^4 cells were seeded on glass coverslips placed in 24-well plates until they formed a confluent monolayer. Cells were fixed with 4% paraformaldehyde (PFA), quenched in 50 mM ammonium chloride and permeabilized in 0.5% Triton-X-100 for 15 minutes. After blocking for 1 h in 3% w/v BSA and 5% v/v normal goat serum in PBS, cells were stained with primary antibodies (Table 5) diluted in blocking solution overnight. Fluorophore conjugated secondary antibodies were diluted in blocking solution and incubated for 1 hour at room temperature (RT). Nuclei were stained with DAPI using a 1:1000 dilution in DPBS for 30 min at RT. After washing in ddH_2O coverslips were mounted on glass slides using Fluoromount-G (Southern Biotech) and dried overnight in the dark. Slides were stored at 4 °C and imaged with a epifluorescence microscope (Zeiss Axiovert 200M) and analyzed in AxioVision 4 software.

2.2.14 Fluorescent activated cell sorting

iPSCs were harvested as single cells using TrypLE. 5×10^4 cells were centrifuged at 300 g for 5 min and the pellet was resuspended in 40 µl staining solution (DPBS with 0.5% BSA a 2 mM EDTA supplemented with 10% FCR blocking solution (Miltenyi Biotec). Antibodies for surface marker staining (CD144-FITC-human clone REA199, CD31-APC-human clone AC128 (Table 6) were added (1:50) and incubated for 10 min at 4°C in the dark. Upon a washing step and resuspension in DPBS with 0.5% BSA 2 mM EDTA cells were measured by MACSQuant VYB (Miltenyi Biotec) and analyzed by FCS Express V6 software.

2.2.15 Quantitative Real-Time PCR

Cells were washed once with DPBS and RNA was isolated using NucleoSpin RNA II (Macherey-Nagel) according to manufacturer instructions. The amount of 0.5-1 µg RNA was reverse transcribed into cDNA using M-MLV reverse transcriptase and random primers (NEB) according the protocol described in Table 12 and Table 13. qRT-PCR was performed with 2.5 ng cDNA using PCR Luna Universal qPCR Master Mix (NEB) and specific primers listed in Table 8 according the program listed in Table **14**. Expression levels were assessed by StepOne Plus, and StepOne Software 2.3 (Applied Biosystems) and measured in technical triplicates. Target gene expression was quantified relative to the housekeeping gene *RSP9* using the ΔΔCT method including primer efficiency (Pfaffl, 2001).

Table 12: cDNA synthesis

Mix	Reagent	Volume	Company
cDNA synthesis mix1	RNA (total 500 – 1000 ng)	0,5-1 µg	
	ddH_20	ad 14,5 µl	Macherey-Nagel
	Random Primer	0,5 µl	NEB
cDNA synthesis mix2	5 x M-MLV (buffer)	5 µl	NEB
	dNTPs (10 µM)	1,25 µl	NEB
	RNAsin	0,5 µl	NEB
	M-MLV-RT (Reverse Transcriptase)	1,0 µl	NEB
	ddH_20	17,25 µl	Macherey-Nagel

Table 13: Cycler program for cDNA synthesis

Step	Process	Time	Temperature
1	Denaturation and Oligo Annealing (Mix1)	5 min	70°C
2	cool down	10 min	4°C
3	cDNA synthesis (add Mix2)	60 min	37°C
4	cDNA synthesis	∞	4°C

Table 14: Cycler program for quantitative real-time PCR

Step	Process	Time	Temperature
1	Denaturation	10 min	95°C
2	Amplification	15 s	95°C
Repeat of step 2 for 39 cycles			
3	Dissociation curve	15 sec	95°C
4		15 sec	60°C
5	Cooling	∞	4°C

2.2.16 RNA-Sequencing: Library preparation and sequencing

8 x 10^4 iECs per well were seeded in 12 well plate and grown to confluence generated from 4 biological independent iPSC lines. Two independent experiments of ligand and SMKI treatment were performed for each line. Upon starvation, ligand stimulation and SMKI treatment cells were lysed and RNA was isolated according to manufacturer instructions (Macherey-Nagel). The following processing was performed by Genewiz, Leipzig, Germany. RNA samples were quantified using Qubit 2.0 Fluorometer (Life Technologies) and RNA integrity was checked with Agilent Fragment Analyzer (Agilent Technologies). RNA sequencing library preparations used the NEBNext Ultra II Directional RNA Library Prep Kit for Illumina by following manufacturer's recommendations (NEB). Briefly, mRNAs were first enriched with Oligod(T) beads. Enriched mRNAs were fragmented for 10 minutes at 94°C. First strand and second

strand cDNA were subsequently synthesized. cDNA fragments were end-repaired and adenylated at 3'ends, and universal adapters were ligated to cDNA fragments, followed by index addition and library enrichment with limited cycle PCR. The sequencing libraries were validated on the Agilent Fragment Analyzer (Agilent Technologies), and quantified by using Qubit 2.0 Fluorometer (Invitrogen). The sequencing libraries were loaded on the Illumina NovaSeq 6000 instrument according to manufacturer's instructions. Clustering was performed directly on the NovaSeq before sequencing. clustered on one lane of a flowcell. After clustering, the flowcell was loaded on the Illumina NovaSeq 6000 instrument according to manufacturer's instructions. The samples were sequenced using a 2 x 150 Paired End (PE) configuration. Image analysis and base calling were conducted by the NovaSeq Control Software. Raw sequence data (.bcl files) generated from Illumina NovaSeq was converted into fastq files and de-multiplexed using Illumina's bcl2fastq 2.19 software. One mis-match was allowed for index sequence identification.

2.2.17 **RNA-Sequencing: Data analysis**

The sequencing data was uploaded to the Galaxy web platform and the public server at *usegalaxy.eu* was used to analyze the data (Afgan et al., 2018). Quality of raw reads was performed with FastQC before data was mapped to the reference genome (hg38) using STAR mapper (Dobin et al., 2013). Alignment quality was assessed with MultiQC (Ewels et al., 2016) and RNA-Seq alignments were assembled into potential transcripts by StringTie (Kovaka et al., 2019). This output was used to analyze differential gene expression with DESeq2 (Love et al., 2014). Cutoff for differentially expressed genes was a logarithmic fold change of $\geq$0.58 and with an adjusted p value of 0.05. Shared differentially expressed genes in both FOP donors were assessed with BioVenn (Hulsen et al., 2008). Z-score calculation and generation of heatmaps was performed with the „pheatmap" package in RStudio. Functional enrichment and clustering was performed with DAVID Bioinformatic Resources 6.8 (Huang et al., 2009a, 2009b) and applying Benjamini correction.

2.2.18 **Statistical analysis and data presentation**

In this study four iPSC lines and were used representing independent biological replicates from two healthy controls (WT) and two FOP donors harboring the ALK2 R206H mutation. Experimental replicates are presented for each donor separately or grouped with the biological replicate. Statistical analysis and data illustrations were

performed with GraphPad Prism 8 (GraphPad Software Inc.). Normal distribution of data sets n < 5 were tested with the Shapiro-Wilk normality test. Data sets n ≥ 5 were tested additionally with the Kolmogorov Smirnov test for normality. In cases of failure to reject the null hypothesis, the ANOVA and Bonferroni or Student´s *t*-test were used to check for statistical significance under the normality assumption. Upon rejection of non-parametric tests were used. P-values lower than 0.05 were considered statistically significant (*P < 0.05, **P < 0.01, ***P < 0.001, ****P < 0.0001). Details about the RNA-Seq data analysis is described in chapter 2.2.17.

2.2.19 **Graphical design**

Graphical Schemes were created with BioRender.com. or in Microsoft PowerPoint. The Figures were assembled and labeled in Adobe® Photoshop (Adobe Systems). Densiometric protein level quantification and fluorescent microscopy image analysis was performed with the software Image J.

3. Results

ActivinA induced SMAD1/5 signaling in an iPSC derived EC model of Fibrodysplasia ossificans Progressiva (FOP) can be rescued by the drug candidate Saracatinib

(Hildebrandt *et al.*, Stem Cell Reviews and Reports, in press 2020)

3.1 Establishment of a FOP endothelial cell model

For the investigation of Activin receptor-like kinase 2 (ALK2) signaling in FOP endothelium, it was aimed to establish a FOP endothelial cell (EC) disease model. Due to the risk to trigger heterotopic ossification (HO) upon tissue biopsy sampling and the limited number of patients of the rare disease, the establishment of FOP patient models has been challenging. Induced pluripotent stem cells (iPSCs) enable the generation of healthy and diseased human cell types of various human tissues via directed differentiation methods, which overcome the restrictions of further patient material and the limited expansion potential of primary cells *in vitro*.

Recently, the Berlin Institute of Health (BIH) Center for Regenerative Therapies (BCRT) generated iPSC from two FOP patients harboring the ALK2 R206H mutation (FOP-1, FOP-2) and two healthy controls (WT-1, WT-2) (Hildebrand et al., 2016; Rossbach et al., 2017, 2016) (Figure 3.1A). Thus, a collaboration was started to use iPSC technology for the generation of a FOP EC model. The iPSCs were generated from urine samples of FOP patients. In brief, renal epithelial cells were isolated from urine of four donors, which were reprogrammed by transient expression of OCT3/4, SOX2, KLF4 and cMYC (Yamanaka factors) using Sendai Virus (Fusaki et al., 2009) (Figure 3.1A). The four iPSC lines are listed in the global human iPSC registry (https://hpscreg.eu) and express characteristic pluripotency markers such as OCT4, SSEA4 and are capable to differentiate into the three germ layers (Hildebrand et al., 2016; Rossbach et al., 2017, 2016).

In this study, iPSCs were cultured and maintained in feeder-free, serum-free defined conditions and showed the typical stem cell morphology, with a high nucleus to cytoplasm ratio and colony growth phenotype (Figure 3.1B).

3.1.1 **WT and FOP iPSCs show differential SMAD responses**

The pluripotent and proliferative ability of iPSCs *in vitro* enables the generation of diverse tissue cell types derived from one of three germ layer (Liu et al., 2020). The maintenance of pluripotency requires tightly and controlled culture conditions (daily medium change) with defined medium and even manual removal of spontaneous differentiated cells (Chen et al., 2014). Moreover, iPSC colonies are typically passaged as small clumps, which is more tedious and time consuming but promotes viability and pluripotency compared to single cell culture of most other cell systems (Marinho et al., 2015). Proper maintenance enables the orchestration of multiple signaling cascades towards pluripotency. Changes in signaling responses can direct stem cells towards spontaneous differentiation to distinct germ layers and eventually create populations of specific cell types (Rao and Greber, 2017). The Bone Morphogenetic Protein (BMP) and Transforming Growth Factor β (TGFβ) signaling pathways are known to contribute to maintain pluripotency and to direct differentiation (Mullen and Wrana, 2017).

Here, BMP, Activin, and TGFβ signal responses were analyzed by the assessment of phosphorylated SMAD proteins in WT and FOP iPSCs. Therefore, iPSCs were treated with the ALK2 specific BMP ligand BMP6, which showed a dose-dependent phosphorylation of SMAD1/5 in both WT and FOP iPSCs (Figure 3.1D). All four iPSC lines responded to ActivinA with a dose-dependent increase in SMAD2 phosphorylation (Figure 3.1C). Interestingly, a similar pattern of SMAD2 phosphorylation was also observed upon BMP6 treatment in WT and FOP iPSCs (Figure 3.1D**)**. However, SMAD1/5 phosphorylation by ActivinA was only seen in FOP but not in WT iPSCs (Figure 3.1C). Treatment of WT and FOP iPSCs with TGFβ showed a canonical response with phosphorylated SMAD2 (pSMAD2) levels and no phosphorylation of SMAD1/5 (Figure 3.1E).

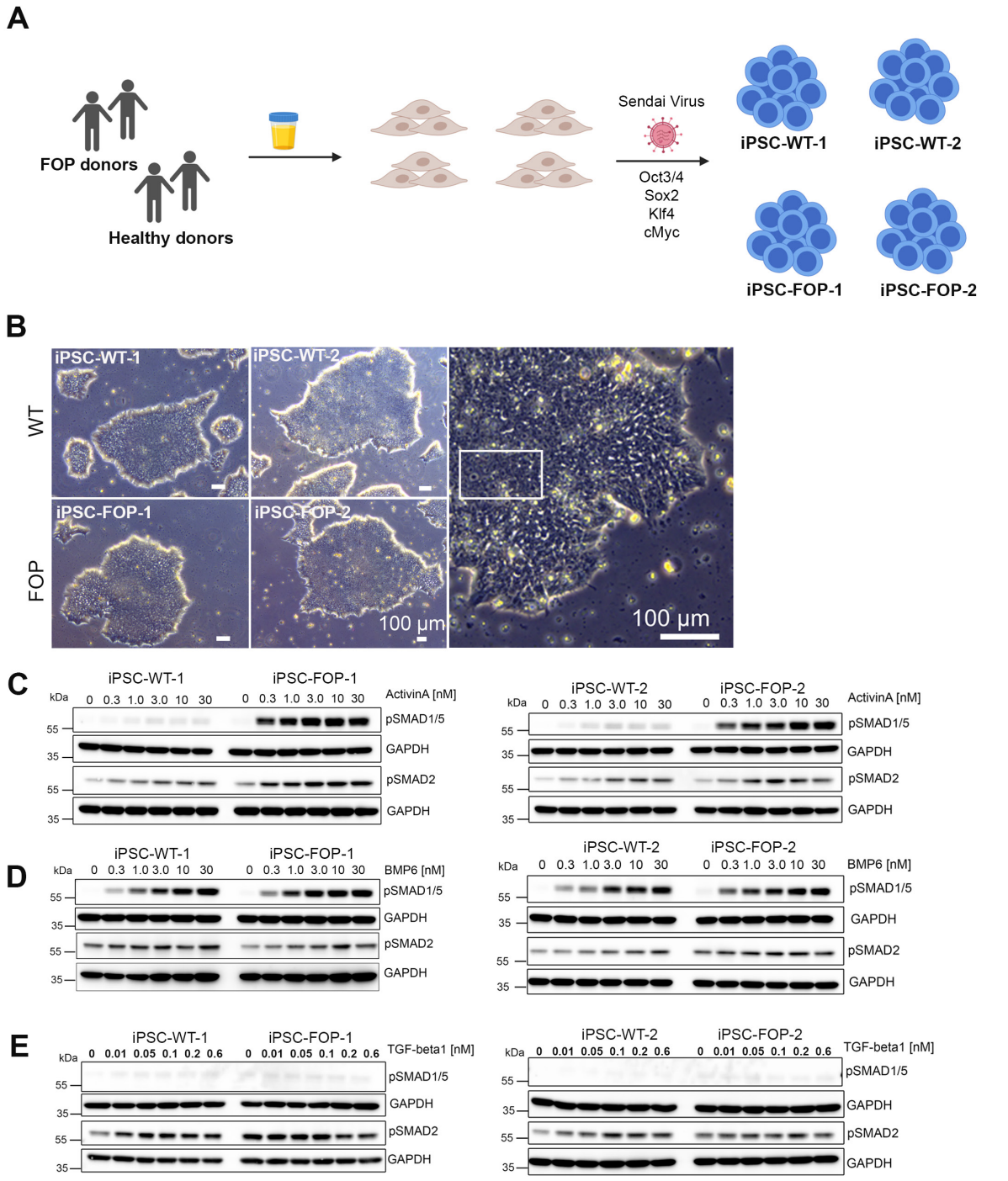

Figure 3.1. WT and FOP iPSC show differential SMAD responses. (**A**) Graphical Scheme of iPSC generation from urine cells using integration free sendai virus for transient expression of the *Yamanaka Factors*. (**B**) Phase contrast images of WT and FOP iPSC colony morphology. (**C-E**) Representative Western Blot of iPSC after stimulation with different doses of ActivinA, BMP6 and TGFβ. Data C-D is derived from (Hildebrandt et.al., Stem Cell Rev Rep, in press 2020).

3.1.2 Establishment of an optimized method to differentiate iPSCs to endothelial cells

ECs can be generation from iPSCs via directed differentiation using diverse strategies, which aim to mimic developmental conditions *in vitro* (Williams and Wu., 2019). Based on aberrant ActivinA/SMAD1/5 signaling in FOP iPSCs, a EC differentiation protocol devoid of exogenous ActivinA (Patsch et al., 2015) was adjusted and optimized. Moreover, to overcome initial cell passage dependent variations in differentiation efficiency (10-80%), the EC differentiation method was combined with a controlled cryopreservation method (Wong et al., 2017) to immediately initiate differentiation upon thawing (Figure 3.2A). Therefore, iPSC colonies were harvested, separated to a single cell suspension from which defined numbers were cryopreserved in an automated step-wise temperature-controlled freezer machine. Upon thawing, iPSCs were directly seeded for differentiation (Figure 3.2B). On day 1, mesoderm was induced by BMP4 and the Glycogen Synthase Kinase 3- β (GSK3-β) inhibitor CHIR99021. GSK3-β inhibition activates the canonical beta-catenin/Wnt pathway. Balanced Wnt signaling is essential for stem cell pluripotency but also for differentiation (Sokol, 2011). Therefore, optimal CHIR99021concentration and cell density was defined for each iPSC line by measuring the differentiation efficiency, which was defined as the amount of generated EC fraction using VE-Cadherin/CD144 as a marker in Fluorescence-activated cell sorting (FACS) analysis (Figure 3.3). Three different CHIR concentrations (5,6,7 µM) and two different cell numbers ($2x10^5$ or $3x10^5$ per 6-well) were tested. The combination, which generated the highest amount of EC fraction is framed with a blue square for each donor (Figure 3.3) and are listed in the table below (Table 15). In brief, the cell number $3x10^5$ achieved the best results for the iPSC donors WT-2, FOP-1, FOP-2 and $2x10^5$ for FOP-1. The CHIR concentration of 6 µM resulted in differentiation efficiency of iPSC donors WT-1, WT-1, FOP-2 and 7 µM for donor FOP. Both, WT and FOP iPSC differentiated to ECs with efficiencies of up to ~80% (Figure 3.2C). On day 4, endothelial specification of mesodermal cells was achieved by Vascular Endothelial Growth Factor A (VEGFA) and Forskolin (Figure 3.2A, B). Forskolin increases cellular cyclic adenosine monophosphate (cAMP) levels which enhance EC differentiation via upregulation of the VEGFA signaling receptor VEGFR2 and co-receptor Neuropilin1 (NRP1) (Yamamizu et al., 2009).

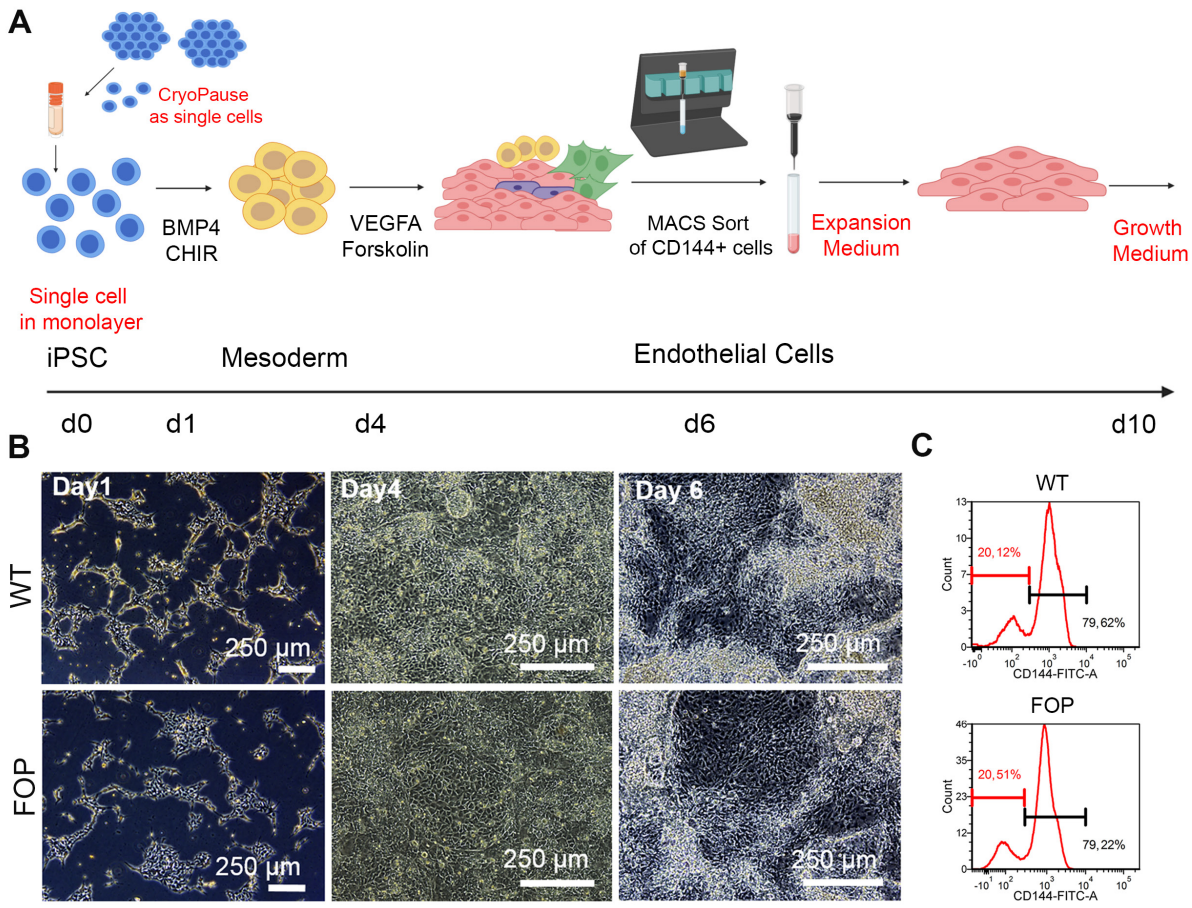

Figure 3.2. Generation of Endothelial Cells from iPSCs (iECs).
(**A**) Workflow of iEC differentiation with modification in red. (**B**) Phase contrast images of cells at different stages during differentiation. (**C**) iEC differentiation efficiency analysis by FACS of CD144+ cells after the MACS sort on day 10.

Mechanistically, cAMP binds and activates protein kinases A (PKA), which was suggested to mediate the upregulation of NRP1 and VEGFR2 (Yamamizu et al., 2009).Thus, Forskolin enhances the sensitivity of progenitors to VEGFA via upregulation of VEGFR2 in endothelial lineage differentiation (Dyer and Patterson, 2010). The EC fraction was purified by Magnetic Activated Cell Sorting (MACS) using magnetic labeled antibodies against VE-Cadherin/CD144. For initial expansion and maturation of $CD144^{+}$ cells, optimal culture conditions were established and assessed by endothelial marker expression using FACS.

The highest and most robust EC marker expression was achieved when culturing CD144+ cells in endothelial growth medium (EGM-2) supplemented with 20% Fetal Calf Serum (FCS) and the TGFβ type I receptor inhibitor SB431542 on gelatin coated culture dishes. SB431542 sustains *ID1* expression, which is required for endothelial cell commitment and proliferation (James et al., 2010). Subsequently iPSC derived ECs were cultured in normal growth medium without SB431542 supplementation.

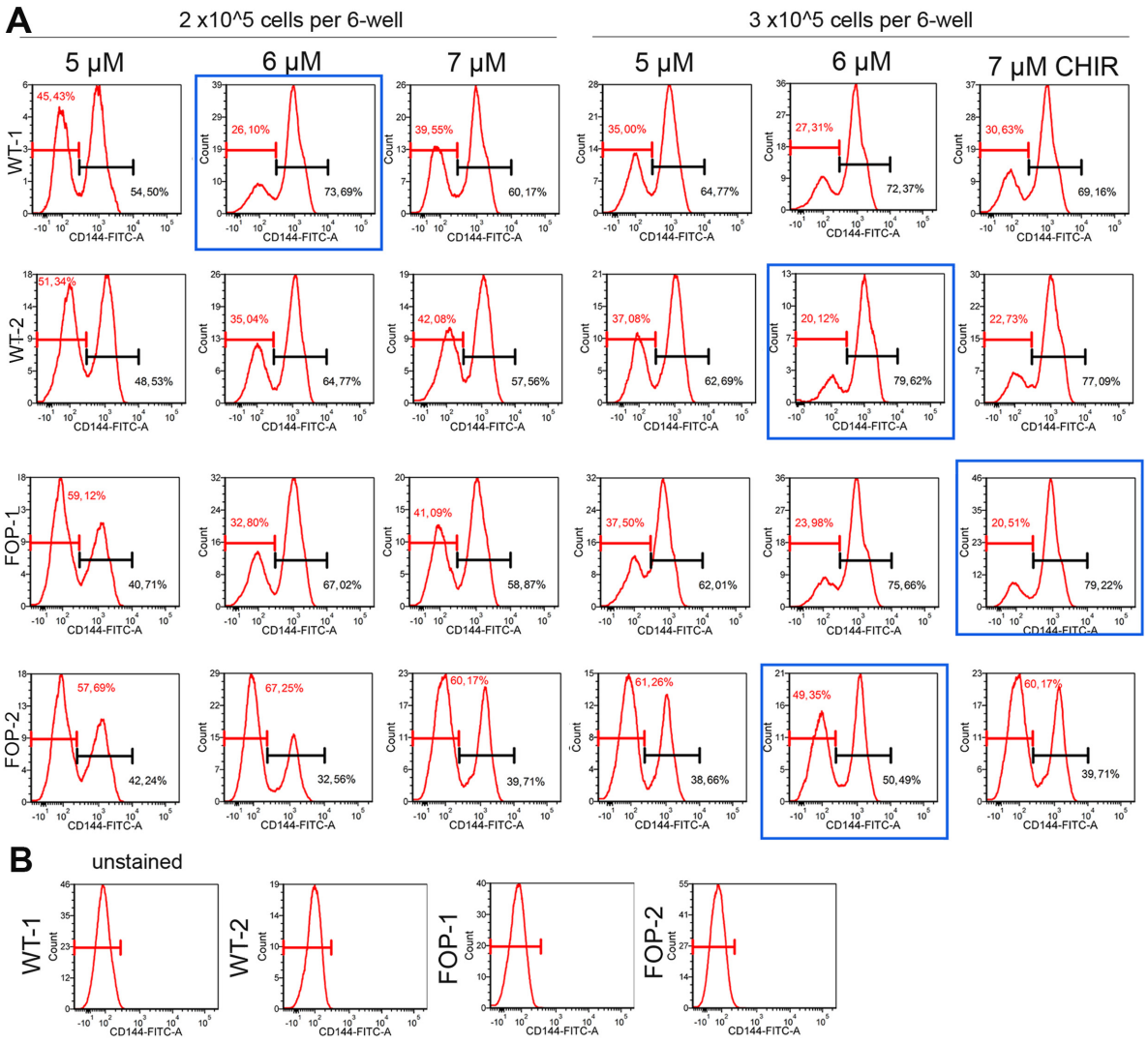

Figure 3.3 Establishment of endothelial differentiation conditions for iPSC lines. (**A**) Optimization of cell density and concentration of the GSK3-β inhibitor CHIR to achieve optimal iEC differentiation efficiency, which was assessed by FACS analysis of CD144+ cells after the MACS sort on day 10 for each of the two WT and two FOP iPSC lines. Experimental conditions with the highest iEC differentiation efficiency are framed with a blue square.(**B**) FACS analysisi of unstained controls.

Table 15 Optimized cell numbers and GSK3-β inhibitor (CHIR99021) concentration for endothelial differentiation of four iPSC donors.

	iPSC-WT-1	iPSC-WT-2	iPSC-FOP-1	iPSC-FOP-2
CHIR99021	6 µM	6 µM	7 µM	6 µM
Cell number/ 6-well	$2x10^5$	$3x10^5$	$3x10^5$	$3x10^5$

3.1.3 WT and FOP iPSC derived ECs are functional and express endothelial markers comparable to primary ECs

After successful generation of robust amounts of iPSC derived ECs, from now on called iECs, complementary methods were used to characterize the endothelial identity of WT and FOP iECs in comparison to primary ECs, using Human Umbilical Vein Endothelial Cells (HUVECs). WT and FOP iECs formed dense monolayers (Figure 3.4A), showed junctional marker expression of VE-Cadherin and PECAM-1 comparable to primary ECs (HUVECs), which was analyzed by immunofluorescence stainings (Figure 3.4A), FACS (Figure 3.4B), and Real Time Polymerase Chain Reaction (RT-PCR) (Figure 3.4C). Moreover, additional EC markers were analyzed by RT-PCR and revealed that WT and FOP iECs robustly expressed *VEGFR1*, *VEGFR2* (*KDR*), von Willebrand factor (*vWF*) and Neuropillin (*NRP1*) (Figure 3.4C). Interestingly, some endothelial markers, such as *VEGFR1* and *KDR* were much higher expressed in iECs compared to HUVECs.

The vascular system is comprised of arterial, venous and lymphatic vessels and is characterized by functional heterogeneity and tissue-specific vascular beds. Thus, primary ECs exhibit heterogenous features and function depending on their vascular origin. Up to date, vascular bed identity has been barely addressed in differentiation protocols of iPSCs to ECs (Williams and Wu, 2019), including the method adapted for this study (Patsch et al., 2015). Therefore, it was asked, if the here generated iECs show any vessel specific properties. Thus, the expression of arterial and venous markers was assessed in iECs compared to primary ECs of vein or artery origin using HUVECs and Human Umbilical Artery Endothelial Cells (HUAECs) (Figure 3.5). Expression of the arterial markers Ephrin B2 (*EFNB2),* Hes related Enhancer protein 2 (*HEY2)* and the Netrin receptor *UNC5B* confirmed arterial identity in HUAECs, which were also expressed by WT and FOP iECs (Figure 3.5A). Mean expression values for all arterial markers were even higher in iECs compared to HUAECs. However, WT and FOP iECs also expressed the venous markers *COUP-Transcription factor II, EPHB4* and Inhibitor of Differentiation (*ID1)* (Figure 3.5B). HUVECs showed the highest mean expression of all venous markers compared to HUAECs and iECs. In sum, WT and FOP iECs robustly expressed arterial markers comparable or even higher to primary HUAECs but also show venous marker expression, which indicates a pre-mature not terminally defined EC identity.

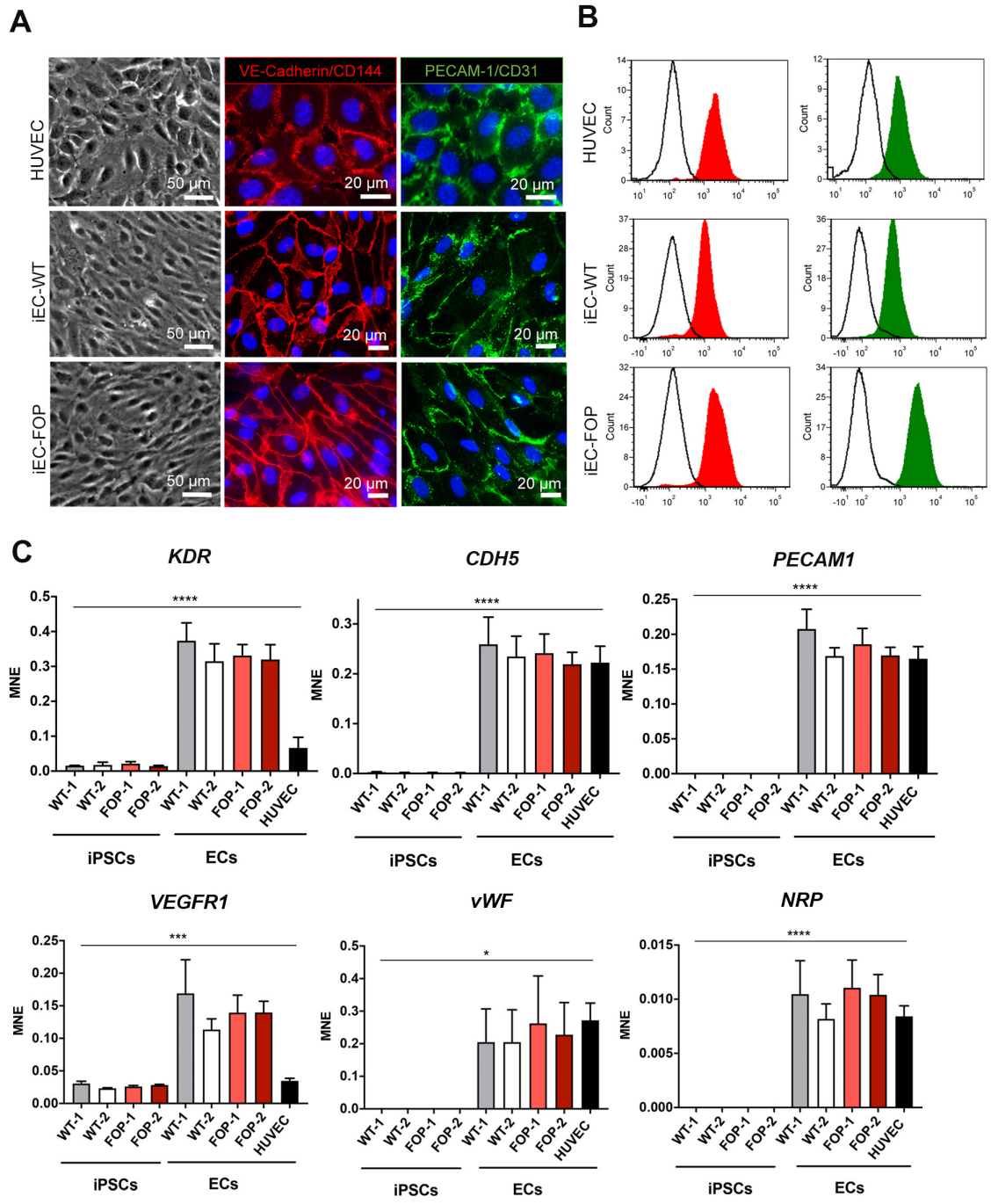

Figure 3.4 WT and FOP iECs express endothelial markers.
(**A**) Phase contrast and immunofluorescence staining of EC markers CD144 and CD31 (iEC WT-1, FOP-1, HUVEC). (**B**) FACS analysis of EC markers CD144 and CD31 (WT-1, FOP-1, HUVEC). (**C**) RT-PCR of EC marker expression in WT and FOP iPSCs compared to iECs (n=4). Data is represented as mean normalized expression (MNE) ± Standard Deviation, * p<0.05,** p<0.01, ***p<0.001, ****p< 0.0001 significance was calculated using one-way ANOVA. Modified from (Hildebrandt et.al., Stem Cell Rev Rep, in press 2020).

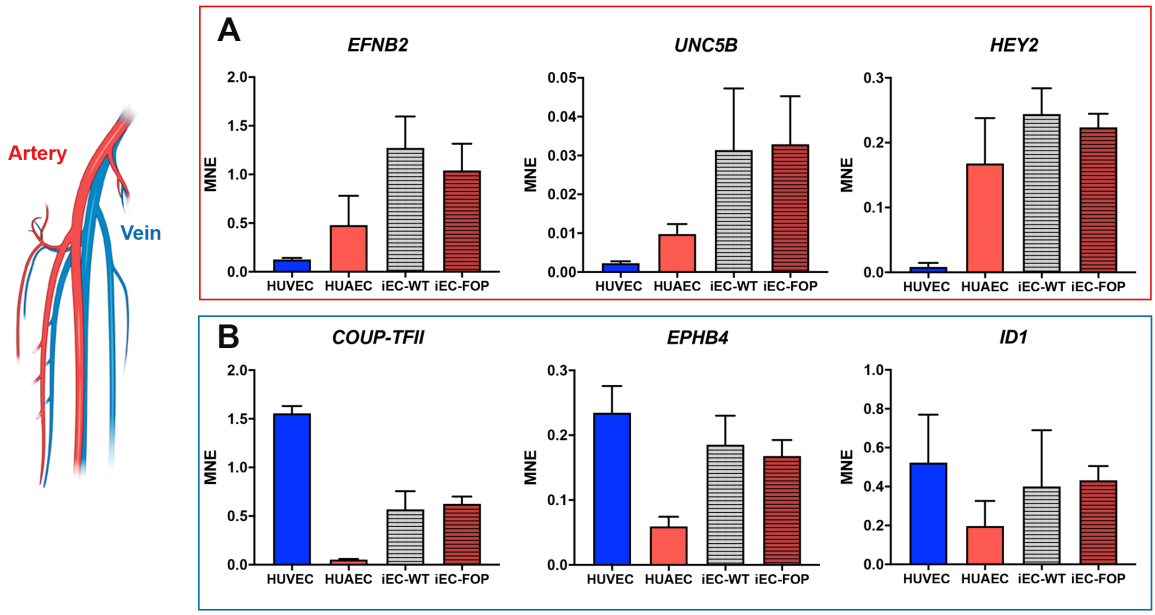

Figure 3.5 Arteriovenous identity of iECs. (**A-B**) RT-PCR of arterial (red box) and venous (blue box) marker expression in WT and FOP iECs (n=4) compared to primary vein (HUVECs) (n=3) and arterial ECs (HUAECs) (n=3). Data is represented as mean normalized expression (MNE) ± Standard Deviation (SD).

To test the functionality of WT and FOP iECs *in vitro*, the ability of iECs to form a functional endothelial barrier was assessed by impedance measurements. For more detailed method description see **3.8.1**. Therefore, iECs were grown to confluence on gold electrode arrays. WT and FOP iECs barrier formation was validated by constant resistance values, derived from impedance measurement at 4000 Hz (Figure 3.6A,B). Treatment with the known permeability inducing factor VEGFA caused disruption of cell-cell junctions as observed by resistance reduction with a subsequent recovery to baseline, similar to HUVECs (Figure 3.6B).

Moreover, it was determined whether iECs respond to pro-inflammatory Tumor Necrosis Factor-α (TNF-α) with a pro-adhesive phenotype as in native vasculature. Indeed, TNF-α treatment for 2 hours resulted in enhanced expression of intracellular adhesion molecule-1 (*ICAM-1*) in iECs (Figure 3.6D). In addition, the ability of iECs to form tubular structures was validated *in vitro* in a 3D-like environment using Matrigel (Figure 3.6C,E).

In summary, these findings show that WT and FOP iPSCs can be differentiated in high efficiencies to functional ECs without obvious genotype differences in the here assessed EC characteristics.

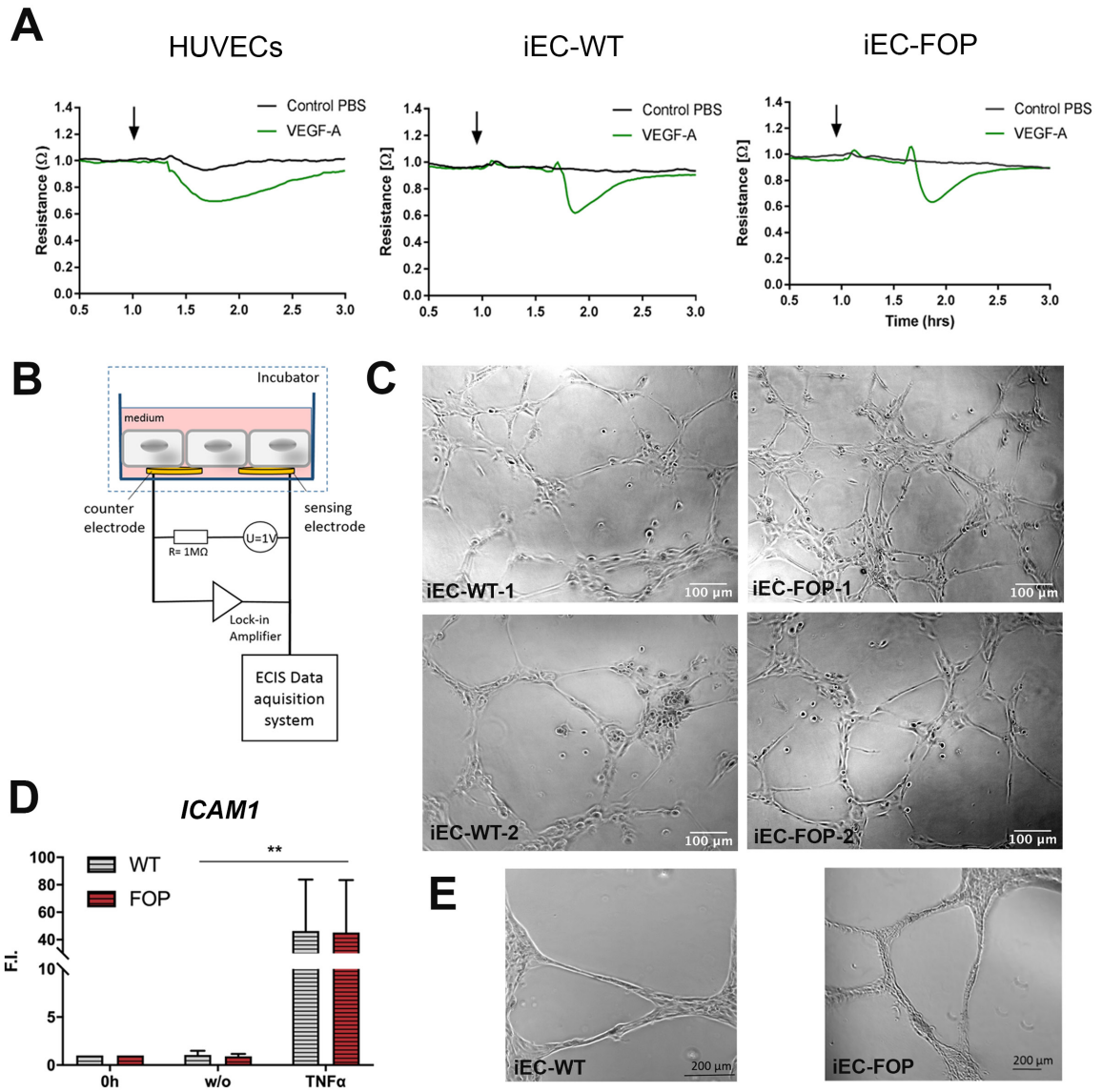

Figure 3.6 iECs show in vitro functionality. (**A**) Representative VEGFA induced endothelial permeability in iECs and HUVECs. Cells were seeded on gold electrode arrays 72 hours before measurement and grown to confluency. Cells were starved 4-6 hours before stimulation with VEGFA (2 nM). Impedance was measured at 4000 Hz and is depicted as resistance, normalized to 1 hour time point before stimulation. (**B**) Schematic cross section of an Electric Cell-Substrate Impedance Sensing (ECIS) culture well. ECs are seeded on top of sensing and counter gold electrodes in cell culture arrays until cells have formed a confluent monolayer. During measurement the electrodes are connected to a lock-in amplifier and a constant alternating current signal is applied via a 1 MΩ resistor. (**C,E**) Representative phase contrast images of tube like structures formed by WT and FOP iECs on Matrigel after 24 hours. (**D**) RT-PCR of *ICAM1* expression BMP upon 2 hours TNFα (0.6 nM) treatment in iECs (n=2). Data is shown as mean fold induction (F.I.) ± SD ** p<0.01 significance was calculated relative to unstimulated (w/o) using two-way ANOVA. (SD: Standard Deviation) Modified from (Hildebrandt et.al., Stem Cell Rev Rep, in press 2020).

3.2 Endothelial differentiation of iPSCs changes the BMP and TGFβ receptor expression profile

3.2.1 ALK2 becomes upregulated upon endothelial differentiation of iPSCs

After differentiation of FOP patient iPSCs into ECs the FOP causing point mutation in the *ALK2*/*ACVR1* locus was confirmed by genotyping PCR (Figure 3.7C). Moreover, expression of *ALK2* in iPSCs was assessed by qPCR, which was even upregulated during EC differentiation of iPSCs (Figure 3.7A). Interestingly, *ALK2* and *ALK1* where the only BMP/TGFβ type I receptors showing upregulated expression during EC differentiation. Using specific primers, *ALK2* expression was further dissected in *ALK2-WT* and mutant *ALK2-R206H* transcripts.

The *ALK2-WT* transcript was expressed in WT and FOP iPSC but became only upregulated in WT upon endothelial differentiation to iECs (Figure 3.7B). As expected the mutant *ALK2-R206H* transcript was only expressed in FOP iPSCs and becomes even upregulated upon differentiation to FOP iECs with more elevated expression in FOP donor 2 compared to donor 1 (Figure 3.7B).

Thus, in FOP iPSC only the mutant *ALK2-R206H* transcript became upregulated upon endothelial differentiation, suggesting an unequal stoichiometry between ALK2-WT and ALK2-R206H in FOP iECs.

The other BMP type I receptors ALK3 and ALK6 did not change expression levels in iPSCs upon EC differentiation. Among the TGFβ type I receptors the ALK5 expression was reduced in iECs compared to iPSCs (Figure 3.7D). ALK7 was expressed in iPSCs but showed no expression upon endothelial differentiation (Figure 3.7D).

The preferred type I receptor ALK4 for ActivinA signaling showed equal expression in both iPSC and iEC lineages (Figure 3.7B).

Among the type II receptors the expression of BMPR2 and TGFBR2 receptors was highly increased in iECs compared to iPSCs, whereas in iPSC ACVR2A/B were higher expressed (Figure 3.7F).

In sum, *ALK1*, *ALK2, BMPR2 and TGFBR2* became upregulated upon endothelial differentiation. *ALK2-WT* transcript was expressed in both WT and FOP iPSC but in FOP only the ALK2 mutant transcript became upregulated after differentiation to FOP iECs.

Additionally, selected co-receptors were analyzed as its tissue specific expression contributes to fine tuning of BMP and TGFβ signal transduction. Endoglin is a known EC marker and functions as a co-receptor for BMP9 and BMP10 signaling in the endothelium and also binds other BMPs as well as Activin and TGFβ (Nickel et al., 2018). Consequently, Endoglin (*ENG*) became highly upregulated upon endothelial differentiation of iPSCs (Figure 3.7G). TGFBR3, also known as Betaglycan is more ubiquitously expressed in human tissues, which is also confirmed by unchanged expression in iPSCs compared to iECs (Figure 3.7G). Cripto (*TDGF1*) acts as co-receptor for Activin and Nodal signaling and is mainly expressed in embryonic tissues (Nickel et al., 2018). Accordingly, was high *TDGF1* expression observed in iPSCs with minimal expression detected in iECs (Figure 3.7G). Based on recent discoveries in the Knaus lab (Dissertation Jatzlau Jerome, 2019) the expression of *UNC5B*, an arterial BMP co-receptor, was also analyzed and was robustly expressed in iECs but also to the same extend in iPSCs (Figure 3.7G).

In sum, among the co-receptors, only Endoglin became highly upregulated whereas Cripto became downregulated upon endothelial differentiation of iPSCs.

Collectively, no significant changes of receptor expression levels were detected between WT and FOP iECs except higher *ALK2-WT* transcript expression in WT iECs compared to FOP iECs.

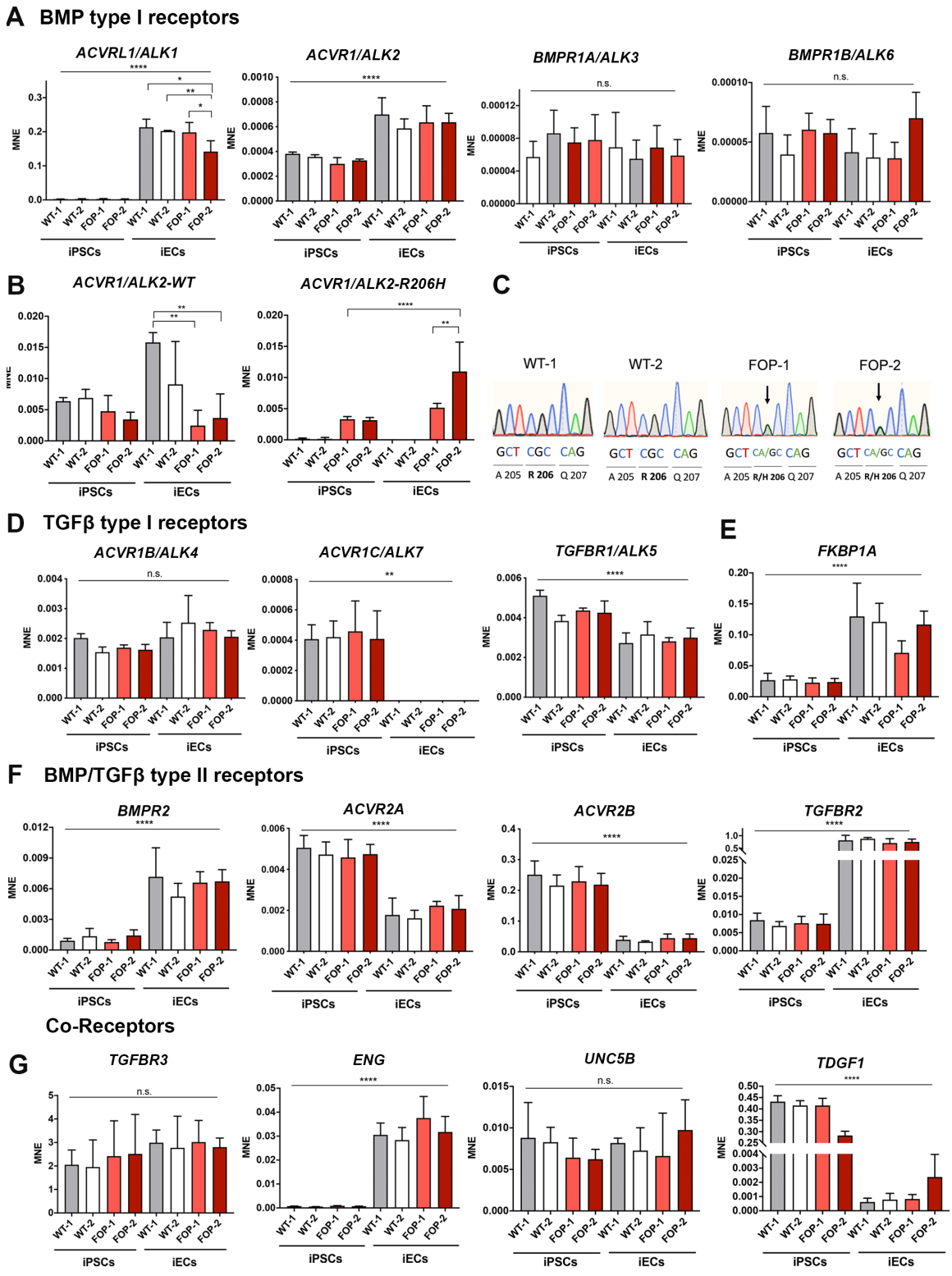

Figure 3.7 Endothelial differentiation of iPSC changes BMP and TGFβ receptor expression profiles. (**A,B, D-G**) RT-PCR of BMP and TGFβ receptor and co-receptor expression in WT and FOP iPSCs compared to iECs cultured in full medium (n=3-4). Data is shown as MNE ± SD. (**C**) Sequencing of genomic DNA of iECs from 4 donors at locus of *ACVR1* R206H mutation. Arrows indicate point mutation. * p<0.05,** p<0.01, ***p<0.001, ****p< 0.0001 significance was calculated using one-way ANOVA. (MNE: mean normalized expression; SD: Standard Deviation). Modified from (Hildebrandt et.al., Stem Cell Rev Rep, in press 2020).

3.2.2 **iECs show an endothelial BMP/TGFβ receptor expression profile**

Mean normalized expression (MNE) values from RT-PCR analysis may give an indication of transcript amounts from different genes. However, the RT-PCR methodology is limited to assess whole transcript abundance in a biological sample and whether one receptor is more expressed than the other. Receptor transcript amounts give an indication about possible protein receptor levels on the membrane. Comparison of relative expression levels of different receptors enable an approximation, which receptor signaling complexes may form among the pleiotropic combinatorial possibilities. In order to estimate transcript abundance of different receptors, data from transcriptome analysis was generated by RNA Sequencing (RNASeq) for iECs and compared to data from HUVECs (Mendez et al., in preparation) and publicly available data from iPSCs, which was retrieved from the Gene Expression Omnibus (GEO) database (Figure 3.8).

RNASeq of iECs revealed an EC specific BMP/TGFβ receptor expression profile comparable to HUVECs with *ALK1* (*ACVR1L*) as the most expressed type I receptor and *BMPR2* and *TGBR2* as the most expressed type II receptors (Figure 3.8A-C). After *ALK1* is *ALK2 (ACVR1)* the second most expressed BMP type I receptor in HUVECs (3 donors) and WT-2 and FOP-2 iECs whereas ALK6 (*BMPR1B*) showed no and ALK3 (*BMPR1A*) minor expression (Figure 3.8A-C). Interestingly, the other donor pair WT-1 and FOP-1 showed equal expression of ALK2 *(ACVR1)* and ALK3 (*BMPR1A*) but also no ALK6 (*BMPR1B*) expression (Figure 3.8A,B). Among TGFβ type I receptors, only ALK4 (*ACVR1B*) and ALK5 (*TGFBR1*) were expressed in iECs and HUVECs. But in HUVECs the amounts of ALK5 (*TGFBR1*) and ALK4 (*ACVR1B*) were lower compared to ALK2 *(ACVR1),* whereas in iECs ALK4 and ALK5 are equally expressed as ALK2 or even higher (Figure 3.8A-C).

Compared to ECs iPSCs showed a different receptor expression profile (Figure 3.8D). iPSCs only expressed the BMP type I receptors ALK3 (*BMPR1B*) and ALK2 (*ACVR1*) (Figure 3.8D). As ECs, iPSC expressed the TGF receptors ALK4 (*ACVR1B*) and ALK5 (*TGFBR1*). All type II receptors were expressed in iPSC, but by far ACVR2B showed the highest levels (Figure 3.8D). Interestingly, the expression levels of co-receptors were more heterogenous between iEC donors, HUVECs and iPSCs (Figure 3.8). Endoglin (*ENG*) and Neuropillins (*NRP1, NRP2*) showed the highest expression in both iECs and HUVECs whereas only *NRP2* is expressed in iPSCs (Figure 3.8). For example, Betaglycan was only robustly expressed in iECs. Additionally, *UNC5B,*

BAMBI and *c-KIT* were expressed in iECs and iPSCs, but only minorly detected in HUVECs. In contrast to ECs Cripto (*TDGF1)* showed the highest mean expression among the co-receptor in iPSCs confirming the RT-PCR results (Figure 3.7).

In summary, transcript expression profiles of ALK1 (*ACVR1L*), ALK2 (ACVR1) and *BMPR2* as well as *TGFBR2* of iECs were comparable to HUVECs, whereas expression levels of other receptors and co-receptor were more heterogenous indicating vascular bed specificity. In contrast, iPSCs showed a distinct characteristic receptor expression profile with high ALK3 (*BMPR1B*) and *ACVR2B* expression accompanied with high expression of the co-receptor Cripto (*TDGF1*).

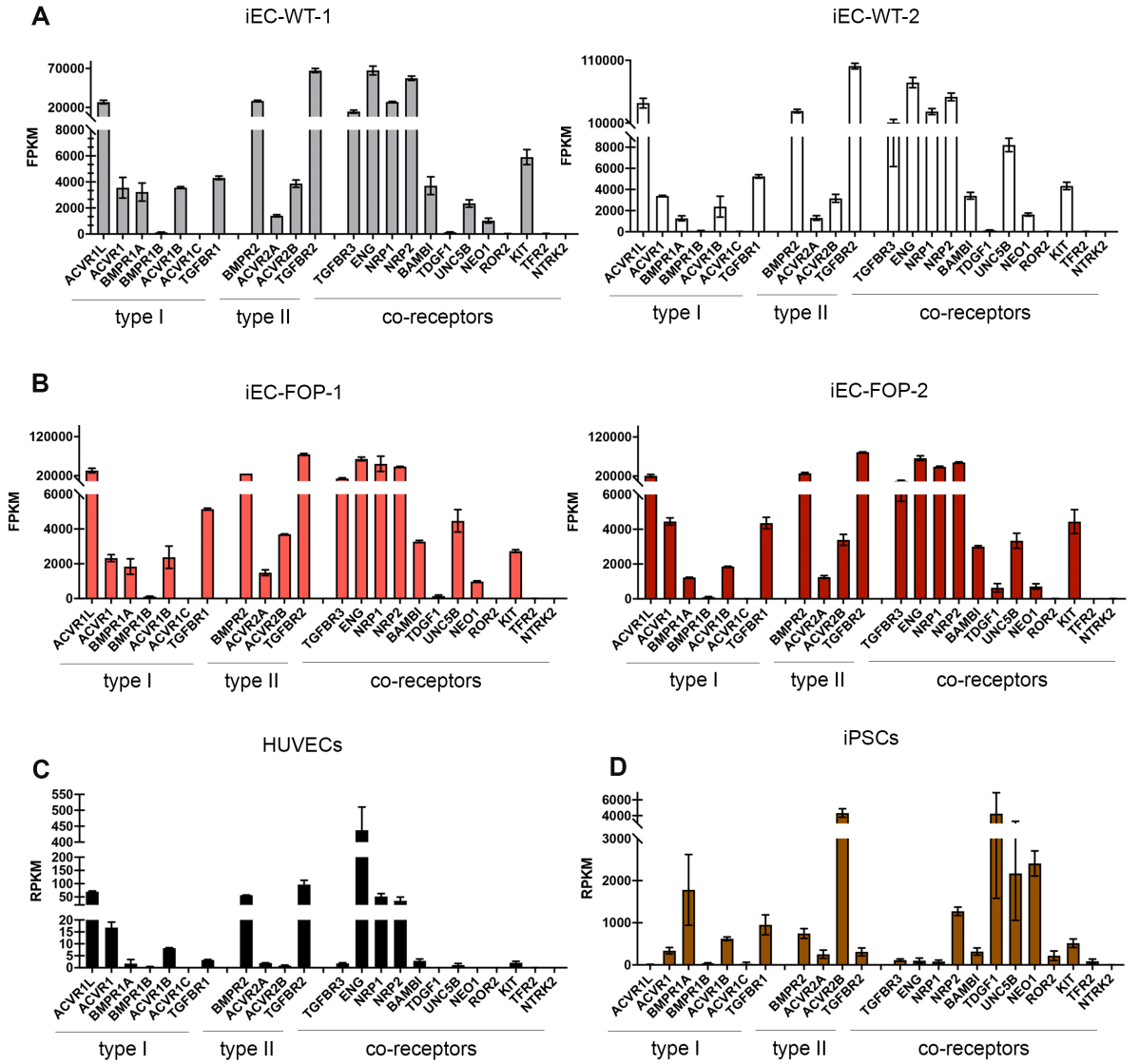

Figure 3.8 Endothelial Cells have a specific BMP and TGFβ transcriptome. Transcript expression levels of BMP and TGFβ receptors and co-receptors shown as mean FPKM (Fragments Per Kilobase of transcript per Million reads mapped) or RPKM (Reads Per Kilobase of transcript per Million reads mapped) values ± SD of RNASeq data of (**A-B**) WT and FOP iECs (n=2), (**C**) HUVECs (n=3) and (**D**) iPSCs (n=3). RNASeq data of iECs is derived from (Hildebrandt et.al., Stem Cell Rev Rep, in press 2020) and HUVEC data is derived internally from (Mendez et al., in preparation) and iPSC from the public GEO database (ID: GSE141136). (SD: Standard Deviation).

3.3 FOP iECs gain aberrant SMAD responses

3.3.1 **ActivinA and BMP6 are the most expressed ligands in iECs**

After analysis of the BMP and TGFβ receptor expression levels in the FOP iEC disease model the TGFβ family ligand expression was analyzed. Transcriptomics revealed that among the Activin/BMP ligands, *INHBA* (ActivinA) and *BMP6* showed the highest expression in iECs (Figure 3.9). By far *TGFβ1* was the most expressed ligand among the TGFβ family. The same ligand expression pattern was also observed in HUVECs, indicating a characteristic ligand expression pattern for ECs (Figure 3.9A-C).

This is supported by the comparison with iPSCs, which show differential expression pattern of the TGFβ ligand family (Figure 3.9D). In iPSCs, *BMP7* showed the highest expression among the BMP ligands. Only minor *INHBA* and *BMP6* expression was detected, but interestingly *NODAL and LEFTY1/2* were upregulated compared to ECs. *TGFβ1* is also robustly expressed in iPSC but the highest expression was observed for *GDF11* (Figure 3.9D).

In sum, *TGFB1*, *BMP6* and *INHBA* (ActivinA) are the most expressed ligands among the BMP, Activin and TGFβ ligand classes in iECs and HUVECs and became highly upregulated upon endothelial differentiation of iPSCs, which was confirmed by RT-PCR (Figure 3.9E,F).

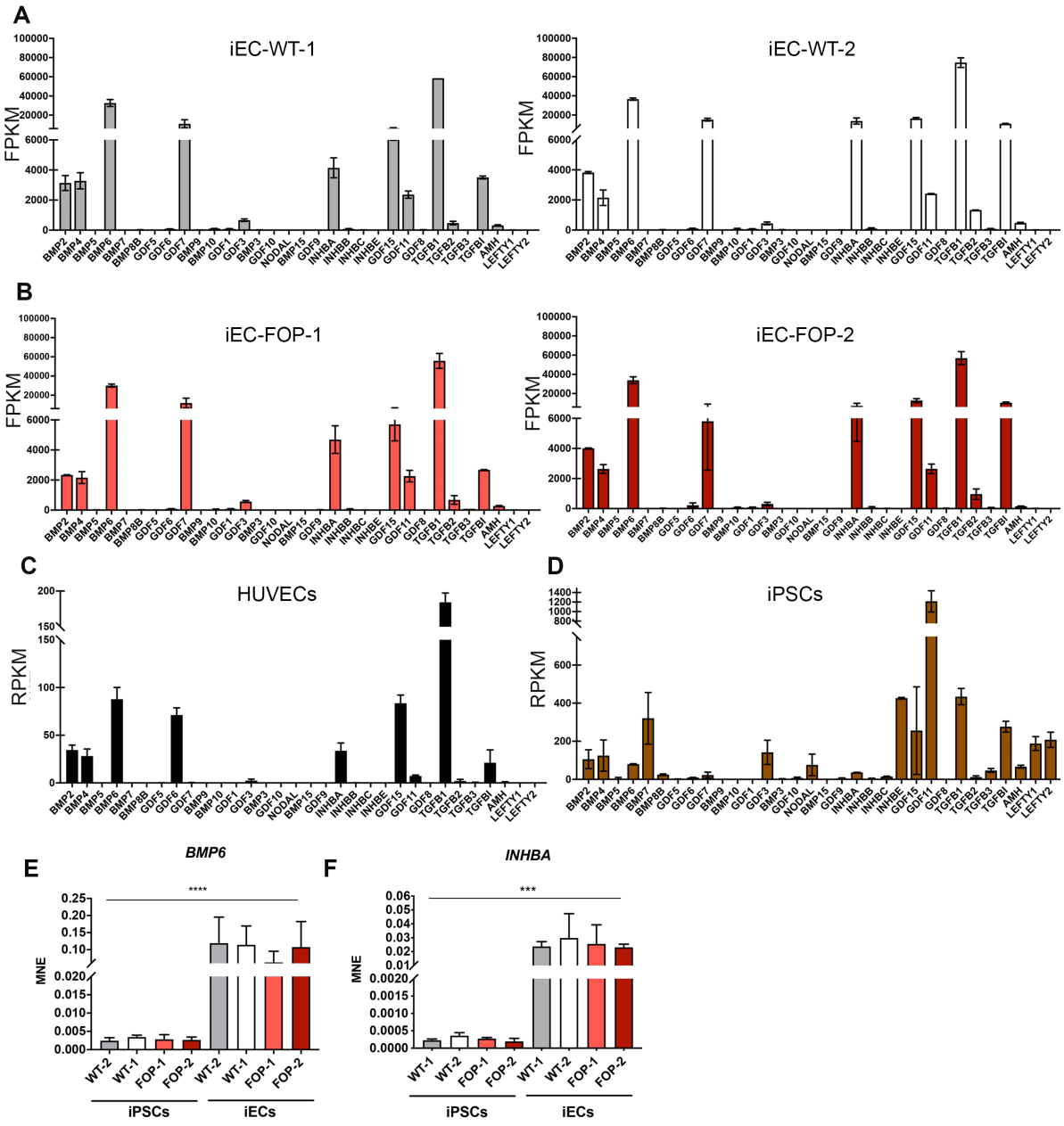

Figure 3.9 ActivinA and BMP6 become upregulated upon endothelial differentiation of iPSCs. Transcript expression levels of TGFβ family ligands are shown as mean FPKM (Fragments Per Kilobase of transcript per Million reads mapped) or RPKM (Reads Per Kilobase of transcript per Million reads mapped) values ± SD of RNASeq data from (**A-B**) WT and FOP iECs (n=2), (**C**) HUVECs (n=3) and (**D**) iPSCs (n=3). RNA Seq data of iECs is derived from (Hildebrandt et.al., Stem Cell Rev Rep, in press 2020) and HUVEC data is derived internally from (Mendez et al., in preparation) and iPSC from the public GEO database (ID: GSE141136). (**E-F**) RT-PCR of BMP6 (n=4) and INHBA (ActivinA) (n=3) expression in WT and FOP iPSCs compared to iECs cultured in full medium. Data is shown as MNE ± SD. ***p<0.001, ****p< 0.0001 significance was calculated using one-way ANOVA. (SD: Standard Deviation; MNE: Mean Normalized Expression). A-B is derived from (Hildebrandt et.al., Stem Cell Rev Rep, in press 2020).

3.3.2 **FOP iECs gain a SMAD1/5 response to ActivinA**

Next, the signaling responses of the BMP, Activin, and TGFβ ligand classed were investigated in iECs. BMP6 induced phosphorylation of SMAD1/5 in both, WT and FOP iECs in a similar dose-dependent manner with slightly higher sensitivity in FOP iECs at 3 nM and 10 nM, indicating hypersensitive signaling (Figure 3.10B and Figure 3.11C). Interestingly, high BMP6 concentrations also induced phosphorylation of SMAD2 in FOP iECs (Figure 3.10B). ActivinA increased SMAD2 phosphorylation in both WT and FOP iECs. In contrast, strong phosphorylation of SMAD1/5 was exclusively seen in FOP iECs but not in WT iECs (Figure 3.10A).

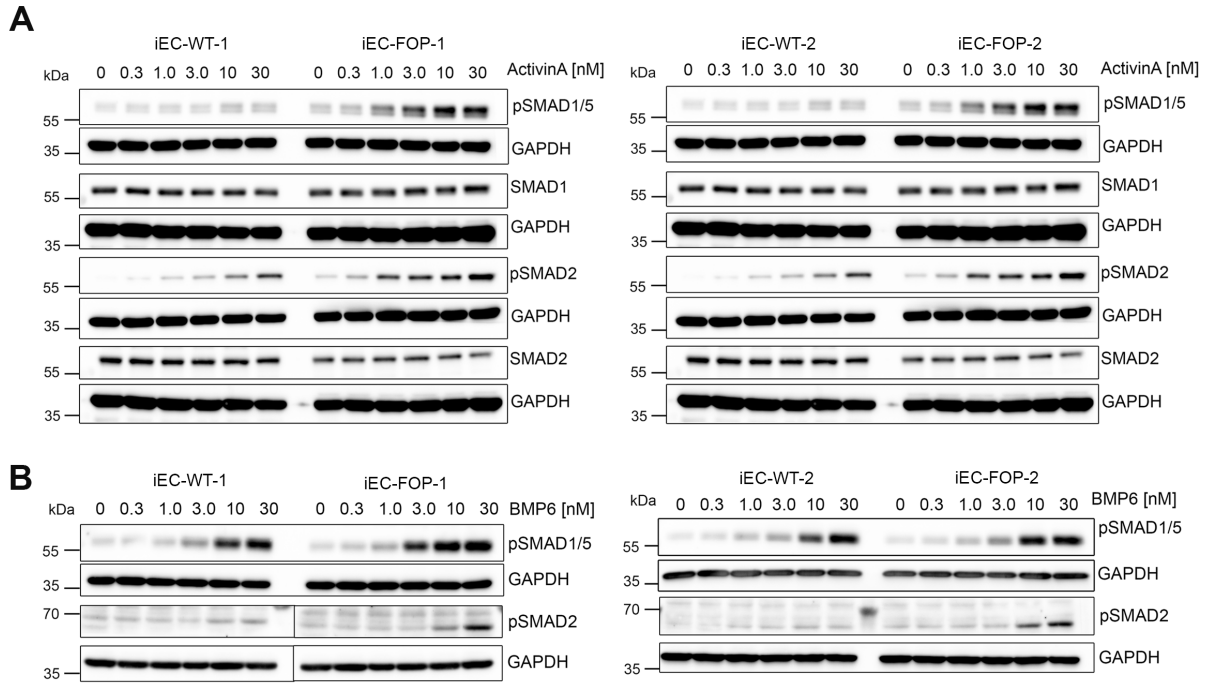

Figure 3.10 ActivinA induces phosphorylation of SMAD1/5 only in FOP iECs. (**A**) Representative Western Blot of protein lysates from WT and FOP iECs after stimulation with different doses of ActivinA, for 30 min. (**B**) Representative Western Blot of lysates from iECs after stimulation with different doses of BMP6 for 30 min. Modified from (Hildebrandt et.al., Stem Cell Rev Rep, in press 2020).

Aberrant ActivinA signaling was confirmed on SMAD1/5 target gene expression (*ID1/2/3)* in FOP iECs only, while BMP6 induced expression of *ID1/2/3* in WT and FOP iECs (Figure 3.11A), which was also confirmed on ID1 protein levels (Figure 3.11B). Additionally, BMP9 induced BMP signaling in WT and FOP iECs was assessed on *ID1/2/3* gene transcription (Figure 3.11A), which was confirmed on pSMAD1/5 levels (Figure 3.12A). Even though, pSMAD1/5 levels were already saturated at low concentrations of BMP9, it upregulated *ID1/2/3* gene transcription with the same fold

change as BMP6, about five-fold increase of *ID1/ID2* expression and two-fold for *ID3* expression (Figure 3.11A). Of note, for BMP target gene transcription analysis ligand concentrations of 5 nM for BMP6 and 0.1 nM for BMP9 were used, which were sufficient to induce a clear pSMAD1/5 response.

Moreover, it was analyzed whether TGFβ is also able to induce BMP signaling as it was observed for ActivinA. *ID1/2/3* expression did not change significantly upon TGFβ stimulation in WT and FOP iECs (Figure 3.11A). However, mean expression levels were always higher in TGFβ treated FOP iECs compared to WT iECs but without significance. *ID2* expression was even increased 2-fold by TGFβ compared to the control (w/o) in FOP iECs (Figure 3.11A). But this could not be confirmed on pSMAD1/5 levels (Figure 3.12C).

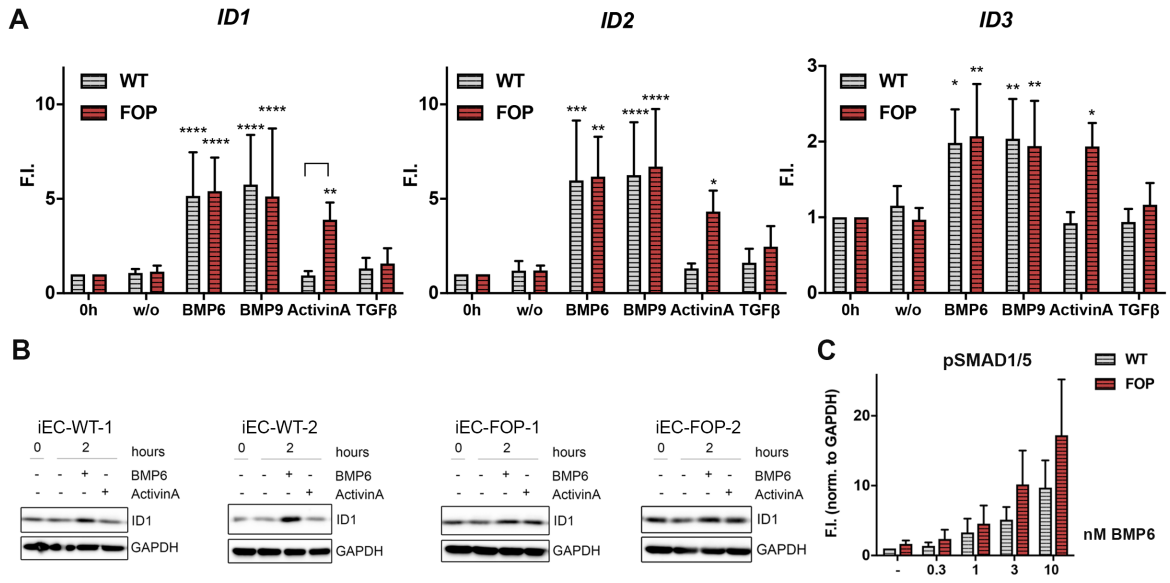

Figure 3.11 ActivinA induces transcription of BMP target genes only in FOP iECs. (**A**) RT-PCR of BMP target gene (ID1/2/3) expression upon BMP6, ActivinA (5 nM), BMP9 (0.1 nM) and TGFβ (0.2 nM) treatment of WT and FOP iECs (n=3-7) for 2 hours. Data is shown as mean F.I. ± SD. (**B**) Western Blot analysis of ID1 protein levels in protein lysates from WT and FOP iECs after 2 hours BMP6 and ActivinA treatment (**C**) Densiometric quantification of pSMAD1/5 protein levels relative to GAPDH of BMP6 treated WT and FOP iECs (n=3). Significance was calculated using two-way ANOVA relative to unstimulated (w/o) *p<0.05, ** p<0.01, ***p<0.001, ****p< 0.0001). (SD: Standard Deviation; F.I: Fold Induction). Modified from (Hildebrandt et.al., Stem Cell Rev Rep, in press 2020).

Compared to BMP6 and BMP9, WT and FOP iECs were not responsive to BMP2. But interestingly, very high BMP2 concentrations of 30 nM were able to induce phosphorylation of SMAD1/5 only in FOP iECs (Figure 3.12B).

Collectively, only FOP iECs gained a SMAD1/5 response to ActivinA and a SMAD2 response to BMP6. Thus, the generated FOP iEC disease model in this study is characterized by aberrant BMP6 and ActivinA SMAD signaling responses.

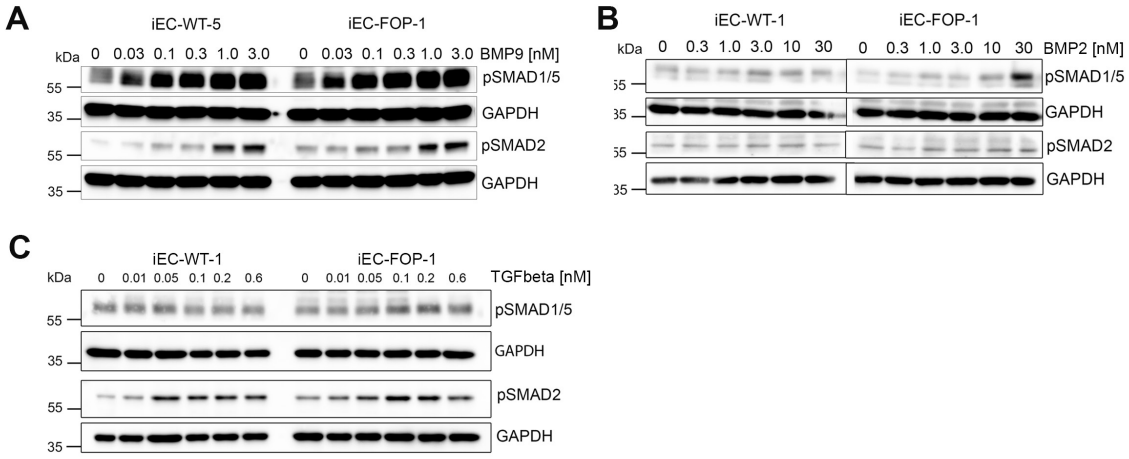

Figure 3.12 Responsiveness of FOP and WT iECs to other ligand groups of the TGFβ ligand family. Representative Western Blot of protein lysates from WT and FOP iECs after stimulation with different doses of (**A**) BMP9 (**B**) BMP2 and (**C**) TGFβ for 30 min.

3.4 ActivinA indirectly modifies the activity of the non-SMAD target AKT in FOP iECs

Based on aberrant SMAD responses by BMP6 and ActivinA in FOP iECs it was examined if these ligands also induce aberrations in non-SMAD signaling responses. Treatment of different concentrations with ActivinA did not induce phosphorylation of Protein kinase B (AKT) in WT or FOP iECs (Figure 3.13A). However, treatment of iECs with 10 nM ActivinA (or higher) resulted in reduced pAKT protein levels only in FOP iECs but not in WT iECs (Figure 3.13A). Time kinetic experiments showed that 10 nM ActivinA reduced phosphorylated AKT (pAKT) protein levels after 60 min and significantly after 120 min in both FOP donors but not in WT iECs (Figure 3.13B,C,F). BMP6 also reduced pAKT levels in FOP iECs but in contrast to ActivinA also in WT iECs (Figure 3.13D,E,F). Pre-treatment with the ALK2 targeting kinase inhibitor K02288 prevented BMP6 induced reduction of pAKT in WT and FOP iECs (Figure 3.13E,F), suggesting an ALK2 dependent effect. This is supported by the observation that the FOP specific reduction of pAKT by ActivinA was significantly rescued by K02288 in FOP iECs (Figure 3.13E,F).

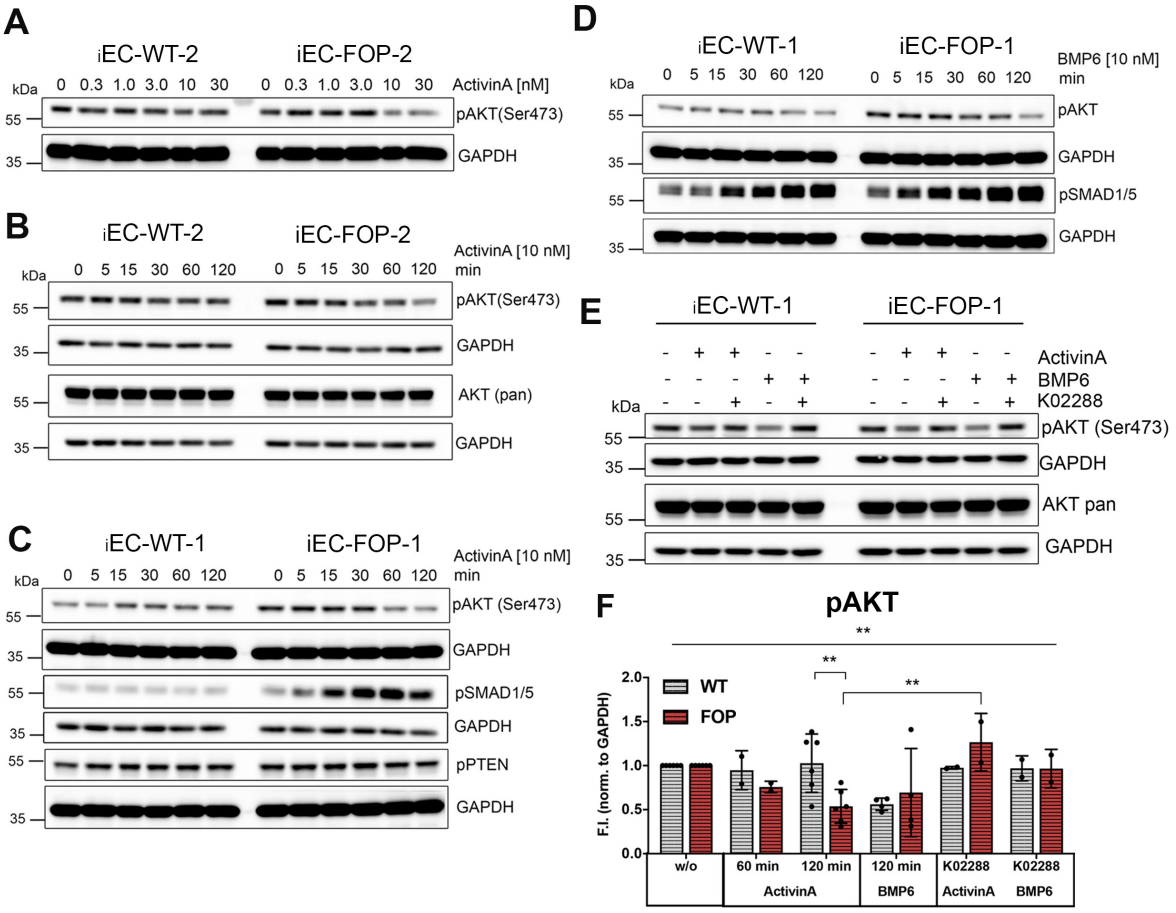

Figure 3.13 ActivinA reduces phosphorylated AKT levels in an ALK2 dependent manner only in FOP iECs.
(**A**) Representative Western Blot of protein lysates from WT and FOP iECs after stimulation with different doses of ActivinA, for 30 min. (**B-C**) Western Blot of protein lysates from FOP iECs after stimulation with ActivinA (10 nM) for different time points. (**D**) Western Blot of protein lysates from FOP iECs after stimulation with BMP6 (10 nM) for different time points. (**E**) Representative Western Blot of protein lysates from WT and FOP iECs pretreated with K02288 (0.5 µM) and stimulation with ActivinA or BMP6 (10 nM) for 120 min. (**F**) Densiometric quantification of phosphorylated (p) AKT protein levels relative to GAPDH in WT and FOP iECs after ActivinA and BMP6 treatment. Including pretreatment with the ALK1/ALK2 inhibitor K02288 (0.5 µM) for 1 hour with subsequent ligand stimulation. Data is shown as mean F.I. ± SD. (SD: Standard Deviation; F.I: Fold Induction).

In addition to AKT the p38 mitogen-activated protein kinase was analyzed upon BMP6 (10 nM) and ActivinA (10 nM) treatment. Whereas, TNFα as a positive control induced phosphorylation of p38, there was no change in p38 phosphorylation observed after treatment with BMP or ActivinA (Figure 3.14B)**.** This was confirmed by treating iECs with increasing concentrations of BMP6, which did not lead to phosphorylation of p38 (Figure 3.14A).

In sum, ActivinA did not activate the non-SMAD pathways of AKT and p38. However, ActivinA reduced phosphorylated AKT protein levels in FOP iECs, which was also confirmed for BMP6 in WT and FOP iECs.

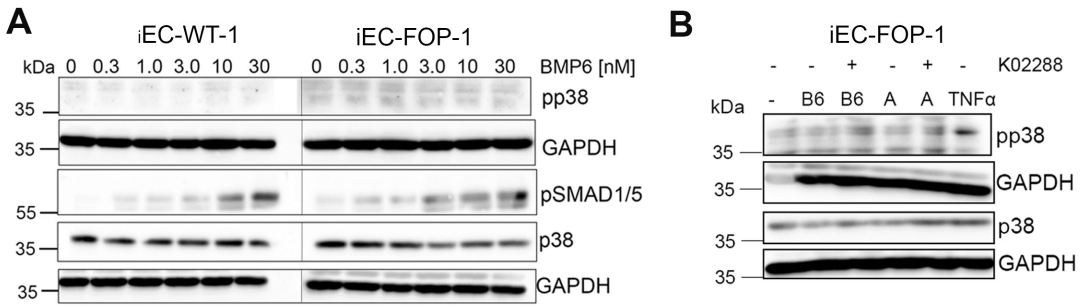

Figure 3.14 ActivinA has no influence on p38 activation. (**A**) Representative Western Blot of protein lysates from WT and FOP iECs after stimulation with different doses of BMP6 for 30 min. (**B**) Western Blot of protein lysates from FOP iECs pretreated with K02288 (0.5 µM) and stimulation with BMP6 (B6) (10 nM), ActivinA (A) (10 nM), TNFα.(0.6 nM).

3.5 Contribution of type I receptors and FKBP12 to aberrant SMAD responses

3.5.1 The ActivinA/SMAD1/5 response in FOP iECs is ALK2 dependent but independent of Activin type I receptors

The ActivinA induced phosphorylation of SMAD1/5 in FOP iECs was validated in a time kinetic experiment showing the earliest response after 30 min, a peak after 60 min and a decrease after 120 min (Figure 3.15A). Phosphorylated SMAD1/5 levels reduced earlier in FOP-2 iECs (Figure 3.15A).

To verify the contribution of type I receptors to ActivinA/SMAD1/5 signaling, iECs were pretreated with K02288, a specific ALK1/ALK2 kinase inhibitor or SB431542, an ALK4/ALK5/ALK7 kinase inhibitor (Figure 3.15B). iECs were pretreated with respective kinase inhibitors 1 hour before ligand stimulation.

As observed in previous results, ActivinA treatment caused only phosphorylation of SMAD1/5 in FOP iECs and this was efficiently prevented by the pretreatment with K02288 (Figure 3.15C), indicating an ALK2 dependent effect. In comparison, K02288 pre-treatment was also performed upon stimulation with BMP6, which prevented induction of SMAD1/5 phosphorylation in both WT and FOP iECs (Figure 3.15C). To investigate whether ActivinA/SMAD1/5 signaling in FOP iECs is dependent on Activin type I receptors, iECs were pretreated with different doses of SB431542 and stimulated with ActivinA. ActivinA induced SMAD2 phosphorylation was already inhibited at the lowest dose of SB431542 (Figure 3.15D). However, Activin induced phosphorylation of SMAD1/5 remained unchanged even when FOP iECs were pretreated with high

concentrations of SB431542 (Figure 3.15D). Thus, the signaling complex transducing aberrant ActivinA/SMAD1/5 responses is independent of ALK4/5/7 but dependent on ALK2.

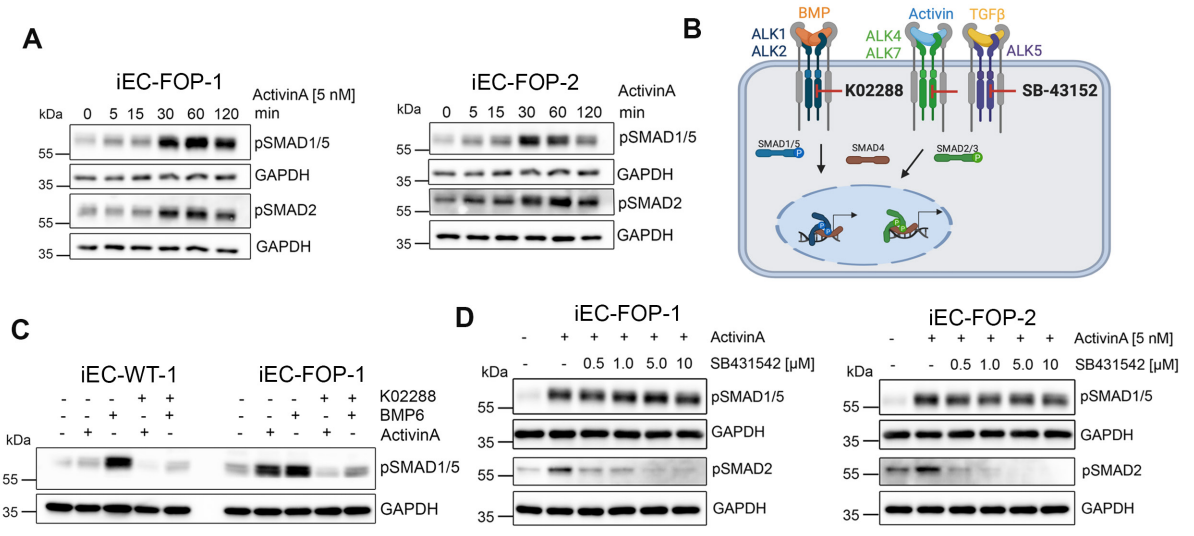

Figure 3.15 The ActivinA SMAD1/5 response in FOP iECs is ALK2 dependent but independent of Activin type I receptors. (**A**) Western Blot of protein lysates from FOP iECs after stimulation with ActivinA (5 nM) for different time points. (**B**) Scheme of kinase inhibitors targeting BMP or TGFβ type I receptors. (**C**) Representative Western Blot of protein lysates from WT and FOP iEC pretreated with ALK1/ALK2 inhibitor K02288 (0.5 μM) and treatment with BMP6, ActivinA for 30 min. (**D**) Western Blot of FOP iECs pretreated with different doses of ALK4/5/7 inhibitor SB431542 and treatment with ActivinA for 30 min. Modified from (Hildebrandt et.al., Stem Cell Rev Rep, in press 2020).

3.5.2 High BMP6 concentrations induced a TGFβ type I receptor dependent SMAD2 response in FOP iECs

Specific kinase inhibitors were also used to verify type I receptor contribution to BMP6 induced SMAD2 signaling in FOP iECs. As shown in (Figure 3.10B**),** BMP6 induced the phosphorylation of SMAD2 (pSMAD2) in FOP iECs at concentrations of 10 nM or higher (Figure 3.10B**).** This effect was even more pronounced at 30 nM of BMP6 and showed a significant increase of pSMAD2 protein levels in FOP iECs compared to unstimulated condition and BMP6 treated WT iECs (Figure 3.16A,B). BMP6/SMAD2 signaling in FOP iECs was confirmed on target gene transcription (*NEDD9*), which also showed a minor effect in WT iECs but without significance (Figure 3.16C). Pretreatment with SB431542 (Figure 3.15B) prevented SMAD2 phosphorylation by BMP6 (Figure 3.16A,B), which indicates the formation of mixed receptor complexes at high BMP6 concentrations in FOP iECs.

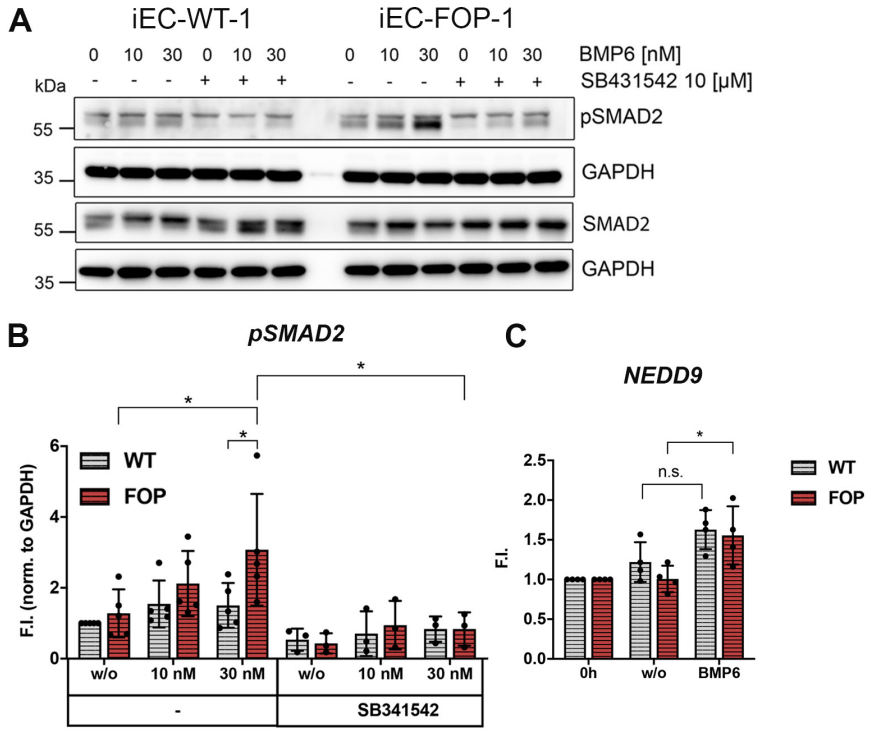

Figure 3.16 BMP6 induced SMAD2 phosphorylation is dependent on TGFβ type I receptors. (**A**) Representative Western Blot of WT and FOP iECs pretreated with ALK4/5/7 inhibitors SB431542 (10 µM) and treatment with BMP6 for 30 min. (**B**) Densiometric quantification of phosphorylated (p) SMAD2 protein levels relative to GAPDH in WT and FOP iECs after BMP6 treatment. Including pretreatment with the SB431542 inhibitor (10 µM) for 1 hour and subsequent ligand stimulation. **(C**) RT-PCR of the SMAD2/3 target gene upon 2 hours BMP6 (30 nM) treatment of iECs. Data is shown as mean F.I. ± SD. (SD: Standard Deviation; F.I: Fold Induction).

3.5.3 **Inhibition of FKBP12 increases basal SMAD1/5 signaling in FOP iECs**

The FK506-binding protein 12 (FKBP12) binds the un-phosphorylated glycine-serine rich (GS) domain of BMP and TGFβ type I receptors to suppress the kinase activity (Wang et al., 1996) (in more detail described in chapter 1.7.5). Concepts explaining hypersensitivity of mutant ALK2 suggested its impaired interaction with FKBP12 (Chaikuad et al., 2012; Shen et al., 2009; Song et al., 2010; van Dinther et al., 2010). Thus, it was analyzed whether inhibition of FKBP12 with FK506, a GS domain binding competitor, modifies BMP signaling in WT and FOP iECs (Figure 3.17B). Therefore, BMP target gene transcription of *ID1* was analyzed (Figure 3.17A).

FK506 treatment increased basal (w/o) levels of *ID1* expression only in FOP iECs, but not in WT iECs (Figure 3.17A), which confirms above mentioned concepts of hypersensitivity without ligand addition. Pretreatment with FK506 and subsequent stimulation with BMP6 only slightly increased mean *ID1* expression compared to BMP6 treatment alone, which was not significant (Figure 3.17A). The same was observed for ActivinA induced *ID1* expression in presence of FK506 (Figure 3.17A). TGFβ did not

induce *ID1* expression confirming previous shown results (Figure 3.17A). Even though *ID1* expression increased upon pretreatment with FK506 and subsequent TGFβ stimulation, the increase was equal to pretreatment with FK506 only (Figure 3.17A). Interestingly, FK506 pre-treated WT iECs showed a minor increase of *ID1* expression upon ActivinA treatment (Figure 3.17B). However, ActivinA induced *ID1* expression to a much lesser extent (~0.4 fold) in FK506 treated WT iECs compared to FOP iECs (~4 fold) (Figure 3.17A), suggesting that additional mechanisms are involved in ActivinA/SMAD1/5 signaling in FOP.

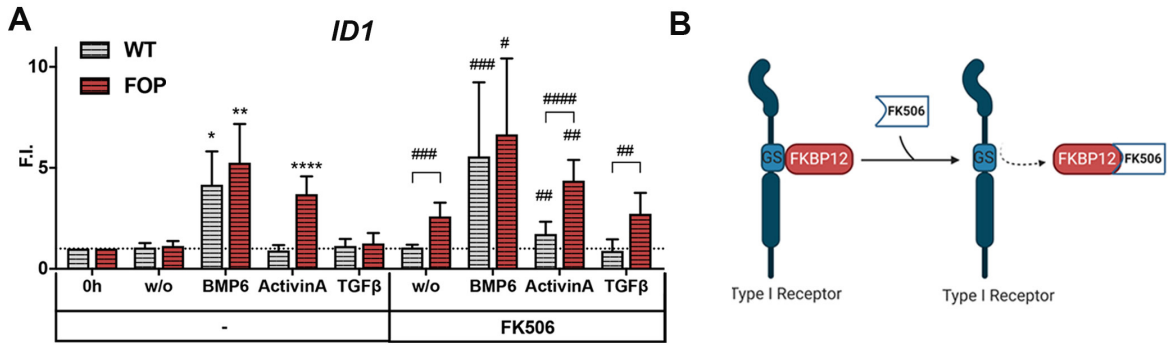

Figure 3.17 Inhibition of FKBP12 increases basal BMP target gene transcription. (**A**) RT-PCR of *ID1* expression of +/- FK506 (1 µM) pretreated (1 hour) WT and FOP iECs with subsequent stimulation of BMP6, ActivinA (5 nM) (n=4-6) and TGFβ (0.2 nM) (n=2) for 2 hours. Data is shown as mean F.I. ± SD. (**B**) Schematic illustration of the effect of FK506 on FKBP12 and type I receptors. * p<0.05,** p<0.01, ***p<0.001, ****p< 0.0001 significance was calculated relative to unstimulated (w/o) if not indicated otherwise, ##p<0.01, ###p<0.001,####p<0.0001 significance of FK506 treated samples to unstimulated (w/o) using two-way ANOVA. (SD: Standard Deviation; F.I: Fold Induction).

Influence of FK506 treatment on BMP signaling was additionally analyzed on pSMAD1/5 protein levels. Increased basal BMP signaling upon FK506 treatment was confirmed by pSMAD1/5 levels in FOP iECs compared to WT iECs (Figure 3.18A).
FK506 pretreatment increased ligand induced (BMP6, ActivinA, TGFβ) mean pSMAD1/5 levels in WT and FOP iECs but not significantly compared to ligand treatment only (Figure 3.18B-G). This is in line with *ID1* expression results, which showed no significant increase between pretreatment of FK506 and subsequent ligand stimulation and ligand treatment only (Figure 3.17A). Except for FK506 treated WT iECs, which showed minor upregulation of *ID1* upon ActivinA stimulation (Figure 3.17A). This trend was also observed upstream on pSMAD1/5 protein levels but was not significant (Figure 3.18C).

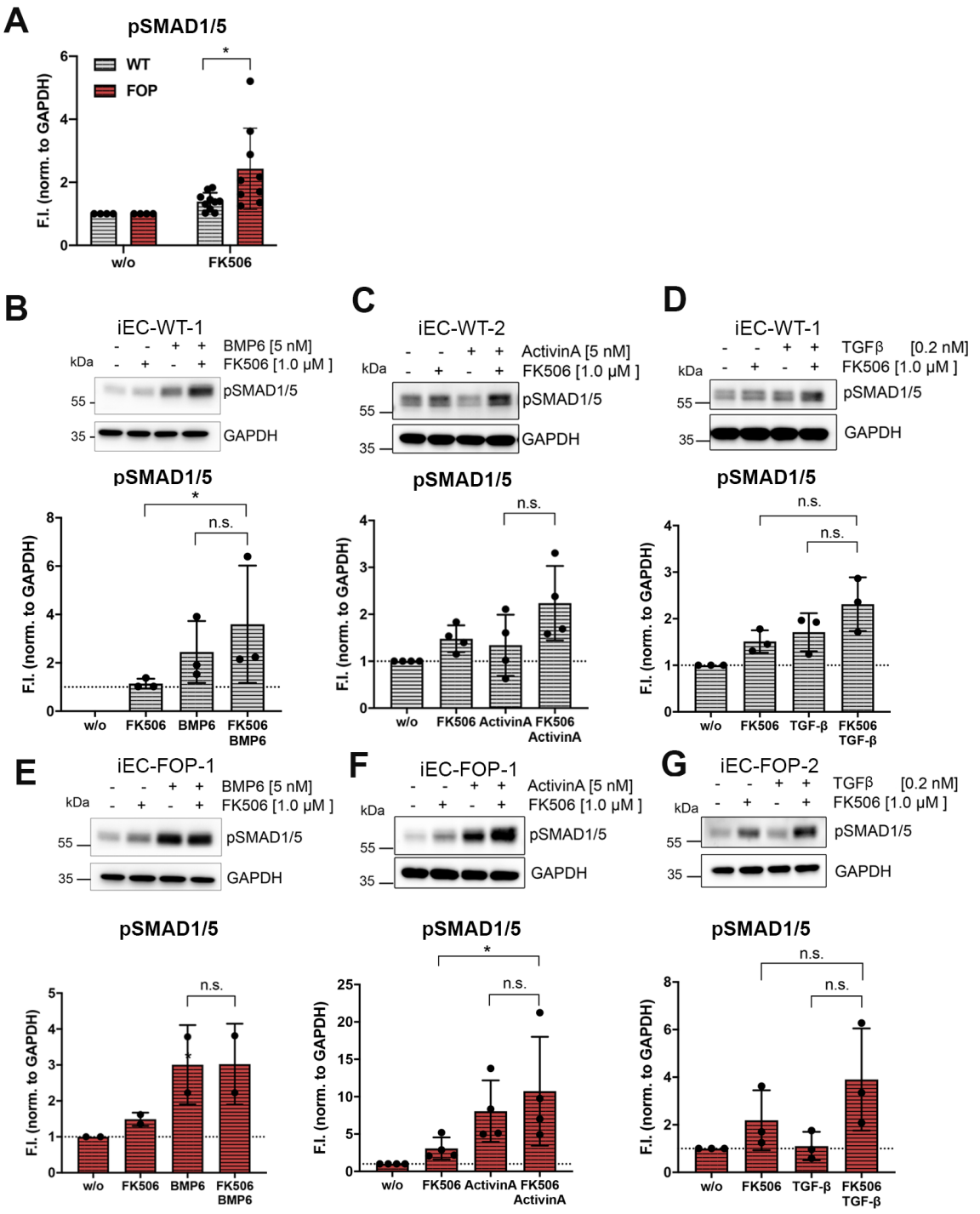

Figure 3.18 Inhibition of FKBP12 increases basal pSMAD1/5 levels. (**A**) Densiometric quantification of phosphorylated (p) SMAD1/5 protein levels relative to GAPDH in FK506 (1 µM) pretreated (1 hour) WT and FOP iECs. (**B-G**) Representative Western Blot and densiometric quantification of pSMAD1/5 levels relative to GAPDH of FK506 pretreated (1 hour) WT or FOP iECs stimulated with indicated ligands (BMP6, ActivinA (5 nM) or TGFβ (0.2 nM). Data is shown as mean F.I. ± SD. For A * $p<0.05$ significance was calculated using Student´s t-Test. (B-G) * $p<0.05$ significance was calculated using the non-parametric Kruskal-Wallis Test. (SD: Standard Deviation; F.I: Fold Induction).

To further validate, that inhibition of FKBP12 enables WT iECs to gain ActivinA dependent activation of SMAD1/5 signaling, a knock-down of the *FKBP12* (*FKBP1A*) mRNA was performed. Efficient knockdown of *FKBP12* was demonstrated by two si-RNA concentrations, which robustly reduced FKBP12 protein amounts compared to scrambled control siRNA (si-scr) (Figure 3.19A,B). After 48 hours of *FKBP12* knock-down, WT iECs were treated with ActivinA (10 nM) for 30 min but no pSMAD1/5 induction was detected (Figure 3.19A,B).

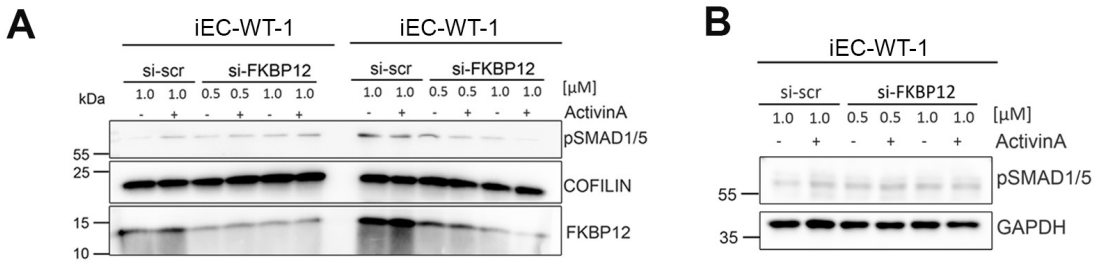

Figure 3.19 Knock-down of FKBP12 does not change ActivinA SMAD1/5 response in WT iECs. After 48 hour treatment with two different siRNAs (scrambled (scr), FKBP1A) WT iECs were starved and treated with ActivinA (10 nM) for 30 min. Representative Western Blots of protein lysates from WT iECs of n=3 independent experiments. (**A**) Detection of proteins upon knock-down by Western Blot: FKBP12, pSMAD1/5 and COFILIN as a housekeeper protein. (**B**) Western Blot detection of pSMAD1/5 and GAPDH as a housekeeper upon FKBP12 knockdown.

In summary, inhibitor experiments demonstrated that ActivinA/SMAD1/5 signaling is equally dependent on ALK2 as BMP6/SMAD1/5 signaling but independent on Activin type I receptors. Moreover, inhibition of FKBP12 is not sufficient to enable a gain of robust ActivinA/SMAD1/5 signaling in WT iECs. This was further supported by FKBP12 knock-down experiments and suggest that other mechanisms facilitate aberrant activation of SMAD1/5 by ActivinA in FOP.

3.6 RNA-Seq reveals a specific FOP transcriptome induced by ActivinA

To investigate the consequences of the observed aberrant ActivinA signaling in FOP iECs the transcriptional responses mediated by the phosphorylated SMADs were further analyzed. Therefore, a comprehensive whole transcriptome analysis was performed using RNA sequencing (RNASeq). Differential gene expression was analyzed between ActivinA (2 hours, 5 nM) and untreated WT and FOP iECs using experimental replicates of each donor (Figure 3.20A).

3.6.1 ActivinA upregulates SMAD2/3 target genes in iECs and additional genes only in FOP iECs

Two independent FOP donors were stimulated with ActivinA and shared 212 differentially expressed genes (DEG) (Figure 3.20B), whereof 64 showed a fold change (FC) of ≥ 1.5. Those genes were subjected to hierarchical cluster analysis comparing WT and FOP (Figure 3.20C). The z-score indicates that most genes in FOP iECs were up- and only few were downregulated by ActivinA (Cluster a, b). In WT iECs, cluster a and b did not show any significant regulation upon ActivinA treatment except of sub-cluster b1, which included the SMAD2/3 target genes *PMEPA1/TMEPAI* and *NEDD9* (Figure 3.20C). In contrast, cluster b2 included SMAD1/5 target genes, such as *ID1, ID3* and *SMAD6*) (Figure 3.20C). This indicates that ActivinA signaling leads to classical SMAD2/3 target gene transcription in WT and FOP iECs, whereas in FOP iECs additional genes were upregulated, including classical BMP/SMAD1/5 target genes.

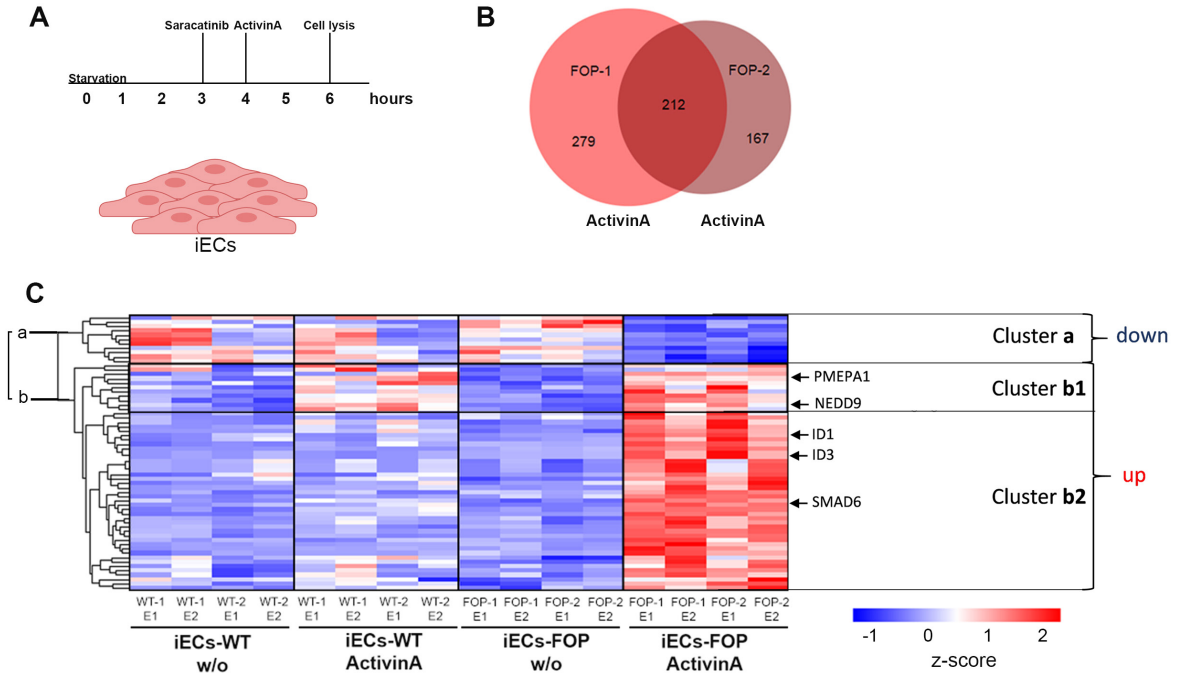

Figure 3.20 ActivinA induces a FOP-specific transcriptome in iECs. (**A**) Experimental setup: RNA Sequencing (RNASeq) of four iEC lines, starved for 4 hours and stimulated for 2 hours with 5 nM ActivinA from two independent experiments. (**B**) Venn diagram of RNASeq data presenting the number of differentially expressed genes (DEG) in both iEC donors (FOP-1 and FOP-2) stimulated with ActivinA. (**C**) Hierarchical clustering of shared DEG in both FOP donors (adjusted p-value<0.05; -0.58≤ log2FC ≥0.58) of ActivinA treated and untreated (w/o) iECs. Heatmap color coding shows z-score of DEG (red=high; blue=low). Labeling „up", „down" refers to DEG in FOP iECs upon ActivinA treatment. Fold Change=FC, E=Experiment). Modified from (Hildebrandt et.al., Stem Cell Rev Rep, in press 2020).

3.6.2 **ActivinA induced genes in FOP iECs are involved in blood vessel formation and activation of BMP and NOTCH pathways**

Subsequent functional gene ontology (GO) annotation analysis revealed significant association between upregulated genes and the BMP signaling pathway only in ActivinA treated FOP iECs (Figure 3.21A)**.** Whereas the TGFβ pathway was identified for upregulated genes (FC of ≥ 1.5) in both WT and FOP iECs upon ActivinA treatment (Figure 3.21A). Interestingly, the NOTCH signaling pathway was also identified in the enriched gene transcripts of ActivinA treated FOP iECs (Figure 3.21A). The integration of BMP and NOTCH signaling is known to regulate vascular patterning of sprouting blood vessels (Beets et al., 2013). And indeed, the GO analysis associated biological processes related to blood vessel and vascular development only with the enriched gene set of ActivinA treated FOP iECs (Figure 3.21B and Figure 3.22A). Moreover, ventricular septum development, which involves Endothelial to Mesenchymal Transition (EndMT) was among the high significant GO terms ($p \leq 0.01$) and only associated with ActivinA treated FOP iECs (Figure 3.21B).

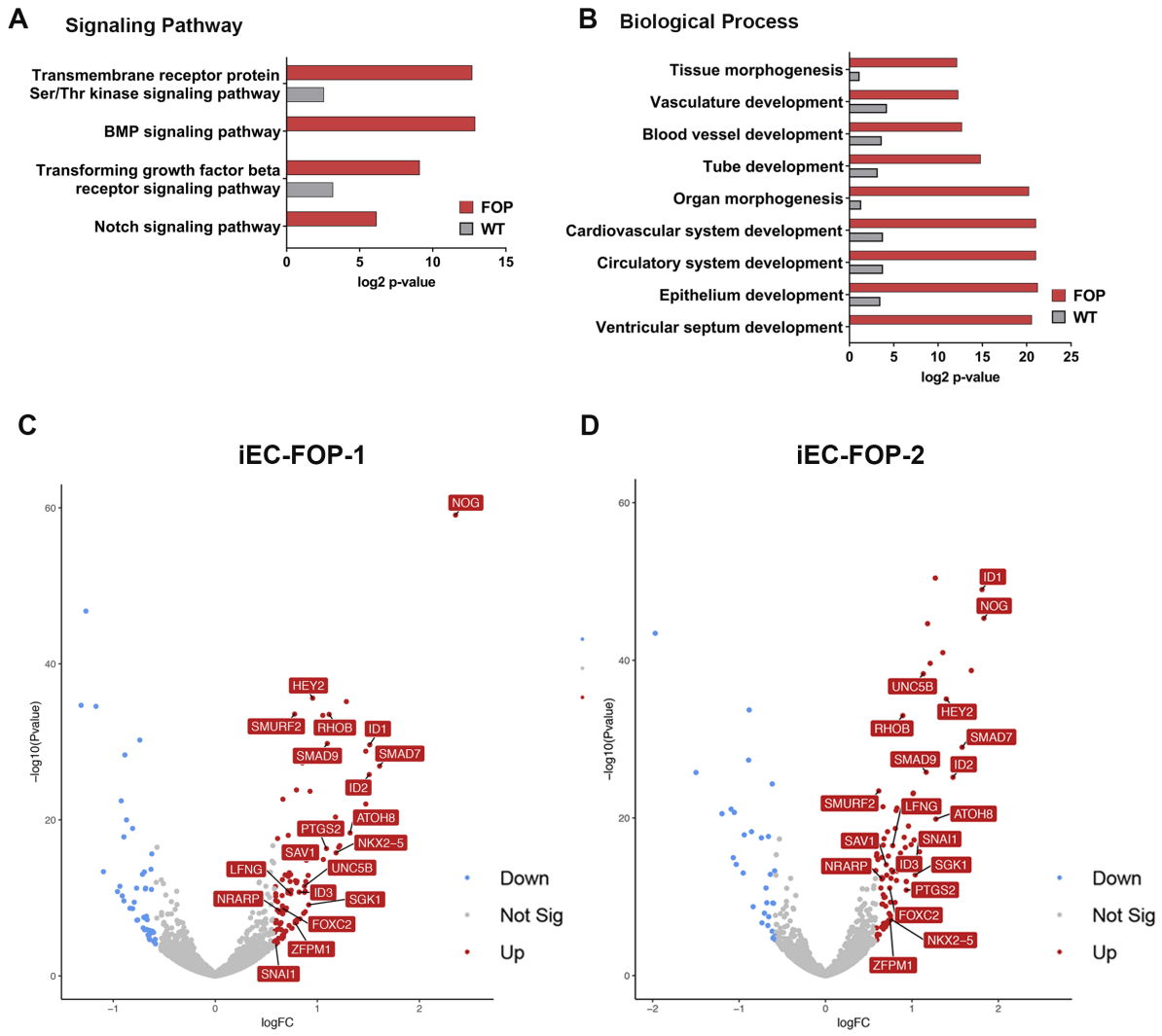

Figure 3.21 The ActivinA induced transcriptome is associated with blood vessel formation and BMP, NOTCH pathway activation. (**A-B**) Selected GO terms of shared upregulated genes in ActivinA treated FOP iECs and respective WT values. Depiction of log2 p-value with Benjamini correction. Value is 0 if GO term was not identified. (**C-D**) Volcano Plot of DEG of ActivinA treated FOP iECs. Genes (adjusted p value<0.05; 0.58≤ log2FC ≥0.58), up-/downregulation is indicated by color. Genes associated with GO terms are labeled. (DEG: Differentially expressed genes). Fold Change=FC. Modified from (Hildebrandt et.al., Stem Cell Rev Rep, in press 2020).

GO analysis of upregulated genes in WT iECs identified TGFβ signaling as the main associated pathway and the only significant biological function was related to general cell communication ($p \leq 0.05$) (Figure 3.22B).

Taken together, ActivinA induced phosphorylation of SMAD1/5 only in FOP iECs. This resulted downstream in the activation of a FOP specific transcriptome in both FOP donors consisting of highly enriched genes (FC of ≥ 1.5) (e.g. *ID1, NOG, HEY2, LFNG, UNC5B* (Figure 3.21C,D), which are involved in blood vessel as well as cardiac development and associated pathway activation of BMP and NOTCH.

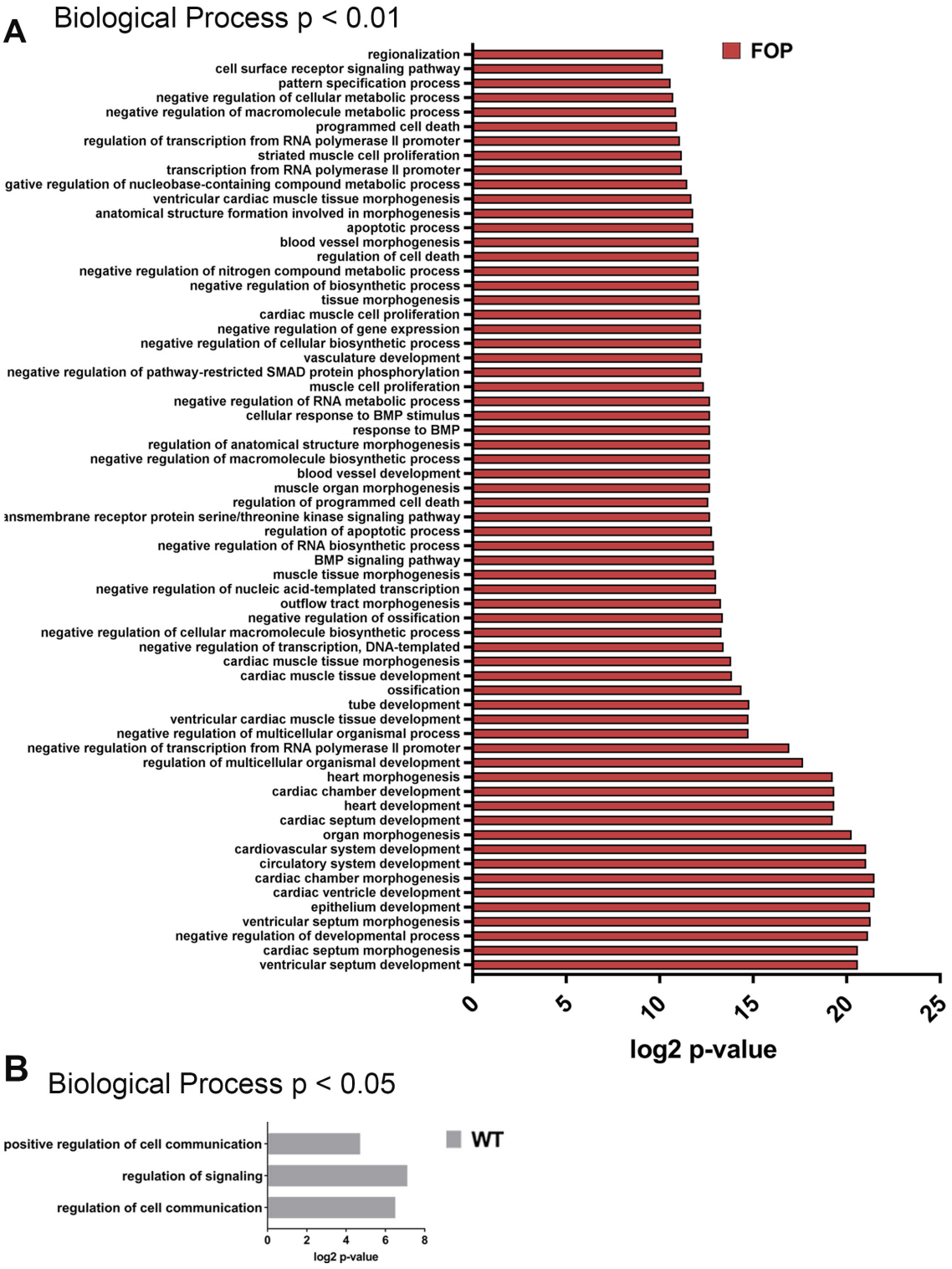

Figure 3.22 ActivinA induced transcriptome of FOP iECs is associated with additional biological functions compared to WT iECs. (**A**) GO terms of upregulated genes in ActivinA treated FOP iECs. Depiction of log2 p-value of Benjamini correction (cut-off at adjusted p-value<0.01). (**B**) GO terms of upregulated genes in ActivinA treated WT iECs. Depiction of all log2 p-values of Benjamini correction (adjusted p-value<0.05). Modified from (Hildebrandt et.al., Stem Cell Rev Rep, in press 2020).

3.6.3 **ActivinA upregulates the same target genes as BMP6 in FOP iECs**

To confirm FOP specific gene transcription by ActivinA and to further dissect whether BMP6 mediates the same downstream transcriptional responses, iECs were treated with BMP6 at the same concentration as ActivinA (5 nM) in independent experiments (Figure 3.23)**.** For comparison iEC were additionally stimulated with BMP9 (0.1 nM). Moreover, iECs were treatment with the ALK2 kinase inhibitor Saracatinib before ligand stimulation, which will be described and explained in more detail in the next paragraph.

RT-PCR analysis confirmed that classical BMP target genes (*SMAD6, SMAD9, NOG,* ID1/2/3, *SMAD7)* were upregulated by BMP6 and BMP9 in WT and FOP iECs (Figure **3.23**). For SMAD6 the BMP induced expression was significantly higher in FOP iECs compared to WT iECs (Figure 3.23B).

In contrast, ActivinA activated BMP target genes in FOP iECs only (Figure 3.23B). Moreover, ActivinA upregulated genes related to NOTCH signaling such as the related ligands *JAG1/JAG2* and the NOTCH target genes *NRARP*, *HEY2* and *HEYL* in FOP iECs only (Figure 3.23C). In addition, genes related to blood vessel formation, such as the endothelial guidance receptor *UNC5B* were upregulated by ActivinA only in FOP iECs but not in WT iECs, whereas BMP6 and BMP9 upregulated these genes with similar fold changes in both WT and FOP iECs (Figure 3.23A,C). Importantly, pretreatment with Saracatinib rescued the differential gene expression by ActivinA in FOP iECs similar to WT levels (Figure 3.23).

GO analysis revealed that associated genes with pathway activation of BMP and NOTCH are involved in blood vessel development. Formation of new blood vessels is characterized by dynamic tip and stalk cell shuffling, which enables blood vessel branching (Chen et al., 2019). Tip and stalk cell identity is defined by the transcriptional profile in addition to morphological and functional characteristics. Transcriptional regulation of specific genes, involved in VEGF and NOTCH pathways contribute to tip and stalk cell selection (Blanco and Gerhardt, 2013). Interestingly, tip cell associated genes such as the NOTCH ligand *DLL4* and *VEGFR2* (*KDR*) were downregulated by ActivinA only in FOP iECs, whereas stalk cell associated genes such as *JAG1, HEY2* and *HEYL* were upregulated (Figure 3.23A,C). In accordance with ActivinA, BMP6 downregulation tip cell and upregulated stalk cell related genes in FOP iECs but additionally in WT iECs (Figure 3.23A,C). BMP6 induced reduction of *KDR* was even stronger in FOP iECs, compared to WT iECs (Figure 3.23A).

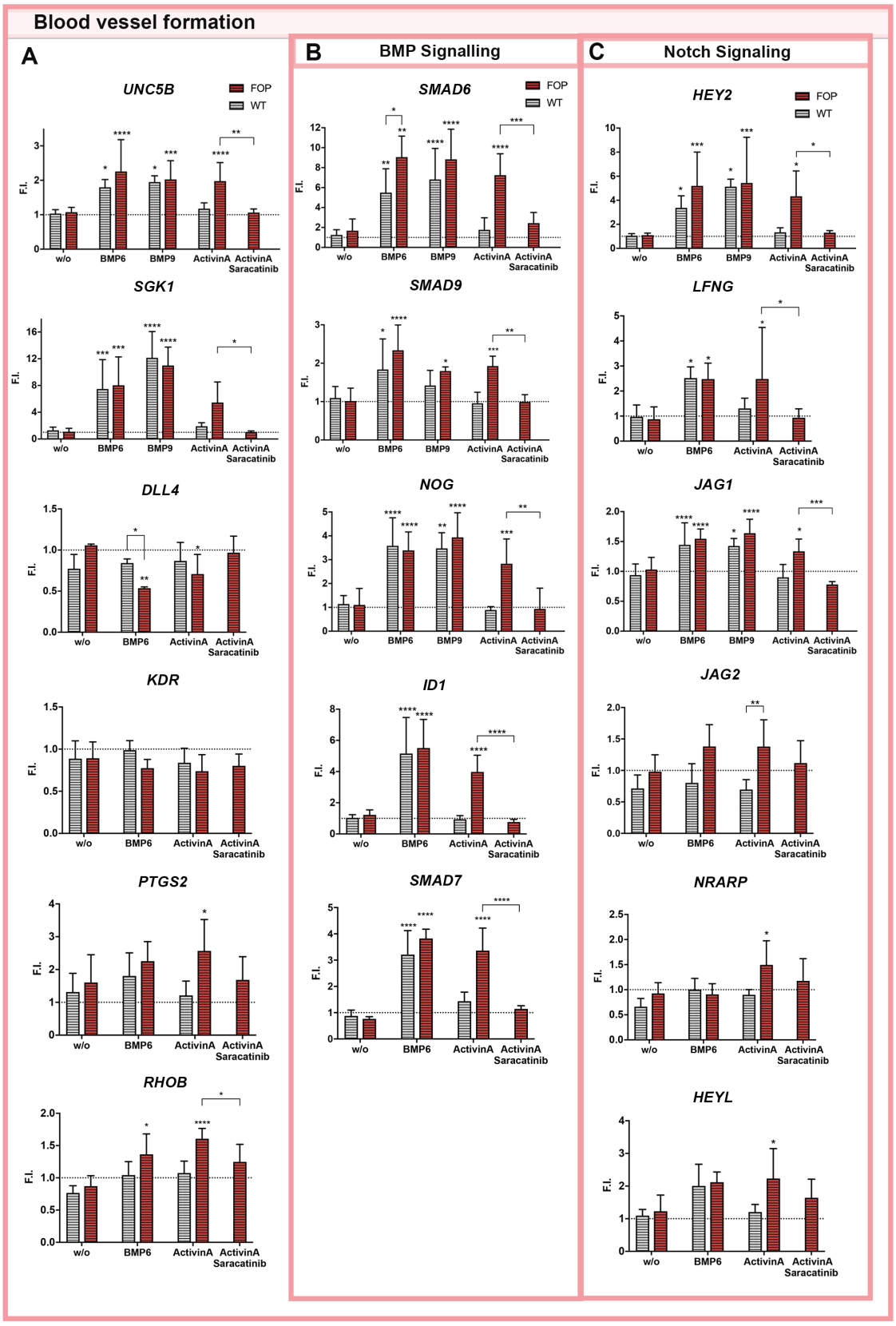

Figure 3.23 ActivinA upregulates the same target genes as BMP6 in FOP iECs. RT-PCR validation of RNASeq target groups upon 1 hour pretreatment with Saracatinib (0.2 µM) and 2 hour ActivinA (5 nM) (n=3-6), BMP6 (5 nM) (n=2-4), BMP9 (0.1 nM) (n=2). treatment in iECs (n=3-6). (**A-C**) Genes are associated with Blood vessel formation and additionally with (**B**) BMP Signaling and (**C**) NOTCH Signaling. Data is normalized to the 0 hour time point (dotted line) and is represented as mean Fold induction (F.I.) ± SD. * p<0.05, ** p<0.01, ***p<0.001, ****p< 0.0001. Significance was calculated relative to unstimulated (w/o) using two-way ANOVA. (SD: Standard Deviation) Modified from (Hildebrandt et.al., Stem Cell Rev Rep, in press 2020).

Interestingly, the NOTCH target gene *NRARP* was only significantly induced by ActivinA in FOP iECs and not by BMP6 in either FOP or WT iECs (Figure 3.23C). To a lesser extent this was also observed for *PTGS2* encoding the Cyclooxygenase COX 2, which is also involved in angiogenesis (Gately and Li, 2004) (Figure 3.23A).
In sum, ActivinA upregulated the same genes as BMP6 and BMP9 only in FOP iECs, suggesting that ActivinA transduces a BMP-like response.

3.6.4 **ActivinA upregulates EndMT associated genes only in FOP iECs**

Based on the identification of ventricular septum development among the high significant GO terms ($p \leq 0.01$) in ActivinA treated FOP iECs (Figure 3.21B), associated genes were analyzed further. The ventricular septum derives from cushion tissue, which underwent EndMT and forms the dividing wall separating the lower heart chambers (ventricle) (Kovacic et al., 2012). EndMT is initiated by the activation of transcription factors, such as SNAI1, SLUG, TWIST, ZEB and MSX1/2 resulting in the repression of endothelial markers and the activation of mesenchymal markers (Chen et al., 2008; Gong et al., 2017; Weinstein et al., 2020). EndMT transcriptional markers were extracted from the RNASeq differential analysis (Figure 3.24A). Only the transcription factor *SNAI1, MSX2* and *FOXC2* were among the significant differential expressed genes ($p< 0.05$) between untreated and ActivinA treated FOP iECs (Figure 3.24A,B). *SNAI1* was among the highly enriched genes (FC of ≥ 1.5) as depicted in the volcano plot previously (Figure 3.21C,D).
The significant hits were confirmed by RT-PCR analysis and additionally analyzed upon stimulation of iECs with BMP6 (Figure 3.24B). ActivinA treatment induced gene expression of *SNAI1* and *MSX2* only in FOP iECs, whereas *FOXC2* was upregulated in both WT and FOP iECs. BMP6 upregulated *SNAI1*, *MSX2* and *FOXC2* significantly in FOP iECs but in WT iECs only *FOXC2* was significantly upregulated (Figure 3.24B). The pretreatment of Saracatinib reduced the induction of *SNAI1*, *FOXC2* and *MSX2* by ActivinA to WT levels (Figure 3.24B).
EndMT associated transcription factors such as *SNAI2* directly repress the expression of genes encoding for junctional proteins (Lamouille et al., 2014). This results in a *Cadherin switch* during EndMT, which promotes the upregulation of Neural Cadherin (N-Cadherin), which facilitates weaker cell-cell interaction thereby promoting migratory characteristics of mesenchymal cells. N-Cadherin (*CDH2*) becomes upregulated via *TWIST* mediated mechanisms but independent of SNAIL (Lamouille et al., 2014; Yang et al., 2012). Therefore, it was analyzed whether ActivinA treatment represses the

expression of the endothelial adherens junction proteins VE-Cadherin (*CDH5*) and PECAM1 and whether it induces N-Cadherin expression.

WT and FOP iECs were stimulated for 2, 6, 24 and 48 hours with ActivinA, which did not lead to changes in the expression of *PECAM1* or *CDH5* (Figure 3.24C). Interestingly, the mean expression values increased over time but were in average higher in WT iECs compared to FOP iECs for all time points independent of ligand stimulation. In addition, N-Cadherin (*CDH2)* expression was assessed after 24-hour ActivinA treatment which showed unchanged and similar levels in WT and FOP iECs (Figure 3.24D). Thus, ActivinA upregulated EndMT associated transcription factors in FOP iECs, which did not result in long-term modification of junctional gene expression.

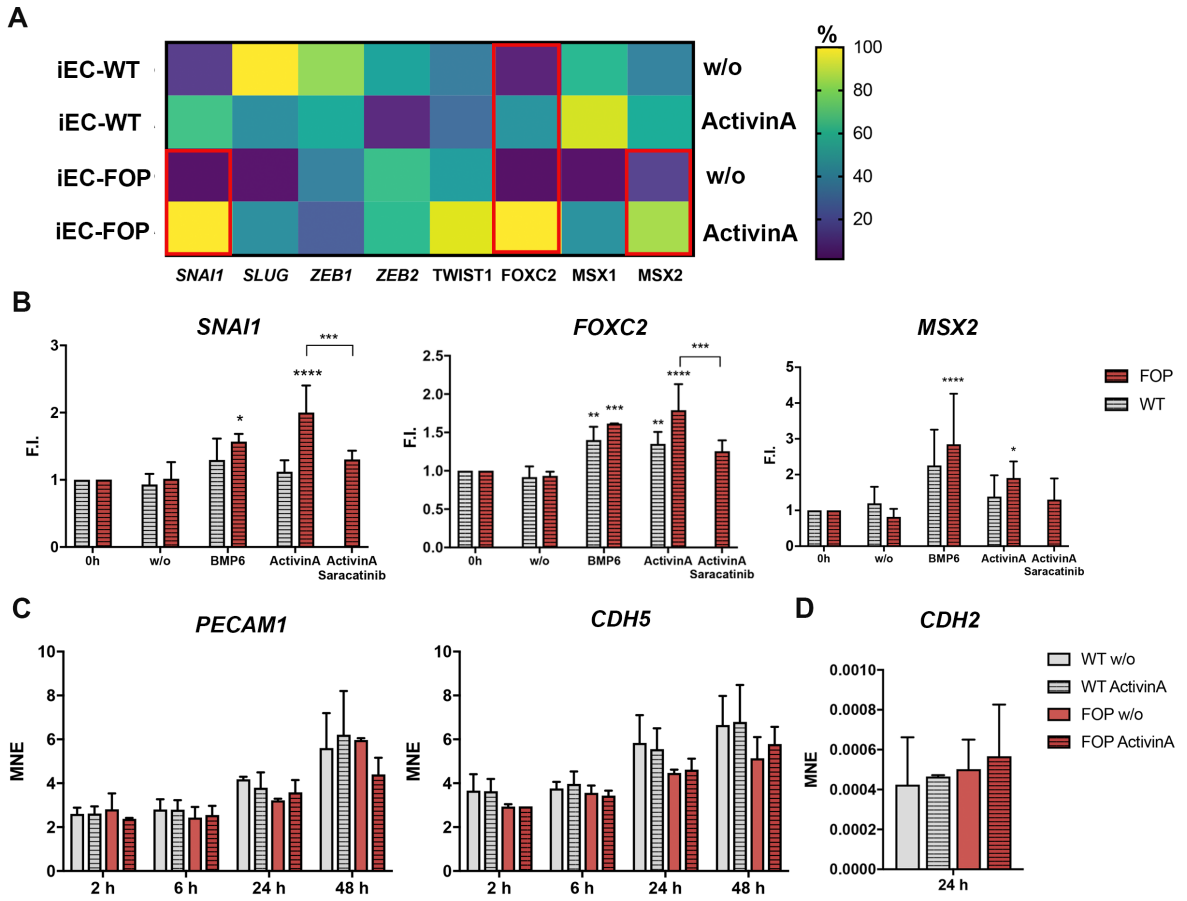

Figure 3.24 ActivinA induces EndMT transcriptional markers in FOP iECs. (**A**) Transcript expression levels from RNASeq data of EndMT markers were normalized for each gene to the smallest FPKM (Fragments Per Kilobase of transcript per Million reads mapped) value among the four samples (WT/FOP, w/o, ActivinA) shown in %. Red squares mark the conditions, which were significant in DEG analysis using DESeq2. (**B**) Validation of significant RNASeq EndMT targets by RT-PCR of WT and FOP iECs pretreated with Saracatinib (0.2 µM) and 2 hours ActivinA (5 nM) (n=4), BMP6 (5 nM) (n=2) stimulation. Data is represented as mean F.I. ± SD. (**C**) Analysis of EC junctions by RT-PCR of WT and FOP iECs stimulated with ActivinA for 2, 6,24 and 48 hours. (**D**) Analysis of EndMT junctional marker N-Cadherin by RT-PCR in WT and FOP iECs stimulated with ActivinA for 24 hours. Data is represented as MNE ± SD. * p<0.05, ** p<0.01, ***p<0.001, ****p< 0.0001. Significance was calculated relative to unstimulated (w/o) using two-way ANOVA. (DEG: Differentially expressed gene; F.I.: fold induction; MNE: mean normalized expression; SD: Standard Deviation).

In summary, aberrant ActivinA signaling resulted downstream in the activation of a FOP specific transcriptome consisting of highly upregulated genes, which are involved in blood vessel formation, stalk cell identity, EndMT and associated pathway activation of BMP and Notch. Most genes could be equally induced by BMP6 and BMP9 in WT and FOP iECs, suggesting that ActivinA transduced am BMP-like response only in FOP iECs. The BMP6 response for the BMP target gene SMAD6 and tip cell marker KDR was even stronger in FOP iECs compared to WT iECs, which indicates hyperactivated BMP signaling in FOP iECs.

3.7 Establishment of drug testing in the FOP iEC disease model

After the validation of the *in vitro* endothelial FOP disease model (iECs), it was discovered that aberrant ActivinA/SMAD1/5 signaling resulted in a FOP specific transcriptome in FOP iECs compared to healthy controls. The ActivinA/SMAD1/5 responses recapitulate an important pathogenic mechanism in FOP (Hatsell et al., 2015; Hino et al., 2015), which indicates that ECs may represent a disease relevant cell type. The ALK2-dependent pathological signaling (over-activation of SMAD1/5 signaling) is thought to trigger HO in FOP. Drug testing approaches have focused on phenotypes related to HO or directly on ALK2 function as reviewed in (Wentworth et al., 2019). Advances in drug development to target the pathway on different levels: Such as specific ligand neutralizing antibodies (Hatsell et al., 2015), kinase inhibitors of the catalytic domain of ALK2 (Mohedas et al., 2013; Sanvitale et al., 2013; Yu et al., 2008a, 2008b) or SMAD1/5 modulating agents, such as the retinoic acid receptor γ (RARγ) agonist palovarotene (Shimono et al., 2010) (Figure 3.25A). Based on the immediate aberrant ActivinA/SMAD1/5 signaling read-out (phosphorylation of SMADs after 30 min) and the transcriptional consequences in FOP iECs (after 2 hours), it was asked if these alterations could be rescued by inhibiting ALK2 kinase activity.

3.7.1 Saracatinib is a BMP signaling inhibitor and prevents SMAD1/5 responses in FOP iECs

The tyrosine kinase inhibitor Saracatinib (AZD-0530) was used for drug testing in the iEC model (Figure 3.25B). Saracatinib was initially developed for the treatment of cancer as a dual Tyrosine protein kinase inhibitor targeting SRC and ABL (Hennequin et al., 2006). However, its additional inhibitory effect on BMP type I receptors (Lewis and Prywes, 2013) (Figure 3.25B) and HO (Hino et al., 2018) (Yu et al 2016) introduced Saracatinib as a potential drug candidate for FOP (Wentworth et al., 2019). The effect

of Saracatinib on FOP endothelium has not been investigated yet. Here, it was focused on early mechanistic actions of Saracatinib on endogenous ALK2 signaling responses. iECs were pretreated with Saracatinib for 1 hour and after 30 min of ActivinA stimulation pSMAD1/5 levels were analyzed. Saracatinib efficiently prevented ActivinA induced phosphorylation of SMAD1/5 in a concentration dependent manner in FOP iECs (Figure 3.25B,C). When higher concentrations of Saracatinib were used, pSMAD2 by ActivinA was slightly reduced at 0.5 µM for FOP donor 1 and at 1.0 µM for FOP donor 2 (Figure 3.25B,C). This was supported by an experiment with TGFβ stimulation, where pretreatment of Saracatinib at 1.0 µM slightly reduced pSMAD2 levels (Figure 3.25G). However, at 0.2 nM, Saracatinib inhibited ActivinA/SMAD1/5 signaling in both FOP donors, whereas SMAD2/3 signaling was unaffected, which was confirmed on pSMAD protein levels and target gene transcription (Figure 3.27, Figure **3.25**B,C)**.** Thus, 0.2 nM were used for subsequent experiments. In contrast to pSMAD levels, pSRC levels remained unaffected by Saracatinib treatment even at high concentration (Figure 3.25I). Next, it was asked whether Saracatinib also inhibits BMP6 induced phosphorylation of SMAD1/5 in the same manner. Therefore, WT and FOP iECs were pretreated with different concentrations of Saracatinib as above and subsequently stimulated with BMP6 for 30 min. Saracatinib also efficiently prevented BMP6 induced phosphorylation of SMAD1/5 in a concentration dependent manner in WT and FOP iECs (Figure 3.25D,E). The concentration dependent effect of Saracatinib pretreatment in BMP6 stimulated FOP iECs was in line with ActivinA treated FOP iECs. At a concentration of 0.05 µM Saracatinib pretreatment showed a reduction in pSMAD1/5 levels for both ligands (BMP6 and ActivinA) (Figure 3.25B-E). Based on the analysis that ALK1 showed the highest expression among type I receptors in iECs, the effect of Saracatinib on ALK1 signaling was investigated. Therefore, FOP iECs were treated with the ALK1 high affinity ligand BMP9 upon pretreatment with a concentration series of Saracatinib. BMP9 induced phosphorylation of SMAD1/5 was only prevented when Saracatinib concentrations of 0.5 µM or higher were used (Figure 3.25J). This indicates, that higher concentrations of Saracatinib are necessary to prevent BMP9/SMAD1/5 signaling in comparison to BMP6 or ActivinA/SMAD1/5 signaling in FOP iECs. This is in line with a different type I receptor kinase inhibitor (K02288), which showed that the application of higher concentrations (2.0 µM) is necessary to prevent BMP9/SMAD1/5 signaling in comparison to BMP6/SMAD1/5 signaling (0.5 µM) (Figure 3.25H).

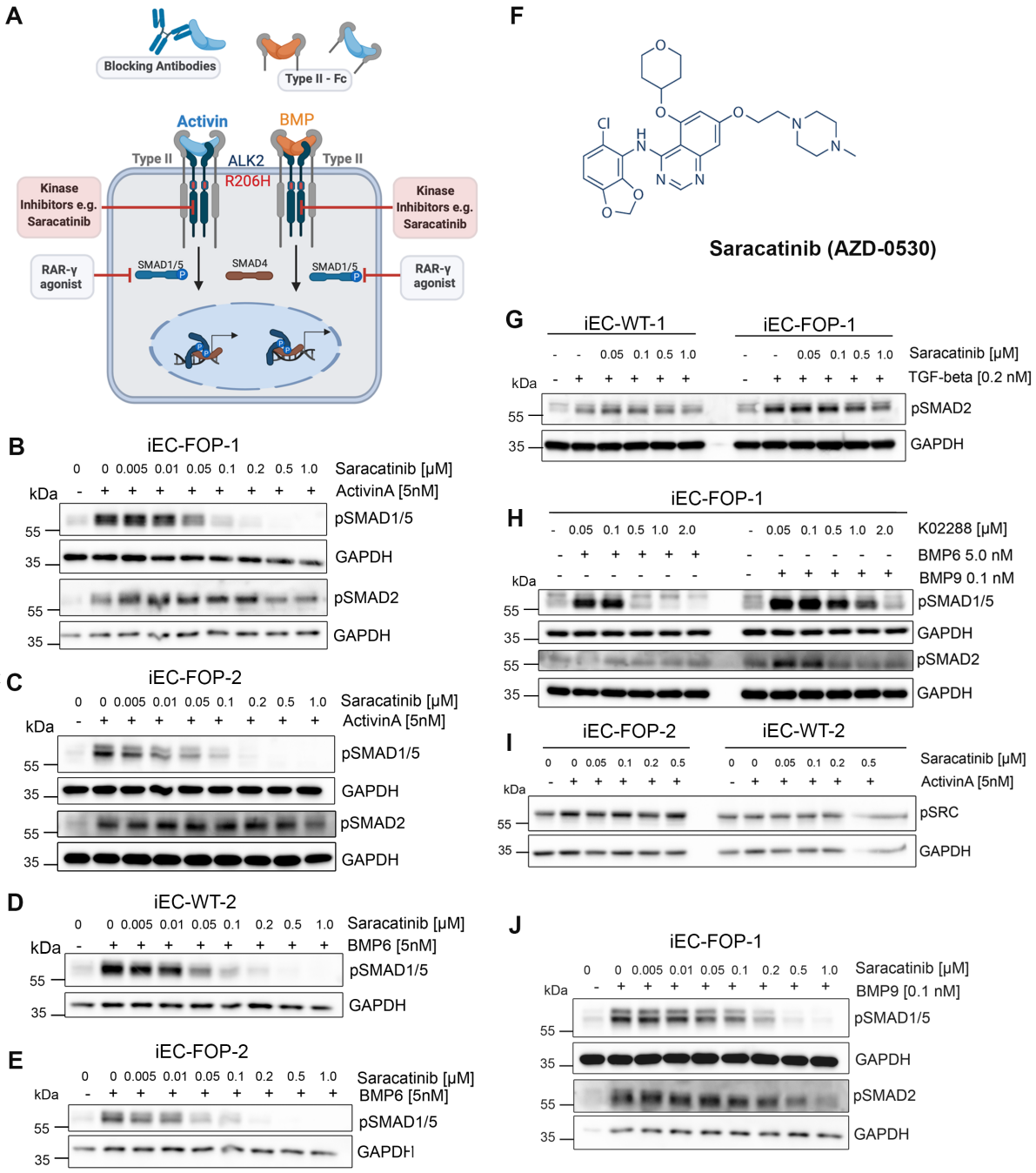

Figure 3.25 Using BMP type I receptor specific kinase inhibitors for drug testing in the FOP iEC disease model.
(**A**) Schematic depiction of strategies to target ALK2 signaling on different levels of the BMP pathway in context of FOP. (**B-C**) Representative Western Blot of protein lysates from iECs using both FOP donor. iECs were pretreated with different concentrations of Saracatinib and stimulation with ActivinA (5 nM) for 30 min. (**D-E**) WT and FOP iECs pretreated with different concentrations of Saracatinib and stimulation with BMP6 (5 nM) for 30 min. (**F**) Chemical Structure of Saracatinib derived from supplier selleckchem.com/products/AZD0530.html (**G**) WT and FOP iECs pretreated with different concentrations of Saracatinib and stimulation with TGFβ (0.2 nM) for 30 min. (**H**) FOP iECs pretreated with different concentrations of K02288 and stimulation with BMP6 (5 nM) or BMP9 (0.1 nM) for 30 min. (**I**) WT and FOP iECs pretreated with different concentrations of Saracatinib and stimulation with ActivinA (5 nM) for 30 min. (**J**) WT and FOP iECs pretreated with different concentrations of Saracatinib and stimulation with BMP9 (0.1 nM) for 30 min. B,C is derived from (Hildebrandt et.al., Stem Cell Rev Rep, in press 2020).

3.7.2 **Saracatinib prevents BMP6 induced SMAD2 signaling and rescues ActivinA induced reduction of phosphorylated AKT**

In addition to aberrant induced SMAD1/5 responses, it was examined if Saracatinib was also able to prevent aberrant BMP6/SMAD2 and dephosphorylation of AKT in FOP iECs. FOP iECs were pretreated with Saracatinib as described above and indeed phosphorylation of SMAD2 and target gene transcription (*NEDD9*) by BMP6 was prevented (Figure 3.26A,B). Thus, BMP6 induced SMAD2 phosphorylation is not only dependent on TGFβ type I receptors, as shown in (Figure 3.16) but also on ALK2. Moreover, Saracatinib prevented also the reduction of phosphorylated AKT protein levels by BMP6 in WT and FOP iECs and by ActivinA in both FOP iEC donors (Figure 3.26C-E).

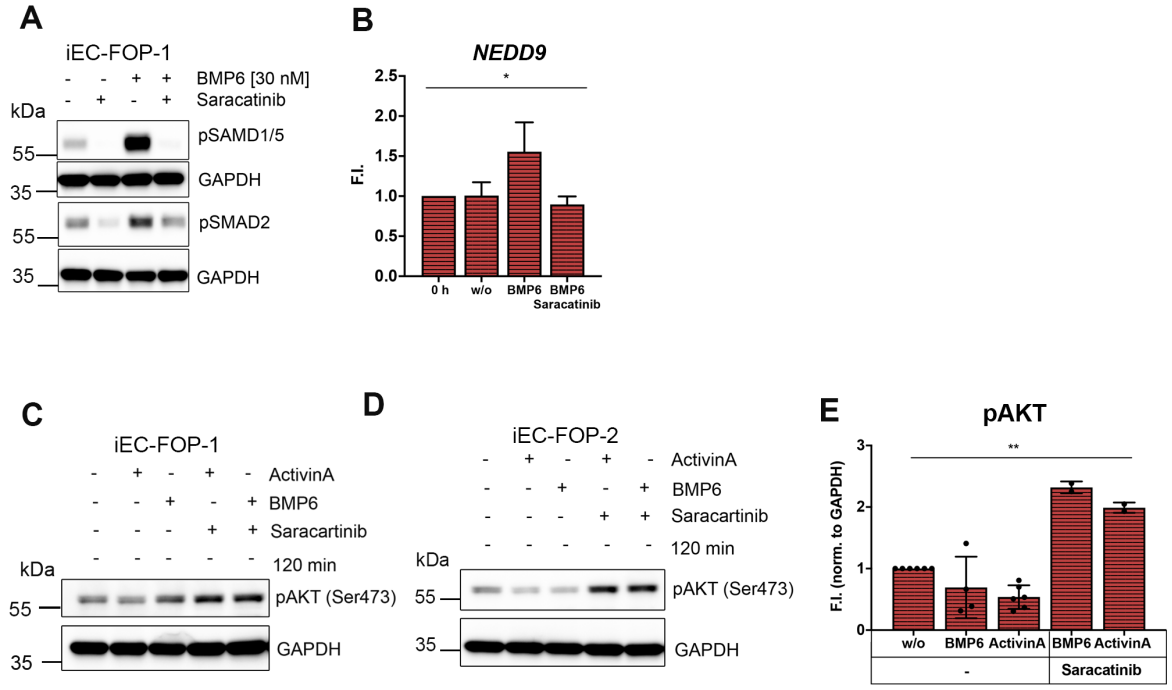

Figure 3.26 Saracatinib prevents aberrant SMAD2 responses by BMP6 and rescues reduction of phosphorylated AKT levels by ActivinA in FOP iECs.(**A**) Representative Western Blot of of iECs pretreated with Saracatinib (1 hour) and BMP6 30 min. (**B**) RT-PCR of SMAD2/3 target gene expression of FOP iECs pretreated with Saracatinib (0.2 µM) (n=2) (1 hour) and BMP6 (30 nM) (n=4) for 2 hours. (**C-E**) Representative Western Blot of protein lysates from FOP iECs pretreated with Saracatinib (0.2 µM) (1 hour) and BMP6 and ActivinA for 120 min and (**E**) densiometric quantification of pAKT levels normalized to GAPDH. ** p<0.01 significance was calculated using the non-parametric Kruskal-Wallis Test. Data is represented as mean F.I. ± SD. (F.I.: fold induction; SD: Standard Deviation)

3.7.3 The kinase inhibitor Saracatinib rescues the ActivinA/SMAD1/5 downstream transcriptional profile in FOP iECs

After establishment of an appropriate Saracatinib concentration, which maintained ActivinA induced SMAD2 phosphorylation but prevented aberrant phosphorylation of SMAD1/5 in FOP iECs (Figure 3.27A), it was investigated if pretreatment with Saracatinib is sufficient to prevent the ActivinA downstream responses on gene transcription. Pretreatment with Saracatinib successfully prevented aberrant activation of BMP target gene (*ID1*) transcription in FOP iECs (Figure 3.27B). Of note, Saracatinib preserved ActivinA induced transcription of the SMAD2/3 target genes *NEDD9* and *PMEPA1* in WT and FOP iECs (Figure 3.27B-D), which confirmed pSMAD2 analysis (Figure 3.27A).

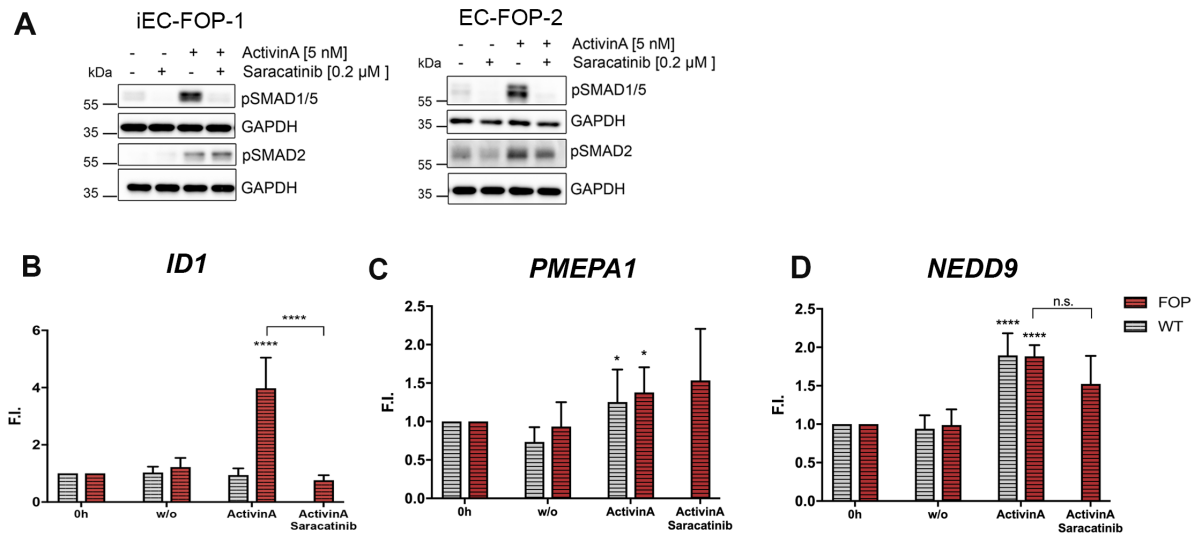

Figure 3.27 Saracatinib prevents aberrant ActivinA/SMAD1/5 responses but maintains SMAD2 signaling in FOP iECs.
(**A**) Representative Western Blot of both FOP donor iECs pretreated with Saracatinib (0.2 µM) and ActivinA (5 nM). (**B-D**) Analysis of downstream target gene effects by Saracatinib pretreatment and ActivinA (5 nM) stimulation using RT-PCR. (B) n=8, (C) (n=4-6), (D) (n=4). Data is represented as mean F.I. ± SD. * p<0.05, ** p<0.01, ***p<0.001, ****p< 0.0001. Significance was calculated relative to unstimulated (w/o) using two-way ANOVA. (F.I.: fold induction; SD: Standard Deviation). Modified from (Hildebrandt et.al., Stem Cell Rev Rep, in press 2020).

To investigate if Saracatinib can rescue the entire FOP specific transcriptome induced by ActivinA, pretreated FOP iECs with Saracatinib were subjected to RNA Sequencing (Figure 3.28A).

Indeed, independent hierarchical cluster analysis of RNASeq data demonstrated rescue of the transcriptional profile induced by ActivinA in FOP iECs (Figure 3.28B cluster a) to WT level after Saracatinib treatment (Figure 3.28B cluster b1 and b2). Of

note, Saracatinib preserved ActivinA induced transcription of the SMAD2/3 target genes in WT and FOP iECs (Figure 3.28B cluster II). Validation by qPCR confirmed that Saracatinib prevented the aberrant activation of genes by ActivinA involved in blood vessel formation, EndMT and associated pathway activation of BMP and Notch (see former Figure 3.23 and Figure 3.24).

In summary, drug testing in the new established FOP endothelial disease model revealed mechanistic insight about the potential drug candidate Saracatinib in FOP endothelium. Saracatinib successfully prevented aberrant ActivinA induced SMAD1/5 phosphorylation and rescued the downstream FOP specific transcriptome to WT expression levels in FOP iECs. Moreover, Saracatinb treatment successfully prevented additional signaling aberrations in SMAD2 and AKT responses in FOP iECs.

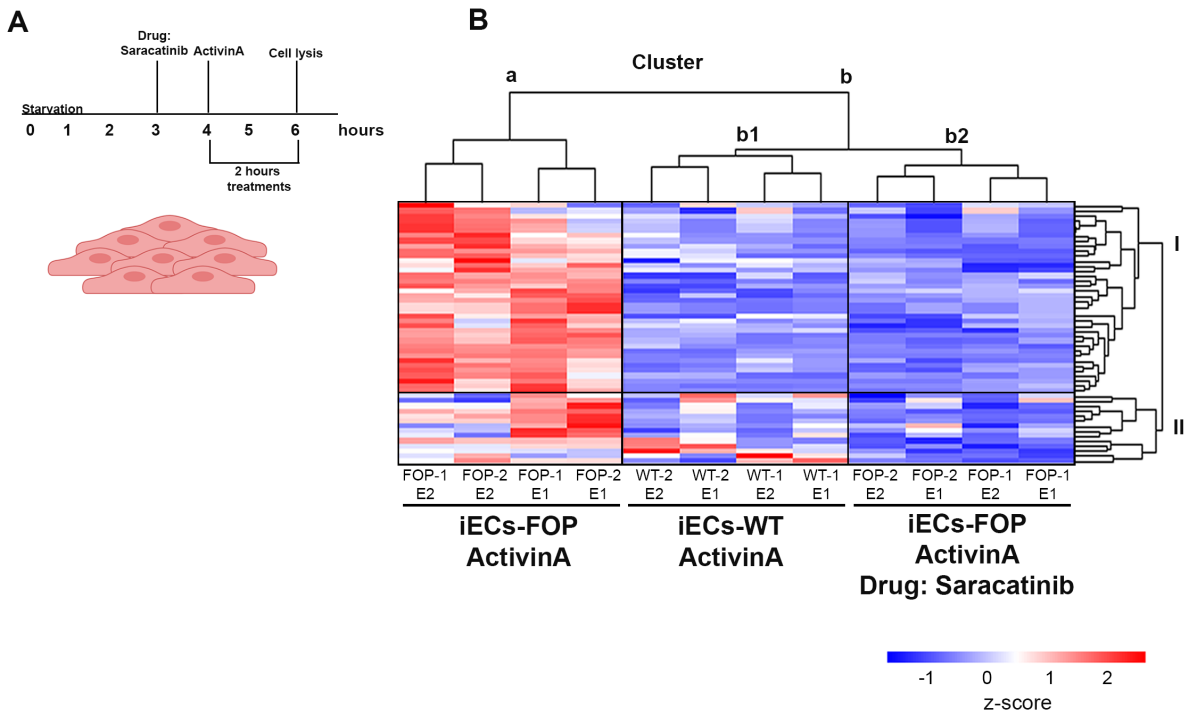

Figure 3.28 Saracatinib rescues the ActivinA induced transcriptome in FOP iECs to WT levels. (**A**) Experimental setup: RNA Seq of 4 iEC lines from two independent experiments, starved for 4 hours, pretreated with Saracatinib and stimulated for 2 hours with 5 nM ActivinA. (**B**) Independent hierarchical clustering of upregulated genes (adjusted p-value<0.05; log2FC ≥0.58) of FOP iECs in comparison to WT and Saracatinib pretreated FOP iECs upon ActivinA (5 nM) treatment. Heatmap color coding shows z-score (red=high; blue=low). Modified from (Hildebrandt et.al., Stem Cell Rev Rep, in press 2020).

3.8 Functional consequences of aberrant ActivinA signaling in FOP iECs

In previous chapters the establishment of an endothelial FOP disease model from patient iPSCs (iECs) was described and it was shown that FOP iECs recapitulate the pathogenic mechanism of aberrant ActivinA/SMAD1/5 signaling. Based on advances in FOP mouse models, it is thought that ActivinA dependent signaling is the main trigger of HO in FOP (Hatsell et al., 2015; Lees-Shepard et al., 2018).

Whether observed vascular aberrations in FOP patient biopsies (Ware et al., 2019) are connected to aberrant ActivinA/SMAD1/5 signaling is not known. Thus, functional consequences of aberrant ActivinA/SMAD1/5 signaling were analyzed in the endothelial FOP *in vitro* model as ECs are a major component of the vasculature. Investigation of the transcriptome of ActivinA treated FOP iECs already revealed that the upregulated genes are associated with blood vessel formation and stalk cell identity (see chapter 3.6)**.** The formation of new blood vessels postnatally is mostly mediated via angiogenesis. Angiogenesis is a multi-stage physiological process and occurs during growth but also in pathological conditions, such as wound healing and disease. Moreover, angiogenesis is an essential process in endochondral bone formation (see chapters 1.3 and 1.4). In fact, early pre-osseous HO lesions in FOP patient biopsies are highly angiogenic (Ware et al., 2019) (see chapter 1.6.3).

The multiple stages in angiogenesis involve complex, coordinated processes such as loosening of cell-cell junctional contacts of the endothelial barrier and sprout elongation, which are orchestrated by multiple signaling pathways. In addition to VEGF and NOTCH, BMP signaling controls multiple stages in angiogenesis (García de Vinuesa et al., 2016; Jin et al., 2014) as it was shown by previous studies in the Knaus lab for the regulation of tip and stalk competence (Benn et al., 2017) and barrier integrity (Benn et al., 2016).

Therefore, it was asked if ActivinA influences angiogenic processes of FOP iECs, which was addressed by functional *in vitro* assays of endothelial barrier and sprout formation.

3.8.1 **Influence of ActivinA on endothelial barrier integrity**

First, endothelial barrier function/permeability was analyzed *in vitro* as the initiation of angiogenesis requires the reduction in barrier integrity by the loosening of cell-cell junctions. Here, iECs were seeded on gold electrode arrays to form a dense endothelial barrier (Figure 3.29A,C). Phase contrast microscopy was used to confirm proper barrier formation on gold electrodes (circle) (Figure 3.29C). The cell membranes have insulating properties and create a resistance towards the electrical current flow. The application of alternating current (AC) instead of direct current (DC) enables the measurement of the impedance at different frequencies. Lower AC frequencies (e.g. 4000 Hz) allow the measurement of the current flow under and between the cells, which represents the quality and function of the endothelial barrier. Resistance as part of impedance measurement describes barrier function best (Szulcek et al., 2014).
Thus, barrier function was assessed by resistance, which was normalized to the time point at one hour before ligand stimulation.

VEGFA induces a short and long-term permeability of iEC barriers

As validated by impedance measurements of iEC characterization (Figure 3.6), WT and FOP iECs form tight barriers and show short-term reduced barrier integrity after 1.5 hours upon stimulation with the permeability inducing and angiogenic factor VEGFA, which lasts approximately for 1 hour until base line recovery (Figure 3.29E). Interestingly, long-term barrier integrity assessment identified a second response of VEGFA, which lasted 24 hours without recovery (Figure 3.29E).
Quantification of VEGFA induced permeability after 6 hours revealed a significant reduced mean resistance in WT (27%) and FOP (21%) iECs by VEGFA compared to controls (Figure 3.29F).
At the 24 hours time point, VEGFA treatment reduced mean resistance of about 27-30% in both WT and FOP iECs compared to the baseline. However, compared to untreated controls (w/o) the effect of VEGFA was only significant in WT iECs (27%) and much stronger compared to FOP iECs (15%) (Figure 3.29G).
Importantly, FOP iECs showed a significant reduced baseline resistance (w/o) compared to WT iECs /w/o) (Figure 3.29G). Indicating that WT iEC barriers maintain more stable in starvation conditions compared to FOP iECs.

ActivinA destabilizes the endothelial barrier integrity

Next, WT and FOP iECs were treated with different concentrations of ActivinA. Untreated WT and FOP iEC barriers remained at constant resistance levels, which even increased in WT iECs (Figure 3.29B). ActivinA treatment decreased resistance in a concentration dependent manner in FOP iECs. Concentrations of 10 and 30 nM ActivinA only started to reduce resistance after approximately 5 hours after stimulation (6 hour time point) (Figure 3.29B). In contrast, resistance values in WT iECs did not decrease markedly below 1.0. However, compared to the control (w/o (PBS treated)), which increased, ActivinA also reduced resistance in a concentration dependent manner in WT iECs (Figure 3.29B).

Quantification of ActivinA (10 nM) treated WT and FOP iEC monolayers revealed that the mean resistance was reduced by 8.0% in FOP iECs and 0% in WT iECs at the 6 hour time point (Figure 3.29F). After 24 hours the ActivinA effect was more pronounced in FOP iECs and reduced the mean resistance to the same extend as VEGFA (Figure 3.29G).

For comparison WT and FOP iECs were also treated with BMP6 at the same concentration as ActivinA. Only in FOP iECs BMP6 reduced mean resistance after 6 hours (Figure 3.29F), which was confirmed for the 24 hour time point (Figure 3.29G). In WT iECs, only long-term BMP6 treatment resulted in a significant reduction of resistance (Figure 3.29G).

Pretreatment with the kinase inhibitor K02288 before BMP6 or Activin stimulation increased mean resistance values to control levels (w/o) (Figure 3.29F,G), indicating an ALK2 dependent mechanism. Moreover, Saracatinib pretreatment rescued ActivinA treated FOP iEC resistance to baseline levels (Figure 3.29F,G).

The effect of ActivinA on VEGFA induced permeability

Only in FOP iECs, ActivinA reduced the mean resistance as strong as VEGFA after long-term treatment. Whereas in WT iECs VEGFA alone showed the strongest effect (Figure 3.29F,G). To analyze the effect of ActivinA on VEGFA induced permeability, a co-treatment was performed. In FOP iECs co-treatment of ActivinA and VEGFA decreased the mean resistance to the same extend as VEGFA (or ActivinA) treatment alone, whereas in WT iECs single VEGFA treatment was stronger (Figure 3.29G).

Thus, co-treatment with ActivinA slightly reduced VEGFA reduced barrier resistance only in WT iECs.

Collectively, the ligand induced reduction in resistance of iECs indicate destabilization of endothelial barrier integrity and function by BMP6 and ActivinA.

In sum, short-term BMP6 treatment reduced endothelial barrier integrity only in FOP iECs, whereas long-term BMP6 treatment resulted in reduced barrier integrity of both WT and FOP iECs.

ActivinA long-term treatment showed a trend of reduced endothelial barrier integrity and only in FOP iECs this effect was as strong as VEGFA alone or in co-treatment.

In WT iECs, VEGFA caused the strongest reduction in barrier resistance, which was slightly impaired by co-treatment with ActivinA. Reduction in barrier integrity by BMP6 and ActivinA could be increased by specific kinase inhibitors, indicating contribution of ALK2 in this process.

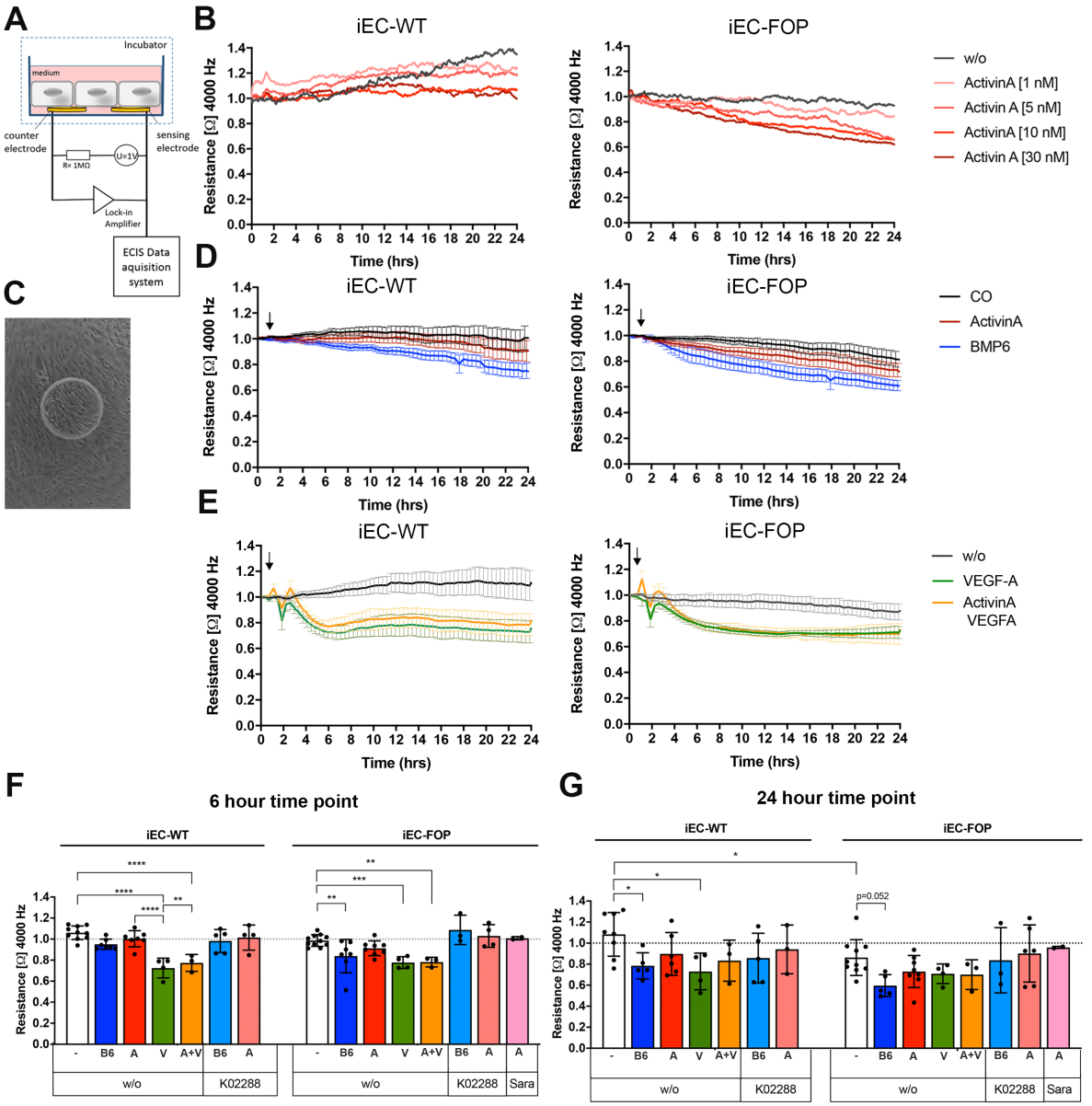

Figure 3.29 Influence of ActivinA on iEC barrier integrity. iECs were seeded on gold electrode arrays 72 hours before measurement and grown to confluency. Cells were starved 4-6 hours before stimulation with indicated growth factors. Impedance was measured at 4000 Hz and is depicted as Resistance and normalized to 1 hour time point before stimulation. (**A**) Schematic cross section of an Electric Cell-Substrate Impedance Sensing (ECIS) culture well. ECs are seeded on top of sensing and counter gold electrodes in cell culture arrays until cells have formed a confluent monolayer. During measurement the electrodes are connected to a lock-in amplifier and a constant alternating current signal is applied via a 1 MΩ resistor. (**B**) ECIS kinetic measurement of WT and FOP iECs treated with different doses of ActivinA. (**C**) Phase contrast image of dense iEC monolayer on one gold electrode (circle). (**D-E**) ECIS kinetic measurement of WT and FOP iECs treated with ActivinA and BMP6 (10nM) (n=7-9), VEGFA (2 nM) (n=3-6). Resistance is depicted as mean F.I. ± SEM. (**F-G**) Quantification of resistance values of specific time points (6 and 24 hours). Resistance is depicted as mean F.I. ± SD. K02288 inhibitor was applied 1 hour before ligand stimulation (0.5 µM) (ActivinA (A); BMP6 (B6); VEGFA (V)). * p<0.05, ** p<0.01, ***p<0.001, ****p< 0.0001. Significance was calculated using two-way ANOVA. (F.I.: Fold Induction; SD: Standard Deviation).

ActivinA induced destabilization of iEC monolayers is independent of SRC and VE-Cadherin

Reduction in measured resistance in an ECIS experiment, represents increased current flow under and between the cells, which indicates changes in cell-cell contact formation. Recently, BMP6 induced permeability by internalization and SRC mediated phosphorylation of VE-Cadherin was shown in venous ECs, which was ALK2 dependent (Benn et al., 2016). Even though the reduction of ActivinA and BMP6 on iEC barrier function was not very strong, the effect of both ligands on SRC and VE-Cadherin was analyzed.

Short-term (30 min) treatment of BMP6, ActivinA (including BMP2 and TGFβ) did not induce phosphorylation of SRC or VE-Cadherin in WT or FOP iECs (Figure 3.30E,F). Based on the long-term effect of ActivinA and BMP6 on iEC barrier function SRC and VE-Cadherin levels were analyzed upon ligand treatment for 2, 6 and 24 hours. Also upon long-term stimulation, BMP6 and ActivinA did not induce phosphorylation of SRC or VE-Cadherin in WT or FOP iECs (Figure 3.30A,B). Moreover, the total protein levels of the junctional protein VE-Cadherin did not change upon ligand treatment (Figure 3.30A,B). This is supported by gene expression analysis, including PECAM-1, which was not significantly changed upon ActivinA treatment in iEC (see previous Figure 3.24). Moreover, differentially expressed gene (DEG) analysis between untreated and ActivinA treated iECs and between WT and FOP using RNASeq data did not identify any differentially regulated genes encoding junctional proteins.

However, the previously observed reduction of pAKT levels by ActivinA were confirmed after 2 hours and lasted even until 24 hours in FOP iECs. (Figure 3.30A,B and Figure 3.30C,D). After 24 hours, control pAKT levels were only reduced in FOP iECs (Figure 3.30A,B and Figure 3.30C,D). The kinetic pattern of pAKT levels was in line with the reduction of the measured resistance of FOP iEC monolayers, indicating an involvement of AKT in endothelial barrier integrity. Interestingly, recent evidence suggests that long-term barrier instability is associated with decreased pAKT levels (Gao et al., 2017).

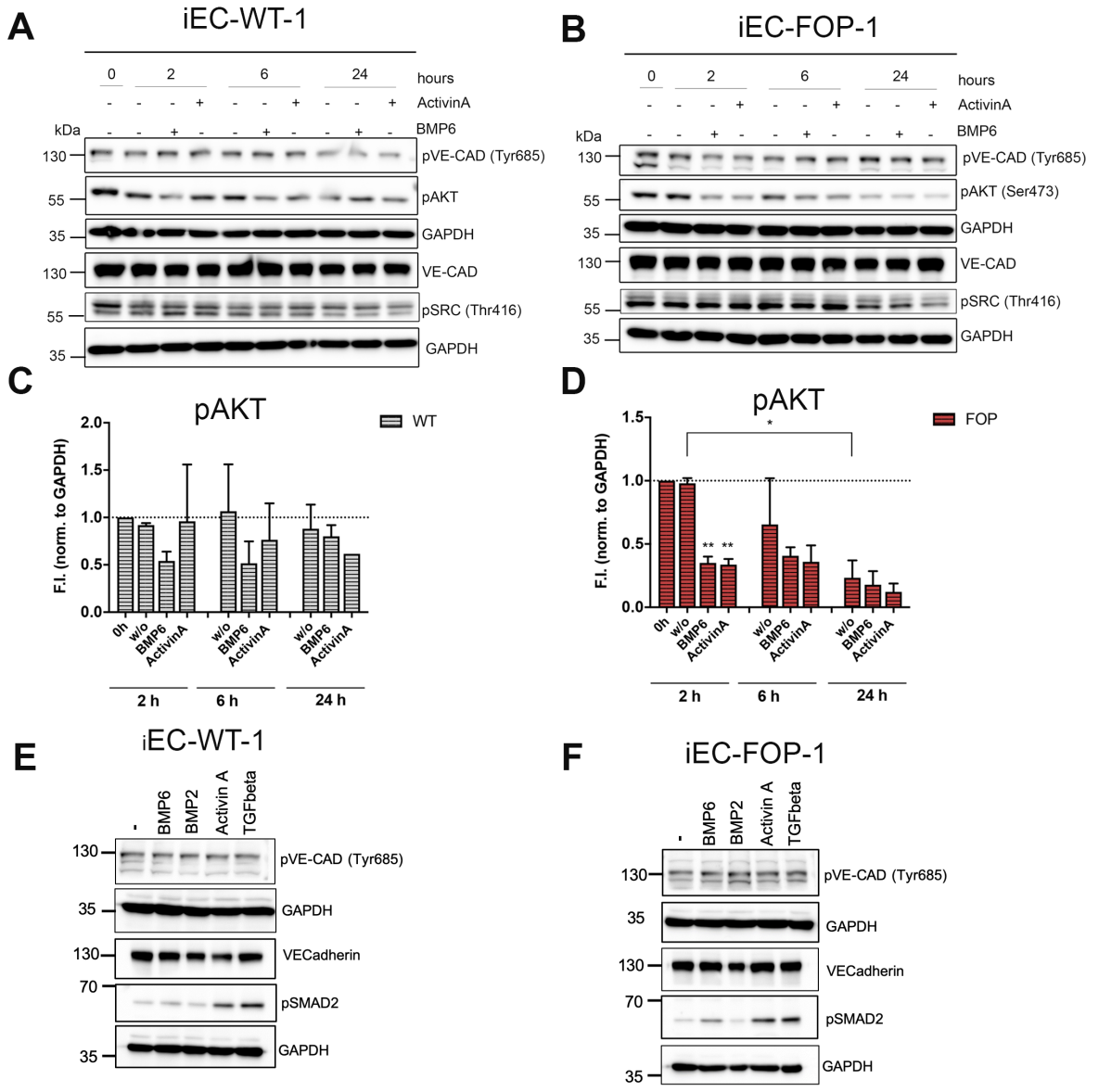

Figure 3.30 ActivinA and BMP6 do not activate SRC and VE-Cadherin.
(**A-B**) Western Blot of protein lysates from WT (**A**) and FOP iECs (**B**) after long-term treatment with ActivinA and BMP6 (10 nM) for different time points. (**C-D**) Densiometric quantification of phosphorylated (p) AKT levels normalized to GAPDH after ActivinA, BMP6 treatment of WT and FOP iECs for different time points. Data is shown as mean ± SD. (**E-F**) Western Blot of protein lysates from WT (E) and FOP iECs (F) after short-term treatment with BMP6, BMP2, ActivinA (5 nM) and TGFβ (0.2 nM). (SD: Standard Deviation). * p<0.05, ** p<0.01. Significance was calculated using one-way ANOVA. (F.I.: Fold Induction; SD: Standard Deviation).

Identification of two endothelial barrier modulators in the ActivinA induced FOP transcriptome

Even though RNASeq analysis of ActivinA treated iECs for 2 hours did not identify any differentially regulated genes encoding junctional proteins, two other interesting candidate genes were identified, which are associated with endothelial barrier integrity: ***TCIM*** (Transcriptional and immune response regulator) and ***ADM*** (Pro-adrenomedullin) (Figure 3.31).

TCIM and *ADM* were among the five most differentially expressed genes upon ActivinA stimulation in both FOP iEC donors (Figure 3.31A,B).

ID1, SMAD6, SMAD7, NOGGIN (NOG) and *TCIM* had the highest fold change (FC of ≥ 2.8) of the upregulated genes among the 212 shared DEG ($p<0.05$), after ActivinA stimulation in both FOP iEC donors (Figure 3.31A,B).

The five most downregulated genes with the highest fold change (FC of ≥ 1.8) consisted of different gene candidates in each FOP iEC donor, except the genes *ADM* and *DEPP1* (Decidual protein induced by progesterone), which were shared between both FOP iEC donors (Figure 3.31A,B).

The top five upregulated genes in both FOP iEC donors belong to classical BMP target genes except TCIM. **TCIM** (TC-1: Thyroid Cancer 1) is a small monomeric protein, originally discovered as an upregulated gene in thyroid cancer (Chua et al., 2000; Sunde et al., 2004). Interestingly, one study analyzed the role of TCIM in the endothelium and suggested TCIM as a novel endothelial inflammatory regulator, which enhances endothelial monocyte adhesion and permeability in overexpression (Kim et al., 2009). Thus, ActivinA induced upregulation of *TCIM* may contribute to the reduced barrier function of FOP iEC monolayers.

In addition, the ActivinA induced downregulation of the peptide hormone **ADM** could also contribute to the ActivinA induced permeability in FOP iECs. ADM belongs to adrenomedullin family, which is associated with barrier-stabilizing effects (García-Ponce et al., 2016). In fact, ADM was shown to reduce endothelial hyperpermeability in a dose dependent manner (Hippenstiel et al., 2002). FOP specific upregulation of *TCIM* expression and downregulation of *ADM* by ActivinA was validated by RT-PCR (Figure 3.31C,D).

BMP6 treatment regulated *TCIM* and *ADM* expression in a similar manner as ActivinA in FOP iECs and additionally also in WT iECs (Figure 3.31C,D). Of note, basal ADM expression levels were lower in FOP iECs compared to WT iECs (Figure 3.31D).

Importantly, pretreatment with Saracatinib resuced induction of *TCIM* and reduction of *ADM* by ActivinA in FOP iECs (Figure 3.31C,D).

Collectively, ActivinA triggered destabilization of iEC monolayers was independent of direct activation of SRC and VE-Cadherin but indicated an association with reduced pAKT levels (Figure 3.30). The reduction of iEC barrier function after 4 hours may involve transcriptional dependent mechanism, such as the contribution of the ActivinA regulated genes *TCIM* and *ADM*.

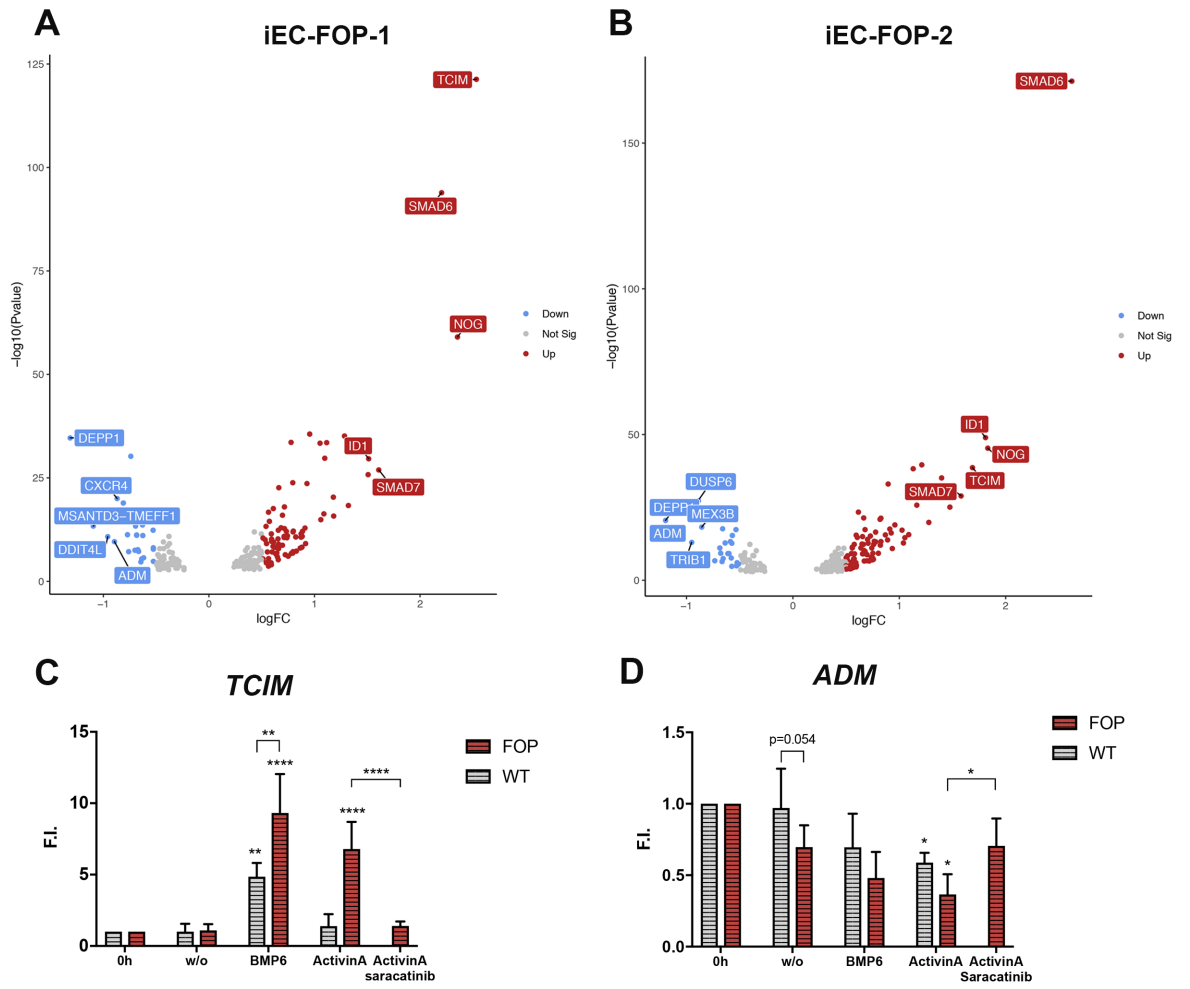

Figure 3.31 Two top deregulated genes of ActivinA treated iECs are associated with endothelial barrier function. (**A-B**) Volcano Plot of DEG of ActivinA treated FOP iECs. Genes (adjusted p value<0.05; 0.58≤ log2FC ≥0.58), up-/downregulation is indicated by color. Genes with highest fold change (FC) are labeled: (blue: log2FC≤-0.9), (red: log2FC≥1.51), (DEG: Differentially expressed genes). (**C-D**) RT-PCR validation of RNASeq target groups upon 1 hour pretreatment with Saracatinib (0.2 µM) and 2 hour ActivinA (5 nM) (n=4-5), BMP6 (5 nM) (n=2) treatment in iECs. * p<0.05, ** p<0.01, ***p<0.001, ****p< 0.0001. Significance was calculated using two-way ANOVA. (F.I.: Fold Induction; SD: Standard Deviation).

3.8.2 **Influence of ActivinA on Sprouting Angiogenesis**

Measurement of endothelial barrier function indicated that ActivinA long-term treatment destabilized endothelial barrier integrity. To analyze whether the effect of ActivinA on iEC monolayers (2D) also influences the formation of endothelial sprouts (3D) *in vitro*, a Sprouting Angiogenesis assay was performed.

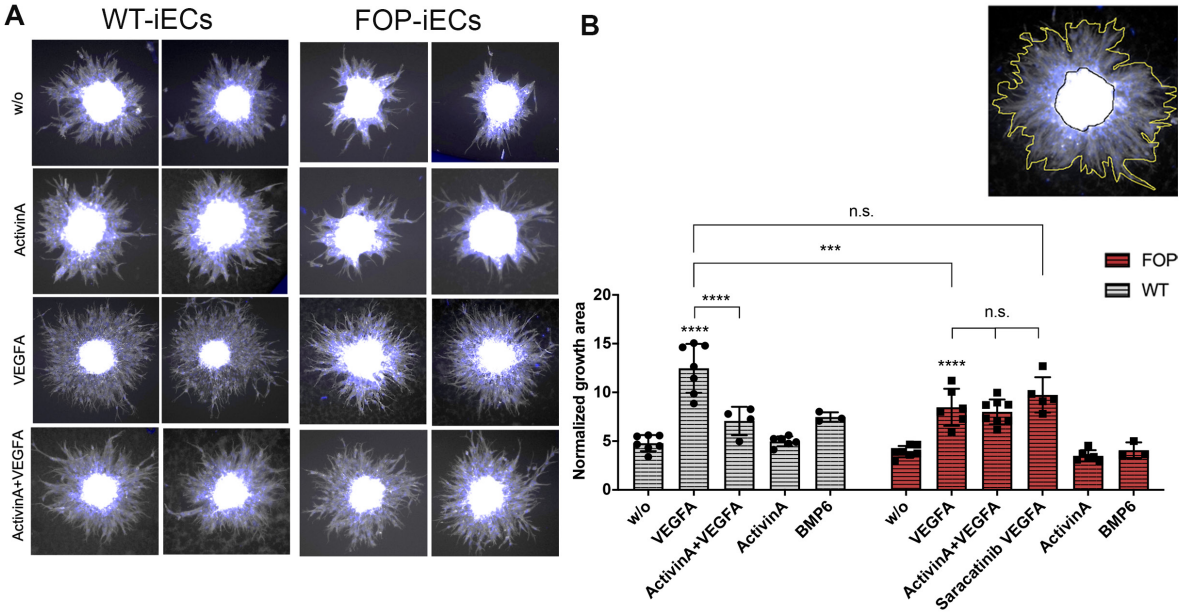

Figure 3.32 ActivinA impairs VEGFA induced angiogenesis only in WT iECs. (**A**) Representative images of epifluorescence imaged iEC spheroids stained with phalloidin and DAPI after 24 hours treatment with respective growth factors (VEGFA (5 nM), ActivinA, BMP6 (10 nM)). (**B**) Spheroid outgrowth area (SOA) was measured and normalized to spheroid size using ImageJ. Data is represented as mean F.I. ± SD of two WT and two FOP donors from two independent experiments with n>3 spheroids per condition. (F.I.: Fold Induction; SD: Standard Deviation, ***p<0.001, ****p< 0.0001. Significance was calculated using two-way ANOVA.

WT and FOP iEC spheroids were generated and seeded for sprout formation on growth factor reduced Matrigel for 24 hours in starvation conditions supplemented with growth factors or PBS as control. The spheroid outgrowth area (SOA) was measured and normalized to spheroid size. Stimulation with VEGFA potently induced the outgrowth of endothelial sprouts in both genotypes (Figure 3.32A). But interestingly, the quantification of the relative outgrowth area revealed that VEGFA induced more outgrowth in WT iECs compared to FOP iECs (Figure 3.32B). Thus, VEGFA induced sprouting outgrowth was significantly different between WT and FOP iECs (Figure 3.32B). Importantly, this difference was not significant anymore when FOP iECs were pre-treated with Saracatinib (Figure 3.32B). ActivinA treatment did not induce endothelial sprouting compared to the controls (w/o) in both genotypes

(Figure 3.32A,B). BMP6 only induced a minor increase in WT iECs compared to untreated controls (w/o) (Figure 3.32A,B).

To assess whether the aberrant ActivinA signaling in FOP versus WT iECs may influence VEGFA induced angiogenesis, a co-treatment was performed.

VEGFA induced sprouting outgrowth was markedly reduced in WT iECs in presence of ActivinA (Figure 3.32B). In contrast, ActivinA did not reduce the VEGFA induced sprouting outgrowth in FOP iECs, which remained at similar induction levels compared to VEGFA only treatment (Figure 3.32B). In sum, FOP iECs showed reduced VEGFA induced sprouting compared to WT iECs. However, ActivinA only impaired VEGFA induced angiogenesis in WT iECs and not FOP iECs.

3.9 Under Fluid Shear Stress WT iECs gain aberrant ActivinA/SMAD1/5 signaling

Previous investigations were conducted in static *in vitro* settings, however the vasculature *in vivo* is normally exposed to mechanical forces, such as fluid shear stress (FSS) by blood flow which integrate into growth factor signal transduction (Givens and Tzima, 2016). FSS was applied to iEC in full medium condition to analyze ActivinA signaling in a more physiological setting. Therefore, iEC were seeded on µ-slides for 2 days to form a tight endothelial monolayer (Figure 3.33A-C).

Arterial FSS ranges from 10-50 dyn/cm^2 and in venous circulation only up to 20 dyn/cm^2 (Givens and Tzima, 2016). iECs were exposed to intermediate FSS range of 30 dyn/cm^2. After 24 hours FSS in full medium, iEC monolayers were morphologically analyzed by phase contrast microscopy in comparison to static controls and before the application of FSS (Figure 3.33C). WT and FOP iECs formed dense monolayers in all conditions. Compared to static control iECs exposed to 24h FSS showed similar morphology and no alignment to the flow direction (Figure 3.33C). Interestingly, morphologic differences of cellular shape and size were also observed independent of FSS between “Before FSS” and “static”, indicating a growth effect upon 24 hours incubation in full medium (Figure 3.33C).

After application of FSS for 24 hours, ActivinA was added to the full medium and FSS was continued for 1 hour in presence of ActivinA. Subsequently iECs were lysed and ActivinA signaling was analyzed (Figure 3.33B). In the first experiment ActivinA treatment (10 nM) induced canonical SMAD2 phosphorylation in static and under FSS in WT and FOP iECs, whereas pSMAD1/5 levels in the static condition remained

unchanged upon ActivinA treatment. FSS alone reduced basal pSMAD1/5 levels in WT and FOP iECs (Figure 3.33D). FSS and ActivinA treatment highly increased pSMAD1/5 levels in FOP iECs (Figure 3.33D), confirming the aberrant ActivinA/SMAD1/5 signaling from previous investigations under static, starvation conditions. Unexpectedly, WT iECs also increased pSMAD1/5 levels upon ActivinA stimulation under FSS (Figure 3.33D). Moreover, FSS alone minorly increased phosphorylated AKT levels whereas no phosphorylated AKT was observed in in static conditions. ActivinA treatment did not induce phosphorylation of AKT in static conditions, however under FSS phosphorylated AKT levels strongly increased in both WT and FOP iECs (Figure 3.33C).

Based on the strong effect of 10 nM ActivinA in full medium conditions, subsequent experiments were performed with 3 nM ActivinA. Physiological levels of ActivinA in human serum were reported in concentrations of 0,0042-0,049 nM (de Kretser et al., 2013; Harada et al., 1996), which are elevated during pregnancy (0,4 nM) (Harada et al., 1996). Current knowledge suggests that ActivinA serum levels in FOP patients are not elevated (Hildebrand et al., 2017a).

ActivinA induced aberrant SMAD1/5 signaling under FSS was confirmed for all WT and FOP donors in independent experiments (Figure 3.33F). The quantification revealed that ActivinA equally increased pSMAD1/5 levels in both WT and FOP iECs under FSS (Figure 3.33G). Minor activation of SMAD1/5 was also observed in static, full medium conditions in WT and FOP iECs (Figure 3.33G**)**. Thus ActivinA/SMAD1/5 signaling was confirmed on BMP target gene transcription (*ID1*) under static and FSS condition in WT and FOP iECs (Figure 3.33E). This indicates that ActivinA may induce SMAD1/5 responses in WT iECs also independent of FSS bur requiring full medium conditions.

Next, it was analyzed if changes in the intracellular type I receptor inhibitor FKBP12 (*FKBP1A*) or ALK2 expression were responsible for the gain in ActivinA/SMAD1/5 response in WT iECs in full medium and under FSS (Figure 3.33E). Even though FOP iECs showed slightly lower levels of *ALK2* and *FKBP1A* expression in each condition, no significant differences could be assessed.

Collectively, FOP iECs showed robust aberrant SMAD1/5 signaling in static starvation conditions and in full medium under FSS. In contrast, WT iECs only respond robustly to ActivinA with SMAD1/5 signaling in full medium under FSS. This indicates, that ActivinA/SMAD1/5 signaling is highly context dependent and favored but not limited to ALK2-R206H expressing cells. This is supported by recent evidence of

ActivinA/SMAD1/5 signaling in ALK2-WT expressing myeloma cells (Olsen et al., 2020, 2018). However, it remains a task of future studies to determine the context dependent co-factor(s), which mediate the formation of an active ActivinA-ALK2 receptor complex transducing SMAD1/5 signals.

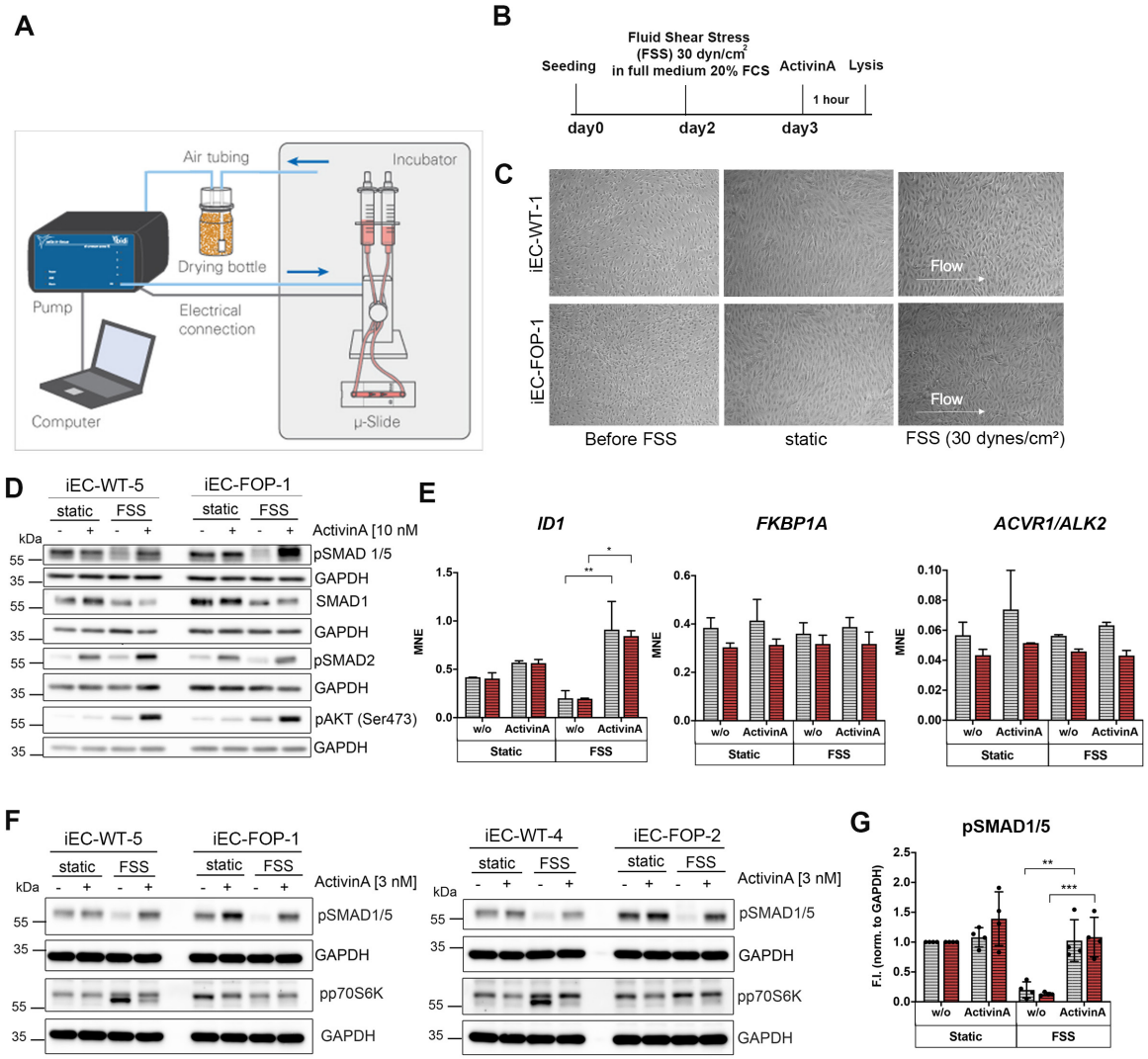

Figure 3.33 WT iECs gain ActivinA/SMAD1/5 signaling in full medium and under FSS conditions. (**A**) Scheme depicting the Fluid Shear Stress (FSS) experimental setup using the ibidi pneumatic pump system (image retrieved from ibidi.de). (**B**) iECs were seeded on µ-slides 48 hours before application of FSS for 24 hours after a 6 hour ramp phase to reach step-wise 30 dyne/cm^2 in full medium. iECs under FSS in full medium were exposed to ActivinA for 1 hour. (**C**) Phase contrast images of iEC on µ-slides before and after FSS as well as in control static conditions. (**D**) Western Blot of protein lysates of iECs after above described experimental conditions using 10 nM ActivinA. (**E**) RT-PCR of *ID1, FKBP1A* and *ALK2* from RNA of iECs under above described FSS conditions using 3 nM ActivinA (n=2) (**F**) Representative Western Blot of protein lysates of iECs after above described experimental conditions using 3 nM ActivinA. (**G**) Densiometric quantification of pSMAD1/5 protein levels relative to GAPDH of Western Blots in F.

4. Discussion

Episodic extraskeletal bone formation in soft tissue by heterotopic ossification (HO) is a major clinical hallmark in the rare disease Fibrodysplasia Ossificans Progressiva (FOP). Independent of the location and initial triggers, ectopic bone in FOP forms via a complex-multi-stage process, which mimics the developmental process of endochondral bone formation. Bone as a highly vascularized organ is not only supplied with gases and nutrients by blood vessels, in fact increasing evidence from recent years show that angiogenic processes are essential for bone formation in development and postnatally (Sivaraj and Adams, 2016). Blockage or loss of the pro-angiogenic factor Vascular Endothelial Growth Factor A (VEGFA) impairs endochondral bone formation by disturbed vascular patterning, decreased chondrocyte differentiation and ossification (Gerber et al., 1999; Liu and Olsen, 2014; Maes et al., 2002). This is also evident for ectopic bone formation: very recent studies demonstrated that VEGFA is critical for HO (Hwang et al., 2019) and confirmed that HO lesions are highly angiogenic (Cocks et al., 2017; Hwang et al., 2019; Kaplan et al., 1993; Shore and Kaplan, 2010). Importantly, FOP patient biopsy analysis uncovered even increased vessel number in HO lesions compared to non-hereditary HO (Ware et al., 2019).

Moreover, the endothelium has remarkable plasticity. Endothelial to mesenchymal transition (EndMT) is not only observed in heart development but also a hallmark of several pathologies ranging from atherosclerosis, tissue fibrosis and HO (Dejana et al., 2017). Human FOP biopsies of HO lesions showed co-expression of endothelial and osteogenic markers (Medici et al., 2010).

However, it remains elusive, which mechanisms orchestrate the endothelium in ectopic bone formation and which signals are responsible for the aberrant vascular phenotype in FOP lesions.

FOP is caused by gain of function mutations in the BMP type 1 receptor ALK2 (ACVR1) with R206H being the most common point mutation located in the intracellular glycine-serine (GS) rich domain (Shore et al., 2006). Mutant receptors lead to hyperactivated SMAD1/5 signaling in response to BMPs (Shen et al., 2009) and aberrantly transduce SMAD1/5 signaling in response to ActivinA (Hatsell et al., 2015; Hino et al., 2015). In FOP mice, blocking of ActivinA prevents HO indicating a central role of this ligand in

the disease (Hatsell et al., 2015). Whether ActivinA causes the vascular phenotype observed in human FOP biopsies is unknown.

In the present study a patient derived endothelial cell (EC) model was generated by using induced Pluripotent Stem Cells (iPSCs) in a combinatorial cryopreservation and differentiation method. FOP iPSC derived EC (iECs) recapitulated the pathological aberrant ActivinA/SMAD1/5 signaling. A comprehensive transcriptome analysis of ActivinA treated FOP ECs identified a FOP-specific genetic profile interlinking ActivinA with BMP/NOTCH pathways, blood vessel formation and EndMT markers. Drug testing in the FOP endothelial disease model showed that the kinase inhibitor Saracatinib rescued the ActivinA-induced transcriptome in FOP iECs to WT levels, suggesting a preventive effect on aberrant vascularization in early HO lesions in FOP.

4.1 Patient iPSCs enable the generation of a FOP disease model

The establishment of patient-derived models of FOP has been challenging due to the limited number of patients and the risk to trigger HO upon tissue biopsy sampling. To overcome restrictions and challenges of primary patient material and the limitations of overexpression approaches in established EC models, induced Pluripotent Stem Cells (iPSCs) generated from FOP patients were used (Hildebrand et al., 2016). iPSCs are a versatile cell model, which enables the generation of specific cells types of various tissues in unlimited numbers carrying the patient specific mutations and have become an important technology for rare diseases (Anderson and Francis, 2018).

The here used FOP iPSCs harboring the ALK2 R206H mutation (FOP-1, FOP-2) and two healthy controls (WT-1, WT-2) were previously characterized and validated according pluripotency and differentiation capacity in all three germ layers (Hildebrand et al., 2016b; Rossbach et al., 2017, 2016). However, a characterization of iPSC SMAD responses was lacking. Therefore, SMAD responses of FOP iPSCs in comparison to WT iPSCs were analyzed here.

4.1.1 iPSCs show robust SMAD2 signaling – a hallmark of pluripotency and differentiation potential

Activation of SMAD2 was analyzed in iPSCs as SMAD2/3 signaling is essential for stem cell self-renewal, pluripotency maintenance (James et al., 2005; Xiao et al., 2006) but also to induce endoderm differentiation (Mullen and Wrana, 2017; Yang and Jiang, 2020). Analysis of SMAD2 is sufficient because it plays a more significant role in maintaining pluripotency in ESC (Mullen and Wrana, 2017;Yumoto et al., 2013).

SMAD2 directly binds to the promoter of the pluripotency transcription factor NANOG and enhances its transcription in ESCs (Vallier et al., 2009; Xu et al., 2008). Moreover, OCT4 and NANOG form complexes with SMAD2 in ESCs and jointly regulate a subset of their target genes including the expression of pluripotency genes (Beyer et al., 2013; Brown et al., 2011;Vallier et al., 2009). Recent evidence shows that SMAD2/3 also interact with epigenetic modifiers to control pluripotency gene transcription via permissive or repressive chromatin environments (Yang and Jiang, 2020). However, SMAD2/3 activation also induces endoderm differentiation by direct binding to endoderm specifiers such as *SOX17* (Kim et al., 2011).

Differences in SMAD2/3 signaling intensity is crucial for divergent regulation of pluripotency and differentiation (Yang and Jiang, 2020). Whereas low ActivinA concentrations (5 ng/ml) maintain ESC pluripotency (Xiao et al., 2006), high ActivinA concentrations (50-100 ng/ml) lead to endoderm differentiation (Kim et al., 2011; Mullen and Wrana, 2017; Yang and Jiang, 2020).

Here, it was confirmed that WT and FOP iPSCs are capable to respond with increased SMAD2 phosphorylation intensity to higher ligand concentrations of TGFβ and ActivinA (Figure 3.1). WT and FOP iPSCs were already sensitive to small concentrations of ActivinA (0.3 nM) and TGFβ (0.001 nM) (Figure 3.1). A high sensitivity towards ActivinA is in line with the high *ACVR2B* receptor expression levels in iPSCs (Figure 3.8). Compared to *ACVR2B* the high affinity receptor for TGFβ (*TGFBR2*) is relatively low expressed. Respective type I receptors (*ALK4* (*ACVR1B*) and *ALK5* (*TGFBR1*)) showed similar expression levels (Figure 3.8). Both, TGFBR2 and ACVR2B bind their ligands with very high affinities (Aykul and Martinez-Hackert, 2016).

However, TGFBR2 only binds TGFβ ligands the ACVR2B binds to multiple ligands with high affinity, including Activin class ligands but also certain BMPs, such as BMP9 (Aykul and Martinez-Hackert, 2016; Townson et al., 2012). Thus, ACVR2B is likely higher expressed in iPSC compared to TGFBR2 to enable signaling complex formation with diverse ligand groups.

4.1.2 Aberrant ActivinA/SMAD1/5 responses in FOP iPSCs may impair their fate

In addition to SMAD2 phosphorylation ActivinA also induced SMAD1/5 phosphorylation, but only in FOP iPSCs (Figure 3.1C). Thus, already FOP iPSCs show the disease characteristic aberrant ActivinA/SMAD1/5 signaling. This is in line with one previous study showing ActivinA/SMAD1/5 in FOP iPSCs (Barruet et al., 2016) using the FOP iPSCs generated from (Matsumoto et al., 2013).

However, ActivinA responses of iPSC generated from other FOP patients remain unknown (Cai et al., 2015; Hamasaki et al., 2012; Hayashi et al., 2016; Sánchez-Duffhues et al., 2019b).

For comparison TGFβ only induced SMAD2 phosphorylation in FOP and WT iPSCs (Figure 3.1E), which suggests that aberrant SMAD1/5 signaling in FOP iPSCs is specific to ActivinA. In contrast to SMAD2/3 signaling, SMAD1/5 signaling in human iPSCs or ESCs is associated with mesodermal differentiation (Faial et al., 2015). Several studies showed that BMP4 signaling is a key inducer of mesoderm in human ESCs (Bernardo et al., 2011; Patsch et al., 2015; Yang et al., 2008; Zhang et al., 2008). SMAD1 binds to the *NANOG* promoter in human ESCs but in contrast to SMAD2/3, NANOG promoter activity is decreased by SMAD1/5/8 signaling, thereby reducing pluripotency (Xu et al., 2008). In addition, the mesodermal transcription factor Brachyury (BRA) interacts with SMAD1 and the cooperative action is essential for mesodermal differentiation (Faial et al., 2015; Messenger et al., 2005).

This indicates, that aberrant ActivinA/SMAD1/5 signaling may result in reduced pluripotency of FOP iPSC when cultured in ActivinA containing iPSC growth medium, such as PluriSTEM (Dakhore et al., 2018). Of note, the iPSC culture medium used here (E8-Medium formulation) contained TGFβ but no ActivinA (Chen et al., 2011; Dakhore et al., 2018).

Thus, FOP iPSC should not be cultured in ActivinA cultured growth medium.

4.2 Establishment of a new FOP endothelial cell model by a combinatorial cryopreservation and differentiation method without ActivinA

Patient iPSCs were used to generate FOP ECs (iECs) aiming to model the human FOP endothelium. Based on aberrant ActivinA/SMAD1/5 signaling in FOP iPSCs, a EC differentiation protocol devoid of exogenous ActivinA (Patsch et al., 2015) was adjusted and optimized (Hildebrandt et al., Stem Cell Rev Rep, in press 2020).

The first experiments indicated a high degree of variability in differentiation efficiency (10-80%) independent of the donor, which most likely occurred due to different iPSC passage numbers.

To overcome this problem, the iPSC EC differentiation method was combined with the controlled cryopreservation method *CryoPause* (Wong et al., 2017) (described in chapter 3.1.2). With this method iPSCs could be immediately seeded for differentiation after thawing. Thus, a batch of cryopreserved iPSCs enables that the same cell population can be used for several differentiations, which successfully reduced the passage variability in differentiation efficiency for each donor.

Current literature suggests, that this study represents the first method combining iPSC *CryoPause* by Wong *et al.* with subsequent endothelial differentiation. Recently, *CryoPause* was also combined with the differentiation of iPSCs into midbrain dopaminergic neural progenitor cells and improved the reproducibility of neuronal differentiation (Drummond et al., 2020).

Experimental variability is still a major challenge in studies using iPSC-derived models (Volpato and Webber, 2020). Compared to immortalized cell lines and other primary cells, iPSC and ESCs require more demanding culture conditions to maintain cell viability and pluripotency. iPSC derivation and directed differentiation methods are complex multistep processes lasting for several days and thus small variations accumulate and cause significant different outcomes (Popp et al., 2018; Volpato and Webber, 2020). The main sources and effects of variation in iPSC cultures are based on the genetic background of different donors, somatic mutations but also routine cell culturing, such as passage number, growth rate and culture medium (Volpato and Webber, 2020).

Thus, the beneficial effect of *CryoPause* likely underlies the reduction of technical but also biological variability such as gene expression or cell cycle status.

Moreover, this method did not only reduce variability in EC differentiation, it also circumvents regular iPSC culture and maintenance between different EC differentiation experiments. Besides experimental advantages, this combined method also improved logistic and organizational hurdles for our particular collaborative project at two lab locations, which may also be useful for other projects.

In future projects, efficiency and reproducibility could be further optimized by the generation of isogenic controls from FOP iPSC by correcting the ALK2 point mutation using genome editing, such as CRISPR/Cas9.

However, even though genome editing methods have been continuously improved, homologues dependent recombination (HDR), which is required for Knock In approaches remain challenging and have lower efficiencies compared to targeted Knock Outs (Liu et al., 2019). So far, the first FOP iPSC rescue for gene correction was performed by traditional bacterial artificial chromosome (BAC)-based homologous recombination (Matsumoto et al., 2015). Another interesting approach simultaneously reprogrammed FOP foreskin fibroblasts and corrected the ALK2-R206H mutation by delivering reprogramming vectors together with CRISPR (Clustered Regularly Interspaced Short Palindromic Repeats)/Cas9 vector-based reagents including a single-stranded oligodeoxynucleotide for gene repair (Kim et al., 2016).

4.2.1 **ActivinA is not required to generate ECs from iPSCs**

Methodological differences between the FOP iEC differentiation protocol presented here (Hildebrandt et al., Stem Cell Rev Rep, in press 2020) and previous studies (Barruet et al., 2016; Cai et al., 2015) include distinct EC isolation markers and monolayer versus embryoid body (EB) formation approaches (Figure 4.1). Those may account for lower differentiation efficiencies (up to 30%) as well as reduced viability and EC marker expression in previous studies (Barruet et al., 2016; Cai et al., 2015). FOP iECs generated here showed efficiencies up to 80% and no impaired EC characteristics. In addition, a key difference to previous iEC generation methods of previous studies is the usage of exogenous ActivinA for mesoderm induction (Barruet et al., 2016; Cai et al., 2015) (Figure 4.1)**.** Here, it was demonstrated that FOP iPSCs show aberrant ActivinA/SMAD1/5 signaling, therefore in this study mesoderm was induced exclusively with BMP4 (without ActivinA supplementation) (Hildebrandt et al., Stem Cell Rev Rep, in press 2020 (Patsch et al., 2015), while above mentioned studies used established methods for iEC generation (with exogenous ActivinA and BMP4) (Orlova et al., 2014; White et al., 2013).

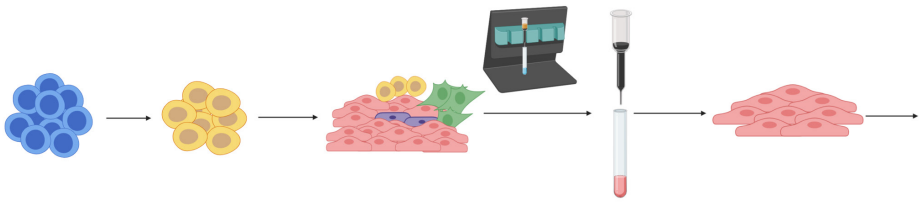

	iPSC Seeding	Mesoderm Induction	Endothelial Cell Specification	Endothelial Cell Enrichment	Endothelial Cell Expansion	Endothelial Cell Maintenance
Hildebrandt *et al.*, SCRR, in press 2020	Single cell Monolayer from thawed iPSC Geltrex	Day 1 - BMP4 (25 ng/ml) CHIR (6-7 µM)	Day 4 VEGFA (200 ng/ml) Forskolin (2 µM)	Day 6 CD144+ MACS sort	EBM-2 (Lonza)+ VEGFA,FGF2,Heparin, Ascorbic Acid, IGF, EGF 20% FCS SB431542 0.1% Gelatin	EBM-2 (PromoCell)+ VEGFA,FGF2,Heparin, Ascorbic Acid, IGF, EGF 20% FCS SB431542 0.1% Gelatin
Barruet E. *et al.*, 2016	Embryoid Body from passaged iPSC	Day 1 ActivinA (3.6 ng/ml) BMP4 (12 ng/ml) bFGF (5 ng/ml)	Day 4 VEGFA 2ng/ml bFGF 2ng/ml	Day 6 KDR+/CD31+ FACS sort	ECM (ScienCell)+ 5% FBS 1% ECGS Fibronectin	ECM (ScienCell)+ 5% FBS 1% ECGS Fibronectin
Cai J. *et al.*, *2015*	Colony Monolayer from passaged iPSC Matrigel	Day 1 ActivinA (25ng/ml) BMP4 (30 ng/ml) VEGFA (30ng/ml), CHIR (1.5 µM)	Day 4 VEGFA (30ng/ml) SB431542 (10µM)	Day 10 CD31+ MACS sort	hEC-SFM (ThermoFisher)+ 1% Plasma VEGFA FGF2 0.1% Gelatin	hEC-SFM (ThermoFisher)+ 1% Plasma VEGFA FGF2 0.1% Gelatin

Figure 4.1 Methodological differences between FOP iPSC derived EC models. Summarized methodological differences between the endothelial FOP model presented here Hildebrandt et al., Stem Cell Rev Rep in press 2020 and others (Barruet et al., 2016; Cai et al., 2015).

ActivinA is frequently used in addition to BMP4 for mesoderm induction of PSCs. This is most likely based on early studies in amphibians, which show ActivinA and FGF2 as critical mesoderm inducers in Xenopus development (Cornell and Kimelman, 1994; LaBonne and Whitman, 1994). However, in human ESCs the effect of ActivinA has mainly been shown to maintain pluripotency (Xiao et al., 2006) or to induce endoderm differentiation at high concentrations (D'Amour et al., 2005) as explained previously (see chapter 4.1.1). There is also evidence that ActivinA treatment induces mesoderm formation by increasing *BRA* and other mesodermal genes, however it is dependent on the presence of BMP4 (Cerdan et al., 2012; Ludovic Vallier et al., 2009). Interestingly SB431542 treatment revealed that Activin/TGFβ type I receptor activity is required for BMP4 induced mesoderm in human ESCs (Zhang et al., 2008). Based on the herein observed BMP6/SMAD2- and SMAD1/5-responses in WT and FOP iPSCs, I propose that SMAD2 and SMAD1/5 responses are required for mesoderm induction, which can be both induced by BMP and do not require ActivinA.

BMP6/SMAD2 responses in iPSCs are likely transduced via heteromeric receptor complexes including Activin/TGFβ type I receptors as shown for BMP6 induced pSMAD2 in FOP iECs. The presence of different type I receptors in the same receptor

complex has been reported previously: For example in Bmp2-Bmp7 heterodimer activated BMP signaling in zebrafish embryos (Little and Mullins, 2009) or in TGFβ induced SMAD2/3 and SMAD1 signaling in ECs (Goumans et al., 2002). Moreover, BMP4 induced mesoderm formation in human ESCs only requires endogenous FGF2 signaling (via ERK) and no exogenous co-treatment with FGF2 (Bernardo et al., 2011). Thus, exogenous BMP4 is sufficient for mesoderm induction in PSCs (Patsch et al., 2015; Zhang et al., 2008). This is supported by *Bmp4* murine knock out models, showing that BMP4 is required for mesoderm development (Winnier et al., 1995). In contrast, mesoderm forms normally in ActivinA (*Inhba*) and *Acvr2* deficient mice (Matzuk et al., 1995a, 1995b; Oh and Li, 1997).

In contrast to BMP4 exogenous ActivinA is not essential for mesoderm development but it may promote mesoderm formation of PSCs *in vitro* when co-treated with BMP4. In context of FOP, ActivinA only activated SMAD1/5 responses in FOP iPSCs, which may impair the iPSC fate in comparison to WT iPSCs. Interestingly, EC differentiation with ActivinA alone only abolished iEC formation (number of PECAM+/VEGFR2+ cells) of WT iPSCs (Barruet et al., 2016). It is likely that aberant activation of SMAD1/5 by ActivinA resulted in mesoderm formation in FOP iPSCs, which might compensate the lack of BMP4/SMAD1/5 responses, not seen in WT iPSCs. As previously described, SMAD1 interacts with BRA and cooperatively induces mesodermal genes (Faial et al., 2015; Messenger et al., 2005). This is supported by the study of Cai et al., which reported increased BRA expression three days after mesoderm induction (including BMP4+ActivinA) in FOP iPSCs (Cai et al., 2015). But in contrast to Barruet et al., iEC formation (PECAM+ cells) of FOP iPSCs was reduced compared to WT iPSCs (Cai et al., 2015). The underlying mechanisms of these differences remain unknown but are likely caused by different ActivinA ligand concentrations and other differences in both EC differentiation methods (Figure 4.1).

Collectively, both studies clearly demonstrate an impact of exogenous ActivinA supplementation on FOP versus WT iEC differentiation. Since exogenous ActivinA is not required for iEC generation, mesoderm induction for **FOP iEC generation** should be performed in **absence of exogenous ActivinA**, as presented here.

4.2.2 **WT and FOP iECs show endothelial functionality**

The here generated iECs were analyzed for EC identity by a series of complementary methods demonstrating EC marker expression and functionality comparable to primary isolated Human Umbilical Vein Endothelial Cells (HUVECs) (Hildebrandt et al., Stem Cell Rev Rep, in press 2020).

In addition to endothelial markers, the expression of ligands and receptors of the TGFβ superfamily was analyzed. No differences in receptor expression levels between WT and FOP iECs was detected. This is in accordance with findings from another WT and FOP iEC model (Barruet et al., 2016). Recently, FOP ECFCs were reported to have increased expression levels of ALK1, ALK4, BMPR2 and the co-receptor Cripto-1 (Sánchez-Duffhues et al., 2019c). However, these effects were not very strong and heterogenous among the donors. Interestingly, RT-PCR and RNA-Seq revealed that Cripto-1 (*TDGF1*) was also higher expressed in one FOP iEC donor (FOP-2) (Figure 3.7 and Figure 3.8), suggesting donor specific effects, which may account for the phenotypic heterogeneity in FOP. Collectively, WT and FOP iECs showed no functional differences in the here assessed EC characteristics. A similar conclusion was reached by Barruet et al., but noted reduced VE-Cadherin levels in FOP iECs (Barruet et al., 2016). In contrast, Cai et al., observed reduced viability and senescence of FOP iECs (Cai et al., 2015). The single observations of impaired FOP iEC characteristics suggest rather a cell model specific effect (e.g. culture conditions, iEC generation method (+ActivinA) see chapter 4.2.1) than a general feature of FOP endothelium.

This is supported by FOP pathology, which hasn´t reported any chronic vascular abnormalities. However, vascular abnormalities were observed locally in lesioned tissues of episodic HO in FOP biopsies, indicating the presence of responsible trigger(s), which act in a time and space dependent manner.

4.2.3 **The vascular bed specificity of iECs is undefined**

In comparison to primary venous ECs (HUVECs), the expression of the *VEGFR1* and *VEGFR2* was even higher in iECs. This could be based on endothelial heterogeneity derived from different vascular beds. In fact, HUVECs were shown to have lower surface density of VEGFR2 in comparison to microvascular ECs (Imoukhuede and Popel, 2011). However, the vascular bed specificity of iECs generated *de novo* is rather undefined. Most differentiations methods up to date generate heterogenous

populations of ECs (Paik et al., 2018; Rufaihah et al., 2013; Williams Ian M. and Wu Joseph C., 2019). This is in line with the analysis of arterial versus venous EC identity in this study, which showed robust arterial markers but also venous marker expression in iECs (Figure 3.5). Current strategies, to advance iEC generation into more vessel and tissue specific cell types include triggers of signaling pathways associated with endothelial specification. For example, VEGFA and NOTCH signaling are key inducers of arterial differentiation. Thus, endothelial progenitors from iPSCs can be directed by defined VEGFA concentrations to more arterial- (high) or venous-like (low) lineages as shown in recent differentiation methods (Rosa et al., 2019; Sriram et al., 2015). However, EC specification requires a number of additional environmental triggers such as mechanical triggers by Fluid Shear Stress (FSS) (Sivarapatna et al., 2015), substrate stiffness (Xue et al., 2017) and hypoxia (Kusuma et al., 2014). Xue *et al*. proposed that based on distinct tissue stiffness between arteries and veins differentiation of endothelial progenitors to arterial ECs requires a stiffer environment compared to venous ECs (Xue et al., 2018, 2017). Based on the pre-mature arteriovenous EC identity of the iECs generated here, the protocol could be further optimized by adjusting VEGFA concentrations and by including mechanical triggers (FSS and/or substrate stiffness) to further specify arterial or venous iEC identity. In addition to arteriovenous identity, ECs have a tissue specific vascular bed identity, which is characterized by specific morphology, expression profiles, functional responses such as permeability, leucocyte adhesion and vasoconstriction (Aird, 2012). Up to date, most differentiation protocols lack vascular bed specificity except the adjustment to generate blood-brain barrier like ECs from iPSCs (Appelt-Menzel et al., 2020; Williams Ian M. and Wu Joseph C., 2019). The generation of other specialized ECs such as capillary ECs has been limited and deeper understanding of vascular bed specific development will enhance the generation of those cell types *in vitro* (Williams Ian M. and Wu Joseph C., 2019). But in fact, EC phenotypes vary not only between different organs, even in specialized tissue structures the vascular tree is composed of specialized ECs. For disease modeling of FOP, directed iPSC differentiation of type H vessel ECs would be of interest. Type H vessel were discovered as unique vessel subtypes in coupling osteogenesis and angiogenesis (Kusumbe et al., 2014) but their developmental path remains unknown.

In sum, a new FOP disease model was established with optimized conditions to investigate ALK2 signaling responses in FOP endothelium (Figure 4.2A), which will be discussed in more detail in the following paragraphs.

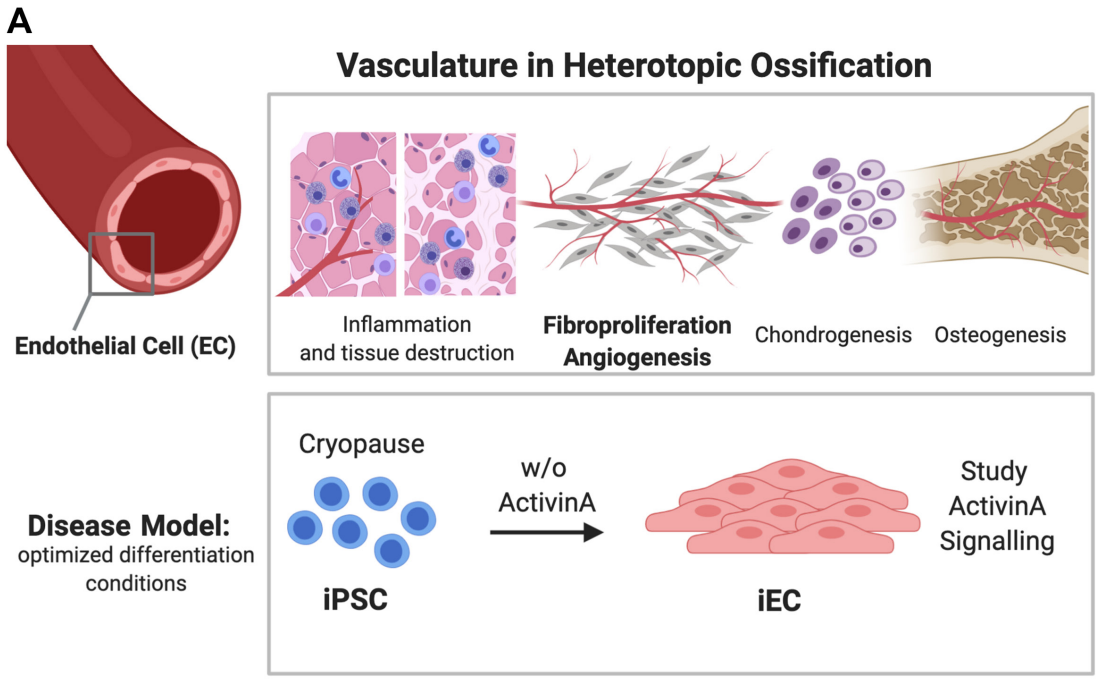

Figure 4.2 Generation of a new FOP endothelial model. (**A**) Depiction of the dynamic vasculature changes in the multi-stage process of HO. Usage of iPSCs to model FOP endothelium with iECs for the investigation of ActivinA signaling. Modified from (Hildebrandt et al., Stem Cell Rev Rep, in press 2020).

4.3 FOP iECs gain aberrant SMAD responses

ALK2 and *ALK1* where the only BMP/TGFβ type I receptors showing upregulated expression during EC differentiation.

This indicates an important functional role for ALK2 in the endothelium, which has been highlighted in recent studies from the Knaus lab and others in context of endothelial survival, permeability, sprouting angiogenesis, vascular branching and monocyte recruitment (Benn et al., 2017; Benn et al., 2016; Lee et al., 2017; Medici et al., 2010; Mitrofan et al., 2017; Wang et al., 2005; Yao et al., 2008). However, its function remains less understood compared to the well-studied ALK1 receptor in the endothelium.

BMP6, the ALK2 signaling ligand showed by far the highest expression among the BMP ligands and ActivinA was the only expressed candidate among the Activin ligand class. Both ligands became highly upregulated upon endothelial differentiation of iPSCs. This suggests that the WT and FOP endothelium produce ActivinA and BMP6 already in steady state independent of external triggers.

However, whether the ligand expression results in synthesis of active ligands, which bind to respective receptors on cell surfaces in HO lesion remains unknown. Ligand interaction with pro-domains, ECM components or antagonists may interfere with ligand activity (Sengle et al., 2011, 2008) (see chapters 1.7.1 and 1.7.4). In contrast to pro-TGFβ1, which requires an ECM and integrin-driven mechanical activation to achieve full signaling activity (Shi et al., 2011), pro-ActivinA or pro-BMP9 have equal signaling activity compared to the mature ligand forms (Mi et al., 2015; X. Wang et al., 2016). However, the prodomain of ActivinA facilitates binding to heparan proteoglycans of the ECM, which is suggested to regulate ActivinA localization and thereby accessibility within tissues (Li et al., 2010). The exact localization of ActivinA in lesioned tissue in FOP remains unknown. But very recently, it was identified that ActivinA was upregulated in a fibroblast population of lesioned tissue upon trauma in FOP mice (Hwang et al., 2020). Fibroblasts proliferate in early pre-osseous HO lesions accompanied by neovascularization (Shore and Kaplan, 2010), which highlights the importance to study ActivinA on FOP endothelium (Figure 4.2B).
Interestingly, in a mouse model of non-genetic HO the expression of several ligands was enriched (BMP2, BMP4, TGFβ1, Activin) in distinct cell types (Hwang et al., 2020). To model signaling responses of active ligands, which represent possible local triggers in lesioned tissues of episodic HO in FOP, iECs were treated with recombinant ligands, including BMP2, BMP6, TGFβ and ActivinA.

4.3.1 **FOP iECs gain ActivinA/SMAD1/5 responses**

Investigation of ActivinA signaling in the here generated FOP endothelial model revealed that only FOP iECs gained ActivinA/SMAD1/5 signaling (Figure 4.2B) (Hildebrandt et al., Stem Cell Rev Rep, in press 2020).
In 2015, Activins were discovered to aberrantly activate SMAD1/5 responses in ALK2-R206H expressing cells (Hatsell et al., 2015; Hino et al., 2015), which was confirmed for all FOP causing mutations in overexpression studies (Haupt et al., 2018). However, the tissue and cell types which gain ActivinA/SMAD1/5 responsiveness endogenously remains poorly understood. The blocking of ActivinA in FOP mice prevents HO, indicating a central role of this ligand in ectopic bone formation (Hatsell et al., 2015; Lees-Shepard et al., 2018; Upadhyay et al., 2017). Thus, FOP iECs recapitulate an important pathogenic mechanism of FOP, which suggests that ECs represent a disease relevant cell type involved in ectopic bone formation (Figure 4.2A).

This is supported by a recent study showing ActivinA/SMAD1/5 signaling in primary endothelial progenitor cells (ECFCs) isolated from peripheral blood of FOP patients (Sánchez-Duffhues et al., 2019c). This indicates, that the here established FOP iECs resemble primary FOP ECs characteristics, providing a valuable, readily available source. The iECs presented here differ from a previous iPSC study, which showed no ActivinA/SMAD1/5 signaling in FOP iECs (Barruet et al., 2016), suggesting that those iECs may not contribute to ActivinA dependent processes in FOP pathogenesis.

4.3.2 **ActivinA/SMAD1/5 signaling is mediated by ALK2**

The underlying mechanism of ActivinA/SMAD1/5 signaling is not fully understood. Here, kinase inhibitor experiments in FOP iECs suggest ALK2 dependency and independency of ALK4/ALK5/ALK7 (Hildebrandt et al., Stem Cell Rev Rep, in press 2020), which is in line with ALK2 and ALK4 knockdown studies in FOP iMSCs (Hino et al., 2015). Interestingly, besides high efficient binding of ActivinA to endogenous ALK2 and ALK4, early crosslinking studies demonstrated ActivinA binding in lower efficiencies to the type I receptors ALK1, ALK5 and ALK6 when overexpressed with type II receptors (ten Dijke et al., 1994a). This suggests that ActivinA may also engage those type I receptors when sufficiently expressed in human tissues, such as ALK1 in the endothelium. The here applied kinase inhibitors K02288 and Saracatinib were more sensitive to ALK2 signaling at the used concentrations but additional targeting of ALK1 cannot be excluded. Thus, potential contribution of ALK1 in endothelial ActivinA/SMAD1/5 could be further clarified by knockdown experiments in the future.
Knockdown experiments targeting type II receptors in FOP iMSCs revealed that ActivinA/SMAD1/5 signaling could only be abrogated when both, ACVR2A and BMPR2 were targeted, suggesting an involvement of both receptors in aberrant ActivinA signaling (Hino et al., 2015). This is supported by earlier work, which demonstrated that type II receptor cooperation (ACVR2A, BMPR2) is essential for ALK2-mutant signaling and even independent of type II receptor kinase activity (Bagarova et al., 2013). This suggests that the scaffolding with type II receptors is crucial and may be sufficient to form a functional signaling complex with ALK2-mutant receptors. Interestingly, knock down of ACVR2B did not reduce ActivinA/SMAD1/5 signaling in FOP iMSCs (Hino et al., 2015). Generally ActivinA has no preference in forming a complex with ACVR2A over ACVR2B (Goebel et al., 2019a), which is supported by similar binding affinities of ActivinA to ACVR2A and ACVR2B (Aykul and Martinez-Hackert, 2016; Hino et al., 2015). This indicates that mutant ALK2 may preferentially

form a complex with ACVR2A. However, knowledge about the interactions of ALK2-WT and ALK2-mutant with ACVR2A/B or BMPR2 are lacking.

Thus, it remains to be shown whether ALK2-R206H facilitates distinct complex formation with ACVR2A, ACVR2B or BMPR2 compared to ALK2-WT in presence of ActivinA. Ongoing Patch- Fluorescence recovery after photobleaching (FRAP) experiments distinguish between transient and stable receptor interaction on cellular membranes and will shed light on ALK2 complex formation with respective type II receptors and the effect of ActivinA (Ongoing cooperation with Prof. Yoav Henis and Szófia Szilágyi, Tel Aviv University, Israel). The important role for type II receptors in ActivinA/SMAD1/5 signaling is further supported by their requirement to facilitate ActivinA binding to ALK2.

4.3.3 **Binding to ActivinA is a general property of ALK2**

In fact, binding of ALK2 to ActivinA in complex with ACVR2A/B was already described when ALK2 was initially identified as an Activin type I receptor (Attisano et al., 1993; Tsuchida et al., 1993). About 30 years ago ALK2 was relabeled as a BMP type I receptor due to its inability to activate SMAD2/3 and this is likely the reason why the cellular consequences of ALK2 binding to ActivinA have remained largely unexplored until today. Recently, Activins have been recognized as competing ligands for ALK2 binding, which antagonize BMP6, BMP7 and BMP9 (Aykul et al., 2020; Hatsell et al., 2015; Martinez-Hackert et al., 2020; Olsen et al., 2015). Receptor binding competition represents an additional mechanism to fine tune complex signaling responses (Martinez-Hackert et al., 2020). In FOP, ALK2-WT-ActivinA complexes dampen the ActivinA triggered HO response as demonstrated by ALK2-WT removal in FOP mice, which exaggerated the amount of HO (Lees-Shepard et al., 2018). Therefore, it is suggested that ActivinA utilizes not only ALK4 as its type I receptor for SMAD2/3 signaling but also engages ALK2 to form non-signaling complexes (NSCs) (Aykul et al., 2020). This is supported by the here analyzed transcriptome of ActivinA treated WT iECs, which only included a few SMAD2/3 target genes and was not associated to endothelial related functions upon gene ontology analysis (Figure 3.20 and Figure 3.22). Here, it was demonstrated that FOP iECs express *ALK2-WT* and mutant *ALK2-R206H* transcripts, suggesting that ActivinA forms also NSCs with ALK2-WT in FOP iECs. Targeted deletion of the WT allele in FOP iECs e.g. by CRISPR/Cas9 could be used to proof that ALK2-WT-ActivinA complexes dampen ActivinA/SMAD1/5 signaling in FOP iECs. Conclusively, binding of ActivinA in complex with type II receptors is a

general property of ALK2 and is independent of the intracellular FOP causing mutations in ALK2.

Consequently, it has been proposed that the neofunction of mutant ALK2 in FOP to transduce ActivinA/SMAD1/5 signaling compared to ALK2-WT is not caused by newly acquired binding to ActivinA (Hatsell et al., 2015).

Very recently structural modeling predictions pinpointed the ALK2 binding to ActivinA to the **finger two tip loop** (**F2TL**) (amino acids 406-409) of ActivinA (Aykul et al., 2020). Moreover, the structures of ALK4 and ALK5 suggest a four amino acid extension in the β4-β5 loop, which mediates specificity for the Activin ligand class through interaction with the ligand fingertip, which is not observed in structures of ALK1, ALK3 or ALK6 (Gipson et al., 2020; Goebel et al., 2019a). Thus, fingertip interactions via β4-β5 loop define receptor specificity and discriminate BMP and Activin type I receptors. Further attempts to crystalize the ALK2 extracellular structure could prove that ALK2 also possesses an extension in the β4-β5 loop.

For the investigation of ALK2 binding to ActivinA Aykul et al. designed ActivinA muteins of the F2TL region, which were able to engage ALK4 for complex formation but not ALK2. Interestingly, those ActivinA muteins were still capable to activate SMAD1/5 signaling in ALK2-R206H expressing cells (Aykul et al., 2020), suggesting that ActivinA/SMAD1/5 signaling is either (1) independent on ActivinA binding to ALK2-R206H or (2) is dependent on binding of ALK2-R206H to ActivinA but at sites different from the F2TL compared to ALK2-WT. Crosslinking experiments revealed that the binding affinity of ActivinA to ALK2-R206H in presence of type II receptors was slightly enhanced compared to ALK2-WT (Hino et al., 2015) (Figure 4.3B, orange label 2). This rather suggests that ALK2-R206H binds ActivinA at different critical contact points (Figure 4.3,orange label 1). Moreover, experiments with ALK2 truncation mutants lacking the ligand binding domain (LBD) demonstrated that ActivinA/SMAD1/5 signaling of ALK2-R206H requires the LBD as for the ALK2 signaling ligands BMP6 and BMP7 (Hildebrand et al., 2017b). Future studies with ALK2-R206H LBD mutants and truncations may shed light on critical extracellular interaction sites. Since ALK2 WT and ALK2-R206H consist of the same LBD the different binding properties to ActivinA could be mediated by a different geometrical orientation of ALK2-R206H when forming a complex with (specific) type II receptors (Figure 4.3B, orange label 4). In sum, **ALK2** binds BMP and Activin ligands and thus should be categorized as a dual

receptor, namely **BMP/Activin type I receptor**. Whether binding of Activin is changed for FOP ALK2 mutants is an interesting question for future research.

Especially the observed ligand flexibility of ActivinA, which resulted in the crystallization of multiple conformations (Greenwald et al., 2004; Thompson et al., 2003) suggests an additional functional model to modify receptor binding specificity of Activins compared to BMPs.

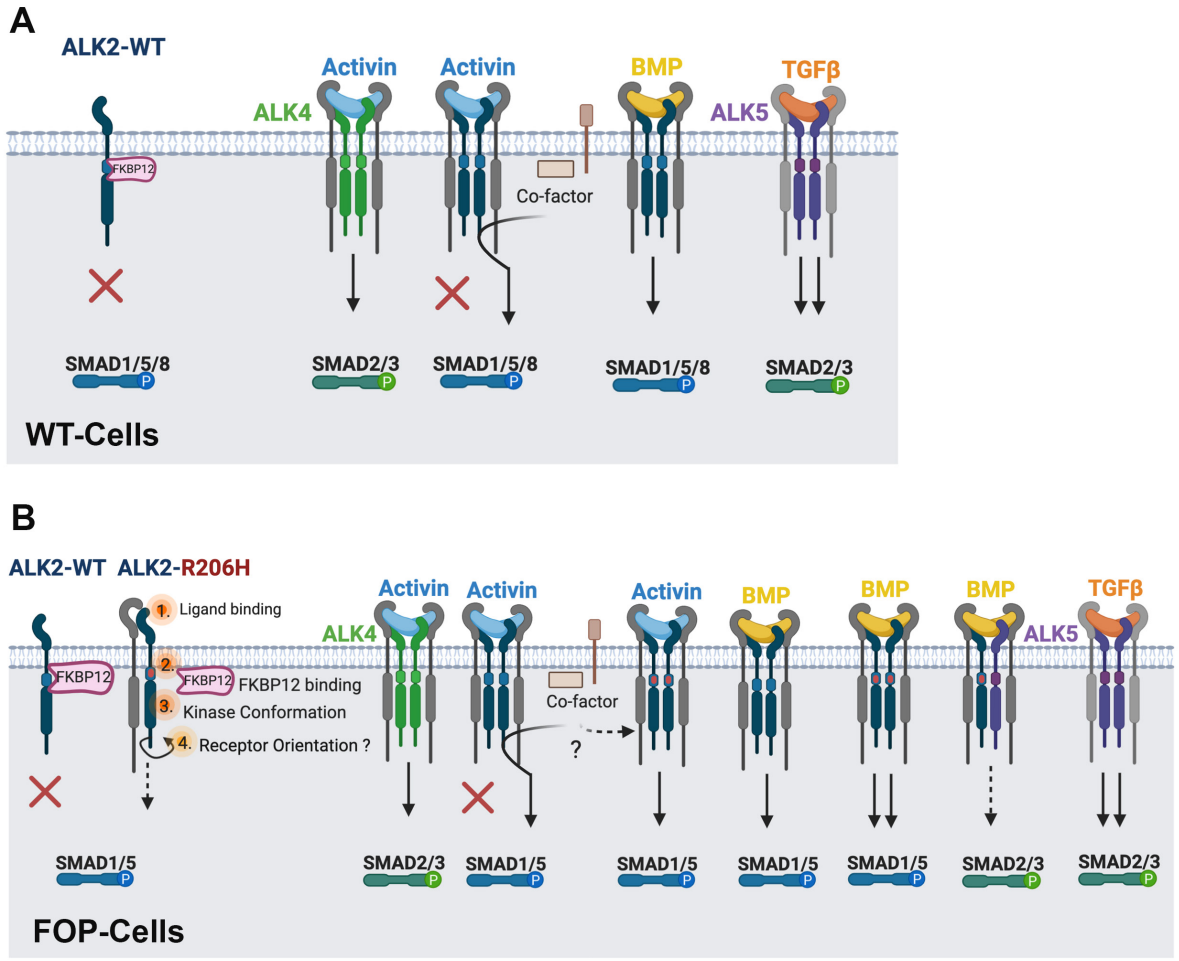

Figure 4.3 The FOP point mutation causes aberrant signaling responses. Proposed model of Activin, BMP and TGFβ responses in WT and FOP cells based on knowledge from the literature and new insight from the present study. (**A**) WT-cells: In absence of ligand FKBP12 keeps type I receptor kinases in an inactive state e.g as displayed for ALK2. FKBP12 becomes dissociated upon ligand receptor complex formation. ALK2 can form a SMAD1/5 signaling complex with BMP6 and a non-signaling complex with ActivinA and respective type II receptors (ACVR2A/B, BMPR2 in grey). In addition, ActivinA can form a SMAD2/3 signaling complex with ALK4. Based on competitive binding of ActivinA to ALK4 or ALK2 and shared type II receptors with BMP6, ActivinA/SMAD2/3 signaling is suggested to be weaker compared to TGFβ/SMAD2/3 signaling involving ALK5 and TGFBR2. (**B**) FOP cells containing ALK2-WT and ALK2-R206H: Compared to ALK2-WT, ALK2-R206H breaks critical inhibitory interactions, which destabilize the inactive conformation of the ALK2 kinase (**orange label 3**) and facilitates reduced binding to FKBP12 resulting in ligand-independent hypersensitive signaling (**orange label 2**). ALK2-WT can form ligand receptor complexes as described in B. ALK2 binds ActivinA and it is suggested that ALK2-R206H may bind ActivinA differently (**orange label 1**), which might be facilitated by a different receptor orientation (**orange label 4**). In addition, ALK2-R206H favors the formation of ActivinA/SMAD1/5 signaling complexes. It is unknown if potential co-factors mediating ALK2-WT ActivinA/SMAD1/5 signaling are also involved in ActivinA-ALK2-R206H complexes. ALK2-R206H transduces BMP6 signals stronger (hypersensitive signaling). At high BMP6 concentrations (dashed arrow) ALK2-R206H cells may also transduce SMAD2/3 responses. As suggested for WT cells (see B) is TGFβ/SMAD2/3 signaling stronger compared to ActivinA/SMAD2/3 signaling.

4.3.4 Inhibition of FKBP12 is not sufficient to convert ALK2 into an ActivinA/SMAD1/5 signaling receptor

The FOP mutations localize around the GS domain and the ATP pocket of the kinase domain, which have been predicted to break critical inhibitory interactions, which destabilize the inactive state of the ALK2 kinase (Figure 4.3B, orange label 3) (Botello-Smith et al., 2017; Chaikuad et al., 2012; Groppe et al., 2007). Biochemical studies confirmed reduced binding of the inhibitory FK506 binding protein 12 (FKBP12) to ALK2 leading to hypersensitive signaling (Figure 4.3B, orange label 2) (Chaikuad et al., 2012; Fukuda et al., 2009; Shen et al., 2009; Song et al., 2010; van Dinther et al., 2010).

Here, treatment with the FKBP12 inhibitor FK506 increased basal pSMAD1/5 levels and *ID1* expression only in FOP iECs, but not in WT iECs and thereby confirms ALK2-R206H hypersensitivity without ligand addition (Figure 3.17A). Another study confirmed that the hypersensitivity of all FOP causing ALK2 mutants is indeed ligand-independent by using LBD deletion constructs (Haupt et al., 2018). Ligand stimulation and subsequent phosphorylation of the type I receptor GS domain by type II receptors releases FKBP12 and activates type I receptor kinases (Wang et al., 1996, 1994) as also demonstrated for mutant ALK2 and FKBP12 (Machiya et al., 2018). In line with this, inhibition of FKBP12 by FK506 treatment did not significantly increase SMAD1/5 signaling after BMP6 and ActivinA ligand treatment in FOP iECs, likely because the ligand concentration was already high enough to completely release FKBP12.

However, at lower ligand doses FK506 may further increase signaling responses in iECs. This is in line with an early study demonstrating that FK506 increased signaling only at low doses of TGFβ whereas high doses had no effect (Wang et al., 1996).

Interestingly, a minor ActivinA/SMAD1/5 downstream response was observed in FK506 pretreatment WT iECs suggesting that the conversion of an inactive ALK2-ActivinA complex to an active signaling complex could be mediated by FKBP12.

This confirms an earlier study using the same FK506 concentration (Hino et al., 2015) but is contradictory to another study (Hatsell et al., 2015), which is likely due to the usage of lower FK506 concentrations. However, the ActivinA response in FK506 pretreated WT iECs was not nearly as strong as in FOP iECs and was not significantly confirmed upstream on phosphorylated SMAD1/5 protein levels.

Moreover, knock-down of FKBP12 in WT iECs did not enable ActivinA/SMAD1/5 responses. It is likely that the minor Activin/SMAD1/5 response in FK506 treated WT iECs resulted from the inhibition of another FK506 binding protein.

Interestingly, **FKBP12** has a close homolog, named **FKBP12.6** with 83% sequence identity (Tong and Jiang, 2015), which was crystalized in complex with ALK2 (PDB ID: 4C02) and thus also interacts with ALK2. Therefore, in addition to FKBP12 a knockdown of FKBP12.6 WT iECs should be performed in future studies.

Collectively, the minor effects of FKBP12 inhibition on ActivinA responses and recent findings that FKBP12 overexpression did not rescue aberrant signaling of mutant ALK2 (Machiya et al., 2018) suggest that additional or other co-factor(s) contribute to ActivinA/SMAD1/5 signaling.

4.3.5 **ActivinA/SMAD1/5 signaling is not limited to FOP**

That additional factors than FKBP12 contribute to ActivinA/SMAD1/5 signaling is further supported by the unexpected observation that WT iECs gained ActvinA/SMAD1/5 signaling to the same extent as FOP iECs in full medium and under fluid shear stress (FSS) after 24 hours (Figure 3.33). The activation of SMAD1/5 signaling by ActivinA was already visible in static full medium condition and to a higher extend under FSS (Figure 3.33). The expression of FKBP12 or ALK2 did not change under this condition and suggests that other, so far unknown co-factors are modified which mediate ActivinA/SMAD1/5 signaling in WT iECs. However, mechanical forces, such as FSS modulate not only transcription but in fact integrate on several levels of the TGFβ/BMP pathway in ECs, such as receptors, SMADs but also cytoskeletal and chromatin re-organization (reviewed in Hiepen et al., 2020). For example in venous ECs it was demonstrated that FSS enhanced association of ALK1 and Endoglin, which increased BMP9-ALK1 signaling (Baeyens et al., 2016). Thus, it is tempting to speculate that FSS may modulate ActivinA receptor complex formation in comparison to static conditions.

In sum, the observation that WT iECs also gain ActivinA/SMAD1/5 signaling emphasize that ActivinA/SMAD1/5 responses are not limited to FOP. However, based on the observations that under starvation conditions only FOP iECs showed ActivinA/SMAD1/5 signaling, it can be concluded that FOP iECs are susceptible for ActivinA/SMAD1/5 responses in conditions not permissive for WT iECs.

Increasing evidence suggests that under certain cellular context, Activins induce SMAD1/5 signaling also in ALK2 WT cells such as myeloma cells (Olsen et al., 2018),

hepatocytes (Besson-Fournier et al., 2012; Canali et al., 2016) and in iMEFs under ectopic ALK2-WT expression (Haupt et al., 2018) (Figure 4.3A).

It is not known whether ActivinA transduces SMAD1/5 responses via the same signaling mechanism in WT and FOP iECs. Current evidence suggest mechanistic similarities of ActivinA/SMAD1/5 signaling in ALK2 WT and FOP cells, demonstrating that the signaling complex requires ALK2 and is independent of ALK4, ALK5, ALK7 expression and kinase activity (Canali et al., 2016; Hino et al., 2015; Olsen et al., 2020). The requirement of certain type II receptors is less clear. Upon Knockdown of BMPR2 ActivinA/SMAD1/5 responses were reduced in FOP iMSCs and potentiated in myeloma cells and hepatocytes (Canali et al., 2016; Olsen et al., 2018).

In line with the observations in myeloma cells is the proposed role of BMPR2 as a gatekeeper, which protected the endothelial hybrid cell line EAHy926 from a gain in ActivinA/SMAD1/5 responsiveness (Hiepen et al., 2019). This study of the Knaus lab from Hiepen, Jatzlau, Hildebrandt *et al*., showed that the gain of ActivinA/SMAD1/5 signaling in BMPR2 deficient EAHy926 was also dependent on ALK1/ALK2 and independent of ALK4, ALK5 and ALK7 (unpublished), thereby confirming the above-mentioned result here and from others. Further understanding of the underlying mechanism how ALK2-WT iECs gain ActivinA/SMAD1/5 signaling may also shed light on the mechanistic action of ActivinA in FOP.

The Holien group recently proposed a general **dual specificity mechanism for Activins** via Activin-SMAD2/3 and BMP-SMAD1/5 type I receptors (Olsen et al., 2020). However, the **context dependent factors**, which mediate ActivinA non-signaling complexes into active SMAD1/5 signaling complexes remain elusive. Moreover, the physiological and pathophysiology role of aberrant Activin/SMAD1/5 mechanisms remain incompletely understood and should be addresses in future research. In FOP, ActivinA/SMAD1/5 signaling has been defined as the main pathogenic mechanism driving ectopic bone formation.

In ALK2-WT hepatocytes ActivinB/SMAD1/5 signaling is suggested to have a physiological role in hepicidin induction during inflammation, which causes reduction of iron blood levels and is associated with anemia (Canali et al., 2016).

In context of myeloma, ActivinA and Activin B induced ALK2-WT-mediated SMAD1/5 responses are associated with myeloma cell death (Olsen et al., 2018).

Future Activin studies should always analyze both SMAD2/3 and SMAD1/5 downstream responses to underpin the concept of dual Activin signaling and to increase the knowledge about aberrant Activin/SMAD1/5 signaling,

4.3.6 **ActivinA and TGFβ transduce SMAD1/5 differently**

Interestingly, TGFβ a ligand of the same family, also transduces SMAD1/5 responses by a mechanism termed **lateral signaling** (see chapter 1.11). TGFβ/SMAD1/5 signaling is transduced by complexes comprised of TGFBR2, ALK5 and the BMP type I receptor ALK1/2 in ECs and ALK2/3 in epithelial cells (Byfield and Roberts, 2004; Daly et al., 2008; Goumans et al., 2003, 2002; Hiepen et al., 2019; Ramachandran et al., 2018). In contrast to ActivinA/SMAD1/5 signaling all TGFβ/SMAD1/5 responses were shown to be dependent on ALK5, suggesting two distinct mechanisms.

4.3.7 **Potential secondary factors in endothelial ActivinA/SMAD1/5 signaling**

The observation that ActivinA/SMAD1/5 signaling in FOP iECs also occurs under certain cellular context in WT iECs suggests that **secondary factor(s)** independent of the ALK2-R206H mutation mediate the aberrant ActivinA mechanism.

It is tempting to speculate that a **co-receptor** becomes upregulated, which modulates ligand-receptor sensitivity and the formation of an active ALK2-ActivinA signaling complex. ActivinA binding was reported for the co-receptors Endoglin (Barbara et al., 1999) and Cripto1 (Gray et al., 2003) in presence of type II receptors. FSS dependent enhancement of ALK1 signaling via Endoglin in ECs (Baeyens et al., 2016) suggest that Endoglin may also contribute to ActivinA/SMAD1/5 signaling under FSS in WT iECs. Moreover, co-receptor binding to ActivinA could potentially convert non-signaling ActivinA-ALK2 complexes for activation by displacement of FKBP12 from the ALK2 GS domain, which destabilizes the inactive receptor kinase.

The co-receptors BAMBI and Betaglycan modulate Activin signaling via indirect mechanisms independent of direct ligand binding. Betaglycan binds with high affinities to Inhibins and enhances binding to Activin type II receptors and thereby antagonize ActivinA signaling (Lewis et al., 2000).

BAMBI is suggested to modulate Activin, BMP and TGFβ signaling through interaction with type I and type II receptors (Nickel et al., 2018; Onichtchouk et al., 1999). Interestingly, BAMBI interacts with all type I receptors except for ALK2 and inhibited the downstream signaling of constitutive active (ca) type I receptors (Onichtchouk et al., 1999). Moreover, to a lower extent BAMBI also inhibited the signaling of (ca)ALK2,

indicating a gain in interaction of BAMBI with caALK2 compared to ALK2-WT (Onichtchouk et al., 1999). It is tempting to speculate that caALK2 or other gain of function ALK2 mutants related to FOP may gain interactions with Bambi compared to ALK2-WT. Thus, in addition to ACVR2A (Onichtchouk et al., 1999) BAMBI may also interact with mutant ALK2, which should be addressed in future studies including the consequences for ActivinA induced SMAD responses in presence or absence of BAMBI.

The dynamic transcriptional regulation of BAMBI further highlights this co-receptor as an interesting candidate to modulate (ActivinA) signaling responses in space and time. BMP7 and hypoxia were shown to upregulate BAMBI expression (Higashihori et al., 2008; Raykhel et al., 2018) whereas FGF1 and FGF2 (Higashihori et al., 2008; Luo et al., 2012) were shown to downregulate BAMBI. Early human FOP lesions are hypoxic, which is thought to promote HO (Wang et al., 2016). BMP and FGF signaling control chondrocyte proliferation and hypertrophic differentiation (Minina et al., 2002; Yoon et al., 2006), which are essential processes in endochondral ossification (see chapter 1.3) during HO in FOP. FGF2 is also a growth factor for endothelial function (Yang et al., 2015) and a main component in the full medium condition of the observed ActivinA/SMAD1/5 signaling in WT iECs. Moreover, synergism and antagonism between FGF and the TGFβ family has been reported on different levels of the signaling cascade (Derynck and Budi, 2019; Schliermann and Nickel, 2018).

In sum, the transcriptional regulation of co-receptors and their role in ActivinA/SMAD1/5 signaling should be analyzed further in WT and FOP iECs.

4.3.8 **FOP iECs foster aberrant BMP/SMAD responses**

Hypersensitive SMAD1/5 signaling in response to BMP ligands (Chaikuad et al., 2012; Fukuda et al., 2009; Haupt et al., 2018; Shen et al., 2009; Song et al., 2010; van Dinther et al., 2010) was discovered much earlier than aberrant ActivinA/SMAD1/5 signaling in FOP (Hatsell et al., 2015; Hino et al., 2015).

In line with the concept of hypersensitive BMP signaling in FOP, BMP6 showed a trend towards increased SMAD1/5 signaling in FOP iECs compared to WT iECs (Figure **3.11**). On *ID1/ID2/ID3* target gene transcription the trend of increased BMP6/SMAD1/5 signaling was not observed (Figure 3.11). Chromatin Immunoprecipitation Sequencing (ChIP-Seq) defined *IDs* as high affinity BMP target genes, based on a higher number of SMAD1/5 binding element (SBE/GC-SBE) motifs with shorter relative distance (Morikawa et al., 2011). Thus, *ID* genes are not an optimal sensor for small changes

in SMAD signaling strength. In comparison SMAD6, which was described as a low affinity SMAD1/5 target gene (Morikawa et al., 2011), requires high levels of phosphorylated SMAD1/5 and is therefore a better indicator of aberrant SMAD1/5 signaling in FOP. Indeed, SMAD6 was significantly higher upregulated in FOP compared to WT iECs after BMP6 stimulation. Thus, FOP iECs recapitulate hypersensitive BMP signaling on pSMAD1/5 levels and selected BMP target gene transcription.

FOP iECs gain BMP2/SMAD1/5 signaling

BMP2 did not induce SMAD1/5 signaling in iECs. This finding is supported by low expression levels of the BMP2 high affinity type I receptors ALK6 and ALK3. While there was no detectable expression of ALK6, some ALK3 expression was measurable in iECs but likely in insufficient amounts to foster BMP2/SMAD1/5 signaling. This data is in line with a recent study, demonstrating that BMP2/SMAD1/5 signaling is vascular bed specific and dependent on high expression levels of ALK3 and ALK6 (Benn et al., 2017). Recently, it was demonstrated that ALK3 mediated SMAD1/5 signaling regulated venous identity during zebrafish and murine development (Neal et al., 2019) Compared to its type I receptors (ALK3, ALK6), BMP2 has low affinity to type II receptors (Heinecke et al., 2009). Consequently, BMP2 did not bind BMPR2 homodimers in cross-linking experiments when ALK3, ALK6 were not co-expressed (Gilboa et al., 2000). However, at high ligand concentrations (20 nM), BMP2 binds weakly to BMPR2 (Gilboa et al., 2000). Interestingly, very high BMP2 concentrations (30 nM) induced phosphorylation of SMAD1/5 only in FOP iECs (Figure 3.12) suggesting a BMP2 signaling complex involving ALK2-R206H. Compared to ALK3 and ALK6, BMPR2 is highly expressed in iECs. Thus, increased interaction of ALK2-R206H with BMPR2 or with the much lower expressed ALK3 is likely the underlying reason why a functional BMP2/SMAD1/5 signaling complex only forms in FOP iECs.

FOP iECs gain BMP6/SMAD2 signaling

In addition to BMP6/SMAD1/5 signaling, high concentrations of BMP6 also activated SMAD2 signaling in FOP iECs. The usage of selective kinase inhibitors (SB434142, Saracatinib) indicated that BMP6 activated SMAD2 via heteromeric receptor complex formation comprising of ALK2 and ALK5 or ALK4. It was reported that ALK5 interacts with ALK2-R206H and with ALK2-WT upon BMP4 stimulation in HUVECs (Medici et al., 2010). This suggests that BMP6/SMAD2 signaling in FOP iECs and the minor trend in WT iECs is mediated via ALK2 and ALK5. The Type II receptor composition of those heteromeric receptor complexes remains unknown. BMP2 induced SMAD2 signaling was suggested to be mediated via heteromeric complex formation comprised of TGFBR2/ALK5 and ALK3 in epithelial cells (Holtzhausen et al., 2014).

BMP9/SMAD2 signaling is a general mechanism in the endothelium

BMP9 induced SMAD1/5 signaling very potently in iECs. In addition, higher concentrations of BMP9 (1.0 nM) also activated SMAD2 signaling in iECs.

BMP9/SMAD2 signaling has been observed in other WT ECs such as Human Pulmonary Artery Endothelial Cells (HPAECs), HUAECs and HUVEC derived EA.hy926 (Hiepen et al., 2019; Jatzlau Jerome, 2019; Park et al., 2012). Moreover, BMP9/SMAD2 responses are not limited to the endothelium and were also reported in in chondrocytes (van Caam et al., 2015) and fibroblasts (Muñoz-Félix et al., 2016) suggesting a general signaling mechanism of BMP9.

Knockdown and receptor kinase inhibitor experiments suggest that ALK1 is essential for BMP9/SMAD2 signaling in ECs (Jatzlau Jerome, 2019; Upton et al., 2009). Whether ALK5 is part of the BMP9/SMAD2 signaling complex remains unclear.

ALK5 Knockdown experiments by Upton et al. suggested that BMP9/SMAD2 responses are independent of ALK5. In contrast, another study suggested ALK5 contribution to BMP9/SMAD2 signaling based on kinase inhibitor (SB-431542) experiments in HUAECs (Jatzlau Jerome, 2019). However, the kinase inhibitor SB-431542 also targets the Activin type I receptors. Thus, BMP9/SMAD2 signaling may also be transduced via ALK4. This assumption is supported by the observation that a Knockdown of the Activin type II receptor ACVR2 reduced BMP9/SMAD2 phosphorylation to a greater extent compared to a BMPR2 knockdown (Upton et al., 2009). In fact, BMP9 has equal high affinity to ACVR2B as ALK1 (Townson et al., 2012).

In sum, based on current evidence I suggest that BMP9/SMAD2 signaling is likely mediated by a complex consisting of ALK1, ALK4 and Activin type II receptors (ACVR2A/B).
For experimental validation of this assumption, studies with targeted receptor deletion as well as complementary experiments should be performed. Moreover, the functional consequences of BMP induced SMAD2 signaling in ECs remain unclear.

4.3.9 **Understudied signaling diversity of the TGFβ superfamily**

Traditionally, the analysis of cellular SMAD1/5 versus SMAD2/3 responses has been determined by the specificity of the used ligands to certain type I receptors (BMP type I receptors for SMAD1/5/8; Activin and TGFβ type I receptors for SMAD2/3 (see chapter 1.7.6). However, increasing evidence suggests that TGFβ family ligands may also signal via heteromeric receptor complexes in a context dependent manner.
These signaling modes are referred to as ***lateral signaling*** for TGFβ (Goumans et al., 2003, 2002) or as ***dual specificity*** for Activins (Olsen et al., 2020). The context may underly receptor expression levels, ligand availability, affinity and/or co-factors.
This study and others suggest that **ALK2** is an important component of those signaling complexes, which transduces Activin/SMAD1/5 responses (Alessi Wolken et al., 2018; Olsen et al., 2020) (see chapter 3.3), TGFβ/SMAD1/5 (Daly et al., 2008; Hiepen et al., 2019; Ramachandran et al., 2018) and BMP/SMAD2/3 (Medici et al., 2010) signaling (see chapter 3.3). Especially in respect to ActivinA this study and others suggest that underlying co-factors mediate Activin/SMAD1/5 signaling, which are still unknown (Olsen et al., 2020). The here collectively termed ***aberrant* SMAD responses** were shown to involve heteromeric receptor complex formation, which was favored by mutant ALK2 but under certain context also observed for WT ALK2.
Thus, *aberrant* SMAD signaling responses are not limited to FOP and may represent a general mechanism to fine tune complex signaling responses in diverse tissue and physiological context. By heteromeric receptor complex formation the diversity of signaling responses from over 30 ligands to a limited number of receptors becomes expanded. This suggests that the activation of both SMAD branches by ligands is **not *aberrant* but rather rare**. Therefore, I propose to generalize the term *dual specificity* for Activin ligands (Olsen et al., 2020) to ***dual SMAD signaling*** for the entire TGFβ ligand family.

Many studies of the past may not have detected *dual SMAD signaling* responses because likely they simply didn't analyze both SMAD branches.
Future investigations are necessary to clarify the underlying molecular mechanism(s) of *dual SMAD signaling* responses by the TGFβ super family and its role in tissue homeostasis and disease.

4.4 ActivinA induces a specific FOP transcriptome in FOP iECs

Downstream effects of ActivinA/SMAD1/5 signaling in human tissue remain poorly understood. This study provides first insight of whole genome responses to ActivinA in ECs and revealed a FOP specific transcriptome in FOP iECs consisting of highly enriched genes associated with blood vessel formation, EndMT and activation of BMP and NOTCH pathways (Hildebrandt et al., Stem Cell Rev Rep, in press 2020).

4.4.1 **ActivinA transduces a BMP like response in FOP iECs**

ActivinA upregulates classical BMP/SMAD1/5 target genes only in FOP iECs, such as *ID1, ID2, ID3, SMAD6, SMAD7* and Noggin, which could be prevented by ALK2 kinase inhibition using Saracatinib (Figure 4.5). The inhibitory SMADs 6 and 7 are negative feedback regulators which inhibit for example the C-terminal phosphorylation of Receptor (R-) SMADs by BMP as well as Activin and TGF type I receptors (see chapter 1.7.6)**.**
In contrast, Noggin is a negative feedback regulator that antagonizes certain BMPs but not ActivinA or TGFβ (Gipson et al., 2020). ActivinA antagonists like Follistatin and Follistatin like proteins were not upregulated after 2 hours of ActivinA stimulation. Follistatin is a direct target gene of ActivinA (Blount et al., 2009) but likely the SMAD2/3 signaling duration and/or intensity was not sufficient to induced Follistatin in these experimental conditions. This suggests that iECs don't activate an early negative feedback mechanism of soluble antagonists, which block the receptor binding of ActivinA. FOP iECs rather stimulate an ActivinA feed forward mechanism by blocking BMPs with Noggin, which represent ALK2 binding competitors for ActivinA (Martinez-Hackert et al., 2020). However, it is not excluded that Follistatin becomes upregulated at later time points, which should be analyzed in iECs.
Here, independent experiments confirmed that ActivinA upregulates the same genes as BMP6 in FOP iECs, indicating that ALK2-R206H lacks ligand specificity by transducing a BMP-like response. This is in line with analyzed ActivinA responses in

FOP mesenchymal stem cells (MCSs) using predefined gene expression profiling by a microarray (Hino et al., 2015).
Collectively, the first whole transcriptome analysis presented here (Hildebrandt et al., Stem Cell Rev Rep, in press 2020) and the microarray by Hino and colleagues (Hino et al., 2015) represent the first studies, which independently analyzed global downstream signaling responses in human FOP patient derived cells.

4.4.2 **ALK2 inhibits canonical Activin/SMAD2/3 signaling**

ActivinA also induced SMAD2/3 signaling via ALK4 in FOP iEC similar to WT iECs (Figure 3.10 and Figure 3.15), which was also observed in previous mentioned MSCs (Hino et al., 2015). But in contrast to SMAD1/5, SMAD2/3 signaling activated only a few target genes, which were not among the high fold change gene clusters (Figure **3.21**C,D). This is in line with principle component analysis (PCA) data of ActivinA treated control MSCs by Hino *et al*., which was close to the untreated controls (Hino et al., 2015). Thus, both gene expression analysis independently support the current model that **WT-ALK2 forms a non-signaling complex** with ActivinA while binding of ActivinA to ALK2-R206H results in an active receptor complex promoting SMAD1/5 signaling (Aykul et al., 2020; Hino et al., 2015) (Hildebrandt et al., Stem Cell Rev Rep, in press 2020). This proposes that **ALK4 competes with WT and mutant ALK2** for complex formation with ActivinA and type II receptors (ACVR2A/B, BMPR2) and may explain why canonical ActivinA-ALK4-SMAD2/3 signaling responses are so weak.
In contrast, the TGFβ induced transcriptome was shown to depend to 75% on canonical SMAD2/3 signaling and only a quarter accounted for lateral TGFβ/SMAD1/5 responses (Ramachandran et al., 2018). This supports previous assumption (see chapter 4.3.6) that ActivinA and TGFβ activate SMAD1/5 via distinct mechanisms. Compared to ActivinA, TGFβ has limited promiscuity and forms complexes only with ALK5 and TGFBR2 and does not compete with BMPs for other type I or type II receptors (Aykul and Martinez-Hackert, 2016; Olsen et al., 2015).
Consequently, I propose that based on receptor availability TGFβ results generally in higher SMAD2/3 signaling intensities compared to ActivinA (Figure 4.4).
This hypothesis ties well with two independent studies, where 10-100 fold smaller TGFβ concentrations induced higher levels of phosphorylated SMAD2 and downstream responses compared to ActivinA in WT MSCs (Hino et al., 2015; Kroon et al., 2017) and FOP MSCs (Hino et al., 2015).

In sum, ActivinA induced BMP target genes via ALK2-R206H-SMAD1/5 only in FOP iECs. In contrast, canonical ActivinA signaling only induced minor target genes via ALK4-SMAD2/3 in WT and FOP iECs, which is possibly based on competitive binding of ALK4 and ALK2 to ActivinA. Moreover, I propose that **ActivinA-ALK2 complexes generally reduce Activin/SMAD2/3 signaling** and thereby discriminate canonical Activin signaling from canonical TGFβ signaling (Figure 4.4).

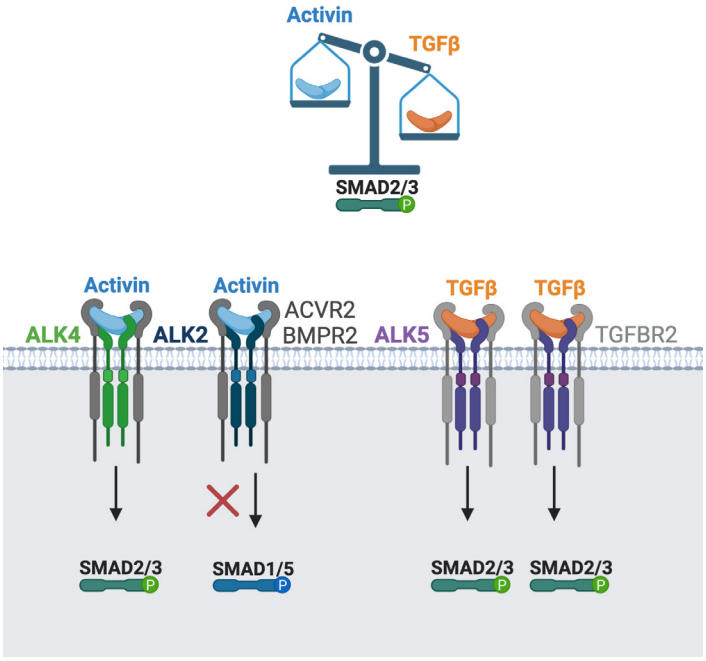

Figure 4.4 ALK2 inhibits canonical Activin/SMAD2/3 signaling. Proposed model for the role of ALK2 in canonical Activin/SMAD2/3 signaling in comparison to TGFβ/signaling. Activin forms complexes with ALK4/7 for canonical SMAD2/3 signaling but also binds to ALK2 for a non-signaling or SMAD1/5 signaling complex using the same type II receptors as ALK4 (ACVR2A/B, BMPR2). Thus, it is proposed that ALK4 competes with ALK2 for complex formation with Activin and type II receptors (ACVR2A/B, BMPR2), which limits the Activin/SMAD2/3 response. In contrast to Activin, TGFβ has limited promiscuity and forms complexes only with ALK5 and TGFBR2 and does not compete with BMPs for other type I or type II receptors. This proposes that Activin-ALK2 complexes generally reduce Activin/SMAD2/3 signaling and thereby discriminate canonical Activin signaling from canonical TGFβ signaling.

4.4.3 ActivinA activates BMP and NOTCH and thereby modifies tip and stalk cell competence of FOP iECs

In addition to BMP target genes, ActivinA also upregulated classical NOTCH target genes (e.g. *JAG1, NRARP*, *HEY2*, *HEYL*), which were regulated by BMP6 in the same manner (Hildebrandt et al., Stem Cell Rev Rep, in press 2020) suggesting a synergism between SMAD1/5 and NOTCH signaling.

Indeed, BMP signaling synergizes and antagonizes with the NOTCH pathway on different levels to control tip and stalk cell identity in angiogenesis (Beets et al., 2013; Larrivée et al., 2012; Mouillesseaux et al., 2016; Moya et al., 2012).

BMP induced SMAD1/5 signaling synergizes with activated NOTCH to induce stalk cell genes, such as the transcriptional repressors HEY1 and HEY2, which downregulate

VEGFR2 expression and thereby repress VEGF signaling and tip cell competence (Larrivée et al., 2012; Moya et al., 2012). Several NOTCH target genes, including *LFNG, JAG1, HEY2,* were confirmed as SMAD1/5 targets by ChIPSeq (Morikawa et al., 2011). BMP and NOTCH regulate selected target genes even cooporately via complex formation of pSMAD1/5 and the NOTCH downstream effector NICD (NOTCH Intracellular Domain) (Itoh et al., 2004), which is suggested to be required in stalk cells for robust target gene expression of both pathways (Moya et al., 2012).

The involvement of SMAD1/5 signaling in promoting stalk cell identity and repressing tip cell identity was recently shown to be mediated by ALK2 in HUVECs (Benn et al., 2017). This is in line with the stalk cell gene induction (*JAG1, HEY2, HEYL*) and repression of the tip cell genes (*DLL4* and *KDR)* by ActivinA in FOP iECs, which was prevented upon ALK2 kinase inhibition with Saracatinib (Figure 4.5).

Thus, ActivinA aberrantly induced ALK2 dependent SMAD1/5 signaling, thereby promoting stalk cell competence and concomitantly repressing tip cell competence.

A very recent study demonstrated in a delicate computational model of early stage angiogenesis that increasing **JAG1** resulted in **pathological vasculature** with thinner and more abundant vessels (Vega et al., 2020). This vascular phenotype is in line with the described vasculature in early pre-osseous HO lesion (Cocks et al., 2017) and suggests that upregulated JAG1 in FOP ECs by ActivinA is involved in the underlying mechanism.

Collectively, these results propose that **Activin/SMAD1/5 signaling** cooperates with the **NOTCH pathway** to **modify tip and stalk cell competence in the FOP endothelium** and represents the first report interlinking ActivinA with NOTCH in context of FOP.

Interestingly, EC-specific disruption of NOTCH signaling in mice impaired postnatal growth of a specific bone vessel type and thereby reduced osteogenesis postnatally (Ramasamy et al., 2014), suggesting that ActivinA could promote coupled angiogenesis and osteogenesis in FOP lesions via NOTCH activation. Moreover, active **NOTCH signaling** was shown to be required for **BMP9-induced ectopic bone formation** from MSCs (Cui et al., 2019). The aberrant activation of NOTCH signaling in FOP endothelium may be further promoted by a feed-forward mechanism because endothelial promoter activity of ActivinA is directly induced via binding of the NOTCH downstream mediator RBPJ (Chang et al., 2011) (Figure 4.6).

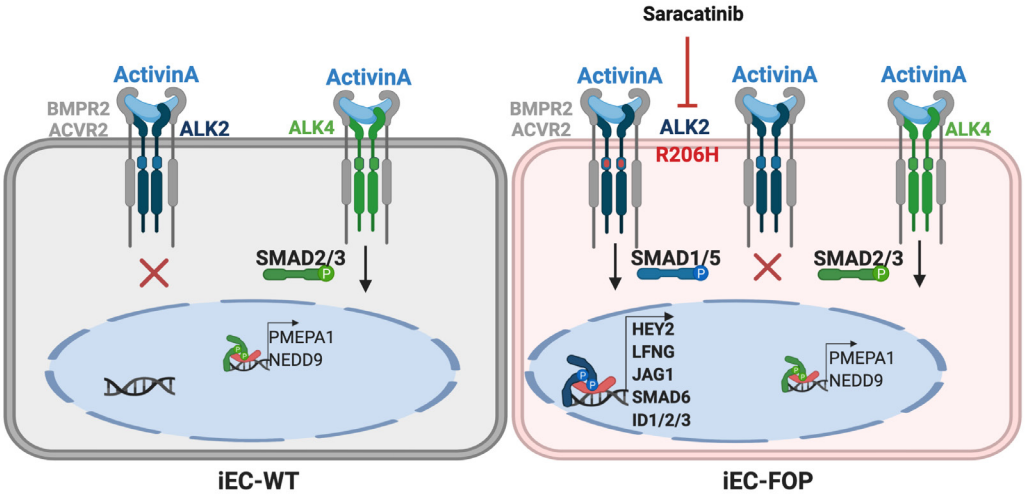

Figure 4.5 ActivinA transduces a BMP-like response only in FOP iECs. ActivinA induces phosphorylation of SMAD1/5 and SMAD2/3 in FOP iECs whereas in WT iECs only SMAD2/3 is phosphorylated. This leads to induction of specific FOP transcriptional profile consisting of target genes related to blood vessel formation and pathways of BMP and NOTCH exemplarily upregulated genes are shown in the nucleus. ALK2 kinase inhibition by Saracatinib prevented ActivinA/SMAD1/5 signaling in FOP iECs. It is suggested that ActivinA primes FOP iECs differently compared to WT iECs, which may result in functional changes and impact the outcome of secondary triggers.

4.5 The ActivinA induced transcriptome primes FOP iECs for angiogenesis and EndMT

Collectively, stalk cell identity and pathway activation of BMP and NOTCH in ActivinA treated FOP iECs suggest that ActivinA may aberrantly trigger new blood vessel formation via sprouting angiogenesis in FOP. This was supported by gene ontology analysis, which associated blood vessel formation and vascular development only with the ActivinA induced transcriptome of FOP iECs (Hildebrandt et al., Stem Cell Rev Rep, in press 2020).

In fact, vascularization precedes bone formation and is also coupled to ossification in bone homeostasis and repair, orchestrated by pro-angiogenic factors such as VEGFA (Grosso et al., 2017). Endochondral ossification in bone healing and angiogenesis is inhibited when VEGF was blocked and enhanced in presence of exogenous VEGFA (Street et al., 2002). Heterotopic bone is formed by endochondral ossification and a recent study demonstrated that loss of mesenchymal VEGFA also reduced trauma induced HO (Hwang et al., 2019). This highlights the **interlink of angiogenesis and osteogenesis in HO**, which is also evident by the high vascularity of human HO lesions prior ossification (Cocks et al., 2017; Kaplan et al., 1993). However, the role of BMP signaling in this context remains poorly understood.

4.5.1 **FOP iECs lack the anti-angiogenic effect of ActivinA**

Here, gene ontology analysis identified blood vessel formation and vascular development only in the ActivinA induced transcriptome of FOP iECs suggesting involvement of the activated SMAD1/5 branch.

Indeed, SMAD1/5 signaling is essential for the developing vasculature and phosphorylated SMAD1/5 levels are ubiquitously detected in vascular cells (Moya et al., 2012). However, SMAD1/5 transcriptional activity is dynamic during blood vessel formation, such as *ID1* expression, which was only observed transiently in early stalk cells and absent in tip cells (Moya et al., 2012). Notably, a dynamic model in blood vessel development suggests that pSMAD1/5 activates distinct target genes in single ECs thereby pre-patterning the endothelium for tip/stalk cell mediated sprouting (Moya et al., 2012).

*Thus, I propose that **ActivinA** acts as a **1st trigger** that induces a FOP specific transcriptome via ALK2/SMAD1/5 signaling, which pre-patterns the FOP endothelium, affecting tip/stalk cell shuffling leading to **pathological angiogenesis** in presence of VEGFA (**2nd trigger**) in early HO lesions* (Figure 4.6).

This hypothesis is supported by an 3D sprouting angiogenesis experiment *in vitro*, which revealed that ActivinA modulates endothelial sprouting differently in FOP iECs compared to WT iECs. ActivinA alone had no effect but reduced VEGFA induced sprout outgrowth only in WT iECs, suggesting that ActivinA normally has an inhibitory function on new blood vessel formation which is not active for the FOP endothelium. This is in line with the literature, which reported ActivinA mostly anti-angiogenic and as an inhibitor of EC growth (Breit et al., 2000; Kaneda et al., 2011; Maeshima et al., 2011; McCarthy and Bicknell, 1993).

Thus, the ActivinA induced transcriptome may indeed prime the FOP endothelium pro-angiogenic instead of antagonizing the **second trigger** hit by VEGFA.

This is further supported by the destabilizing effect on endothelial barrier integrity after long term ActivinA treatment. In presence of VEGFA, ActivinA slightly counteracted the destabilizing effect of VEGFA on the endothelial barrier in WT iECs but not in FOP iECs. Endothelial barrier disruption is essential for angiogenesis and represents an early characteristic stage in the multi-step process (Adair and Montani, 2010; Gerhardt, 2008; Ribatti and Crivellato, 2012).

Interestingly, **deregulated BMP signaling** due to mutations in ALK1 and Endoglin results in the vascular pathology hereditary hemorrhagic telangiectasia (**HHT**), which

predisposes the formation of malformed, immature leaky vessels (Roman and Hinck, 2017). The variable age of onset and severity of HHT also suggest a 2nd hit model, in which aberrant ALK1 signaling primes the endothelium and 2nd triggers eventually initiate pathological angiogenesis and/or remodeling resulting in leaky vessels.
Moreover, the association of the **ActivinA binding co-receptor Endoglin** to vessel wall hemostasis and HHT (Park et al., 2009; Rossi et al., 2018; Salles-Crawley et al., 2014) suggest a potential involvement of Endoglin in the destabilizing effects of ActivinA on the endothelial barrier.

4.5.2 Implications for ActivinA in the FOP specific vascular phenotype of HO lesions

Interestingly, the increased vessel number, are and size in FOP lesions was not observed in non-hereditary HO lesions, distinguishing both pathologies (Ware et al., 2019). That genetic versus non-hereditary HO underlie separate mechanisms is also supported by recent evidence that ActivinA does not induce post-traumatic HO in WT mice (Hwang et al., 2020). Interestingly, the study revealed that ActivinA was upregulated in both FOP and non-hereditary pre-osseous HO lesions but originated from different cell types. In FOP lesions **ActivinA was only upregulated in fibroblasts** (Hwang et al., 2020), which are crucial in normal wound healing (Bainbridge, 2013) and are present in early pre-osseous FOP lesions accompanied by neovascularization. In fact, the angiogenic fibroproliferative stage transitions normal wound healing to endochondral bone formation in FOP (Shore and Kaplan, 2010).
This highlights the relevance to investigate ActivinA effects on FOP vasculature further. The here generated **iECs** could be used to **model human vascularized, fibroproliferative lesions** in future co-culture experiments with fibroblasts. Via indirect co-culture experiments using trans-well inserts secreted factors could be analyzed. Moreover, a 3D co-culture sprouting angiogenesis assay (Shah et al., 2019) using fibroblasts and ECs could be performed to firstly model angiogenic fibroproliferation in FOP lesions.
Collectively, fibroblasts as the origin of ActivinA in HO expands the above-mentioned hypothesis in time and space.
Thus, ActivinA may derive from invading fibroblasts in early pre-osseous FOP lesions and thereby trigger pathological angiogenesis in HO.

Moreover, the here demonstrated **FOP specific ActivinA effects** on **iEC ALK2 signaling** may contribute to the **underlying molecular mechanism** of the **aberrant vascular phenotype in human FOP lesions**, which is not observed in non-genetic HO (Figure 4.6).

The role of ActivinA in non-hereditary HO lesions upon poly-trauma remains unknown. Recent evidence demonstrated ActivinA as a negative regulator of muscle mass (Latres et al., 2017). ActivinA inhibition with a specific antibody increased muscle mass in mice, suggesting ActivinA as a modulator in muscle growth and regeneration (Latres et al., 2017).

Nevertheless, antibodies that neutralized ALK2 and interestingly also ALK3 reduced also non-hereditary HO (Hwang et al., 2020) highlighting the crucial role of **ALK2** and **BMP signaling in both HO forms**, which likely become activated by different triggers in both pathologies.

4.5.3 **Implications for EndMT**

EndMT is characterized by the expression of several transcription factors (e.g. SNAIL, SLUG, ZEB, TWIST), which trigger ECs to disintegrate from the endothelial barrier to become migratory mesenchymal cells by downregulation of endothelial and junctional markers (Ma et al., 2020). The ActivinA induced FOP transcriptome was associated with ventricular septum development involving EndMT (Kovacic et al., 2012) and classical EndMT transcriptional markers (e.g. **SNAI1, MSX2**) were identified. Moreover, the FOP specific upregulation of the NOTCH ligand JAG1 in iECs was shown to induce EndMT in microvascular ECs (Noseda et al., 2004). Moreover, strong **JAG1** expression in endocardial cushions suggested even the requirement of JAG1 in developmental EndMT (Luxán Guillermo et al., 2016; Noseda et al., 2004).

However, ActivinA did not reduce the expression of genes encoding cell-junction proteins (VE-Cadherin (*CDH5*), *PECAM1*) in FOP iECs, suggesting that ActivinA only induces **partial-EndMT** and **requires 2nd trigger(s)**.

Interestingly, primary ECFCs from FOP patients were demonstrated to undergo EndMT only in presence of the inflammatory trigger TNFα (Sánchez-Duffhues et al., 2019c). Generally, inflammatory cytokines have been suggested to corporately induce EndMT with TGFβ family members (Sánchez-Duffhues et al., 2019a).

Compared to TGFβ, TNFα alone even repressed more efficiently the expression of *CDH5* and *PECAM1* in human aortic ECs (Sánchez-Duffhues et al., 2019a).

Thus, similar as for angiogenesis, **ActivinA** may **prime FOP iEC** for enhanced TNFα induced **EndMT** (Figure 4.6).

In sum, ActivinA induced SMAD1/5 signaling only in FOP iECs resulting in a FOP transcriptome which activates BMP and NOTCH pathways and is associated with angiogenesis and EndMT.

ActivinA induced only partial EndMT and alterations in angiogenesis were only observed in presence of VEGFA, which suggests a **second hit model** for **pathological endothelial function in FOP** (Figure 4.6).

Here, **VEGFA** and inflammatory triggers such as **TNFα** are suggested to induce pathological angiogenesis and EndMT respectively as **2nd hit triggers** (Figure 4.6).

That EndMT may occur in human FOP lesion is supported by co-expression of the endothelial marker vWF and osteochondrogenic markers in patient biopsies (Medici et al., 2010). However, based on different Cre and HO mouse models the role of ECs in ectopic bone formation remain controversial (Lees-Shepard and Goldhamer, 2018) and requires more investigations.

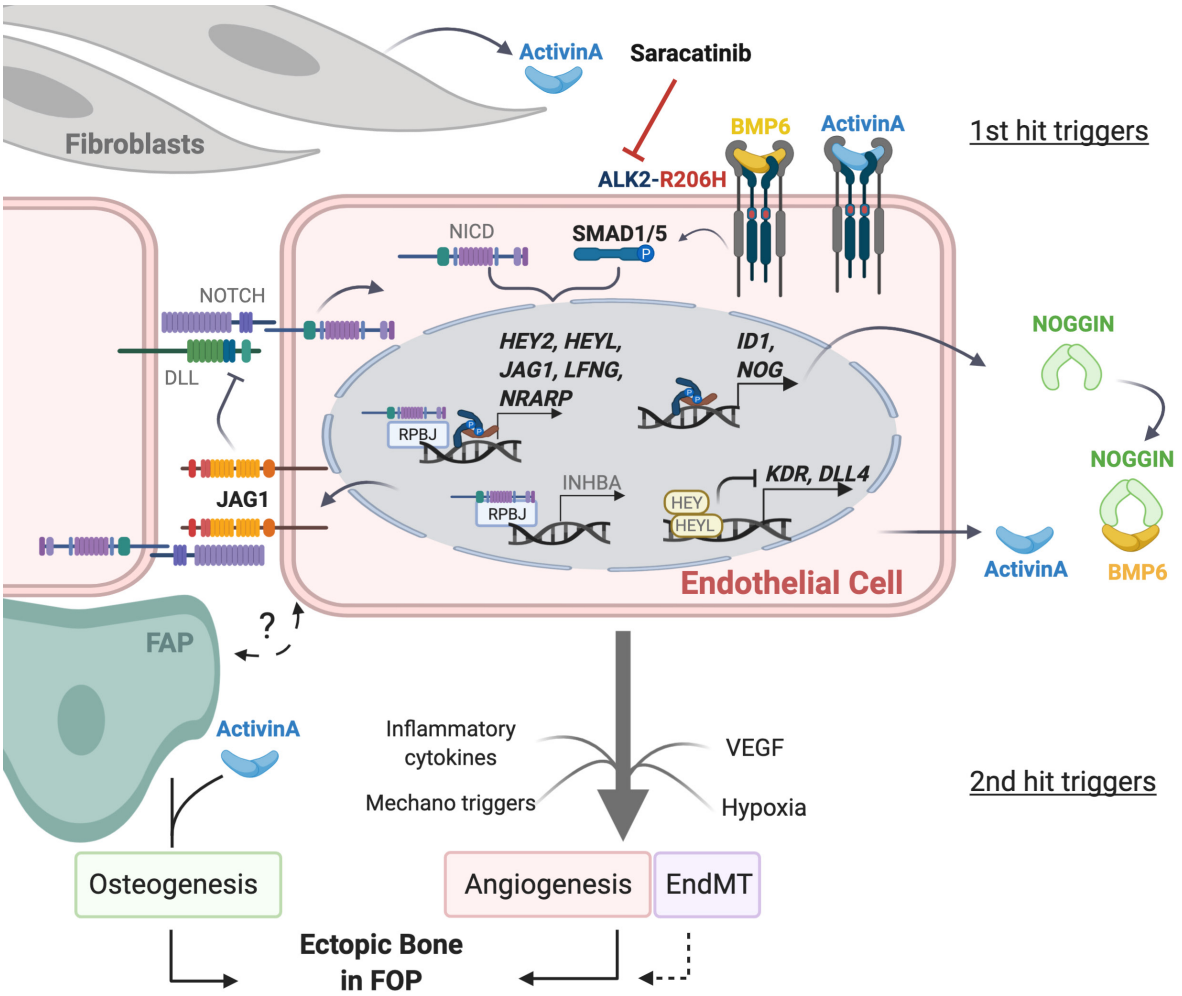

Figure 4.6 Model of early endothelial ActivinA signaling and its consequences on Endothelial Cell function in the angiogenic and fibroproliferative stage of FOP lesions.
Initial inflammation in skeletal muscle tissue in FOP lesions is followed by a **fibroproliferative angiogenic transition stage**, and subsequent endochondral bone formation. Fibroblasts in FOP lesions upregulate ActivinA (Hwang et al., 2020) suggesting that fibroblast derived ActivinA induces aberrant SMAD1/5 signaling in FOP ECs resulting in a FOP specific transcriptome interlinking ActivinA with BMP/NOTCH pathways, blood vessel formation and EndMT. Moreover, the activation of only the BMP binding antagonist (Noggin) in the transcriptome suggests a feed forward mechanism for ActivinA signaling by removing BMPs as ALK2 binding competitors. BMP6 stimulation upregulated the same genes as ActivinA, indicating that ActivinA transduces a BMP like response and that **BMP6** can also function as a **1st trigger**. Importantly, FOP iECs expressed BMP6 and ActivinA suggesting autocrine signaling. Since ActivinA induced only partial EndMT and alterations in angiogenesis were only observed in presence of VEGFA a **second hit model** for pathological endothelial function in FOP is suggested:
I propose that the ActivinA induced FOP specific transcriptome (1st trigger) pre-patterns the FOP endothelium and thereby challenges endothelial identity and plasticity, which leads to ***pathological angiogenesis and EndMT*** *in presence of 2nd triggers.*
Drug treatment of FOP endothelial disease model with the kinase inhibitor **Saracatinib** prevented aberrant signaling responses and rescued the ActivinA-induced transcriptome in FOP iECs to WT levels, suggesting a preventive effect on aberrant vascularization in early HO lesions in FOP
The role of ECs in ectopic bone formation remains controversial (Lees-Shepard and Goldhamer, 2018). But co-expression of the endothelial marker vWF and osteochondrogenic markers in patient biopsies suggest that EndMT may occur in human FOP lesions (Medici et al., 2010).
Fibro/adipogenic progenitors (**FAPs**) in the muscle interstitium represent a major progenitor cell type in ectopic bone formation in FOP (Lees-Shepard et al., 2018). FAPs closely associate with blood vessels in skeletal muscle (see **Figure 1.9**) (Uezumi et al., 2010). However, a potential crosstalk between FAPs and the vasculature remains unexplored.

4.6 Implications for a crosstalk between ALK2 and VEGF signaling

Interestingly, the VEGFA induced sprouting outgrowth is reduced in FOP iECs, which could be partially rescued by targeting ALK2. This indicates, an ALK2 dependent crosstalk with VEGFA signaling and suggests impaired angiogenesis capacity of FOP iECs representing an interesting topic for future work.

Whether this potential crosstalk occurs upstream on the receptor level or by ALK2 induced target genes remains unknown. ALK2 mediated crosstalk with VEGFA should be further validated by complementary analysis of up and downstream targets from both signaling pathways in a time resolved manner. Crosstalk of VEGF and BMP signaling on the transcriptional level has been observed previously.

Haploinsufficient *Alk1* mice (HHT model) have reduced Vegfr1 levels, which is suggested to cause the hypersprouting phenotype in retinal angiogenesis (Thalgott Jérémy H. et al., 2018). Moreover, Vegfa levels were elevated in *Alk1* deficient mice (Shao et al., 2009). This is in line with increased VEGFA plasma levels in HHT patients with mutations in either *Endoglin* or *ALK1* (Sadick et al., 2005b, 2005a).

Mechanistic analysis suggest that VEGFA expression is enhanced via TGFβ/ALK5/SMAD2 signaling and reduced by BMP9/ALK1/SMAD1 in aortic ECs (Shao et al., 2009). Thus, aberrations in SMAD responses modulate VEGFA expression. In general, most adult tissues express low levels of **VEGFA** and it becomes **upregulated** in **pathological conditions** such as inflammation, wound healing, bone repair and tumor formation (Nagy et al., 2007). A classical inducer of VEGFA expression in pathological angiogenesis is hypoxia via the hypoxia-inducible factor (HIF) (Nagy et al., 2007).

Upregulated VEGF in bone formation and regeneration has a dual role by promoting new blood vessel formation but also stimulating osteogenesis and thereby couples angiogenesis and osteogenesis (Grosso et al., 2017). As mentioned previously VEGFA is required for proper bone repair and regeneration (Hu and Olsen, 2016) and ectopic bone formation (Hwang et al., 2019). VEGFA is expressed by ECs but also by osteogenic cells and in particular maturating osteoblasts are thought to be the main source of VEGFA in bone formation (Hu and Olsen, 2016). Recently, MSCs were identified as the main source of VEGFA in ectopic bone formation (Hwang et al., 2019). Moreover, it was suggested that VEGFA promotes (ectopic) bone formation synergistically with BMP2 (Kempen et al., 2009; Wang et al., 2018) but whether this is

mediated by direct signaling crosstalk remains unknown and should be addressed in future studies.

VEGFA expression levels were not modified in FOP iEC after 2 hours ActivinA treatment. Interestingly, it was reported that FOP monocytes show highly increased VEGFA secretion upon inflammatory triggers compared to controls (Barruet et al., 2018), suggesting that ALK2 signaling modifies VEGFA expression context-dependently.

In sum, current evidence suggests a SMAD dependent crosstalk of BMP and VEGF signaling on the transcriptional level, which should be investigated further.

Monocytic VEGFA upregulation suggests recruitment of ECs by monocytes in FOP lesions, which may mediate the transmission from inflammation to angiogenesis and fibroproliferation (Figure 4.2A).

4.7 Endothelial barrier disruption initiates angiogenesis, Inflammation and EndMT – possible implications for FOP

The endothelium forms a dynamic semi-permeable barrier between the blood and the tissue. In homeostasis basal permeability enables exchange by diffusion of small molecules (< 40 kDa) and gases but prevents extravasation of larger molecules and cells (Claesson-Welsh, 2015; Egawa et al., 2013). During inflammation, edema, wound healing or diseases vascular permeability dramatically increases, mediated by acute (short-term) or chronic (long-term) exposure to permeabilizing factors, particularly VEGF, which enables the influx of larger molecules and cells (Nagy et al., 2008). Moreover, the dissolution of cell-cell contacts facilitate the loosening and migration of selected cells of the endothelial barrier and thus is essential for the initiation of new blood vessel formation in angiogenesis, wound healing (Tonnesen et al., 2000) and also for EndMT (Sánchez-Duffhues et al., 2018).

The multi-stage process of HO in FOP is characterized by several above mentioned tissue responses such as inflammation, edema formation, angiogenesis (Shore and Kaplan, 2010) and also suggested to involve EndMT (Medici et al., 2010; Sánchez-Duffhues et al., 2019c). Thus, any aberration in FOP endothelial barrier function may help to unreveal the underlying mechanisms of several stages in HO.

Here, long-term BMP6 treatment triggered destabilization of WT and FOP iEC monolayers in an ALK2 dependent manner and a trend was also observed for ActivinA

in FOP iECs (Figure 3.29). This is in line with a recent study of BMP6 induced permeability in venous ECs via ALK2 (Benn et al., 2016).

However, ActivinA and BMP6 induced permeability of iEC monolayers was independent of direct activation of SRC and VE-Cadherin, which is in contrast to the previous mentioned study (Benn et al., 2016). The complex underlying mechanisms destabilizing endothelial barriers are diverse, involving junctional rearrangements cytoskeletal dynamics and also vary between vascular bed specificities (Claesson-Welsh, 2015; Goddard and Iruela-Arispe, 2013). Moreover, the short and long-term induced permeability by VEGFA in WT and FOP iECs with a short recovery even suggest two distinct underlying mechanisms, which was observed previously in microvascular ECs (Gao et al., 2017). The authors suggested that the early VEGFA induced barrier disruption was SRC dependent whereas the long term effect was mediated by **AKT** (Gao et al., 2017). AKT1 kinase is essential for vascular function and *Akt1* deficient mice have enhanced angiogenic responses with impaired blood vessel maturation and increased vascular permeability (Chen et al., 2005).

Importantly, long-term TGFβ induced barrier disruption was suggested to be mediated via inhibition of AKT phosphorylation (Ser 473) (Chen et al., 2005). This is in line with the analysis of iEC barriers: ActivinA long term treatment also resulted in reduced phosphorylated AKT levels in FOP iECs, which was confirmed for BMP6 in WT and FOP iECs. The kinetic pattern of pAKT levels were in line with the reduction of the measured resistance of FOP iEC monolayers, suggesting an involvement of AKT in endothelial barrier integrity. Thus, ActivinA inhibition of AKT activity could be associated with increased angiogenesis in pre-osseous FOP lesions.

Even though most mechanisms in the regulation of endothelial barriers are non-transcriptional and show direct effects on kinases and junctional proteins, long term effects on barrier disruption as shown here suggest that transcriptional targets are involved, which is supported by several reports (Clark et al., 2015; Goddard and Iruela-Arispe, 2013). Highly upregulated ***TCIM*** and downregulated ***ADM*** were identified as potential endothelial barrier modulators in the ActivinA induced FOP transcriptome and were confirmed to depend on ALK2 (see Figure 3.31). Both hits were associated with endothelial permeability previously (Hippenstiel et al., 2002; Kim et al., 2009) and should be analyzed by rescue experiments in FOP iEC barrier function further.

Interestingly, overexpression of TCIM was shown to induce **edema formation** in zebrafish and to increase endothelial inflammatory mediators, monocyte adhesion and

permeability in human arterial ECs (Kim et al., 2009). In contrast, the peptide hormone ADM stabilizes endothelial barriers. ADM reduced endothelial hyperpermeability in HUVECs dose dependently and blocked edema formation in rabbit lungs (Hippenstiel et al., 2002). Thus, it is tempting to speculate that TCIM and ADM could contribute to permeability in edema formation in FOP lesions.

4.8 Saracatinib rescues aberrant signaling responses in FOP iECs

4.8.1 Saracatinib is an efficient ALK2 inhibitor and prevents aberrant signaling responses in FOP iECs

The ALK2-dependent over-activation of SMAD1/5 signaling is thought to trigger HO in FOP. Thus, activation of SMAD1/5 responses in iECs by ActivinA recapitulate an important pathogenic molecular mechanism in FOP (Hatsell et al., 2015; Hino et al., 2015). Drug testing approaches have focused on phenotypes related to HO or directly on ALK2 function as reviewed in (Wentworth et al., 2019). Based on the early read out of aberrant ActivinA signaling in the iEC disease model, the mechanistic action of the investigational drug candidate Saracatinib was analyzed, which directly targets the ALK2 kinase (Kitoh, 2020).

Saracatinib, initially discovered as a tyrosine kinase inhibitor and developed for the treatment of cancer (Hennequin et al., 2006) was later extended as an inhibitor for BMP type I receptors (Lewis and Prywes, 2013) and HO (Hino et al., 2018; Wentworth et al., 2019; Yu et al., 2016). From 2007 until today 33 clinical trials have been completed with Saracatinib (clinicaltrials.gov). Saracatinib has been reported to be well tolerated by patients (Baird et al., 2020) but due to insufficient efficacy in several therapeutic applications in clinical trials, Saracatinib hasn’t received any drug approval for any indication up to date. As a repurposed drug a first phase II clinical trial was recently initated to assess the efficacy of Saracatinib in HO prevention in FOP patients, named *STOPFOP* (NCT04307953).

Very recently, the related comprehensive pre-clinical study describing Saracatinib as a candidate for ALK2 inhibition to prevent HO in FOP has been published on a preprint server (Williams et al., 2020). The authors demonstrate the identification of Saracatinib in a library screen of clinically tested small molecules and solved the crystal structure of Saracatinib in complex with ALK2 kinase showing that Saracatinib interacts with the ATP-binding pocket (Williams et al., 2020).

However, the effect of Saracatinib on FOP ECs has not been reported yet. In the present study Saracatinib efficiently inhibited aberrant ALK2 signaling in both FOP donors in response to ActivinA on phosphorylated SMAD levels and downstream target gene transcription (Hildebrandt et al., Stem Cell Rev Rep, in press 2020). Moreover, Saracatinib prevented aberrant BMP6/SMAD2 responses and rescued ActivinA induced reduction of phosphorylated AKT. BMP6 signaling responses were inhibited by Saracatinib in both WT and FOP iECs (Hildebrandt et al., Stem Cell Rev Rep, in press 2020) (Figure 3.25). This is in line with recent data from the above mentioned preprint demonstrating Saracatinib induced inhibition of BMP6/SMAD1/5 responses in WT and FOP cells and inhibition of ActivinA/SMAD1/5 responses in FOP cells (Williams et al., 2020). Thus, Saracatinib is an ALK2 inhibitor and prevents ALK2 activation independent of the ligand.

Interestingly, a recent study developed macrocyclic compounds (OD36, OD52), which were even more effective to block ActivinA/SMAD1/5 responses compared to BMP6 (Sánchez-Duffhues et al., 2019c). Thus, remaining BMP6 responses could be mediated by ALK2-WT since the macrocyclic compounds showed enhanced activity for mutant ALK2-R206H (Sánchez-Duffhues et al., 2019c).

Interestingly, the macrocyclic compounds also blocked BMP9 signaling more efficiently compared to BMP6 (Sánchez-Duffhues et al., 2019c). Here, higher concentrated Saracatinib (>0.5 µM) also inhibited BMP9 induced SMAD1/5 and SMAD2 signaling. This indicates off-target effects to ALK1 at high doses, which is in line with *in vitro* kinase assays with Saracatinib (Lewis and Prywes, 2013) and the macrocyclic compounds (Sánchez-Duffhues et al., 2019c). However, increasing evidence suggest that ALK2 also binds BMP9 and mediates signaling (Olsen et al., 2018, 2015; Salmon et al., 2020).

At concentrations of 0.5 µM or higher, Saracatinib also slightly reduced pSMAD2 levels upon BMP9 and ActivinA treatment, which is in line with reported reduced CAGA reporter activity by another study using 0.1 µM (Hino et al., 2018). This indicates minor concentration dependent ALK4 and ALK5 off target by Saracatinib.

In the iEC model Saracatinib inhibited ActivinA/SMAD1/5 signaling in both FOP donors, whereas SMAD2/3 signaling was unaffected at 0.2 µM, which was also confirmed on target gene transcription. This supports the clinical trial design of *STOPFOP*, treating patients with a dose of 0.1 µM Saracatinib (NCT04307953). Moreover, Saracatinib, originally discovered to target SRC kinases, was not affective

to inhibit SRC activity in iECs at low doses (up to 0.5 µM), which is in line with reported SRC inhibition at 5 µM (Cavalloni et al., 2012).
Collectively, Saracatinib efficiently inhibits ALK2 signaling at minimal dose, whereas higher doses increase off-target effects to other kinases.
This highlights the importance of optimal dosing aiming to achieve efficacy and low side effects, which remains to be shown for Saracatinib in FOP patients in near future.

4.8.2 ALK2 kinase inhibitors as potential therapeutic drugs to prevent HO in FOP

Importantly, Saracatinib successfully restored the ActivinA induced FOP transcriptome to WT expression levels and counteracted impaired endothelial function of FOP iECs, suggesting a preventive effect of Saracatinib on aberrant vascularization in early HO lesions in FOP (Hildebrandt et al., Stem Cell Rev Rep, in press 2020). This is supported by an independent clinical model of biliary tract carcinoma showing that Saracatinib inhibited tumor angiogenesis *in vivo* (Cavalloni et al., 2012). But the authors used in latter study high doses of Saracatinib, suggesting that ALK1 and SRC were targeted in addition to ALK2 in this context.
Besides target specificity, for clinical applications in humans, kinase inhibitors have to withstand a safety evaluation with low off target effects on essential systemic physiological functions. For example LDN-212854 showed increased selectivity for ALK2 than to ALK1 compared to Saracatinib but treatment with LDN-212854 in mice was associated with weight loss up to 25% relative to vehicle controls, whereas Saracatinib was well tolerated, as demonstrated in the patent by (Yu et al., 2016). The data from FOP iECs suggest that Saracatinib prevents aberrant ALK2 signaling responses in the vasculature of FOP patients and contributes to a better understanding of the specific mechanistic action of Saracatinib in human tissues.
Thus, the here established FOP iECs represent a powerful patient model for further studies on disease mechanism(s) under endogenous receptor levels and for drug testing.
Besides Saracatinib, the toolbox of compounds targeting the ALK2 kinase has been expanded through discovery of BLU-782 (IPN60130), BCX9250, KER-047 (IFOPA, n.d.), including the previous mentioned macrocyclic inhibitors (Sánchez-Duffhues et al., 2019c). Thus, **iECs** could be also applied for **drug comparison** and to investigate **patient specific differences**. In fact, disease progression is very heterogenous among FOP patients and the underlying causes remain unknown. Moreover, most pre-

clinical evaluation of compound activity was performed in models with the most common ALK2 mutation R206H, excluding the other FOP causing mutations.

This highlights the potential iPSC derived human disease models for **personalized medicine** approaches for patient specific **compound screening platforms** and pre-clinical testings. Although there is no effective treatment for FOP approved today, within the time frame of this project the clinical trials in FOP excitingly increased from 1 to 8. The majority includes 5 clinical trials with small molecule kinase inhibitors from which Saracatinib as a repurposed drug will be the first kinase inhibitor tested in a phase II trial in FOP patients (Figure 4.7)**.** The efficacy and safety of those drugs remains to be shown in near future and optimally a range of treatment strategies will become available to ensure the best treatment strategies for individual FOP patients. Besides prevention of ectopic bone formation, it will be interesting to determine if these treatment options are also beneficial to reduce or prevent the degenerative joint disease (see chapter 1.6.1) (Kaplan et al., 2020) which is associated with the life-threatening thoratic insufficiency in FOP patients (Kaplan et al., 2010; Towler et al., 2020).

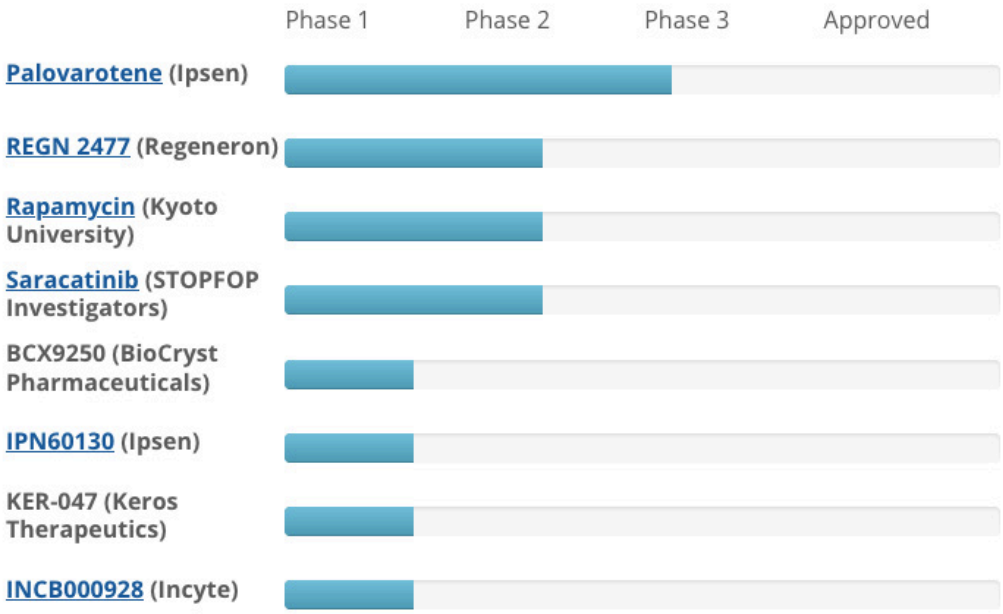

Figure 4.7 Ongoing Clinical Trials in FOP. After promising findings in basic research and pre-clinical animal testing an integral part of drug development includes clinical trial research in humans. Currently, no drug has been approved for FOP but 8 investigational drugs are in clinical studies. For clinical testing a drug is first evaluated for dosing and safety in healthy volunteers (Phase 1). In a proof of concept study efficacy and continued safety assessment is performed in the patient target group, optimally in a randomized controlled trial format (Phase 2). In a confirmatory study efficacy and safety is analyzed in a more heterogenous and often larger patient target group (Phase 3). Authorities, such as the European Medicines Agency (EMA) in Europe or the Food and Drug Administration (FDA) in the US. Assess and evaluate the benefit and risk of novel drugs to decide on its approval. Graph was retrieved from the International FOP Association (IFOPA) (https://www.ifopa.org/ongoing_clinical_trials_in_fop).

4.9 Conclusion

In the present study a new FOP patient derived endothelial cell model was generated by using iPSCs in a combinatorial cryopreservation and differentiation method. FOP iECs recapitulated the pathomechanism of aberrant ActivinA/SMAD1/5 signaling and a comprehensive transcriptome analysis identified a FOP-specific genetic profile interlinking ActivinA with BMP/NOTCH pathways, blood vessel formation and EndMT. Collectively, the results propose a model in which ActivinA primes FOP ECs in favor of pathological angiogenesis and EndMT in presence of angiogenic and inflammatory factors as 2nd triggers.

The model is in line with FOP pathology, which is characterized by episodic *flare ups* from which 20% do not result in heterotopic bone (Eekhoff et al., 2018). This suggests that besides the ALK2 mutation additional triggers are involved, which represent a critical switch to induce bone formation or not. Those triggers likely create a pro-osteogenic niche in the lesioned tissue, including a pro-angiogenic environment as observed in FOP patient biopsies, which show even increased vascularity compared to non-hereditary lesions prior ectopic bone formation (Cocks et al., 2017; Ware et al., 2019). The here investigated aberrant ActivinA and BMP effects on ALK2 signaling and angiogenic processes of FOP ECs contribute to a better understanding of the underlying molecular mechanism of the differential vascular phenotype in FOP lesions. Drug testing in the FOP endothelial disease model showed that the kinase inhibitor Saracatinib rescued the ActivinA induced transcriptome to WT levels, suggesting a preventive effect on angiogenesis in early HO lesions in FOP.

The tight interlink of osteogenesis and angiogenesis and the requirement of pro-angiogenic factors in ectopic bone formation (Hwang et al., 2019) suggest further investigations (e.g. with the iECs model) on anti-angiogenic therapies for FOP.

The results in this study support that ALK2 is an essential component of the ActivinA/SMAD1/5 signaling complex whereas ALK4 is not required. It remains to be shown, how ActivinA/SMAD1/5 signaling is favored by mutant ALK2 and which co-factors enable it for WT ALK2. The results here and from others suggest that reduced binding of FKBP12 is not sufficient to convert the ActivinA-ALK2 into a signaling complex. In conclusion, this work strengthens the role of ECs as a disease relevant cell type in FOP, which indirectly and/or directly contributes to each stage of ectopic bone formation.

4.10 Future perspectives

4.10.1 Investigation of the ActivinA/SMAD1/5 signaling complex in WT and FOP iECs

Besides ALK2, little is known about the composition of the ActivinA/SMAD1/5 signaling receptor complex. Type II receptors are essential for ALK2 signaling (Bagarova et al., 2013) but which type II receptor(s) form a complex with ActivinA and ALK2 remains incompletely understood. It remains to be shown whether ALK2-R206H facilitates distinct complex formation with ACVR2A, ACVR2B or BMPR2 compared to ALK2-WT in presence of ActivinA. Ongoing, type II receptor knockdown experiments remain challenging due to lack of specific antibodies for knockdown validation. Generally, due to the lack of specific antibodies for most BMP and TGFβ receptors the primary cell model with endogenous receptor expression is limited for interaction studies and high-resolution microscopy. Strategies and efforts to generate an endogenously ALK2-GFP tagged iPSC line in an Einstein Kickbox collaboration is described in the appendix (see chapter 5.1). Based on the limitation of endogenous systems, traditional overexpression construct encoding tagged receptors offer additional methods to unravel the composition of ligand receptor complexes.

As mentioned in chapter 4.3.2 ongoing Patch-FRAP experiments with tagged receptors in overexpression will shed light on ALK2 complex formation with respective type II receptors and the effect of ActivinA (Ongoing cooperation with Prof. Yoav Henis and Szófia Szilágyi, Tel Aviv University, Israel).

Moreover, the recently expanded tool-box of fluorescently labeled ligands in the Knaus group (J. Jatzlau, P. Knaus in cooperation with M. Hyvönen, University of Cambridge, UK and J. Broichhagen, FMP, Berlin) represent useful tools to visualize ligand binding on endogenous receptors but also to investigate ligand-receptor interaction by using fluorescently tagged receptors and co-receptors in Stimulated Emission Depletion (STED) microscopy.

In addition, the unexpected discovery of ActivinA/SMAD1/5 signaling in WT iECs in full medium conditions suggests a context dependent *switch* from ActivinA-ALK2 non-signaling to SMAD1/5 signaling complexes and offers a promising experimental model to explore the co-factor X, which controls this switch.

4.10.2 Potential contribution of iECs to a future human FOP organoid

In the previous chapters it was highlighted that ECs contribute to each stage of ectopic bone formation in FOP ranging from inflammation and coupled angiogenesis, osteogenesis. Thereby the vasculature undergoes dynamic changes, which have been barely modeled with human systems.

According the mechanistic and functional investigations of the here generated FOP EC disease model, it is proposed that the aberrant ActivinA/SMAD1/5 signaling responses induce a transcriptome, which pre-patterns the FOP endothelium favoring initiation of pathogenic angiogenesis in early HO lesions. Potentially, this underlying molecular mechanism contributes to the vascular phenotype found in HO lesions of FOP patients. However, to functionally recapitulate the complex vascular phenotype in FOP lesions during HO, iECs should be integrated in more advanced 3D organoid models. Recent progress in skeletal muscle organoid models (Maffioletti et al., 2018) could be used to establish a first human FOP organoid from patient iPSCs for future studies. Maffioletti et al., generated artificial muscle with characteristics of human skeletal muscle tissue containing myofibers, satellite cells and integrated isogenic ECs and pericytes derived from the same iPSC donors used for myogenic differentiation, which could be implanted in mice (Maffioletti et al., 2018).

It is a question for future research to investigate if a human FOP skeletal muscle organoid would also recapitulate the observed muscle resident progenitor cells of ectopic bone in FOP mice (e.g. FAPs). In fact, until now the different progenitor cell populations have been solely described in FOP mouse models (Dey et al., 2016; Lees-Shepard et al., 2018; Medici et al., 2010). Human FOP organoids with human FAP populations would also offer a model to study the above depicted interaction of ECs and FAPs.

4.10.3 Potential role of the Endothelial Barrier in preventing enhanced BMP signaling and (trans)-differentiation

In this study it was shown that FOP iECs have increased basal permeability compared to WT controls. FOP basal permeability could be further enhanced upon BMP6 and ActivinA stimulation. This suggests, that permeability is favored in the FOP endothelium. This is supported by early electron microscopy of human FOP lesions showing that vessels are leaky and hemorrhagic (el-Labban et al., 1995).

Since the here observed effects in the *in vitro* setting were not very strong, permeability measurements should be validated in more physiological conditions, using full medium

and co-cultured mural cells, such as pericytes. Pericytes contribute to vessel stability and aberrant TGF/BMP signaling has been suggested to induce defective endothelial-mural cell interaction impairing vessel stability and permeability (Thalgott et al., 2015). Local leakiness of FOP vasculature would enable permeability of blood plasma proteins (e.g BMPs, Activins), which would boost or even trigger the aberrant bone formation in soft tissues. This aspect is of particular interest in respect of a recent study, which demonstrated that circulating BMPs (e.g BMP4, BMP7) in the blood stream can be further cleaved N-terminally by serum proteases (thrombin, plasmin), which result in “Super BMPs” with 30-fold more potency (Wagner et al., 2017).

Accordingly, it can be hypothesized that growth factor transmission from blood into the tissue by vascular leakage would further enhance BMP signaling in lesioned tissue in FOP. In a limb model, the super BMPs induced cell cycle re-entry and dedifferentiation of skeletal muscle (Wagner et al., 2017) suggesting that enhanced BMP signaling impairs cellular fate of mature tissue or in other words, cellular plasticity.

A study of (Murgai et al., in preparation) confirmed this observation for murine myoblasts *in vitro*. Moreover, in an embryonic *in vivo* model of enhanced BMP signaling (Noggin deficient mice) the authors observed trans-differentiation capabilities of myogenic cells to other mesodermal lineages, including osteogenic and chondrogenic cells. Whether, cell cycle re-entry and dedifferentiation of skeletal muscle with trans-differentiation capabilities also occurs in adult mammals with enhanced BMP signaling, for example in FOP mice, is unknown.

It is tempting to speculate, that vascular leakage contributes to episodic excessive BMP signaling in FOP lesions by opening the barrier for blood derived BMPs, super BMPs and Activins, which hit ALK2 expressing cells and thereby induce (trans)-differentiation in skeletal muscle. Importantly, FAPs, which are considered as the major progenitor cell population in HO in FOP were reported to accumulate around blood vessels in skeletal tissue (Uezumi et al., 2010) (see Figure 1.9 and Figure 4.6). This, indicates direct contact of ECs to FAPs, which facilitates short diffusion distance of blood derived growth factures upon vascular leakage.

4.10.4 **Mechanical cues as additional triggers in FOP**

Even though HO often becomes initiated spontaneously in FOP patients, it is also triggered by minor trauma. In non-hereditary forms of HO, trauma and injury represents a major inducer of the aberrant tissue repair process. In general, proper tissue repair and regeneration is not only controlled by biochemical signals but also by mechanical forces (Tsata and Beis, 2020). Increasing evidence suggests a crosstalk of the BMP signaling pathway with mechanical forces such as tension, compression, shear force and substrate stiffness, which has been mostly studied in the context of bone formation and remodeling as reviewed in (da Silva Madaleno et al., 2020). However, also the endothelium is exposed to multiple mechanical forces, which orchestrate with TGFβ and BMP to control endothelial function (Hiepen et al., 2020).

Interestingly, two recent studies demonstrated that the FOP causing ALK2 mutation R206H elevated cellular mechanical signaling and altered mechanosensing as well as tissue stiffness in HO (Haupt et al., 2019; Stanley et al., 2019).

The elevated tissue stiffness in murine FOP lesions (Haupt et al., 2019) suggests a modulation of mechanical properties during HO. The composition of extracellular matrix (ECM) proteins modulates tissue stiffening and becomes for example temporary replaced to provide instructive cues for progenitor cells in amphibian limb regeneration (Calve et al., 2010). Interestingly, in the above mentioned embryonic *in vivo* model of enhanced BMP signaling (Noggin deficient mice) (see chapter 4.10.3) the trans-differentiation of myogenic cells into osteochondrogenic lineages was accompanied by changes in ECM proteins, such as Tenascin-C (Murgai et al., in preparation). The ECM components in human HO biopsies are still unknown and it would be interesting to analyze if for example Tenascin becomes upregulated.

Murine FOP *in vitro* and *in vivo* models indicate that the collagen composition at the fibroproliferative stage is altered (Haupt et al., 2019). The fibroproliferative stage in HO is highly angiogenic (Shore and Kaplan, 2010) and the property of ECs to sense substrate stiffness in crosstalk with TGFβ/BMP signaling (Hiepen et al., 2020) suggests that an altered ECM composition may modulate endothelial signaling and cellular fate in FOP. Moreover, ECs themselves also modulate mechanical forces and ECM stiffness as a result of unbalanced TGFβ/BMP signaling responses, as recently demonstrated for BMPR2 deficient ECs (Hiepen et al., 2019).

Whether FOP ECs modulate and transduce mechanical stimuli differently is unknown. It is tempting to speculate that those cues further modulate signaling overactivation by BMPs and Activins and represents an interesting question for future research.

The iEC experiments under Fluid Shear Stress (FSS), in which WT iECs also gain ActivinA/SMAD1/5 signaling, suggest that FSS may integrate in signaling responses by modulating ActivinA receptor complex formation.

In fact, a complete understanding of the FOP lesion niche, which directs FOP progenitors to aberrant endochondral bone formation requires not only the mechanistic investigation of growth factor signaling. To the same extend the knowledge about ECM composition and the ultimately connected mechanical cues and their transduction in cellular function are of great importance.

As stated by a recent review, `**cells live in a complex world**´ and only the comprehensive integration of the above mentioned context will reveal the actual signaling state and ultimately cell function in tissue context (Stricker et al., 2017). Consequently, the here generated **versatile FOP endothelial cell model** can be ***put into context*** by using more physiological cell culture conditions with incorporated mechanical and biochemical triggers in space and time in future.

5. Appendix

5.1 Visualization of the endogenous BMP receptor ALK2 in endothelial cells using CRISPR/Cas9 and iPSC technology (Einstein Kickbox: *iPSC-GenEd*)

The ability to generate induced pluripotent stem cells (iPSCs) from somatic cells provides tremendous opportunities to establish *in vitro* disease models. The discovery of the Clustered Regularly Interspaced Short Palindromic Repeats (CRISPR)/Cas9 technology has improved to introduce precise changes in the genome of iPSCs. Bone morphogenetic protein (BMP) signal transduction requires two receptor types (type I and type II), which form heterotetrameric complexes. Besides receptor oligomerization and binding affinities of ligands, the localization of BMP receptors in distinct plasma membrane domains contribute to signaling specificity.

Previous studies demonstrated the impact of lateral mobility of BMP receptors within distinct plasma membrane domains on their signaling specificity using single particle tracking microscopy (Guzman et al., 2012). The localization and lateral mobility of ALK2 within the plasma membrane remains unknown.

Subcellular localization defines the access of proteins to interaction partners and enables the integration of proteins into functional biological domains. Up to date, endogenous subcellular localization and functionality of transmembrane receptors is a major unsolved question in the field of growth factor signaling. Due to a lack for functional specific antibodies, subcellular localization and functionality of BMP receptors are still limited to overexpression studies, which may lead to aberrant receptor localization and thereby restricts clinical translation of research findings. Interestingly, overexpression studies indicated alterations in the subcellular distribution of ALK2 due to the R206H mutation (Song et al., 2010b).

As patient material of rare diseases and other primary cell models, such as endothelial cells (ECs), are limited due to their availability and mortality in culture, iPSC technology was used approach the question about the subcellular function of mutant and WT ALK2 receptor.

Thus, the aim was to take advantage of the genome editing technology CRISPR/Cas9 to generate an endogenously Green Fluorescent Protein (GFP) tagged ALK2 iPSC line

(ALK2-meGFP iPSC) for direct receptor visualization by super-resolution microscopy. The N-terminal GFP tag enables the possibilities to enhance the signal with GFP specific nanobodies, that are suitable for super resolution microscopy. As an outlook, it is aimed to use the ALK2-meGFP iPSC line for the endothelial differentiation from iPSC as established and described in chapter 3.1. The usage of WT and FOP iPSCs enables to study endogenous ALK2 location and functionality in disease relevant cell types such as ECs for the first time. Shedding light of ALK2 subcellular localization accelerates the understanding of BMP receptor biology and is beneficial for the development of targeted treatment strategies in FOP. The pluripotency and immortality of the genetically engineered cell model enables the production of various cell types for future projects addressing ALK2 receptor functionality in regenerative mechanisms. ALK2-meGFP expression and localization could be potentially followed during differentiation from the stem cell fate to the formation of a specialized cell type.

5.1.1 **CRISPR/Cas9 strategy to generate an ALK2-meGFP iPSC line**

To assess functionality of the ALK2 N-terminal GFP tagged fusion protein in terms of signaling capabilities (e.g. ligand binding, receptor complex formation) an overexpression construct according the genetic design was generated beforehand (Figure **5.1**A). The ALK2-GFP fusion protein was designed with a flexible glycine linker to monomeric enhanced (me)GFP at the N-terminus (Figure 5.1B). Therefore, GFP insertion had to be targeted to exon 2 for GFP insertion after the signal peptide (Figure **5.1**A). In general, as a tag, monomeric enhanced GFP (EGFP) was chosen in order to prevent the dimerization of GFP fusion proteins. Moreover, it enables the possibilities to further enhance the signal with GFP specific nanobodies, that are suitable for super-resolution microscopy and single particle tracking (Fridy et al., 2014; Platonova et al., 2015). A N-terminal hemagglutinin (HA)-tagged human (h) WT ALK2 overexpression construct referred as control. Furthermore, hALK2-WT-HA was used as a cloning template to replace the HA tag by a meGFP tag by site directed mutagenesis including different linker sequences. Linkers with variable length and amino acid (AA) composition, distinguishing between flexible (F) and rigid (R) linkers were located between the ligand binding domain and the meGFP. The fusion protein hALK2-WT-mEGFP-L1 localized at the plasma membrane as confirmed with fluorescent microscopy (Figure 5.1C) and had the expected size as shown in Western Blot analysis (Figure 5.1D).

Signaling properties were assessed by the BMP Responsive Element (BRE) luciferase reporter assay, an artificial promoter construct of the BMP target gene *ID1*. C2C12 cells overexpressing differently tagged ALK2 receptors were stimulated with BMP6 for 6 hours (Figure 5.1E). Overexpression of HA-tagged ALK2 receptor and mEGFP-tagged receptor increased the promoter activity with and without BMP6 stimulation in comparison to the control (ß-galactosidase overexpression). Some linker designs impaired BMP6 induced signaling responses, whereas the flexible (F) linker F1 (containing three glycines) performed best for WT and FOP ALK2-mEGFP in comparison to HA tagged ALK2 controls (Figure 5.1E). Finally, the CRISPR donor repair template was constructed according the validated GFP-F1 linker design genetic design for functional GFP tagged ALK2.

In sum, N-terminal GFP tagged ALK2 receptor functionality requires a flexible glycine linker to monomeric enhanced (me)GFP. This highlights the importance of functionality testing's of tagged receptor proteins with proper linker designs.

Targeted nucleases are powerful tools for mediating genome alteration with high precision. The RNA-guided Cas9 nuclease from the microbial CRISPR adaptive immune system can be used to facilitate efficient genome engineering in eukaryotic cells by simply specifying a 20-nt targeting sequence within its guide RNA (gRNA). The gRNA consists of the sequence specific CRISPR (cr) RNA and transactivating tracrRNA. The 20-nt guide sequence within the gRNA must immediately precede a 5′-NGG PAM, and base pairs with the opposite strand to mediate Cas9 cleavage at ~3 bp upstream of the protospacer adjacent motif (PAM) (Ran et al., 2013). The online CRISPR Design Tool (http://tools.genome-engineering.org) was used to design the two target gRNAs *in silico* for human ALK2. First, gRNAs were designed to target the exon 2 for GFP insertion after the signal peptide of the *ALK2* locus (Figure 5.1F). The chosen gRNAs were cloned into the commercially available CRISPR px459 V2 (hSpCas9-2A-Puro V2.0) and additionally in the pEF1a-Cas9-GFP expression vector as described (Ran et al., 2013). In brief, phosphorylation and annealing was performed harboring a BbsI overhang. Afterwards, BbsI (#R0539S, NEB) digestion and ligation was performed according manufacturer's instructions and the plasmids were validated by Sanger sequencing.

The aim was to transfect the cells with the CRISPR targeting constructs, followed by an enrichment of Cas9+ cells by a GFP sort. As with other designer nuclease technologies such as Zink Finger Nucleases (ZFNs) and Transcription Activator-like

Effector Nucleases (TALENs), Cas9 facilitates targeted DNA double stranded breaks DSBs at specific loci of interest in the mammalian genome and stimulate genome editing via non-homologous end-joining (NHEJ) or homology-directed repair (HDR) (Ran et al., 2013). While the NHEJ pathway for DNA damage repair can lead to frameshift mutations in exon regions that will lead to a knockout of the target gene, insertions of foreign DNA fragments (Knock In) are mediated by the HDR pathway. Traditionally, targeted DNA modifications require the use of plasmid-based donor repair templates that contain homology arms flanking the site of alteration (Smithies et al., 1985; Thomas et al., 1986). The homology arms on each side can vary in length, but are typically longer than 500 base pairs (bp) (Hasty et al., 1991; Thomas et al., 1986). This method was used to generate large modifications by insertion of a GFP. For the GFP Knock In approach, repair templates were designed and cloned which compose of 600bp homologues arms framing monomeric enhanced GFP (meGFP) and a flexible linker sequence, from now on referred as GFP-Repair Template/Plasmid 1 or 2 dependent on the gRNA (Figure 5.1A). The 600 bp homology arms were amplified from bacterial artificial chromosome (BAC) by *Phusion* polymerase-based PCR. The homology arms were cloned via restriction cloning in a self-cleavable repair plasmid Tial1 (Lackner et al., 2015) resulting in a GFP tag framed by the homology arms which is flanked by two tial1 recognition sites, as well as a U6 promoter driving the expression of the tial1 gRNA. Consequently, the tag of interest will be released upon co-expression of Cas9 from px459 V2 and spontaneously integrated at the site specified by the genomic gRNA. gRNAs were validated for activity based on efficient DNA cleavage using *in vitro* cleavage of target DNA with ribonucleoprotein (RNP) complex. *ALK2* target sequence (1250 bp) was amplified by PCR from genomic iPSC DNA (QuickExtract™ DNA Extraction Solution) using specific primers, which was incubated with the Cas9 RNP complex (recombinant Cas9 protein, gRNA, tracrRNA). After incubation the DNA was separated on an agarose gel and showed the noncleaved product (1250 bp) and the successful cleavage products of gRNA1 (659 bp, 588 pb) and gRNA2 (641 bp, 606 bp) (Figure 5.1G). Thus, both designed gRNAs are functional and show DNA cleavage at the ALK2 target site in a cell free context (*in vitro*).

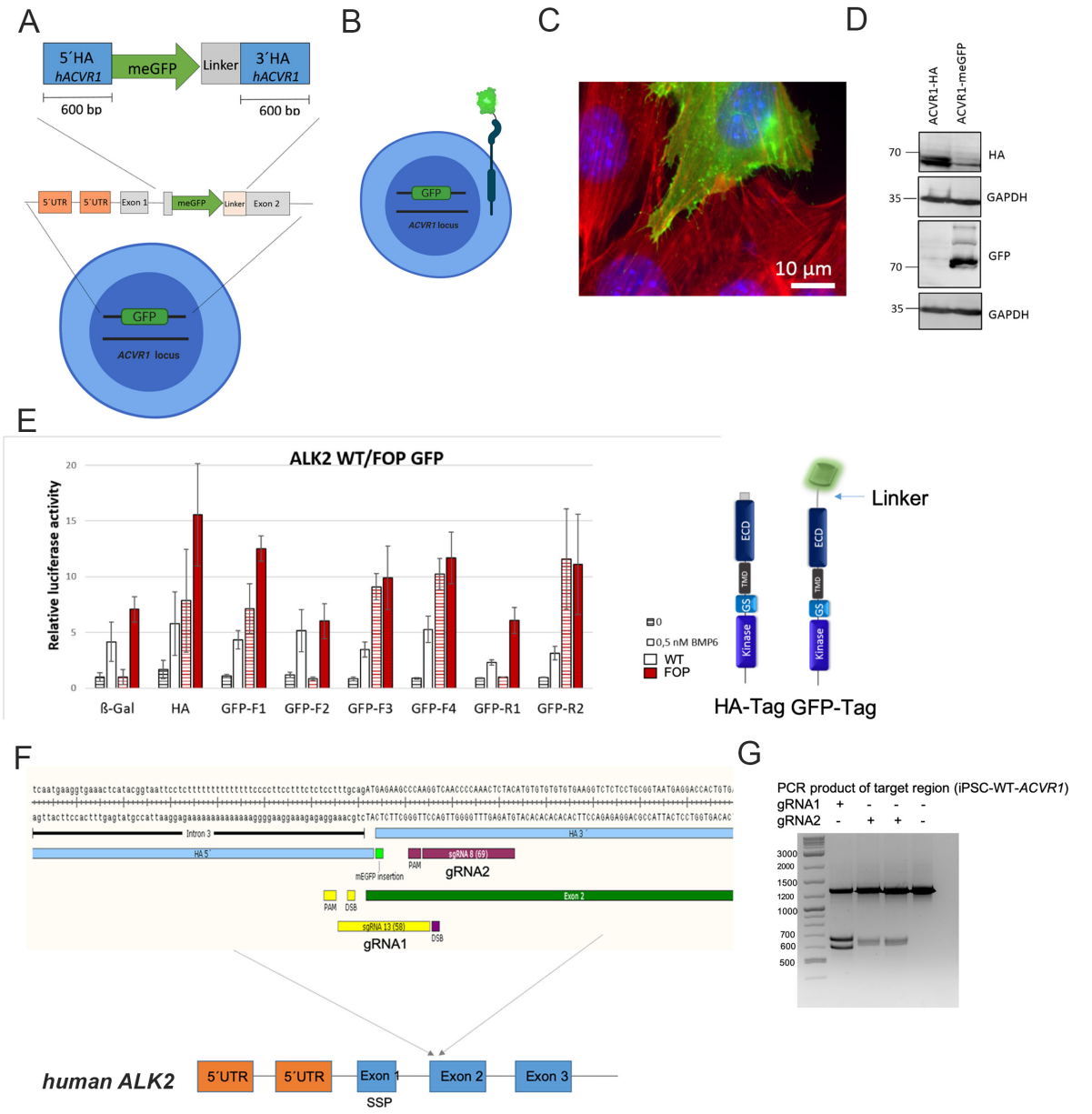

Figure 5.1 CRISPR/Cas9 strategy to generate an ALK2-meGFP iPSC line. (A) Scheme of the GFP knock-in strategy targeting the human *ALK2* (*ACVR1*) locus, showing the repair construct design with meGFP and a flexible linker sequence, framed with 600 bp homology arms (HA) on both sides with the insertion site at exon 2. (B) Schematic illustration of the N-terminal meGFP tagged ALK2 transmembrane protein. (C) Membrane localization for ALK2-F1-mEGFP was confirmed by fluorescence microscopy in C2C12 cells (D) and the expected protein size was shown in Western Blot analysis. (E) Functionality testing of WT/R206H ALK2-meGFP fusion protein comparing different linker sequences F (flexible linker); R (rigid linker)) in overexpression for signaling functionality using BMP Responsive Element (BRE) reporter gene assay in comparison to HA-tagged ALK2 in C2C12 cells. (F) Scheme depicting the mechanism of CRISPR-Cas9-induced DNA double strand breaks and cloning of the necessary components gRNA, Cas9 in an overexpression plasmid including a GFP gene (pEF1a-Cas9-GFP-gRNA1, pEF1a-Cas9-GFP-gRNA2) and the respective GFP repair templates for homology-directed repair (G) CRISPR/Cas9 targeting strategy approach, showing two different gRNAs targeting exon 2 of the ALK2 gene after exon 1 coding for the signal peptide (SSP) (H) Validation of gRNA activity for efficient DNA cleavage using *in vitro* cleavage of target DNA with ribonucleoprotein (RNP) complex. Target sequence (1250 bp) was amplified by PCR from genomic iPSC DNA using specific primers, which was incubated with the Cas9 RNP complex (Cas9, gRNA, tacrRNA). Product was separated on an agarose gel and shows the noncleaved product (1250 bp) and the cleavage products of gRNA1 (659 bp, 588 bp) and gRNA2 (641 bp, 606 bp).

5.1.2 Establishment of delivery and screening method for CRISPR/Cas9 in iPSCs

In order to deliver the CRISPR reagents (gRNA, GFP repair template, Cas9) into iPSCs, two different electroporation-based transfection methods were established (Figure 5.2A). 1. Cas9 ribonucleoprotein (RNP) complex, containing the gRNA (sequence specific CRISPR (cr) RNA and transactivating (tracr) RNA), recombinant Cas9 and the GFP repair plasmid (GFP coding sequence framed by 600 bp homologues target sequence). 2. Cas9 overexpression plasmid containing Cas9 gene and the gRNA and the repair plasmid (GFP coding sequence framed by 600 bp homologues target sequence) (Figure 5.2A). Transfection efficiency was quantified by Flourescence Activated Cell Sorting (FACS). To evaluate the transfection efficiency of the Cas9 ribonucleoprotein complex a fluorescently labeled tracrRNA was used. Upon transfection of the Cas9 ribonucleoprotein complex, including the labeled tracrRNA by electroporation the cells were thoroughly washed and analyzed by FACS. Delivery of CRISPR reagents using ribonucleoprotein complex by electroporation achieved transfection efficiencies up to 99% of the fluorescent labeled tracrRNA (Figure 5.2B), which indicates that the CRISPR reagents can be successfully delivered in iPSCs by electroporation. Delivery of labeled tracrRNA was also confirmed by fluorescence microscopy (Figure 5.2D). However, screening for GFP positive iPSC clones 2-4 days after transfection with Fluorescence High Content Screener (HCS) (Opera Phenix HCS) did not detect GFP positive iPSC colonies.

Additionally, a genotyping PCR with specific primer pairs was established to detect the insertion of the meGFP fragment in cells (positive clones) within a cell population (Figure 5.2C). Genotyping PCR using the primer pairs 1,2 and 3,4, which detect meGFP insertion in Exon 2 of the ALK2 locus only showed a PCR product in the transfection condition containing the meGFP repair vector (Figure 5.2C). This indicates the generation of ALK2-meGFP positive clones within the cell population by CRISPR Cas9. As a negative control, to exclude false positive clone detection, a genotyping PCR was also performed using only the repair plasmid as PCR templates. Unspecific bands were detected, however at different size as for the conditions using the CRISPR Cas9 reagents (Figure 5.2C). Primer pair 1,4 would also detect a complete GFP insertion as the product size would increase by the size of inserted GFP (714 bp) (Figure 5.2C).

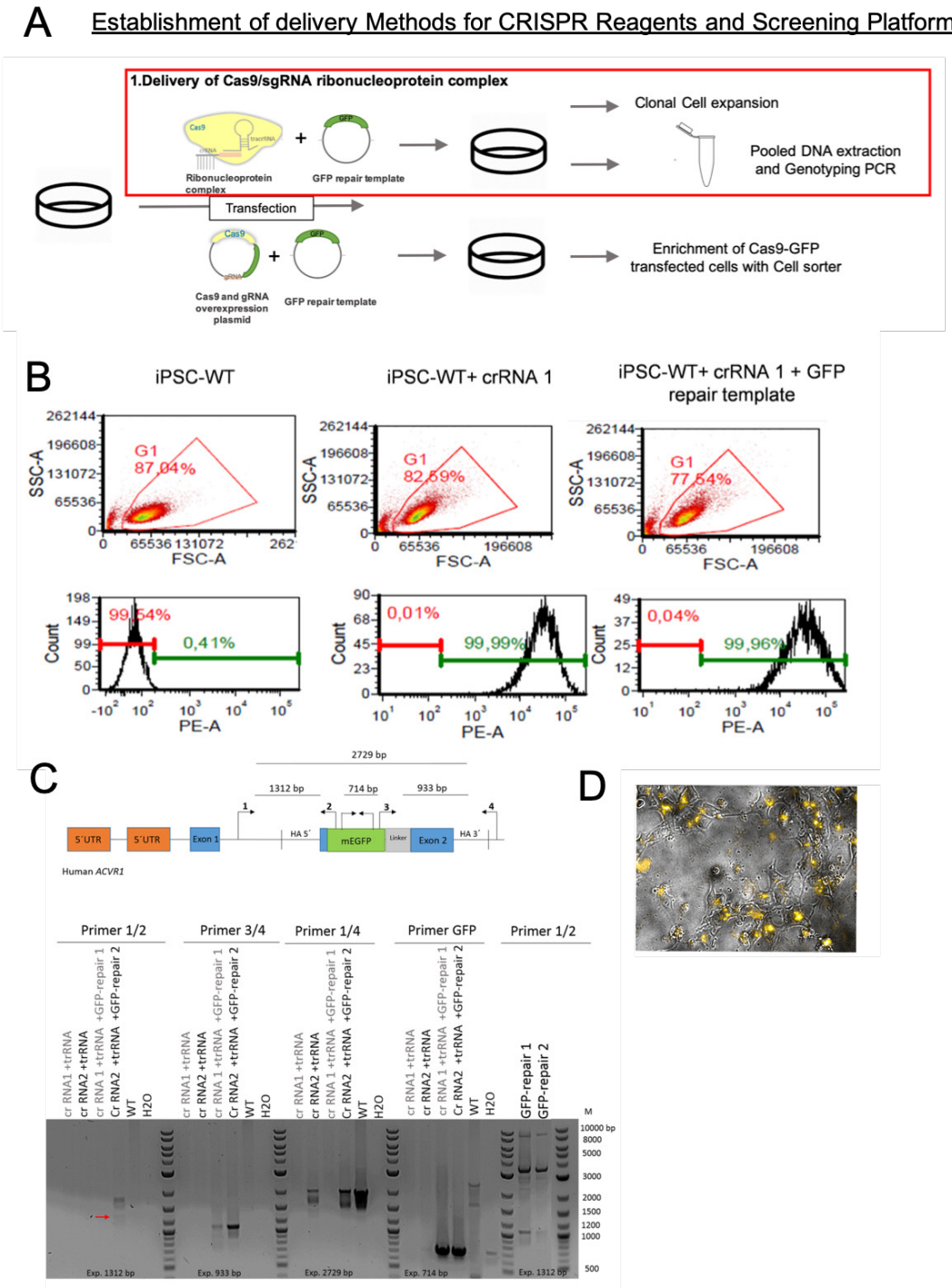

Figure 5.2 Establishment of delivery and screening methods for CRISPR/Cas9 in iPSC using the Ribonucleoprotein complex. (**A**) Working scheme to deliver CRSPR reagents and to screen for CRISPR events in iPSC. CRISPR/Cas9 reagents (gRNA (sequence specific CRISPR RNA) and trans-activating tracrRNA), Cas9 nuclease and GFP repair plasmid) were transfected in iPSC using electroporation by two different delivery methods. Following data is based on the 1. Delivery method using the ribonucleoprotein complex (framed with a red square). (**B**) Transfection of Ribonucleoprotein complex in iPSCs. Transfection efficiency was analyzed by FACS using a fluorescently labeled tracrRNA. (**D**) Analysis of positive clones by genotyping PCR. Four specific primers were designed to detect the insertion of the GFP fragment (positive clones) in a cell population. Genomic DNA was isolated of iPSCs 48 hours after transfection of the ribonucleoprotein complex containing gRNA1 or gRNA2 with and without the GFP repair plasmid (see labeling). Primer 1 and 4 were designed outside of the homology region contained in the repair plasmid. As an additional control genotyping PCR using exemplarily primer 1 and 2 was performed only on the repair plasmids as a template. (**D**) Representative image of immunofluorescence microscopy showing iPSC transfected with labeled tracrRNA (Alt-R CRISPR-Cas9 tracrRNA-ATTO550). Kristin Fischer and Valeria Fernandez Vallone contributed to these experiments.

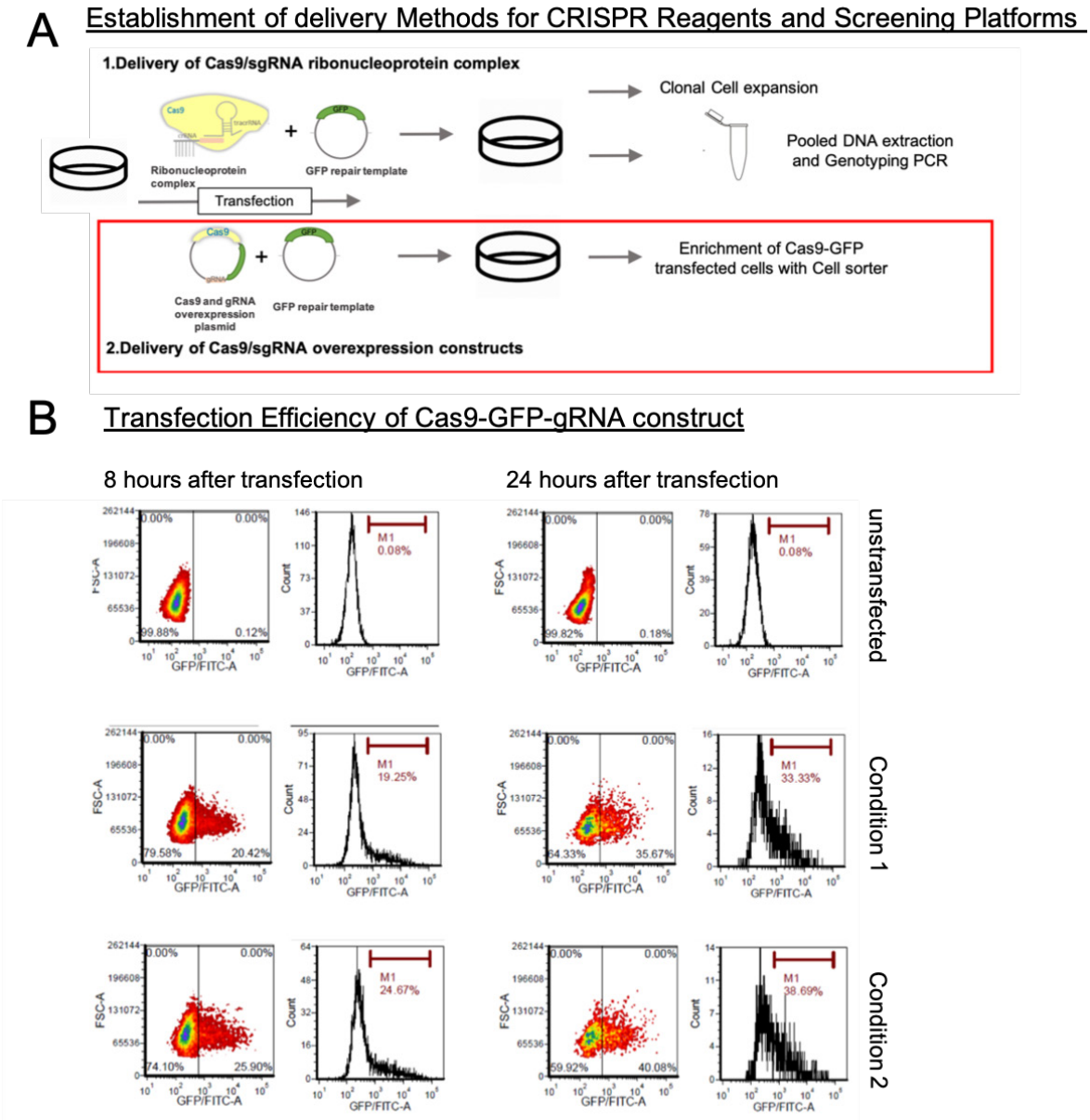

Figure 5.3 Establishment of delivery and screening method for CRISPR/Cas9 in iPSC using Cas9-GFP overexpression constructs. (**A**) Working scheme to deliver CRSPR reagents and to screen for CRISPR events in iPSC. CRISPR/Cas9 reagents were transfected in iPSC using electroporation by two different delivery methods. Following data is based on the 2. Delivery method using Cas9/gRNA overexpression constructs (framed with a red square). (**B**) Transfection of overexpression constructs (pEF1a-Cas9-GFP-gRNA, GFP repair plasmid; condition 1: 8 µg; condition2: 10µg) in iPSCs. Transfection efficiency was analyzed by FACS of iPSCs transfected with the Cas9-GFP-gRNA construct and the respective GFP repair template using different total plasmid DNA amounts. Kristin Fischer and Valeria Fernandez Vallone contributed to these experiments.

In this condition, the size of the product did not increase in the cell population containing the ribonucleoprotein complex and the GFP repair plasmid compared to WT cells (Figure 5.2C). This is not surprising, as product detection by electrophoresis on an agarose gel is not sensitive enough to detect individual positive clones in a cell population and indicating at the same time a very low Knock In efficiency.

In parallel an alternative delivery method 2. was established using transient overexpression of plasmids including a GFP reporter to enrich Cas9 transfected cells

(Figure 5.3A). iPSCs were transfected with two different plasmid DNA concentrations (pEF1a-cas9-GFP-gRNA, GFP-Repair Template) in 1:1 ratio by electroporation (AMAXA Nucleofector, Roche). Transfection efficiency was assessed by measuring GFP positive cells using FACS, which reached up to 39% (Figure 5.3B). Thus, about 40% of transfected iPSCs successfully overexpressed Cas9 and respective gRNA. Based on the robust GFP expression, iPSCs overexpressing Cas9 were enriched by GFP using a cell sorter 24 hours after transfection. GFP expression in the positive iPSC fraction was confirmed by FACS analysis and the positive cell fraction was replated in a well of a 12-well plate (Figure 5.4A). Four days after the sort single iPSC were vital and have formed characteristic cell colonies. Automated Fluorescence High Content Screener (HCS) was used for detection of GFP positive colonies but except single unspecific signals of none iPSC structures, no GFP positive iPSC colonies were detected (Figure 5.5C).

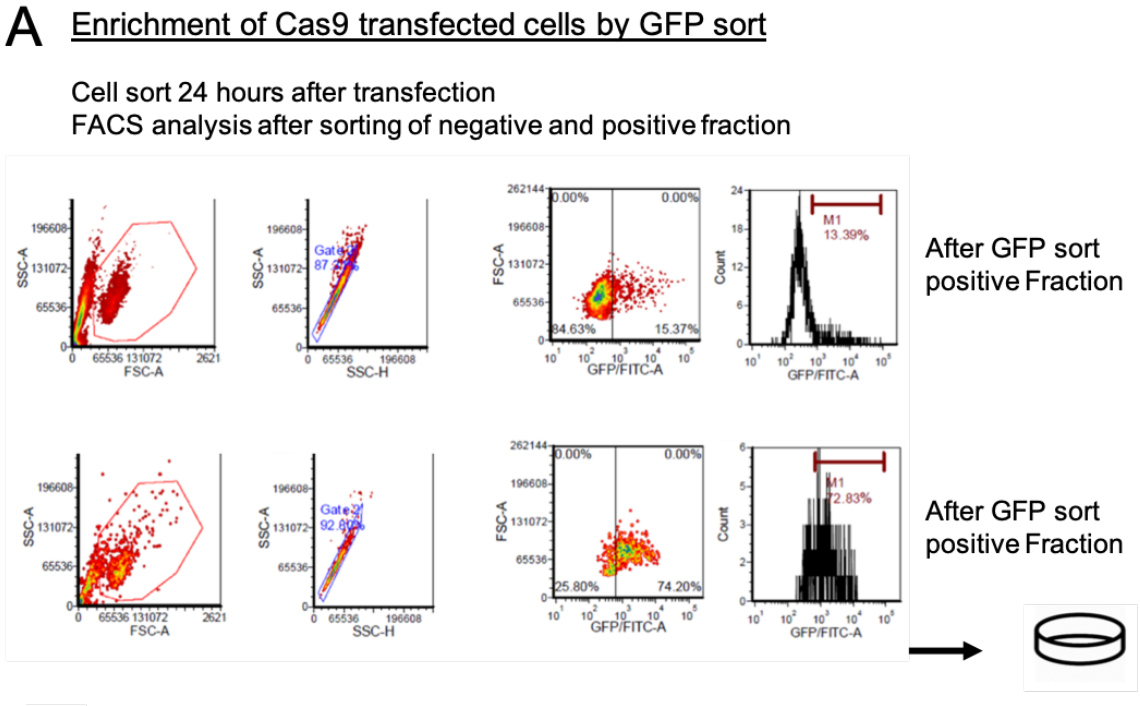

Figure 5.4 Enrichment of Cas9 transfected cells by GFP sort. (**A**) Transfected cells with Cas9-GFP-gRNA1 construct were enriched using a cell sorter (MACSQuant Tyto). Sorted cells were analyzed by FACS and replated into wells of a 12-well plate. Kristin Fischer and Valeria Fernandez Vallone contributed to these experiments.

In addition, 24 hours after transfection GFP sorted iPSCs were stained with a labeled (AlexaFluor647) GFP antibody to increase the GFP signal of possible positive clones. About 1.5 million stained with the anti-GFP were analyzed by FACS but no positive signal was detected (Figure 5.5A). To confirm the functionality of the anti-GFP antibody, an iPSC-GFP reporter line was stained as a positive control. Here, iPSC-GFP reporter cells were successfully stained with the GFP antibody using the same dilution (Figure 5.5B). Thus, enrichment of Cas9 transfected cells via cell sorting did not enhance the Knock In efficiency as no ALK2-GFP positive iPSC colonies could be detected. One possible reason for that could be that the gRNAs do not cut the genomic target DNA at the *ALK2* gene locus in iPSCs as efficiently as in a cell free environment as shown before (Figure 5.1G). Consequently, the gRNA cutting efficiency was analyzed in cellular context using a restriction digest screening. Therefore, CRISPR reagents were transfected as described above and 24 hours later genomic DNA was isolated, the target sequence was amplified by PCR and subjected to specific restriction enzymes, which recognize the uncut targeting site of gRNA1 and gRNA2 (Figure 5.6). WT controls (untransfected) show the expected band pattern of StyI digest. For HincII an additional band was observed above 1200bp, which may represent remaining uncut PCR product (1291 bp) (Figure 5.6). The restriction digest of cells transfected with CRISPR reagent did not show any different band pattern compared to WT controls (Figure 5.6). This indicates, that the of CRISPR/Cas9 mediated cutting efficiency on genomic DNA in iPSCs of gRNA1 and 2 is either too low and requires a more sensitive method for detection or does not happen at all. Based on the validated functionality of gRNA1 and 2 in a cell free context *in vitro*, it is suggested that the *ALK2* DNA locus in the cellular environment may not be accessible. In fact, the targeting efficiency of gRNAs varies widely between target loci based on the chromatin structure, which is independent of the targeting sequence (Lee et al., 2016).

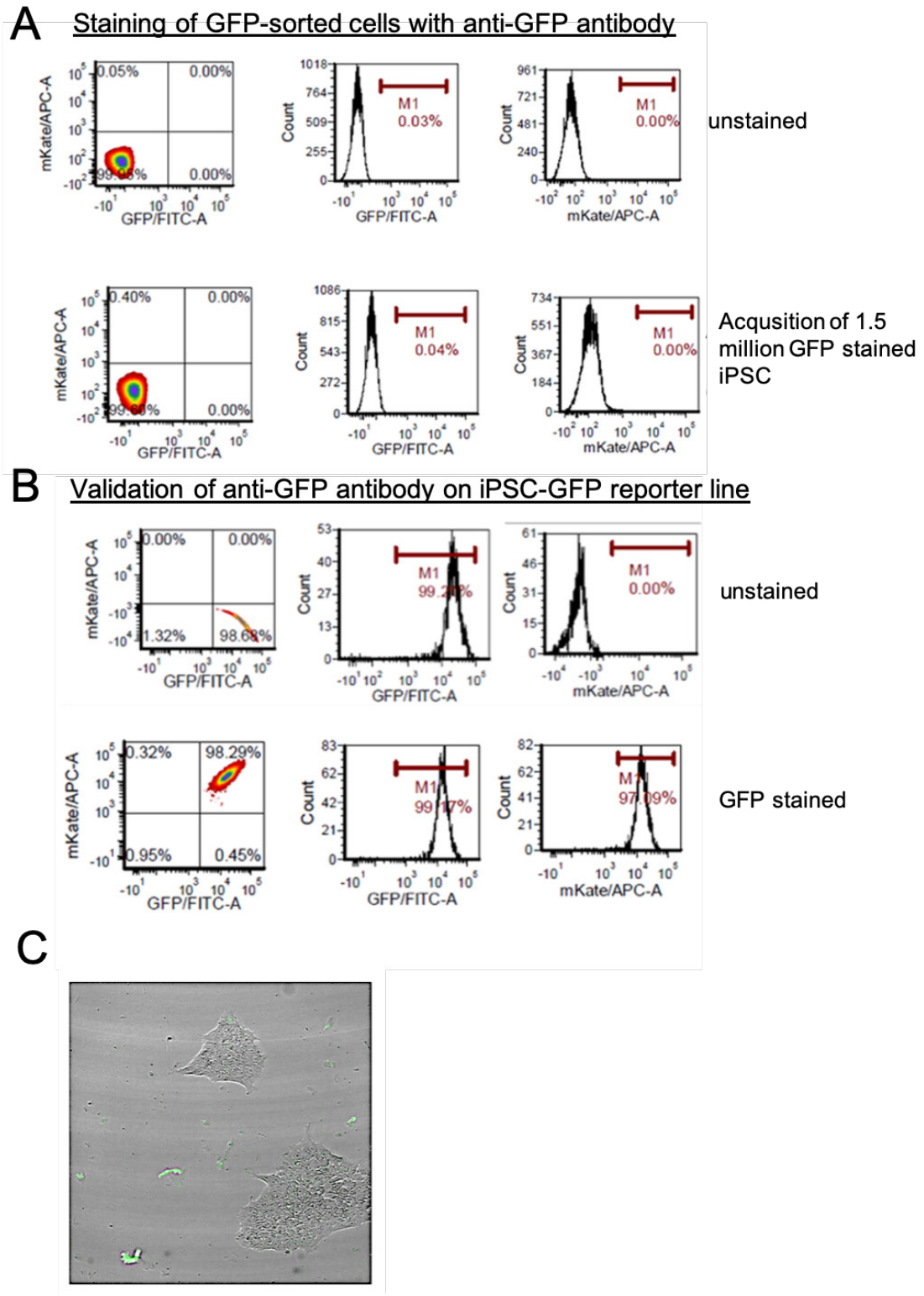

Figure 5.5 Anti-GFP staining after delivery of CRSPR reagents (**A**) Staining of GFP sorted iPSCs with an Alexa Fluor 647 (APC) labelled anti GFP antibody (1:1000) and subsequent FACS analysis in the APC channel. (**B**) Validation of Alexa Fluor 647 (APC) labelled anti GFP antibody (1:1000) on a GFP iPSC reporter line by FACS analysis. (**C**) Representative Image of automated screening for GFP positive iPSC clones 4 days after sorting with Fluorescence High Content Screener (HCS) (Opera Phenix HCS). Kristin Fischer and Valeria Fernandez Vallone contributed to these experiments.

Collectively, two independent delivery method of the CRISPR/Cas9 reagents and a screening platform were successfully established in iPSCs. The targeting activity of two distinct guide RNAs was validated in a cell-free environment. However, the targeting activity could not be confirmed in the cellular context using plasmid overexpression. For future experiments the following aspects should be considered. First, analysis of gRNA cutting efficiency upon using restriction digest screening should be also performed on RNP transfected iPSCs. In general, analysis of single clones early after transfection may increase the sensitivity to detect positive clones (with DSB or GFP insertion). The design of alternative gRNAs is limited in the N-terminal GFP tagging approach as the targeting frame is small due to proximity of the insertion to the splice site of exon 2 and the signal peptide. A C-terminal tagging may be an additional option and would also allow the insertion of a floxed selection cassette. However, N-terminal tagging is preferred for most imaging methods. If successful CRISPR/Cas9 mediated DSB could be detected at the ALK2 locus targeted by gRNA1 and gRNA2 additional experiments should be performed to increase the likelihood of Knock In events. Knock In efficiencies can be below 1% based on the preferred non-homologous end joining (NHEJ) DNA repair mechanism after a DSB over homology-directed repair (HDR) (Song et al., 2016). Small molecules inhibiting NHEJ and upscaling of the experiments can be used to increase Knock In efficiencies. Moreover, it should be considered that epigenetic modifications such as DNA methylation may cause silencing of transgenes as GFP (Krishnan et al., 2006).

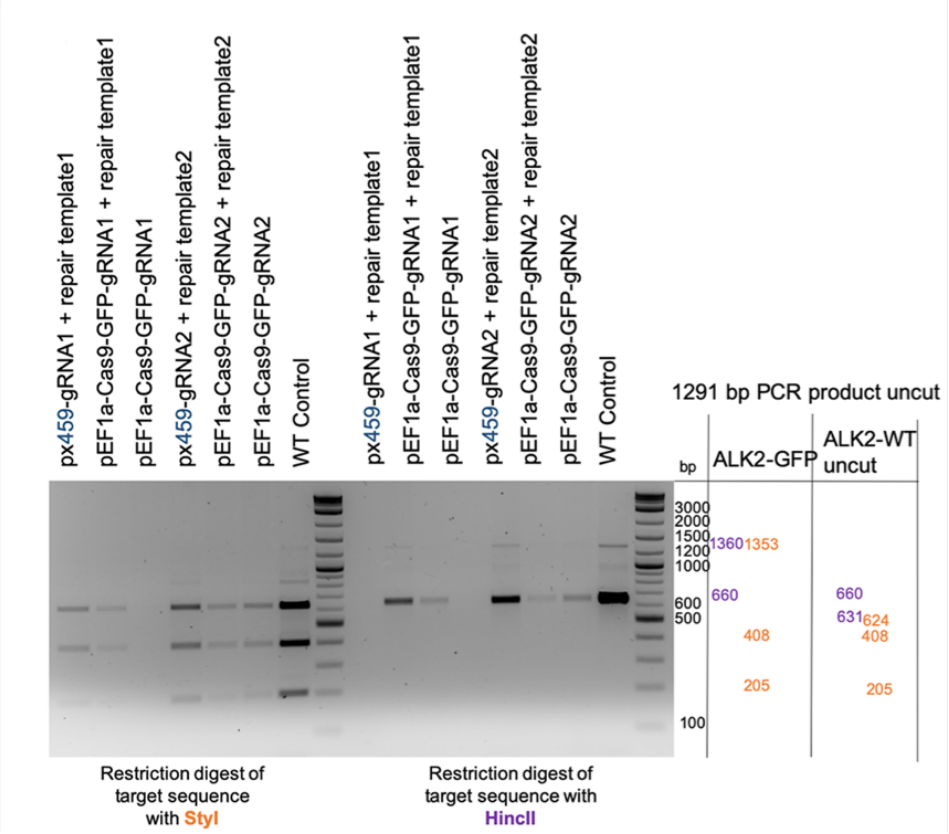

Figure 5.6 Analysis of gRNA cutting efficiency in iPSCs. Analysis of gRNA cutting efficiency upon transfection of CRISPR reagents into iPSCs using restriction digest screening. Genomic DNA of iPSCs was isolated and incubated with specific restriction enzymes recognizing the uncut targeting site of gRNA1 and gRNA2. Digested DNA was separated on an agarose gel and expected band pattern of ALK2-WT (uncut) and ALK2-GFP upon digest with StyI (orange) or HincII (purple) are indicated on the right. Kristin Fischer and Valeria Fernandez Vallone contributed to these experiments.

5.2 ActivinA upregulates the novel BMP target gene *TCIM* in FOP iECs

TCIM (Transcriptional and immune response regulator) was identified as one of the most upregulated genes upon ActivinA treatment in FOP iECs only. In FOP-1 iECs *TCIM* represented the gene with the highest fold change induction (see chapter 3.6 Figure 3.31A,B). The other four most deregulated genes consisted of classical BMP target genes (*ID1, SMAD6, SMAD7, NOG)* ($p<0.05$, FC of ≥ 2.8). However, a search in a Chromatin Immunoprecipitation DNA-Sequencing (ChiPSeq) data list from HUVECs revealed *TCIM* as a direct SMAD1/5 target gene. The loci of *TCIM,* also named as *C8orf4,* was bound by SMAD1/5 after 2 hour of BMP9 stimulation (Morikawa et al., 2011). This binding was HUVEC specific as *TCIM* was not regulated in PASMCs (arterial smooth muscle cells) with the same experimental conditions (Morikawa et al., 2011). The authors did not comment on TCIM or validated the BMP induced *TCIM* expression in HUVECs further.

In general, further investigations of *TCIM* as an endothelial specific BMP target gene are lacking. Originally, TCIM 1, also named (TC-1: Thyroid Cancer 1), was discovered as an highly upregulated gene in thyroid cancer (Chua et al., 2000; Sunde et al., 2004) and shown to induce the expression of downstream genes in cancer cells, involved in proliferation and invasiveness (Jung et al., 2006; Kim et al., 2006). However, besides its discovery in cancer the knowledge about TCIM and its physiological role is limited. It was reported that TCIM is a small monomeric protein with a putative nuclear localization signal, which positively regulates Wnt signaling by interacting with the transcriptional Wnt antagonist Chibby (Jung et al., 2006). TCIM is conserved among vertebrates. Zebrafish has two *Tcim* homologous, where one was predominantly expressed in the developing blood vessels and the other in hematopoietic precursor cells (Kim et al., 2009). This study investigated TCIM further in context of the human endothelium and showed that basal *TCIM* expression levels were low and became upregulated by inflammatory cytokines such as TNFα and IL-1β using HAECs (Human Aortic Endothelial Cells), which was NF-κB-dependent (Kim et al., 2009). Moreover, TCIM itself modified NF-κB signaling by enhancing DNA binding activity and nuclear translocation of NF-κB in human umbilical vein endothelial cells (HUVECs) and HAECs and induced inflammatory cytokine expression when overexpressed. In line with this, resulted a knockdown of *TCIM* in reduced inflammatory cytokine expression levels

(Kim et al., 2009). As a functional consequence monocyte adhesion and endothelial permeability was shown to be increased, which was mediated by increased *ICAM1* expression when TCIM was overexpressed. Moreover, *TCIM* RNA injection in zebrafish caused edema formation. Thus, the authors suggested TCIM as a novel endothelial inflammatory regulator and a potential therapeutic target for vascular inflammatory diseases (Kim et al., 2009).

Based on the identification of TCIM as a FOP specific target gene in ActivinA treated FOP iECs, regulation of *TCIM* gene expression was analyzed further.

First, *TCIM* induced expression by ActivinA in FOP iECs was confirmed by RT-PCR (Figure 5.7A). As a positive control TNFα was used. Whereas ActivinA increased *TCIM* already by 4-fold, showed TNFα an induction up to 20-fold (Figure 5.7I), which confirmed previous reported upregulation of TCIM by TNFα in ECs (Kim et al., 2009). Moreover, *TCIM* is also upregulated by BMP6 treatment in both WT iECs and FOP iECs (Figure 5.7A). This supports the ChiPSeq data by Morikawa *et al*. and confirms *TCIM* as a SMAD1/5 target gene, which is aberrantly induced by ActivinA/SMAD1/5 signaling in FOP iECs. Moreover, ActivinA induced *TCIM* transcription is ALK2 dependent as shown by a pretreatment with Saracatinib (Figure 5.7A).

Based on previous evidence that *TCIM* transcription is dependent on NF-κB signaling WT and FOP iECs were pretreated with a NF-κB signaling inhibitor (BMS-345541) before ligand stimulation. Indeed, ligand (ActivinA, BMP6, TNFα) induced *TCIM* induction in WT and FOP iECs could be completely blocked by a pretreatment with BMS-345541 (Figure 5.7A,I). BMS-345541 targets the inhibitory-κB-kinase complex (IKK), which is required for NF-κB activation (Israël, 2010). A titration experiment with different concentrations of BMS-345541 showed that 5 µM is sufficient to inhibit *TCIM* expression by ActivinA in FOP iECs whereas ActivinA induced *ID1* expression levels remained unaffected (Figure 5.7D,F). This was confirmed on pSMAD1/5 protein levels, which were not impaired even when concentrations up to 10 µM BMS-345541 were used (Figure 5.7B). For WT iECs the results indicated that 2.5 µM are proffered to block BMP6 induced *TCIM* expression without impairment of *ID1* expression (Figure **5.7**E,G).

This suggests, that transcriptional regulation of *TCIM* by BMP6 and ActivinA in iECs is not only dependent on ALK2 signaling but also NF-κB dependent, which is in line with NF-κB dependent *TCIM* induction by TNFα and IL-1β in HAECs (Kim et al., 2009) as

also confirmed here for TNFα in iECs (Figure 5.7I). This suggests a crosstalk of ALK2 and NF-κB-signaling. Interestingly, ActivinA also upregulated the inhibitor of kappa B-like protein *(NFKBI),* which was also observed upon BMP6 treatment in WT and FOP iECs (Figure 5.7C).

Remarkably, analysis of RNASeq Data of HUVECs under FSS revealed that *TCIM* is induced after 24 hours of low and high FSS (Figure 5.7J), which indicates a mechanosensitive transcriptional regulation of *TCIM*.

In sum, *TCIM* represents an interesting endothelial specific BMP target gene, which is aberrantly regulated in the FOP endothelium by ActivinA. Especially the role of TCIM in context of endothelial inflammation should be analyzed further in context of FOP. Even though initial experiments did not show an upregulation of the potential TCIM downstream target *ICAM1* after long term ActivinA stimulation (Figure 5.7H). *TCIM* knockdown approaches and co-treatment with inflammatory triggers may shed light on the role of TCIM in FOP endothelium. Moreover, future investigations should also focus on the role of *TCIM* as a general endothelial specific BMP target gene with a putative role in mechanotransduction.

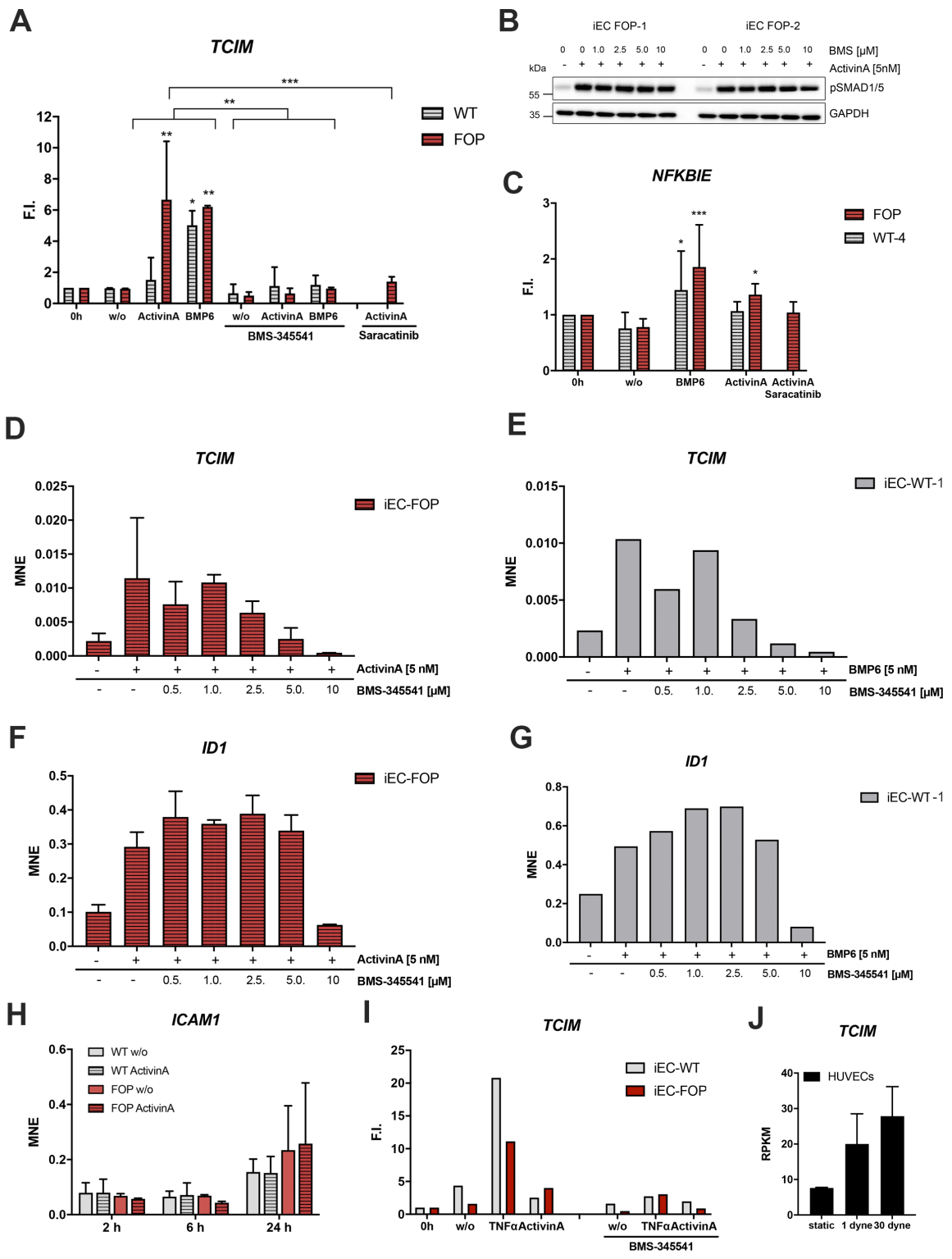

Figure 5.7 ActivinA upregulates the novel endothelial BMP target gene *TCIM* in FOP iECs. (**A**) RT-PCR validation of RNASeq target upon 1 hour pretreatment with Saracatinib (0.2 μM) or BMS-345541 (10 μM) and 2 hour ActivinA (5 nM), BMP6 (5 nM) treatment in iECs. (**B**) Western Blot of protein lysates of FOP iECs pretreated with different doses of BMS-345541 for one hour and subsequent stimulation with ActivinA (5 nM) for 30 min. (**C**) RT-PCR of RNA from 1 hour pretreatment with Saracatinib and 2 hours ActivinA in iECs. **(D-G)** RT-PCR of RNA from iECs pretreated with different doses of BMS-345541 for one hour and subsequent stimulation with ActivinA (5 nM) for 2 hours. (**H**) RT-PCR of ActivinA treated WT and FOP iECs. (**I**) RT-PCR of RNA from 1 hour pretreatment with BMS-345541 (10 μM) and 2 hour ActivinA (5 nM) or TNFα (0.6 nM) treatment in iECs. (**J**) RPKM (Reads Per Kilobase of transcript per Million reads mapped) values were retrieved from RNASeq experiment of Mendez *et al.,* unpublished. In brief. HUVECs were seeded on μ-slides 48 hours before application of FSS for 24 hours after a 5 hours ramp phase to reach step-wise 1.0 or 30 dyne/cm^2 in full medium.

6. List of Abbreviations

ABL kinase	Abelson murine leukemia viral oncogene homolog 1
ACVR2A/B	Activin receptor type 2A/B
ADM	Adrenomedullin
AKT	Protein kinase B
ALK1-7	Activin Receptor-Like Kinase
AMH	Anti-Mullerian hormone
AMHR2	Anti-Mullerian hormone receptor type 2
BAECs	Bovine Aortic Endothelial Cells
BAMBI	BMP and activin membrane-bound inhibitor
BISC	BMP-induced signaling complex
BMP	bone morphogenetic protein
BMPR2	BMP receptor type 2
BMPRs	BMP receptors
bp	base pairs
BRA	Brachyury
BRE-Luc	BMP responsive element luciferase reporter
BSA	bovine serum albumin
cAMP	cyclic adenosine monophosphate
C-terminus	carboxy-terminus
CDH2	N-Cadherin
CDH5	VE-Cadherin
cDNA	complementary deoxyribonucleic acid
ChIP-Seq	sequencing of immunoprecipitated chromatin
cm²	cubic centimeter
Coup-TFII	Chicken ovalbumin upstream promoter-transcription factor II
CRISPR	Clustered Regularly Interspaced Short Palindromic Repeats
Ct	threshold cycle
DAPI	4′,6-Diamidino-2-phenylindole dihydrochloride
dH2O	double distilled water
DIPG	Diffuse intrinsic pontine glioma
DLL1-4	Delta-like1-4
DMEM	Dulbecco's modified Eagle's medium
DMSO	dimethyl sulfoxide
DNA	deoxyribonucleic acid
dNTP	deoxyribonucleotide triphosphate
EC	endothelial cells
ECD	extracellular domain
ECFCs	endothelial colony forming cells

ECIS	Electric Cell-Substrate Impedance Sensing
ECM	extracellular matrix
EDTA	ethylenediaminetetraacetic acid
EGFL7	epidermal growth factor-like domain 7
EGR1	Early growth response protein 1
EndMT	Endothelial to mesenchymal transition
ENG	Endoglin
EPC	Endothelial Progenitor Cells
EPC	Endothelial progenitor Cells
Ephb4	Ephrin type-B receptor 4
ERK	extracellular signal-regulated kinases
ESC	Embryonic stem cell
et al. (lat.)	et altera; and others
FBS	fetal bovine serum
FGF	Fibroblast growth factor
FI	Fold induction
FKBP12	FK506 binding protein
FOP	Fibrodysplasia ossificans progressive
FOXC2	Forkhead Box C2
FRAP	Fluorescence recovery after photobleaching
FSS	fluid shear stress
g	gram / gravity
GDFs	Growth and Differentiation Factors
GSK3-β	Glycogen Synthase Kinase 3- β
gRNA	guide RNA
GS-Box/Domain	glycine serine-rich domain
h	hour
HAEC	Human Aortic Endothelial Cells
HDAC	histone deacetylases
HDMEC	Human Dermal Microvascular Endothelial Cells
HES1	hairy and enhancer of split-1
hESC-ECs	Human Embryonic-Stem-cell-derived Endothelial Cells
HEY1/2	Hairy/enhancer-of-split related with YRPW motif protein 1/2
HEYL	Hairy/enhancer-of-split related with YRPW motif like
HHT	Hereditary hemorrhagic telangiectasia
HHT	hereditary haemorrhagic telangiectasia
HIF1	Hypoxia-inducible factor 1
HJV	Hemojuvelin
HLX	H2.0-like homeo box transcription factor
HMEC	human microvascular endothelial cells
HO	Heterotopic Ossification
hpf	hours post fertilization
HSP27	heat shock protein 27

HUAEC	Human Umbilical Arterial Endothelial Cells
HUVEC	Human Umbilical Vein Endothelial Cells
ID1-4	Inhibitor of Differentiation 1-4
IDR	interdigital region
iEC	induced pluripotent stem cell derived endothelial cell
Ig	immunoglobulin
iMEF	immortalized mouse embryonic fibroblasts
iMSC	induced mesenchymal stem cell
iPSC	induced pluripotent stem cell
JAG1/2	Jagged1/2
JNK	c-Jun N-terminal kinases
KD	kinase domain
KLF	Krüppel-like Factor
L	liter
LAP	Latency Associated Peptide
LATS1	Large tumor suppressor kinase 1
LBD	Ligand binding domain
LSS	laminar shear stress
LTBP	latent TGFβ binding protein
MACS	Magnetic Activated Cell Sorting
MAML	Mastermind-like protein
MAPK	mitogen-activated protein kinase
MCAM	melanoma cell adhesion molecule
MEF2	myocyte enhancer factor-2
MEK5	mitogen-activated protein kinase kinase 5
MMPs	Matrix metalloproteinases
mEpiSCs	mouse epiblast stem cells
Mfsd2a	Major facilitator superfamily domain-containing protein 2
min	minute
ml	milliliter
mm	millimeter
mM	millimolar
MMPs	matrix metalloproteases
mRNA	messenger-RNA
MSCs	mesenchymal stem cells
MSX2	Msh Homeobox 2
MuSK	Muscle-Specific Kinase
MW	molecular weight
MyoX	myosin X
N-terminus	amino-terminus
NECD	NOTCH extracellular domain
NEDD9	Developmentally Down-Regulated 9
NEO	Neogenin

ng	nanogram
NHEJ	Non-homologous end joining
NICD	intracellular domain of NOTCH
NMD	nonsense-mediated decay
NOG	Noggin
NOG	noggin
NRARP	NOTCH Regulated Ankyrin Repeat Protein
NRP1/2	Neuropilin1/2
OCT4	Octamer-binding transcription factor 4
OSR1	odd-skipped related transcription factor 1/2
PAEC	pulmonary arterial endothelial cells
PAH	Pulmonary arterial hypertension
PAH	pulmonary arterial hypertension
PAM	Protospacer adjacent motif
PBS	phosphate buffered saline
PCR	polymerase chain reaction
PECAM1	Platelet endothelial cell adhesion molecule
PFA	paraformaldehyde
PFCs	preformed complexes
pH	potentia Hydrogenii
RHOB	Ras homolog family member B
PI3K	phosphoinositide 3-kinase
PMEPA1	Prostate Transmembrane Protein, Androgen Induced 1
RBPJ	Recombination signal binding protein for immunoglobulin kappa J region
RGMs	repulsive guidance molecules
PTGS2	Prostaglandin-endoperoxide synthase 2
RNA	ribonucleic acid
RNA-Seq	RNA-Sequencing
Robo1-4	Roundabout homolog 1-4
ROCK	Rho-associated protein kinase
rpm	rounds per minute
Rrs	regulatory enhancer regions
RUNX2	Runt-related transcription factor 2
SBE	SMAD binding element
SCF	stem cell factor
scr	scrambled
scRNA-seq	Single-cell RNA sequencing
SD	Standard deviation
SDS	sodium dodecyl sulfate
siRNA	small interfering RNA
SLUG/SNAI2	Zinc finger protein SNAI2
SMAD	Mothers against decapentaplegic homolog
SMAD	Sons of mothers against decapentaplegic

SNAI1	Zinc finger protein SNAI1
SNAI1	Snail
SOX2	sex determining region box 2
SP	signal peptide
SRC	Proto-oncogene tyrosine -protein kinase Src
SSEA4	Anti-stage specific embryonic antigen 4
TCIM	Transcriptional And Immune Response Regulator
TGFβ	Transforming growth factor β
TMD	transmembrane domain
TWIST	Twist-related protein 1
TGFBR2	TGFβ receptor 2
UNC5B	Uncoordinated 5B
VEGF	vascular endothelial growth factor
VEGFR	Vascular endothelial growth facor receptor
WT	Wildtype
µ	micro
µg	microgram
µl	microliter
µm	micrometer
µM	micromole
°C	degree Celsius

7. Bibliography

Adair, T.H., Montani, J.-P., 2010. Overview of Angiogenesis, Angiogenesis. Morgan & Claypool Life Sciences.

Afgan, E., Baker, D., Batut, B., van den Beek, M., Bouvier, D., Čech, M., Chilton, J., Clements, D., Coraor, N., Grüning, B.A., Guerler, A., Hillman-Jackson, J., Hiltemann, S., Jalili, V., Rasche, H., Soranzo, N., Goecks, J., Taylor, J., Nekrutenko, A., Blankenberg, D., 2018. The Galaxy platform for accessible, reproducible and collaborative biomedical analyses: 2018 update. Nucleic Acids Res 46, W537–W544. https://doi.org/10.1093/nar/gky379

Afrakhte, M., Morén, A., Jossan, S., Itoh, S., Sampath, K., Westermark, B., Heldin, C.-H., Heldin, N.-E., ten Dijke, P., 1998. Induction of Inhibitory Smad6 and Smad7 mRNA by TGF-β Family Members. Biochemical and Biophysical Research Communications 249, 505–511. https://doi.org/10.1006/bbrc.1998.9170

Agarwal, S., Loder, S., Cholok, D., Peterson, J., Li, J., Fireman, D., Breuler, C., Hsieh, H.S., Ranganathan, K., Hwang, C., Drake, J., Li, S., Chan, C.K., Longaker, M.T., Levi, B., 2016. Local and Circulating Endothelial Cells Undergo Endothelial to Mesenchymal Transition (EndMT) in Response to Musculoskeletal Injury. Sci Rep 6, 32514. https://doi.org/10.1038/srep32514

Agarwal, S., Loder, S.J., Cholok, D., Peterson, J., Li, J., Breuler, C., Cameron Brownley, R., Hsin Sung, H., Chung, M.T., Kamiya, N., Li, S., Zhao, B., Kaartinen, V., Davis, T.A., Qureshi, A.T., Schipani, E., Mishina, Y., Levi, B., 2017. Scleraxis-Lineage Cells Contribute to Ectopic Bone Formation in Muscle and Tendon. Stem Cells 35, 705–710. https://doi.org/10.1002/stem.2515

Aird, W.C., 2012. Endothelial Cell Heterogeneity. Cold Spring Harb Perspect Med 2. https://doi.org/10.1101/cshperspect.a006429

Akiyama, I., Yoshino, O., Osuga, Y., Shi, J., Harada, M., Koga, K., Hirota, Y., Hirata, T., Fujii, T., Saito, S., Kozuma, S., 2014. Bone Morphogenetic Protein 7 Increased Vascular Endothelial Growth Factor (VEGF)-A Expression in Human Granulosa Cells and VEGF Receptor Expression in Endothelial Cells. Reprod Sci 21, 477–482. https://doi.org/10.1177/1933719113503411

Alarcón, C., Zaromytidou, A.-I., Xi, Q., Gao, S., Yu, J., Fujisawa, S., Barlas, A., Miller, A.N., Manova-Todorova, K., Macias, M.J., Sapkota, G., Pan, D., Massagué, J., 2009. Nuclear CDKs Drive Smad Transcriptional Activation and Turnover in BMP and TGF-β Pathways. Cell 139, 757–769. https://doi.org/10.1016/j.cell.2009.09.035

Al-Bari, A.A., Mamun, A.A., 2020. Current advances in regulation of bone homeostasis. FASEB BioAdvances 2, 668–679. https://doi.org/10.1096/fba.2020-00058

Alessi Wolken, D.M., Idone, V., Hatsell, S.J., Yu, P.B., Economides, A.N., 2018. The obligatory role of Activin A in the formation of heterotopic bone in Fibrodysplasia Ossificans Progressiva. Bone, Heterotopic Ossification 109, 210–217. https://doi.org/10.1016/j.bone.2017.06.011

Alitalo, K., Tammela, T., Petrova, T.V., 2005. Lymphangiogenesis in development and human disease. Nature 438, 946–953. https://doi.org/10.1038/nature04480

Allendorph, G.P., Vale, W.W., Choe, S., 2006. Structure of the ternary signaling complex of a TGF-beta superfamily member. Proc. Natl. Acad. Sci. U.S.A. 103, 7643–7648. https://doi.org/10.1073/pnas.0602558103

Alt, A., Miguel-Romero, L., Donderis, J., Aristorena, M., Blanco, F.J., Round, A., Rubio, V., Bernabeu, C., Marina, A., 2012. Structural and Functional Insights into Endoglin Ligand Recognition and Binding. PLOS ONE 7, e29948. https://doi.org/10.1371/journal.pone.0029948

Anderson, R.H., Francis, K.R., 2018. Modeling rare diseases with induced pluripotent stem cell technology. Mol Cell Probes 40, 52–59. https://doi.org/10.1016/j.mcp.2018.01.001

Andres, A.-C., Djonov, V., 2010. The Mammary Gland Vasculature Revisited. J Mammary Gland Biol Neoplasia 15, 319–328. https://doi.org/10.1007/s10911-010-9186-9

Andriopoulou, P., Navarro, P., Zanetti, A., Lampugnani, M.G., Dejana, E., 1999. Histamine induces tyrosine phosphorylation of endothelial cell-to-cell adherens junctions. Arterioscler. Thromb. Vasc. Biol. 19, 2286–2297. https://doi.org/10.1161/01.atv.19.10.2286

Angelini, D.J., Hyun, S.-W., Grigoryev, D.N., Garg, P., Gong, P., Singh, I.S., Passaniti, A., Hasday, J.D., Goldblum, S.E., 2006. TNF-alpha increases tyrosine phosphorylation of vascular endothelial cadherin and opens the paracellular pathway through fyn activation in human lung endothelia. Am. J. Physiol. Lung Cell Mol. Physiol. 291, L1232-1245. https://doi.org/10.1152/ajplung.00109.2006

Apostolou, E., Stadtfeld, M., 2018. Cellular trajectories and molecular mechanisms of iPSC reprogramming. Current Opinion in Genetics & Development 52, 77–85. https://doi.org/10.1016/j.gde.2018.06.002

Appelt-Menzel, A., Oerter, S., Mathew, S., Haferkamp, U., Hartmann, C., Jung, M., Neuhaus, W., Pless, O., 2020. Human iPSC-Derived Blood-Brain Barrier Models: Valuable Tools for Preclinical Drug Discovery and Development? Curr Protoc Stem Cell Biol 55, e122. https://doi.org/10.1002/cpsc.122

Apte, R.S., Chen, D.S., Ferrara, N., 2019. VEGF in Signaling and Disease: Beyond Discovery and Development. Cell 176, 1248–1264. https://doi.org/10.1016/j.cell.2019.01.021

Aragón, E., Wang, Q., Zou, Y., Morgani, S.M., Ruiz, L., Kaczmarska, Z., Su, J., Torner, C., Tian, L., Hu, J., Shu, W., Agrawal, S., Gomes, T., Márquez, J.A., Hadjantonakis, A.-K., Macias, M.J., Massagué, J., 2019. Structural basis for distinct roles of SMAD2 and SMAD3 in FOXH1 pioneer-directed TGF-β signaling. Genes Dev 33, 1506–1524. https://doi.org/10.1101/gad.330837.119

Asahara, T., Murohara, T., Sullivan, A., Silver, M., van der Zee, R., Li, T., Witzenbichler, B., Schatteman, G., Isner, J.M., 1997. Isolation of putative progenitor endothelial cells for angiogenesis. Science 275, 964–967. https://doi.org/10.1126/science.275.5302.964

Asano, K., Sakata, A., Shibuya, H., Kitagawa, M., Teshima, K., Kato, Y., Sasaki, Y., Kutara, K., Seki, M., Edamura, K., Sato, T., Tanaka, S., 2006. Fibrodysplasia ossificans progressiva-like condition in a cat. J. Vet. Med. Sci. 68, 1003–1006. https://doi.org/10.1292/jvms.68.1003

Aspalter, I.M., Gordon, E., Dubrac, A., Ragab, A., Narloch, J., Vizán, P., Geudens, I., Collins, R.T., Franco, C.A., Abrahams, C.L., Thurston, G., Fruttiger, M.,

Rosewell, I., Eichmann, A., Gerhardt, H., 2015. Alk1 and Alk5 inhibition by Nrp1 controls vascular sprouting downstream of Notch. Nat Commun 6, 7264. https://doi.org/10.1038/ncomms8264

Attisano, L., Cárcamo, J., Ventura, F., Weis, F.M.B., Massagué, J., Wrana, J.L., 1993. Identification of human activin and TGFβ type I receptors that form heteromeric kinase complexes with type II receptors. Cell 75, 671–680. https://doi.org/10.1016/0092-8674(93)90488-C

Attisano, L., Wrana, J.L., Montalvo, E., Massagué, J., 1996. Activation of signalling by the activin receptor complex. Mol. Cell. Biol. 16, 1066–1073. https://doi.org/10.1128/mcb.16.3.1066

Ausprunk, D.H., Folkman, J., 1977. Migration and proliferation of endothelial cells in preformed and newly formed blood vessels during tumor angiogenesis. Microvasc. Res. 14, 53–65. https://doi.org/10.1016/0026-2862(77)90141-8

Aykul, S., Corpina, R.A., Goebel, E.J., Cunanan, C.J., Dimitriou, A., Kim, H., Zhang, Q., Rafique, A., Leidich, R., Wang, X., McClain, J., Jimenez, J., Nannuru, K.C., Rothman, N.J., Lees-Shepard, J.B., Martinez-Hackert, E., Murphy, A.J., Thompson, T.B., Economides, A.N., Idone, V., 2020. Activin A forms a non-signaling complex with ACVR1 and type II Activin/BMP receptors via its finger 2 tip loop [WWW Document]. eLife. https://doi.org/10.7554/eLife.54582

Aykul, S., Martinez-Hackert, E., 2019. High-Throughput, Biosensor-Based Approach to Examine Bone Morphogenetic Protein (BMP)–Receptor Interactions. Methods Mol Biol 1891, 37–49. https://doi.org/10.1007/978-1-4939-8904-1_5

Aykul, S., Martinez-Hackert, E., 2016. Transforming Growth Factor-β Family Ligands Can Function as Antagonists by Competing for Type II Receptor Binding. J. Biol. Chem. 291, 10792–10804. https://doi.org/10.1074/jbc.M115.713487

Aykul, S., Parenti, A., Chu, K.Y., Reske, J., Floer, M., Ralston, A., Martinez-Hackert, E., 2017. Biochemical and Cellular Analysis Reveals Ligand Binding Specificities, a Molecular Basis for Ligand Recognition, and Membrane Association-dependent Activities of Cripto-1 and Cryptic. J. Biol. Chem. 292, 4138–4151. https://doi.org/10.1074/jbc.M116.747501

Baeyens, N., Larrivée, B., Ola, R., Hayward-Piatkowskyi, B., Dubrac, A., Huang, B., Ross, T.D., Coon, B.G., Min, E., Tsarfati, M., Tong, H., Eichmann, A., Schwartz, M.A., 2016. Defective fluid shear stress mechanotransduction mediates hereditary hemorrhagic telangiectasia. J Cell Biol 214, 807–816. https://doi.org/10.1083/jcb.201603106

Bagarova, J., Vonner, A.J., Armstrong, K.A., Börgermann, J., Lai, C.S.C., Deng, D.Y., Beppu, H., Alfano, I., Filippakopoulos, P., Morrell, N.W., Bullock, A.N., Knaus, P., Mishina, Y., Yu, P.B., 2013. Constitutively Active ALK2 Receptor Mutants Require Type II Receptor Cooperation. Mol Cell Biol 33, 2413–2424. https://doi.org/10.1128/MCB.01595-12

Bainbridge, P., 2013. Wound healing and the role of fibroblasts. J Wound Care 22, 407–408, 410–412. https://doi.org/10.12968/jowc.2013.22.8.407

Baird, K., Glod, J., Steinberg, S.M., Reinke, D., Pressey, J.G., Mascarenhas, L., Federman, N., Marina, N., Chawla, S., Lagmay, J.P., Goldberg, J., Milhem, M., Loeb, D.M., Butrynski, J.E., Turpin, B., Staddon, A., Spunt, S.L., Jones, R.L., Rodler, E.T., Schuetze, S.M., Okuno, S.H., Helman, L., 2020. Results of a Randomized, Double-Blinded, Placebo-Controlled, Phase 2.5 Study of Saracatinib (AZD0530), in Patients with Recurrent Osteosarcoma Localized to the Lung. Sarcoma 2020. https://doi.org/10.1155/2020/7935475

Barbara, N.P., Wrana, J.L., Letarte, M., 1999. Endoglin is an accessory protein that interacts with the signaling receptor complex of multiple members of the

transforming growth factor-beta superfamily. J. Biol. Chem. 274, 584–594. https://doi.org/10.1074/jbc.274.2.584

Barruet, E., Hsiao, E.C., 2018. Application of human induced pluripotent stem cells to model fibrodysplasia ossificans progressiva. Bone, Heterotopic Ossification 109, 162–167. https://doi.org/10.1016/j.bone.2017.07.003

Barruet, E., Morales, B.M., Cain, C.J., Ton, A.N., Wentworth, K.L., Chan, T.V., Moody, T.A., Haks, M.C., Ottenhoff, T.H.M., Hellman, J., Nakamura, M.C., Hsiao, E.C., 2018. NF-κB/MAPK activation underlies ACVR1-mediated inflammation in human heterotopic ossification. JCI Insight 3. https://doi.org/10.1172/jci.insight.122958

Barruet, E., Morales, B.M., Lwin, W., White, M.P., Theodoris, C.V., Kim, H., Urrutia, A., Wong, S.A., Srivastava, D., Hsiao, E.C., 2016. The ACVR1 R206H mutation found in fibrodysplasia ossificans progressiva increases human induced pluripotent stem cell-derived endothelial cell formation and collagen production through BMP-mediated SMAD1/5/8 signaling. Stem Cell Res Ther 7, 115. https://doi.org/10.1186/s13287-016-0372-6

Baujat, G., Choquet, R., Bouée, S., Jeanbat, V., Courouve, L., Ruel, A., Michot, C., Le Quan Sang, K.-H., Lapidus, D., Messiaen, C., Landais, P., Cormier-Daire, V., 2017. Prevalence of fibrodysplasia ossificans progressiva (FOP) in France: an estimate based on a record linkage of two national databases. Orphanet Journal of Rare Diseases 12, 123. https://doi.org/10.1186/s13023-017-0674-5

Bautch, V.L., 2019. Bone morphogenetic protein and blood vessels: new insights into endothelial cell junction regulation. Curr Opin Hematol 26, 154–160. https://doi.org/10.1097/MOH.0000000000000492

Beets, K., Huylebroeck, D., Moya, I.M., Umans, L., Zwijsen, A., 2013. Robustness in angiogenesis: notch and BMP shaping waves. Trends Genet. 29, 140–149. https://doi.org/10.1016/j.tig.2012.11.008

Benedito, R., Roca, C., Sörensen, I., Adams, S., Gossler, A., Fruttiger, M., Adams, R.H., 2009. The notch ligands Dll4 and Jagged1 have opposing effects on angiogenesis. Cell 137, 1124–1135. https://doi.org/10.1016/j.cell.2009.03.025

Benn, A., Bredow, C., Casanova, I., Vukičević, S., Knaus, P., 2016. VE-cadherin facilitates BMP-induced endothelial cell permeability and signaling. J. Cell. Sci. 129, 206–218. https://doi.org/10.1242/jcs.179960

Benn, A., Haupt, J., Hildebrandt, S., Kaehler, C., Knaus, P., 2017. Physiological and Pathological Consequences of Vascular BMP Signaling, in: Bone Morphogenetic Proteins: Systems Biology Regulators, Progress in Inflammation Research. Springer, Cham, pp. 367–407. https://doi.org/10.1007/978-3-319-47507-3_17

Benn, A., Hiepen, C., Osterland, M., Schutte, C., Zwijsen, A., Knaus, P., 2017. Role of bone morphogenetic proteins in sprouting angiogenesis: differential BMP receptor-dependent signaling pathways balance stalk vs. tip cell competence. FASEB J 31, 4720–4733. https://doi.org/10.1096/fj.201700193RR

Bernard, D.J., Lee, K.B., Santos, M.M., 2006. Activin B can signal through both ALK4 and ALK7 in gonadotrope cells. Reprod. Biol. Endocrinol. 4, 52. https://doi.org/10.1186/1477-7827-4-52

Bernardo, A.S., Faial, T., Gardner, L., Niakan, K.K., Ortmann, D., Senner, C.E., Callery, E.M., Trotter, M.W., Hemberger, M., Smith, J.C., Bardwell, L., Moffett, A., Pedersen, R.A., 2011. BRACHYURY and CDX2 Mediate BMP-Induced Differentiation of Human and Mouse Pluripotent Stem Cells into Embryonic and Extraembryonic Lineages. Cell Stem Cell 9, 144–155. https://doi.org/10.1016/j.stem.2011.06.015

Besson-Fournier, C., Latour, C., Kautz, L., Bertrand, J., Ganz, T., Roth, M.-P., Coppin, H., 2012. Induction of activin B by inflammatory stimuli up-regulates expression of the iron-regulatory peptide hepcidin through Smad1/5/8 signaling. Blood 120, 431–439. https://doi.org/10.1182/blood-2012-02-411470

Beyer, T.A., Weiss, A., Khomchuk, Y., Huang, K., Ogunjimi, A.A., Varelas, X., Wrana, J.L., 2013. Switch Enhancers Interpret TGF-β and Hippo Signaling to Control Cell Fate in Human Embryonic Stem Cells. Cell Reports 5, 1611–1624. https://doi.org/10.1016/j.celrep.2013.11.021

Bilic, J., Izpisua Belmonte, J.C., 2012. Concise review: Induced pluripotent stem cells versus embryonic stem cells: close enough or yet too far apart? Stem Cells (Dayton, Ohio) 30, 33–41. https://doi.org/10.1002/stem.700

Blanco, R., Gerhardt, H., 2013. VEGF and Notch in Tip and Stalk Cell Selection. Cold Spring Harb Perspect Med 3. https://doi.org/10.1101/cshperspect.a006569

Blount, A.L., Schmidt, K., Justice, N.J., Vale, W.W., Fischer, W.H., Bilezikjian, L.M., 2009. FoxL2 and Smad3 Coordinately Regulate Follistatin Gene Transcription. J Biol Chem 284, 7631–7645. https://doi.org/10.1074/jbc.M806676200

Bocharov, E.V., Korzhnev, D.M., Blommers, M.J.J., Arvinte, T., Orekhov, V.Y., Billeter, M., Arseniev, A.S., 2002. Dynamics-modulated biological activity of transforming growth factor beta3. J. Biol. Chem. 277, 46273–46279. https://doi.org/10.1074/jbc.M206274200

Borggrefe, T., Oswald, F., 2009. The Notch signaling pathway: transcriptional regulation at Notch target genes. Cell. Mol. Life Sci. 66, 1631–1646. https://doi.org/10.1007/s00018-009-8668-7

Botello-Smith, W.M., Alsamarah, A., Chatterjee, P., Xie, C., Lacroix, J.J., Hao, J., Luo, Y., 2017. Polymodal allosteric regulation of Type 1 Serine/Threonine Kinase Receptors via a conserved electrostatic lock. PLOS Computational Biology 13, e1005711. https://doi.org/10.1371/journal.pcbi.1005711

Boyd, N.L., Dhara, S.K., Rekaya, R., Godbey, E.A., Hasneen, K., Rao, R.R., West, F.D., Gerwe, B.A., Stice, S.L., 2007. BMP4 promotes formation of primitive vascular networks in human embryonic stem cell-derived embryoid bodies. Exp. Biol. Med. (Maywood) 232, 833–843.

Breeland, G., Sinkler, M.A., Menezes, R.G., 2020. Embryology, Bone Ossification, in: StatPearls. StatPearls Publishing, Treasure Island (FL).

Breit, S., Ashman, K., Wilting, J., Rössler, J., Hatzi, E., Fotsis, T., Schweigerer, L., 2000. The N-myc Oncogene in Human Neuroblastoma Cells: Down-Regulation of an Angiogenesis Inhibitor Identified as Activin A. Cancer Res 60, 4596–4601.

Brown, M.A., Zhao, Q., Baker, K.A., Naik, C., Chen, C., Pukac, L., Singh, M., Tsareva, T., Parice, Y., Mahoney, A., Roschke, V., Sanyal, I., Choe, S., 2005. Crystal structure of BMP-9 and functional interactions with pro-region and receptors. J. Biol. Chem. 280, 25111–25118. https://doi.org/10.1074/jbc.M503328200

Brown, S., Teo, A., Pauklin, S., Hannan, N., Cho, C.H.-H., Lim, B., Vardy, L., Dunn, N.R., Trotter, M., Pedersen, R., Vallier, L., 2011. Activin/Nodal Signaling Controls Divergent Transcriptional Networks in Human Embryonic Stem Cells and in Endoderm Progenitors. STEM CELLS 29, 1176–1185. https://doi.org/10.1002/stem.666

Brummel, T.J., Twombly, V., Marqués, G., Wrana, J.L., Newfeld, S.J., Attisano, L., Massagué, J., O'Connor, M.B., Gelbart, W.M., 1994. Characterization and relationship of Dpp receptors encoded by the saxophone and thick veins

genes in Drosophila. Cell 78, 251–261. https://doi.org/10.1016/0092-8674(94)90295-x

Byfield, S.D., Roberts, A.B., 2004. Lateral signaling enhances TGF-beta response complexity. Trends Cell Biol. 14, 107–111. https://doi.org/10.1016/j.tcb.2004.01.001

Cai, J., Orlova, V.V., Cai, X., Eekhoff, E.M.W., Zhang, K., Pei, D., Pan, G., Mummery, C.L., ten Dijke, P., 2015. Induced Pluripotent Stem Cells to Model Human Fibrodysplasia Ossificans Progressiva. Stem Cell Reports 5, 963–970. https://doi.org/10.1016/j.stemcr.2015.10.020

Calve, S., Odelberg, S.J., Simon, H.-G., 2010. A transitional extracellular matrix instructs cell behavior during muscle regeneration. Dev Biol 344, 259–271. https://doi.org/10.1016/j.ydbio.2010.05.007

Campinho, P., Vilfan, A., Vermot, J., 2020. Blood Flow Forces in Shaping the Vascular System: A Focus on Endothelial Cell Behavior. Front. Physiol. 11. https://doi.org/10.3389/fphys.2020.00552

Canali, S., Core, A.B., Zumbrennen-Bullough, K.B., Merkulova, M., Wang, C.-Y., Schneyer, A.L., Pietrangelo, A., Babitt, J.L., 2016. Activin B Induces Noncanonical SMAD1/5/8 Signaling via BMP Type I Receptors in Hepatocytes: Evidence for a Role in Hepcidin Induction by Inflammation in Male Mice. Endocrinology 157, 1146–1162. https://doi.org/10.1210/en.2015-1747

Cárcamo, J., Weis, F.M., Ventura, F., Wieser, R., Wrana, J.L., Attisano, L., Massagué, J., 1994. Type I receptors specify growth-inhibitory and transcriptional responses to transforming growth factor beta and activin. Molecular and Cellular Biology 14, 3810–3821. https://doi.org/10.1128/MCB.14.6.3810

Cash, J.N., Rejon, C.A., McPherron, A.C., Bernard, D.J., Thompson, T.B., 2009. The structure of myostatin:follistatin 288: insights into receptor utilization and heparin binding. EMBO J 28, 2662–2676. https://doi.org/10.1038/emboj.2009.205

Castonguay, R., Werner, E.D., Matthews, R.G., Presman, E., Mulivor, A.W., Solban, N., Sako, D., Pearsall, R.S., Underwood, K.W., Seehra, J., Kumar, R., Grinberg, A.V., 2011. Soluble endoglin specifically binds bone morphogenetic proteins 9 and 10 via its orphan domain, inhibits blood vessel formation, and suppresses tumor growth. J. Biol. Chem. 286, 30034–30046. https://doi.org/10.1074/jbc.M111.260133

Cavalloni, G., Peraldo-Neia, C., Sarotto, I., Gammaitoni, L., Migliardi, G., Soster, M., Marchiò, S., Aglietta, M., Leone, F., 2012. Antitumor activity of Src inhibitor saracatinib (AZD-0530) in preclinical models of biliary tract carcinomas. Mol Cancer Ther 11, 1528–1538. https://doi.org/10.1158/1535-7163.MCT-11-1020

Cerdan, C., McIntyre, B.A.S., Mechael, R., Levadoux-Martin, M., Yang, J., Lee, J.B., Bhatia, M., 2012. Activin A Promotes Hematopoietic Fated Mesoderm Development Through Upregulation of Brachyury in Human Embryonic Stem Cells. Stem Cells Dev 21, 2866–2877. https://doi.org/10.1089/scd.2012.0053

Chadwick, K., Wang, L., Li, L., Menendez, P., Murdoch, B., Rouleau, A., Bhatia, M., 2003. Cytokines and BMP-4 promote hematopoietic differentiation of human embryonic stem cells. Blood 102, 906–915. https://doi.org/10.1182/blood-2003-03-0832

Chaikuad, A., Alfano, I., Kerr, G., Sanvitale, C.E., Boergermann, J.H., Triffitt, J.T., Delft, F. von, Knapp, S., Knaus, P., Bullock, A.N., 2012. Structure of the Bone Morphogenetic Protein Receptor ALK2 and Implications for Fibrodysplasia

Ossificans Progressiva. J. Biol. Chem. 287, 36990–36998. https://doi.org/10.1074/jbc.M112.365932
Chaikuad, A., Bullock, A.N., 2016. Structural Basis of Intracellular TGF-β Signaling: Receptors and Smads. Cold Spring Harb Perspect Biol 8, a022111. https://doi.org/10.1101/cshperspect.a022111
Chakkalakal, S.A., Zhang, D., Culbert, A.L., Convente, M.R., Caron, R.J., Wright, A.C., Maidment, A.D.A., Kaplan, F.S., Shore, E.M., 2012. An Acvr1 R206H knock-in mouse has fibrodysplasia ossificans progressiva. J Bone Miner Res 27, 1746–1756. https://doi.org/10.1002/jbmr.1637
Chal, J., Oginuma, M., Al Tanoury, Z., Gobert, B., Sumara, O., Hick, A., Bousson, F., Zidouni, Y., Mursch, C., Moncuquet, P., Tassy, O., Vincent, S., Miyanari, A., Bera, A., Garnier, J.-M., Guevara, G., Hestin, M., Kennedy, L., Hayashi, S., Drayton, B., Cherrier, T., Gayraud-Morel, B., Gussoni, E., Relaix, F., Tajbakhsh, S., Pourquié, O., 2015. Differentiation of pluripotent stem cells to muscle fiber to model Duchenne muscular dystrophy. Nature Biotechnology 33, 962–969. https://doi.org/10.1038/nbt.3297
Chambers, S.M., Qi, Y., Mica, Y., Lee, G., Zhang, X.-J., Niu, L., Bilsland, J., Cao, L., Stevens, E., Whiting, P., Shi, S.-H., Studer, L., 2012. Combined small-molecule inhibition accelerates developmental timing and converts human pluripotent stem cells into nociceptors. Nature Biotechnology 30, 715–720. https://doi.org/10.1038/nbt.2249
Chang, A.C.Y., Fu, Y., Garside, V.C., Niessen, K., Chang, L., Fuller, M., Setiadi, A., Smrz, J., Kyle, A., Minchinton, A., Marra, M., Hoodless, P.A., Karsan, A., 2011. Notch initiates the endothelial-to-mesenchymal transition in the atrioventricular canal through autocrine activation of soluble guanylyl cyclase. Dev. Cell 21, 288–300. https://doi.org/10.1016/j.devcel.2011.06.022
Chappell, J.C., Bautch, V.L., 2010. Vascular development: genetic mechanisms and links to vascular disease. Curr Top Dev Biol 90, 43–72. https://doi.org/10.1016/S0070-2153(10)90002-1
Chavkin, N.W., Hirschi, K.K., 2020. Single Cell Analysis in Vascular Biology. Front. Cardiovasc. Med. 7. https://doi.org/10.3389/fcvm.2020.00042
Cheifetz, S., Like, B., Massagué, J., 1986. Cellular distribution of type I and type II receptors for transforming growth factor-beta. J Biol Chem 261, 9972–9978.
Chen, G., Gulbranson, D.R., Hou, Z., Bolin, J.M., Ruotti, V., Probasco, M.D., Smuga-Otto, K., Howden, S.E., Diol, N.R., Propson, N.E., Wagner, R., Lee, G.O., Antosiewicz-Bourget, J., Teng, J.M.C., Thomson, J.A., 2011. Chemically defined conditions for human iPSC derivation and culture. Nat Methods 8, 424–429. https://doi.org/10.1038/nmeth.1593
Chen, J., Somanath, P.R., Razorenova, O., Chen, W.S., Hay, N., Bornstein, P., Byzova, T.V., 2005. Akt1 regulates pathological angiogenesis, vascular maturation and permeability in vivo. Nat Med 11, 1188–1196. https://doi.org/10.1038/nm1307
Chen, K.G., Mallon, B.S., McKay, R.D.G., Robey, P.G., 2014. Human Pluripotent Stem Cell Culture: Considerations for Maintenance, Expansion, and Therapeutics. Cell Stem Cell 14, 13–26. https://doi.org/10.1016/j.stem.2013.12.005
Chen, W., Xia, P., Wang, H., Tu, J., Liang, X., Zhang, X., Li, L., 2019. The endothelial tip-stalk cell selection and shuffling during angiogenesis. J Cell Commun Signal 13, 291–301. https://doi.org/10.1007/s12079-019-00511-z
Chen, Y.-H., Ishii, M., Sucov, H.M., Maxson, R.E., 2008. Msx1 and Msx2are required for endothelial-mesenchymal transformation of the atrioventricular cushions

and patterning of the atrioventricular myocardium. BMC Developmental Biology 8, 75. https://doi.org/10.1186/1471-213X-8-75
Chowdhury, F., Li, I.T.S., Ngo, T.T.M., Leslie, B.J., Kim, B.C., Sokoloski, J.E., Weiland, E., Wang, X., Chemla, Y.R., Lohman, T.M., Ha, T., 2016. Defining Single Molecular Forces Required for Notch Activation Using Nano Yoyo. Nano Lett. 16, 3892–3897. https://doi.org/10.1021/acs.nanolett.6b01403
Chua, E.L., Young, L., Wu, W.M., Turtle, J.R., Dong, Q., 2000. Cloning of TC-1 (C8orf4), a novel gene found to be overexpressed in thyroid cancer. Genomics 69, 342–347. https://doi.org/10.1006/geno.2000.6348
Chung, A.S., Lee, J., Ferrara, N., 2010. Targeting the tumour vasculature: insights from physiological angiogenesis. Nat Rev Cancer 10, 505–514. https://doi.org/10.1038/nrc2868
Chung, U.-I., 2004. Essential role of hypertrophic chondrocytes in endochondral bone development. Endocr. J. 51, 19–24. https://doi.org/10.1507/endocrj.51.19
Chung, Y.S., Zhang, W.J., Arentson, E., Kingsley, P.D., Palis, J., Choi, K., 2002. Lineage analysis of the hemangioblast as defined by FLK1 and SCL expression. Development 129, 5511–5520. https://doi.org/10.1242/dev.00149
Clackson, T., Wells, J.A., 1995. A hot spot of binding energy in a hormone-receptor interface. Science 267, 383–386. https://doi.org/10.1126/science.7529940
Claesson-Welsh, L., 2015. Vascular permeability--the essentials. Ups. J. Med. Sci. 120, 135–143.
Clark, P.R., Kim, R.K., Pober, J.S., Kluger, M.S., 2015. Tumor Necrosis Factor Disrupts Claudin-5 Endothelial Tight Junction Barriers in Two Distinct NF-κB-Dependent Phases. PLoS One 10. https://doi.org/10.1371/journal.pone.0120075
Cocks, M., Mohan, A., Meyers, C.A., Ding, C., Levi, B., McCarthy, E., James, A.W., 2017. Vascular patterning in human heterotopic ossification. Hum Pathol 63, 165–170. https://doi.org/10.1016/j.humpath.2017.03.005
Cohen, P., Alessi, D.R., 2013. Kinase Drug Discovery – What's Next in the Field? ACS Chem Biol 8, 96–104. https://doi.org/10.1021/cb300610s
Constam, D.B., 2014. Regulation of TGFβ and related signals by precursor processing. Seminars in Cell & Developmental Biology, RNA biogenesis & TGFβ signalling in embryonic development 32, 85–97. https://doi.org/10.1016/j.semcdb.2014.01.008
Cornell, R.A., Kimelman, D., 1994. Activin-mediated mesoderm induction requires FGF. Development 120, 453–462.
Cotton, T.R., Fischer, G., Wang, X., McCoy, J.C., Czepnik, M., Thompson, T.B., Hyvönen, M., 2018. Structure of the human myostatin precursor and determinants of growth factor latency. EMBO J 37, 367–383. https://doi.org/10.15252/embj.201797883
Cowin, S.C., Cardoso, L., 2015. Blood and interstitial flow in the hierarchical pore space architecture of bone tissue. J Biomech 48, 842–854. https://doi.org/10.1016/j.jbiomech.2014.12.013
Cui, J., Zhang, W., Huang, E., Wang, J., Liao, J., Li, R., Yu, X., Zhao, C., Zeng, Z., Shu, Y., Zhang, R., Yan, S., Lei, J., Yang, C., Wu, K., Wu, Y., Huang, S., Ji, X., Li, A., Gong, C., Yuan, C., Zhang, L., Liu, W., Huang, B., Feng, Y., An, L., Zhang, B., Dai, Z., Shen, Y., Luo, W., Wang, X., Huang, A., Luu, H.H., Reid, R.R., Wolf, J.M., Thinakaran, G., Lee, M.J., He, T.-C., 2019. BMP9-induced osteoblastic differentiation requires functional Notch signaling in mesenchymal stem cells. Laboratory Investigation 99, 58–71. https://doi.org/10.1038/s41374-018-0087-7

da Silva Madaleno, C., Jatzlau, J., Knaus, P., 2020. BMP signalling in a mechanical context – Implications for bone biology. Bone 137, 115416. https://doi.org/10.1016/j.bone.2020.115416

Dakhore, S., Nayer, B., Hasegawa, K., 2018. Human Pluripotent Stem Cell Culture: Current Status, Challenges, and Advancement. Stem Cells Int 2018. https://doi.org/10.1155/2018/7396905

Daly, A.C., Randall, R.A., Hill, C.S., 2008. Transforming growth factor beta-induced Smad1/5 phosphorylation in epithelial cells is mediated by novel receptor complexes and is essential for anchorage-independent growth. Mol. Cell. Biol. 28, 6889–6902. https://doi.org/10.1128/MCB.01192-08

D'Amour, K.A., Agulnick, A.D., Eliazer, S., Kelly, O.G., Kroon, E., Baetge, E.E., 2005. Efficient differentiation of human embryonic stem cells to definitive endoderm. Nat. Biotechnol. 23, 1534–1541. https://doi.org/10.1038/nbt1163

Danielpour, D., 2000. Iodination of TGF-beta, TGF-beta-receptor crosslinking, and immunoprecipitation of TGF-beta-receptor complexes. Methods Mol Biol 142, 29–37. https://doi.org/10.1385/1-59259-053-5:29

David, L., Mallet, C., Keramidas, M., Lamandé, N., Gasc, J.-M., Dupuis-Girod, S., Plauchu, H., Feige, J.-J., Bailly, S., 2008. Bone morphogenetic protein-9 is a circulating vascular quiescence factor. Circ. Res. 102, 914–922. https://doi.org/10.1161/CIRCRESAHA.107.165530

David, L., Mallet, C., Mazerbourg, S., Feige, J.-J., Bailly, S., 2007. Identification of BMP9 and BMP10 as functional activators of the orphan activin receptor-like kinase 1 (ALK1) in endothelial cells. Blood 109, 1953–1961. https://doi.org/10.1182/blood-2006-07-034124

de Castro, N.P., Rangel, M.C., Nagaoka, T., Salomon, D.S., Bianco, C., 2010. Cripto-1: an embryonic gene that promotes tumorigenesis. Future Oncol 6, 1127–1142. https://doi.org/10.2217/fon.10.68

De Crescenzo, G., Hinck, C.S., Shu, Z., Zúñiga, J., Yang, J., Tang, Y., Baardsnes, J., Mendoza, V., Sun, L., López-Casillas, F., O'Connor-McCourt, M., Hinck, A.P., 2006. Three key residues underlie the differential affinity of the TGFbeta isoforms for the TGFbeta type II receptor. J. Mol. Biol. 355, 47–62. https://doi.org/10.1016/j.jmb.2005.10.022

de Kretser, D.M., Bensley, J.G., Pettilä, V., Linko, R., Hedger, M.P., Hayward, S., Allan, C.A., McLachlan, R.I., Ludlow, H., Phillips, D.J., 2013. Serum activin A and B levels predict outcome in patients with acute respiratory failure: a prospective cohort study. Crit Care 17, R263. https://doi.org/10.1186/cc13093

de Vries, C., Escobedo, J.A., Ueno, H., Houck, K., Ferrara, N., Williams, L.T., 1992. The fms-like tyrosine kinase, a receptor for vascular endothelial growth factor. Science 255, 989–991. https://doi.org/10.1126/science.1312256

de Vries, T.J., Schoenmaker, T., Micha, D., Hogervorst, J., Bouskla, S., Forouzanfar, T., Pals, G., Netelenbos, C., Eekhoff, E.M.W., Bravenboer, N., 2018. Periodontal ligament fibroblasts as a cell model to study osteogenesis and osteoclastogenesis in fibrodysplasia ossificans progressiva. Bone 109, 168–177. https://doi.org/10.1016/j.bone.2017.07.007

Dejana, E., Hirschi, K.K., Simons, M., 2017. The molecular basis of endothelial cell plasticity. Nature Communications 8, 14361. https://doi.org/10.1038/ncomms14361

Del Amo-Maestro, L., Marino-Puertas, L., Goulas, T., Gomis-Rüth, F.X., 2019. Recombinant production, purification, crystallization, and structure analysis of human transforming growth factor β2 in a new conformation. Sci Rep 9, 8660. https://doi.org/10.1038/s41598-019-44943-4

Dennler, S., Itoh, S., Vivien, D., ten Dijke, P., Huet, S., Gauthier, J.-M., 1998. Direct binding of Smad3 and Smad4 to critical TGFβ-inducible elements in the promoter of human plasminogen activator inhibitor-type 1 gene. The EMBO Journal 17, 3091–3100. https://doi.org/10.1093/emboj/17.11.3091

Derynck, R., Budi, E.H., 2019. Specificity, versatility, and control of TGF-β family signaling. Sci. Signal. 12. https://doi.org/10.1126/scisignal.aav5183

Derynck, R., Zhang, Y.E., 2003. Smad-dependent and Smad-independent pathways in TGF-beta family signalling. Nature 425, 577–584. https://doi.org/10.1038/nature02006

Descamps, B., Emanueli, C., 2012. Vascular differentiation from embryonic stem cells: novel technologies and therapeutic promises. Vascul Pharmacol 56, 267–79. https://doi.org/10.1016/j.vph.2012.03.007

Dey, D., Bagarova, J., Hatsell, S.J., Armstrong, K.A., Huang, L., Ermann, J., Vonner, A.J., Shen, Y., Mohedas, A.H., Lee, A., Eekhoff, E.M., van Schie, A., Demay, M.B., Keller, C., Wagers, A.J., Economides, A.N., Yu, P.B., 2016. Two tissue-resident progenitor lineages drive distinct phenotypes of heterotopic ossification. Sci Transl Med 8, 366ra163. https://doi.org/10.1126/scitranslmed.aaf1090

Dobin, A., Davis, C.A., Schlesinger, F., Drenkow, J., Zaleski, C., Jha, S., Batut, P., Chaisson, M., Gingeras, T.R., 2013. STAR: ultrafast universal RNA-seq aligner. Bioinformatics 29, 15–21. https://doi.org/10.1093/bioinformatics/bts635

Dörpholz, G., Murgai, A., Jatzlau, J., Horbelt, D., Belverdi, M.P., Heroven, C., Schreiber, I., Wendel, G., Ruschke, K., Stricker, S., Knaus, P., 2017. IRS4, a novel modulator of BMP/Smad and Akt signalling during early muscle differentiation. Scientific Reports 7, 8778. https://doi.org/10.1038/s41598-017-08676-6

Drissi, M.H., Li, X., Sheu, T.J., Zuscik, M.J., Schwarz, E.M., Puzas, J.E., Rosier, R.N., O'Keefe, R.J., 2003. Runx2/Cbfa1 stimulation by retinoic acid is potentiated by BMP2 signaling through interaction with Smad1 on the collagen X promoter in chondrocytes. J. Cell. Biochem. 90, 1287–1298. https://doi.org/10.1002/jcb.10677

Drummond, N.J., Singh Dolt, K., Canham, M.A., Kilbride, P., Morris, G.J., Kunath, T., 2020. Cryopreservation of Human Midbrain Dopaminergic Neural Progenitor Cells Poised for Neuronal Differentiation. Front Cell Dev Biol 8, 578907. https://doi.org/10.3389/fcell.2020.578907

Dyer, L.A., Patterson, C., 2010. Development of the Endothelium: An Emphasis on Heterogeneity. Semin Thromb Hemost 36, 227–235. https://doi.org/10.1055/s-0030-1253446

Dyer, M.A., Farrington, S.M., Mohn, D., Munday, J.R., Baron, M.H., 2001. Indian hedgehog activates hematopoiesis and vasculogenesis and can respecify prospective neurectodermal cell fate in the mouse embryo. Development 128, 1717–1730.

Ebisawa, T., Tada, K., Kitajima, I., Tojo, K., Sampath, T.K., Kawabata, M., Miyazono, K., Imamura, T., 1999. Characterization of bone morphogenetic protein-6 signaling pathways in osteoblast differentiation. J. Cell. Sci. 112 (Pt 20), 3519–3527.

Ebner, R., Chen, R.H., Lawler, S., Zioncheck, T., Derynck, R., 1993. Determination of type I receptor specificity by the type II receptors for TGF-beta or activin. Science 262, 900–902. https://doi.org/10.1126/science.8235612

Eekhoff, E.M.W., Botman, E., Coen Netelenbos, J., de Graaf, P., Bravenboer, N., Micha, D., Pals, G., de Vries, T.J., Schoenmaker, T., Hoebink, M.,

Lammertsma, A.A., Raijmakers, P., 2018. [18F]NaF PET/CT scan as an early marker of heterotopic ossification in fibrodysplasia ossificans progressiva. Bone 109, 143–146. https://doi.org/10.1016/j.bone.2017.08.012

Egawa, G., Nakamizo, S., Natsuaki, Y., Doi, H., Miyachi, Y., Kabashima, K., 2013. Intravital analysis of vascular permeability in mice using two-photon microscopy. Sci Rep 3. https://doi.org/10.1038/srep01932

Einhorn, T.A., Gerstenfeld, L.C., 2015. Fracture healing: mechanisms and interventions. Nat Rev Rheumatol 11, 45–54. https://doi.org/10.1038/nrrheum.2014.164

Eisenberg, L.M., Markwald, R.R., 1995. Molecular regulation of atrioventricular valvuloseptal morphogenesis. Circ. Res. 77, 1–6.

el-Labban, N.G., Hopper, C., Barber, P., 1995. Ultrastructural finding of vascular degeneration in fibrodysplasia ossificans progressiva (FOP). J Oral Pathol Med 24, 125–129. https://doi.org/10.1111/j.1600-0714.1995.tb01152.x

Evrard, S.M., Lecce, L., Michelis, K.C., Nomura-Kitabayashi, A., Pandey, G., Purushothaman, K.-R., d'Escamard, V., Li, J.R., Hadri, L., Fujitani, K., Moreno, P.R., Benard, L., Rimmele, P., Cohain, A., Mecham, B., Randolph, G.J., Nabel, E.G., Hajjar, R., Fuster, V., Boehm, M., Kovacic, J.C., 2016. Endothelial to mesenchymal transition is common in atherosclerotic lesions and is associated with plaque instability. Nature Communications 7, 11853. https://doi.org/10.1038/ncomms11853

Ewels, P., Magnusson, M., Lundin, S., Käller, M., 2016. MultiQC: summarize analysis results for multiple tools and samples in a single report. Bioinformatics 32, 3047–3048. https://doi.org/10.1093/bioinformatics/btw354

Faial, T., Bernardo, A.S., Mendjan, S., Diamanti, E., Ortmann, D., Gentsch, G.E., Mascetti, V.L., Trotter, M.W.B., Smith, J.C., Pedersen, R.A., 2015. Brachyury and SMAD signalling collaboratively orchestrate distinct mesoderm and endoderm gene regulatory networks in differentiating human embryonic stem cells. Development 142, 2121–2135. https://doi.org/10.1242/dev.117838

Fang, J., Hirschi, K., 2019. Molecular regulation of arteriovenous endothelial cell specification. F1000Res 8. https://doi.org/10.12688/f1000research.16701.1

Fathi, A., Eisa-Beygi, S., Baharvand, H., 2017. Signaling Molecules Governing Pluripotency and Early Lineage Commitments in Human Pluripotent Stem Cells. Cell J 19, 194–203. https://doi.org/10.22074/cellj.2016.3915

Feng, X.H., Derynck, R., 1997. A kinase subdomain of transforming growth factor-beta (TGF-beta) type I receptor determines the TGF-beta intracellular signaling specificity. EMBO J. 16, 3912–3923. https://doi.org/10.1093/emboj/16.13.3912

Ferrara, N., Carver-Moore, K., Chen, H., Dowd, M., Lu, L., O'Shea, K.S., Powell-Braxton, L., Hillan, K.J., Moore, M.W., 1996. Heterozygous embryonic lethality induced by targeted inactivation of the VEGF gene. Nature 380, 439–442. https://doi.org/10.1038/380439a0

Filipowska, J., Tomaszewski, K.A., Niedźwiedzki, Ł., Walocha, J.A., Niedźwiedzki, T., 2017. The role of vasculature in bone development, regeneration and proper systemic functioning. Angiogenesis 20, 291–302. https://doi.org/10.1007/s10456-017-9541-1

Fiori, J.L., Billings, P.C., de la Peña, L.S., Kaplan, F.S., Shore, E.M., 2006. Dysregulation of the BMP-p38 MAPK signaling pathway in cells from patients with fibrodysplasia ossificans progressiva (FOP). Journal of Bone and Mineral Research: The Official Journal of the American Society for Bone and Mineral Research 21, 902–909. https://doi.org/10.1359/jbmr.060215

Franzén, P., ten Dijke, P., Ichijo, H., Yamashita, H., Schulz, P., Heldin, C.-H., Miyazono, K., 1993. Cloning of a TGFβ type I receptor that forms a heteromeric complex with the TGFβ type II receptor. Cell 75, 681–692. https://doi.org/10.1016/0092-8674(93)90489-D

Fridy, P.C., Li, Y., Keegan, S., Thompson, M.K., Nudelman, I., Scheid, J.F., Oeffinger, M., Nussenzweig, M.C., Fenyö, D., Chait, B.T., Rout, M.P., 2014. A robust pipeline for rapid production of versatile nanobody repertoires. Nat. Methods 11, 1253–1260. https://doi.org/10.1038/nmeth.3170

Fukuda, T., Kohda, M., Kanomata, K., Nojima, J., Nakamura, A., Kamizono, J., Noguchi, Y., Iwakiri, K., Kondo, T., Kurose, J., Endo, K., Awakura, T., Fukushi, J., Nakashima, Y., Chiyonobu, T., Kawara, A., Nishida, Y., Wada, I., Akita, M., Komori, T., Nakayama, K., Nanba, A., Maruki, Y., Yoda, T., Tomoda, H., Yu, P.B., Shore, E.M., Kaplan, F.S., Miyazono, K., Matsuoka, M., Ikebuchi, K., Ohtake, A., Oda, H., Jimi, E., Owan, I., Okazaki, Y., Katagiri, T., 2009. Constitutively activated ALK2 and increased SMAD1/5 cooperatively induce bone morphogenetic protein signaling in fibrodysplasia ossificans progressiva. J. Biol. Chem. 284, 7149–7156. https://doi.org/10.1074/jbc.M801681200

Fukuda, T., Scott, G., Komatsu, Y., Araya, R., Kawano, M., Ray, M.K., Yamada, M., Mishina, Y., 2006. Generation of a mouse with conditionally activated signaling through the BMP receptor, ALK2. Genesis 44, 159–167. https://doi.org/10.1002/dvg.20201

Fusaki, N., Ban, H., Nishiyama, A., Saeki, K., Hasegawa, M., 2009. Efficient induction of transgene-free human pluripotent stem cells using a vector based on Sendai virus, an RNA virus that does not integrate into the host genome. Proc Jpn Acad Ser B Phys Biol Sci 85, 348–362. https://doi.org/10.2183/pjab.85.348

Gao, F., Sabbineni, H., Artham, S., Somanath, P.R., 2017. Modulation of long-term endothelial-barrier integrity is conditional to the cross-talk between Akt and Src signaling. J. Cell. Physiol. 232, 2599–2609. https://doi.org/10.1002/jcp.25791

García de Vinuesa, A., Abdelilah-Seyfried, S., Knaus, P., Zwijsen, A., Bailly, S., 2016. BMP signaling in vascular biology and dysfunction. Cytokine Growth Factor Rev. 27, 65–79. https://doi.org/10.1016/j.cytogfr.2015.12.005

García-Ponce, A., Chánez Paredes, S., Castro Ochoa, K.F., Schnoor, M., 2016. Regulation of endothelial and epithelial barrier functions by peptide hormones of the adrenomedullin family. Tissue Barriers 4. https://doi.org/10.1080/21688370.2016.1228439

Gately, S., Li, W.W., 2004. Multiple roles of COX-2 in tumor angiogenesis: a target for antiangiogenic therapy. Semin Oncol 31, 2–11. https://doi.org/10.1053/j.seminoncol.2004.03.040

Gavard, J., Gutkind, J.S., 2006. VEGF controls endothelial-cell permeability by promoting the beta-arrestin-dependent endocytosis of VE-cadherin. Nat. Cell Biol. 8, 1223–1234. https://doi.org/10.1038/ncb1486

Gerber, H.-P., Vu, T.H., Ryan, A.M., Kowalski, J., Werb, Z., Ferrara, N., 1999. VEGF couples hypertrophic cartilage remodeling, ossification and angiogenesis during endochondral bone formation. Nature Medicine 5, 623–628. https://doi.org/10.1038/9467

Gerhardt, H., 2008. VEGF and endothelial guidance in angiogenic sprouting. Organogenesis 4, 241–246.

Gilboa, L., Nohe, A., Geissendörfer, T., Sebald, W., Henis, Y.I., Knaus, P., 2000. Bone Morphogenetic Protein Receptor Complexes on the Surface of Live

Cells: A New Oligomerization Mode for Serine/Threonine Kinase Receptors. Mol Biol Cell 11, 1023–1035.
Giles, P.B., Candy, C.L., Fleming, P.A., Owens, R.W., Scott Argraves, W., Drake, C.J., 2005. VEGF directs newly gastrulated mesoderm to the endothelial lineage. Developmental Biology 279, 169–178. https://doi.org/10.1016/j.ydbio.2004.12.011
Gipson, G.R., Goebel, E.J., Hart, K.N., Kappes, E.C., Kattamuri, C., McCoy, J.C., Thompson, T.B., 2020. Structural perspective of BMP ligands and signaling. Bone 140, 115549. https://doi.org/10.1016/j.bone.2020.115549
Givens, C., Tzima, E., 2016. Endothelial Mechanosignaling: Does One Sensor Fit All? Antioxid. Redox Signal. 25, 373–388. https://doi.org/10.1089/ars.2015.6493
Glaser, D.L., Kaplan, F.S., 2005. Treatment considerations for the management of fibrodysplasia ossificans progressiva. Clinic Rev Bone Miner Metab 3, 243–250. https://doi.org/10.1385/BMM:3:3-4:243
Glinka, Y., Stoilova, S., Mohammed, N., Prud'homme, G.J., 2011. Neuropilin-1 exerts co-receptor function for TGF-beta-1 on the membrane of cancer cells and enhances responses to both latent and active TGF-beta. Carcinogenesis 32, 613–621. https://doi.org/10.1093/carcin/bgq281
Goddard, L.M., Iruela-Arispe, M.L., 2013. Cellular and molecular regulation of vascular permeability. Thromb. Haemost. 109, 407–415. https://doi.org/10.1160/TH12-09-0678
Goebel, E.J., Corpina, R.A., Hinck, C.S., Czepnik, M., Castonguay, R., Grenha, R., Boisvert, A., Miklossy, G., Fullerton, P.T., Matzuk, M.M., Idone, V.J., Economides, A.N., Kumar, R., Hinck, A.P., Thompson, T.B., 2019a. Structural characterization of an activin class ternary receptor complex reveals a third paradigm for receptor specificity. Proc. Natl. Acad. Sci. U.S.A. 116, 15505–15513. https://doi.org/10.1073/pnas.1906253116
Goebel, E.J., Hart, K.N., McCoy, J.C., Thompson, T.B., 2019b. Structural biology of the TGFβ family. Exp. Biol. Med. (Maywood) 244, 1530–1546. https://doi.org/10.1177/1535370219880894
Gomez-Puerto, M.C., Iyengar, P.V., García de Vinuesa, A., ten Dijke, P., Sanchez-Duffhues, G., 2019. Bone morphogenetic protein receptor signal transduction in human disease. J Pathol 247, 9–20. https://doi.org/10.1002/path.5170
Gong, H., Lyu, X., Wang, Q., Hu, M., Zhang, X., 2017. Endothelial to mesenchymal transition in the cardiovascular system. Life Sciences 184, 95–102. https://doi.org/10.1016/j.lfs.2017.07.014
Góth, M.I., Hubina, E., Raptis, S., Nagy, G.M., Tóth, B.E., 2003. Physiological and pathological angiogenesis in the endocrine system. Microsc Res Tech 60, 98–106. https://doi.org/10.1002/jemt.10248
Goumans, M.-J., Liu, Z., ten Dijke, P., 2009. TGF-β signaling in vascular biology and dysfunction. Cell Research 19, 116–127. https://doi.org/10.1038/cr.2008.326
Goumans, M.J., Mummery, C., 2000. Functional analysis of the TGFbeta receptor/Smad pathway through gene ablation in mice. Int. J. Dev. Biol. 44, 253–265.
Goumans, M.-J., Valdimarsdottir, G., Itoh, S., Lebrin, F., Larsson, J., Mummery, C., Karlsson, S., ten Dijke, P., 2003. Activin Receptor-like Kinase (ALK)1 Is an Antagonistic Mediator of Lateral TGFβ/ALK5 Signaling. Molecular Cell 12, 817–828. https://doi.org/10.1016/S1097-2765(03)00386-1
Goumans, M.-J., Valdimarsdottir, G., Itoh, S., Rosendahl, A., Sideras, P., ten Dijke, P., 2002. Balancing the activation state of the endothelium via two distinct

TGF-beta type I receptors. EMBO J. 21, 1743–1753. https://doi.org/10.1093/emboj/21.7.1743

Gray, P.C., Harrison, C.A., Vale, W., 2003. Cripto forms a complex with activin and type II activin receptors and can block activin signaling. Proc Natl Acad Sci U S A 100, 5193–5198. https://doi.org/10.1073/pnas.0531290100

Gray, P.C., Shani, G., Aung, K., Kelber, J., Vale, W., 2006. Cripto binds transforming growth factor beta (TGF-beta) and inhibits TGF-beta signaling. Mol. Cell. Biol. 26, 9268–9278. https://doi.org/10.1128/MCB.01168-06

Greenwald, J., Vega, M.E., Allendorph, G.P., Fischer, W.H., Vale, W., Choe, S., 2004. A flexible activin explains the membrane-dependent cooperative assembly of TGF-beta family receptors. Mol. Cell 15, 485–489. https://doi.org/10.1016/j.molcel.2004.07.011

Grgurevic, L., Pecina, M., Vukicevic, S., 2017. Marshall R. Urist and the discovery of bone morphogenetic proteins. International Orthopaedics (SICOT) 41, 1065–1069. https://doi.org/10.1007/s00264-017-3402-9

Groppe, J., Greenwald, J., Wiater, E., Rodriguez-Leon, J., Economides, A.N., Kwiatkowski, W., Affolter, M., Vale, W.W., Belmonte, J.C.I., Choe, S., 2002. Structural basis of BMP signalling inhibition by the cystine knot protein Noggin. Nature 420, 636–642. https://doi.org/10.1038/nature01245

Groppe, J., Hinck, C.S., Samavarchi-Tehrani, P., Zubieta, C., Schuermann, J.P., Taylor, A.B., Schwarz, P.M., Wrana, J.L., Hinck, A.P., 2008. Cooperative assembly of TGF-beta superfamily signaling complexes is mediated by two disparate mechanisms and distinct modes of receptor binding. Mol. Cell 29, 157–168. https://doi.org/10.1016/j.molcel.2007.11.039

Groppe, J.C., Shore, E.M., Kaplan, F.S., 2007. Functional modeling of the ACVR1 (R206H) mutation in FOP. Clin. Orthop. Relat. Res. 462, 87–92. https://doi.org/10.1097/BLO.0b013e318126c049

Grosso, A., Burger, M.G., Lunger, A., Schaefer, D.J., Banfi, A., Di Maggio, N., 2017. It Takes Two to Tango: Coupling of Angiogenesis and Osteogenesis for Bone Regeneration. Front Bioeng Biotechnol 5. https://doi.org/10.3389/fbioe.2017.00068

Gu, Z., Reynolds, E.M., Song, J., Lei, H., Feijen, A., Yu, L., He, W., MacLaughlin, D.T., Raaij, J. van den E., Donahoe, P.K., Li, E., 1999. The type I serine/threonine kinase receptor ActRIA (ALK2) is required for gastrulation of the mouse embryo. Development 126, 2551–2561.

Guerrero-Esteo, M., Sanchez-Elsner, T., Letamendia, A., Bernabeu, C., 2002. Extracellular and cytoplasmic domains of endoglin interact with the transforming growth factor-beta receptors I and II. J. Biol. Chem. 277, 29197–29209. https://doi.org/10.1074/jbc.M111991200

Guilliard, M.J., 2001. Fibrodysplasia ossificans in a German shepherd dog. J Small Anim Pract 42, 550–553. https://doi.org/10.1111/j.1748-5827.2001.tb06026.x

Guzman, A., Femiak, M.Z.-, Boergermann, J.H., Paschkowsky, S., Kreuzaler, P.A., Fratzl, P., Harms, G.S., Knaus, P., 2012. SMAD versus Non-SMAD Signaling Is Determined by Lateral Mobility of Bone Morphogenetic Protein (BMP) Receptors. J Biol Chem 287, 39492–39504. https://doi.org/10.1074/jbc.M112.387639

Hamasaki, M., Hashizume, Y., Yamada, Y., Katayama, T., Hohjoh, H., Fusaki, N., Nakashima, Y., Furuya, H., Haga, N., Takami, Y., Era, T., 2012. Pathogenic Mutation of ALK2 Inhibits Induced Pluripotent Stem Cell Reprogramming and Maintenance: Mechanisms of Reprogramming and Strategy for Drug

Identification. STEM CELLS 30, 2437–2449. https://doi.org/10.1002/stem.1221
Hankenson, K.D., Dishowitz, M., Gray, C., Schenker, M., 2011. Angiogenesis in Bone Regeneration. Injury 42, 556–561. https://doi.org/10.1016/j.injury.2011.03.035
Harada, K., Shintani, Y., Sakamoto, Y., Wakatsuki, M., Shitsukawa, K., Saito, S., 1996. Serum immunoreactive activin A levels in normal subjects and patients with various diseases. J Clin Endocrinol Metab 81, 2125–2130. https://doi.org/10.1210/jcem.81.6.8964839
Harrington, A.E., Morris-Triggs, S.A., Ruotolo, B.T., Robinson, C.V., Ohnuma, S.-I., Hyvönen, M., 2006. Structural basis for the inhibition of activin signalling by follistatin. EMBO J 25, 1035–1045. https://doi.org/10.1038/sj.emboj.7601000
Hartung, A., Bitton-Worms, K., Rechtman, M.M., Wenzel, V., Boergermann, J.H., Hassel, S., Henis, Y.I., Knaus, P., 2006. Different Routes of Bone Morphogenic Protein (BMP) Receptor Endocytosis Influence BMP Signaling. Mol Cell Biol 26, 7791–7805. https://doi.org/10.1128/MCB.00022-06
Hassel, S., Eichner, A., Yakymovych, M., Hellman, U., Knaus, P., Souchelnytskyi, S., 2004. Proteins associated with type II bone morphogenetic protein receptor (BMPR-II) and identified by two-dimensional gel electrophoresis and mass spectrometry. Proteomics 4, 1346–1358. https://doi.org/10.1002/pmic.200300770
Hasty, P., Rivera-Pérez, J., Bradley, A., 1991. The length of homology required for gene targeting in embryonic stem cells. Mol Cell Biol 11, 5586–5591.
Hata, A., Chen, Y.-G., 2016. TGF-β Signaling from Receptors to Smads. Cold Spring Harb Perspect Biol 8. https://doi.org/10.1101/cshperspect.a022061
Hatsell, S.J., Idone, V., Wolken, D.M.A., Huang, L., Kim, H.J., Wang, L., Wen, X., Nannuru, K.C., Jimenez, J., Xie, L., Das, N., Makhoul, G., Chernomorsky, R., D'Ambrosio, D., Corpina, R.A., Schoenherr, C.J., Feeley, K., Yu, P.B., Yancopoulos, G.D., Murphy, A.J., Economides, A.N., 2015. ACVR1R206H receptor mutation causes fibrodysplasia ossificans progressiva by imparting responsiveness to activin A. Sci Transl Med 7, 303ra137. https://doi.org/10.1126/scitranslmed.aac4358
Hattner, R., Epker, B.N., Frost, H.M., 1965. Suggested sequential mode of control of changes in cell behaviour in adult bone remodelling. Nature 206, 489–490. https://doi.org/10.1038/206489a0
Haupt, J., Deichsel, A., Stange, K., Ast, C., Bocciardi, R., Ravazzolo, R., Di Rocco, M., Ferrari, P., Landi, A., Kaplan, F.S., Shore, E.M., Reissner, C., Seemann, P., 2014. ACVR1 p.Q207E causes classic fibrodysplasia ossificans progressiva and is functionally distinct from the engineered constitutively active ACVR1 p.Q207D variant. Hum Mol Genet 23, 5364–5377. https://doi.org/10.1093/hmg/ddu255
Haupt, J., Stanley, A., McLeod, C.M., Cosgrove, B.D., Culbert, A.L., Wang, L., Mourkioti, F., Mauck, R.L., Shore, E.M., 2019. ACVR1(R206H) FOP mutation alters mechanosensing and tissue stiffness during heterotopic ossification. Mol Biol Cell 30, 17–29. https://doi.org/10.1091/mbc.E18-05-0311
Haupt, J., Xu, M., Shore, E.M., 2018. Variable signaling activity by FOP ACVR1 mutations. Bone 109, 232–240. https://doi.org/10.1016/j.bone.2017.10.027
Hayashi, Y., Hsiao, E.C., Sami, S., Lancero, M., Schlieve, C.R., Nguyen, T., Yano, K., Nagahashi, A., Ikeya, M., Matsumoto, Y., Nishimura, K., Fukuda, A., Hisatake, K., Tomoda, K., Asaka, I., Toguchida, J., Conklin, B.R., Yamanaka, S., 2016. BMP-SMAD-ID promotes reprogramming to pluripotency by

inhibiting p16/INK4A-dependent senescence. Proc Natl Acad Sci U S A 113, 13057–13062. https://doi.org/10.1073/pnas.1603668113
He, C., Chen, X., 2005. Transcription regulation of the vegf gene by the BMP/Smad pathway in the angioblast of zebrafish embryos. Biochem. Biophys. Res. Commun. 329, 324–330. https://doi.org/10.1016/j.bbrc.2005.01.133
Heinecke, K., Seher, A., Schmitz, W., Mueller, T.D., Sebald, W., Nickel, J., 2009. Receptor oligomerization and beyond: a case study in bone morphogenetic proteins. BMC Biol. 7, 59. https://doi.org/10.1186/1741-7007-7-59
Hellström, M., Phng, L.-K., Hofmann, J.J., Wallgard, E., Coultas, L., Lindblom, P., Alva, J., Nilsson, A.-K., Karlsson, L., Gaiano, N., Yoon, K., Rossant, J., Iruela-Arispe, M.L., Kalén, M., Gerhardt, H., Betsholtz, C., 2007. Dll4 signalling through Notch1 regulates formation of tip cells during angiogenesis. Nature 445, 776–780. https://doi.org/10.1038/nature05571
Henderson, A.M., Wang, S.J., Taylor, A.C., Aitkenhead, M., Hughes, C.C., 2001. The basic helix-loop-helix transcription factor HESR1 regulates endothelial cell tube formation. J. Biol. Chem. 276, 6169–6176. https://doi.org/10.1074/jbc.M008506200
Hennequin, L.F., Allen, J., Breed, J., Curwen, J., Fennell, M., Green, T.P., Lambert-van der Brempt, C., Morgentin, R., Norman, R.A., Olivier, A., Otterbein, L., Plé, P.A., Warin, N., Costello, G., 2006. N-(5-chloro-1,3-benzodioxol-4-yl)-7-[2-(4-methylpiperazin-1-yl)ethoxy]-5- (tetrahydro-2H-pyran-4-yloxy)quinazolin-4-amine, a novel, highly selective, orally available, dual-specific c-Src/Abl kinase inhibitor. J. Med. Chem. 49, 6465–6488. https://doi.org/10.1021/jm060434q
Hiepen, C., Benn, A., Denkis, A., Lukonin, I., Weise, C., Boergermann, J.H., Knaus, P., 2014. BMP2-induced chemotaxis requires PI3K p55γ/p110α-dependent phosphatidylinositol (3,4,5)-triphosphate production and LL5β recruitment at the cytocortex. BMC Biol 12, 43. https://doi.org/10.1186/1741-7007-12-43
Hiepen, C., Jatzlau, J., Hildebrandt, S., Kampfrath, B., Goktas, M., Murgai, A., Camacho, J.L.C., Haag, R., Ruppert, C., Sengle, G., Cavalcanti-Adam, E.A., Blank, K.G., Knaus, P., 2019. BMPR2 acts as a gatekeeper to protect endothelial cells from increased TGFβ responses and altered cell mechanics. PLOS Biology 17, e3000557. https://doi.org/10.1371/journal.pbio.3000557
Hiepen, C., Mendez, P.-L., Knaus, P., 2020. It Takes Two to Tango: Endothelial TGFβ/BMP Signaling Crosstalk with Mechanobiology. Cells 9, 1965. https://doi.org/10.3390/cells9091965
Higashihori, N., Song, Y., Richman, J.M., 2008. Expression and regulation of the decoy bone morphogenetic protein receptor BAMBI in the developing avian face. Developmental Dynamics 237, 1500–1508. https://doi.org/10.1002/dvdy.21529
Hildebrand, L., Gaber, T., Kühnen, P., Morhart, R., Unterbörsch, H., Schomburg, L., Seemann, P., 2017a. Trace element and cytokine concentrations in patients with Fibrodysplasia Ossificans Progressiva (FOP): A case control study. J Trace Elem Med Biol 39, 186–192. https://doi.org/10.1016/j.jtemb.2016.10.001
Hildebrand, L., Rossbach, B., Kühnen, P., Gossen, M., Kurtz, A., Reinke, P., Seemann, P., Stachelscheid, H., 2016. Generation of integration free induced pluripotent stem cells from fibrodysplasia ossificans progressiva (FOP) patients from urine samples. Stem Cell Research 16, 54–58. https://doi.org/10.1016/j.scr.2015.11.017
Hildebrand, L., Stange, K., Deichsel, A., Gossen, M., Seemann, P., 2017b. The Fibrodysplasia Ossificans Progressiva (FOP) mutation p.R206H in ACVR1

confers an altered ligand response. Cellular Signalling 29, 23–30. https://doi.org/10.1016/j.cellsig.2016.10.001

Hildebrandt, S., Kampfrath, B., Fischer, K., Hildebrand, L., Haupt, J., Stachelscheid, H., Knaus, P., 2020. ActivinA induced SMAD1/5 signaling in an iPSC derived EC model of Fibrodysplasia ossificans Progressiva (FOP) can be rescued by the drug candidate Saracatinib. Stem Cell Reviews and Reports. (in press)

Hinck, A.P., 2012. Structural studies of the TGF-βs and their receptors – insights into evolution of the TGF-β superfamily. FEBS Letters, Sorting the TGF-β Labyrinth 586, 1860–1870. https://doi.org/10.1016/j.febslet.2012.05.028

Hinck, A.P., Mueller, T.D., Springer, T.A., 2016. Structural Biology and Evolution of the TGF-β Family. Cold Spring Harb Perspect Biol 8. https://doi.org/10.1101/cshperspect.a022103

Hino, K., Ikeya, M., Horigome, K., Matsumoto, Y., Ebise, H., Nishio, M., Sekiguchi, K., Shibata, M., Nagata, S., Matsuda, S., Toguchida, J., 2015. Neofunction of ACVR1 in fibrodysplasia ossificans progressiva. Proc. Natl. Acad. Sci. U.S.A. 112, 15438–15443. https://doi.org/10.1073/pnas.1510540112

Hino, K., Zhao, C., Horigome, K., Nishio, M., Okanishi, Y., Nagata, S., Komura, S., Yamada, Y., Toguchida, J., Ohta, A., Ikeya, M., 2018. An mTOR Signaling Modulator Suppressed Heterotopic Ossification of Fibrodysplasia Ossificans Progressiva. Stem Cell Reports 11, 1106–1119. https://doi.org/10.1016/j.stemcr.2018.10.007

Hippenstiel, S., Witzenrath, M., Schmeck, B., Hocke, A., Krisp, M., Krüll, M., Seybold, J., Seeger, W., Rascher, W., Schütte, H., Suttorp, N., 2002. Adrenomedullin reduces endothelial hyperpermeability. Circ. Res. 91, 618–625. https://doi.org/10.1161/01.res.0000036603.61868.f9

Hoeman, C.M., Cordero, F.J., Hu, G., Misuraca, K., Romero, M.M., Cardona, H.J., Nazarian, J., Hashizume, R., McLendon, R., Yu, P., Procissi, D., Gadd, S., Becher, O.J., 2019. ACVR1 R206H cooperates with H3.1K27M in promoting diffuse intrinsic pontine glioma pathogenesis. Nature Communications 10, 1023. https://doi.org/10.1038/s41467-019-08823-9

Hofmann, J.J., Iruela-Arispe, M.L., 2007. Notch Expression Patterns in the Retina: An Eye on Receptor-Ligand Distribution during Angiogenesis. Gene Expr Patterns 7, 461–470. https://doi.org/10.1016/j.modgep.2006.11.002

Hofmann, M., Heineke, J., 2018. The Impact of Endothelial Transcription Factors in Sprouting Angiogenesis, in: Marmé, D. (Ed.), Tumor Angiogenesis: A Key Target for Cancer Therapy. Springer International Publishing, Cham, pp. 1–18. https://doi.org/10.1007/978-3-319-31215-6_38-1

Holtzhausen, A., Golzio, C., How, T., Lee, Y.-H., Schiemann, W.P., Katsanis, N., Blobe, G.C., 2014. Novel bone morphogenetic protein signaling through Smad2 and Smad3 to regulate cancer progression and development. FASEB J 28, 1248–1267. https://doi.org/10.1096/fj.13-239178

Hong, J.H., Lee, G.T., Lee, J.H., Kwon, S.J., Park, S.H., Kim, S.J., Kim, I.Y., 2009. Effect of bone morphogenetic protein-6 on macrophages. Immunology 128, e442–e450. https://doi.org/10.1111/j.1365-2567.2008.02998.x

Hu, D.P., Ferro, F., Yang, F., Taylor, A.J., Chang, W., Miclau, T., Marcucio, R.S., Bahney, C.S., 2017. Cartilage to bone transformation during fracture healing is coordinated by the invading vasculature and induction of the core pluripotency genes. Development 144, 221–234. https://doi.org/10.1242/dev.130807

Hu, K., Olsen, B.R., 2016. Osteoblast-derived VEGF regulates osteoblast differentiation and bone formation during bone repair. J Clin Invest 126, 509–526. https://doi.org/10.1172/JCI82585

Huang, D.W., Sherman, B.T., Lempicki, R.A., 2009a. Bioinformatics enrichment tools: paths toward the comprehensive functional analysis of large gene lists. Nucleic Acids Res. 37, 1–13. https://doi.org/10.1093/nar/gkn923

Huang, D.W., Sherman, B.T., Lempicki, R.A., 2009b. Systematic and integrative analysis of large gene lists using DAVID bioinformatics resources. Nat Protoc 4, 44–57. https://doi.org/10.1038/nprot.2008.211

Hulsen, T., de Vlieg, J., Alkema, W., 2008. BioVenn – a web application for the comparison and visualization of biological lists using area-proportional Venn diagrams. BMC Genomics 9, 488. https://doi.org/10.1186/1471-2164-9-488

Hüning, I., Gillessen-Kaesbach, G., 2014. Fibrodysplasia Ossificans Progressiva: Clinical Course, Genetic Mutations and Genotype-Phenotype Correlation. Mol Syndromol 5, 201–211. https://doi.org/10.1159/000365770

Huse, M., Chen, Y.G., Massagué, J., Kuriyan, J., 1999. Crystal structure of the cytoplasmic domain of the type I TGF beta receptor in complex with FKBP12. Cell 96, 425–436. https://doi.org/10.1016/s0092-8674(00)80555-3

Hwang, C., Marini, S., Huber, A.K., Stepien, D.M., Sorkin, M., Loder, S., Pagani, C.A., Li, John, Visser, N.D., Vasquez, K., Garada, M.A., Li, S., Xu, J., Hsu, C.-Y., Yu, P.B., James, A.W., Mishina, Y., Agarwal, S., Li, Jun, Levi, B., 2019. Mesenchymal VEGFA induces aberrant differentiation in heterotopic ossification. Bone Res 7, 1–17. https://doi.org/10.1038/s41413-019-0075-6

Hwang, C., Pagani, C.A., Das, N., Marini, S., Huber, A.K., Xie, L., Jimenez, J., Brydges, S., Lim, W., Nannuru, K., Murphy, A.J., Economides, A.N., Hatsell, S.J., Levi, B., 2020. Activin A does not drive post-traumatic heterotopic ossification. Bone 115473. https://doi.org/10.1016/j.bone.2020.115473

IFOPA, n.d. Ongoing Clinical Trials in FOP [WWW Document]. IFOPA - International Fibrodysplasia Ossificans Progressiva Association. URL https://www.ifopa.org/ongoing_clinical_trials_in_fop (accessed 12.2.20).

Imoukhuede, P.I., Popel, A.S., 2011. Quantification and cell-to-cell variation of vascular endothelial growth factor receptors. Exp Cell Res 317, 955–965. https://doi.org/10.1016/j.yexcr.2010.12.014

Inman, G.J., Nicolás, F.J., Hill, C.S., 2002. Nucleocytoplasmic Shuttling of Smads 2, 3, and 4 Permits Sensing of TGF-β Receptor Activity. Molecular Cell 10, 283–294. https://doi.org/10.1016/S1097-2765(02)00585-3

Ishida, W., Hamamoto, T., Kusanagi, K., Yagi, K., Kawabata, M., Takehara, K., Sampath, T.K., Kato, M., Miyazono, K., 2000. Smad6 is a Smad1/5-induced smad inhibitor. Characterization of bone morphogenetic protein-responsive element in the mouse Smad6 promoter. J. Biol. Chem. 275, 6075–6079. https://doi.org/10.1074/jbc.275.9.6075

Iso, T., Kedes, L., Hamamori, Y., 2003. HES and HERP families: multiple effectors of the Notch signaling pathway. J. Cell. Physiol. 194, 237–255. https://doi.org/10.1002/jcp.10208

Israël, A., 2010. The IKK Complex, a Central Regulator of NF-κB Activation. Cold Spring Harb Perspect Biol 2. https://doi.org/10.1101/cshperspect.a000158

Itoh, F., Itoh, S., Goumans, M.-J., Valdimarsdottir, G., Iso, T., Dotto, G.P., Hamamori, Y., Kedes, L., Kato, M., ten Dijke Pt, P., 2004. Synergy and antagonism between Notch and BMP receptor signaling pathways in endothelial cells. EMBO J. 23, 541–551. https://doi.org/10.1038/sj.emboj.7600065

Iyer, S., Ferreri, D.M., DeCocco, N.C., Minnear, F.L., Vincent, P.A., 2004. VE-cadherin-p120 interaction is required for maintenance of endothelial barrier function. Am. J. Physiol. Lung Cell Mol. Physiol. 286, L1143-1153. https://doi.org/10.1152/ajplung.00305.2003

Jakobsson, L., Franco, C.A., Bentley, K., Collins, R.T., Ponsioen, B., Aspalter, I.M., Rosewell, I., Busse, M., Thurston, G., Medvinsky, A., Schulte-Merker, S., Gerhardt, H., 2010. Endothelial cells dynamically compete for the tip cell position during angiogenic sprouting. Nat. Cell Biol. 12, 943–953. https://doi.org/10.1038/ncb2103

James, D., Levine, A.J., Besser, D., Hemmati-Brivanlou, A., 2005. TGFbeta/activin/nodal signaling is necessary for the maintenance of pluripotency in human embryonic stem cells. Development 132, 1273–1282. https://doi.org/10.1242/dev.01706

James, D., Nam, H., Seandel, M., Nolan, D., Janovitz, T., Tomishima, M., Studer, L., Lee, G., Lyden, D., Benezra, R., Zaninovic, N., Rosenwaks, Z., Rabbany, S.Y., Rafii, S., 2010. Expansion and maintenance of human embryonic stem cell-derived endothelial cells by TGFbeta inhibition is Id1 dependent. Nat. Biotechnol. 28, 161–166. https://doi.org/10.1038/nbt.1605

Jatzlau Jerome, 2019. GUIDING BMP-SIGNALING: UNC5B AS ARTERIAL BMP CO-RECEPTOR.

Jiang, X., Nicolls, M.R., Tian, W., Rockson, S.G., 2018. Lymphatic Dysfunction, Leukotrienes, and Lymphedema. Annu. Rev. Physiol. 80, 49–70. https://doi.org/10.1146/annurev-physiol-022516-034008

Jin, Y., Kaluza, D., Jakobsson, L., 2014. VEGF, Notch and TGFβ/BMPs in regulation of sprouting angiogenesis and vascular patterning. Biochem. Soc. Trans. 42, 1576–1583. https://doi.org/10.1042/BST20140231

Joe, A.W., Yi, L., Natarajan, A., Le Grand, F., So, L., Wang, J., Rudnicki, M.A., Rossi, F.M., 2010. Muscle injury activates resident fibro/adipogenic progenitors that facilitate myogenesis. Nat Cell Biol 12, 153–63. https://doi.org/10.1038/ncb2015

Johnson, K.E., Makanji, Y., Temple-Smith, P., Kelly, E.K., Barton, P.A., Al-Musawi, S.L., Mueller, T.D., Walton, K.L., Harrison, C.A., 2016. Biological activity and in vivo half-life of pro-activin A in male rats. Molecular and Cellular Endocrinology 422, 84–92. https://doi.org/10.1016/j.mce.2015.12.007

Jörnvall, H., Blokzijl, A., ten Dijke, P., Ibáñez, C.F., 2001. The orphan receptor serine/threonine kinase ALK7 signals arrest of proliferation and morphological differentiation in a neuronal cell line. J. Biol. Chem. 276, 5140–5146. https://doi.org/10.1074/jbc.M005200200

Joziasse, I.C., Smith, K.A., Chocron, S., van Dinther, M., Guryev, V., van de Smagt, J.J., Cuppen, E., ten Dijke, P., Mulder, B.J., Maslen, C.L., Reshey, B., Doevendans, P.A., Bakkers, J., 2011. ALK2 mutation in a patient with Down's syndrome and a congenital heart defect. Eur J Hum Genet 19, 389–393. https://doi.org/10.1038/ejhg.2010.224

Jung, Y., Bang, S., Choi, K., Kim, E., Kim, Y., Kim, J., Park, J., Koo, H., Moon, R.T., Song, K., Lee, I., 2006. TC1 (C8orf4) Enhances the Wnt/β-Catenin Pathway by Relieving Antagonistic Activity of Chibby. Cancer Res 66, 723–728. https://doi.org/10.1158/0008-5472.CAN-05-3124

Kan, L., Kessler, J.A., 2011. Animal Models of Typical Heterotopic Ossification. J Biomed Biotechnol 2011. https://doi.org/10.1155/2011/309287

Kaneda, H., Arao, T., Matsumoto, K., De Velasco, M.A., Tamura, D., Aomatsu, K., Kudo, K., Sakai, K., Nagai, T., Fujita, Y., Tanaka, K., Yanagihara, K., Yamada,

Y., Okamoto, I., Nakagawa, K., Nishio, K., 2011. Activin A inhibits vascular endothelial cell growth and suppresses tumour angiogenesis in gastric cancer. Br. J. Cancer 105, 1210–1217. https://doi.org/10.1038/bjc.2011.348

Kaplan, F.S., Al Mukaddam, M., Stanley, A., Towler, O.W., Shore, E.M., 2020. Fibrodysplasia ossificans progressiva (FOP): A disorder of osteochondrogenesis. Bone 140, 115539. https://doi.org/10.1016/j.bone.2020.115539

Kaplan, F.S., Le Merrer, M., Glaser, D.L., Pignolo, R.J., Goldsby, R., Kitterman, J.A., Groppe, J., Shore, E.M., 2008. Fibrodysplasia ossificans progressiva. Best Pract Res Clin Rheumatol 22, 191–205. https://doi.org/10.1016/j.berh.2007.11.007

Kaplan, F.S., Tabas, J.A., Gannon, F.H., Finkel, G., Hahn, G.V., Zasloff, M.A., 1993. The histopathology of fibrodysplasia ossificans progressiva. An endochondral process. J Bone Joint Surg Am 75, 220–230. https://doi.org/10.2106/00004623-199302000-00009

Kaplan, F.S., Tabas, J.A., Zasloff, M.A., 1990. Fibrodysplasia ossificans progressiva: A clue from the fly? Calcif Tissue Int 47, 117–125. https://doi.org/10.1007/BF02555995

Kaplan, F.S., Zasloff, M.A., Kitterman, J.A., Shore, E.M., Hong, C.C., Rocke, D.M., 2010. Early Mortality and Cardiorespiratory Failure in Patients with Fibrodysplasia Ossificans Progressiva. JBJS 92, 686–691. https://doi.org/10.2106/JBJS.I.00705

Kaplan, J., Kaplan, F.S., Shore, E.M., 2012. Restoration of normal BMP signaling levels and osteogenic differentiation in FOP mesenchymal progenitor cells by mutant allele-specific targeting. Gene Ther 19, 786–790. https://doi.org/10.1038/gt.2011.152

Kappas, N.C., Zeng, G., Chappell, J.C., Kearney, J.B., Hazarika, S., Kallianos, K.G., Patterson, C., Annex, B.H., Bautch, V.L., 2008. The VEGF receptor Flt-1 spatially modulates Flk-1 signaling and blood vessel branching. J. Cell Biol. 181, 847–858. https://doi.org/10.1083/jcb.200709114

Katagiri, T., Tsukamoto, S., Kuratani, M., 2018. Heterotopic bone induction via BMP signaling: Potential therapeutic targets for fibrodysplasia ossificans progressiva. Bone, Heterotopic Ossification 109, 241–250. https://doi.org/10.1016/j.bone.2017.07.024

Keighron, C., Lyons, C.J., Creane, M., O'Brien, T., Liew, A., 2018. Recent Advances in Endothelial Progenitor Cells Toward Their Use in Clinical Translation. Front Med (Lausanne) 5, 354. https://doi.org/10.3389/fmed.2018.00354

Keller, S., Nickel, J., Zhang, J.-L., Sebald, W., Mueller, T.D., 2004. Molecular recognition of BMP-2 and BMP receptor IA. Nat. Struct. Mol. Biol. 11, 481–488. https://doi.org/10.1038/nsmb756

Kempen, D.H.R., Lu, L., Heijink, A., Hefferan, T.E., Creemers, L.B., Maran, A., Yaszemski, M.J., Dhert, W.J.A., 2009. Effect of local sequential VEGF and BMP-2 delivery on ectopic and orthotopic bone regeneration. Biomaterials 30, 2816–2825. https://doi.org/10.1016/j.biomaterials.2009.01.031

Kennedy, M., D'Souza, S.L., Lynch-Kattman, M., Schwantz, S., Keller, G., 2007. Development of the hemangioblast defines the onset of hematopoiesis in human ES cell differentiation cultures. Blood 109, 2679–2687. https://doi.org/10.1182/blood-2006-09-047704

Kerr, G., Sheldon, H., Chaikuad, A., Alfano, I., von Delft, F., Bullock, A.N., Harris, A.L., 2015. A small molecule targeting ALK1 prevents Notch cooperativity and

inhibits functional angiogenesis. Angiogenesis 18, 209–217. https://doi.org/10.1007/s10456-014-9457-y

Kim, B., Koo, H., Yang, S., Bang, S., Jung, Y., Kim, Y., Kim, J., Park, J., Moon, R.T., Song, K., Lee, I., 2006. TC1(C8orf4) correlates with Wnt/beta-catenin target genes and aggressive biological behavior in gastric cancer. Clinical Cancer Research: An Official Journal of the American Association for Cancer Research 12, 3541–3548. https://doi.org/10.1158/1078-0432.CCR-05-2440

Kim, B.-Y., Jeong, S., Lee, S.-Y., Lee, S.M., Gweon, E.J., Ahn, H., Kim, J., Chung, S.-K., 2016. Concurrent progress of reprogramming and gene correction to overcome therapeutic limitation of mutant ALK2-iPSC. Experimental & Molecular Medicine 48, e237–e237. https://doi.org/10.1038/emm.2016.43

Kim, Jungtae, Kim, Y., Kim, H.-T., Kim, D.W., Ha, Y., Kim, Jihun, Kim, C.-H., Lee, I., Song, K., 2009. TC1(C8orf4) is a novel endothelial inflammatory regulator enhancing NF-kappaB activity. J. Immunol. 183, 3996–4002. https://doi.org/10.4049/jimmunol.0900956

Kim, R.Y., Robertson, E.J., Solloway, M.J., 2001. Bmp6 and Bmp7 Are Required for Cushion Formation and Septation in the Developing Mouse Heart. Developmental Biology 235, 449–466. https://doi.org/10.1006/dbio.2001.0284

Kim, S.W., Yoon, S.-J., Chuong, E., Oyolu, C., Wills, A.E., Gupta, R., Baker, J., 2011. Chromatin and transcriptional signatures for Nodal signaling during endoderm formation in hESCs. Developmental Biology 357, 492–504. https://doi.org/10.1016/j.ydbio.2011.06.009

Kinsella, M.G., Fitzharris, T.P., 1980. Origin of cushion tissue in the developing chick heart: cinematographic recordings of in situ formation. Science 207, 1359–1360.

Kirkbride, K.C., Townsend, T.A., Bruinsma, M.W., Barnett, J.V., Blobe, G.C., 2008. Bone Morphogenetic Proteins Signal through the Transforming Growth Factor-β Type III Receptor. J. Biol. Chem. 283, 7628–7637. https://doi.org/10.1074/jbc.M704883200

Kishigami, S., Mishina, Y., 2005. BMP signaling and early embryonic patterning. Cytokine Growth Factor Rev. 16, 265–278. https://doi.org/10.1016/j.cytogfr.2005.04.002

Kitoh, H., 2020. Clinical Aspects and Current Therapeutic Approaches for FOP. Biomedicines 8, 325. https://doi.org/10.3390/biomedicines8090325

Klein, D., 2018. iPSCs-based generation of vascular cells: reprogramming approaches and applications. Cell. Mol. Life Sci. 75, 1411–1433. https://doi.org/10.1007/s00018-017-2730-7

Koch, S., Claesson-Welsh, L., 2012. Signal Transduction by Vascular Endothelial Growth Factor Receptors. Cold Spring Harb Perspect Med 2. https://doi.org/10.1101/cshperspect.a006502

Koenig, B.B., Cook, J.S., Wolsing, D.H., Ting, J., Tiesman, J.P., Correa, P.E., Olson, C.A., Pecquet, A.L., Ventura, F., Grant, R.A., Chen, G.-X., Wrana, J.L., Massagué, J., Rosenbaum, J.S., 1994. Characterization and cloning of a receptor for BMP-2 and BMP-4 from NIH 3T3 cells. Molecular and Cellular Biology 14, 5961–5974. https://doi.org/10.1128/MCB.14.9.5961

Korn, C., Augustin, H.G., 2015. Mechanisms of Vessel Pruning and Regression. Dev. Cell 34, 5–17. https://doi.org/10.1016/j.devcel.2015.06.004

Kornev, A.P., Haste, N.M., Taylor, S.S., Eyck, L.F.T., 2006. Surface comparison of active and inactive protein kinases identifies a conserved activation mechanism. Proc. Natl. Acad. Sci. U.S.A. 103, 17783–17788. https://doi.org/10.1073/pnas.0607656103

Kosaki, R., Gebbia, M., Kosaki, K., Lewin, M., Bowers, P., Towbin, J.A., Casey, B., 1999. Left-right axis malformations associated with mutations in ACVR2B, the gene for human activin receptor type IIB. Am. J. Med. Genet. 82, 70–76. https://doi.org/10.1002/(sici)1096-8628(19990101)82:1<70::aid-ajmg14>3.0.co;2-y

Kovacic Jason C., Mercader Nadia, Torres Miguel, Boehm Manfred, Fuster Valentin, 2012. Epithelial-to-Mesenchymal and Endothelial-to-Mesenchymal Transition. Circulation 125, 1795–1808. https://doi.org/10.1161/CIRCULATIONAHA.111.040352

Kovaka, S., Zimin, A.V., Pertea, G.M., Razaghi, R., Salzberg, S.L., Pertea, M., 2019. Transcriptome assembly from long-read RNA-seq alignments with StringTie2. Genome Biology 20, 278. https://doi.org/10.1186/s13059-019-1910-1

Kovall, R.A., Gebelein, B., Sprinzak, D., Kopan, R., 2017. The Canonical Notch Signaling Pathway: Structural and Biochemical Insights into Shape, Sugar, and Force. Developmental Cell 41, 228–241. https://doi.org/10.1016/j.devcel.2017.04.001

Krishnan, M., Park, J.M., Cao, F., Wang, D., Paulmurugan, R., Tseng, J.R., Gonzalgo, M.L., Gambhir, S.S., Wu, J.C., 2006. Effects of Epigenetic Modulation on Reporter Gene Expression: Implications for Stem Cell Imaging. FASEB J 20, 106–108. https://doi.org/10.1096/fj.05-4551fje

Kronenberg, H.M., 2003. Developmental regulation of the growth plate. Nature 423, 332–336. https://doi.org/10.1038/nature01657

Kroon, L.M.G. de, Davidson, E.N.B., Narcisi, R., Farrell, E., Kraan, P.M. van der, van Osch, G.J.V.M., 2017. Activin and Nodal Are Not Suitable Alternatives to TGFβ for Chondrogenic Differentiation of Mesenchymal Stem Cells. Cartilage 8, 432–438. https://doi.org/10.1177/1947603516667585

Kume, T., 2010. Specification of arterial, venous, and lymphatic endothelial cells during embryonic development. Histol Histopathol 25, 637–646.

Kusuma, S., Peijnenburg, E., Patel, P., Gerecht, S., 2014. Low oxygen tension enhances endothelial fate of human pluripotent stem cells. Arterioscler Thromb Vasc Biol 34, 913–920. https://doi.org/10.1161/ATVBAHA.114.303274

Kusumbe, A.P., Ramasamy, S.K., Adams, R.H., 2014. Coupling of angiogenesis and osteogenesis by a specific vessel subtype in bone. Nature 507, 323–328. https://doi.org/10.1038/nature13145

Kusumbe, A.P., Ramasamy, S.K., Starsichova, A., Adams, R.H., 2015. Sample preparation for high-resolution 3D confocal imaging of mouse skeletal tissue. Nature Protocols 10, 1904–1914. https://doi.org/10.1038/nprot.2015.125

LaBonne, C., Whitman, M., 1994. Mesoderm induction by activin requires FGF-mediated intracellular signals. Development 120, 463–472.

LaBonty, M., Pray, N., Yelick, P.C., 2017. A Zebrafish Model of Human Fibrodysplasia Ossificans Progressiva. Zebrafish 14, 293–304. https://doi.org/10.1089/zeb.2016.1398

LaBonty, M., Yelick, P.C., 2018. Animal models of Fibrodysplasia Ossificans Progressiva. Dev Dyn 247, 279–288. https://doi.org/10.1002/dvdy.24606

Lackner, D.H., Carré, A., Guzzardo, P.M., Banning, C., Mangena, R., Henley, T., Oberndorfer, S., Gapp, B.V., Nijman, S.M.B., Brummelkamp, T.R., Bürckstümmer, T., 2015. A generic strategy for CRISPR-Cas9-mediated gene tagging. Nature Communications 6, ncomms10237. https://doi.org/10.1038/ncomms10237

Lamouille, S., Xu, J., Derynck, R., 2014. Molecular mechanisms of epithelial–mesenchymal transition. Nat Rev Mol Cell Biol 15, 178–196. https://doi.org/10.1038/nrm3758

Lampugnani, M.G., Corada, M., Caveda, L., Breviario, F., Ayalon, O., Geiger, B., Dejana, E., 1995. The molecular organization of endothelial cell to cell junctions: differential association of plakoglobin, beta-catenin, and alpha-catenin with vascular endothelial cadherin (VE-cadherin). J. Cell Biol. 129, 203–217.

Lanahan, A.A., Hermans, K., Claes, F., Kerley-Hamilton, J.S., Zhuang, Z.W., Giordano, F.J., Carmeliet, P., Simons, M., 2010. VEGF receptor 2 endocytic trafficking regulates arterial morphogenesis. Dev Cell 18, 713–724. https://doi.org/10.1016/j.devcel.2010.02.016

Langen, U.H., Pitulescu, M.E., Kim, J.M., Enriquez-Gasca, R., Sivaraj, K.K., Kusumbe, A.P., Singh, A., Di Russo, J., Bixel, M.G., Zhou, B., Sorokin, L., Vaquerizas, J.M., Adams, R.H., 2017. Cell-matrix signals specify bone endothelial cells during developmental osteogenesis. Nat Cell Biol 19, 189–201. https://doi.org/10.1038/ncb3476

Langenfeld, E.M., Langenfeld, J., 2004. Bone Morphogenetic Protein-2 Stimulates Angiogenesis in Developing Tumors11NIH K22 grant CA91919-01A1 and UMDNJ Foundation to J. Langenfeld. Mol Cancer Res 2, 141–149.

Larrivée, B., Prahst, C., Gordon, E., del Toro, R., Mathivet, T., Duarte, A., Simons, M., Eichmann, A., 2012. ALK1 signaling inhibits angiogenesis by cooperating with the Notch pathway. Dev Cell 22, 489–500. https://doi.org/10.1016/j.devcel.2012.02.005

Latres, E., Mastaitis, J., Fury, W., Miloscio, L., Trejos, J., Pangilinan, J., Okamoto, H., Cavino, K., Na, E., Papatheodorou, A., Willer, T., Bai, Y., Hae Kim, J., Rafique, A., Jaspers, S., Stitt, T., Murphy, A.J., Yancopoulos, G.D., Gromada, J., 2017. Activin A more prominently regulates muscle mass in primates than does GDF8. Nature Communications 8, 15153. https://doi.org/10.1038/ncomms15153

Le, V.Q., Wharton, K.A., 2012. Hyperactive BMP signaling induced by ALK2R206H requires type II receptor function in a Drosophila model for classic fibrodysplasia ossificans progressiva. Developmental Dynamics 241, 200–214. https://doi.org/10.1002/dvdy.22779

Lebrin, F., Goumans, M.-J., Jonker, L., Carvalho, R.L.C., Valdimarsdottir, G., Thorikay, M., Mummery, C., Arthur, H.M., ten Dijke, P., 2004. Endoglin promotes endothelial cell proliferation and TGF-beta/ALK1 signal transduction. EMBO J. 23, 4018–4028. https://doi.org/10.1038/sj.emboj.7600386

Lee, C.M., Davis, T.H., Deshmukh, H., Bao, G., 2016. 131. Chromatin-Dependent Loci Accessibility Affects CRISPR-Cas9 Targeting Efficiency. Molecular Therapy 24, S54. https://doi.org/10.1016/S1525-0016(16)32940-9

Lee, H.-W., Chong, D.C., Ola, R., Dunworth, W.P., Meadows, S., Ka, J., Kaartinen, V.M., Qyang, Y., Cleaver, O., Bautch, V.L., Eichmann, A., Jin, S.-W., 2017. Alk2/ACVR1 and Alk3/BMPR1A Provide Essential Function for Bone Morphogenetic Protein-Induced Retinal Angiogenesis. Arterioscler. Thromb. Vasc. Biol. 37, 657–663. https://doi.org/10.1161/ATVBAHA.116.308422

Lees-Shepard, J.B., Goldhamer, D.J., 2018. Stem cells and heterotopic ossification: Lessons from animal models. Bone 109, 178–186. https://doi.org/10.1016/j.bone.2018.01.029

Lees-Shepard, J.B., Yamamoto, M., Biswas, A.A., Stoessel, S.J., Nicholas, S.-A.E., Cogswell, C.A., Devarakonda, P.M., Schneider, M.J., Cummins, S.M.,

Legendre, N.P., Yamamoto, S., Kaartinen, V., Hunter, J.W., Goldhamer, D.J., 2018. Activin-dependent signaling in fibro/adipogenic progenitors causes fibrodysplasia ossificans progressiva. Nat Commun 9, 471. https://doi.org/10.1038/s41467-018-02872-2

Letamendía, A., Lastres, P., Botella, L.M., Raab, U., Langa, C., Velasco, B., Attisano, L., Bernabeu, C., 1998. Role of endoglin in cellular responses to transforming growth factor-beta. A comparative study with betaglycan. J. Biol. Chem. 273, 33011–33019.

Lewis, K.A., Gray, P.C., Blount, A.L., MacConell, L.A., Wiater, E., Bilezikjian, L.M., Vale, W., 2000. Betaglycan binds inhibin and can mediate functional antagonism of activin signalling. Nature 404, 411–414. https://doi.org/10.1038/35006129

Lewis, T.C., Prywes, R., 2013. Serum regulation of Id1 expression by a BMP pathway and BMP responsive element. Biochim. Biophys. Acta 1829, 1147–1159. https://doi.org/10.1016/j.bbagrm.2013.08.002

Li, S., Shimono, C., Norioka, N., Nakano, I., Okubo, T., Yagi, Y., Hayashi, M., Sato, Y., Fujisaki, H., Hattori, S., Sugiura, N., Kimata, K., Sekiguchi, K., 2010. Activin A binds to perlecan through its pro-region that has heparin/heparan sulfate binding activity. J. Biol. Chem. 285, 36645–36655. https://doi.org/10.1074/jbc.M110.177865

Lian, X., Zhang, J., Azarin, S.M., Zhu, K., Hazeltine, L.B., Bao, X., Hsiao, C., Kamp, T.J., Palecek, S.P., 2013. Directed cardiomyocyte differentiation from human pluripotent stem cells by modulating Wnt/β-catenin signaling under fully defined conditions. Nature Protocols 8, 162–175. https://doi.org/10.1038/nprot.2012.150

Lin, H.Y., Wang, X.F., Ng-Eaton, E., Weinberg, R.A., Lodish, H.F., 1992. Expression cloning of the TGF-beta type II receptor, a functional transmembrane serine/threonine kinase. Cell 68, 775–785. https://doi.org/10.1016/0092-8674(92)90152-3

Ling, N., Ying, S.Y., Ueno, N., Shimasaki, S., Esch, F., Hotta, M., Guillemin, R., 1986. Pituitary FSH is released by a heterodimer of the beta-subunits from the two forms of inhibin. Nature 321, 779–782. https://doi.org/10.1038/321779a0

Little, S.C., Mullins, M.C., 2009. Bone morphogenetic protein heterodimers assemble heteromeric type I receptor complexes to pattern the dorsoventral axis. Nat Cell Biol 11, 637–643. https://doi.org/10.1038/ncb1870

Liu, G., David, B.T., Trawczynski, M., Fessler, R.G., 2020. Advances in Pluripotent Stem Cells: History, Mechanisms, Technologies, and Applications. Stem Cell Rev and Rep 16, 3–32. https://doi.org/10.1007/s12015-019-09935-x

Liu, M., Rehman, S., Tang, X., Gu, K., Fan, Q., Chen, D., Ma, W., 2019. Methodologies for Improving HDR Efficiency. Front. Genet. 9. https://doi.org/10.3389/fgene.2018.00691

Liu, Y., Olsen, B.R., 2014. Distinct VEGF Functions During Bone Development and Homeostasis. Arch. Immunol. Ther. Exp. 62, 363–368. https://doi.org/10.1007/s00005-014-0285-y

Lo, R.S., Chen, Y.G., Shi, Y., Pavletich, N.P., Massagué, J., 1998. The L3 loop: a structural motif determining specific interactions between SMAD proteins and TGF-beta receptors. EMBO J 17, 996–1005. https://doi.org/10.1093/emboj/17.4.996

Lobov, I.B., Renard, R.A., Papadopoulos, N., Gale, N.W., Thurston, G., Yancopoulos, G.D., Wiegand, S.J., 2007. Delta-like ligand 4 (Dll4) is induced by VEGF as a

negative regulator of angiogenic sprouting. Proc. Natl. Acad. Sci. U.S.A. 104, 3219–3224. https://doi.org/10.1073/pnas.0611206104

Logan, M., Martin, J.F., Nagy, A., Lobe, C., Olson, E.N., Tabin, C.J., 2002. Expression of Cre Recombinase in the developing mouse limb bud driven by a Prxl enhancer. Genesis 33, 77–80. https://doi.org/10.1002/gene.10092

López-Casillas, F., Wrana, J.L., Massagué, J., 1993. Betaglycan presents ligand to the TGF beta signaling receptor. Cell 73, 1435–1444. https://doi.org/10.1016/0092-8674(93)90368-z

Lounev, V.Y., Ramachandran, R., Wosczyna, M.N., Yamamoto, M., Maidment, A.D.A., Shore, E.M., Glaser, D.L., Goldhamer, D.J., Kaplan, F.S., 2009. Identification of progenitor cells that contribute to heterotopic skeletogenesis. J Bone Joint Surg Am 91, 652–663. https://doi.org/10.2106/JBJS.H.01177

Love, M.I., Huber, W., Anders, S., 2014. Moderated estimation of fold change and dispersion for RNA-seq data with DESeq2. Genome Biol. 15, 550. https://doi.org/10.1186/s13059-014-0550-8

Lucarelli, P., Schilling, M., Kreutz, C., Vlasov, A., Boehm, M.E., Iwamoto, N., Steiert, B., Lattermann, S., Wäsch, M., Stepath, M., Matter, M.S., Heikenwälder, M., Hoffmann, K., Deharde, D., Damm, G., Seehofer, D., Muciek, M., Gretz, N., Lehmann, W.D., Timmer, J., Klingmüller, U., 2018. Resolving the Combinatorial Complexity of Smad Protein Complex Formation and Its Link to Gene Expression. Cell Syst 6, 75-89.e11. https://doi.org/10.1016/j.cels.2017.11.010

Luo, X., Hutley, L.J., Webster, J.A., Kim, Y.-H., Liu, D.-F., Newell, F.S., Widberg, C.H., Bachmann, A., Turner, N., Schmitz-Peiffer, C., Prins, J.B., Yang, G.-S., Whitehead, J.P., 2012. Identification of BMP and Activin Membrane-Bound Inhibitor (BAMBI) as a Potent Negative Regulator of Adipogenesis and Modulator of Autocrine/Paracrine Adipogenic Factors. Diabetes 61, 124–136. https://doi.org/10.2337/db11-0998

Luxán Guillermo, D'Amato Gaetano, MacGrogan Donal, de la Pompa José Luis, 2016. Endocardial Notch Signaling in Cardiac Development and Disease. Circulation Research 118, e1–e18. https://doi.org/10.1161/CIRCRESAHA.115.305350

Ma, J., Sánchez-Duffhues, G., Goumans, M.-J., ten Dijke, P., 2020. TGF-β-Induced Endothelial to Mesenchymal Transition in Disease and Tissue Engineering. Front. Cell Dev. Biol. 8. https://doi.org/10.3389/fcell.2020.00260

Machiya, A., Tsukamoto, S., Ohte, S., Kuratani, M., Fujimoto, M., Kumagai, K., Osawa, K., Suda, N., Bullock, A.N., Katagiri, T., 2018. Effects of FKBP12 and type II BMP receptors on signal transduction by ALK2 activating mutations associated with genetic disorders. Bone 111, 101–108. https://doi.org/10.1016/j.bone.2018.03.015

Macias, M.J., Martin-Malpartida, P., Massagué, J., 2015. Structural determinants of SMAD function in TGF-β signaling. Trends Biochem Sci 40, 296–308. https://doi.org/10.1016/j.tibs.2015.03.012

Macías-Silva, M., Hoodless, P.A., Tang, S.J., Buchwald, M., Wrana, J.L., 1998. Specific activation of Smad1 signaling pathways by the BMP7 type I receptor, ALK2. J. Biol. Chem. 273, 25628–25636. https://doi.org/10.1074/jbc.273.40.25628

Mack, J.J., Iruela-Arispe, M.L., 2018. NOTCH regulation of the endothelial cell phenotype. Current Opinion in Hematology 25, 212–218. https://doi.org/10.1097/MOH.0000000000000425

Maes, C., Carmeliet, P., Moermans, K., Stockmans, I., Smets, N., Collen, D., Bouillon, R., Carmeliet, G., 2002. Impaired angiogenesis and endochondral bone formation in mice lacking the vascular endothelial growth factor isoforms VEGF164 and VEGF188. Mechanisms of Development 111, 61–73. https://doi.org/10.1016/S0925-4773(01)00601-3

Maes, C., Goossens, S., Bartunkova, S., Drogat, B., Coenegrachts, L., Stockmans, I., Moermans, K., Nyabi, O., Haigh, K., Naessens, M., Haenebalcke, L., Tuckermann, J.P., Tjwa, M., Carmeliet, P., Mandic, V., David, J.-P., Behrens, A., Nagy, A., Carmeliet, G., Haigh, J.J., 2010. Increased skeletal VEGF enhances β-catenin activity and results in excessively ossified bones. The EMBO Journal 29, 424–441. https://doi.org/10.1038/emboj.2009.361

Maeshima, K., Kojima, I., Kishi, S., 2011. The Role of activin A in Angiogenesis. Invest. Ophthalmol. Vis. Sci. 52, 4839–4839.

Maffioletti, S.M., Sarcar, S., Henderson, A.B.H., Mannhardt, I., Pinton, L., Moyle, L.A., Steele-Stallard, H., Cappellari, O., Wells, K.E., Ferrari, G., Mitchell, J.S., Tyzack, G.E., Kotiadis, V.N., Khedr, M., Ragazzi, M., Wang, W., Duchen, M.R., Patani, R., Zammit, P.S., Wells, D.J., Eschenhagen, T., Tedesco, F.S., 2018. Three-Dimensional Human iPSC-Derived Artificial Skeletal Muscles Model Muscular Dystrophies and Enable Multilineage Tissue Engineering. Cell Rep 23, 899–908. https://doi.org/10.1016/j.celrep.2018.03.091

Man, S., Sanchez Duffhues, G., ten Dijke, P., Baker, D., 2019. The therapeutic potential of targeting the endothelial-to-mesenchymal transition. Angiogenesis 22, 3–13. https://doi.org/10.1007/s10456-018-9639-0

Manolagas, S.C., Parfitt, A.M., 2010. WHAT OLD MEANS TO BONE. Trends Endocrinol Metab 21, 369–374. https://doi.org/10.1016/j.tem.2010.01.010

Marinho, P.A., Chailangkarn, T., Muotri, A.R., 2015. Systematic optimization of human pluripotent stem cells media using Design of Experiments. Scientific Reports 5, 9834. https://doi.org/10.1038/srep09834

Marsell, R., Einhorn, T.A., 2011. THE BIOLOGY OF FRACTURE HEALING. Injury 42, 551–555. https://doi.org/10.1016/j.injury.2011.03.031

Martinez-Hackert, E., Sundan, A., Holien, T., 2020. Receptor binding competition: A paradigm for regulating TGF-β family action. Cytokine & Growth Factor Reviews. https://doi.org/10.1016/j.cytogfr.2020.09.003

Martin-Malpartida, P., Batet, M., Kaczmarska, Z., Freier, R., Gomes, T., Aragón, E., Zou, Y., Wang, Q., Xi, Q., Ruiz, L., Vea, A., Márquez, J.A., Massagué, J., Macias, M.J., 2017. Structural basis for genome wide recognition of 5-bp GC motifs by SMAD transcription factors. Nature Communications 8, 2070. https://doi.org/10.1038/s41467-017-02054-6

Massagué, J., Like, B., 1985. Cellular receptors for type beta transforming growth factor. Ligand binding and affinity labeling in human and rodent cell lines. J Biol Chem 260, 2636–2645.

Matsumoto, Y., Hayashi, Y., Schlieve, C.R., Ikeya, M., Kim, H., Nguyen, T.D., Sami, S., Baba, S., Barruet, E., Nasu, A., Asaka, I., Otsuka, T., Yamanaka, S., Conklin, B.R., Toguchida, J., Hsiao, E.C., 2013. Induced pluripotent stem cells from patients with human fibrodysplasia ossificans progressiva show increased mineralization and cartilage formation. Orphanet J Rare Dis 8, 190. https://doi.org/10.1186/1750-1172-8-190

Matsumoto, Y., Ikeya, M., Hino, K., Horigome, K., Fukuta, M., Watanabe, M., Nagata, S., Yamamoto, T., Otsuka, T., Toguchida, J., 2015. New Protocol to Optimize iPS Cells for Genome Analysis of Fibrodysplasia Ossificans Progressiva. STEM CELLS 33, 1730–1742. https://doi.org/10.1002/stem.1981

Matzuk, M.M., Kumar, T.R., Bradley, A., 1995a. Different phenotypes for mice deficient in either activins or activin receptor type II. Nature 374, 356–360. https://doi.org/10.1038/374356a0

Matzuk, M.M., Kumar, T.R., Vassalli, A., Bickenbach, J.R., Roop, D.R., Jaenisch, R., Bradley, A., 1995b. Functional analysis of activins during mammalian development. Nature 374, 354–356. https://doi.org/10.1038/374354a0

McCarthy, S.A., Bicknell, R., 1993. Inhibition of vascular endothelial cell growth by activin-A. J. Biol. Chem. 268, 23066–23071.

McKusick, V.A., 1959. Hereditary Disorders of Connective Tissue. Bull N Y Acad Med 35, 143–156.

Medici, D., Shore, E.M., Lounev, V.Y., Kaplan, F.S., Kalluri, R., Olsen, B.R., 2010. Conversion of vascular endothelial cells into multipotent stem-like cells. Nat Med 16, 1400–6. https://doi.org/10.1038/nm.2252

Mellor, S.L., Ball, E.M.A., O'Connor, A.E., Ethier, J.-F., Cranfield, M., Schmitt, J.F., Phillips, D.J., Groome, N.P., Risbridger, G.P., 2003. Activin betaC-subunit heterodimers provide a new mechanism of regulating activin levels in the prostate. Endocrinology 144, 4410–4419. https://doi.org/10.1210/en.2003-0225

Mellor, S.L., Cranfield, M., Ries, R., Pedersen, J., Cancilla, B., de Kretser, D., Groome, N.P., Mason, A.J., Risbridger, G.P., 2000. Localization of activin beta(A)-, beta(B)-, and beta(C)-subunits in humanprostate and evidence for formation of new activin heterodimers of beta(C)-subunit. J. Clin. Endocrinol. Metab. 85, 4851–4858. https://doi.org/10.1210/jcem.85.12.7052

Mendoza, V., Vilchis-Landeros, M.M., Mendoza-Hernández, G., Huang, T., Villarreal, M.M., Hinck, A.P., López-Casillas, F., Montiel, J.-L., 2009. Betaglycan has two independent domains required for high affinity TGF-β binding: proteolytic cleavage separates the domains and inactivates the neutralizing activity of the soluble receptor. Biochemistry 48, 11755–11765. https://doi.org/10.1021/bi901528w

Messenger, N.J., Kabitschke, C., Andrews, R., Grimmer, D., Miguel, R.N., Blundell, T.L., Smith, J.C., Wardle, F.C., 2005. Functional Specificity of the Xenopus T-Domain Protein Brachyury Is Conferred by Its Ability to Interact with Smad1. Developmental Cell 8, 599–610. https://doi.org/10.1016/j.devcel.2005.03.001

Meyers, C., Lisiecki, J., Miller, S., Levin, A., Fayad, L., Ding, C., Sono, T., McCarthy, E., Levi, B., James, A.W., 2019. Heterotopic Ossification: A Comprehensive Review. JBMR Plus 3, e10172. https://doi.org/10.1002/jbm4.10172

Mi, L.-Z., Brown, C.T., Gao, Y., Tian, Y., Le, V.Q., Walz, T., Springer, T.A., 2015. Structure of bone morphogenetic protein 9 procomplex. Proc. Natl. Acad. Sci. U.S.A. 112, 3710–3715. https://doi.org/10.1073/pnas.1501303112

Micha, D., Voermans, E., Eekhoff, M.E.W., van Essen, H.W., Zandieh-Doulabi, B., Netelenbos, C., Rustemeyer, T., Sistermans, E.A., Pals, G., Bravenboer, N., 2016. Inhibition of TGFβ signaling decreases osteogenic differentiation of fibrodysplasia ossificans progressiva fibroblasts in a novel in vitro model of the disease. Bone 84, 169–180. https://doi.org/10.1016/j.bone.2016.01.004

Minina, E., Kreschel, C., Naski, M.C., Ornitz, D.M., Vortkamp, A., 2002. Interaction of FGF, Ihh/Pthlh, and BMP signaling integrates chondrocyte proliferation and hypertrophic differentiation. Dev Cell 3, 439–449. https://doi.org/10.1016/s1534-5807(02)00261-7

Mishina, Y., Crombie, R., Bradley, A., Behringer, R.R., 1999. Multiple roles for activin-like kinase-2 signaling during mouse embryogenesis. Dev. Biol. 213, 314–326. https://doi.org/10.1006/dbio.1999.9378

Mishina, Y., Suzuki, A., Ueno, N., Behringer, R.R., 1995. Bmpr encodes a type I bone morphogenetic protein receptor that is essential for gastrulation during mouse embryogenesis. Genes Dev. 9, 3027–3037. https://doi.org/10.1101/gad.9.24.3027

Mitrofan, C.-G., Appleby, S.L., Nash, G.B., Mallat, Z., Chilvers, E.R., Upton, P.D., Morrell, N.W., 2017. Bone morphogenetic protein 9 (BMP9) and BMP10 enhance tumor necrosis factor-α-induced monocyte recruitment to the vascular endothelium mainly via activin receptor-like kinase 2. J Biol Chem 292, 13714–13726. https://doi.org/10.1074/jbc.M117.778506

Miyazawa, K., Miyazono, K., 2017. Regulation of TGF-β Family Signaling by Inhibitory Smads. Cold Spring Harb Perspect Biol 9. https://doi.org/10.1101/cshperspect.a022095

Mohedas, A.H., Xing, X., Armstrong, K.A., Bullock, A.N., Cuny, G.D., Yu, P.B., 2013. Development of an ALK2-biased BMP type I receptor kinase inhibitor. ACS Chem Biol 8, 1291–1302. https://doi.org/10.1021/cb300655w

Moonen, J.-R.A.J., Krenning, G., Brinker, M.G.L., Koerts, J.A., van Luyn, M.J.A., Harmsen, M.C., 2010. Endothelial progenitor cells give rise to pro-angiogenic smooth muscle-like progeny. Cardiovasc. Res. 86, 506–515. https://doi.org/10.1093/cvr/cvq012

Morales-Piga, A., Bachiller-Corral, F.J., Sánchez-Duffhues, G., 2014. Is “fibrodysplasia ossificans progressiva” a vascular disease? A groundbreaking pathogenic model. Reumatol Clin 10, 389–395. https://doi.org/10.1016/j.reuma.2014.05.001

Morikawa, M., Koinuma, D., Miyazono, K., Heldin, C.-H., 2013. Genome-wide mechanisms of Smad binding. Oncogene 32, 1609–1615. https://doi.org/10.1038/onc.2012.191

Morikawa, M., Koinuma, D., Tsutsumi, S., Vasilaki, E., Kanki, Y., Heldin, C.-H., Aburatani, H., Miyazono, K., 2011. ChIP-seq reveals cell type-specific binding patterns of BMP-specific Smads and a novel binding motif. Nucleic Acids Res. 39, 8712–8727. https://doi.org/10.1093/nar/gkr572

Mortzfeld, B.M., Taubenheim, J., Klimovich, A.V., Fraune, S., Rosenstiel, P., Bosch, T.C.G., 2019. Temperature and insulin signaling regulate body size in Hydra by the Wnt and TGF-beta pathways. Nature Communications 10, 3257. https://doi.org/10.1038/s41467-019-11136-6

Moskowitz, I.P., Wang, J., Peterson, M.A., Pu, W.T., Mackinnon, A.C., Oxburgh, L., Chu, G.C., Sarkar, M., Berul, C., Smoot, L., Robertson, E.J., Schwartz, R., Seidman, J.G., Seidman, C.E., 2011. Transcription factor genes Smad4 and Gata4 cooperatively regulate cardiac valve development. [corrected]. Proc. Natl. Acad. Sci. U.S.A. 108, 4006–4011. https://doi.org/10.1073/pnas.1019025108

Mossahebi-Mohammadi, M., Quan, M., Zhang, J.-S., Li, X., 2020. FGF Signaling Pathway: A Key Regulator of Stem Cell Pluripotency. Front Cell Dev Biol 8. https://doi.org/10.3389/fcell.2020.00079

Mouillesseaux, K.P., Wiley, D.S., Saunders, L.M., Wylie, L.A., Kushner, E.J., Chong, D.C., Citrin, K.M., Barber, A.T., Park, Y., Kim, J.-D., Samsa, L.A., Kim, J., Liu, J., Jin, S.-W., Bautch, V.L., 2016. Notch regulates BMP responsiveness and lateral branching in vessel networks via SMAD6. Nat Commun 7, 1–12. https://doi.org/10.1038/ncomms13247

Moya, I.M., Umans, L., Maas, E., Pereira, P.N.G., Beets, K., Francis, A., Sents, W., Robertson, E.J., Mummery, C.L., Huylebroeck, D., Zwijsen, A., 2012. Stalk cell

phenotype depends on integration of Notch and Smad1/5 signaling cascades. Dev. Cell 22, 501–514. https://doi.org/10.1016/j.devcel.2012.01.007
Mueller, T.D., Nickel, J., 2012. Promiscuity and specificity in BMP receptor activation. FEBS Letters, Sorting the TGF-β Labyrinth 586, 1846–1859. https://doi.org/10.1016/j.febslet.2012.02.043
Mullen, A.C., Wrana, J.L., 2017. TGF-β Family Signaling in Embryonic and Somatic Stem-Cell Renewal and Differentiation. Cold Spring Harb Perspect Biol 9. https://doi.org/10.1101/cshperspect.a022186
Muñoz-Félix, J.M., Cuesta, C., Perretta-Tejedor, N., Subileau, M., López-Hernández, F.J., López-Novoa, J.M., Martínez-Salgado, C., 2016. Identification of bone morphogenetic protein 9 (BMP9) as a novel profibrotic factor in vitro. Cellular Signalling 28, 1252–1261. https://doi.org/10.1016/j.cellsig.2016.05.015
Nagarajan, R.P., Zhang, J., Li, W., Chen, Y., 1999. Regulation of Smad7 promoter by direct association with Smad3 and Smad4. J. Biol. Chem. 274, 33412–33418. https://doi.org/10.1074/jbc.274.47.33412
Nagy, J.A., Benjamin, L., Zeng, H., Dvorak, A.M., Dvorak, H.F., 2008. Vascular permeability, vascular hyperpermeability and angiogenesis. Angiogenesis 11, 109–119. https://doi.org/10.1007/s10456-008-9099-z
Nagy, J.A., Dvorak, A.M., Dvorak, H.F., 2007. VEGF-A and the induction of pathological angiogenesis. Annu Rev Pathol 2, 251–275. https://doi.org/10.1146/annurev.pathol.2.010506.134925
Naito, H., Iba, T., Takakura, N., 2020. Mechanisms of new blood-vessel formation and proliferative heterogeneity of endothelial cells. Int Immunol 32, 295–305. https://doi.org/10.1093/intimm/dxaa008
Namwanje, M., Brown, C.W., 2016. Activins and Inhibins: Roles in Development, Physiology, and Disease. Cold Spring Harb Perspect Biol 8. https://doi.org/10.1101/cshperspect.a021881
Neal, A., Nornes, S., Payne, S., Wallace, M.D., Fritzsche, M., Louphrasitthiphol, P., Wilkinson, R.N., Chouliaras, K.M., Liu, K., Plant, K., Sholapurkar, R., Ratnayaka, I., Herzog, W., Bond, G., Chico, T., Bou-Gharios, G., De Val, S., 2019. Venous identity requires BMP signalling through ALK3. Nature Communications 10, 453. https://doi.org/10.1038/s41467-019-08315-w
Nickel, J., Kotzsch, A., Sebald, W., Mueller, T.D., 2005. A single residue of GDF-5 defines binding specificity to BMP receptor IB. J. Mol. Biol. 349, 933–947. https://doi.org/10.1016/j.jmb.2005.04.015
Nickel, J., ten Dijke, P., Mueller, T.D., 2018. TGF-β family co-receptor function and signaling. Acta Biochim Biophys Sin (Shanghai) 50, 12–36. https://doi.org/10.1093/abbs/gmx126
Niethamer, T.K., Stabler, C.T., Leach, J.P., Zepp, J.A., Morley, M.P., Babu, A., Zhou, S., Morrisey, E.E., 2020. Defining the role of pulmonary endothelial cell heterogeneity in the response to acute lung injury. Elife 9. https://doi.org/10.7554/eLife.53072
Nimmagadda, S., Geetha Loganathan, P., Huang, R., Scaal, M., Schmidt, C., Christ, B., 2005. BMP4 and noggin control embryonic blood vessel formation by antagonistic regulation of VEGFR-2 (Quek1) expression. Dev. Biol. 280, 100–110. https://doi.org/10.1016/j.ydbio.2005.01.005
Nohe, A., Hassel, S., Ehrlich, M., Neubauer, F., Sebald, W., Henis, Y.I., Knaus, P., 2002. The mode of bone morphogenetic protein (BMP) receptor oligomerization determines different BMP-2 signaling pathways. J. Biol. Chem. 277, 5330–5338. https://doi.org/10.1074/jbc.M102750200

Nolan, K., Kattamuri, C., Rankin, S.A., Read, R.J., Zorn, A.M., Thompson, T.B., 2016. Structure of Gremlin-2 in Complex with GDF5 Gives Insight into DAN-Family-Mediated BMP Antagonism. Cell Rep 16, 2077–2086. https://doi.org/10.1016/j.celrep.2016.07.046

Noseda, M., McLean, G., Niessen, K., Chang, L., Pollet, I., Montpetit, R., Shahidi, R., Dorovini-Zis, K., Li, L., Beckstead, B., Durand, R.E., Hoodless, P.A., Karsan, A., 2004. Notch activation results in phenotypic and functional changes consistent with endothelial-to-mesenchymal transformation. Circ Res 94, 910–917. https://doi.org/10.1161/01.RES.0000124300.76171.C9

Oh, S.P., Li, E., 1997. The signaling pathway mediated by the type IIB activin receptor controls axial patterning and lateral asymmetry in the mouse. Genes Dev. 11, 1812–1826. https://doi.org/10.1101/gad.11.14.1812

Oh, S. Paul, Seki, T., Goss, K.A., Imamura, T., Yi, Y., Donahoe, P.K., Li, L., Miyazono, K., ten Dijke, P., Kim, S., Li, E., 2000. Activin receptor-like kinase 1 modulates transforming growth factor-β1 signaling in the regulation of angiogenesis. Proc Natl Acad Sci U S A 97, 2626–2631.

Olsen, O.E., Hella, H., Elsaadi, S., Jacobi, C., Martinez-Hackert, E., Holien, T., 2020. Activins as Dual Specificity TGF-β Family Molecules: SMAD-Activation via Activin- and BMP-Type 1 Receptors. Biomolecules 10, 519. https://doi.org/10.3390/biom10040519

Olsen, O.E., Sankar, M., Elsaadi, S., Hella, H., Buene, G., Darvekar, S.R., Misund, K., Katagiri, T., Knaus, P., Holien, T., 2018b. BMPR2 inhibits activin and BMP signaling via wild-type ALK2. J Cell Sci 131. https://doi.org/10.1242/jcs.213512

Olsen, O.E., Wader, K.F., Hella, H., Mylin, A.K., Turesson, I., Nesthus, I., Waage, A., Sundan, A., Holien, T., 2015. Activin A inhibits BMP-signaling by binding ACVR2A and ACVR2B. Cell Commun. Signal 13, 27. https://doi.org/10.1186/s12964-015-0104-z

Onichtchouk, D., Chen, Y.G., Dosch, R., Gawantka, V., Delius, H., Massagué, J., Niehrs, C., 1999. Silencing of TGF-beta signalling by the pseudoreceptor BAMBI. Nature 401, 480–485. https://doi.org/10.1038/46794

Orlova, V.V., van den Hil, F.E., Petrus-Reurer, S., Drabsch, Y., Ten Dijke, P., Mummery, C.L., 2014. Generation, expansion and functional analysis of endothelial cells and pericytes derived from human pluripotent stem cells. Nat Protoc 9, 1514–1531. https://doi.org/10.1038/nprot.2014.102

Paik, D.T., Tian, L., Lee, J., Sayed, N., Chen, I.Y., Rhee, S., Rhee, J.-W., Kim, Y., Wirka, R.C., Buikema, J.W., Wu, S.M., Red-Horse, K., Quertermous, T., Wu, J.C., 2018. Large-Scale Single-Cell RNA-Seq Reveals Molecular Signatures of Heterogeneous Populations of Human Induced Pluripotent Stem Cell-Derived Endothelial Cells. Circ Res 123, 443–450. https://doi.org/10.1161/CIRCRESAHA.118.312913

Pardali, E., Goumans, M.-J., ten Dijke, P., 2010. Signaling by members of the TGF-beta family in vascular morphogenesis and disease. Trends Cell Biol. 20, 556–567. https://doi.org/10.1016/j.tcb.2010.06.006

Park, C., Afrikanova, I., Chung, Y.S., Zhang, W.J., Arentson, E., Fong, G. hua, Rosendahl, A., Choi, K., 2004. A hierarchical order of factors in the generation of FLK1- and SCL-expressing hematopoietic and endothelial progenitors from embryonic stem cells. Development 131, 2749–2762. https://doi.org/10.1242/dev.01130

Park, J.E.S., Shao, D., Upton, P.D., deSouza, P., Adcock, I.M., Davies, R.J., Morrell, N.W., Griffiths, M.J.D., Wort, S.J., 2012. BMP-9 Induced Endothelial Cell Tubule Formation and Inhibition of Migration Involves Smad1 Driven

Endothelin-1 Production. PLOS ONE 7, e30075. https://doi.org/10.1371/journal.pone.0030075

Park, S.O., Wankhede, M., Lee, Y.J., Choi, E.-J., Fliess, N., Choe, S.-W., Oh, S.-H., Walter, G., Raizada, M.K., Sorg, B.S., Oh, S.P., 2009. Real-time imaging of de novo arteriovenous malformation in a mouse model of hereditary hemorrhagic telangiectasia. J Clin Invest 119, 3487–3496. https://doi.org/10.1172/JCI39482

Patsch, C., Challet-Meylan, L., Thoma, E.C., Urich, E., Heckel, T., O'Sullivan, J.F., Grainger, S.J., Kapp, F.G., Sun, L., Christensen, K., Xia, Y., Florido, M.H.C., He, W., Pan, W., Prummer, M., Warren, C.R., Jakob-Roetne, R., Certa, U., Jagasia, R., Freskgård, P.-O., Adatto, I., Kling, D., Huang, P., Zon, L.I., Chaikof, E.L., Gerszten, R.E., Graf, M., Iacone, R., Cowan, C.A., 2015. Generation of vascular endothelial and smooth muscle cells from human pluripotent stem cells. Nature Cell Biology 17, 994–1003. https://doi.org/10.1038/ncb3205

Pedrosa, A.-R., Trindade, A., Fernandes, A.-C., Carvalho, C., Gigante, J., Tavares, A.T., Diéguez-Hurtado, R., Yagita, H., Adams, R.H., Duarte, A., 2015. Endothelial Jagged1 antagonizes Dll4 regulation of endothelial branching and promotes vascular maturation downstream of Dll4/Notch1. Arterioscler. Thromb. Vasc. Biol. 35, 1134–1146. https://doi.org/10.1161/ATVBAHA.114.304741

Pepinsky, B., Gong, B.-J., Gao, Y., Lehmann, A., Ferrant, J., Amatucci, J., Sun, Y., Bush, M., Walz, T., Pederson, N., Cameron, T., Wen, D., 2017. A Prodomain Fragment from the Proteolytic Activation of Growth Differentiation Factor 11 Remains Associated with the Mature Growth Factor and Keeps It Soluble. Biochemistry 56, 4405–4418. https://doi.org/10.1021/acs.biochem.7b00302

Pera, M.F., Andrade, J., Houssami, S., Reubinoff, B., Trounson, A., Stanley, E.G., Ward-van Oostwaard, D., Mummery, C., 2004. Regulation of human embryonic stem cell differentiation by BMP-2 and its antagonist noggin. J Cell Sci 117, 1269–1280. https://doi.org/10.1242/jcs.00970

Persson, U., Izumi, H., Souchelnytskyi, S., Itoh, S., Grimsby, S., Engström, U., Heldin, C.H., Funa, K., ten Dijke, P., 1998. The L45 loop in type I receptors for TGF-beta family members is a critical determinant in specifying Smad isoform activation. FEBS Lett. 434, 83–87. https://doi.org/10.1016/s0014-5793(98)00954-5

Peterson, J.R., De La Rosa, S., Sun, H., Eboda, O., Cilwa, K.E., Donneys, A., Morris, M., Buchman, S.R., Cederna, P.S., Krebsbach, P.H., Wang, S.C., Levi, B., 2014. Burn Injury Enhances Bone Formation in Heterotopic Ossification Model. Ann Surg 259, 993–998. https://doi.org/10.1097/SLA.0b013e318291da85

Pettersen, E.F., Goddard, T.D., Huang, C.C., Couch, G.S., Greenblatt, D.M., Meng, E.C., Ferrin, T.E., 2004. UCSF Chimera--a visualization system for exploratory research and analysis. J Comput Chem 25, 1605–1612. https://doi.org/10.1002/jcc.20084

Pfaffl, M.W., 2001. A new mathematical model for relative quantification in real-time RT-PCR. Nucleic Acids Res. 29, e45. https://doi.org/10.1093/nar/29.9.e45

Phng, L.-K., Gerhardt, H., 2009. Angiogenesis: A Team Effort Coordinated by Notch. Developmental Cell 16, 196–208. https://doi.org/10.1016/j.devcel.2009.01.015

Pickup, M.W., Owens, P., Moses, H.L., 2017. TGF-β, Bone Morphogenetic Protein, and Activin Signaling and the Tumor Microenvironment. Cold Spring Harb Perspect Biol 9. https://doi.org/10.1101/cshperspect.a022285

Piek, E., Afrakhte, M., Sampath, K., van Zoelen, E.J., Heldin, C.H., ten Dijke, P., 1999. Functional antagonism between activin and osteogenic protein-1 in human embryonal carcinoma cells. J. Cell. Physiol. 180, 141–149. https://doi.org/10.1002/(SICI)1097-4652(199908)180:2<141::AID-JCP1>3.0.CO;2-I

Piera-Velazquez, S., Jimenez, S.A., 2019. Endothelial to Mesenchymal Transition: Role in Physiology and in the Pathogenesis of Human Diseases. Physiol. Rev. 99, 1281–1324. https://doi.org/10.1152/physrev.00021.2018

Pignolo, R.J., Foley, K.L., 2005. Nonhereditary heterotopic ossification Implications for Injury, Arthropathy, and Aging. Clinic Rev Bone Miner Metab 3, 261–266. https://doi.org/10.1385/BMM:3:3-4:261

Platonova, E., Winterflood, C.M., Junemann, A., Albrecht, D., Faix, J., Ewers, H., 2015. Single-molecule microscopy of molecules tagged with GFP or RFP derivatives in mammalian cells using nanobody binders. Methods, Super-resolution Light Microscopy 88, 89–97. https://doi.org/10.1016/j.ymeth.2015.06.018

Popp, B., Krumbiegel, M., Grosch, J., Sommer, A., Uebe, S., Kohl, Z., Plötz, S., Farrell, M., Trautmann, U., Kraus, C., Ekici, A.B., Asadollahi, R., Regensburger, M., Günther, K., Rauch, A., Edenhofer, F., Winkler, J., Winner, B., Reis, A., 2018. Need for high-resolution Genetic Analysis in iPSC: Results and Lessons from the ForIPS Consortium. Scientific Reports 8, 17201. https://doi.org/10.1038/s41598-018-35506-0

Prahst, C., Héroult, M., Lanahan, A.A., Uziel, N., Kessler, O., Shraga-Heled, N., Simons, M., Neufeld, G., Augustin, H.G., 2008. Neuropilin-1-VEGFR-2 Complexing Requires the PDZ-binding Domain of Neuropilin-1. J. Biol. Chem. 283, 25110–25114. https://doi.org/10.1074/jbc.C800137200

Prummel, K.D., Nieuwenhuize, S., Mosimann, C., 2020. The lateral plate mesoderm. Development 147. https://doi.org/10.1242/dev.175059

Racacho, L., Byrnes, A.M., MacDonald, H., Dranse, H.J., Nikkel, S.M., Allanson, J., Rosser, E., Underhill, T.M., Bulman, D.E., 2015. Two novel disease-causing variants in BMPR1B are associated with brachydactyly type A1. Eur J Hum Genet 23, 1640–1645. https://doi.org/10.1038/ejhg.2015.38

Radaev, S., Zou, Z., Huang, T., Lafer, E.M., Hinck, A.P., Sun, P.D., 2010. Ternary complex of transforming growth factor-beta1 reveals isoform-specific ligand recognition and receptor recruitment in the superfamily. J Biol Chem 285, 14806–14814. https://doi.org/10.1074/jbc.M109.079921

Ramachandran, A., Vizán, P., Das, D., Chakravarty, P., Vogt, J., Rogers, K.W., Müller, P., Hinck, A.P., Sapkota, G.P., Hill, C.S., 2018. TGF-β uses a novel mode of receptor activation to phosphorylate SMAD1/5 and induce epithelial-to-mesenchymal transition. eLife 7, e31756. https://doi.org/10.7554/eLife.31756

Ramasamy, S.K., Kusumbe, A.P., Wang, L., Adams, R.H., 2014. Endothelial Notch activity promotes angiogenesis and osteogenesis in bone. Nature 507, 376–380. https://doi.org/10.1038/nature13146

Ramoshebi, L.N., Ripamonti, U., 2000. Osteogenic protein-1, a bone morphogenetic protein, induces angiogenesis in the chick chorioallantoic membrane and synergizes with basic fibroblast growth factor and transforming growth factor-beta1. Anat. Rec. 259, 97–107. https://doi.org/10.1002/(SICI)1097-0185(20000501)259:1<97::AID-AR11>3.0.CO;2-O

Ran, F.A., Hsu, P.D., Wright, J., Agarwala, V., Scott, D.A., Zhang, F., 2013. Genome engineering using the CRISPR-Cas9 system. Nat Protoc 8, 2281–2308. https://doi.org/10.1038/nprot.2013.143

Rao, J., Greber, B., 2017. Concise Review: Signaling Control of Early Fate Decisions Around the Human Pluripotent Stem Cell State. STEM CELLS 35, 277–283. https://doi.org/10.1002/stem.2527

Raykhel, I., Moafi, F., Myllymäki, S.M., Greciano, P.G., Matlin, K.S., Moyano, J.V., Manninen, A., Myllyharju, J., 2018. BAMBI is a novel HIF1-dependent modulator of TGFβ-mediated disruption of cell polarity during hypoxia. J Cell Sci 131. https://doi.org/10.1242/jcs.210906

Reissmann, E., Jörnvall, H., Blokzijl, A., Andersson, O., Chang, C., Minchiotti, G., Persico, M.G., Ibáñez, C.F., Brivanlou, A.H., 2001. The orphan receptor ALK7 and the Activin receptor ALK4 mediate signaling by Nodal proteins during vertebrate development. Genes Dev 15, 2010–2022. https://doi.org/10.1101/gad.201801

Rejon, C.A., Hancock, M.A., Li, Y.N., Thompson, T.B., Hébert, T.E., Bernard, D.J., 2013. Activins bind and signal via bone morphogenetic protein receptor type II (BMPR2) in immortalized gonadotrope-like cells. Cell. Signal. 25, 2717–2726. https://doi.org/10.1016/j.cellsig.2013.09.002

Ren, R., Charles, P.C., Zhang, C., Wu, Y., Wang, H., Patterson, C., 2007. Gene expression profiles identify a role for cyclooxygenase 2-dependent prostanoid generation in BMP6-induced angiogenic responses. Blood 109, 2847–2853. https://doi.org/10.1182/blood-2006-08-039743

Ribatti, D., Crivellato, E., 2012. “Sprouting angiogenesis”, a reappraisal. Developmental Biology 372, 157–165. https://doi.org/10.1016/j.ydbio.2012.09.018

Ricard, N., Ciais, D., Levet, S., Subileau, M., Mallet, C., Zimmers, T.A., Lee, S.-J., Bidart, M., Feige, J.-J., Bailly, S., 2012. BMP9 and BMP10 are critical for postnatal retinal vascular remodeling. Blood 119, 6162–6171. https://doi.org/10.1182/blood-2012-01-407593

Ricard, N., Simons, M., 2015. When It Is Better to Regress: Dynamics of Vascular Pruning. PLOS Biology 13, e1002148. https://doi.org/10.1371/journal.pbio.1002148

Richter, A., Alexdottir, M.S., Magnus, S.H., Richter, T.R., Morikawa, M., Zwijsen, A., Valdimarsdottir, G., 2019. EGFL7 Mediates BMP9-Induced Sprouting Angiogenesis of Endothelial Cells Derived from Human Embryonic Stem Cells. Stem Cell Reports 12, 1250–1259. https://doi.org/10.1016/j.stemcr.2019.04.022

Richter, A., Valdimarsdottir, L., Hrafnkelsdottir, H.E., Runarsson, J.F., Omarsdottir, A.R., Oostwaard, D.W., Mummery, C., Valdimarsdottir, G., 2014. BMP4 Promotes EMT and Mesodermal Commitment in Human Embryonic Stem Cells via SLUG and MSX2. STEM CELLS 32, 636–648. https://doi.org/10.1002/stem.1592

Robinson, C.J., Stringer, S.E., 2001. The splice variants of vascular endothelial growth factor (VEGF) and their receptors. J. Cell. Sci. 114, 853–865.

Rocha, S.F., Adams, R.H., 2009. Molecular differentiation and specialization of vascular beds. Angiogenesis 12, 139–147. https://doi.org/10.1007/s10456-009-9132-x

Rodriguez, C., Chen, F., Weinberg, R.A., Lodish, H.F., 1995. Cooperative binding of transforming growth factor (TGF)-beta 2 to the types I and II TGF-beta

receptors. J. Biol. Chem. 270, 15919–15922. https://doi.org/10.1074/jbc.270.27.15919

Roman, B.L., Hinck, A.P., 2017. ALK1 signaling in development and disease: new paradigms. Cell Mol Life Sci 74, 4539–4560. https://doi.org/10.1007/s00018-017-2636-4

Rosa, S., Praça, C., Pitrez, P.R., Gouveia, P.J., Aranguren, X.L., Ricotti, L., Ferreira, L.S., 2019. Functional characterization of iPSC-derived arterial- and venous-like endothelial cells. Sci Rep 9, 1–15. https://doi.org/10.1038/s41598-019-40417-9

Rosenzweig, B.L., Imamura, T., Okadome, T., Cox, G.N., Yamashita, H., ten Dijke, P., Heldin, C.H., Miyazono, K., 1995. Cloning and characterization of a human type II receptor for bone morphogenetic proteins. Proc Natl Acad Sci U S A 92, 7632–7636.

Rossbach, B., Hildebrand, L., El-Ahmad, L., Stachelscheid, H., Reinke, P., Kurtz, A., 2017. Generation of a human induced pluripotent stem cell line from urinary cells of a healthy donor using integration free Sendai virus technology. Stem Cell Research 21, 167–170. https://doi.org/10.1016/j.scr.2016.09.002

Rossbach, B., Hildebrand, L., El-Ahmad, L., Stachelscheid, H., Reinke, P., Kurtz, A., 2016. Generation of a human induced pluripotent stem cell line from urinary cells of a healthy donor using an integration free vector. Stem Cell Research 16, 314–317. https://doi.org/10.1016/j.scr.2015.12.018

Rossi, E., Pericacho, M., Bachelot-Loza, C., Pidard, D., Gaussem, P., Poirault-Chassac, S., Blanco, F.J., Langa, C., González-Manchón, C., Novoa, J.M.L., Smadja, D.M., Bernabeu, C., 2018. Human endoglin as a potential new partner involved in platelet–endothelium interactions. Cell. Mol. Life Sci. 75, 1269–1284. https://doi.org/10.1007/s00018-017-2694-7

Rothhammer, T., Bataille, F., Spruss, T., Eissner, G., Bosserhoff, A.-K., 2007. Functional implication of BMP4 expression on angiogenesis in malignant melanoma. Oncogene 26, 4158–4170. https://doi.org/10.1038/sj.onc.1210182

Rufaihah, A.J., Huang, N.F., Kim, J., Herold, J., Volz, K.S., Park, T.S., Lee, J.C., Zambidis, E.T., Reijo-Pera, R., Cooke, J.P., 2013. Human induced pluripotent stem cell-derived endothelial cells exhibit functional heterogeneity. Am J Transl Res 5, 21–35.

Rydén, M., Imamura, T., Jörnvall, H., Belluardo, N., Neveu, I., Trupp, M., Okadome, T., ten Dijke, P., Ibáñez, C.F., 1996. A novel type I receptor serine-threonine kinase predominantly expressed in the adult central nervous system. J. Biol. Chem. 271, 30603–30609. https://doi.org/10.1074/jbc.271.48.30603

Sadick, H., Naim, R., Gössler, U., Hörmann, K., Riedel, F., 2005a. Angiogenesis in hereditary hemorrhagic telangiectasia: VEGF165 plasma concentration in correlation to the VEGF expression and microvessel density. Int J Mol Med 15, 15–19.

Sadick, H., Riedel, F., Naim, R., Goessler, U., Hörmann, K., Hafner, M., Lux, A., 2005b. Patients with hereditary hemorrhagic telangiectasia have increased plasma levels of vascular endothelial growth factor and transforming growth factor-beta1 as well as high ALK1 tissue expression. Haematologica 90, 818–828.

Saito, T., Bokhove, M., Croci, R., Zamora-Caballero, S., Han, L., Letarte, M., de Sanctis, D., Jovine, L., 2017. Structural Basis of the Human Endoglin-BMP9 Interaction: Insights into BMP Signaling and HHT1. Cell Rep 19, 1917–1928. https://doi.org/10.1016/j.celrep.2017.05.011

Sakaki-Yumoto, M., Liu, J., Ramalho-Santos, M., Yoshida, N., Derynck, R., 2013. Smad2 Is Essential for Maintenance of the Human and Mouse Primed Pluripotent Stem Cell State. J Biol Chem 288, 18546–18560. https://doi.org/10.1074/jbc.M112.446591

Sala, L.F.L., Pozzi, L.M., McAloose, D., Kaplan, F.S., Shore, E.M., Kompanje, E.J.O., Sidor, I.F., Musmeci, L., Uhart, M.M., 2012. Severe soft tissue ossification in a southern right whale Eubalaena australis. Dis Aquat Organ 102, 149–156. https://doi.org/10.3354/dao02538

Salikhova, A., Wang, L., Lanahan, A.A., Liu, M., Simons, M., Leenders, W.P.J., Mukhopadhyay, D., Horowitz, A., 2008. Vascular endothelial growth factor and semaphorin induce neuropilin-1 endocytosis via separate pathways. Circ Res 103, e71-79. https://doi.org/10.1161/CIRCRESAHA.108.183327

Salles-Crawley, I.I., Monkman, J.H., Ahnström, J., Lane, D.A., Crawley, J.T.B., 2014. Vessel wall BAMBI contributes to hemostasis and thrombus stability. Blood 123, 2873–2881. https://doi.org/10.1182/blood-2013-10-534024

Salmon, R.M., Guo, J., Wood, J.H., Tong, Z., Beech, J.S., Lawera, A., Yu, M., Grainger, D.J., Reckless, J., Morrell, N.W., Li, W., 2020. Molecular basis of ALK1-mediated signalling by BMP9/BMP10 and their prodomain-bound forms. Nature Communications 11, 1621. https://doi.org/10.1038/s41467-020-15425-3

Sánchez-Duffhues, G., de Vinuesa, A.G., Lindeman, J.H., Mulder-Stapel, A., DeRuiter, M.C., Van Munsteren, C., Goumans, M.-J., Hierck, B.P., Ten Dijke, P., 2015. SLUG is expressed in endothelial cells lacking primary cilia to promote cellular calcification. Arterioscler. Thromb. Vasc. Biol. 35, 616–627. https://doi.org/10.1161/ATVBAHA.115.305268

Sánchez-Duffhues, G., García de Vinuesa, A., Ten Dijke, P., 2018. Endothelial-to-mesenchymal transition in cardiovascular diseases: Developmental signaling pathways gone awry. Dev. Dyn. 247, 492–508. https://doi.org/10.1002/dvdy.24589

Sánchez-Duffhues, G., García de Vinuesa, A., van de Pol, V., Geerts, M.E., de Vries, M.R., Janson, S.G., van Dam, H., Lindeman, J.H., Goumans, M., ten Dijke, P., 2019a. Inflammation induces endothelial-to-mesenchymal transition and promotes vascular calcification through downregulation of BMPR2. J Pathol 247, 333–346. https://doi.org/10.1002/path.5193

Sánchez-Duffhues, G., Mikkers, H., de Jong, D., Szuhai, K., de Vries, T.J., Freund, C., Bravenboer, N., van Es, R.J.J., Netelenbos, J.C., Goumans, M.-J., Eekhoff, E.M.W., Ten Dijke, P., 2019b. Generation of Fibrodysplasia ossificans progressiva and control integration free iPSC lines from periodontal ligament fibroblasts. Stem Cell Res 41, 101639. https://doi.org/10.1016/j.scr.2019.101639

Sánchez-Duffhues, G., Williams, E., Benderitter, P., Orlova, V., van Wijhe, M., Garcia de Vinuesa, A., Kerr, G., Caradec, J., Lodder, K., de Boer, H.C., Goumans, M., Eekhoff, E.M.W., Morales-Piga, A., Bachiller-Corral, J., Koolwijk, P., Bullock, A.N., Hoflack, J., ten Dijke, P., 2019c. Development of Macrocycle Kinase Inhibitors for ALK2 Using Fibrodysplasia Ossificans Progressiva-Derived Endothelial Cells. JBMR Plus 3. https://doi.org/10.1002/jbm4.10230

Sánchez-Duffhues, G., Williams, E., Goumans, M.-J., Heldin, C.-H., ten Dijke, P., 2020. Bone morphogenetic protein receptors: Structure, function and targeting by selective small molecule kinase inhibitors. Bone 138, 115472. https://doi.org/10.1016/j.bone.2020.115472

Sanvitale, C.E., Kerr, G., Chaikuad, A., Ramel, M.-C., Mohedas, A.H., Reichert, S., Wang, Y., Triffitt, J.T., Cuny, G.D., Yu, P.B., Hill, C.S., Bullock, A.N., 2013. A new class of small molecule inhibitor of BMP signaling. PLoS ONE 8, e62721. https://doi.org/10.1371/journal.pone.0062721

Saremba, S., Nickel, J., Seher, A., Kotzsch, A., Sebald, W., Mueller, T.D., 2008. Type I receptor binding of bone morphogenetic protein 6 is dependent on N-glycosylation of the ligand. FEBS J. 275, 172–183. https://doi.org/10.1111/j.1742-4658.2007.06187.x

Scharpfenecker, M., van Dinther, M., Liu, Z., van Bezooijen, R.L., Zhao, Q., Pukac, L., Löwik, C.W.G.M., ten Dijke, P., 2007. BMP-9 signals via ALK1 and inhibits bFGF-induced endothelial cell proliferation and VEGF-stimulated angiogenesis. J. Cell. Sci. 120, 964–972. https://doi.org/10.1242/jcs.002949

Schliermann, A., Nickel, J., 2018. Unraveling the Connection between Fibroblast Growth Factor and Bone Morphogenetic Protein Signaling. Int J Mol Sci 19. https://doi.org/10.3390/ijms19103220

Schuldiner, M., Yanuka, O., Itskovitz-Eldor, J., Melton, D.A., Benvenisty, N., 2000. Effects of eight growth factors on the differentiation of cells derived from human embryonic stem cells. Proceedings of the National Academy of Sciences of the United States of America 97, 11307–11312. https://doi.org/10.1073/pnas.97.21.11307

Seeherman, H.J., Berasi, S.P., Brown, C.T., Martinez, R.X., Juo, Z.S., Jelinsky, S., Cain, M.J., Grode, J., Tumelty, K.E., Bohner, M., Grinberg, O., Orr, N., Shoseyov, O., Eyckmans, J., Chen, C., Morales, P.R., Wilson, C.G., Vanderploeg, E.J., Wozney, J.M., 2019. A BMP/activin A chimera is superior to native BMPs and induces bone repair in nonhuman primates when delivered in a composite matrix. Science Translational Medicine 11, eaar4953. https://doi.org/10.1126/scitranslmed.aar4953

Seher, A., Lagler, C., Stühmer, T., Müller-Richter, U.D.A., Kübler, A.C., Sebald, W., Müller, T.D., Nickel, J., 2017. Utilizing BMP-2 muteins for treatment of multiple myeloma. PLOS ONE 12, e0174884. https://doi.org/10.1371/journal.pone.0174884

Seibold, H.R., Davis, C.L., 1967. Generalized myositis ossificans (familial) in pigs. Pathol Vet 4, 79–88. https://doi.org/10.1177/030098586700400108

Sengle, G., Charbonneau, N.L., Ono, R.N., Sasaki, T., Alvarez, J., Keene, D.R., Bächinger, H.P., Sakai, L.Y., 2008. Targeting of bone morphogenetic protein growth factor complexes to fibrillin. J. Biol. Chem. 283, 13874–13888. https://doi.org/10.1074/jbc.M707820200

Sengle, G., Ono, R.N., Sasaki, T., Sakai, L.Y., 2011. Prodomains of Transforming Growth Factor β (TGFβ) Superfamily Members Specify Different Functions. J Biol Chem 286, 5087–5099. https://doi.org/10.1074/jbc.M110.188615

Setchell, B.P., Jacks, F., 1974. Inhibin-like activity in rete testis fluid. J. Endocrinol. 62, 675–676. https://doi.org/10.1677/joe.0.0620675

Shah, S., Lee, H., Park, Y.H., Jeon, E., Chung, H.K., Lee, E.S., Shim, J.H., Kang, K.-T., 2019. Three-dimensional Angiogenesis Assay System using Co-culture Spheroids Formed by Endothelial Colony Forming Cells and Mesenchymal Stem Cells. JoVE (Journal of Visualized Experiments) e60032. https://doi.org/10.3791/60032

Shalaby, F., Rossant, J., Yamaguchi, T.P., Gertsenstein, M., Wu, X.F., Breitman, M.L., Schuh, A.C., 1995. Failure of blood-island formation and vasculogenesis in Flk-1-deficient mice. Nature 376, 62–66. https://doi.org/10.1038/376062a0

Shao, E.S., Lin, L., Yao, Y., Boström, K.I., 2009. Expression of vascular endothelial growth factor is coordinately regulated by the activin-like kinase receptors 1 and 5 in endothelial cells. Blood 114, 2197–2206. https://doi.org/10.1182/blood-2009-01-199166

Shelton, M., Metz, J., Liu, J., Carpenedo, R.L., Demers, S.-P., Stanford, W.L., Skerjanc, I.S., 2014. Derivation and Expansion of PAX7-Positive Muscle Progenitors from Human and Mouse Embryonic Stem Cells. Stem Cell Reports 3, 516–529. https://doi.org/10.1016/j.stemcr.2014.07.001

Shen, Q., Little, S.C., Xu, M., Haupt, J., Ast, C., Katagiri, T., Mundlos, S., Seemann, P., Kaplan, F.S., Mullins, M.C., Shore, E.M., 2009. The fibrodysplasia ossificans progressiva R206H ACVR1 mutation activates BMP-independent chondrogenesis and zebrafish embryo ventralization. J. Clin. Invest. 119, 3462–3472. https://doi.org/10.1172/JCI37412

Shi, M., Zhu, J., Wang, R., Chen, X., Mi, L., Walz, T., Springer, T.A., 2011. Latent TGF-β structure and activation. Nature 474, 343–349. https://doi.org/10.1038/nature10152

Shimono, K., Morrison, T.N., Tung, W., Chandraratna, R.A., Williams, J.A., Iwamoto, M., Pacifici, M., 2010. Inhibition of ectopic bone formation by a selective retinoic acid receptor alpha-agonist: a new therapy for heterotopic ossification? J. Orthop. Res. 28, 271–277. https://doi.org/10.1002/jor.20985

Shimono, K., Tung, W., Macolino, C., Chi, A.H.-T., Didizian, J.J., Mundy, C., Chandraratna, R.A., Mishina, Y., Iwamoto, M.E., Pacifici, M., Iwamoto, M., 2011. Potent Inhibition of Heterotopic Ossification by Nuclear Retinoic Acid Receptor γ Agonists. Nat Med 17, 454–460. https://doi.org/10.1038/nm.2334

Shore, E.M., Feldman, G.J., Xu, M., Kaplan, F.S., 2005. The genetics of fibrodysplasia ossificans progressiva. Clinic Rev Bone Miner Metab 3, 201–204. https://doi.org/10.1385/BMM:3:3-4:201

Shore, E.M., Kaplan, F.S., 2010. Inherited human diseases of heterotopic bone formation. Nat Rev Rheumatol 6, 518–27. https://doi.org/10.1038/nrrheum.2010.122

Shore, Eileen M., Xu, M., Feldman, G.J., Fenstermacher, D.A., Cho, T.-J., Choi, I.H., Connor, J.M., Delai, P., Glaser, D.L., LeMerrer, M., Morhart, R., Rogers, J.G., Smith, R., Triffitt, J.T., Urtizberea, J.A., Zasloff, M., Brown, M.A., Kaplan, F.S., 2006. A recurrent mutation in the BMP type I receptor ACVR1 causes inherited and sporadic fibrodysplasia ossificans progressiva. Nat Genet 38, 525–527. https://doi.org/10.1038/ng1783

Sivaraj, K.K., Adams, R.H., 2016. Blood vessel formation and function in bone. Development 143, 2706–2715. https://doi.org/10.1242/dev.136861

Sivarapatna, A., Ghaedi, M., Le, A.V., Mendez, J.J., Qyang, Y., Niklason, L.E., 2015. Arterial specification of endothelial cells derived from human induced pluripotent stem cells in a biomimetic flow bioreactor. Biomaterials 53, 621–633. https://doi.org/10.1016/j.biomaterials.2015.02.121

Skawina, A., Litwin, J.A., Gorczyca, J., Miodoński, A.J., 1994. Blood vessels in epiphyseal cartilage of human fetal femoral bone: a scanning electron microscopic study of corrosion casts. Anat Embryol 189, 457–462. https://doi.org/10.1007/BF00185441

Smith, K.A., Joziasse, I.C., Chocron, S., van Dinther, M., Guryev, V., Verhoeven, M.C., Rehmann, H., van der Smagt, J.J., Doevendans, P.A., Cuppen, E., Mulder, B.J., Ten Dijke, P., Bakkers, J., 2009. Dominant-negative ALK2 allele associates with congenital heart defects. Circulation 119, 3062–3069. https://doi.org/10.1161/CIRCULATIONAHA.108.843714

Smithies, O., Gregg, R.G., Boggs, S.S., Koralewski, M.A., Kucherlapati, R.S., 1985. Insertion of DNA sequences into the human chromosomal beta-globin locus by homologous recombination. Nature 317, 230–234.

Sokol, S.Y., 2011. Maintaining embryonic stem cell pluripotency with Wnt signaling. Development 138, 4341–4350. https://doi.org/10.1242/dev.066209

Somekawa, S., Imagawa, K., Hayashi, H., Sakabe, M., Ioka, T., Sato, G.E., Inada, K., Iwamoto, T., Mori, T., Uemura, S., Nakagawa, O., Saito, Y., 2012. Tmem100, an ALK1 receptor signaling-dependent gene essential for arterial endothelium differentiation and vascular morphogenesis. Proc. Natl. Acad. Sci. U.S.A. 109, 12064–12069. https://doi.org/10.1073/pnas.1207210109

Song, G.-A., Kim, H.-J., Woo, K.-M., Baek, J.-H., Kim, G.-S., Choi, J.-Y., Ryoo, H.-M., 2010. Molecular consequences of the ACVR1(R206H) mutation of fibrodysplasia ossificans progressiva. J. Biol. Chem. 285, 22542–22553. https://doi.org/10.1074/jbc.M109.094557

Song, J., Yang, D., Xu, J., Zhu, T., Chen, Y.E., Zhang, J., 2016. RS-1 enhances CRISPR/Cas9- and TALEN-mediated knock-in efficiency. Nature Communications 7, 10548. https://doi.org/10.1038/ncomms10548

Sriram, G., Tan, J.Y., Islam, I., Rufaihah, A.J., Cao, T., 2015. Efficient differentiation of human embryonic stem cells to arterial and venous endothelial cells under feeder- and serum-free conditions. Stem Cell Res Ther 6, 261. https://doi.org/10.1186/s13287-015-0260-5

Stange, K., Désir, J., Kakar, N., Mueller, T.D., Budde, B.S., Gordon, C.T., Horn, D., Seemann, P., Borck, G., 2015. A hypomorphic BMPR1B mutation causes du Pan acromesomelic dysplasia. Orphanet Journal of Rare Diseases 10, 84. https://doi.org/10.1186/s13023-015-0299-5

Stanley, A., Heo, S., Mauck, R.L., Mourkioti, F., Shore, E.M., 2019. Elevated BMP and Mechanical Signaling Through YAP1/RhoA Poises FOP Mesenchymal Progenitors for Osteogenesis. Journal of Bone and Mineral Research 34, 1894–1909. https://doi.org/10.1002/jbmr.3760

Stickens, D., Behonick, D.J., Ortega, N., Heyer, B., Hartenstein, B., Yu, Y., Fosang, A.J., Schorpp-Kistner, M., Angel, P., Werb, Z., 2004. Altered endochondral bone development in matrix metalloproteinase 13-deficient mice. Development 131, 5883–5895. https://doi.org/10.1242/dev.01461

Street, J., Bao, M., deGuzman, L., Bunting, S., Peale, F.V., Ferrara, N., Steinmetz, H., Hoeffel, J., Cleland, J.L., Daugherty, A., Bruggen, N. van, Redmond, H.P., Carano, R.A.D., Filvaroff, E.H., 2002. Vascular endothelial growth factor stimulates bone repair by promoting angiogenesis and bone turnover. PNAS 99, 9656–9661. https://doi.org/10.1073/pnas.152324099

Stricker, S., Knaus, P., Simon, H.-G., 2017. Putting Cells into Context. Front Cell Dev Biol 5. https://doi.org/10.3389/fcell.2017.00032

Stumm, J., Vallecillo-García, P., Vom Hofe-Schneider, S., Ollitrault, D., Schrewe, H., Economides, A.N., Marazzi, G., Sassoon, D.A., Stricker, S., 2018. Odd skipped-related 1 (Osr1) identifies muscle-interstitial fibro-adipogenic progenitors (FAPs) activated by acute injury. Stem Cell Research 32, 8–16. https://doi.org/10.1016/j.scr.2018.08.010

Suda, R.K., Billings, P.C., Egan, K.P., Kim, J.H., McCarrick-Walmsley, R., Glaser, D.L., Porter, D.L., Shore, E.M., Pignolo, R.J., 2009. Circulating osteogenic precursor cells in heterotopic bone formation. Stem Cells 27, 2209–19. https://doi.org/10.1002/stem.150

Sun, J., Liu, Y.-H., Chen, H., Nguyen, M.P., Mishina, Y., Upperman, J.S., Ford, H.R., Shi, W., 2007. Deficient Alk3-mediated BMP signaling causes prenatal

omphalocele-like defect. Biochem Biophys Res Commun 360, 238–243. https://doi.org/10.1016/j.bbrc.2007.06.049

Sun, Z., Li, X., Massena, S., Kutschera, S., Padhan, N., Gualandi, L., Sundvold-Gjerstad, V., Gustafsson, K., Choy, W.W., Zang, G., Quach, M., Jansson, L., Phillipson, M., Abid, M.R., Spurkland, A., Claesson-Welsh, L., 2012. VEGFR2 induces c-Src signaling and vascular permeability in vivo via the adaptor protein TSAd. J. Exp. Med. 209, 1363–1377. https://doi.org/10.1084/jem.20111343

Sunde, M., McGrath, K.C.Y., Young, L., Matthews, J.M., Chua, E.L., Mackay, J.P., Death, A.K., 2004. TC-1 is a novel tumorigenic and natively disordered protein associated with thyroid cancer. Cancer Res. 64, 2766–2773. https://doi.org/10.1158/0008-5472.can-03-2093

Suzuki, Y., Ohga, N., Morishita, Y., Hida, K., Miyazono, K., Watabe, T., 2010. BMP-9 induces proliferation of multiple types of endothelial cells in vitro and in vivo. J. Cell. Sci. 123, 1684–1692. https://doi.org/10.1242/jcs.061556

Szulcek, R., Bogaard, H.J., van Nieuw Amerongen, G.P., 2014. Electric Cell-substrate Impedance Sensing for the Quantification of Endothelial Proliferation, Barrier Function, and Motility. J Vis Exp. https://doi.org/10.3791/51300

Takahashi, K., Okita, K., Nakagawa, M., Yamanaka, S., 2007. Induction of pluripotent stem cells from fibroblast cultures. Nature Protocols 2, 3081–3089. https://doi.org/10.1038/nprot.2007.418

Takahashi, K., Yamanaka, S., 2016. A decade of transcription factor-mediated reprogramming to pluripotency. Nature Reviews Molecular Cell Biology 17, 183–193. https://doi.org/10.1038/nrm.2016.8

Takahashi, K., Yamanaka, S., 2006. Induction of Pluripotent Stem Cells from Mouse Embryonic and Adult Fibroblast Cultures by Defined Factors. Cell 126, 663–676. https://doi.org/10.1016/j.cell.2006.07.024

Taylor, A.M., Bordoni, B., 2020. Histology, Blood Vascular System, in: StatPearls. StatPearls Publishing, Treasure Island (FL).

ten Dijke, P., Yamashita, H., Ichijo, H., Franzén, P., Laiho, M., Miyazono, K., Heldin, C.H., 1994a. Characterization of type I receptors for transforming growth factor-beta and activin. Science 264, 101–104. https://doi.org/10.1126/science.8140412

ten Dijke, P., Yamashita, H., Sampath, T.K., Reddi, A.H., Estevez, M., Riddle, D.L., Ichijo, H., Heldin, C.H., Miyazono, K., 1994b. Identification of type I receptors for osteogenic protein-1 and bone morphogenetic protein-4. J. Biol. Chem. 269, 16985–16988.

Terman, B.I., Dougher-Vermazen, M., Carrion, M.E., Dimitrov, D., Armellino, D.C., Gospodarowicz, D., Böhlen, P., 1992. Identification of the KDR tyrosine kinase as a receptor for vascular endothelial cell growth factor. Biochem. Biophys. Res. Commun. 187, 1579–1586. https://doi.org/10.1016/0006-291x(92)90483-2

Thalgott, J., Dos-Santos-Luis, D., Lebrin, F., 2015. Pericytes as targets in hereditary hemorrhagic telangiectasia. Front Genet 6. https://doi.org/10.3389/fgene.2015.00037

Thalgott Jérémy H., Dos-Santos-Luis Damien, Hosman Anna E., Martin Sabrina, Lamandé Noël, Bracquart Diane, Srun Samly, Galaris Georgios, de Boer Hetty C., Tual-Chalot Simon, Kroon Steven, Arthur Helen M., Cao Yihai, Snijder Repke J., Disch Frans, Mager Johannes J., Rabelink Ton J., Mummery Christine L., Raymond Karine, Lebrin Franck, 2018. Decreased Expression of

Vascular Endothelial Growth Factor Receptor 1 Contributes to the Pathogenesis of Hereditary Hemorrhagic Telangiectasia Type 2. Circulation 138, 2698–2712. https://doi.org/10.1161/CIRCULATIONAHA.117.033062

The Nobel Prize in Physiology or Medicine 2012 [WWW Document], n.d. . NobelPrize.org. URL https://www.nobelprize.org/prizes/medicine/2012/press-release/ (accessed 12.9.20).

Thomas, K.R., Folger, K.R., Capecchi, M.R., 1986. High frequency targeting of genes to specific sites in the mammalian genome. Cell 44, 419–428.

Thomas, P.S., Sridurongrit, S., Ruiz-Lozano, P., Kaartinen, V., 2012. Deficient Signaling via Alk2 (Acvr1) Leads to Bicuspid Aortic Valve Development. PLOS ONE 7, e35539. https://doi.org/10.1371/journal.pone.0035539

Thompson, T.B., Lerch, T.F., Cook, R.W., Woodruff, T.K., Jardetzky, T.S., 2005b. The Structure of the Follistatin:Activin Complex Reveals Antagonism of Both Type I and Type II Receptor Binding. Developmental Cell 9, 535–543. https://doi.org/10.1016/j.devcel.2005.09.008

Thompson, T.B., Woodruff, T.K., Jardetzky, T.S., 2003. Structures of an ActRIIB:activin A complex reveal a novel binding mode for TGF-β ligand:receptor interactions. EMBO J 22, 1555–1566. https://doi.org/10.1093/emboj/cdg156

Thompson, T.J., Owens, P.D., Wilson, D.J., 1989. Intramembranous osteogenesis and angiogenesis in the chick embryo. J Anat 166, 55–65.

Tirone, M., Giovenzana, A., Vallone, A., Zordan, P., Sormani, M., Nicolosi, P.A., Meneveri, R., Gigliotti, C.R., Spinelli, A.E., Bocciardi, R., Ravazzolo, R., Cifola, I., Brunelli, S., 2019. Severe Heterotopic Ossification in the Skeletal Muscle and Endothelial Cells Recruitment to Chondrogenesis Are Enhanced by Monocyte/Macrophage Depletion. Front Immunol 10. https://doi.org/10.3389/fimmu.2019.01640

Tong, M., Jiang, Y., 2015. FK506-Binding Proteins and Their Diverse Functions. CMP 9, 48–65. https://doi.org/10.2174/1874467208666150519113541

Tonnesen, M.G., Feng, X., Clark, R.A., 2000. Angiogenesis in wound healing. J Investig Dermatol Symp Proc 5, 40–46. https://doi.org/10.1046/j.1087-0024.2000.00014.x

Topper, J.N., Cai, J., Qiu, Y., Anderson, K.R., Xu, Y.Y., Deeds, J.D., Feeley, R., Gimeno, C.J., Woolf, E.A., Tayber, O., Mays, G.G., Sampson, B.A., Schoen, F.J., Gimbrone, M.A., Falb, D., 1997. Vascular MADs: two novel MAD-related genes selectively inducible by flow in human vascular endothelium. Proc. Natl. Acad. Sci. U.S.A. 94, 9314–9319. https://doi.org/10.1073/pnas.94.17.9314

Towbin, J.A., 2015. Vascular Genetical Embryology, in: Lanzer, P. (Ed.), PanVascular Medicine. Springer, Berlin, Heidelberg, pp. 3–26. https://doi.org/10.1007/978-3-642-37078-6_1

Towler, O.W., Shore, E.M., Kaplan, F.S., 2020. Skeletal malformations and developmental arthropathy in individuals who have fibrodysplasia ossificans progressiva. Bone 130, 115116. https://doi.org/10.1016/j.bone.2019.115116

Townson, S.A., Martinez-Hackert, E., Greppi, C., Lowden, P., Sako, D., Liu, J., Ucran, J.A., Liharska, K., Underwood, K.W., Seehra, J., Kumar, R., Grinberg, A.V., 2012. Specificity and Structure of a High Affinity Activin Receptor-like Kinase 1 (ALK1) Signaling Complex. J Biol Chem 287, 27313–27325. https://doi.org/10.1074/jbc.M112.377960

Tremblay, K.D., Dunn, N.R., Robertson, E.J., 2001. Mouse embryos lacking Smad1 signals display defects in extra-embryonic tissues and germ cell formation. Development 128, 3609–3621.

Tsata, V., Beis, D., 2020. In Full Force. Mechanotransduction and Morphogenesis during Homeostasis and Tissue Regeneration. J Cardiovasc Dev Dis 7. https://doi.org/10.3390/jcdd7040040

Tsuchida, K., Mathews, L.S., Vale, W.W., 1993. Cloning and characterization of a transmembrane serine kinase that acts as an activin type I receptor. Proc Natl Acad Sci U S A 90, 11242–11246.

Tsuchida, K., Nakatani, M., Yamakawa, N., Hashimoto, O., Hasegawa, Y., Sugino, H., 2004. Activin isoforms signal through type I receptor serine/threonine kinase ALK7. Mol. Cell. Endocrinol. 220, 59–65. https://doi.org/10.1016/j.mce.2004.03.009

Udan, R.S., Culver, J.C., Dickinson, M.E., 2013. Understanding vascular development. Wiley Interdiscip Rev Dev Biol 2, 327–346. https://doi.org/10.1002/wdev.91

Uezumi, A., Fukada, S., Yamamoto, N., Ikemoto-Uezumi, M., Nakatani, M., Morita, M., Yamaguchi, A., Yamada, H., Nishino, I., Hamada, Y., Tsuchida, K., 2014. Identification and characterization of PDGFRα+ mesenchymal progenitors in human skeletal muscle. Cell Death Dis 5, e1186. https://doi.org/10.1038/cddis.2014.161

Uezumi, A., Fukada, S., Yamamoto, N., Takeda, S., Tsuchida, K., 2010. Mesenchymal progenitors distinct from satellite cells contribute to ectopic fat cell formation in skeletal muscle. Nat Cell Biol 12, 143–52. https://doi.org/10.1038/ncb2014

Uezumi, Akiyoshi, Ikemoto-Uezumi, M., Tsuchida, K., 2014. Roles of nonmyogenic mesenchymal progenitors in pathogenesis and regeneration of skeletal muscle. Front Physiol 5. https://doi.org/10.3389/fphys.2014.00068

Upadhyay, J., Xie, L., Huang, L., Das, N., Stewart, R.C., Lyon, M.C., Palmer, K., Rajamani, S., Graul, C., Lobo, M., Wellman, T.J., Soares, E.J., Silva, M.D., Hesterman, J., Wang, L., Wen, X., Qian, X., Nannuru, K., Idone, V., Murphy, A.J., Economides, A.N., Hatsell, S.J., 2017. The Expansion of Heterotopic Bone in Fibrodysplasia Ossificans Progressiva Is Activin A-Dependent. J. Bone Miner. Res. 32, 2489–2499. https://doi.org/10.1002/jbmr.3235

Upton, P.D., Davies, R.J., Trembath, R.C., Morrell, N.W., 2009. Bone morphogenetic protein (BMP) and activin type II receptors balance BMP9 signals mediated by activin receptor-like kinase-1 in human pulmonary artery endothelial cells. J Biol Chem 284, 15794–15804. https://doi.org/10.1074/jbc.M109.002881

Urist, M.R., 1965. Bone: formation by autoinduction. Science 150, 893–899. https://doi.org/10.1126/science.150.3698.893

Valdimarsdottir, G., Goumans, M.-J., Rosendahl, A., Brugman, M., Itoh, S., Lebrin, F., Sideras, P., ten Dijke, P., 2002. Stimulation of Id1 expression by bone morphogenetic protein is sufficient and necessary for bone morphogenetic protein-induced activation of endothelial cells. Circulation 106, 2263–2270. https://doi.org/10.1161/01.cir.0000033830.36431.46

Valdimarsdottir Gudrun, Goumans Marie-José, Rosendahl Alexander, Brugman Martijn, Itoh Susumu, Lebrin Franck, Sideras Paschalis, ten Dijke Peter, 2002. Stimulation of Id1 Expression by Bone Morphogenetic Protein Is Sufficient and Necessary for Bone Morphogenetic Protein–Induced Activation of Endothelial Cells. Circulation 106, 2263–2270. https://doi.org/10.1161/01.CIR.0000033830.36431.46

Valentine, B.A., George, C., Randolph, J.F., Center, S.A., Fuhrer, L., Beck, K.A., 1992. Fibrodysplasia ossificans progressiva in the cat. A case report. J. Vet. Intern. Med. 6, 335–340. https://doi.org/10.1111/j.1939-1676.1992.tb00366.x

Vallecillo-García, P., Orgeur, M., vom Hofe-Schneider, S., Stumm, J., Kappert, V., Ibrahim, D.M., Börno, S.T., Hayashi, S., Relaix, F., Hildebrandt, K., Sengle, G., Koch, M., Timmermann, B., Marazzi, G., Sassoon, D.A., Duprez, D., Stricker, S., 2017. Odd skipped-related 1 identifies a population of embryonic fibro-adipogenic progenitors regulating myogenesis during limb development. Nature Communications 8, 1218. https://doi.org/10.1038/s41467-017-01120-3

Vallier, L., Mendjan, S., Brown, S., Chng, Z., Teo, A., Smithers, L.E., Trotter, M.W., Cho, C.H., Martinez, A., Rugg-Gunn, P., Brons, G., Pedersen, R.A., 2009. Activin/Nodal signalling maintains pluripotency by controlling Nanog expression. Development 136, 1339–49. https://doi.org/10.1242/dev.033951

Vallier, Ludovic, Touboul, T., Chng, Z., Brimpari, M., Hannan, N., Millan, E., Smithers, L.E., Trotter, M., Rugg-Gunn, P., Weber, A., Pedersen, R.A., 2009. Early Cell Fate Decisions of Human Embryonic Stem Cells and Mouse Epiblast Stem Cells Are Controlled by the Same Signalling Pathways. PLoS One 4. https://doi.org/10.1371/journal.pone.0006082

van Caam, A., Blaney Davidson, E., Garcia de Vinuesa, A., van Geffen, E., van den Berg, W., Goumans, M.-J., ten Dijke, P., van der Kraan, P., 2015. The high affinity ALK1-ligand BMP9 induces a hypertrophy-like state in chondrocytes that is antagonized by TGFβ1. Osteoarthritis and Cartilage 23, 985–995. https://doi.org/10.1016/j.joca.2015.02.007

van Dinther, M., Visser, N., de Gorter, D.J.J., Doorn, J., Goumans, M.-J., de Boer, J., ten Dijke, P., 2010. ALK2 R206H mutation linked to fibrodysplasia ossificans progressiva confers constitutive activity to the BMP type I receptor and sensitizes mesenchymal cells to BMP-induced osteoblast differentiation and bone formation. J. Bone Miner. Res. 25, 1208–1215. https://doi.org/10.1359/jbmr.091110

van Meeteren, L.A., Thorikay, M., Bergqvist, S., Pardali, E., Stampino, C.G., Hu-Lowe, D., Goumans, M.-J., ten Dijke, P., 2012. Anti-human activin receptor-like kinase 1 (ALK1) antibody attenuates bone morphogenetic protein 9 (BMP9)-induced ALK1 signaling and interferes with endothelial cell sprouting. J. Biol. Chem. 287, 18551–18561. https://doi.org/10.1074/jbc.M111.338103

Van Varik, B., Rennenberg, R., Reutelingsperger, C., Kroon, A., de Leeuw, P., Schurgers, L.J., 2012. Mechanisms of arterial remodeling: lessons from genetic diseases. Front. Genet. 3. https://doi.org/10.3389/fgene.2012.00290

Vega, R., Carretero, M., Travasso, R.D.M., Bonilla, L.L., 2020. Notch signaling and taxis mechanisms regulate early stage angiogenesis: A mathematical and computational model. PLOS Computational Biology 16, e1006919. https://doi.org/10.1371/journal.pcbi.1006919

Vieira, J.M., Ruhrberg, C., Schwarz, Q., 2010. VEGF receptor signaling in vertebrate development. Organogenesis 6, 97–106.

Volpato, V., Webber, C., 2020. Addressing variability in iPSC-derived models of human disease: guidelines to promote reproducibility. Dis Model Mech 13. https://doi.org/10.1242/dmm.042317

Wagner, I., Wang, H., Weissert, P.M., Straube, W.L., Shevchenko, Anna, Gentzel, M., Brito, G., Tazaki, A., Oliveira, C., Sugiura, T., Shevchenko, Andrej, Simon, A., Drechsel, D.N., Tanaka, E.M., 2017. Serum Proteases Potentiate BMP-Induced Cell Cycle Re-entry of Dedifferentiating Muscle Cells during Newt Limb Regeneration. Dev Cell 40, 608-617.e6. https://doi.org/10.1016/j.devcel.2017.03.002

Wakayama, Y., Fukuhara, S., Ando, K., Matsuda, M., Mochizuki, N., 2015. Cdc42 mediates Bmp-induced sprouting angiogenesis through Fmnl3-driven

assembly of endothelial filopodia in zebrafish. Dev. Cell 32, 109–122. https://doi.org/10.1016/j.devcel.2014.11.024

Wakefield, L.M., Smith, D.M., Broz, S., Jackson, M., Levinson, A.D., Sporn, M.B., 1989. Recombinant TGF-beta 1 is synthesized as a two-component latent complex that shares some structural features with the native platelet latent TGF-beta 1 complex. Growth Factors 1, 203–218. https://doi.org/10.3109/08977198908997997

Wallez, Y., Cand, F., Cruzalegui, F., Wernstedt, C., Souchelnytskyi, S., Vilgrain, I., Huber, P., 2007. Src kinase phosphorylates vascular endothelial-cadherin in response to vascular endothelial growth factor: identification of tyrosine 685 as the unique target site. Oncogene 26, 1067–1077. https://doi.org/10.1038/sj.onc.1209855

Wang, H., Lindborg, C., Lounev, V., Kim, J.-H., McCarrick-Walmsley, R., Xu, M., Mangiavini, L., Groppe, J.C., Shore, E.M., Schipani, E., Kaplan, F.S., Pignolo, R.J., 2016. Cellular Hypoxia Promotes Heterotopic Ossification by Amplifying BMP Signaling. J. Bone Miner. Res. 31, 1652–1665. https://doi.org/10.1002/jbmr.2848

Wang, J., Sridurongrit, S., Dudas, M., Thomas, P., Nagy, A., Schneider, M.D., Epstein, J.A., Kaartinen, V., 2005. Atrioventricular cushion transformation is mediated by ALK2 in the developing mouse heart. Dev. Biol. 286, 299–310. https://doi.org/10.1016/j.ydbio.2005.07.035

Wang, R.N., Green, J., Wang, Z., Deng, Y., Qiao, M., Peabody, M., Zhang, Q., Ye, J., Yan, Z., Denduluri, S., Idowu, O., Li, M., Shen, C., Hu, A., Haydon, R.C., Kang, R., Mok, J., Lee, M.J., Luu, H.L., Shi, L.L., 2014. Bone Morphogenetic Protein (BMP) signaling in development and human diseases. Genes & Diseases 1, 87–105. https://doi.org/10.1016/j.gendis.2014.07.005

Wang, T., Donahoe, P.K., Zervos, A.S., 1994. Specific interaction of type I receptors of the TGF-beta family with the immunophilin FKBP-12. Science 265, 674–676. https://doi.org/10.1126/science.7518616

Wang, T., Guo, S., Zhang, H., 2018. Synergistic Effects of Controlled-Released BMP-2 and VEGF from nHAC/PLGAs Scaffold on Osteogenesis. Biomed Res Int 2018. https://doi.org/10.1155/2018/3516463

Wang, T., Li, B.-Y., Danielson, P.D., Shah, P.C., Rockwell, S., Lechleider, R.J., Martin, J., Manganaro, T., Donahoe, P.K., 1996. The Immunophilin FKBP12 Functions as a Common Inhibitor of the TGFβ Family Type I Receptors. Cell 86, 435–444. https://doi.org/10.1016/S0092-8674(00)80116-6

Wang, X., Fischer, G., Hyvönen, M., 2016. Structure and activation of pro-activin A. Nature Communications 7, 12052. https://doi.org/10.1038/ncomms12052

Wang, X.F., Lin, H.Y., Ng-Eaton, E., Downward, J., Lodish, H.F., Weinberg, R.A., 1991. Expression cloning and characterization of the TGF-beta type III receptor. Cell 67, 797–805.

Ware, A.D., Brewer, N., Meyers, C., Morris, C., McCarthy, E., Shore, E.M., James, A.W., 2019b. Differential Vascularity in Genetic and Nonhereditary Heterotopic Ossification. Int J Surg Pathol 27, 859–867. https://doi.org/10.1177/1066896919857135

Warren, H.B., Carpenter, J.L., 1984. Fibrodysplasia ossificans in three cats. Vet. Pathol. 21, 495–499. https://doi.org/10.1177/030098588402100507

Watabe, T., Miyazono, K., 2009. Roles of TGF-β family signaling in stem cell renewal and differentiation. Cell Research 19, 103–115. https://doi.org/10.1038/cr.2008.323

Watanabe, R., Yamada, Y., Ihara, Y., Someya, Y., Kubota, A., Kagimoto, S., Kuroe, A., Iwakura, T., Shen, Z.-P., Inada, A., Adachi, T., Ban, N., Miyawaki, K., Sunaga, Y., Tsuda, K., Seino, Y., 1999. The MH1 Domains of Smad2 and Smad3 Are Involved in the Regulation of the ALK7 Signals. Biochemical and Biophysical Research Communications 254, 707–712. https://doi.org/10.1006/bbrc.1998.0118

Watson, E.C., Grant, Z.L., Coultas, L., 2017. Endothelial cell apoptosis in angiogenesis and vessel regression. Cell. Mol. Life Sci. 74, 4387–4403. https://doi.org/10.1007/s00018-017-2577-y

Weber, D., Kotzsch, A., Nickel, J., Harth, S., Seher, A., Mueller, U., Sebald, W., Mueller, T.D., 2007. A silent H-bond can be mutationally activated for high-affinity interaction of BMP-2 and activin type IIB receptor. BMC Struct. Biol. 7, 6. https://doi.org/10.1186/1472-6807-7-6

Weinstein, N., Mendoza, L., Álvarez-Buylla, E.R., 2020. A Computational Model of the Endothelial to Mesenchymal Transition. Front. Genet. 11. https://doi.org/10.3389/fgene.2020.00040

Wentworth, K.L., Masharani, U., Hsiao, E.C., 2019. Therapeutic advances for blocking heterotopic ossification in fibrodysplasia ossificans progressiva. Br J Clin Pharmacol 85, 1180–1187. https://doi.org/10.1111/bcp.13823

Wessel, F., Winderlich, M., Holm, M., Frye, M., Rivera-Galdos, R., Vockel, M., Linnepe, R., Ipe, U., Stadtmann, A., Zarbock, A., Nottebaum, A.F., Vestweber, D., 2014. Leukocyte extravasation and vascular permeability are each controlled in vivo by different tyrosine residues of VE-cadherin. Nat. Immunol. 15, 223–230. https://doi.org/10.1038/ni.2824

White, M.P., Rufaihah, A.J., Liu, L., Ghebremariam, Y.T., Ivey, K.N., Cooke, J.P., Srivastava, D., 2013. Limited gene expression variation in human embryonic stem cell and induced pluripotent stem cell-derived endothelial cells. Stem Cells 31, 92–103. https://doi.org/10.1002/stem.1267

White, T.D., Black, M.T., Folkens, P.A., 2011. Human Osteology. Academic Press.

Wieser, R., Wrana, J.L., Massagué, J., 1995. GS domain mutations that constitutively activate T beta R-I, the downstream signaling component in the TGF-beta receptor complex. EMBO J. 14, 2199–2208.

Wiley, D.M., Kim, J.-D., Hao, J., Hong, C.C., Bautch, V.L., Jin, S.-W., 2011. Distinct signalling pathways regulate sprouting angiogenesis from the dorsal aorta and the axial vein. Nature Cell Biology 13, 686–692. https://doi.org/10.1038/ncb2232

Williams, E., Bagarova, J., Kerr, G., Xia, D.-D., Place, E.S., Dey, D., Shen, Y., Bocobo, G.A., Mohedas, A.H., Huang, X., Sanderson, P.E., Lee, A., Zheng, W., Economides, A.N., Smith, J.C., Yu, P.B., Bullock, A.N., 2020. Saracatinib is an efficacious clinical candidate for fibrodysplasia ossificans progressiva. bioRxiv 2020.10.29.360370. https://doi.org/10.1101/2020.10.29.360370

Williams Ian M., Wu Joseph C., 2019. Generation of Endothelial Cells From Human Pluripotent Stem Cells. Arteriosclerosis, Thrombosis, and Vascular Biology 39, 1317–1329. https://doi.org/10.1161/ATVBAHA.119.312265

Willis, S.A., Zimmerman, C.M., Li, L.I., Mathews, L.S., 1996. Formation and activation by phosphorylation of activin receptor complexes. Mol Endocrinol 10, 367–379. https://doi.org/10.1210/mend.10.4.8721982

Winnier, G., Blessing, M., Labosky, P.A., Hogan, B.L., 1995. Bone morphogenetic protein-4 is required for mesoderm formation and patterning in the mouse. Genes Dev. 9, 2105–2116. https://doi.org/10.1101/gad.9.17.2105

Wolfman, N.M., McPherron, A.C., Pappano, W.N., Davies, M.V., Song, K., Tomkinson, K.N., Wright, J.F., Zhao, L., Sebald, S.M., Greenspan, D.S., Lee, S.-J., 2003. Activation of latent myostatin by the BMP-1/tolloid family of metalloproteinases. Proc. Natl. Acad. Sci. U.S.A. 100, 15842–15846. https://doi.org/10.1073/pnas.2534946100

Wong, K.G., Ryan, S.D., Ramnarine, K., Rosen, S.A., Mann, S.E., Kulick, A., De Stanchina, E., Müller, F.-J., Kacmarczyk, T.J., Zhang, C., Betel, D., Tomishima, M.J., 2017. CryoPause: A New Method to Immediately Initiate Experiments after Cryopreservation of Pluripotent Stem Cells. Stem Cell Reports 9, 355–365. https://doi.org/10.1016/j.stemcr.2017.05.010

Wosczyna, Michael N., Biswas, A.A., Cogswell, C.A., Goldhamer, D.J., 2012. Multipotent progenitors resident in the skeletal muscle interstitium exhibit robust BMP-dependent osteogenic activity and mediate heterotopic ossification. J Bone Miner Res 27, 1004–1017. https://doi.org/10.1002/jbmr.1562

Wozney, J.M., Rosen, V., Celeste, A.J., Mitsock, L.M., Whitters, M.J., Kriz, R.W., Hewick, R.M., Wang, E.A., 1988. Novel regulators of bone formation: molecular clones and activities. Science 242, 1528–1534. https://doi.org/10.1126/science.3201241

Wrana, J.L., Attisano, L., Cárcamo, J., Zentella, A., Doody, J., Laiho, M., Wang, X.F., Massagué, J., 1992. TGF beta signals through a heteromeric protein kinase receptor complex. Cell 71, 1003–1014. https://doi.org/10.1016/0092-8674(92)90395-s

Xiao, L., Yuan, X., Sharkis, S.J., 2006. Activin A Maintains Self-Renewal and Regulates Fibroblast Growth Factor, Wnt, and Bone Morphogenic Protein Pathways in Human Embryonic Stem Cells. STEM CELLS 24, 1476–1486. https://doi.org/10.1634/stemcells.2005-0299

Xiao, Z., Liu, X., Henis, Y.I., Lodish, H.F., 2000. A distinct nuclear localization signal in the N terminus of Smad 3 determines its ligand-induced nuclear translocation. PNAS 97, 7853–7858. https://doi.org/10.1073/pnas.97.14.7853

Xu, R.-H., Peck, R.M., Li, D.S., Feng, X., Ludwig, T., Thomson, J.A., 2005. Basic FGF and suppression of BMP signaling sustain undifferentiated proliferation of human ES cells. Nature Methods 2, 185–190. https://doi.org/10.1038/nmeth744

Xu, R.-H., Sampsell-Barron, T.L., Gu, F., Root, S., Peck, R.M., Pan, G., Yu, J., Antosiewicz-Bourget, J., Tian, S., Stewart, R., Thomson, J.A., 2008. NANOG is a direct target of TGFbeta/activin-mediated SMAD signaling in human ESCs. Cell Stem Cell 3, 196–206. https://doi.org/10.1016/j.stem.2008.07.001

Xue, C., Huang, Q., Zhang, T., Zhao, D., Ma, Q., Tian, T., Cai, X., 2018. Matrix stiffness regulates arteriovenous differentiation of endothelial progenitor cells during vasculogenesis in nude mice. Cell Prolif 52. https://doi.org/10.1111/cpr.12557

Xue, C., Zhang, T., Xie, X., Zhang, Q., Zhang, S., Zhu, B., Lin, Y., Cai, X., 2017. Substrate stiffness regulates arterial-venous differentiation of endothelial progenitor cells via the Ras/Mek pathway. Biochim Biophys Acta Mol Cell Res 1864, 1799–1808. https://doi.org/10.1016/j.bbamcr.2017.07.006

Yadin, D., Knaus, P., Mueller, T.D., 2016. Structural insights into BMP receptors: Specificity, activation and inhibition. Cytokine Growth Factor Rev. 27, 13–34. https://doi.org/10.1016/j.cytogfr.2015.11.005

Yagi, K., Goto, D., Hamamoto, T., Takenoshita, S., Kato, M., Miyazono, K., 1999. Alternatively spliced variant of Smad2 lacking exon 3. Comparison with wild-

type Smad2 and Smad3. J. Biol. Chem. 274, 703–709. https://doi.org/10.1074/jbc.274.2.703

Yamaji, N., Celeste, A.J., Thies, R.S., Song, J.J., Bernier, S.M., Goltzman, D., Lyons, K.M., Nove, J., Rosen, V., Wozney, J.M., 1994. A Mammalian Serine/Threonine Kinase Receptor Specifically Binds BMP-2 and BMP-4. Biochemical and Biophysical Research Communications 205, 1944–1951. https://doi.org/10.1006/bbrc.1994.2898

Yamamizu, K., Kawasaki, K., Katayama, S., Watabe, T., Yamashita, J.K., 2009. Enhancement of vascular progenitor potential by protein kinase A through dual induction of Flk-1 and Neuropilin-1. Blood 114, 3707–3716. https://doi.org/10.1182/blood-2008-12-195750

Yamashita, H., ten Dijke, P., Huylebroeck, D., Sampath, T.K., Andries, M., Smith, J.C., Heldin, C.H., Miyazono, K., 1995. Osteogenic protein-1 binds to activin type II receptors and induces certain activin-like effects. J Cell Biol 130, 217–226. https://doi.org/10.1083/jcb.130.1.217

Yang, F., Sun, L., Li, Q., Han, X., Lei, L., Zhang, H., Shang, Y., 2012. SET8 promotes epithelial-mesenchymal transition and confers TWIST dual transcriptional activities. EMBO J. 31, 110–123. https://doi.org/10.1038/emboj.2011.364

Yang, J., Jiang, W., 2020. The Role of SMAD2/3 in Human Embryonic Stem Cells. Front. Cell Dev. Biol. 8. https://doi.org/10.3389/fcell.2020.00653

Yang, L., Soonpaa, M.H., Adler, E.D., Roepke, T.K., Kattman, S.J., Kennedy, M., Henckaerts, E., Bonham, K., Abbott, G.W., Linden, R.M., Field, L.J., Keller, G.M., 2008. Human cardiovascular progenitor cells develop from a KDR + embryonic-stem-cell-derived population. Nature 453, 524–528. https://doi.org/10.1038/nature06894

Yang, X., Liaw, L., Prudovsky, I., Brooks, P.C., Vary, C., Oxburgh, L., Friesel, R., 2015. Fibroblast Growth Factor Signaling in the Vasculature. Curr Atheroscler Rep 17, 509. https://doi.org/10.1007/s11883-015-0509-6

Yao, Y., Shao, E.S., Jumabay, M., Shahbazian, A., Ji, S., Boström, K.I., 2008. High-density lipoproteins affect endothelial BMP-signaling by modulating expression of the activin-like kinase receptor 1 and 2. Arterioscler Thromb Vasc Biol 28, 2266–2274. https://doi.org/10.1161/ATVBAHA.108.176958

Ye, L., Jiang, W.G., 2016. Bone morphogenetic proteins in tumour associated angiogenesis and implication in cancer therapies. Cancer Letters 380, 586–597. https://doi.org/10.1016/j.canlet.2015.10.036

Yeo, J.-C., Ng, H.-H., 2013. The transcriptional regulation of pluripotency. Cell Research 23, 20–32. https://doi.org/10.1038/cr.2012.172

Ying, Q.-L., Nichols, J., Chambers, I., Smith, A., 2003. BMP Induction of Id Proteins Suppresses Differentiation and Sustains Embryonic Stem Cell Self-Renewal in Collaboration with STAT3. Cell 115, 281–292. https://doi.org/10.1016/S0092-8674(03)00847-X

Yoon, B.S., Pogue, R., Ovchinnikov, D.A., Yoshii, I., Mishina, Y., Behringer, R.R., Lyons, K.M., 2006. BMPs regulate multiple aspects of growth-plate chondrogenesis through opposing actions on FGF pathways. Development 133, 4667–4678. https://doi.org/10.1242/dev.02680

Yoshimatsu, Y., Watabe, T., 2011. Roles of TGF-β signals in endothelial-mesenchymal transition during cardiac fibrosis. Int J Inflam 2011, 724080. https://doi.org/10.4061/2011/724080

Yu, P.B., BAGAROVA, J., DEY, D., 2016. Methods and compositions for the treatment or prevention of abnormal bone formation in a soft tissue. WO2016130897A1.

Yu, P.B., Deng, D.Y., Lai, C.S., Hong, C.C., Cuny, G.D., Bouxsein, M.L., Hong, D.W., McManus, P.M., Katagiri, T., Sachidanandan, C., Kamiya, N., Fukuda, T., Mishina, Y., Peterson, R.T., Bloch, K.D., 2008a. BMP type I receptor inhibition reduces heterotopic [corrected] ossification. Nat. Med. 14, 1363–1369. https://doi.org/10.1038/nm.1888

Yu, P.B., Hong, C.C., Sachidanandan, C., Babitt, J.L., Deng, D.Y., Hoyng, S.A., Lin, H.Y., Bloch, K.D., Peterson, R.T., 2008b. Dorsomorphin inhibits BMP signals required for embryogenesis and iron metabolism. Nat. Chem. Biol. 4, 33–41. https://doi.org/10.1038/nchembio.2007.54

Zeisberg, E.M., Tarnavski, O., Zeisberg, M., Dorfman, A.L., McMullen, J.R., Gustafsson, E., Chandraker, A., Yuan, X., Pu, W.T., Roberts, A.B., Neilson, E.G., Sayegh, M.H., Izumo, S., Kalluri, R., 2007. Endothelial-to-mesenchymal transition contributes to cardiac fibrosis. Nat Med 13, 952–961. https://doi.org/10.1038/nm1613

Zelzer, E., McLean, W., Ng, Y.-S., Fukai, N., Reginato, A.M., Lovejoy, S., D'Amore, P.A., Olsen, B.R., 2002. Skeletal defects in VEGF120/120 mice reveal multiple roles for VEGF in skeletogenesis. Development 129, 1893–1904.

Zhang, H., Bradley, A., 1996. Mice deficient for BMP2 are nonviable and have defects in amnion/chorion and cardiac development. Development 122, 2977–2986.

Zhang, P., Li, J., Tan, Z., Wang, C., Liu, T., Chen, L., Yong, J., Jiang, W., Sun, X., Du, L., Ding, M., Deng, H., 2008. Short-term BMP-4 treatment initiates mesoderm induction in human embryonic stem cells. Blood 111, 1933–1941. https://doi.org/10.1182/blood-2007-02-074120

Zhang, P., Yan, X., Chen, Y., Yang, Z., Han, H., 2014. Notch signaling in blood vessels: from morphogenesis to homeostasis. Sci. China Life Sci. 57, 774–780. https://doi.org/10.1007/s11427-014-4716-0

Zhang, S.C., Wernig, M., Duncan, I.D., Brüstle, O., Thomson, J.A., 2001. In vitro differentiation of transplantable neural precursors from human embryonic stem cells. Nature Biotechnology 19, 1129–1133. https://doi.org/10.1038/nbt1201-1129

Zhang, Y.E., 2017. Non-Smad Signaling Pathways of the TGF-β Family. Cold Spring Harb Perspect Biol 9. https://doi.org/10.1101/cshperspect.a022129

Zhou, Q., Heinke, J., Vargas, A., Winnik, S., Krauss, T., Bode, C., Patterson, C., Moser, M., 2007. ERK signaling is a central regulator for BMP-4 dependent capillary sprouting. Cardiovasc. Res. 76, 390–399. https://doi.org/10.1016/j.cardiores.2007.08.003

Zhu, J., Lin, S.J., Zou, C., Makanji, Y., Jardetzky, T.S., Woodruff, T.K., 2012. Inhibin α-Subunit N Terminus Interacts with Activin Type IB Receptor to Disrupt Activin Signaling. J Biol Chem 287, 8060–8070. https://doi.org/10.1074/jbc.M111.293381

Zijlstra, A., Aimes, R.T., Zhu, D., Regazzoni, K., Kupriyanova, T., Seandel, M., Deryugina, E.I., Quigley, J.P., 2004. Collagenolysis-dependent Angiogenesis Mediated by Matrix Metalloproteinase-13 (Collagenase-3). J. Biol. Chem. 279, 27633–27645. https://doi.org/10.1074/jbc.M313617200

8. Statement of Authorship

Hiermit versichere ich, dass ich die hier vorliegende Doktorarbeit selbstständig und lediglich unter Benutzung der angegebenen Quellen und Hilfsmittel verfasst habe. Ich versichere außerdem, dass die vorliegende Arbeit weder in dieser noch in einer anderen Form einem anderen Prüfungsverfahren zugrunde gelegen hat.

Berlin, 22.12.2020

Susanne Hildebrandt

9. Acknowledgement

Am Ende dieser Arbeit möchte ich gern auf die letzten fünf Jahre zurückblicken und Danke sagen! Allegorisch gesehen startete dieses Promotionsprojekt noch ganz unreif, wie eine Vorläuferzelle, dessen Ausrichtung und Spezialisierung noch offen war. Durch den Kontakt und Input von wichtigen Wegbegleitern und Wegbegleiterinnen entstand eine Nische, die mit stetigem Wissensaustausch und Wachstumsfaktoren die Entwicklung eines gestärkten und spezialisierten vaskulären Netzwerks ermöglichte.
Den initialen Trigger für den komplexen, mehrstufigen Entwicklungsprozess verdanke ich vor allem meiner Doktormutter Frau **Prof. Dr. Petra Knaus**. Ich erinnere mich noch gut an unser erstes Gespräch anlässlich meiner Initiativbewerbung, wo Sie mir von einer seltenen Knochenerkrankung berichtete und sich sicher war, dass dies eine passende Projektrichtung für mich sei. In der Tat hörte ich zu diesem Zeitpunkt das erste Mal von der seltenen Erkrankung Fibrodysplasia Ossificans Progressiva (FOP), die ganz im Sinne der BMPs, neben dem Knochen, in weitaus mehr Geweben eine Rolle spielt. Von Anfang an beeindruckte mich Petras Enthusiasmus für die Rezeptorbiologie und ich schätze die anfängliche Projektfokussierung auf die ALK2 Rezeptorfunktion. Dies setzte eine wertvolle Basis um das spätere Krankheitsmodell von Patientenzellen mit molekularer Ausrichtung erfolgreich entwickeln zu können. Ich möchte mich ganz herzlich bei Petra für die Möglichkeit der Anfertigung dieses vielseitigen Promotionsprojekts in ihrem Labor und die wissenschaftliche Betreuung bedanken. Der stetige wissenschaftliche und persönliche Austausch mit Ihr und die Vermittlung von hilfreichen Kontakten in der Forschungslandschaft hat dieses Projekt geformt und gestaltet. Danke, für die Offenheit und Begeisterung neuen Dingen gegenüber. Daraus resultierten neue Labormethoden, Nachhaltigkeitsinitiativen und diverse Kollaborationen.
Zusätzlich bedanke ich mich für den wertvollen Austausch mit meinen Zweitgutachter
Herrn **Prof. Sigmar Stricker**. Das Feedback in den Mentoring Meetings war immer sehr hilfreich, um das Projekt weiter zu formen und vor allem in der Endphase die Key Findings und Novelty für die Verfassung der Publikation herauszustellen.
Des Weiteren bedanke ich mich bei Frau **Dr. Julia Haupt**. Wir teilten das Labor (leider nur) in meinem ersten Promotionsjahr, in dem ich überwiegend Plasmide klonierte. Dank Julia erhielt ich wertvolles Wissen und Einblicke in die FOP Thematik die über die Molekularbiologie hinausragte. Sie bestärkte mich darin, den Austausch auf Patiententreffen wahrzunehmen und initiierte den Kontakt zu Patientenzellmaterial an der Charité. Aus der ersten beeindruckenden Teilnahme des Jahrestreffens vom deutschen FOP e.V im Jahre 2017 entstand eine erfreuliche Zusammenarbeit auf persönlicher und beruflicher Ebene, die sogar in eine gemeinsame Antragsstellung mündete. Herzlicher Dank geht an **Ralf Fischer mit Familie** und allen **Freunden und Förderern des FOP e.V**, der auch unsere Forschung finanziell unterstützt. Ich bedanke mich für die jährliche Einladung und die Herausforderung meine Forschungsergebnisse einfachverständlich vorzutragen. Der anschließende Austausch generierte neue Ideen und Anregungen.
Für die Bereitstellung der FOP Patientenzellen bedanke ich mich bei **Prof. Dr. Petra Seemann** und **Dr. Laura Hildebrand**. Die hilfreichen Diskussionen mit Laura zu Beginn des Projekts mündeten sogar in die erfolgreiche Einwerbung von Drittmitteln über ein BSRT Joint Projekt. Zusätzlich danke ich **Dr. Bella Roßbach** und **Dr. Kurtz** für die Bereitstellung der Kontrollstammzelllinien.

Für das Stammzellprojekt wurde eine neue Kooperation mit **Dr. Harald Stachelscheid** gestartet werden, bei dem ich bereits als Bachelorstudentin die Stammzellkultur lernte. Ich bedanke mich für die Möglichkeit die Stammzellarbeiten bei Ihm im Labor durchzuführen und das er mit Rat und Tat dieses Projekt förderte und voranbrachte. Danke, an die Unterstützung seines gesamten **Stammzelllaborteams**, welches die Zusammenarbeit an zwei Laborstandorten machbar und reibungsloser gestaltete. Großen Dank an **Kristin Fischer**, die mit Enthusiasmus und technischer Unterstützung die Endotheldifferenzierung maßgeblich mit vorangetrieben hat.
Danke auch an **Tanja Fisch** für die Unterstützung der FACS Messungen und **Dr. Valeria Fernandez Vallone**, die bei unserem Kickbox iPSC ALK2-GFP Projekt motivierend mitwirkte. In diesem Zusammenhang bedanke ich mich für die Finanzierungsmöglichkeiten an der BSRT, Charité und dem ECRT. Daraus wurden Forschungsprojekte vorangetrieben, neu initiiert und ich konnte Weiterbildungsangebote wahrnehmen.
Vor allem danke ich **Dr. Sabine Bartosch** und **Bianca Kühn**, die mir administrativ und beratend zur Seite standen. Zusätzlich danke ich auch der Frauenförderung des Fachbereichs BCP der Freien Universität Berlin, der Dahlem Research School und **Simone Schlender**, die über den SFB958 meine Forschung und Weiterbildung unterstützte.
Großer Dank geht an die **Kollegen und Kolleginnen der gesamten AG Knaus** mit denen ich in den letzten Jahren zusammenarbeiten durfte. Vielen Dank an meine Benchkollegen
Dr. Jerome Jatzlau und **Vladimir Ugorets**, mit denen ich so manchen Abend mit bestelltem Essen im Institut verbrachte und tiefgründig wissenschaftliche wie auch welt-sozialpolitische Gespräche führte. Unterstützung, gepaart mit einem Lachen half in so manch frustrationsreichen Momenten. Herzlicher Dank geht an **Branka Kampfrath**, die in dem Forschungsprojekt tatkräftigt mitgearbeitet und mitgefiebert hat. Ich danke den Post Docs:
Dr. Christian Hiepen, **Dr. Maria Reichenbach**, **Dr. Gina Dörpholz** und **Dr. David Yadin** für wertvolles Feedback mit anspruchsvollen Seminarfragen und die Weitergabe von methodischer Expertise, die das Projekt vorangetrieben haben. Danke an Maria für die gemeinsame Durchführung der Flowexperimenten und danke an Chris und Jerome für die Zusammenarbeit im spanenden EAhy-PAH Projekt. Zusätzlich danke ich **Mounir Benamar** für die Unterstützung bei den Spheroid Assays und **Paul Mendez** für den Austausch über RNASeq Auswertungsmethoden. Ein herzliches Danke geht an **Nadine Großmann**, die Verstärkung und neue Inspiration in unsere FOP Forschung mit einfließen lassen hat. Mit Freude erinnere ich mich an unsere gemeinsame Teilnahme an diversen Rare Disease Veranstaltungen bei denen der leibliche Genuss meist nie zu kurz kam.
Für die Unterstützung im Labormanagement und lockeren Austausch auf der Treppe im Institut danke ich **Anna Jarek** und **Sonja Niedrig**. Ein großes Danke auch an **Katharina Hoffmann**, die für viele Vertrags-, Bestell- und Versandherausforderungen unersetzlich war und gepaart mit Ihrer lebhaften Art, Mut zugesprochen und Erfolge gefeiert hat. Danke auch an die zuverlässige, administrative Unterstützung von **Marina Filatova** in der AG Knaus und den KollegInnen **Yunyun Xiao**, **Nurcan Hastar**, **Mustafa Ilhan** und **Carolina Da Silva Madaleno**.
Aus dem Biochemie Institut möchte ich noch **Reinmar Undeutsch** für seine IT Unterstützung danken und **Dr. Arunima Murgai** für den interessanten Austausch und unsere unvergessliche Reise nach Japan für die BMP Konferenz, auf der wir die tolle Möglichkeit bekamen einen Vortrag über unsere Forschung zu halten.
In diesem Zusammenhang möchte ich mich auch bei der gesamten **FOP/ALK2 Forschungscommunity** bedanken, die mich zu Beginn an mit Ihrem Fachwissen, Forschungsmodellen und persönlichen Engagement für die Grundlagenforschung und

Translation inspirierte. Besonders der persönliche Austausch beispielsweise auf Fachtagungen mit **Dr. Toril Holien**, **Prof. Gudrun Valdimarsdóttir**, **Prof. Fred Kaplan**, **Prof. Eileen Shore**, **Dr. Gonzalo Sánchez-Duffhues** bereicherte meine Doktorarbeit mit neuem Wissen und Ideen.
In diesem Zusammenhang sind auch dankend die Besuche von Fachexperten aus Petras Forschungsnetzwerk wie **Prof. Marko Hyvönen** und **Prof. Christoph Winkler** und die laufende, spannende Kooperation mit **Prof. Joav Henis** und **Szofia Szilagyi** hervorzuheben.
Last but not least bedanke ich mich bei meiner **Familie und meinen Freunden**, die mir in all den Jahren der Ausbildung zur Seite standen und die nötige Abwechslung und Selbstreflektion stimulierten. Besonders meiner **Mutter**, die mich immer bestärkte neue Herausforderungen zu wagen, Selbstvertrauen zu gewinnen und auch Möglichkeiten in fremden Gewässern wahrzunehmen. Ich danke für die Unterstützung meiner **Schwester Sandra mit Familie**, die mich früh inspirierte neue Wege einzuschlagen und mir bei Entscheidungsfindungen zur Seite stand. Ich möchte mich auch herzlich bei meinem **Bruder Stephan** bedanken, der immer für eine Überraschung gut ist und mir mit einem Schnuckepaket den Endspurt versüßte. Lieben Dank für die Gedanken und Worte meiner langjährigen Freundin **Marga** aus der Ferne.
Ich danke meinen Studienfreundinnen **Rejzka** und **Lili**, die mich stets mit Rat und Tat unterstützen und mit denen ich zugleich Abenteuer, Abwechslung und Entspannung teilen kann. Von Herzen und ohne viel Worte danke ich besonders **Knut** für seine Liebe und Unterstützung in allen Lebenslagen. Die gemeinsamen Pausen haben mir viele arbeitsintensive Tage versüßt.
Anknüpfend an die Worte zu Beginn, verbleibt ein maturiertes vaskuläres Netzwerk, auf das ich mit Stolz und Dankbarkeit blicke und freue mich auf weitere Zweige, die daraus wachsen werden.

10. List of publications

10.1 Journal articles

Hildebrandt S., Kampfrath B., Fischer K., Hildebrand L., Haupt J., Stachelscheid H., Knaus P. "ActivinA induced SMAD1/5 signaling in an iPSC derived EC model of Fibrodysplasia ossificans Progressiva (FOP) can be rescued by the drug candidate Saracatinib", Stem Cell Reviews and Reports, 2020, in press

Hiepen C., Jatzlau J., **Hildebrandt S**., Kampfrath B., Goktas M., Murgai A., Cuellar Camacho J.L., Haag R., Ruppert C., Sengle G., Cavalcanti-Adam E.A., Blank K., Knaus P. BMPR2 acts as a gatekeeper to protect endothelial cells from increased TGFβ responses and altered cell mechanics", 2019, PLOS Biology

Hildebrandt S., Baschant U., Thiele S., Tuckermann J.,Hofbauer L.C.,Rauner M. „Glucocorticoids supress Wnt16 expression in osteolasts in vitro and in vivo", 2018, Nature Scientific Reports

Benn A., Haupt J., **Hildebrandt S.**, Kähler C., Knaus P. "Physiological and pathological consequences of vascular BMP signaling". Bone Morphogenetic Proteins: Systems Biology Regulators, edited by Vukicevic Slobodan and Sampath Kuber T, 2017, Springer Publishers

10.2 Oral Presentations

Talks

2017-2019 Annual German FOP patient meeting, Valbert, Germany

"Die Rolle des ALK2 Rezeptors in der Blugefäßinnenwand-mögliche Auswirkungen auf den Beginn der heterotopen Ossifikation"

09/2019 Tel Aviv University-Freie Universität Berlin Joint workshop, Berlin

"Using an iPSC approach to study BMP/TGFbeta signaling in endothelial cells in context of FOP."

12/2018 Berlin-Brandenburg School for regenerative Therapies (BSRT) Symposium, Berlin Germany

Hildebrandt S., Haupt J., Jatzlau J., Hildebrand L., Stachelscheid H., Knaus P "How a small failure in the BMP receptor ACVR1 primes endothelial cells to contribute to heterotopic bone formation in FOP"

10/2018 12th International BMP Conference, Tokyo, Japan

Hildebrandt S., Haupt J., Jatzlau J., Hildebrand L., Stachelscheid H., Knaus P. „Role of the BMP receptor ACVR1/ALK2 in endothelial cells derived from iPSC of FOP patients"

07/2017 Biochemistry Retreat, Freie Universität Berlin

Presenting research projects of the group of Prof. Petra Knaus

Hiepen C., Jatzlau J., **Hildebrandt S.** "Bone/Body Morphogenetic Protein signal transduction"

04/2015 4th Joint meeting of European Calcified Tissue Society (ECTS) & International Bone and Mineral Society (IBMS), Rotterdam, The Netherlands

Hildebrandt S., Thiele S., Baschant U., Salbach-Hirsch J., Tuckermann J., Hofbauer L. C, Rauner M. "Wnt16 promotes osteoblastogenesis and is negatively regulated by glucocorticoids *in vitro* and *in vivo*", Awarded a New Investigator Award

Poster Presentations

08/2017 TGFβ Meeting, Uppsala University, Sweden

Hildebrandt S., Haupt J., Jatzlau J., Hildebrand L., Stachelscheid H., Knaus P. „Generation of iPSC derived ECs and an endogenous ACVR1-GFP cell line"

12/2017 BSRT Symposium

Hildebrandt S., Haupt J., Jatzlau J., Hildebrand L., Stachelscheid H., Knaus P. „Generation of iPSC derived ECs and an endogenous ACVR1-GFP cell line"

11. Grants and fellowships

11/2019 Travel stipend to attend the FOP Drug Development Forum, USA
International FOP Association (IFOPA)

10/2018 Travel stipend to attend 12th International BMP Conference, Japan
University of Tokyo

01/2019 Young Scientist Kickbox Seed Grant for innovative research ideas
Hildebrandt S., Stachelscheid H., Knaus P. "Visualization of the endogenous BMP receptor ALK2 in endothelial cells using CRISPR/Cas9 and iPSC technology"
(Einstein Kickbox: *iPSC-GenEd*)
10.000 € consumable grant, Einstein Center for Regenerative Therapies

03/2018 Young Scientist Kickbox Seed Grant for innovative research ideas
Hildebrandt S., Stachelscheid H., Knaus P. "Visualization of the endogenous BMP receptor ALK2 in endothelial cells using CRISPR/Cas9 and iPSC technology"
(Einstein Kickbox: *iPSC-GenEd*)
5.000 € consumable grant, Einstein Center for Regenerative Therapies

07/2016 BSRT Joint Research Grant for collaboration with fellow PhD students
Hildebrandt S. Hildebrand L. "Contribution of endothelial cells to the initialization of flare-ups in Fibrodysplasia Ossificans Progressiva"
10.000 € consumable grant, Berlin-Brandenburg School for Regenerative Therapies

12. Curriculum vitae

For reasons of data protection the curriculum vitae is not published in the electronic version.